ANTIMALARIAL ACTIVITY OF AMINOGUANIDINES

By

Alina R. Krollenbrock

A DISSERTATION

Presented to the Department of Physiology & Pharmacology
and the Oregon Health & Science University
School of Medicine
in partial fulfillment of
the requirements for the degree of

Doctor of Philosophy

June 2022

School of Medicine

Oregon Health & Science University

CERTIFICATE OF APPROVAL

This is to certify that the PhD dissertation of

Alina Krollenbrock

has been approved

_____
Mentor/Advisor

_____
Member

_____
Member

_____
Member

_____
Member

Table of Contents

Table of Contents 1
List of Figures 4
List of Tables 7
List of Schemes 9
Acknowledgements 11
Abstract 13
Chapter 1 : Introduction 15
Malaria 15
Malaria Disease Burden 15
Malaria Life Cycle 16
Human Plasmodium Parasites 20
Global Eradication of Malaria 22
Chemical Therapy and Prophylaxis of Malaria 22
Vector Control Strategies 26
A Malaria Vaccine 28
Aminoguanidines 30
Robenidine: a veterinary anticoccidial drug 31
Aminoguanidines in other Pathogens 32
Chemical Modification of Robenidine 33
Aminoguanidines in Malaria 34
Conclusion 35
Chapter 2 : Experimental 36
Chemical Synthesis 36
General Chemistry – Materials and Instruments 36
Synthesis of Aminoguanidines 37
Preparation of Aminoguanidine Free Bases 71
Preparation of Aminoguanidine Phosphate Salts 71
Synthesis of Endochin-Like Quinolones 71
Biology and Experiments 78
General Biology - Parasite Culture and Drug Sensitivity 79
IC_{50} Determination by the Fluorescence-Based SYBR Green Assay 79
Variations on the SYBR Green Assay 80

HepG2 Cytotoxicity Assay....81
In Vivo Efficacy against Blood Stage Murine Malaria....82
Murine Microsomal Stability....83
Pharmacokinetics Profile of Compound **1**....83
In vivo Blood Stage Prophylaxis of ELQ Prodrugs in Murine Malaria....84
Pharmacokinetics of ELQ Prodrugs....84
Protein Target Identification with a Photoactivatable Probe....85
Chapter 3 : Robenidine Analogs are Potent Antimalarials in Drug-Resistant *Plasmodium falciparum*....87
Introduction....87
Results and Discussion....88
The aminoguanidine robenidine is an effective antimalarial in vitro....88
Synthesis of aminoguanidine robenidine analogs....89
Structure activity relationships of aminoguanidines in vitro....90
Aminoguanidines retain in vitro activity in drug-resistant strains of malaria....94
Aminoguanidines have high in vitro therapeutic indices....95
Aminoguanidines do not show Atovaquone synergy observed with linear biguanides....96
Aminoguanidine activity is concentration dependent but not time dependent....99
Lead aminoguanidines have high in vivo efficacy in a mouse model of malaria....100
1 is a highly potent antimalarial in vitro and in vivo....102
Murine microsomal stability of aminoguanidines correlates with in vivo activity....103
Conclusion....104
Chapter 4 : Structure Activity Relationships and Drug Action of the Aminoguanidines in Malaria....106
Introduction....106
Results and Discussion....107
Visual Appearance of Plasmodium Parasites Treated with Compound **1**....107
Synergy of Compound **1** with Commercial Antimalarial Drugs....108
Aminoguanidines in Synchronous Blood Stage Parasites....110
Pharmacokinetics of Compound **1**....112
Major Modifications to the Aminoguanidine Structure....115
In vitro Activity of Bicyclic and Heterocyclic Aminoguanidines....118
Analogs of Compound **1** and Compound **16**....123
Chemical Tools to Probe the Aminoguanidine Mechanism of Action....127
Alternative Salts of Aminoguanidines....131

In vivo Activity of Selected Aminoguanidines 133
Metabolic Stability of Aminoguanidines 135
Probing the Aminoguanidine Mechanism of Action 137
Chapter 5 : Alkoxycarbonate Ester Prodrugs of the Antimalarial ELQ-300 for Intramuscular Injection 142
Introduction 142
Results and Discussion 145
Synthesis of Alkoxycarbonate Ester Prodrugs 145
Physiochemical Properties of Alkoxycarbonate Ester Prodrugs 147
On-Target in vitro Antimalarial Activity of Alkoxycarbonate Ester Prodrugs 151
In vivo Blood Stage Prophylaxis of Intramuscular ELQ-331 and ELQ-492 153
Long-Term Pharmacokinetics of ELQ-331, ELQ-494, and ELQ-495 154
Conclusion 156
Chapter 6 : Conclusion 158
Summary and Conclusions 158
Future Directions 160
Down-selection of a Preclinical Aminoguanidine Drug Candidate 160
Exploration of the Aminoguanidine Drug Action 161
Aminoguanidines in Other Pathogens 163
References 165
Appendix 1: ^{1}H and ^{13}C NMR Spectra 189

List of Figures

Figure 1-1: Global Distribution of Malaria per 1000 people (WHO 2018). 16

Figure 1-2: The life cycle of *Plasmodium* parasites including the mosquito stage, liver stage, and erythrocytic cycle (Medicines for Malaria Venture). 17

Figure 1-3: *Plasmodium falciparum* Tm-90C2B parasites in human erythrocytes a: ring stage, b: trophozoite, c: schizont containing merozoites and a digestive vacuole that contains hemozoin. Images were captured by the author on a light microscope at 1000X magnification. 18

Figure 1-4: A high-resolution image of a *Plasmodium* parasite inside a host erythrocyte in which the apicoplast and a digestive vacuole containing hemozoin are visible (image from Medicines for Malaria Venture, mmv.org). 19

Figure 1-5: Selected antimalarial drugs; a: piperaquine, b: mefloquine, c: artemisinin, d: primaquine, e: proguanil, f: atovaquone, g: ELQ-300. 26

Figure 1-6: a: Robenidine, b: NCL195, c: CGP40215A. 32

Figure 3-1: a: Robenidine; b: compound **1**. 88

Figure 3-2: IC_{50} curve of robenidine in D6 compared with chloroquine. Y values represent fluorescence relative to untreated controls. 89

Figure 3-3: a: proguanil is converted to cycloguanil *in vivo* by a mechanism involving the abstraction of the proton shown in red, b: LT-31 cannot cyclize by the same mechanism because a tert-butyl group is used in place of proguanil's isopropyl group, c: the aminoguanidine **13** is structurally similar to LT-31. 97

Figure 3-4: The concentration-response curve of the linear biguanide LT-31 shifts significantly from the drug-sensitive D6 *P. falciparum* strain to the drug-resistant A6 strain. Activity is restored in A6 with the addition of 10 nM atovaquone (ATQ). Conversely, the

concentration-response curves of the aminoguanidines **13** and **16** do not shift significantly between the three test conditions.....98

Figure 3-5: Inhibition of *P. falciparum* Dd2 growth by 16 (green) and 21 (purple) at 48 hr (dotted curves), 72 hr (dashed curves), and 96 hr (solid curves) time points.....100

Figure 4-1: Light microscope images of Geimsa-stained blood smears of *P. falciparum* Tm90-C2B-infected erythrocytes; a: untreated parasites; b: parasites incubated for 24 hr with 400 nM **1**.....108

Figure 4-2: Isobolograms measuring the synergy of **1** with Atovaquone (left), Chloroquine (center), and ELQ-300 (right) in *P. falciparum* Tm90-C2B.....109

Figure 4-3: IC_{50} curves of **1**, **16**, atovaquone (ATQ), and chloroquine (CQ) in parasites synchronized to the ring stage or the trophozoite stage. *P. falciparum* D6 (top) parasites are drug sensitive, while Dd2 parasites are chloroquine resistant but atovaquone sensitive. 111

Figure 4-4: Plasma concentration-time curves for oral and IV **1**. 113

Figure 4-5: The notation of positions around pyridine, naphthalene, and quinoline ring systems. Pyridine and naphthalene are symmetrical and have some positions which are chemically equivalent. Quinoline is asymmetrical and has no chemically equivalent positions. 121

Figure 4-6: Top: a rhodamine fluorescence image (180 sec exposure) of a gel containing *P. falciparum* Tm90-C2B lysates incubated with the probe compound **86**. Lane 1 contains all blue ladder. Sample 1 (lanes 2 and 9) contained lysates with none of the probe compound. Sample 2 (lanes 3 and 10) was incubated with 0.1 μM of the probe, Sample 3 (lanes 4 and 11) with 1 μM, Sample 4 (lanes 5 and 12) with 10 μM, and Sample 5 (lanes 6 and 13) with 100 μM. Sample 6 (lanes 7 and 14) was also incubated with 100 μM of the probe but received no UV irradiation. Lanes 8 and 14 had no samples added. Bottom: a Coomassie Blue stain of the above gel showing the protein contents of the parasite lysates.....139

Figure 5-1: a: an ester, b: a carbonate ester, c: an alkoxycarbonate ester, d: ELQ-300, an antimalarial drug candidate, e: ELQ-331, an alkoxycarbonate ester prodrug of ELQ-300.145

Figure 5-2: Top: melting points of the alkoxycarbonate ester prodrug series. Bottom: sesame oil solubility of the alkoxycarbonate ester prodrug series. The x axis of both graphs refers to the number of carbon atoms in the terminal alkyl chain of the pro-moiety (Scheme A1, R group). 148

Figure 5-3: Solubility testing of alkoxycarbonate ester prodrugs.....150

Figure 5-4: IC_{50} curves of alkoxycarbonate ester prodrugs of ELQ-300 in Dd2 (ELQ-300-sensitive) and D1 (ELQ-300-resistant) *P. falciparum*.....151

Figure 5-5: Long-term pharmacokinetics of ELQ-300 after dosing IM with the alkoxycarbonate ester prodrugs ELQ-331, ELQ-494, or ELQ-495 (Image from Smilkstein 2019). 155

Figure 6-1: Color spectrum of the aminoguanidine library (other compounds were colorless). Top: pure aminoguanidine hydrochloride salts. Bottom: aminoguanidines at 10 mM in DMSO.....163

List of Tables

Table 1-1: Features of the human malaria parasites.....20

Table 3-1: Aminoguanidine halogen series and antimalarial drugs[a].....92

Table 3-2: Aminoguanidine methyl, methoxy, fluoromethyl, fluoromethoxy, and nitrile series[a]..93

Table 3-3: Other aminoguanidines[a] 94

Table 3-4: Atovaquone synergy of aminoguanidines and the linear biguanide LT-31 99

Table 3-5: *Pf* Dd2 IC_{50} of 16 and 21 vs drug incubation length[a] 100

Table 3-6: *in vivo* ED_{50} and ED_{90} of lead aminoguanidines[a] 102

Table 3-7: Murine Microsomal Stability of Aminoguanidines[a].....103

Table 4-1: Mean FICs of **1** combined with Atovaquone, Chloroquine, or ELQ-300 110

Table 4-2: IC_{50}s of **1**, **16**, atovaquone, and chloroquine in synchronous parasites. 112

Table 4-3: Plasma concentration of IV and oral **1** over time in CD1 mice.....113

Table 4-4: Pharmacokinetic parameters of **1**. 114

Table 4-5: *in vitro* activity of carbohydrazides, thiocarbohydrazides, and other modified aminoguanidines.....116

Table 4-6: *in vitro* activity of bicyclic and heterocyclic aminoguanidines.....119

Table 4-7: *in vitro* activity of analogs of **1** and **16**. 123

Table 4-8: *in vitro* antimalarial activity of aminoguanidine chemical tools. 129

Table 4-9: *in vitro* activity of alternative salts of aminoguanidines. 132

Table 4-10: Day 5 *in vivo* inhibition of parasites at 5 mg/kg/day.....134

Table 4-11: ED_{50} values of selected aminoguanidines. 135

Table 4-12: Murine microsomal stability of selected aminoguanidines. 136

Table 5-1: Physiochemical Properties of Alkoxycarbonate Ester Prodrugs of ELQ-300 149

Table 5-2: Solubility of alkoxycarbonate ester prodrugs in IM injection vehicles 150

Table 5-3: *in vitro* activity of alkoxycarbonate ester prodrugs of ELQ-300.....152

Table 5-4: *in vivo* prophylactic activity of alkoxycarbonate ester prodrugs of ELQ-300 153

List of Schemes

Scheme 3-1: A general synthesis of aminoguanidine robenidine analogs. Compounds were prepared by refluxing benzaldehydes or acetophenones with 1,3-diaminoguanidine hydrochloride in ethanol. 90

Scheme 4-1: General synthesis of aminoguanidines, carbohydrazides, and thiocarbohydrazides. 116

Scheme 4-2: Synthesis of compounds **74**, **75**, and **76**. **74** was prepared by a substitution reaction with zinc dicyanide catalyzed by palladium tetrakis. **75** and **76** were prepared by the general aminoguanidine synthesis procedure. 125

Scheme 4-3: 77 was prepared with a modified aminoguanidine synthesis procedure. One equivalent each of 3-cyano-4-fluorobenzaldehyde, 4-trifluoromethoxybenzaldehyde, and 1,3-diaminoguanidine were refluxed in ethanol, resulting in a 1:2:1 mixture of 16:77:1. This mixture was separated using reverse phase chromatography with a C-18 stationary phase and MeOH/H_2O mobile phase with 0.5% formic acid. 126

Scheme 4-4: Attempted synthesis of azide aminoguanidines **81** and **82**. Azidobenzaldehydes **79** and **80** were prepared from bromobenzaldehydes via a copper catalyzed substitution reaction using sodium azide, DMEDA, and sodium ascorbate. The corresponding azide aminoguanidines were not produced by the general aminoguanidine synthesis method. .128

Scheme 4-5: Synthesis of the benzophenone aminoguanidines **85** and **86**. 4-Formylbenzaldehyde (**84**) was oxidized from a benzyl alcohol starting material. Two equivalents were combined with 1,3-diaminoguanidine to form the symmetrical benzophenone **85** via the general aminoguanidine synthesis method. One equivalent of **84** was combined with 4-propynoxybenzaldehyde and 1,3-diaminoguanidine to produce a 1:2:1 mixture of **32**:**86**:**85**, which was separated by reverse phase chromatography as with compound **77**. 130

Scheme 5-1: Two step synthesis of alkoxycarbonate ester ELQ=300 prodrugs starting from alcohols, chloromethyl chloroformate, and ELQ-300. R is an unbranched alkyl group ranging from methyl to decyl. 147

Acknowledgements

The research comprising this dissertation would not have been possible without the contributions of many people within and outside of our research group. Their support has allowed me to broaden and deepen my knowledge, skills, and respect for the complexity of the natural world.

Thank you to my mentor Dr. Michael Riscoe for his patience, support and teaching throughout my time in the group. Dr. Riscoe's research group is living proof that the highest quality of scientific research can be performed while never compromising the work-life balance of the people who perform it. I have on more than one occasion referred to Dr. Riscoe as 'the gold standard' for a graduate school mentor.

Thank you to Dr. Yuexin Li for performing the *in vivo* experiments throughout this dissertation as well as some of the cytotoxicity *in vitro* assays. Dr. Li is the definition of a professional when it comes to mouse work.

Thank you to Dr. Aaron Nilsen, Dr. Sovitj Pou, and Dr. Rolf Winter for providing valuable support and troubleshooting for my chemical synthesis. Thank you to Dr. Marty Smilkstein for teaching me the SYBR Green *in vitro* assay and for his thoughtful conceptualization of malaria biochemistry. Thank you also to other past and present members of the Riscoe lab including Lisa Frueh, Dr. Isaac Forquer, Dr. Kayla Sheridan, Galen Miley, Dr. Katherine Liebman, Dr. Alison Stickles, and Mason Handford, all of whom have helped me directly with my work at least once.

Other scientists outside of the Riscoe group have also been instrumental in assisting my dissertation research. Thank you to the staff of Chem Partner for performing metabolic stability and pharmacokinetics experiments for the aminoguanidines, and to the OHSU pharmacokinetics core for assisting with the pharmacokinetics of the ELQs. Thank you to the Portland State University Mass Spec Facility and Rosie Dodean and Samanthi Gedara for performing the HRMS

characterization of the aminoguanidines (Rosie also supplied me with the starting material for compound **37**, which was an intermediate she had previously synthesized for another project). Thank you to Dr. Michael Cohen for allowing me to use his equipment and resources to test my probe compound **86**, and especially to Dr. Anna Duell for very patiently assisting me with the experiments. Thank you also to Dr. Stone Doggett and Dr. Jane Kelly for assisting with the attempted liver-stage bioluminescence imaging, and to Dr. Daniel Marks and Tanya Korzun for supplying us with an emergency stock of luciferin at the last minute.

Thank you to my dissertation advisory committee chair Dr. Scott Landfear, who was also a mentor though my T32 training grant, an experience which was very valuable for exploring my options in a scientific career. Thank you also to my other committee members Dr. Xiangshu Xiao and Dr. Michael Cohen for valuable insights and suggestions at each meeting.

Thank you to my collaborators from next door and across the world. Thank you to Dr. Jennifer Keiser and her student Christian Lotz for their very promising work testing my aminoguanidine library in *Schistosoma*. Similarly, thank you to Dr. Stone Doggett and his lab members Cole Bryant and Dr. Sam Drennan for testing the compounds against *Toxoplasma*.

Thank you to my union, Graduate Researchers United, for fighting for a better standard of living for graduate researchers at OHSU, and particularly to Sam Papadakis, Marc Meadows, Rich Posert, and Danielle Mathieson for bargaining our first contract. Thank you to AFSCME Council 75 for supporting us in this effort.

Finally, thank you to my family. To my parents, who each have PhDs of their own, thank you for encouraging and supporting my interest in science throughout my life. To my wife Ashley, thank you for helping me keep perspective when I become too focused on the small details. To my daughter Everett, thanks for always having a hug and kiss ready when I leave for work and come home. To my son, I can't wait to meet you in two short months!

Abstract

Malaria is a mosquito-borne parasitic disease that has deeply impacted the human population throughout recorded history. The disease burden of malaria has gradually declined over the last few decades due to continuing global efforts towards its eradication. In the past two years however, this trend has unfortunately stalled and reversed as healthcare resources are diverted to address the global COVID-19 pandemic. Though the GSK-developed RTS-S vaccine was recently approved by the WHO for malaria prevention, this tool will not be sufficient on its own to eradicate malaria, particularly as antimalarial drug resistance is rapidly spreading.

To combat drug resistance, novel antimalarial drugs must be developed without susceptibility to existing resistance mechanisms. One approach to discovering novel drug classes is to repurpose molecular scaffolds known to have activity in other disease areas. In the research comprising this dissertation, the veterinary anticoccidial drug robenidine and its derivatives of the aminoguanidine chemotype were investigated as potential antimalarial drugs. Coccidiosis is caused by the *Eimeria* parasite, a close genetic relative of the malaria parasite *Plasmodium*. Despite this relationship and robenidine's commercial use for over 50 years, the aminoguanidines have not been systematically evaluated for antimalarial activity up to this point.

Chapter 1 of this dissertation discusses the malaria parasite including its life cycle and variations among the five human pathogenic species, as well as the state of the field of antimalarial drugs and other eradication techniques. Chapter 2 provides detailed descriptions of the chemical syntheses and experiments discussed throughout the document. Chapter 3 discusses the structure activity relationships of a first set of 38 aminoguanidine compounds and is also published under the same title in ACS Infectious Diseases (Krollenbrock 2020) except for the section on atovaquone synergy which is original to this document. Chapter 4 describes the

structure activity relationships of additional aminoguanidines with broader and more complex structures, as well as several experiments exploring the drug action of the aminoguanidines.

Another unmet need in the global malaria eradication effort is for long-lasting prophylactic drugs. Chapter 5 discusses research on alkoxycarbonate ester prodrugs of the antimalarial endochin-like quinolones (ELQs) and their optimization for delivery by intramuscular injection. The research of this chapter supported a publication in Malaria Journal (Smilkstein 2019) but all data and text are original to this document excluding the figure on the pharmacokinetics of ELQ prodrugs. Chapter 6 provides a brief conclusion summarizing the findings of this research and discussing future directions for the projects.

The research described in this dissertation applies to two chemical scaffolds with excellent potential as antimalarial drugs, the aminoguanidines and the endochin-like quinolones. The aminoguanidines are a novel structural class capable of evading both laboratory generated and clinical drug-resistance mechanisms. The endochin-like quinolones can be formulated as long-acting injectable malaria prophylactics. Both classes may one day be used clinically as tools in the fight for malaria eradication.

Chapter 1 : Introduction

Malaria

Malaria Disease Burden

It is hard to overstate the burden of malaria on human health and wellbeing. Hundreds of millions of cases of the disease are reported each year, resulting in hundreds of thousands of deaths. Though these have gradually declined over the last two decades, this trend has seen an unfortunate and significant reversal in the last two years due to the strain placed on healthcare infrastructure by the global COVID-19 pandemic (Aborode 2021). Whereas in 2019 there were 227 million cases reported, in 2020 there were 241 million (WHO 2021). Deaths due to malaria follow a similar pattern of gradual decline from 2000 to 2019 and a significant uptick from 2019 (558,000 deaths) to 2020 (627,000 deaths). This resurgence can be linked to three major factors: the overwhelming demand placed on the healthcare systems of malaria endemic countries due to COVID-19, the reduction or cancelation of planned malaria eradication programs (such as the distribution of insecticide treated nets) also due to COVID-19, and the emergence and spread of resistance to existing malaria therapies (Weiss 2021).

The majority of malaria cases (95% in 2020) occur in sub-Saharan Africa (Figure 1-1), with other endemic regions present in southeast Asia, and central and South America (WHO 2021). Most deaths due to malaria occur in children under the age of 5, and people with compromised immune systems are also at increased risk for severe and fatal malaria (Alemu 2013). Children are particularly at risk to death due to cerebral malaria (Phillips 1990). Malaria

in pregnant women impacts fetal development, frequently resulting in reduced birth weight and higher incidence of miscarriage (Grunnet 2022).

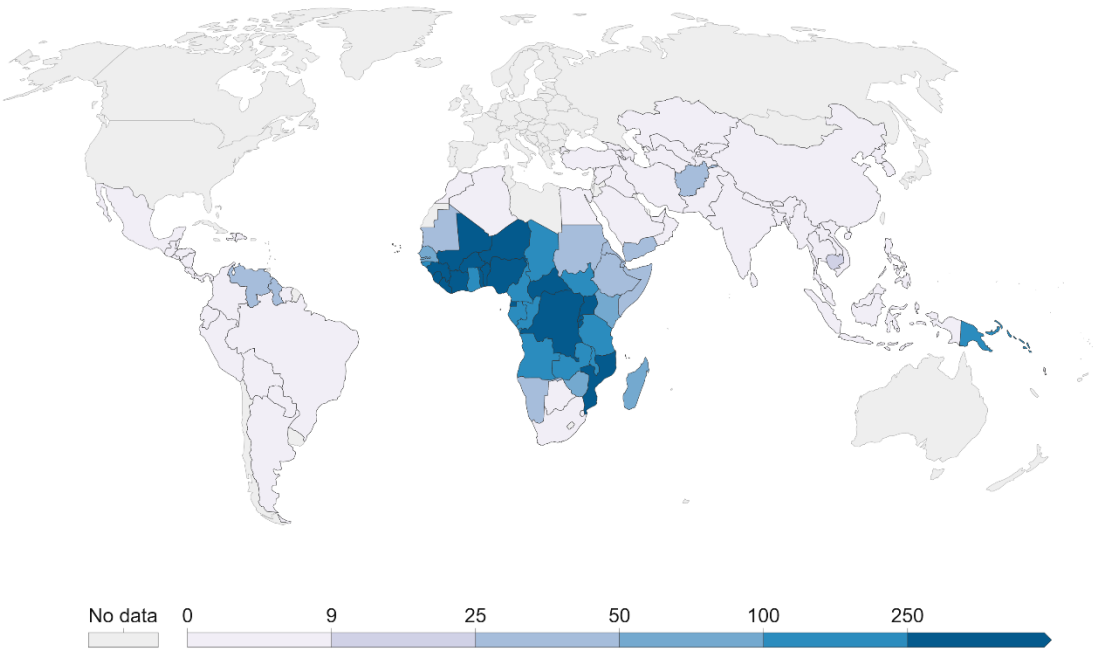

Figure 1-1: Global Distribution of Malaria per 1000 people (WHO 2018).

Malaria Life Cycle

Malaria is a widespread and deadly tropical disease. It is an intracellular protozoan parasite which invades the liver (hepatocytes) and red blood cells (erythrocytes) in the host. The malaria parasite *Plasmodium* is a member of the Apicomplexa phylum, which is also the phylum of other human and animal pathogens such as *Toxoplasma*, *Babesia* and *Eimeria*. This phylum is characterized by the presence of an organelle called the apicoplast, a four-membraned vesicle with a role in host cell invasion (McFadden 2010).

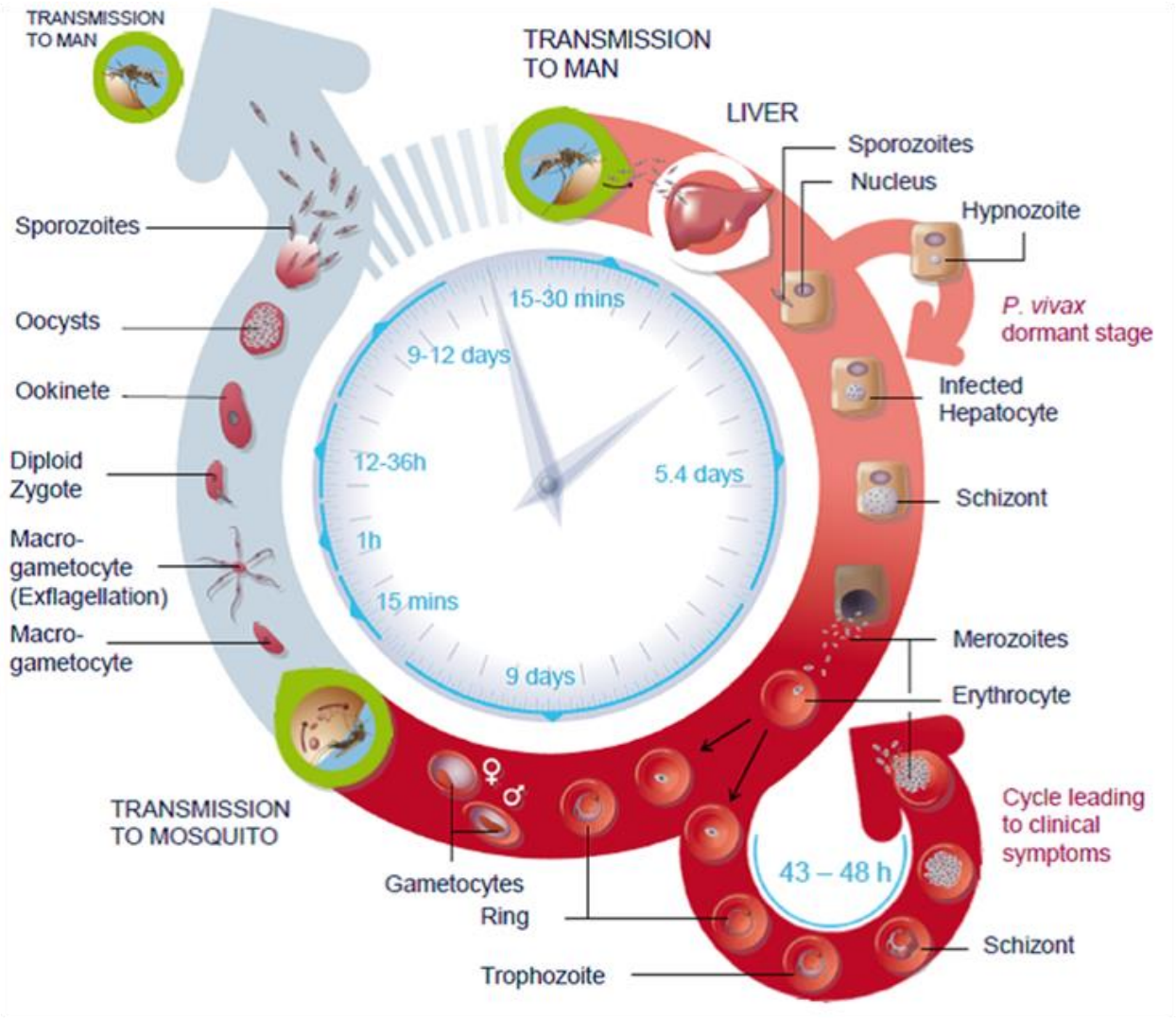

Figure 1-2: The life cycle of *Plasmodium* parasites including the mosquito stage, liver stage, and erythrocytic cycle (Medicines for Malaria Venture).

The malaria parasite has a complex, multi-stage life cycle (Figure 1-2) which can be broadly categorized into the liver stage, blood stage, and mosquito stage. Notably, the parasite requires both the Anopheles mosquito vector and a vertebrate host, which varies from mammals to reptiles to birds depending on the malaria species (Grilo 2016, Templeton 2016). The parasites initially invade in a form called sporozoites, which enter the mammalian host via a bite from the mosquito. In the bloodstream, these sporozoites are quickly carried to the host liver, where they invade host hepatocytes (Meis 1983).

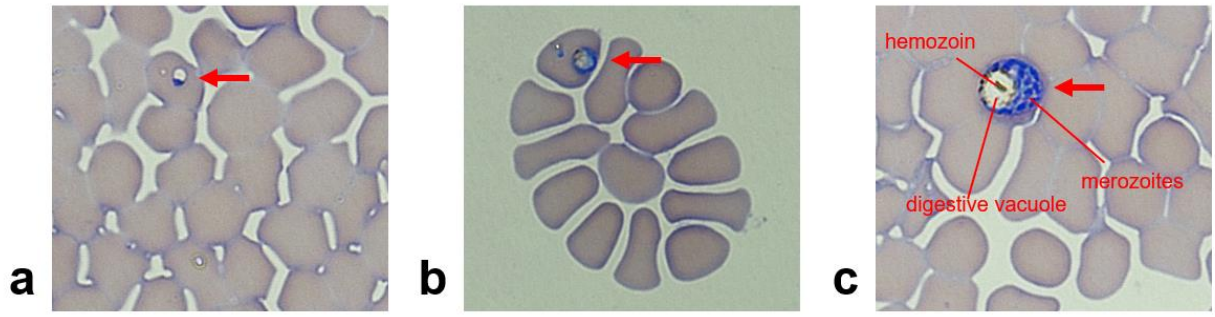

Figure 1-3: *Plasmodium falciparum* Tm-90C2B parasites in human erythrocytes a: ring stage, b: trophozoite, c: schizont containing merozoites and a digestive vacuole that contains hemozoin. Images were captured by the author on a light microscope at 1000X magnification.

After approximately a week of maturation, the parasites leave the hepatocytes as merozoites, which then invade erythrocytes and begin a replication process called the erythrocytic cycle (Dvorak 1975). Inside the blood cells, the parasites undergo a 24- to 72-hour cycle of development and replication, transforming from the small ring stage (Figure 1-3a) to trophozoites (Figure 1-3b) to the larger schizont (Figure 1-3c), which contains many nascent merozoites (Beck 1970). In the course of this growth and development the parasites consume the protein contents of the erythrocyte, primarily hemoglobin. A byproduct of the consumption of hemoglobin by the parasite is the release of the cofactor heme, which is not utilized by the parasite (Slater 1991). Under the acidic conditions of the parasite's digestive vacuole and in the absence of its protein environment, free heme associates into reciprocal dimers, forming inert crystals called hemozoin (Bendrat 1995, Pagola 2000), which can be visualized microscopically in stained smears of parasitized red blood cells (Figure 1-3c, Figure 1-4).

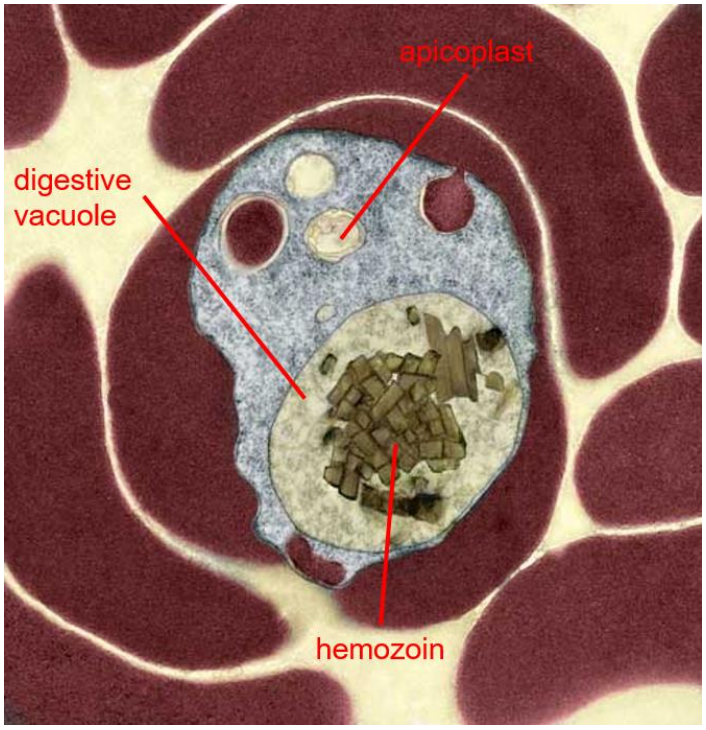

Figure 1-4: A high-resolution image of a *Plasmodium* parasite inside a host erythrocyte in which the apicoplast and a digestive vacuole containing hemozoin are visible (image from Medicines for Malaria Venture, mmv.org).

After one iteration of the erythrocytic cycle, new merozoites are released from the schizont accompanied by lysis of the host erythrocyte. Each merozoite rapidly colonizes a new cell, often within 30 seconds of release (Hadley 1986). This leaves little time for the host immune system to recognize and respond to the pathogen. Typically, the erythrocytic cycle remains synchronized across the whole population of merozoites for a given malaria infection, and at each 48-hour time point a larger number of merozoites is simultaneously released into the bloodstream. Each schizont can release over 20 new merozoites, and consequently the parasitemia, or percentage of erythrocytes containing parasites, can increase 20-fold with each cycle (Fairley 1949).

After sufficient cycles, the host immune system responds to the presence of the pathogen and induces a fever in the host. The immune response is clinically apparent in parallel to the

parasite replication process, as fevers occur on the same 48-hour cycle with increasing severity throughout the course of infection as disease burden increases (Covell 1960).

The erythrocytic cycle is self-sustaining via asexual reproduction, however, a subset of merozoites diverge into a sexual form called gametocytes, and it is these gametocytes which are picked up by mosquitoes during a blood meal (Gwadz 1979). Haploid gametocytes fuse to form diploid zygotes, which proliferate via sexual reproduction in the mosquito midgut. The *Plasmodium* zygotes transform into oocysts which contain many sporozoites. When the sporozoites are released, they travel to the mosquito salivary glands where they can be transferred to a new host when the female mosquito takes another blood meal, completing the *Plasmodium* life cycle (Vaughan 2021).

Human Plasmodium Parasites

Five different species of *Plasmodium* parasites can cause a human malaria infection (Table 1-1). These parasites, which include *P. falciparum*, *P. vivax*, *P. ovale*, *P. malariae*, and *P. knowlesi*, differ in their disease severity and presentation (Miller 2002).

Table 1-1: Features of the human malaria parasites

***Plasmodium* Species**	**Erythrocytic Cycle Length (hr)**	**Erythrocytes Invaded**	**Hypnozoite Formation**	**Disease Severity**
falciparum	48	All Stages	No	Severe
vivax	48	Reticulocytes Only	Yes	Moderate
ovale	48	All Stages	Yes	Moderate
malariae	24	Older Erythrocytes	No	Benign
knowlesi	72	All Stages	No	Moderate

Plasmodium falciparum is the deadliest human malaria pathogen, responsible for nearly all malaria deaths (Gething 2017). It has a 48-hour blood stage cycle and invades erythrocytes of any developmental stage. It is the primary species in sub-Saharan Africa. The increased lethality of this species is related to its unique ability to encode surface adhesion proteins for the host erythrocyte (Wahlgren 2017). Cells producing these proteins adhere to vascular walls where they escape detection by the host immune system. This feature causes the severe symptoms of cerebral malaria, in which infected red blood cells adhere to the arterial wall of particularly narrow cerebral capillaries, causing deadly blockages of blood flow to the brain. Cerebral malaria may also have long lasting consequences for survivors, including cognitive impairment and an increased risk for seizure disorders (John 2008). Vascular wall adhesion also impedes placental blood flow to developing fetuses, leading to low birth weight and other developmental issues (Fried 2017).

The second most common form of malaria is *P. vivax*, the primary species observed in Southeast Asia and South America (Mendis 2001). This species also has a 48-hour erythrocytic cycle. Because *P. vivax* selectively invades immature red blood cells, or reticulocytes, the parasitemia of *vivax* infections has a lower upper limit compared to falciparum malaria (Galinski 2008). This in turn limits disease severity as vivax malaria is only rarely fatal. The more concerning aspect of *vivax* malaria is its ability to enter into a dormant form during the liver stage called a hypnozoite (Adams 2017). Hypnozoites respond to few known antimalarial drugs and can cause disease recrudescence even years after the initial infection. *Vivax* malaria parasites utilize a structural property of reticulocytes called the Duffy coat protein in their attachment and cell invasion mechanism (Chootong 2010). Interestingly, in Africa a large portion of the population is ‘Duffy negative’ rendering intrinsic immunity to this species across much of the continent.

The remaining three *Plasmodium* species are significantly rarer in human infections. *P. ovale* is similar to *P. vivax* in its 48-hour erythrocytic cycle and the ability to form hypnozoites (Collins 2005). *P. knowlesi* is unique in its shorter 24-hr erythrocytic cycle and ability to use either

monkeys or humans as a mammalian host. In southeast Asia where the species is most prevalent, zoonotic infection presents a challenge for eradication in regions where humans and long-tailed macaques cohabitate (Antinori 2012). *P. malariae* has the longest erythrocytic cycle at 72 hours (Oriero 2021) and is considered a benign form of the disease.

Global Eradication of Malaria

Chemical Therapy and Prophylaxis of Malaria

Several different classes of antimalarial drugs have been utilized in modern and traditional medicine for the treatment and prophylaxis of malaria (Figure 1-5). These classes include the 4-aminoquinolines, 8-aminoquinolines, 4-methanoloquinolines, antifolates, antimicrobials, antirespiratory compounds, and artemisinin derivatives.

The 4-aminoquinolines include chloroquine, amodiaquine, and the bis-quinoline piperaquine (Figure 1-5a). These compounds function through an unexpected mode of action involving no drug target in the parasite's biology. Instead, these compounds exploit the residual heme cofactor remaining as a waste product after the parasite consumes hemoglobin within the parasite Achilles' heel, the acidic digestive vacuole (Gluzman 1994). Under untreated conditions, this residual heme associates into crystals called hemozoin which are large enough to be visualized on a light microscope (Figure 1-4). However, when a 4-aminoquinoline drug is present, the drug molecule binds heme as it is liberated during the digestion process and prevents the formation of hemozoin. Enough free drug-heme complexes accumulate that the parasite's digestive vacuole is lysed by osmotic pressure. Without a traditional protein target, it would appear that this drug class would be highly unlikely to produce resistance. Unfortunately, the parasite evades chloroquine and other 4-aminoquinolines via the expression of an efflux

transporter termed the ‘chloroquine resistance transporter’ (Sidhu 2002, Kim 2019). The prevalence and widespread nature of this resistance mechanism has led to the reduction in clinical use of chloroquine, and other members of this class are typically used in combination therapies to evade or delay the onset of resistance.

Another aminoquinoline class, the 8-aminoquinolines primaquine (Figure 1-5d) and tafenoquine, function by a separate mechanism from the 4-aminoquinolines. This mechanism remained unknown for 70 years, but recent evidence indicates that an activated redox active form of primaquine interacts with cytochrome p450 NADH oxoreductase in the human host’s liver and bone marrow and locally produces an excess of hydrogen peroxide and associated oxygen radicals, killing the parasites via oxidative stress (Camarda 2019). This class of antimalarials is particularly effective against the liver stage of malaria, and further is the only class with the ability to kill latent hypnozoites in the liver (Llanos-Cuentas 2019). Accordingly, these compounds are commonly prescribed for malaria caused by *Plasmodium vivax* and *ovale*. A major limitation of this antimalarial class is their potential toxicity for individuals with glucose-6-phosphate-dehydrogenase (G6PDH) deficiency, a condition affecting about 1/6th of the global population (~400 million people) with a concentration in Africa (Carter 2018, Luzzato 2020).

A final quinoline drug class, the 4-quinolinemethanols, function by a mechanism of action which until recently was unknown. Recent studies indicate that these drugs inhibit *Plasmodium* protein synthesis at the 80S ribosomal subunit (Wong 2017). Quinine is a 4-quinolinemethanol used in traditional Peruvian medicine as an extract from the bark of the cinchona tree, and is famously also a component of tonic water (Findlay 1944). The more complex compound mefloquine (Figure 1-5b) is a commonly prescribed antimalarial prophylactic, though taking this drug is associated with undesirable and potentially serious side effects (Weinke 1991). Particularly in patients with psychiatric disorders, melfoquine use can trigger panic attacks, psychosis, and seizures, and these effects can persist for a long time after receiving the drug. Clinical resistance to 4-quinolinemethanols has been shown in Southeast Asia and Africa.

Antifolate antimalarials such as sulfadoxine, pyrimethamine, proguanil (Figure 1-5e), and chlorproguanil function by inhibiting enzymes of the *Plasmodium* folate synthesis pathway, either dihydrofolate reductase (DHFR) or dihydropteroate synthase (DHPS) (Zhang 1991). Sulfadoxine (a DHPS inhibitor) and pyrimethamine (a DHFR inhibitor) are frequently prescribed as an antifolate combination therapy. Notably, the DHFR protein is co-translated with thymidylate synthetase as a dual function enzyme, whereas in humans these enzymes exist separately. Mutations to both *pf*DHFR and *pf*DHPS have arisen in the field which cause antifolate resistance, and for this reason these drugs are more commonly prescribed as components of a drug cocktail (Gutman 2015). Antifolate resistance in malaria parasites is widespread.

Although the malaria parasite is eukaryotic, some antimicrobial compounds such as doxycycline, tetracycline, and clindamycin are also effective antimalarials (Imboden 1950, Grande 1956, de Carvalho 2021). These drugs target the apicoplast organelle, which may lend credence to its theoretical origins as an endosymbiote (Kohler 1997).

Another class of antimalarials are anti-respiratory compounds such as Atovaquone (Figure 1-5f), which target the parasite's mitochondrial electron transport chain. Atovaquone inhibits the *Plasmodium* cytochrome bc_1 (complex III), which in addition to suspending the oxidation of ubiquinol to ubiquinone deprives the parasites of vital precursors of pyrimidine biosynthesis (Davies 1989). Atovaquone rapidly accrues resistance in the clinic and is commonly prescribed as a daily prophylactic in conjunction with the antifolate proguanil as the combination therapy Malarone. Members of the Endochin-like quinolone (ELQ) chemotype described by our group also inhibit cytochrome bc_1, though many of them including the potent antimalarial ELQ-300 (Figure 1-5g) do so at the reductive Q_i binding site rather than the oxidative Q_o site where Atovaquone binds (Stickles 2015). ELQ-331, a prodrug of ELQ-300, is in preclinical development by the Medicines for Malaria Venture (Frueh 2017).

The current last line of defense in complicated malaria cases are artemisinin combination therapies (ACTs), in which artemisinin (Figure 1-5c) or a derivative such as artemether or

artesunate are paired with a partner drug such as piperaquine, lumefantrine, or amodiaquine (Douglas 2010). Artemisinin has been used for centuries in Chinese medicine as an extract from wormwood, but it was not until relatively recently that this compound was identified as the active therapeutic component of the extract and a tentative mechanism of action was described (Tu, 2011). Artemisinin appears to work via the localized production of free radicals resulting from chelation of iron atoms involved in peroxide bridges (Tilley 2016). ACTs rapidly clear parasites from the blood and are effective in drug-resistant strains. However, in 2008 resistance to ACTs was discovered in Southeast Asia, and pan-resistant malaria strains continue to persist in that region (Noedl 2008). Even more concerningly, ACT resistance in sub-Saharan Africa was described in 2021 (Fukuda 2021). The potential devastation caused by the spread of pan-resistant malaria in Africa threatens to undo the efforts of the past decades towards global malaria eradication.

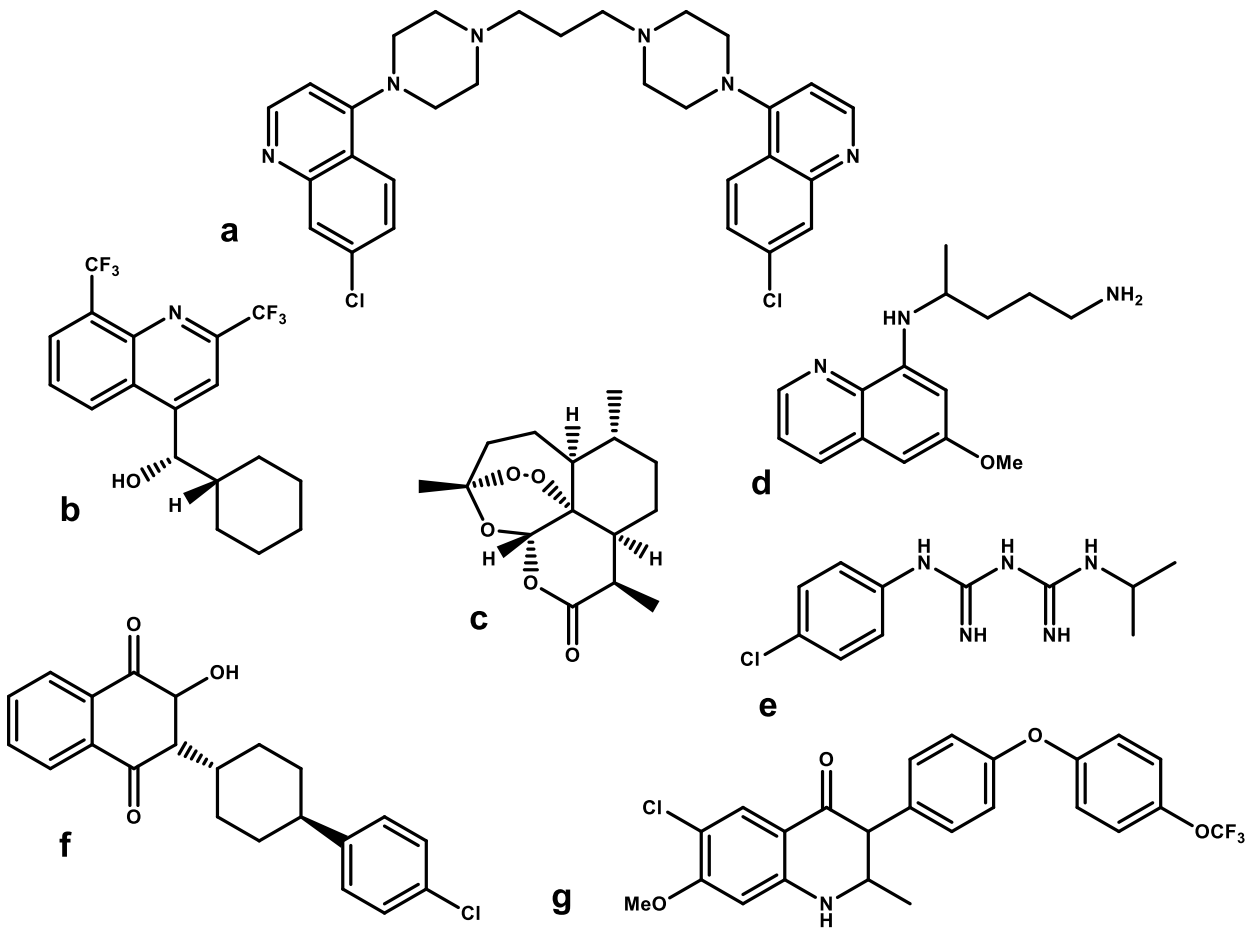

Figure 1-5: Selected antimalarial drugs; a: piperaquine, b: mefloquine, c: artemisinin, d: primaquine, e: proguanil, f: atovaquone, g: ELQ-300.

Vector Control Strategies

Another key component of the fight for malaria eradication is control of the malaria vector, the *Anopheles* mosquito. The two major strategies for vector control focus on indoor spaces and include insecticide treated nets and indoor residual spraying. Other tactics bring vector control to outdoor locations, meeting mosquitoes at their source.

The most common vector control strategy is the distribution of insecticide-treated nets (ITNs) to individuals in malaria endemic regions (Killeen 2007). These nets are used to cover beds and sleeping areas, preventing malaria transmission during sleep. Insecticides used in ITNs

include pyrethroids like permethrin, organochlorines like dichloro-diphenyl-trichloroethane (DDT), organophosphates like malathion, and carbamates like propoxur. One issue with this control strategy is the misuse of ITNs for fishing, which causes environmental damage by depleting small fish with their fine mesh, and leeching of insecticides into waterways. Another concern analogous to drug resistance in *Plasmodium* is selecting for insecticide resistance in Anopheles mosquitoes (Hemingway 2016). All four approved insecticide classes have reported resistance in the field. Chemical treated nets of the near future may include antimalarial compounds to block transmission between hosts. In one study, surface contact with the antimalarial drug atovaquone arrested parasite growth in the midgut of *Anopheles* mosquitoes (Paton 2019).

Another strategy often used in conjunction with ITNs is indoor residual spraying (IRS). In this approach, insecticide solutions are sprayed on the interior walls of homes in malaria endemic areas (Oxborough 2016). This method makes use of a behavioral characteristic of Anopheles mosquitoes, which very commonly land on a wall surface after taking a blood meal. IRS uses the same classes of insecticides as ITNs, and as such is subject to the same concerns about insecticide resistance.

Combating vector transmission in outdoor spaces is a greater challenge and is attempted less commonly in malaria endemic regions because of its relatively high cost (Killeen 2017). Among the approaches to outdoor vector control is large scale larvicidal spraying at mosquito breeding sites in wetlands, preventing the mosquitoes from reaching their adult form. Another strategy is internal or external treatment of livestock with insecticides, as many animals are also targets for Anopheles mosquito biting. Larger outdoor spaces can also be sprayed from the ground or by plane.

A more experimental approach to vector control is the concept of transgenic mosquito release. Anopheles mosquitoes can be genetically engineered to prevent malaria transmission to humans. One example is the development of mosquitoes expressing an anti-*P. falciparum* circumsporozoite protein antibody, which prevents transmission of malaria to humans by attacking

sporozoites in the insects' salivary glands (Yamamoto 2019). In theory, the large-scale release of transgenic mosquitoes would cause the transmission-blocking trait to spread throughout the mosquito population. In practice, the success of this approach relies on the significant assumption that there is no evolutionary fitness cost associated with these genetic modifications. Mathematical models have been developed describing the potential effects of large-scale release of transgenic mosquitos (Rafikov 2008). In 2019 the first major real-world test of this concept was performed in Burkina Faso using a mark-release-recapture study design (Yao 2022). This study, which used sterile male mosquitoes, demonstrated that transgenic mosquitoes had significantly shorter lifespans and decreased mobility compared to wildtype controls. Even if the technological aspects of this approach can be improved upon, its advisability is questionable as there are many potential consequences for the mosquito population, malaria parasite counter-evolution, and the ecological balance of malaria endemic regions.

A Malaria Vaccine

A final strategy for the eradication of malaria is the augmentation of the human immune response with a malaria vaccine. Malaria immunity does not arise easily from simple exposure to the disease, immunity requires over 20 exposures to the pathogen and is never complete sterilizing immunity. Human populations with historical roots in malaria endemic regions have an over-representation of genetic traits which make them more resilient to the disease. The native sub-Saharan African population has a greater population density for sickle cell trait, which is the heterozygous version of sickle cell anemia. This trait is advantageous for malaria prevention because it reduces the parasites' ability to invade erythrocytes successfully. Similarly, a higher percentage of sub-Saharan Africans are negative for the Duffy antigen, effectively making them immune to *Plasmodium vivax*, which requires this protein for cell invasion. Glucose-6-phosphate

dehydrogenase deficiency (G6PDD) is also associated with better malaria outcomes and is more common in the African population.

Researchers have attempted to develop vaccines for malaria for many decades and have run into obstacles that persist even to the present day. One significant challenge is the morphological transformation between the *Plasmodium* life cycle stages; no malaria antigen is present at every stage of the life cycle (Palatnik de Sousa 2020). Other difficulties are shared with those of natural immunity: multiple exposures are required, immunity is short lived, and applies only to a specific strain. This is in part because red blood cells do not present immune-histocompatibility antigens, meaning that the T-cell memory response cannot be engaged. Initially it was believed that exposure to *Plasmodium vivax*, a less deadly species of human malaria, could serve as a form of vaccine, and its immunoprotective capacity was assessed in the mid 20th century (Heidelberger 1946). Another early approach to the malaria vaccine came in 1967 and focused on the *Plasmodium* life cycle stage that first enters the human body, the sporozoite (Nussenzweig 1967). In this study, irradiated sporozoites were demonstrated to protect mice from subsequent infections, but the approach could not be translated to human use. The co-administration of a suspension of mycobacterium in mineral oil called Freund's adjuvant (Ward 1950) improved efficacy in animals, but produced unwanted side-effects ranging from liver degeneration in ducks to injection-site lesions in rhesus monkeys (Nussenzweig 1984). In 1977, a method for culturing parasites of the erythrocytic cycle outside of animal hosts was developed (Trager 1977), which furthered malaria research in all areas including vaccine development. In 1980 the external 'circumsporozoite' protein of sporozoites was determined to be antigenic (Yoshida 1980), and this protein is still a major target for vaccine development. Despite advancing vaccine technology in recent decades, a vaccine with long lasting, broadly active efficacy has proven elusive (Mahmoudi 2017, Matuschewski 2017). The GMZ2 vaccine candidate, which targeted the surface proteins of blood stage merozoites, failed to produce sufficient efficacy in a

phase II trial (Sirima 2016). The Multiple epitope thrombospondin adhesion protein (ME-TRAP) vaccine also failed in phase II (Afolabi 2016).

2021 marked a major milestone in malaria vaccine development when the WHO offered its first ever malaria vaccine approval to GSK's RTS-S vaccine. The biochemical construct used in this vaccine was first developed in the 1980s and consists of a combination of *Plasmodium* sporozoite antigens and hepatitis B viral proteins (Rutgers 1988). In this mixture, the 'repeat domain' (R) and T-cell epitope (T) of the circumsporozoite protein are fused with the surface antigen (S) of hepatitis B to form a single fusion protein. This fusion protein is then combined with HepB surface antigen on its own to form the RTS-S construct, which self-assembles into virus-like particles. Clinical trials were conducted from 2012 to 2019 with varying levels of efficacy and success (Mahmoudi 2017). A three-dose regimen of the vaccine is currently beginning widespread population administration in Malawi, Ghana, and Kenya (WHO 2019).

This vaccine presents an exciting new tool for malaria eradication, but its impact will neither be instantaneous nor complete. Reaching remote populations in malaria endemic regions is challenging even for a one-time intervention, and administering 3 vaccine doses and an additional booster to the same individuals is exponentially more difficult. The intramuscular or intravenous injections required for vaccination also require a higher level of skill for healthcare providers than oral drug administrations. The vaccine also shows reduced efficacy in children, who are most susceptible to malaria fatalities as compared with adults (Olotu 2016). With rapidly spreading drug resistance including the recent emergence of artemisinin resistance in Asia and Africa, it is clear that additional options are desperately needed for treatment and prevention of malaria.

Aminoguanidines

Robenidine: a veterinary anticoccidial drug

Development of new malaria drug classes that can evade existing resistance mechanisms is an urgent global need if elimination and eradication goals are to be achieved. One frequently proven successful approach to the development of novel therapeutics is to begin with a drug for a related parasite or pathogen and refine its structure using medicinal chemistry techniques.

Robenidine (Figure 1-6a), formerly called robenzidene, is a veterinary drug developed in the early 1970s to treat coccidiosis caused by parasites in the *Eimeria* genus (Kantor 1970, Reid 1970, Ryley 1971, Ryley 1972, Wong 1972, Kennett 1974). Robenidine is frequently added to animal feed to prevent and treat coccidiosis in chickens (Berger 1974), other fowl (Long 1978), and rabbits (Peters 1979). *Eimeria* and *Plasmodium*, the parasite responsible for malaria infections, are both members of the Apicomplexan phylum, distinguished by the presence of the apical complex and frequent presence of the apicoplast organelle (Wilson 1996).

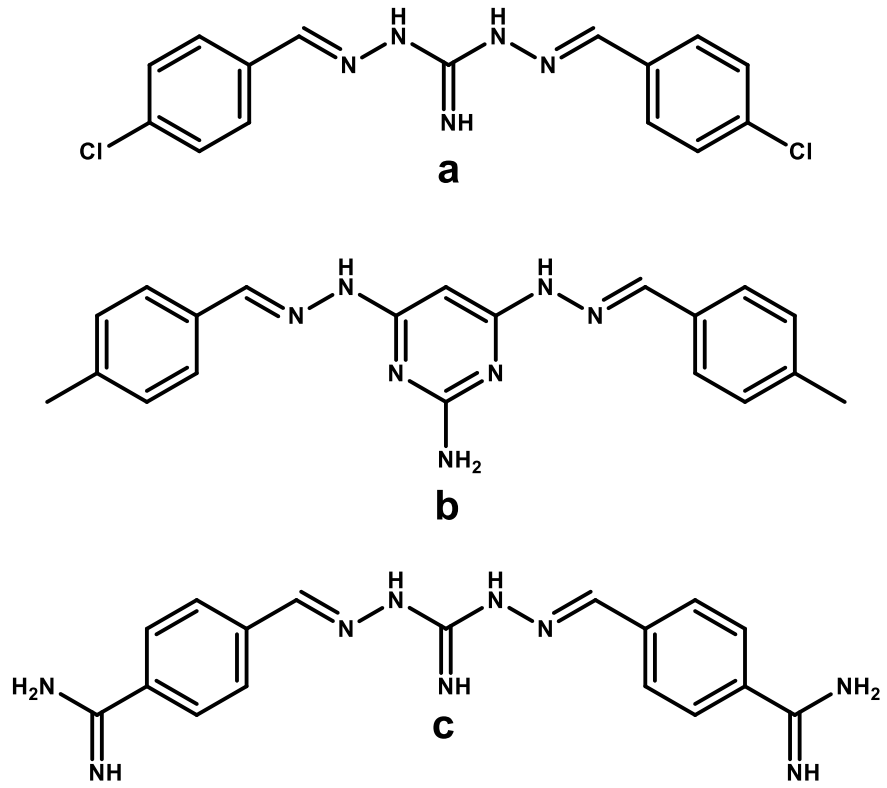

Figure 1-6: a: Robenidine, b: NCL195, c: CGP40215A.

Aminoguanidines in other Pathogens

Robenidine and other aminoguanidines have been evaluated for efficacy against several other protozoan parasites, including *Toxoplasma gondii* (in vitro IC_{50} 0.03 µg/mL for robenidine) (Ito 1974, Krylov 1976, Bakhtari 1988, Ricketts 1993), *Leishmania donovani* (in vitro IC_{50} 18 µM for the analogue CGP 40215A) (Mukhopadhyay 1996), *Babesia microti* (murine in vivo non-recrudescence dose 100 mg/kg/day for oral robenidine) (Yao 2015, Huang 2017), and the trypanosomes, *T. brucei* and *T. cruzi* (in vitro IC_{50} 20 µM for the analogue CGP 40215A) (Bacchi 1996, Brun 2001, Beswick 2006). It has also been tested against microorganisms such as *Lactobacillus* (Puchalski 2020), *E. coli* (Stanley 1996), *Acanthamoeba polyphaga* (Ogbunude 2001), *Goussia carpelli* (Molnar 2007), and several other Gram-positive and Gram-negative bacterial pathogens (Hansen 2009, Claes 2019).

Chemical Modification of Robenidine

Recently, work by Trott and McClusky (Abraham 2016, Ogunniyi 2017, Russell 2018, Russell 2019, Abraham 2019, Khazandi 2019) has further explored the aminoguanidine chemotype of robenidine, applying a medicinal chemistry approach to repurpose the drug for various bacterial pathogens. Their group synthesized a library of structurally diverse di-aryl aminoguanidines and evaluated their efficacy in Methicillin-Resistant *Staphylococcus aureus* (MRSA), Vancomycin Resistant Enterococci (VRE), *E. coli*, and *P. aeruginosa* (Abraham 2016). Their initial study included halogenated, alkylated, hydroxy-, and methoxy- substituted di-aryl aminoguanidines. Among mono-substituted compounds, chlorinated and alkylated aminoguanidines showed the greatest antimicrobial activity. Multi-substitution of active compounds did not improve their activity with the exception of a 2-F, 4-Cl compound which surpassed mono-halogenated parent compounds. Bicyclic and heterocyclic compounds were also evaluated, though these compounds showed little to no antimicrobial activity. Substitution at the benzyl position adjacent to the aminoguanidine core with halogens and small alkyl substituents had a generally positive effect on activity.

A second SAR study from the same group investigated monomeric and asymmetrical aminoguanidines as well as symmetrical di-aryl compounds (Russell 2018). In general, asymmetrical compounds had reduced antimicrobial activity compared with symmetrical counterparts. Monomeric aminoguanidines were inactive without a long alkyl chain at the benzyl position adjacent to the aminoguanidine core. Additional bicyclic and heterocyclic symmetrical aminoguanidines had little antimicrobial activity with the exception of two potent indole compounds. Modification of the central immine nitrogen to oxygen or sulfur eliminated antimicrobial activity, but conversion of the immine component to an isosteric aminopyrimidine ring in a follow-up study demonstrated improved activity over the original aminoguanidines

(Russell 2019). Subsequent research from this group has consequently focused on the aminopyridines such as NCL195 (Figure 1-6b).

Trott and McClusky's research has demonstrated that the aminoguanidine chemical scaffold is amenable to synthetic modification and can successfully be refined for activity against pathogens other than Eimeria. The activity of Robenidine and its aminoguanidine analogs against protozoan parasites remained to be determined.

Aminoguanidines in Malaria

There has been surprisingly little research into the efficacy of robenidine and other aminoguanidines in malaria despite the close genetic ties between *Plasmodium* and *Eimeria*. In the initial disclosure of Robenidine's discovery, the authors mentioned assessing the compound against other parasitic pathogens including the murine malaria species *Plasmodium berghei* (Kantor 1970). No numerical value for its efficacy was included in this publication, but it was described as "*somewhat effective*." No follow-up research was described by this or other research groups to evaluate robenidine in human or non-human malaria.

The 5-nitrogen core structure of robenidine, 1,3-diaminoguanidine, is a known inhibitor of nitric oxide synthase in the mammalian spleen, and suppression of nitric oxide production is associated with evasion of the immune system by malaria parasites (Ahvazi 1995). This indicates that aminoguanidine without aryl substituents may actually worsen malaria infections and increase parasitemia. Aminoguanidine hemisulfate administration elevated malaria infection in mice (Taylor-Robinson 1999).

The di-aryl immine Robenidine analog CGP 40215A (Figure 1-6c), an S-adenosylmethionine decarboxylase inhibitor, was demonstrated to inhibit *Plasmodium falciparum* growth with an IC_{50} of 1.8 µM in an investigation of intracellular polyamine concentrations in *Plasmodium* parasites (Das Gupta 2005). This compound was not shown to affect the polyamine

biosynthesis pathway under study by this group and was consequently not further explored or developed as an antimalarial drug.

To date, no medicinal chemistry efforts have focused on refining and optimizing the aminoguanidine scaffold for antimalarial activity. The research comprising this dissertation represents the first attempt to evaluate structure–activity relationships (SAR) of the aminoguanidine chemotype against malaria parasites.

Conclusion

The work of this dissertation describes the initial validation of a novel class of antimalarial drugs: the aminoguanidines. Many of these molecules have highly potent antimalarial activity *in vitro* which is maintained across multiple drug-resistant strains of *Plasmodium falciparum*. These molecules have little to no cytotoxicity *in vitro* and maintain large *in vitro* therapeutic indices. Several aminoguanidines are also highly effective *in vivo* in murine malaria and have good to excellent metabolic stability. Overall, the aminoguanidine class appears very promising as a potential therapeutic tool in the fight for global malaria eradication.

Chapter 2 : Experimental

Chemical Synthesis

General Chemistry – Materials and Instruments

All solvents, starting materials, and reagents were acquired from commercial sources (Sigma-Aldrich, Combi-Blocks and Ambeed). Robenidine was obtained from Santa Cruz Biotechnology (Santa Cruz, California). All materials were used without further purification. ^{1}H and ^{13}C NMR Spectra were taken on a Bruker 400 MHz instrument and chemical shifts are reported relative to TMS (0.0 ppm). Fluorescence measurements were recorded using a Molecular Devices Spectramax iD3 equipped with Softmax Pro 7 software. Final compounds were measured to be >95% pure by high performance liquid chromatography (HPLC) using an Agilent Technologies 1260 Infinity II system (unless otherwise noted). Gas Chromatography Mass Spectrometry (GCMS) was performed on an Agilent GCMS system including a GC System (7890B), MSD (5977A) and autosampler (7693), and data was visualized and processed using Agilent MassHunter software. High-resolution mass spectrometry (HRMS) using electrospray ionization was performed by the Portland State University BioAnalytical Mass Spectrometry Facility. Melting points were measured using a Stanford Research Systems OptiMelt Automated Melting Point System (model MPA100). Note on compound naming: Names for aminoguanidine compounds 39-86 were generated using ChemDraw Professional v. 18. Names for compounds 1-39 were named using a previous version of ChemDraw and follow slightly different naming conventions without alkene geometry specified. The original names for these compounds are used here to match their published names.

Synthesis of Aminoguanidines

1 *- 2,2'-Bis[(3-cyano-4-fluorophenyl)methylene]carbonimidic Dihydrazide Hydrochloride*

A solution of 3-cyano-4-fluorobenzaldehyde (1.31 g, 8.8 mmol, 2.2 eq.) and 1,3-diaminoguanidine hydrochloride (500 mg, 4 mmol, 1 eq.) in ethanol (5 mL) was refluxed for 16 hr. Diethyl ether (10 mL) was added and the product carbonimidic dihydrazide crashed out of solution as a white solid. The product was filtered, washed with diethyl ether, and recrystallized from methanol as a hydrochloride salt. Yield: 1.54 g, 99 %. ^{1}H NMR (400 MHz, DMSO-d6) δ 12.56 (s, 2H), 8.76 (s, 2H), 8.64 (d, J = 5.63 Hz, 2H), 8.46 (s, 2H), 8.33-8.32 (m, 2H), 7.68 (t, J = 8.92, 2H). ^{13}C NMR (100 MHz, DMSO-d6) δ 164.98, 162.40, 153.57, 146.25, 136.94, 135.95, 133.22, 131.61, 131.57, 117.73, 117.53, 114.22, 101.56, 101.40. HRMS found 352.1111, M+H. MP = 317-319°C.

2 *- 2,2'-Bis[(2-fluorophenyl)methylene]carbonimidic Dihydrazide Hydrochloride*

A solution of 2-fluorobenzaldehyde (1.1 g, 8.8 mmol, 2.2 eq.) and 1,3-diaminoguanidine hydrochloride (500 mg, 4 mmol, 1 eq.) in ethanol (5 mL) was refluxed for 16 hr. Diethyl ether (10 mL) was added and the product carbonimidic dihydrazide crashed out of solution as a white solid. The product was filtered, washed with diethyl ether, and recrystallized from methanol as a hydrochloride salt. Yield: 1.34 g, 99 %. ^{1}H NMR (400 MHz, DMSO-d6) δ 12.54 (s, 2H), 8.72 (s, 2H), 8.64 (s, 2H), 8.36 (dt, J = 7.9, 1.72, 2H), 7.59-7.53 (m, 2H), 7.34 (t, J = 7.9 Hz, 4H). ^{13}C NMR (100 MHz, DMSO-d6) δ 162.21, 159.71, 152.74, 141.62, 132.93, 127.31, 124.75, 120.82, 116.07, 115.86. HRMS found 302.1206, M+H. MP = 293-295°C.

3 *- 2,2'-Bis[(3-fluorophenyl)methylene]carbonimidic Dihydrazide Hydrochloride*

A solution of 3-fluorobenzaldehyde (1.09 g, 8.8 mmol, 2.2 eq.) and 1,3-diaminoguanidine hydrochloride (500 mg, 4 mmol, 1 eq.) in ethanol (5 mL) was refluxed for 16 hr. Diethyl ether (10 mL) was added and the product carbonimidic dihydrazide crashed out of solution as a white solid.

The product was filtered, washed with diethyl ether, and recrystallized from methanol as a hydrochloride salt. Yield: 1.31 g, 97 %. ^{1}H NMR (400 MHz, DMSO-d6) δ 12.56 (s, 2H), 8.69 (s, 2H), 8.48 (s, 2H), 7.98 (d, J = 10.3 Hz, 2H), 7.70(d, 7.6 Hz, 2H), 7.53 (q, J = 7.3, 2H), 7.33 (t, J = 8.3, 2H). ^{13}C NMR (100 MHz, DMSO-d6) δ 164.14, 161.72, 153.47, 148.02, 136.37, 136.28, 131.34, 131,26, 125.37, 118.15, 117.94, 113.89, 113.66. HRMS found 302.1206, M+H. MP = 281-283°C.

4 *- 2,2'-Bis[(4-fluorophenyl)methylene]carbonimidic Dihydrazide Hydrochloride*

A solution of 4-fluorobenzaldehyde (1.09 g, 8.8 mmol, 2.2 eq.) and 1,3-diaminoguanidine hydrochloride (500 mg, 4 mmol, 1 eq.) in ethanol (5 mL) was refluxed for 16 hr. Diethyl ether (10 mL) was added and the product carbonimidic dihydrazide crashed out of solution as a white solid. The product was filtered, washed with diethyl ether, and recrystallized from methanol as a hydrochloride salt. Yield: 1.33 g, 99 %. ^{1}H NMR (400 MHz, DMSO-d6) δ 12.32 (s, 2H), 8.56 (s, 2H), 8.44 (s, 2H), 8.03 (t, J = 6.5 Hz, 4H), 7.34 (t, J = 8.2, 4H). ^{13}C NMR (100 MHz, DMSO-d6) δ 165.24, 162.77, 153.41, 148.14, 130.71, 130.62, 130.48, 130.45, 116.40, 116.19. HRMS found 302.1205, M+H. MP = 295-297°C.

5 *- 2,2'-Bis[(2-chlorophenyl)methylene]carbonimidic Dihydrazide Hydrochloride*

A solution of 2-chlorobenzaldehyde (1.23 g, 8.8 mmol, 2.2 eq.) and 1,3-diaminoguanidine hydrochloride (500 g, 4 mmol, 1 eq.) in ethanol (5 mL) was refluxed for 16 hr. Diethyl ether (10 mL) was added and the product carbonimidic dihydrazide crashed out of solution as a white solid. The product was filtered, washed with diethyl ether, and recrystallized from methanol as a hydrochloride salt. Yield: 1.42 g, 96 %. ^{1}H NMR (400 MHz, DMSO-d6) δ 12.62 (s, 2H), 8.88 (s, 2H), 8.69 (s, 2H), 8.43 (d, J = 7.15 Hz, 2H), 7.58-7.46 (m, 6H). ^{13}C NMR (100 MHz, DMSO-d6) δ 153.19, 145.53, 134.06, 132.77, 131.03, 130.39, 128.51, 127.95. HRMS found 334.0620, M+H. MP = 295-297°C.

6 *- 2,2'-Bis[(3-chlorophenyl)methylene]carbonimidic Dihydrazide Hydrochloride*

A solution of 3-chlorobenzaldehyde (1.23 g, 8.8 mmol, 2.2 eq.) and 1,3-diaminoguanidine hydrochloride (500 g, 4 mmol, 1 eq.) in ethanol (5 mL) was refluxed for 16 hr. Diethyl ether (10 mL) was added and the product carbonimidic dihydrazide crashed out of solution as a white solid. The product was filtered, washed with diethyl ether, and recrystallized from methanol as a hydrochloride salt. Yield: 1.48 g, 100 %. ^{1}H NMR (400 MHz, DMSO-d6) δ 12.39 (s, 2H), 8.69 (s, 2H), 8.43 (s, 2H), 8.17 (s, 2H), 7.83 (d, J = 6.49 Hz, 2H), 7.59-7.50 (m, 2H). . ^{13}C NMR (100 MHz, DMSO-d6) δ 153.40, 147.93, 135.91, 134.27, 131.11. 130.92, 127.71, 127.06. HRMS found 334.0619, M+H. MP = 268-270°C.

7 *- 2,2'-Bis[(2-bromophenyl)methylene]carbonimidic Dihydrazide Hydrochloride*

A solution of 2-bromobenzaldehyde (1.23 g, 8.8 mmol, 2.2 eq.) and 1,3-diaminoguanidine hydrochloride (500 g, 4 mmol, 1 eq.) in ethanol (5 mL) was refluxed for 16 hr. Diethyl ether (10 mL) was added and the product carbonimidic dihydrazide crashed out of solution as a white solid. The product was filtered, washed with diethyl ether, and recrystallized from methanol as a hydrochloride salt. Yield: 1.83 g, 100 %. ^{1}H NMR (400 MHz, DMSO-d6) δ 12.52 (s, 2H), 8.80 (s, 2H), 8.66 (s, 2H), 8.39 (d, J = 7.64 Hz, 2H), 7.73 (d, J = 7.94, 2H), 7.51 (t, J = 7.43 Hz, 2H), 7.43 (t, J = 7.56, 2H). ^{13}C NMR (100 MHz, DMSO-d6) δ 153.21, 133.66, 133.00, 132.53, 128.87, 128.44, 124.44. HRMS found 423.9586, M+H. MP = 279-281°C.

8 *- 2,2'-Bis[(3-bromophenyl)methylene]carbonimidic Dihydrazide Hydrochloride*

A solution of 3-bromobenzaldehyde (1.63 g, 8.8 mmol, 2.2 eq.) and 1,3-diaminoguanidine hydrochloride (500 mg, 4 mmol, 1 eq.) in ethanol (5 mL) was refluxed for 16 hr. Diethyl ether (10 mL) was added and the product carbonimidic dihydrazide crashed out of solution as a white solid. The product was filtered, washed with diethyl ether, and recrystallized from methanol as a

hydrochloride salt. Yield: 1.80 g, 98 %. ^{1}H NMR (400 MHz, DMSO-d6) δ 12.28 (s, 2H), 8.66 (s, 2H), 8.39 (s, 2H), 8.29 (t, J = 3.08 Hz, 2H), 7.87 (d, J = 7.80, 2H), 7.68 (dd, J = 8.00, 2.79, 2H), 7.45 (t, J = 7.86, 2H). ^{13}C NMR (100 MHz, DMSO-d6) δ 136.13, 133.80, 131.34, 129.95, 128.05, 122.83. HRMS found 423.9589, M+H. MP = 258-260°C.

9 *- 2,2'-Bis[(4-bromophenyl)methylene]carbonimidic Dihydrazide Hydrochloride*

A solution of 4-bromobenzaldehyde (1.63 g, 8.8 mmol, 2.2 eq.) and 1,3-diaminoguanidine hydrochloride (500 g, 4 mmol, 1 eq.) in ethanol (5 mL) was refluxed for 16 hr. Diethyl ether (10 mL) was added and the product carbonimidic dihydrazide crashed out of solution as a white solid. The product was filtered, washed with diethyl ether, and recrystallized from methanol as a hydrochloride salt. Yield: 1.73 g, 94 %. ^{1}H NMR (400 MHz, DMSO-d6) δ 12.32 (s, 2H), 8.61 (s, 2H), 8.41 (s, 2H), 7.91 (d, J = 8.24 Hz, 4H), 7.70 (d, J = 8.21, 4H). ^{13}C NMR (100 MHz, DMSO-d6) δ 153.32, 148.29, 133.05, 132.23, 130.23, 124.70. HRMS found 423.9587, M+H. MP = 295-297°C.

10 *- 2,2'-Bis[(4-methylphenyl)methylene]carbonimidic Dihydrazide Hydrochloride*

A solution of 4-methylbenzaldehyde (1.06 g, 8.8 mmol, 2.2 eq.) and 1,3-diaminoguanidine hydrochloride (500 mg, 4 mmol, 1 eq.) in ethanol (5 mL) was refluxed for 16 hr. Diethyl ether (10 mL) was added and the product carbonimidic dihydrazide crashed out of solution as a white solid. The product was filtered, washed with diethyl ether, and recrystallized from methanol as a hydrochloride salt. Yield: 1.11 g, 84 %. ^{1}H NMR (400 MHz, DMSO-d6) δ 12.18 (s, 2H), 8.46 (s, 2H), 8.39 (s, 2H), 7.83 (d, J = 7.8 Hz, 4H), 7.30 (d, J = 7.8 Hz, 4H), 2.37 (s, 6H). ^{13}C NMR (100 MHz, DMSO-d6) δ 152.08, 148.22, 140.13, 130.00, 128.74, 127.24, 20.51. HRMS found 294.1708, M+H. MP = 246-248°C.

11 *- 2,2'-Bis[(4-methoxyphenyl)methylene]carbonimidic Dihydrazide Hydrochloride*

A solution of 4-methoxybenzaldehyde (1.2 g, 8.8 mmol, 2.2 eq.) and 1,3-diaminoguanidine hydrochloride (500 mg, 4 mmol, 1 eq.) in ethanol (5 mL) was refluxed for 16 hr. Diethyl ether (10 mL) was added and the product carbonimidic dihydrazide crashed out of solution as a white solid. The product was filtered, washed with diethyl ether, and recrystallized from methanol as a hydrochloride salt. Yield: 1.37 g, 94 %. ^{1}H NMR (400 MHz, DMSO-d6) δ 12.00 (s, 2H), 8.37 (s, 2H), 8.35 (s, 2H), 7.88 (d, J = 9.1 Hz, 4H), 7.04 (d, J = 9.1 Hz, 4H), 3.83 (s, 6H). ^{13}C NMR (100 MHz, DMSO-d6) δ 181.34, 152.55, 129.56, 125.90, 114.22, 55.38. HRMS found 326.1608, M+H. MP = 218-220°C.

12 *- 2,2'-Bis[(4-trifluoromethylphenyl)methylene]carbonimidic Dihydrazide Hydrochloride*

A solution of trifluoromethylbenzaldehyde (1.53 g, 8.8 mmol, 2.2 eq.) and 1,3-diaminoguanidine hydrochloride (500 mg, 4 mmol, 1 eq.) in ethanol (5 mL) was refluxed for 16 hr. Diethyl ether (10 mL) was added and the product carbonimidic dihydrazide crashed out of solution as a white solid. The product was filtered, washed with diethyl ether, and recrystallized from methanol as a hydrochloride salt. Yield: 1.75 g, 100 %. ^{1}H NMR (400 MHz, DMSO-d6) δ 12.55 (s, 2H), 8.78 (s, 2H), 8.55 (s, 2H), 8.19 (d, J = 7.8 Hz, 4H), 7.85 (d, J = 8.1, 4H). ^{13}C NMR (100 MHz, DMSO-d6) δ 153.12, 147.44, 137.21, 130.44, 130.12, 128.51, 125.5 (d, J = 3.7 Hz), 122.68. HRMS found 402.1140, M+H. MP = 273-275°C.

13 *- 2,2'-Bis[(4-trifluoromethylphenyl)ethylidene]carbonimidic Dihydrazide Hydrochloride*

A solution of 4-trifluoromethylacetophenone (1.65 g, 8.8 mmol, 2.2 eq.) and 1,3-diaminoguanidine hydrochloride (500 mg, 4 mmol, 1 eq.) in ethanol (5 mL) was refluxed for 16 hr. Diethyl ether (10 mL) was added and the product carbonimidic dihydrazide crashed out of solution as a white solid. The product was filtered, washed with diethyl ether, and recrystallized from methanol as a hydrochloride salt. Yield: 1.78 g, 96 %. ^{1}H NMR (400 MHz, DMSO-d6) δ 12.04 (s, 2H), 8.89 (s, 2H), 8.28 (d, J = 7.6 Hz, 4H), 7.81 (d, J = 8.4, 4H), 2.5 (s, 6H). ^{13}C NMR (100 MHz, DMSO-d6) δ

154.75, 141.00, 128.26, 125.6 (d, J = 4.4 Hz), 123.28. HRMS found 430.1455, M+H. MP = 334-336°C.

14 *- 2,2'-Bis[(2-trifluoromethoxyphenyl)methylene]carbonimidic Dihydrazide Hydrochloride*

A solution of 2-trifluoromethoxybenzaldehyde (1.67 g, 8.8 mmol, 2.2 eq.) and 1,3-diaminoguanidine hydrochloride (500 mg, 4 mmol, 1 eq.) in ethanol (5 mL) was refluxed for 16 hr. Diethyl ether (10 mL) was added and the product carbonimidic dihydrazide crashed out of solution as a white solid. The product was filtered, washed with diethyl ether, and recrystallized from methanol as a hydrochloride salt. Yield: 1.87 g, 100 %. ^{1}H NMR (400 MHz, DMSO-d6) δ 12.54 (s, 2H), 8.75 (s, 2H), 8.71 (s, 2H), 8.48 (d, J = 7.8 Hz, 2H), 7.67-7.50 (m, 6H). ^{13}C NMR (100 MHz, DMSO-d6) δ 152.21, 146.36, 131.98, 127.28, 127.14, 125.67, 121.03, 120.74, 118.19. HRMS found 434.1039, M+H. MP = 194-196°C.

15 *- 2,2'-Bis[(3-trifluoromethoxyphenyl)methylene]carbonimidic Dihydrazide Hydrochloride*

A solution of 3-trifluoromethoxybenzaldehyde (835 mg, 4.4 mmol, 2.2 eq.) and 1,3-diaminoguanidine hydrochloride (250 mg, 2 mmol, 1 eq.) in ethanol (5 mL) was refluxed for 16 hr. Diethyl ether (10 mL) was added and the product carbonimidic dihydrazide crashed out of solution as a white solid. The product was filtered, washed with diethyl ether, and recrystallized from methanol as a hydrochloride salt. Yield: 660 mg, 70 %. ^{1}H NMR (400 MHz, DMSO-d6) δ 12.43, (s, 2H), 8.71 (s, 2H), 8.47 (s, 2H), 8.09 (s, 2H), 7.93 (d, J = 7.6 Hz, 2H), 7.63 (t, J = 7.9, 2H), 7.49 (d, J = 8.3 Hz, 2H). ^{13}C NMR (100 MHz, DMSO-d6) δ 153.48, 149.29, 147.93, 136.22, 131.31, 128.06, 123.45, 121.84, 120.13. HRMS found 434.1039, M+H. MP = 241-243°C.

16 *- 2,2'-Bis[(4-trifluoromethoxyphenyl)methylene]carbonimidic Dihydrazide Hydrochloride*

A solution of 4-trifluoromethoxybenzaldehyde (1.67 g, 8.8 mmol, 2.2 eq.) and 1,3-diaminoguanidine hydrochloride (500 mg, 4 mmol, 1 eq.) in ethanol (5 mL) was refluxed for 16 hr.

Diethyl ether (10 mL) was added and the product carbonimidic dihydrazide crashed out of solution as a white solid. The product was filtered, washed with diethyl ether, and recrystallized from methanol as a hydrochloride salt. Yield: 1.03 g, 55 %. ^{1}H NMR (400 MHz, DMSO-d6) δ 12.24 (s, 2H), 8.61 (s, 2H), 8.45 (s, 2H), 8.10 (d, J = 8.9 Hz, 4H), 7.50 (d, J = 8.1 Hz, 4H). ^{13}C NMR (100 MHz, DMSO-d6) δ 150.26, 133.07, 130.34, 121.70. HRMS found 434.1041, M+H. MP = 278-280°C.

17 *- 2,2'-Bis[(4-trifluoromethoxyphenyl)ethylidene]carbonimidic Dihydrazide Hydrochloride*

A solution of 4-trifluoromethoxyacetophenone (1.79 g, 8.8 mmol, 2.2 eq.) and 1,3-diaminoguanidine hydrochloride (500 mg, 4 mmol, 1 eq.) in ethanol (5 mL) was refluxed for 16 hr. Diethyl ether (10 mL) was added and the product carbonimidic dihydrazide crashed out of solution as a white solid. The product was filtered, washed with diethyl ether, and recrystallized from methanol as a hydrochloride salt. Yield: 1.88 g, 95 %. ^{1}H NMR (400 MHz, DMSO-d6) δ 11.91 (s, 2H), 8.78 (s, 2H), 8.19 (d, J = 8.8 Hz, 4H), 7.44 (d, J = 8.1, 4H), 2.46 (s, 6H). ^{13}C NMR (100 MHz, DMSO-d6) δ 154.66, 149.85, 136.38, 129.60, 121.79, 121.17, 119.24, 15.48. HRMS found 462.1352, M+H. MP = 323-325°C.

18 *- 2,2'-Bis[(4-difluoromethoxyphenyl)methylene]carbonimidic Dihydrazide Hydrochloride*

A solution of 4-difluoromethoxybenzaldehyde (757 mg, 4.4 mmol, 2.2 eq.) and 1,3-diaminoguanidine hydrochloride (250 g, 2 mmol, 1 eq.) in ethanol (5 mL) was refluxed for 16 hr. Diethyl ether (10 mL) was added and the product carbonimidic dihydrazide crashed out of solution as a white solid. The product was filtered, washed with diethyl ether, and recrystallized from methanol as a hydrochloride salt. Yield: 0.63 g, 73 %. ^{1}H NMR (400 MHz, DMSO-d6) δ 12.28 (s, 2H), 8.56 (s, 2H), 8.43 (s, 2H), 8.02 (d, J = 8.6, 4H), 7.38 (t, J = 74, 2H), 7.29 (d, J = 8.6 Hz, 4H). ^{13}C NMR (100 MHz, DMSO-d6) δ 153.17, 130.67, 130.22, 119.01, 116.58. HRMS found 398.1231, M+H. MP = 245-247°C.

19 *- 2,2'-Bis[(4-difluoromethoxyphenyl)ethylidene]carbonimidic Dihydrazide Hydrochloride*

A solution of 4-difluoromethoxyacetophenone (818 mg, 4.4 mmol, 2.2 eq.) and 1,3-diaminoguanidine hydrochloride (250 mg, 2 mmol, 1 eq.) in ethanol (5 mL) was refluxed for 16 hr. Diethyl ether (10 mL) was added and the product carbonimidic dihydrazide crashed out of solution as a white solid. The product was filtered, washed with diethyl ether, and recrystallized from methanol as a hydrochloride salt. Yield: 990 mg, 100 %. ^{1}H NMR (400 MHz, DMSO-d6) δ 11.78 (s, 2H), 8.72 (s, 2H), 8.13 (d, J = 8.8 Hz, 4H), 7.36 (t, J = 73.56, 2H), 7.24 (d, J = 8.6, 2H). ^{13}C NMR (100 MHz, DMSO-d6) δ 154.53, 152.90, 152.66, 133.97, 129.39, 119.19, 118.54, 116.62, 114.06, 15.33. HRMS found 426.1538, M+H. MP = 273-275°C.

20 *- 2,2'-Bis[(2-cyanophenyl)methylene]carbonimidic Dihydrazide Hydrochloride*

A solution of 2-cyanobenzaldehyde (1.15 g, 8.8 mmol, 2.2 eq.) and 1,3-diaminoguanidine hydrochloride (500 mg, 4 mmol, 1 eq.) in ethanol (5 mL) was refluxed for 16 hr. Diethyl ether (10 mL) was added and the product carbonimidic dihydrazide crashed out of solution as a white solid. The product was filtered, washed with diethyl ether, and recrystallized from methanol as a hydrochloride salt. Yield: 1.23 g, 88 %. ^{1}H NMR (400 MHz, DMSO-d6) δ 12.88 (s, 2H), 8.8 (s, 2H), 8.74 (s, 2H), 8.52 (d, J = 7.8 Hz, 2H), 7.96 (d, J = 7.8 Hz, 2H), 7.84 (t, J = 7.7 Hz, 2H), 7.68 (t, J = 7.7, 2H), 7.34 (t, J = 50.59, 2H). ^{13}C NMR (100 MHz, DMSO-d6) δ 145.01. 136.32, 133.91, 133.88, 131.56, 127.55, 117.67, 111.51, 56.48, 19.03. HRMS found 316.1301, M+H. MP = 213-215°C.

21 *- 2,2'-Bis[(3-cyanophenyl)methylene]carbonimidic Dihydrazide Hydrochloride*

A solution of 3-cyanobenzaldehyde (1.15 g, 8.8 mmol, 2.2 eq.) and 1,3-diaminoguanidine hydrochloride (500 mg, 4 mmol, 1 eq.) in ethanol (5 mL) was refluxed for 16 hr. Diethyl ether (10 mL) was added and the product carbonimidic dihydrazide crashed out of solution as a white solid.

The product was filtered, washed with diethyl ether, and recrystallized from methanol as a hydrochloride salt. Yield: 1.40 g, 100 %. ^{1}H NMR (400 MHz, DMSO-d6) δ 12.44 (s, 2H), 8.74 (s, 2H), 8.56 (s, 2H), 8.46 (s, 2H), 8.22 (d, J = 8.1 Hz, 2H), 7.95 (d, J = 7.8 Hz, 2H), 7.71 (t, J = 7.6 Hz, 2H). ^{13}C NMR (100 MHz, DMSO-d6) δ 153.60, 147.27, 135.10, 134.21, 133.25, 131.24, 130.50, 118.95, 112.49. HRMS found 316.1300, M+H. MP = 278-280°C.

22 *- 2,2'-Bis[(4-cyanophenyl)methylene]carbonimidic Dihydrazide Hydrochloride*

A solution of 4-cyanobenzaldehyde (1.15 g, 8.8 mmol, 2.2 eq.) and 1,3-diaminoguanidine hydrochloride (500 mg, 4 mmol, 1 eq.) in ethanol (5 mL) was refluxed for 16 hr. Diethyl ether (10 mL) was added and the product carbonimidic dihydrazide crashed out of solution as a white solid. The product was filtered, washed with diethyl ether, and recrystallized from methanol as a hydrochloride salt. Yield: 1.40 g, 100 %. ^{1}H NMR (400 MHz, DMSO-d6) δ 12.69 (s, 2H), 8.79 (s, 2H), 8.52 (s, 2H), 8.17 (d, J = 8.2 Hz, 4H), 7.97 (d, J = 8.3 Hz, 4H). ^{13}C NMR (100 MHz, DMSO-d6) δ 153.64, 147.70, 138.14, 133.11, 128.92, 119.09, 113.05. HRMS found 316.1303, M+H. MP = 303-305°C.

23 *- 2,2'-Bis[(3-cyanophenyl)ethylidene]carbonimidic Dihydrazide Hydrochloride*

A solution of 3-cyanoacetophenone (1.28 g, 8.8 mmol, 2.2 eq.) and 1,3-diaminoguanidine hydrochloride (500 mg, 4 mmol, 1 eq.) in ethanol (5 mL) was refluxed for 16 hr. Diethyl ether (10 mL) was added and the product carbonimidic dihydrazide crashed out of solution as a white solid. The product was filtered, washed with diethyl ether, and recrystallized from methanol as a hydrochloride salt. Yield: 1.40 g, 92 %. ^{1}H NMR (400 MHz, DMSO-d6) δ 11.89 (s, 2H), 8.90 (s, 2H), 8.63 (t, J = 1.44 Hz, 2H), 8.33 (dt, J = 7.75, 1.39, 2H), 7.92 (dt, J = 7.76, 2.44, 2H), 7.67 (t, J = 7.88, 2H), 2.48 (s, 6H). ^{13}C NMR (100 MHz, DMSO-d6) δ 154.70, 152.16, 138.21, 133.59, 132.06, 131.04, 130.09, 119.21, 112.16, 15.29. HRMS found 344.1612, M+H. MP = 304-306°C.

24 *- 2,2'-Bis(phenylmethylene)carbonimidic Dihydrazide Hydrochloride*

A solution of benzaldehyde (933 mg, 8.8 mmol, 2.2 eq.) and 1,3-diaminoguanidine hydrochloride (500 mg, 4 mmol, 1 eq.) in ethanol (5 mL) was refluxed for 16 hr. Diethyl ether (10 mL) was added and the product carbonimidic dihydrazide crashed out of solution as a white solid. The product was filtered, washed with diethyl ether, and recrystallized from methanol as a hydrochloride salt. Yield: 1.19 g, 99 %. ^{1}H NMR (400 MHz, DMSO-d6) δ 12.23 (s, 2H), 8.53 (s, 2H), 8.44 (s, 2H), 7.96-7.94 (m, 4H), 7.50-7.49 (m, 6H). ^{13}C NMR (100 MHz, DMSO-d6) δ 133.27, 130.77, 128.73, 127.86. HRMS found 266.1398, M+H. MP = 245-247°C.

25 *- 2,2'-Bis[(4-phenol)methylene]carbonimidic Dihydrazide Hydrochloride*

A solution of 4-hydroxybenzaldehyde (1.1 g, 8.8 mmol, 2.2 eq.) and 1,3-diaminoguanidine hydrochloride (500 mg, 4 mmol, 1 eq.) in ethanol (5 mL) was refluxed for 16 hr. Diethyl ether (10 mL) was added and the product carbonimidic dihydrazide crashed out of solution as a white solid. The product was filtered, washed with diethyl ether, and recrystallized from methanol as a hydrochloride salt. Yield: 1.33 g, 100 %. ^{1}H NMR (400 MHz, DMSO-d6) δ 11.95 (s, 2H), 10.15 (s, 2H), 8.28 (s, 2H), 7.75 (d, J = 8.1 Hz, 4H), 6.87 (d, J = 8.3, 4H). ^{13}C NMR (100 MHz, DMSO-d6) δ 160.56, 130.15, 124.76, 116.10. HRMS found 298.1296, M+H. MP = 185-187°C.

26 *- 2,2'-Bis[(4-diphenyl)methylene]carbonimidic Dihydrazide Hydrochloride*

A solution of 4-phenylbenzaldehyde (1.60 g, 8.8 mmol, 2.2 eq.) and 1,3-diaminoguanidine hydrochloride (500 mg, 4 mmol, 1 eq.) in ethanol (5 mL) was refluxed for 16 hr. Diethyl ether (10 mL) was added and the product carbonimidic dihydrazide crashed out of solution as a white solid. The product was filtered, washed with diethyl ether, and recrystallized from methanol as a hydrochloride salt. Yield: 1.81 g, 100 %. ^{1}H NMR (400 MHz, DMSO-d6) δ 12.32 (s, 2H), 8.59 (s, 2H), 8.49 (s, 2H), 8.05 (d, J = 7.3 Hz, 2H), 7.81 (d, J = 7.3 Hz, 2H), 7.77 (d, J = 7.6 Hz, 2H), 7.51 (t, J = 7.3 Hz, 2H), 7.42 (t, J = 7.6 Hz, 1H). ^{13}C NMR (100 MHz, DMSO-d6) δ 153.28, 142.71,

139.72, 132.89, 129.52, 128.99, 128.51, 127.42, 127.28. HRMS found 418.2022, M+H. MP = 286-288°C.

27 *- 2,2'-Bis[(4-nitrophenyl)methylene]carbonimidic Dihydrazide Hydrochloride*

A solution of 4-nitrobenzaldehyde (1.33 g, 8.8 mmol, 2.2 eq.) and 1,3-diaminoguanidine hydrochloride (500 mg, 4 mmol, 1 eq.) in ethanol (5 mL) was refluxed for 16 hr. Diethyl ether (10 mL) was added and the product carbonimidic dihydrazide crashed out of solution as a white solid. The product was filtered, washed with diethyl ether, and recrystallized from methanol as a hydrochloride salt. Yield: 1.56 g, 100 %. ^{1}H NMR (400 MHz, DMSO-d6) δ 12.68 (s, 2H), 8.82 (s, 2H), 8.57 (s, 2H), 8.33 (d, J = 8.3 Hz, 4H), 8.24 (d, J = 8.3 Hz, 4H). ^{13}C NMR (100 MHz, DMSO-d6) δ 153.79, 148.78, 147.27, 139.98, 129.35, 124.35. HRMS found 356.1098, M+H. MP = 285-287°C.

28 *- 2,2'-Bis[(4-dimethylaminophenyl)methylene]carbonimidic Dihydrazide Hydrochloride*

A solution of N, N-dimethylaminobenzaldehyde (1.31 g, 8.8 mmol, 2.2 eq.) and 1,3-diaminoguanidine hydrochloride (500 mg, 4 mmol, 1 eq.) in ethanol (5 mL) was refluxed for 16 hr. Diethyl ether (10 mL) was added and the product carbonimidic dihydrazide crashed out of solution as a white solid. The product was filtered, washed with diethyl ether, and recrystallized from methanol as a hydrochloride salt. Yield: 90 mg, 6 %. This compound was chemically unstable in chromatography solvents, but was greater than 80% pure when used in *in vitro* assays. ^{1}H NMR (400 MHz, DMSO-d6) δ 11.74 (s, 2H), 8.22 (s, 2H), 8.14 (s, 2H), 7.71 (d, J = 7.8 Hz, 4H), 6.75 (d, J = 7.8 Hz, 4H), 3.00 (s, 6H). ^{13}C NMR (100 MHz, DMSO-d6) δ 152.50, 152.35, 129.69, 129.41, 121.22, 120.96, 112.01. HRMS found 352.2237, M+H. MP = 132-134°C.

29 *- 2,2'-Bis[(phenyl-4-carbonate)methylene]carbonimidic Dihydrazide Hydrochloride*

A solution of 4-formylphenylcarbonate (1.32 g, 8.8 mmol, 2.2 eq.) and 1,3-diaminoguanidine hydrochloride (500 mg, 4 mmol, 1 eq.) in ethanol (5 mL) was refluxed for 16 hr. Diethyl ether (10 mL) was added and the product carbonimidic dihydrazide crashed out of solution as a white solid. The product was filtered, washed with diethyl ether, and recrystallized from methanol as a hydrochloride salt. Yield: 600 mg, 39 %. ^{1}H NMR (400 MHz, DMSO-d6) δ 13.13 (s, 2H), 12,57 (s, 2H), 8,70 (s, 2H), 8.52 (s, 2H), 8.11 (d, J = 7.7 Hz, 4H), 8.03 (d, J = 7.7 Hz, 4H). ^{13}C NMR (100 MHz, DMSO-d6) δ 193.48, 167.31, 167.02, 153.47, 148.46. 139.35, 137.72, 136.12, 132.79, 130.39, 130.03, 128.40. HRMS found 354.1195, M+H. MP = 336-338°C.

30 *- 2,2'-Bis[(4-carbonamidophenyl)methylene]carbonimidic Dihydrazide Hydrochloride*

A solution of 4-carbonamidobenzaldehyde (655 mg, 4.4 mmol, 2.2 eq.) and 1,3-diaminoguanidine hydrochloride (250 mg, 2 mmol, 1 eq.) in ethanol (5 mL) was refluxed for 16 hr. Diethyl ether (10 mL) was added and the product carbonimidic dihydrazide crashed out of solution as a white solid. The product was filtered, washed with diethyl ether, and recrystallized from methanol as a hydrochloride salt. Yield: 770 mg, 100 %. ^{1}H NMR (400 MHz, DMSO-d6) δ 12.43 (s, 2H), 8.85 (s, 2H), 8.50 (s, 2H), 8.13 (s, 2H), 8.04 (d, J = 7.8 Hz, 4H), 7.98 (d, J = 7.8 Hz, 4H), 7.50 (s, 2H). ^{13}C NMR (100 MHz, DMSO-d6) δ 167.70, 153.41, 148.59, 136.32, 136.26, 128.30, 128.15. HRMS found 352.5100, M+H. MP = 309-311°C.

31 *- 2,2'-Bis[(4-sulphonamidophenyl)methylene]carbonimidic Dihydrazide Hydrochloride*

A solution of 4-sulphonamidobenzaldehyde (814 mg, 4.4 mmol, 2.2 eq.) and 1,3-diaminoguanidine hydrochloride (250 mg, 2 mmol, 1 eq.) in ethanol (5 mL) was refluxed for 16 hr. Diethyl ether (10 mL) was added and the product carbonimidic dihydrazide crashed out of solution as a white solid. The product was filtered, washed with diethyl ether, and recrystallized from methanol as a hydrochloride salt. Yield: 920 mg, 100 %. ^{1}H NMR (400 MHz, DMSO-d6) δ 12.41, (s, 2H), 8.69 (s, 2H), 8.50 (s, 2H), 8.14 (6, J = 7.6 Hz, 4H), 7.91 (d, J = 7.6, 4H), 7.49 (s, 4H). ^{13}C

NMR (100 MHz, DMSO-d6) δ 153.49, 146.00, 136.81, 128.72, 125.43. HRMS found 424.0852, M+H. MP = 285-287°C.

32 *- 2,2'-Bis[(4-propynoxyphenyl)methylene]carbonimidic Dihydrazide Hydrochloride*

A solution of 4-propynoxybenzaldehyde (704 mg, 4.4 mmol, 2.2 eq.) and 1,3-diaminoguanidine hydrochloride (250 g, 2 mmol, 1 eq.) in ethanol (5 mL) was refluxed for 16 hr. Diethyl ether (10 mL) was added and the product carbonimidic dihydrazide crashed out of solution as a white solid. The product was filtered, washed with diethyl ether, and recrystallized from methanol as a hydrochloride salt. Yield: 0.82 g, 100 %. ^{1}H NMR (400 MHz, DMSO-d6) δ 12.19 (s, 2H), 8.42 (s, 2H), 8.37 (s, 2H), 7.91 (d, J = 8.4 Hz, 4H). ^{13}C NMR (100 MHz, DMSO-d6) δ 159.67, 153.09, 129.93, 127.06, 115.56, 79.38, 79.06, 56.09. HRMS found 374.1606, M+H. MP = 217-219°C.

33 *- 2,2'-Bis[(4-morpholinophenyl)methylene]carbonimidic Dihydrazide Hydrochloride*

A solution of 4-morpholinobenzaldehyde (840 mg, 4.4 mmol, 2.2 eq.) and 1,3-diaminoguanidine hydrochloride (250 mg, 2 mmol, 1 eq.) in ethanol (5 mL) was refluxed for 16 hr. Diethyl ether (10 mL) was added and the product carbonimidic dihydrazide crashed out of solution as a white solid. The product was filtered, washed with diethyl ether, and recrystallized from methanol as a hydrochloride salt. Yield: 850 mg, 90 %. ^{1}H NMR (400 MHz, DMSO-d6) δ 11.84 (s, 2H), 8.26 (s, 4H), 7.77 (d, J = 8.1 Hz, 4H), 7.01 (d, J = 8.1 Hz, 4H), 3.75 (s, 8H), 3.24 (s, 8H). ^{13}C NMR (100 MHz, DMSO-d6) δ 153.09, 152.75, 149.18, 129.58, 123.87, 114.5366.40, 47.78. HRMS found 436.2449, M+H. MP = 280-282°C.

34 *- 2,2'-Bis[(3-tetrazole-1-phenyl)methylene]carbonimidic Dihydrazide Hydrochloride*

A solution of 3-tetrazole-1-benzaldehyde (766 mg, 4.4 mmol, 2.2 eq.) and 1,3-diaminoguanidine hydrochloride (250 g, 2 mmol, 1 eq.) in ethanol (5 mL) was refluxed for 16 hr. Diethyl ether (10 mL) was added and the product carbonimidic dihydrazide crashed out of solution as a white solid.

The product was filtered, washed with diethyl ether, and recrystallized from methanol as a hydrochloride salt. Yield: 870 mg, 100 %. This compound was not sufficiently soluble in chromatography solvents to obtain a quantitative purity by HPLC. ^{1}H NMR (400 MHz, DMSO-d6) δ 8.84 (s, 2H), 8.75 (s, 2H), 8.66 (s, 2H), 8.20 (t, J = 9.0 Hz, 4H), 7.76 (t, J = 7.78, 2H). ^{13}C NMR (100 MHz, DMSO-d6) δ 152.27, 147.44, 133.85, 129.83, 129.27, 128.30, 125.70, 124.25. HRMS found 402.1641, M+H. MP = 289-291°C.

35 *- 2,2'-Bis[(4-tetrazole-1-phenyl)methylene]carbonimidic Dihydrazide Hydrochloride*

A solution of 4-tetrazole-1-benzaldehyde (1.53 g, 8.8 mmol, 2.2 eq.) and 1,3-diaminoguanidine hydrochloride (500 mg, 4 mmol, 1 eq.) in ethanol (5 mL) was refluxed for 16 hr. Diethyl ether (10 mL) was added and the product carbonimidic dihydrazide crashed out of solution as a white solid. The product was filtered, washed with diethyl ether, and recrystallized from methanol as a hydrochloride salt. Yield: 1.75 g, 100 %. This compound was not sufficiently soluble in chromatography solvents to obtain a quantitative purity by HPLC. ^{1}H NMR (400 MHz, DMSO-d6) δ 8.70 (s, 2H), 8.52 (s, 2H), 8.20 (s, 8H), 3.47-3.42 (m, 2H), 1.06 (t, J = 7.0 Hz, 2H). ^{13}C NMR (100 MHz, DMSO-d6) δ 153.39, 148.45, 136.23, 129.19, 127.77. HRMS found 402.1641, M+H. MP = 277-279°C.

36 *- 2,2'-Bis{[4-(2,2-difluoro-2,3-dioxazolo)]phenyl}methylene]carbonimidic Dihydrazide Hydrochloride*

A solution of 4-(2,2-difluoro-2,3-dioxazolo)benzaldehyde (820 mg, 4.4 mmol, 2.2 eq.) and 1,3-diaminoguanidine hydrochloride (250 mg, 2 mmol, 1 eq.) in ethanol (5 mL) was refluxed for 16 hr. Diethyl ether (10 mL) was added and the product carbonimidic dihydrazide crashed out of solution as a white solid. The product was filtered, washed with diethyl ether, and recrystallized from methanol as a hydrochloride salt. Yield: 800 mg, 87 %. ^{1}H NMR (400 MHz, DMSO-d6) δ 12.58 (s, 2H), 8.66 (s, 2H), 8.60 (s, 2H), 8.04 (d, J = 7.74 Hz, 2H), 7.52 (dd, J = 7.97, 0.93, 2H), 7.32 (t,

J = 8.12, 2H). ^{13}C NMR (100 MHz, DMSO-d6) δ 142.55, 140.90, 140.27, 130.60, 123.91, 120.71, 116.23, 111.11. HRMS found 426.0814, M+H. MP = 276-278°C.

37 *- 2,2'-Bis[(2,4-dimethoxy-5-chlorophenyl)ethylidene]carbonimidic Dihydrazide Hydrochloride*

A solution of 2,4-dimethoxy-5-chloroacetophenone (655 mg, 4.4 mmol, 2.2 eq.) and 1,3-diaminoguanidine hydrochloride (250 mg, 2 mmol, 1 eq.) in ethanol (5 mL) was refluxed for 16 hr. Diethyl ether (10 mL) was added and the product carbonimidic dihydrazide crashed out of solution as a white solid. The product was filtered, washed with diethyl ether, and recrystallized from methanol as a hydrochloride salt. Yield: 400 mg, 39 %. ^{1}H NMR (400 MHz, DMSO-d6) δ 11.64 (s, 2H), 8.55 (s, 2H), 7.68 (s, 2H), 6.85 (s, 2H), 3.94 (s, 6H), 3.91 (s, 6H), 2.31 (s, 6H),. ^{13}C NMR (100 MHz, DMSO-d6) δ 157.97, 156.84, 154.64, 154.53, 130.97, 130.65, 120.76, 112.75, 98.42, 98.30, 57.21, 56.96, 56.79, 32.07, 19.31. HRMS found 482.1350, M+H. MP = 229-231°C.

38 *– 2-(phenylmethylene), 2'-[(2-fluorophenyl)methylene]carbonimidic Dihydrazide Hydrochloride*

A solution of benzaldehyde (466 mg, 4.4 mmol, 1.1 eq.), 2-fluorobenzaldehyde (546 mg, 4.4 mmol, 1.1 eq.) and 1,3-diaminoguanidine hydrochloride (500 mg, 4 mmol, 1 eq.) in ethanol (5 mL) was refluxed for 16 hr. Diethyl ether (10 mL) was added and the product carbonimidic dihydrazide crashed out of solution as a white solid. The product was filtered, washed with diethyl ether, and recrystallized from methanol as a hydrochloride salt. This product was isolated as a mixture also containing **24** and **2**. **38** was the dominant product accounting for greater than 50% of the total material in the mixture. Yield: 1.27 g mixture, 50 %. ^{1}H NMR (400 MHz, DMSO-d6) δ 12.30 (s, 3H), 8.69 (s, 1H), 8.62 (s, 1H), 8.57 (s, 1H), 8.53 (s, 1H), 8.44 (s, 1H), 8.35 (t, J = 6.5 Hz, 1H), 7.96-7.94 (m, 2H), 7.56 (q, J = 8.1 Hz, 1H), 7.51-7.49 (m, 2H), 7.34 (t, J = 8.1, 2H). ^{13}C NMR (100 MHz, DMSO-d6) δ 133.27, 130.78, 128.74, 127.89, 127.28, 124.80, 115.88. HRMS found 284.1301, M+H. MP = 281-283°C.

39 *– N',2-bis((E)-4-(trifluoromethoxy)benzylidene)hydrazine-1-carbohydrazide Hydrochloride*

A solution of 4-trifluoromethoxybenzaldehyde (1.67 g, 8.8 mmol, 2.2 eq.) and carbohydrazide (360 mg, 4 mmol, 1 eq.) in ethanol (10 mL) was refluxed for 16 hr. Diethyl ether (10 mL) was added and the product carbohydrazide crashed out of solution as a white solid. The product was filtered, washed with diethyl ether, and recrystallized from methanol as a hydrochloride salt. Yield: 940 mg, 50 %. ^{1}H NMR (400 MHz, DMSO-d6) δ 10.85 (s, 2H), 8.21 (s, 2H), 7.88 (d, *J* = 8.2 Hz, 4H), 7.43 (d, *J* = 8.3 Hz, 4H). ^{13}C NMR (100 MHz, DMSO-d6) δ 152.37, 149.27, 134.41, 129.05, 121.70. HRMS found 435.0881, M+H. MP = 207-209 °C.

40 *– N',2-bis((E)-4-(trifluoromethoxy)benzylidene)hydrazine-1-carbothiohydrazide Hydrochloride*

A solution of 4-trifluoromethoxybenzalhehyde (1.67 g, 8.8 mmol, 2.2 eq.) and thiocarbhydrazide (424 mg, 4 mmol, 1 eq.) in ethanol (10 mL) was refluxed for 16 hr. Diethyl ether (10 mL) was added and the product thiocarbohydrazide crashed out of solution as a white solid. The product was filtered, washed with diethyl ether, and recrystallized from methanol as a hydrochloride salt. Yield: 1.5 g, 77 %. ^{1}H NMR (400 MHz, DMSO-d6) δ 11.93 (s, 2H), 10.53 (s, 2H), 8.10-7.99 (m, 4H), 7.54-7.36 (m, 4H). ^{13}C NMR (100 MHz, DMSO-d6) δ 149.66, 141.77, 133.90, 129.87, 121.67. HRMS found 451.0655, M+H. MP = 225-227 °C.

41 *– N',2-bis((E)-3-cyanobenzylidene)hydrazine-1-carbohydrazide Hydrochloride*

A solution of 3-cyanobenzaldehyde (1.15 g, 8.8 mmol, 2.2 eq.) and carbohydrazide (360 mg, 4 mmol, 1 eq.) in ethanol (10 mL) was refluxed for 16 hr. Diethyl ether (10 mL) was added and the product carbohydrazide crashed out of solution as a white solid. The product was filtered, washed with diethyl ether, and recrystallized from methanol as a hydrochloride salt. Yield: 1.4 g, 99 %. ^{1}H NMR (400 MHz, DMSO-d6) δ 11.35-18.88 (m, 2H), 8.33-7.64 (m, 8H). ^{13}C NMR (100 MHz, DMSO-d6) δ 133.06, 130.45. HRMS found 317.1141, M+H, 339.0960, M+Na. MP = 235-237°C.

42 *– N',2-bis((E)-3-cyanobenzylidene)hydrazine-1-carbothiohydrazide Hydrochloride*

A solution of 3-cyanobenzaldehyde (1.15 g, 8.8 mmol, 2.2 eq.) and thiocarbhydrazide (424 mg, 4 mmol, 1 eq.) in ethanol (10 mL) was refluxed for 16 hr. Diethyl ether (10 mL) was added and the product thiocarbohydrazide crashed out of solution as a white solid. The product was filtered, washed with diethyl ether, and recrystallized from methanol as a hydrochloride salt. Yield: 1.28 g, 87 %. ^{1}H NMR (400 MHz, DMSO-d6) δ 12.04 (d, *J* = 129 Hz, 2H), 8.58 (d, *J* = 62.5 Hz, 2H), 8.12 (d, *J* = 8.1 Hz, 2H), 7.90 (d, *J* = 7.7 Hz, 2H), 7.68 (t, *J* = 7.8 Hz, 2H). ^{13}C NMR (100 MHz, DMSO-d6) δ 175.83, 133.06, 130.95, 112.48. HRMS found 333.0912, M+H. MP = 229-231°C.

43 *– N',2-bis((E)-3-cyano-4-fluorobenzylidene)hydrazine-1-carbohydrazide Hydrochloride*

A solution of 2-fluoro-5-formylbenzonitrile (1.31 g, 8.8 mmol, 2.2 eq.) and carbohydrazide (360 mg, 4 mmol, 1 eq.) in ethanol (10 mL) was refluxed for 16 hr. Diethyl ether (10 mL) was added and the product carbohydrazide crashed out of solution as a white solid. The product was filtered, washed with diethyl ether, and recrystallized from methanol as a hydrochloride salt. Yield: 1.51 g, 97 %. ^{1}H NMR (400 MHz, DMSO-d6) δ 11.02 (s, 2H), 8.16 (dt, *J* = 9.0, 3.4 Hz, 2H), 7.62 (t, *J* = 9.0 Hz, 2H). ^{13}C NMR (100 MHz, DMSO-d6) δ 132.22, 101.19. HRMS found 333.0952, M+H. MP = 238-240 °C.

44 *– N',2-bis((E)-3-cyano-4-fluorobenzylidene)hydrazine-1-carbothiohydrazide Hydrochloride*

A solution of 2-fluoro-5-formylbenzonitrile (1.31 g, 8.8 mmol, 2.2 eq.) and thiocarbohydrazide (424 mg, 4 mmol, 1 eq.) in ethanol (10 mL) was refluxed for 16 hr. Diethyl ether (10 mL) was added and the product thiocarbohydrazide crashed out of solution as a white solid. The product was filtered, washed with diethyl ether, and recrystallized from methanol as a hydrochloride salt. Yield: 1.34 g, 83 %. ^{1}H NMR (400 MHz, DMSO-d6) δ 12.20 (s, 2H), 11.87 (s, 2H), 8.61 (d, *J* = 17.1 Hz, 4H), 8.21 (s, 8H), 7.65 (t, *J* = 9.0 Hz, 4H. ^{13}C NMR (100 MHz, DMSO-d6) δ 132.83, 129.68, 101.33. HRMS found 369.0723, M+H. MP = 250-253 °C.

45 *– N',2-bis((E)-4-cyanobenzylidene)hydrazine-1-carbohydrazide Hydrochloride*

A solution of 4-cyanobenzaldehyde (1.15 g, 8.8 mmol, 2.2 eq.) and carbohydrazide (360 mg, 4 mmol, 1 eq.) in ethanol (10 mL) was refluxed for 16 hr. Diethyl ether (10 mL) was added and the product carbohydrazide crashed out of solution as a white solid. The product was filtered, washed with diethyl ether, and recrystallized from methanol as a hydrochloride salt. Yield: 1.2 g, 85 %. ^{1}H NMR (400 MHz, DMSO-d6) δ 11.08 (s, 4H), 8.24 (s, 2H), 8.03 – 7.86 (m, 19H). ^{13}C NMR (100 MHz, DMSO-d6) δ 152.15, 139.51, 133.09, 127.84, 119.25, 111.78. HRMS found 317.1143, M+H. MP = 254-256°C.

46 *– N',2-bis((E)-4-cyanobenzylidene)hydrazine-1-carbothiohydrazide Hydrochloride*

A solution of 4-cyanobenzaldehyde (1.15 g, 8.8 mmol, 2.2 eq.) and thiocarbhydrazide (424 mg, 4 mmol, 1 eq.) in ethanol (10 mL) was refluxed for 16 hr. Diethyl ether (10 mL) was added and the product thiocarbohydrazide crashed out of solution as a white solid. The product was filtered, washed with diethyl ether, and recrystallized from methanol as a hydrochloride salt. Yield: 1.38 g, 93 %. ^{1}H NMR (400 MHz, DMSO-d6) δ 12.26 (s, 2H), 11.91 (s, 2H), 8.66 (s, 2H), 8.19 (s, 2H), 8.07 – 8.00 (m, 7H), 7.93 (d, *J* = 7.5 Hz, 29H), 7.85 (d, *J* = 8.3 Hz, 2H). ^{13}C NMR (100 MHz, DMSO-d6) δ 175.89, 133.19, 119.19, 112.35. HRMS found 333.0913, M+H. MP = 240-242°C.

47 *– (E)-N'-((E)-[1,1'-biphenyl]-4-ylmethylene)-2-([1,1'-biphenyl]-4-ylmethylene)hydrazine-1-carbohydrazide*

A solution of 4-phenylbenzaldehyde (1.6 g, 8.8 mmol, 2.2 eq.) and carbohydrazide (360 mg, 4 mmol, 1 eq.) in ethanol (10 mL) was refluxed for 16 hr. Diethyl ether (10 mL) was added and the product carbohydrazide crashed out of solution as a white solid. The product was filtered, washed with diethyl ether, and recrystallized from methanol as a hydrochloride salt. Yield: 1.41 g, 78 %. ^{1}H NMR (400 MHz, DMSO-d6) δ 10.77 (s, 2H), 8.24 (s, 1H), 7.85 (d, *J* = 8.2 Hz, 4H), 7.80 – 7.65

(m, 8H), 7.54 – 7.44 (m, 4H), 7.44 – 7.35 (m, 2H). ^{13}C NMR (100 MHz, DMSO-d6) δ 141.39, 129.48, 127.86, 127.38, 127.12. HRMS found 419.1864, M+H. MP = 248-250°C.

48 *– (E)-N'-((E)-[1,1'-biphenyl]-4-ylmethylene)-2-([1,1'-biphenyl]-4-ylmethylene)hydrazine-1-carbothiohydrazide*

A solution of 4-phenylbenzaldehyde (1.6 g, 8.8 mmol, 2.2 eq.) and thiocarbhydrazide (424 mg, 4 mmol, 1 eq.) in ethanol (10 mL) was refluxed for 16 hr. Diethyl ether (10 mL) was added and the product thiocarbohydrazide crashed out of solution as a white solid. The product was filtered, washed with diethyl ether, and recrystallized from methanol as a hydrochloride salt. Yield: 1.73 g, 92 %. ^{1}H NMR (400 MHz, DMSO-d6) δ 11.97 (s, 2H), 11.68 (s, 2H), 8.68 (s, 2H), 8.21 (s, 2H), 8.08 – 7.68 (m, 17H), 7.62 – 7.45 (m, 8H), 7.45 – 7.33 (m, 4H). ^{13}C NMR (100 MHz, DMSO-d6) δ 175.21, 142.02, 139.84, 129.51, 128.37, 127.46, 127.18. HRMS found 433.1480, M+. MP = 226-228°C.

49 *– N',2-bis((E)-3-nitrobenzylidene)hydrazine-1-carboximidhydrazide Hydrochloride*

A solution of 3-nitrobenzaldehyde (1.33 g, 8.8 mmol, 2.2 eq.) and 1,3-diaminoguanidine hydrochloride (500 mg, 4 mmol, 1 eq.) in ethanol (10 mL) was refluxed for 16 hr. Diethyl ether (10 mL) was added and the product carbonimidic dihydrazide crashed out of solution as a white solid. The product was filtered, washed with diethyl ether, and recrystallized from methanol as a hydrochloride salt. Yield: 1.51 mg, 97 %. ^{1}H NMR (400 MHz, DMSO-d6) δ 12.39 (s, 2H), 8.89 (s, 0H), 8.85 – 8.77 (m, 5H), 8.55 (s, 3H), 8.40 (dt, *J* = 7.9, 1.3 Hz, 3H), 8.32 (ddd, *J* = 8.2, 2.4, 1.0 Hz, 4H), 7.80 (t, *J* = 8.0 Hz, 3H). ^{13}C NMR (100 MHz, DMSO-d6) δ 148.85, 135.61, 134.65, 130.79, 125.47, 122.49. HRMS found 356.1095, M+H. MP = 271-273 °C.

50 *– 3,3'-((1E,1'E)-((iminomethylene)bis(hydrazin-2-yl-1-ylidene))bis(methaneylylidene))dibenzamide Hydrochloride*

A solution of 3-formylbenzamide (656 mg, 4.4 mmol, 2.2 eq.) and 1,3-diaminoguanidine hydrochloride (250 mg, 2 mmol, 1 eq.) in ethanol (10 mL) was refluxed for 16 hr. Diethyl ether (10 mL) was added and the product carbonimidic dihydrazide crashed out of solution as a white solid. The product was filtered, washed with diethyl ether, and recrystallized from methanol as a hydrochloride salt. Yield: 770 mg, 99 %. ^{1}H NMR (400 MHz, DMSO-d6) δ 12.27 (s, 2H), 8.58 (s, 3H), 8.51 (s, 3H), 8.41 (t, *J* = 1.8 Hz, 4H), 8.30 (s, 0H), 8.15 – 8.01 (m, 9H), 7.97 (dt, *J* = 7.8, 1.4 Hz, 4H), 7.62 – 7.50 (m, 8H). ^{13}C NMR (100 MHz, DMSO-d6) δ 167.74, 135.32, 133.89, 130.74, 130.07, 129.21, 127.42. HRMS found 352.1512, M+H. MP = 237-239 °C.

51 *– N',2-bis(bis(4-chlorophenyl)methylene)hydrazine-1-carboximidhydrazide Hydrochloride*

A solution of 4, 4'-dichlorobenzophenone (2.21 g, 8.8 mmol, 2.2 eq.) and 1,3-diaminoguanidine hydrochloride (500 mg, 4 mmol, 1 eq.) in ethanol (10 mL) was refluxed for 16 hr. Diethyl ether (10 mL) was added and the product carbonimidic dihydrazide crashed out of solution as a white solid. The product was filtered, washed with diethyl ether, and recrystallized from methanol as a hydrochloride salt. Yield: 2.1 mg, 89 %. ^{1}H NMR (400 MHz, DMSO-d6) δ 8.69 (s, 2H), 7.80 – 7.72 (m, 16H), 7.69 – 7.60 (m, 16H), 7.22 (s, 3H), 4.61 (s, 3H). ^{13}C NMR (100 MHz, DMSO-d6) δ 194.10, 160.37, 138.27, 135.83, 131.97, 129.25, 128.98. HRMS found 556.0434, M+H. MP = 149-151°C.

52 *– (E)-N'-((E)-[1,1'-biphenyl]-3-ylmethylene)-2-([1,1'-biphenyl]-3-ylmethylene)hydrazine-1-carboximidhydrazide Hydrochloride*

A solution of 3-phenylbenzaldehyde (802 mg, 4.4 mmol, 2.2 eq.) and 1,3-diaminoguanidine hydrochloride (250 mg, 2 mmol, 1 eq.) in ethanol (10 mL) was refluxed for 16 hr. Diethyl ether (10 mL) was added and the product carbonimidic dihydrazide crashed out of solution as a white solid. The product was filtered, washed with diethyl ether, and recrystallized from methanol as a hydrochloride salt. Yield: 860 mg, 95 %. ^{1}H NMR (400 MHz, DMSO-d6) δ 12.22 (s, 2H), 8.60 (s,

2H), 8.50 (s, 3H), 8.24 (t, *J* = 1.8 Hz, 3H), 7.94 (dt, *J* = 7.8, 1.4 Hz, 3H), 7.78 (dd, *J* = 10.2, 8.3 Hz, 10H), 7.59 (t, *J* = 7.7 Hz, 4H), 7.55 – 7.48 (m, 7H), 7.47 – 7.38 (m, 4H). ^{13}C NMR (100 MHz, DMSO-d6) δ 141.27, 139.94, 134.40, 129.85, 129.56, 129.46, 128.31, 127.53, 127.40, 126.37. HRMS found 418.2020, M+H. MP = 249-251 °C.

53 *– (E)-2-((4'-fluoro-[1,1'-biphenyl]-4-yl)methylene)-N'-((E)-(4'-fluoro-[1,1'-biphenyl]-4-yl)methylene)hydrazine-1-carboximidhydrazide Hydrochloride*

A solution of 4'-fluorobiphenyl-4-carbaldehyde (880 mg, 4.4 mmol, 2.2 eq.) and 1,3-diaminoguanidine hydrochloride (250 mg, 2 mmol, 1 eq.) in ethanol (10 mL) was refluxed for 16 hr. Diethyl ether (10 mL) was added and the product carbonimidic dihydrazide crashed out of solution as a white solid. The product was filtered, washed with diethyl ether, and recrystallized from methanol as a hydrochloride salt. Yield: 920 mg, 94 %. ^{1}H NMR (400 MHz, DMSO-d6) δ 12.23 (s, 2H), 8.57 (s, 3H), 8.47 (s, 4H), 8.08 – 8.01 (m, 10H), 7.87 – 7.76 (m, 20H), 7.39 – 7.28 (m, 10H). ^{13}C NMR (100 MHz, DMSO-d6) δ 163.89, 161.45, 141.64, 136.18, 132.84, 129.39, 129.31, 128.99, 127.36, 116.44, 116.23. HRMS found 454.1830, M+H. MP = 285-287 °C.

54 *– (E)-2-((4'-chloro-[1,1'-biphenyl]-4-yl)methylene)-N'-((E)-(4'-chloro-[1,1'-biphenyl]-4-yl)methylene)hydrazine-1-carboximidhydrazide Hydrochloride*

A solution of 4'-chlorobiphenyl-4-carbaldehyde (955 mg, 4.4 mmol, 2.2 eq.) and 1,3-diaminoguanidine hydrochloride (250 mg, 2 mmol, 1 eq.) in ethanol (10 mL) was refluxed for 16 hr. Diethyl ether (10 mL) was added and the product carbonimidic dihydrazide crashed out of solution as a white solid. The product was filtered, washed with diethyl ether, and recrystallized from methanol as a hydrochloride salt. Yield: 1.04 g, 99 %. ^{1}H NMR (400 MHz, DMSO-d6) δ 12.12 (s, 2H), 8.56 (s, 2H), 8.46 (s, 3H), 8.09 – 8.01 (m, 7H), 7.86 – 7.76 (m, 13H), 7.61 – 7.52 (m, 7H). ^{13}C NMR (100 MHz, DMSO-d6) δ 138.47, 133.40, 129.47, 129.06, 127.38. HRMS found 486.1236, M+H. MP = 288-290 °C.

55 *– (E)-2-((4'-bromo-[1,1'-biphenyl]-4-yl)methylene)-N'-((E)-(4'-bromo-[1,1'-biphenyl]-4-yl)methylene)hydrazine-1-carboximidhydrazide Hydrochloride*

A solution of 4'-bromobiphenyl-4-carbaldehyde (230 mg, 0.88 mmol, 2.2 eq.) and 1,3-diaminoguanidine hydrochloride (50 mg, 0.4 mmol, 1 eq.) in ethanol (10 mL) was refluxed for 16 hr. Diethyl ether (10 mL) was added and the product carbonimidic dihydrazide crashed out of solution as a white solid. The product was filtered, washed with diethyl ether, and recrystallized from methanol as a hydrochloride salt. Yield: 210 mg, 86.2 %. ^{1}H NMR (400 MHz, DMSO-d6) δ 12.11 (s, 2H), 8.54 (s, 2H), 8.45 (s, 3H), 8.08 – 8.01 (m, 7H), 7.86 – 7.78 (m, 7H), 7.78 – 7.65 (m, 14H). ^{13}C NMR (100 MHz, DMSO-d6) δ 138.85, 132.39, 129.37, 129.03, 127.33, 122.03. HRMS found 574.0051, M+H. MP = 296-298 °C.

56 *– (E)-2-((4'-(trifluoromethyl)-[1,1'-biphenyl]-4-yl)methylene)-N'-((E)-(4'-(trifluoromethyl)-[1,1'-biphenyl]-4-yl)methylene)hydrazine-1-carboximidhydrazide Hydrochloride*

A solution of 4'-trifluoromethylbiphenyl-4-carbaldehyde (550 mg, 2.2 mmol, 2.2 eq.) and 1,3-diaminoguanidine hydrochloride (250 mg, 2 mmol, 1 eq.) in ethanol (10 mL) was refluxed for 16 hr. Diethyl ether (10 mL) was added and the product carbonimidic dihydrazide crashed out of solution as a white solid. The product was filtered, washed with diethyl ether, and recrystallized from methanol as a hydrochloride salt. Yield: 570 mg, 97 %. ^{1}H NMR (400 MHz, DMSO-d6) δ 12.15 (s, 2H), 8.59 (s, 2H), 8.48 (s, 2H), 8.14 – 8.06 (m, 6H), 8.03 – 7.96 (m, 6H), 7.93 – 7.82 (m, 13H). ^{13}C NMR (100 MHz, DMSO-d6) δ 129.08, 128.12, 127.87, 126.35. HRMS found 554.1767, M+H. MP = 274-276 °C.

57 *– N',2-bis((E)-4-phenoxybenzylidene)hydrazine-1-carboximidhydrazide Hydrochloride*

A solution of 4-phenoxybenzaldehyde (872 mg, 4.4 mmol, 2.2 eq.) and 1,3-diaminoguanidine hydrochloride (250 mg, 2 mmol, 1 eq.) in ethanol (10 mL) was refluxed for 16 hr. Diethyl ether

(10 mL) was added and the product carbonimidic dihydrazide crashed out of solution as a white solid. The product was filtered, washed with diethyl ether, and recrystallized from methanol as a hydrochloride salt. Yield: 810 mg, 84 %. ^{1}H NMR (400 MHz, DMSO-d6) δ 12.05 (s, 2H), 8.45 (s, 3H), 8.39 (s, 3H), 8.00 – 7.91 (m, 8H), 7.50 – 7.40 (m, 8H), 7.27 – 7.17 (m, 4H), 7.14 – 7.04 (m, 16H). ^{13}C NMR (100 MHz, DMSO-d6) δ 159.49, 156.16, 130.72, 130.33, 128.81, 124.71, 119.79, 118.64. HRMS found 450.1919, M+H. MP = 201-203 °C.

58 *– N',2-bis((E)-4-(4-fluorophenoxy)benzylidene)hydrazine-1-carboximidhydrazide Hydrochloride*

A solution of 4-(4'-fluorophenoxy)benzaldehyde (951 mg, 4.4 mmol, 2.2 eq.) and 1,3-diaminoguanidine hydrochloride (250 mg, 2 mmol, 1 eq.) in ethanol (10 mL) was refluxed for 16 hr. Diethyl ether (10 mL) was added and the product carbonimidic dihydrazide crashed out of solution as a white solid. The product was filtered, washed with diethyl ether, and recrystallized from methanol as a hydrochloride salt. Yield: 930 mg, 89 %. ^{1}H NMR (400 MHz, DMSO-d6) δ 12.04 (s, 2H), 8.45 (s, 3H), 8.38 (s, 3H), 8.04 – 7.90 (m, 9H), 7.34 – 7.23 (m, 8H), 7.21 – 7.11 (m, 9H), 7.10 – 7.02 (m, 8H). ^{13}C NMR (100 MHz, DMSO-d6) δ 159.86, 152.10, 130.34, 128.74, 121.94, 121.86, 118.18, 117.40, 117.17. HRMS found 486.1731, M+H. MP = 220-222 °C.

59 *– N',2-bis((E)-4-(4-chlorophenoxy)benzylidene)hydrazine-1-carboximidhydrazide Hydrochloride*

A solution of 4-(4'-chlorophenoxy)benzaldehyde (1.02 g, 4.4 mmol, 2.2 eq.) and 1,3-diaminoguanidine hydrochloride (250 mg, 2 mmol, 1 eq.) in ethanol (10 mL) was refluxed for 16 hr. Diethyl ether (10 mL) was added and the product carbonimidic dihydrazide crashed out of solution as a white solid. The product was filtered, washed with diethyl ether, and recrystallized from methanol as a hydrochloride salt. Yield: 890 mg, 81 %. ^{1}H NMR (400 MHz, DMSO-d6) δ 12.12 (s, 2H), 8.48 (s, 3H), 8.40 (s, 4H), 8.02 – 7.92 (m, 9H), 7.53 – 7.41 (m, 9H), 7.17 – 7.05 (m,

18H), 3.38 (q, *J* = 7.0 Hz, 6H), 1.09 (t, *J* = 7.0 Hz, 1H). ^{13}C NMR (100 MHz, DMSO-d6) δ 158.99, 155.24, 130.55, 130.40, 129.26, 128.41, 121.40, 118.94. HRMS found 518.1141, M+H. MP = 248-250 °C.

60 – *(E)-N'-((E)-naphthalen-1-ylmethylene)-2-(naphthalen-1-ylmethylene)hydrazine-1-carboximidhydrazide Hydrochloride*

A solution of 1-napthaldehyde (1.37 g, 8.8 mmol, 2.2 eq.) and 1,3-diaminoguanidine hydrochloride (500 mg, 4 mmol, 1 eq.) in ethanol (10 mL) was refluxed for 16 hr. Diethyl ether (10 mL) was added and the product carbonimidic dihydrazide crashed out of solution as a white solid. The product was filtered, washed with diethyl ether, and recrystallized from methanol as a hydrochloride salt. Yield: 1.52 mg, 95 %. ^{1}H NMR (400 MHz, DMSO-d6) δ 12.25 (s, 1H), 9.36 (s, 1H), 8.61 (s, 1H), 8.47 – 8.38 (m, 3H), 8.16 – 8.02 (m, 3H), 7.76 – 7.59 (m, 4H). ^{13}C NMR (100 MHz, DMSO-d6) δ 133.84, 131.69, 131.10, 129.39, 129.03, 127.94, 126.82, 126.71, 126.00, 123.33. HRMS found 366.1704, M+H. MP = 254-256 °C.

61 – *(E)-N'-((E)-naphthalen-2-ylmethylene)-2-(naphthalen-2-ylmethylene)hydrazine-1-carboximidhydrazide Hydrochloride*

A solution of 2-napthaldehyde (1.37 g, 8.8 mmol, 2.2 eq.) and 1,3-diaminoguanidine hydrochloride (500 mg, 4 mmol, 1 eq.) in ethanol (10 mL) was refluxed for 16 hr. Diethyl ether (10 mL) was added and the product carbonimidic dihydrazide crashed out of solution as a white solid. The product was filtered, washed with diethyl ether, and recrystallized from methanol as a hydrochloride salt. Yield: 1.55 g, 97 %. ^{1}H NMR (400 MHz, DMSO-d6) δ 12.37 (s, 2H), 8.63 (s, 6H), 8.36 – 8.26 (m, 9H), 8.06 – 7.95 (m, 14H), 7.67 – 7.56 (m, 9H). ^{13}C NMR (100 MHz, DMSO-d6) δ 134.51, 133.18, 131.58, 130.36, 128.92, 128.84, 128.31, 127.99, 127.36, 123.69. HRMS found 366.1705, M+H. MP = 290-292 °C.

62 – *(E)-N'-((E)-quinolin-2-ylmethylene)-2-(quinolin-2-ylmethylene)hydrazine-1-carboximidhydrazide Hydrochloride*

A solution of 2-quinolinecarboxaldehyde (691 mg, 4.4 mmol, 2.2 eq.) and 1,3-diaminoguanidine hydrochloride (250 mg, 2 mmol, 1 eq.) in ethanol (10 mL) was refluxed for 16 hr. Diethyl ether (10 mL) was added and the product carbonimidic dihydrazide crashed out of solution as a white solid. The product was filtered, washed with diethyl ether, and recrystallized from methanol as a hydrochloride salt. Yield: 780 mg, 97 %. ^{1}H NMR (400 MHz, DMSO-d6) δ 12.69 (s, 2H), 8.87 (s, 4H), 8.64 (s, 6H), 8.58 (d, *J* = 8.6 Hz, 11H), 8.52 (d, *J* = 8.7 Hz, 9H), 8.13 – 8.02 (m, 18H), 7.84 (ddd, *J* = 8.4, 6.9, 1.5 Hz, 9H), 7.69 (ddd, *J* = 8.1, 6.9, 1.2 Hz, 9H). ^{13}C NMR (100 MHz, DMSO-d6) δ 153.32, 128.57, 128.53, 128.21, 118.99. HRMS found 368.1612, M+H. MP = 263-265 °C.

63 – *(E)-N'-((E)-quinolin-3-ylmethylene)-2-(quinolin-3-ylmethylene)hydrazine-1-carboximidhydrazide Hydrochloride*

A solution of 3-quinolinecarboxaldehyde (691 mg, 4.4 mmol, 2.2 eq.) and 1,3-diaminoguanidine hydrochloride (250 mg, 2 mmol, 1 eq.) in ethanol (10 mL) was refluxed for 16 hr. Diethyl ether (10 mL) was added and the product carbonimidic dihydrazide crashed out of solution as a white solid. The product was filtered, washed with diethyl ether, and recrystallized from methanol as a hydrochloride salt. Yield: 720 mg, 89 %. ^{1}H NMR (400 MHz, DMSO-d6) δ 12.50 (s, 1H), 9.65 (d, *J* = 2.1 Hz, 2H), 8.80 – 8.73 (m, 4H), 8.67 (s, 2H), 8.09 (ddd, *J* = 10.0, 8.3, 1.2 Hz, 5H), 7.85 (ddd, *J* = 8.5, 6.9, 1.5 Hz, 3H), 7.70 (ddd, *J* = 8.1, 6.9, 1.2 Hz, 2H). ^{13}C NMR (100 MHz, DMSO-d6) δ 149.40, 148.50, 136.60, 131.30, 129.45, 129.17, 128.00, 127.64, 127.06. HRMS found 368.1613, M+H. MP = 294-296°C.

64 – *(E)-N'-((E)-quinolin-4-ylmethylene)-2-(quinolin-4-ylmethylene)hydrazine-1-carboximidhydrazide Hydrochloride*

A solution of 4-quinolinecarboxaldehyde (691 mg, 4.4 mmol, 2.2 eq.) and 1,3-diaminoguanidine hydrochloride (250 mg, 2 mmol, 1 eq.) in ethanol (10 mL) was refluxed for 16 hr. Diethyl ether (10 mL) was added and the product carbonimidic dihydrazide crashed out of solution as a white solid. The product was filtered, washed with diethyl ether, and recrystallized from methanol as a hydrochloride salt. Yield: 720 mg, 89 %. ^{1}H NMR (400 MHz, DMSO-d6) δ 9.39 (s, 2H), 9.06 (d, *J* = 4.7 Hz, 2H), 8.76 – 8.71 (m, 1H), 8.47 – 8.37 (m, 4H), 8.16 (dd, *J* = 8.4, 1.3 Hz, 2H), 7.90 (ddd, *J* = 8.3, 6.8, 1.4 Hz, 2H), 7.80 (ddd, *J* = 8.3, 6.9, 1.4 Hz, 2H). ^{13}C NMR (100 MHz, DMSO-d6) δ 130.59, 128.24, 125.51, 123.77, 118.72. HRMS found 368.1612, M+H. MP = 254-256 °C.

65 – *(E)-N'-((E)-quinolin-8-ylmethylene)-2-(quinolin-8-ylmethylene)hydrazine-1-carboximidhydrazide Hydrochloride*

A solution of 8-quinolinecarboxaldehyde (691 mg, 4.4 mmol, 2.2 eq.) and 1,3-diaminoguanidine hydrochloride (250 mg, 2 mmol, 1 eq.) in ethanol (10 mL) was refluxed for 16 hr. Diethyl ether (10 mL) was added and the product carbonimidic dihydrazide crashed out of solution as a white solid. The product was filtered, washed with diethyl ether, and recrystallized from methanol as a hydrochloride salt. Yield: 740 mg, 92 %. ^{1}H NMR (400 MHz, DMSO-d6) δ 12.51 (s, 1H), 9.75 (s, 2H), 9.04 (dd, *J* = 4.2, 1.8 Hz, 3H), 8.81 (dd, *J* = 7.4, 1.4 Hz, 3H), 8.70 – 8.65 (m, 2H), 8.50 (dd, *J* = 8.4, 1.8 Hz, 2H), 8.18 (dd, *J* = 8.2, 1.5 Hz, 2H), 7.79 (t, *J* = 7.8 Hz, 2H), 7.68 (dd, *J* = 8.3, 4.2 Hz, 2H). ^{13}C NMR (100 MHz, DMSO-d6) δ 151.19, 145.77, 137.27, 131.42, 130.50, 128.47, 127.44, 126.88, 122.54. HRMS found 368.1612, M+H. MP = 263-265 °C.

66 – *(E)-N'-((E)-pyridin-3-ylmethylene)-2-(pyridin-3-ylmethylene)hydrazine-1-carboximidhydrazide Hydrochloride*

A solution of 3-pyridinecarboxaldehyde (942 mg, 8.8 mmol, 2.2 eq.) and 1,3-diaminoguanidine hydrochloride (500 mg, 4 mmol, 1 eq.) in ethanol (10 mL) was refluxed for 16 hr. Diethyl ether (10 mL) was added and the product carbonimidic dihydrazide crashed out of solution as a white

solid. The product was filtered, washed with diethyl ether, and recrystallized from methanol as a hydrochloride salt. Yield: 1.21 g, 99 %. ^{1}H NMR (400 MHz, DMSO-d6) δ 12.37 (s, 1H), 9.09 (dd, *J* = 2.2, 0.8 Hz, 2H), 8.66 (dt, *J* = 6.5, 3.2 Hz, 3H), 8.48 (s, 2H), 8.40 (dt, *J* = 8.0, 1.9 Hz, 2H), 7.53 (ddd, *J* = 8.0, 4.8, 0.8 Hz, 2H). ^{13}C NMR (100 MHz, DMSO-d6) δ 151.63, 149.64, 135.07, 129.80, 124.33. HRMS found 268.1301, M+H. MP = 177-179°C.

67 *– (E)-N'-((E)-pyridin-4-ylmethylene)-2-(pyridin-4-ylmethylene)hydrazine-1-carboximidhydrazide Hydrochloride*

A solution of 4-pyridinecarboxaldehyde (942 mg, 8.8 mmol, 2.2 eq.) and 1,3-diaminoguanidine hydrochloride (500 mg, 4 mmol, 1 eq.) in ethanol (10 mL) was refluxed for 16 hr. Diethyl ether (10 mL) was added and the product carbonimidic dihydrazide crashed out of solution as a white solid. The product was filtered, washed with diethyl ether, and recrystallized from methanol as a hydrochloride salt. Yield: 905 mg, 75 %. ^{1}H NMR (400 MHz, DMSO-d6) δ 8.83 – 8.76 (m, 6H), 8.70 (s, 2H), 8.47 (s, 2H), 8.19 – 8.12 (m, 6H). ^{13}C NMR (100 MHz, DMSO-d6) δ 147.44, 122.93. HRMS found 268.1301, M+H. MP = 255-257°C.

68 *– (E)-2-((7-chloroquinolin-3-yl)methylene)-N'-((E)-(7-chloroquinolin-3-yl)methylene)hydrazine-1-carboximidhydrazide Hydrochloride*

A solution of 7-chloroquinoline-3-carbaldehyde (84 mg, 0.44 mmol, 2.2 eq.) and 1,3-diaminoguanidine hydrochloride (25 mg, 0.2 mmol, 1 eq.) in ethanol (10 mL) was refluxed for 16 hr. Diethyl ether (10 mL) was added and the product carbonimidic dihydrazide crashed out of solution as a white solid. The product was filtered, washed with diethyl ether, and recrystallized from methanol as a hydrochloride salt. Yield: 72 mg, 76 %. ^{1}H NMR (400 MHz, DMSO-d6) δ 12.41 (s, 1H), 9.68 (d, *J* = 2.0 Hz, 2H), 8.82 – 8.68 (m, 4H), 8.63 (s, 2H), 8.19 – 8.04 (m, 4H), 7.75 (dd, *J* = 8.7, 2.2 Hz, 2H). ^{13}C NMR (100 MHz, DMSO-d6) δ 150.65, 148.76, 131.10, 128.65, 128.26, 126.31. HRMS found 436.0833, M+H. MP = 319-321 °C.

69 *– (E)-2-((7-chloroquinolin-4-yl)methylene)-N'-((E)-(7-chloroquinolin-4-yl)methylene)hydrazine-1-carboximidhydrazide Hydrochloride*

A solution of 7-chloroquinoline-4-carbaldehyde (422 mg, 2.2 mmol, 2.2 eq.) and 1,3-diaminoguanidine hydrochloride (125 mg, 1 mmol, 1 eq.) in ethanol (10 mL) was refluxed for 16 hr. Diethyl ether (10 mL) was added and the product carbonimidic dihydrazide crashed out of solution as a white solid. The product was filtered, washed with diethyl ether, and recrystallized from methanol as a hydrochloride salt. Yield: 400 mg, 85 %. ^{1}H NMR (400 MHz, DMSO-d6) δ 9.35 (s, 3H), 9.07 (d, *J* = 4.6 Hz, 4H), 8.83 (s, 3H), 8.45 (d, *J* = 9.1 Hz, 4H), 8.36 (d, *J* = 4.6 Hz, 4H), 8.17 (d, *J* = 2.2 Hz, 4H), 7.80 (dd, *J* = 9.1, 2.3 Hz, 4H). ^{13}C NMR (100 MHz, DMSO-d6) δ 151.85, 149.09, 145.05, 137.60, 134.93, 128.64, 128.61, 126.11, 124.06, 119.41. HRMS found 436.0833, M+H. MP = 222-224 °C.

70 *– N',2-bis((E)-4-cyano-3-fluorobenzylidene)hydrazine-1-carboximidhydrazide Hydrochloride*

A solution of 2-fluoro-4-formylbenzonitrile (656 mg, 4.4 mmol, 2.2 eq.) and 1,3-diaminoguanidine hydrochloride (250 mg, 2 mmol, 1 eq.) in ethanol (5 mL) was refluxed for 16 hr. Diethyl ether (10 mL) was added and the product carbonimidic dihydrazide crashed out of solution as a white solid. The product was filtered, washed with diethyl ether, and recrystallized from methanol as a hydrochloride salt. Yield: 700 mg, 99 %. ^{1}H NMR (400 MHz, DMSO-d6) δ 12.80 (s, 2H), 8.86 (s, 2H), 8.50 (s, 2H), 8.28 (dd, *J* = 0.8, 1.4 Hz, 2H), 8.06 (dd, *J* = 8.1, 6.8 Hz, 2H), 7.93 (d, *J* = 6.8 Hz, 2H). ^{13}C NMR (100 MHz, DMSO-d6) δ 164.31, 161.78, 141.36, 141.27, 134.91, 134.83, 125.67, 114.83, 114.62, 114.40, 101.79. HRMS found 352.1107, M+H. MP = 293-295°C.

71 *– N',2-bis((E)-4-chloro-3-cyanobenzylidene)hydrazine-1-carboximidhydrazide Hydrochloride*

A solution of 2-chloro-5-formylbenzonitrile (183 mg, 1.1 mmol, 2.2 eq.) and 1,3-diaminoguanidine hydrochloride (63 mg, 0.5 mmol, 1 eq.) in ethanol (5 mL) was refluxed for 16 hr. Diethyl ether (10

mL) was added and the product carbonimidic dihydrazide crashed out of solution as a white solid. The product was filtered, washed with diethyl ether, and recrystallized from methanol as a hydrochloride salt. Yield: 190 mg, 99 %. ^{1}H NMR (400 MHz, DMSO-d6) δ 12.52 (s, 2H), 8.77 (s, 2H), 8.67 (d, *J* = 2.1 Hz, 2H), 8.44 (s, 2H), 8.25 (dd, *J* = 8.6, 2.1 Hz, 2H, 7.89 (d, *J* = 8.5 Hz, 2H). ^{13}C NMR (100 MHz, DMSO-d6) δ 137.16, 134.45, 133.90, 133.46, 130.99, 116.23, 113.15. HRMS found 382.0362, M+. MP = 297-299 °C.

72 *– N',2-bis((E)-3,5-dicyanobenzylidene)hydrazine-1-carboximidhydrazide Hydrochloride*

A solution of 5-formylisopthalonitrile (172 mg, 1.1 mmol, 2.2 eq.) and 1,3-diaminoguanidine hydrochloride (63 mg, 0.5 mmol, 1 eq.) in ethanol (10 mL) was refluxed for 16 hr. Diethyl ether (10 mL) was added and the product carbonimidic dihydrazide crashed out of solution as a white solid. The product was filtered, washed with diethyl ether, and recrystallized from methanol as a hydrochloride salt. Yield: 144 mg, 72 %. ^{1}H NMR (400 MHz, DMSO-d6) δ 12.69 (s, 1H), 8.80 (d, *J* = 1.5 Hz, 4H), 8.54 (t, *J* = 1.5 Hz, 2H), 8.46 (s, 1H). ^{13}C NMR (100 MHz, DMSO-d6) δ 136.50, 135.68, 117.44, 113.83. HRMS found 366.1203, M+H. MP = 312-314 °C.

73 *– N',2-bis((E)-3,4-dicyanobenzylidene)hydrazine-1-carboximidhydrazide Hydrochloride*

A solution of 4-formylpthalonitrile (172 mg, 1.1 mmol, 2.2 eq.) and 1,3-diaminoguanidine hydrochloride (63 mg, 0.5 mmol, 1 eq.) in ethanol (10 mL) was refluxed for 16 hr. Diethyl ether (10 mL) was added and the product carbonimidic dihydrazide crashed out of solution as a white solid. The product was filtered, washed with diethyl ether, and recrystallized from methanol as a hydrochloride salt. Yield: 129 mg, 64 %. ^{1}H NMR (400 MHz, DMSO-d6) δ 12.79 (s, 1H), 8.89 – 8.80 (m, 3H), 8.50 (s, 1H), 8.39 (dd, *J* = 8.2, 1.7 Hz, 2H), 8.26 (d, *J* = 8.1 Hz, 2H). ^{13}C NMR (100 MHz, DMSO-d6) δ 139.10, 134.95, 133.26, 132.44, 116.40, 116.30, 115.68, 115.39. HRMS found 366.1204, M+H. MP = 315-317 °C.

74 – *3-cyano-4-trifluoromethoxybenzaldehyde*

A solution of 3-iodo-4-trifluoromethoxybenzaldehyde (689 mg, 2.18 mmol, 1 eq.) and zinc cyanide (410 mg, 3.5 mmol, 1.5 eq.) in DMF (10 mL) was stirred at room temperature. Tetrakis(triphenylphosphine) Palladium (300 mg, cat.) was added and the mixture was brought to 100 °C for 8 hr. Aqueous potassium carbonate (10%) was added, and the organic components were extracted in ethyl acetate. The product, a pale yellow oil, was purified by wet column chromatography using ethyl acetate and hexane on silica gel. Yield: 104 mg, 22 %. ^{1}H NMR (400 MHz, DMSO-d6) δ 10.06 (d, *J* = 6.7 Hz, 1H), 8.64 – 8.57 (m, 1H), 8.37 (t, *J* = 7.7 Hz, 1H), 7.92 (d, *J* = 8.6 Hz, 1H). ^{13}C NMR (100 MHz, DMSO-d6) δ 190.96, 152.60, 136.47, 135.53, 122.22, 114.06, 107.11. GCMS found 214.0, M+.

75 *– N',2-bis((E)-3-iodo-4-(trifluoromethoxy)benzylidene)hydrazine-1-carboximidhydrazide Hydrochloride*

A solution of 3-iodo-4-trifluoromethoxybenzaldehyde (278 mg, 0.88 mmol, 2.2 eq.) and 1,3-diaminoguanidine hydrochloride (50 mg, 0.4 mmol, 1 eq.) in ethanol (10 mL) was refluxed for 16 hr. Diethyl ether (10 mL) was added and the product carbonimidic dihydrazide crashed out of solution as a white solid. The product was filtered, washed with diethyl ether, and recrystallized from methanol as a hydrochloride salt. Yield: 129 mg, 45 %. ^{1}H NMR (400 MHz, DMSO-d6) δ 12.42 (s, 2H), 8.72 (s, 4H), 8.66 (s, 6H), 8.41 (s, 4H), 8.02 (d, *J* = 8.4 Hz, 6H), 7.54 (s, 4H), 7.20 (s, 1H), 4.60 (s, 1H). ^{13}C NMR (100 MHz, DMSO-d6) δ 150.20, 138.82, 134.61, 130.60, 121.87, 119.22, 92.17. HRMS found 685.8966, M+H. MP = 237-239 °C.

76 *– N',2-bis((E)-3-cyano-4-(trifluoromethoxy)benzylidene)hydrazine-1-carboximidhydrazide Hydrochloride*

A solution of 3-cyano-4-trifluoromethoxybenzaldehyde (95 mg, 0.44 mmol, 2.2 eq.) and 1,3-diaminoguanidine hydrochloride (25 mg, 0.2 mmol, 1 eq.) in ethanol (5 mL) was refluxed for 16

hr. Diethyl ether (10 mL) was added and the product carbonimidic dihydrazide crashed out of solution as a white solid. The product was filtered, washed with diethyl ether, and recrystallized from methanol as a hydrochloride salt. Yield: 45 mg, 43 %. ^{1}H NMR (400 MHz, DMSO-d6) δ 12.50 (s, 1H), 8.77 (d, *J* = 2.2 Hz, 3H), 8.46 (s, 1H), 8.35 (dd, *J* = 8.8, 2.2 Hz, 2H), 7.83 (dq, *J* = 8.7, 1.6 Hz, 2H). ^{13}C NMR (100 MHz, DMSO-d6) δ 135.44, 134.18, 133.44, 114.62, 107.19, 102.74. HRMS found 484.0943, M+H. MP = 292-294 °C.

77 *– N'-((E)-3-cyano-4-fluorobenzylidene)-2-((E)-4-(trifluoromethoxy)benzylidene)hydrazine-1-carboximidhydrazide Hydrochloride*

A solution of 4-trifluoromethoxybenzaldehyde (856 mg, 4.4 mmol, 1.1 eq.), 2-fluoro-5-formylbenzonitrile (650 mg, 4.4 mmol, 1.1 eq.), and 1,3-diaminoguanidine hydrochloride (500 mg, 4 mmol, 1 eq.) in ethanol (10 mL) was refluxed for 16 hr. Diethyl ether (10 mL) was added and the product carbonimidic dihydrazides crashed out of solution as a mixture of white solids. The mixture of products was filtered and washed with diethyl ether. The product was purified by reverse phase wet column chromatography on a C-18 column (Biotage Sfar C-18 30g) using methanol containing 0.5% formic acid and water containing 0.5% formic acid. Yield: 558 mg, 33 %. ^{1}H NMR (400 MHz, DMSO-d6) δ 12.26 (s, 1H), 8.64 (dd, *J* = 6.3, 2.3 Hz, 3H), 8.42 (d, *J* = 10.4 Hz, 2H), 8.32 (ddd, *J* = 8.8, 5.3, 2.2 Hz, 1H), 8.14 – 8.05 (m, 2H), 7.69 (t, *J* = 9.0 Hz, 1H), 7.50 (d, *J* = 8.0 Hz, 2H). ^{13}C NMR (100 MHz, DMSO-d6) δ 133.20, 130.33, 121.72, 114.24. HRMS found 393.1074, M+H. MP = 81-83°C.

78 *– N',2-bis((E)-4-(pentafluorosulfaneyl)benzylidene)hydrazine-1-carboximidhydrazide Hydrochloride*

A solution of 4-(pentafluorosulfanyl)benzaldehyde (255 mg, 1.1 mmol, 2.2 eq.) and 1,3-diaminoguanidine hydrochloride (63 mg, 0.5 mmol, 1 eq.) in ethanol (10 mL) was refluxed for 16 hr. Diethyl ether (10 mL) was added and the product carbonimidic dihydrazide crashed out of

solution as a white solid. The product was filtered, washed with diethyl ether, and recrystallized from methanol as a hydrochloride salt. Yield: 185 mg, 67 %. ^{1}H NMR (400 MHz, DMSO-d6) δ 12.42 (s, 1H), 8.74 (s, 1H), 8.49 (s, 2H), 8.18 (d, *J* = 8.6 Hz, 4H), 8.14 – 7.94 (m, 5H). ^{13}C NMR (100 MHz, DMSO-d6) δ 154.22, 137.52, 129.04, 126.73, 40.62. HRMS found 518.0518, M+H. MP = 264-266 °C.

79 – *3-formylbenzonitrile*

3-Bromobenzaldehyde (1 g, 5.4 mmol, 2 eq), sodium azide (700 mg, 10.8 mmol, 4 eq), sodium ascorbate (53 mg, 0.27 mmol, 0.1 eq), and copper iodide (100 mg, 0.54 mmol, 0.2 eq) were dissolved in 7:3 EtOH: H_2O (10 mL) under argon. N,N'-dimethylethylenediamine (0.9 mL, 0.81 mmol, 0.3 eq) was added and the mixture was heated to reflux for 1.5 hr. Water was added and the product was extracted with dichloromethane. The product, a yellow solid, was purified by wet column chromatography using ethyl acetate and hexanes on silica gel. Yield: 200 mg, 25 %. ^{1}H NMR (400 MHz, DMSO-d6) δ 7.57 (t, *J* = 1.8 Hz, 3H), 7.51 (ddd, *J* = 7.7, 2.2, 1.2 Hz, 3H), 7.43 – 7.24 (m, 8H), 7.24 – 7.03 (m, 6H), 3.24 (ddd, *J* = 8.4, 6.9, 3.0 Hz, 14H), 2.98 (s, 1H), 2.54 – 2.46 (m, 12H), 2.06 (s, 26H), 1.50 (dd, *J* = 8.8, 5.2 Hz, 1H), 1.23 (s, 3H), 0.86 (dt, *J* = 8.5, 7.1 Hz, 1H).. ^{13}C NMR (100 MHz, DMSO-d6) δ 143.84, 143.19, 139.64, 131.66, 130.63, 130.06, 128.55, 126.39, 121.90, 119.67, 119.25, 91.39, 91.10, 70.26, 53.28, 48.23. GCMS found 147.1, M+.

80 – *4-formylbenzonitrile*

4-Bromobenzaldehyde (1 g, 5.4 mmol, 2 eq), sodium azide (700 mg, 10.8 mmol, 4 eq), sodium ascorbate (53 mg, 0.27 mmol, 0.1 eq), and copper iodide (100 mg, 0.54 mmol, 0.2 eq) were dissolved in 7:3 EtOH: H_2O (10 mL) under argon. N,N'-dimethylethylenediamine (0.9 mL, 0.81 mmol, 0.3 eq) was added and the mixture was heated to reflux for 1.5 hr. Water was added and the product was extracted with dichloromethane. The product, a yellow solid, was purified by wet column chromatography using ethyl acetate and hexanes on silica gel. Yield: 450 mg, 57 %. ^{1}H

NMR (400 MHz, DMSO-d6) δ 7.53 (d, *J* = 8.3 Hz, 2H), 7.42 (d, *J* = 8.3 Hz, 1H), 7.34 (d, *J* = 8.3 Hz, 2H), 7.09 (d, *J* = 8.4 Hz, 1H). ^{13}C NMR (100 MHz, DMSO-d6) δ 192.14, 140.26, 139.65, 137.70, 132.79, 131.90, 131.71, 131.47, 131.40, 130.89, 121.78, 120.26, 119.20, 91.34, 91.19, 53.27, 53.21. GCMS found 147.1, M+.

81 *– N',2-bis((E)-3-azidobenzylidene)hydrazine-1-carboximidhydrazide Hydrochloride*

A solution of 3-azidobenzaldehyde (162 mg, 1.1 mmol, 2.2 eq.) and 1,3-diaminoguanidine hydrochloride (63 mg, 0.5 mmol, 1 eq.) in ethanol (10 mL) was refluxed for 16 hr. Diethyl ether (10 mL) was added and an orange, polymer-like substance was afforded containing none of the desired product.

82 *– N',2-bis((E)-4-azidobenzylidene)hydrazine-1-carboximidhydrazide Hydrochloride*

A solution of 4-azidobenzaldehyde (323 mg, 2.2 mmol, 2.2 eq.) and 1,3-diaminoguanidine hydrochloride (125 mg, 1 mmol, 1 eq.) in ethanol (10 mL) was refluxed for 16 hr. Diethyl ether (10 mL) was added and an orange, polymer-like substance was afforded containing none of the desired product.

83 *– (E)-2-((2-oxo-2H-chromen-6-yl)methylene)-N'-((E)-(2-oxo-2H-chromen-6-yl)methylene)hydrazine-1-carboximidhydrazide Hydrochloride*

A solution of coumarin-6-carboxaldehyde (766 mg, 4.4 mmol, 2.2 eq.) and 1,3-diaminoguanidine hydrochloride (250 mg, 2 mmol, 1 eq.) in ethanol (10 mL) was refluxed for 16 hr. Diethyl ether (10 mL) was added and the product carbonimidic dihydrazide crashed out of solution as a white solid. The product was filtered, washed with diethyl ether, and recrystallized from methanol as a hydrochloride salt. Yield: 870 mg, 99 %. ^{1}H NMR (400 MHz, DMSO-d6) δ 12.33 (s, 2H), 8.60 (s, 3H), 8.50 (s, 3H), 8.30 (dd, *J* = 8.7, 2.1 Hz, 4H), 8.21 (d, *J* = 2.1 Hz, 4H), 8.09 (d, *J* = 9.6 Hz, 4H), 7.54 (d, *J* = 8.7 Hz, 4H), 6.59 (d, *J* = 9.6 Hz, 4H). ^{13}C NMR (100 MHz, DMSO-d6) δ 160.04,

155.32, 144.33, 130.99, 130.31, 128.92, 119.40, 117.51. HRMS found 402.1191, M+H. MP = 300-302 °C.

84 – *4-formylbenzophenone*

4-(hydroxymethyl)-benzophenone (424 mg, 2 mmol, 1 eq.) and PCC (432 mg, 2 mmol, 1 eq.) were stirred in dichloromethane (20 mL) over molecular sieves for 16 hr. The product was filtered to remove the molecular sieves and extracted in dichloromethane and brine. The product was purified by wet column chromatography using ethyl acetate and hexane on silica gel. Yield: 280 mg, 67 %. ^{1}H NMR (400 MHz, DMSO-d6) δ 10.15 (s, 1H), 8.14 – 8.05 (m, 2H), 7.95 – 7.89 (m, 2H), 7.89 – 7.67 (m, 4H), 7.60 (t, *J* = 7.7 Hz, 3H). ^{13}C NMR (100 MHz, DMSO-d6) δ 195.84, 193.49, 142.29, 138.81, 136.80, 133.76, 130.50, 130.26, 129.97, 129.23. GCMS found 209.9, M+.

85 *– N',2-bis((E)-4-benzoylbenzylidene)hydrazine-1-carboximidhydrazide Hydrochloride*

A solution of 4-formylbenzophenone (46 mg, 0.22 mmol, 2.2 eq.) and 1,3-diaminoguanidine hydrochloride (12.5 mg, 0.1 mmol, 1 eq.) in ethanol (5 mL) was refluxed for 16 hr. Diethyl ether (10 mL) was added and the product carbonimidic dihydrazide crashed out of solution as a white solid. The product was filtered, washed with diethyl ether, and recrystallized from methanol as a hydrochloride salt. Yield: 50 mg, 98 %. ^{1}H NMR (400 MHz, DMSO-d6) δ 11.93 (s, 2H), 8.14 (s, 3H), 7.97 (d, *J* = 8.1 Hz, 4H), 7.84 – 7.62 (m, 11H), 7.58 (t, *J* = 7.6 Hz, 4H), 6.87 (s, 2H). ^{13}C NMR (100 MHz, DMSO-d6) δ 130.52, 129.98, 129.04. HRMS found 472.1765, M+. MP = 118-120 °C.

86 *– N'-((E)-4-benzoylbenzylidene)-2-((E)-4-(prop-2-yn-1-yloxy)benzylidene)hydrazine-1-carboximidhydrazide Hydrochloride*

A solution of 4-formylbenzophenone (116 mg, 0.55 mmol, 1.1 eq.), 4-propynoxybenzahldehyde (88 mg, 0.55 mmol, 1.1 eq.), and 1,3-diaminoguanidine hydrochloride (63 mg, 0.5 mmol, 1 eq.) in ethanol (5 mL) was refluxed for 16 hr. Diethyl ether (10 mL) was added and the product carbonimidic dihydrazides crashed out of solution as a mixture of white solids. The mixture of products was filtered and washed with diethyl ether. The product was purified by reverse phase wet column chromatography on a C-18 column (Biotage Sfar C-18 30g) using methanol containing 0.5% formic acid and water containing 0.5% formic acid. Yield: 60 mg, 26 %. ^{1}H NMR (400 MHz, DMSO-d6) δ 8.14 (d, *J* = 10.5 Hz, 2H), 8.02 (s, 1H), 8.00 – 7.90 (m, 2H), 7.83 – 7.64 (m, 8H), 7.63 – 7.54 (m, 2H), 7.05 – 6.97 (m, 2H), 6.71 (s, 1H), 4.84 (d, *J* = 2.4 Hz, 2H), 3.60 (t, *J* = 2.4 Hz, 1H). ^{13}C NMR (100 MHz, DMSO-d6) δ 130.52, 129.96, 129.03, 128.52, 115.40, 78.86, 55.97. HRMS found 424.1761, M+H. MP = 61-63 °C.

Preparation of Aminoguanidine Free Bases

Aminoguanidines were prepared synthetically as hydrochloride salts. Aminoguanidine hydrochlorides were dissolved in dichloromethane and an excess of NaOH (2M aqueous) was added while stirring. The free bases were extracted using dichloromethane and dH_2O. Dichloromethane was removed by rotary evaporation to afford the aminoguanidine free bases.

Preparation of Aminoguanidine Phosphate Salts

Aminoguanidine free bases were dissolved in methanol while stirring. One equivalent of phosphoric acid was added and the mixtures were stirred for 20 minutes at room temperature. Methanol was removed by rotary evaporation to afford the aminoguanidine phosphate salts.

Synthesis of Endochin-Like Quinolones

Chloromethyl Methyl Carbonate

Dry methanol (0.44 mL, 11 mmol, 1.1 eq.), triethylamine (2.8 mL, 20 mmol, 2 eq.), and dry THF (60 mL) were combined and cooled to -78 ^{o}C on a dry ice-acetone bath under argon while stirring. Chloromethyl chloroformate (1.29 g, 0.9 mL, 10 mmol, 1 eq.) was added dropwise and the mixture was allowed to warm to room temperature overnight. When the reaction was complete by GCMS, the mixture was filtered and the filtrate was concentrated by rotary evaporation yielding 440 mg (35 %) as a yellow solid. GCMS found 125.1, M+H.

ELQ-487

ELQ-300 (714 mg, 1.5 mmol, 1 eq.) was dissolved in dry DMF (20 mL). Tetrabutylammonium iodide (1.11 g, 3 mmol, 2 eq.) was added, followed by potassium carbonate (414 mg, 3 mmol, 2 eq.) and chloromethyl methyl carbonate (372 mg, 3 mmol, 2 eq.). The mixture was stirred at 60 ^{o}C overnight. The solvent was removed by rotary evaporation and the mixture was redissolved in dichloromethane (20 mL) and washed three times with brine (3 x 20 mL). The organic layer was dried with $MgSO_4$ and the solvent was removed by rotary evaporation. The crude product was purified by flash chromatography using ethyl acetate and hexane on silica gel, yielding 460 mg (54 %) of fine white crystals. ^{1}H NMR (400 MHz, DMSO-d6): δ 7.99 (s, 1H), 7.57 (s, 1H), 7.44 (m, 4H), 7.23 (m, 4H), 5.37 (s, 2H), 4.03 (s, 3H), 3.64 (s, 3H), 2.44 (s, 3H); MP = 124 ^{o}C. GCMS found 563.4, M+.

Chloromethyl Propyl Carbonate

Dry n-propanol (0.83 mL, 11 mmol, 1.1 eq.), triethylamine (2.8 mL, 20 mmol, 2 eq.), and dry THF (60 mL) were combined and cooled to -78 ^{o}C on a dry ice-acetone bath under argon while stirring. Chloromethyl chloroformate (1.29 g, 0.9 mL, 10 mmol, 1 eq.) was added dropwise and the mixture was allowed to warm to room temperature overnight. When the reaction was complete by GCMS, the mixture was filtered and the filtrate was concentrated by rotary evaporation yielding 830 mg (55 %) as a yellow solid. GCMS found 153.1, M+H.

ELQ-488

ELQ-300 (714 mg, 1.5 mmol, 1 eq.) was dissolved in dry DMF (20 mL). Tetrabutylammonium iodide (1.11 g, 3 mmol, 2 eq.) was added, followed by potassium carbonate (414 mg, 3 mmol, 2 eq.) and chloromethyl propyl carbonate (456 mg, 3 mmol, 2 eq.). The mixture was stirred at 60 ^{o}C overnight. The solvent was removed by rotary evaporation and the mixture was redissolved in dichloromethane (20 mL) and washed three times with brine (3 x 20 mL). The organic layer was dried with $MgSO_4$ and the solvent was removed by rotary evaporation. The crude product was purified by flash chromatography using ethyl acetate and hexane on silica gel, yielding 330 mg (37 %) as a white solid. ^{1}H NMR (400 MHz, DMSO-d6): δ 7.98 (s, 1H), 7.57 (s, 1H), 7.45 (m, 4H), 7.21 (m, 4H), 5.35 (s, 2H), 4.03 (s, 3H), 3.94 (t, J = 6.5, 2H), 2.44 (s, 3H), 1.49 (sxt, J = 7, 2H), 0.78 (t, J = 7.3, 3H); MP = 131 ^{o}C. GCMS found 591.4, M+.

Chloromethyl Butyl Carbonate

Dry n-butanol (1.0 mL, 11 mmol, 1.1 eq.), triethylamine (2.8 mL, 20 mmol, 2 eq.), and dry THF (60 mL) were combined and cooled to -78 ^{o}C on a dry ice-acetone bath under argon while stirring. Chloromethyl chloroformate (1.29 g, 0.9 mL, 10 mmol, 1 eq.) was added dropwise and the mixture was allowed to warm to room temperature overnight. When the reaction was complete by GCMS, the mixture was filtered and the filtrate was concentrated by rotary evaporation yielding 1.10 g (66 %) as a yellow solid. GCMS found 167.1, M+H.

ELQ-489

ELQ-300 (714 mg, 1.5 mmol, 1 eq.) was dissolved in dry DMF (20 mL). Tetrabutylammonium iodide (1.11 g, 3 mmol, 2 eq.) was added, followed by potassium carbonate (414 mg, 3 mmol, 2 eq.) and chloromethyl butyl carbonate (498 mg, 3 mmol, 2 eq.). The mixture was stirred at 60 ^{o}C overnight. The solvent was removed by rotary evaporation and the mixture was redissolved in

dichloromethane (20 mL) and washed three times with brine (3 x 20 mL). The organic layer was dried with $MgSO_4$ and the solvent was removed by rotary evaporation. The crude product was purified by flash chromatography using ethyl acetate and hexane on silica gel, yielding 300 mg (33 %) as white crystals. ^{1}H NMR (400 MHz, DMSO-d6): δ 7.99 (s, 1H), 7.55 (s, 1H), 7.44 (m, 4H), 7.21 (m, 4H), 5.35 (s, 2H), 4.03 (s, 3H), 3.98 (t, J = 6.6, 2H), 2.42 (s, 3H), 1.44 (m, 2H), 1.18 (m, 2H), 0.80 (t, J = 7.3, 3H); MP = 95 ^{o}C. GCMS found 605.4, M+.

Chloromethyl Pentyl Carbonate

Dry n-pentanol (1.2 mL, 11 mmol, 1.1 eq.), triethylamine (2.8 mL, 20 mmol, 2 eq.), and dry THF (60 mL) were combined and cooled to -78 ^{o}C on a dry ice-acetone bath under argon while stirring. Chloromethyl chloroformate (1.29 g, 0.9 mL, 10 mmol, 1 eq.) was added dropwise and the mixture was allowed to warm to room temperature overnight. When the reaction was complete by GCMS, the mixture was filtered and the filtrate was concentrated by rotary evaporation yielding 1.47 g (82 %) as a yellow solid. GCMS found 181.2, M+H.

ELQ-490

ELQ-300 (714 mg, 1.5 mmol, 1 eq.) was dissolved in dry DMF (20 mL). Tetrabutylammonium iodide (1.11 g, 3 mmol, 2 eq.) was added, followed by potassium carbonate (414 mg, 3 mmol, 2 eq.) and chloromethyl pentyl carbonate (540 mg, 3 mmol, 2 eq.). The mixture was stirred at 60 ^{o}C overnight. The solvent was removed by rotary evaporation and the mixture was redissolved in dichloromethane (20 mL) and washed three times with brine (3 x 20 mL). The organic layer was dried with $MgSO_4$ and the solvent was removed by rotary evaporation. The crude product was purified by flash chromatography using ethyl acetate and hexane on silica gel, yielding 220 mg (24 %) as white crystals. ^{1}H NMR (400 MHz, DMSO-d6): δ 7.99 (s, 1H), 7.57 (s, 1H), 7.44 (m, 4H), 7.21 (m, 4H), 5.35 (s, 2H), 4.03 (s, 3H), 3.96 (t, J = 6.6, 2H), 2.44 (s, 3H), 1.45 (quin, 2H), 1.17 (m, 4H), 0.80 (t, J = 7.1, 3H); MP = 109 ^{o}C. GCMS found 619.5, M+.

Chloromethyl Hexyl Carbonate

Dry n-hexanol (1.37 mL, 11 mmol, 1.1 eq.), triethylamine (2.8 mL, 20 mmol, 2 eq.), and dry THF (60 mL) were combined and cooled to -78 ^{o}C on a dry ice-acetone bath under argon while stirring. Chloromethyl chloroformate (1.29 g, 0.9 mL, 10 mmol, 1 eq.) was added dropwise and the mixture was allowed to warm to room temperature overnight. When the reaction was complete by GCMS, the mixture was filtered and the filtrate was concentrated by rotary evaporation yielding 1.67 g (86 %) as a yellow solid. GCMS found 195.2, M+H.

ELQ-491

ELQ-300 (714 mg, 1.5 mmol, 1 eq.) was dissolved in dry DMF (20 mL). Tetrabutylammonium iodide (1.11 g, 3 mmol, 2 eq.) was added, followed by potassium carbonate (414 mg, 3 mmol, 2 eq.) and chloromethyl hexyl carbonate (584 mg, 3 mmol, 2 eq.). The mixture was stirred at 60 ^{o}C overnight. The solvent was removed by rotary evaporation and the mixture was redissolved in dichloromethane (20 mL) and washed three times with brine (3 x 20 mL). The organic layer was dried with $MgSO_4$ and the solvent was removed by rotary evaporation. The crude product was purified by flash chromatography using ethyl acetate and hexane on silica gel, yielding 240 mg (25 %) as a white solid. ^{1}H NMR (400 MHz, DMSO-d6): δ 7.99 (s, 1H), 7.55 (s, 1H), 7.44 (m, 4H), 7.20 (m, 4H), 5.35 (s, 2H), 4.03 (s, 3H), 3.96 (t, J = 6.6, 2H), 2.44 (s, 3H), 1.42 (m, 2H), 1.19 (m, 6H), 0.82 (t, J = 7.3, 3H); MP = 79 ^{o}C. GCMS found 633.5, M+.

Chloromethyl Heptyl Carbonate

Dry n-heptanol (1.56 mL, 11 mmol, 1.1 eq.), triethylamine (2.8 mL, 20 mmol, 2 eq.), and dry THF (60 mL) were combined and cooled to -78 ^{o}C on a dry ice-acetone bath under argon while stirring. Chloromethyl chloroformate (1.29 g, 0.9 mL, 10 mmol, 1 eq.) was added dropwise and the mixture was allowed to warm to room temperature overnight. When the reaction was complete by GCMS,

the mixture was filtered and the filtrate was concentrated by rotary evaporation yielding 1.87 g (90 %) as a yellow solid. GCMS found 209.2, M+H.

ELQ-492

ELQ-300 (714 mg, 1.5 mmol, 1 eq.) was dissolved in dry DMF (20 mL). Tetrabutylammonium iodide (1.11 g, 3 mmol, 2 eq.) was added, followed by potassium carbonate (414 mg, 3 mmol, 2 eq.) and chloromethyl heptyl carbonate (624 mg, 3 mmol, 2 eq.). The mixture was stirred at 60 ^{o}C overnight. The solvent was removed by rotary evaporation and the mixture was redissolved in dichloromethane (20 mL) and washed three times with brine (3 x 20 mL). The organic layer was dried with $MgSO_4$ and the solvent was removed by rotary evaporation. The crude product was purified by flash chromatography using ethyl acetate and hexane on silica gel, yielding 170 mg (18 %) as a white solid. ^{1}H NMR (400 MHz, DMSO-d6): δ 7.99 (s, 1H), 7.56 (s, 1H), 7.44 (m, 4H), 7.20 (m, 4H), 5.35 (s, 2H), 4.03 (s, 3H), 3.96 (t, J = 6.6, 2H), 2.44 (s, 3H), 1.45 (m, 2H), 1.20 (m, 8H), 0.83 (t, J = 7.3, 3H); MP = 63 ^{o}C. GCMS found 647.5, M+.

Chloromethyl Octyl Carbonate

Dry n-octanol (1.74 mL, 11 mmol, 1.1 eq.), triethylamine (2.8 mL, 20 mmol, 2 eq.), and dry THF (60 mL) were combined and cooled to -78 ^{o}C on a dry ice-acetone bath under argon while stirring. Chloromethyl chloroformate (1.29 g, 0.9 mL, 10 mmol, 1 eq.) was added dropwise and the mixture was allowed to warm to room temperature overnight. When the reaction was complete by GCMS, the mixture was filtered and the filtrate was concentrated by rotary evaporation yielding 1.71 g (77 %) as a yellow solid. GCMS found 223.2, M+H.

ELQ-493

ELQ-300 (714 mg, 1.5 mmol, 1 eq.) was dissolved in dry DMF (20 mL). Tetrabutylammonium iodide (1.11 g, 3 mmol, 2 eq.) was added, followed by potassium carbonate (414 mg, 3 mmol, 2

eq.) and chloromethyl octyl carbonate (666 mg, 3 mmol, 2 eq.). The mixture was stirred at 60 °C overnight. The solvent was removed by rotary evaporation and the mixture was redissolved in dichloromethane (20 mL) and washed three times with brine (3 x 20 mL). The organic layer was dried with $MgSO_4$ and the solvent was removed by rotary evaporation. The crude product was purified by flash chromatography using ethyl acetate and hexane on silica gel, yielding 310 mg (31 %) as a white solid. ^{1}H NMR (400 MHz, DMSO-d6): δ 7.99 (s, 1H), 7.57 (s, 1H), 7.44 (m, 4H), 7.21 (m, 4H), 5.35 (s, 2H), 4.02 (s, 3H), 3.96 (t, J = 6.6, 2H), 2.44 (s, 3H), 1.44 (m, 2H), 1.21 (m, 10H), 0.84 (t, J = 7, 3H); MP = 54 °C. GCMS found 661.5, M+.

Chloromethyl Nonyl Carbonate

Dry n-nonanol (1.91 mL, 11 mmol, 1.1 eq.), triethylamine (2.8 mL, 20 mmol, 2 eq.), and dry THF (60 mL) were combined and cooled to -78 °C on a dry ice-acetone bath under argon while stirring. Chloromethyl chloroformate (1.29 g, 0.9 mL, 10 mmol, 1 eq.) was added dropwise and the mixture was allowed to warm to room temperature overnight. When the reaction was complete by GCMS, the mixture was filtered and the filtrate was concentrated by rotary evaporation yielding 1.75 g (74 %) as a yellow solid. GCMS found 237.3, M+H.

ELQ-494

ELQ-300 (714 mg, 1.5 mmol, 1 eq.) was dissolved in dry DMF (20 mL). Tetrabutylammonium iodide (1.11 g, 3 mmol, 2 eq.) was added, followed by potassium carbonate (414 mg, 3 mmol, 2 eq.) and chloromethyl nonyl carbonate (708 mg, 3 mmol, 2 eq.). The mixture was stirred at 60 °C overnight. The solvent was removed by rotary evaporation and the mixture was redissolved in dichloromethane (20 mL) and washed three times with brine (3 x 20 mL). The organic layer was dried with $MgSO_4$ and the solvent was removed by rotary evaporation. The crude product was purified by flash chromatography using ethyl acetate and hexane on silica gel, yielding 440 mg (43 %) as a white waxy solid. ^{1}H NMR (400 MHz, DMSO-d6): δ 7.97 (s, 1H), 7.56 (s, 1H), 7.44

(m, 4H), 7.20 (m, 4H), 5.35 (s, 2H), 4.02 (s, 3H), 3.96 (t, J = 6.6, 2H), 2.44 (s, 3H), 1.43 (m, 2H), 1.20 (m, 12H), 0.84 (t, J = 6.6, 3H); MP = 57 ^{o}C. GCMS found 640.5, M-Cl.

Chloromethyl Decyl Carbonate

Dry n-decanol (2.1 mL, 11 mmol, 1.1 eq.), triethylamine (2.8 mL, 20 mmol, 2 eq.), and dry THF (60 mL) were combined and cooled to -78 ^{o}C on a dry ice-acetone bath under argon while stirring. Chloromethyl chloroformate (1.29g, 0.9 mL, 10 mmol, 1 eq.) was added dropwise and the mixture was allowed to warm to room temperature overnight. When the reaction was complete by GCMS, the mixture was filtered and the filtrate was concentrated by rotary evaporation yielding 2.24 g (90 %) as a yellow solid. GCMS found 251.2, M+H.

ELQ-495

ELQ-300 (714 mg, 1.5 mmol, 1 eq.) was dissolved in dry DMF (20 mL). Tetrabutylammonium iodide (1.11 g, 3 mmol, 2 eq.) was added, followed by potassium carbonate (414 mg, 3 mmol, 2 eq.) and chloromethyl decyl carbonate (750 mg, 3 mmol, 2 eq.). The mixture was stirred at 60 ^{o}C overnight. The solvent was removed by rotary evaporation and the mixture was redissolved in dichloromethane (20 mL) and washed three times with brine (3 x 20 mL). The organic layer was dried with $MgSO_4$ and the solvent was removed by rotary evaporation. The crude product was purified by flash chromatography using ethyl acetate and hexane on silica gel, yielding 370 mg (36 %) as a white waxy solid. ^{1}H NMR (400 MHz, DMSO-d6): δ 7.98 (s, 1H), 7.56 (s, 1H), 7.44 (m, 4H), 7.21 (m, 4H), 5.35 (s, 2H), 4.02 (s, 3H), 3.96 (t, J = 6.6, 2H), 2.44 (s, 3H), 1.42 (m, 2H), 1.23 (m, 14H), 0.85 (m, 3H); MP = 55 ^{o}C. GCMS found 654.5, M-Cl.

Biology and Experiments

General Biology - Parasite Culture and Drug Sensitivity

The following parasite strains were used in this study and obtained through BEI Resources, NIAID, NIH. *Plasmodium falciparum*, Strain D6 (MRA-285, originally from Sierra Leone, has modest resistance to mefloquine) (Oduola 1988). Strain Dd2 (MRA-150, originated from Indochina; derived from W2-mef and is resistant to chloroquine, pyrimethamine and mefloquine. *P. falciparum* strain D1 was derived from strain Dd2 and is ELQ-300 resistant. *P. falciparum* strain Tm90-C2B (Thailand; resistant to mefloquine, chloroquine, atovaquone, and pyrimethamine) was obtained directly from the Division of Experimental Therapeutics of Walter Reed Army Institute of Research (WRAIR) in Silver Spring, Maryland, USA (Nilsen 2013). Strain SB1-A6 (MRA-1002, Sierra Leone was derived from D6 clone and is resistant to Atovaquone and ELQ-300 (Smilkstein 2008).

P. falciparum parasites were thawed from frozen stock and cultured in suspended human erythrocytes (Lampire Biological Labs, Pipersville, PA) not more than 28 days old at 2% hematocrit. The culture medium used was RPMI-1640, supplemented with 25 mM HEPES buffer, 25 mg/L gentamicin sulfate, 45 mg/L hypoxanthine, 10 mM glucose, 2 mM glutamine, and 0.5% Albumax II (complete medium) (Trager 1976). Cultures were maintained in a standard low oxygen atmosphere (5% O_2, 5% CO_2, 90% N_2) in an environmental chamber and incubated at 37 °C. Cultures were sub-passaged every 3-4 days into a fresh culture flask containing complete media and erythrocytes.

IC_{50} Determination by the Fluorescence-Based SYBR Green Assay

The aminoguanidine series was assessed for *in vitro* antiplasmodial activity using the fluorescence-based SYBR Green assay described previously by Smilkstein and co-workers (Smilkstein 2004). Compounds were evaluated in quadruplicate in flat-bottomed Costar clear 96-well plates (Model #3585). A two-fold serial dilution of each compound was performed across the columns of the test plates starting with 20 μM and ending with a final untreated column to serve

as control wells. Asynchronous parasite infected erythrocytes in growth media were added to each well for a total volume of 100 µL, final hematocrit of 2%, and initial parasitemia of 0.2%. The commercial malaria drugs atovaquone and chloroquine were used as control drugs. Test plates were incubated for 72 hr at 37 °C in an environmental chamber with a controlled low oxygen atmosphere (5% O_2, 5% CO_2, 90% N_2). After the incubation period, 100 µL SYBR Green I dye-detergent solution was added to each well, and the plates were incubated at ambient temperature and atmosphere in the dark for at least one hour. Fluorescence was read at 497 nm excitation and 520 nm emission bands using a Spectramax iD3 plate reader. Fluorescence readings were normalized with respect to the untreated control wells representing normal parasite growth and plotted against the logarithm of drug concentration. An IC_{50} was determined for each compound by fitting this data to a variable slope nonlinear regression curve using Graphpad Prism software (v. 8).

Variations on the SYBR Green Assay

Variation 1: Time Dependency Experiment

Test plates were prepared as described above. Test plates were incubated for 48, 72, or 96 hr at 37 °C in an environmental chamber with a controlled low oxygen atmosphere (5% O_2, 5% CO_2, 90% N_2). After the incubation period, parasite growth was measured by SYBR Green staining as described above.

Variation 2: Stage Specificity Experiment

Parasite cultures were synchronized using sorbitol as described by Lambros and Vanderberg (Lambros 1979). RPMI media was removed from parasite cultures and replaced with an equal volume of 5% aqueous D-sorbitol. The cultures were incubated for 10-20 minutes at room temperature in sorbitol, which was then removed. The cultures were washed 3 times with RPMI media and then resuspended in media. The cultures were inspected for synchronization to the ring stage by blood smear on the day following sorbitol treatment. The sorbitol treatment was

repeated every 48 hours until tight synchronization was achieved. Test plates for the SYBR Green Assay were prepared, incubated, and stained as described above, using cultures synchronized at either the ring stage or the mid-trophozoite stage.

Variation 3: Synergy Experiment

Drug synergy was measured by fixed-ratio isobolograms as described by Fivelman (Fivelman 2004). Pairs of drugs were combined in the following ratios: 5:0, 1:4, 2:3, 3:2, 4:1, and 0:5. These drug mixtures were applied to test plates as described above, incubated and stained with SYBR Green as described. Variations in the measured IC_{50}s of the drug combinations were plotted on an isobologram to assess for drug synergy vs. antagonism.

Variation 4: Atovaquone-Biguanide Synergy Experiment

RPMI media was removed from *Plasmodium* cultures and replaced with RPMI media containing 10 nM Atovaquone. After culturing parasites with Atovaquone for 1 week to ensure atovaquone resistance, test plates were prepared as described. A second set of test plates were prepared using RPMI media with 10 nM Atovaquone applied to the plates and to prepare drug solutions. Both sets of plates were incubated and stained as described.

HepG2 Cytotoxicity Assay

Compounds were prepared as 10 mM stock solutions in DMSO. Human hepatocarcinoma (HepG2) cells were maintained in culture at 37 °C in a humidified 5% CO_2 atmosphere in RPMI-1640 medium containing 10% fetal bovine serum. HepG2 cells were added to each well of flat bottom 96-well tissue culture plates at an initial density of 2×10^4 cells per well, and an initial volume of 160 µL complete medium per well. After an overnight incubation at 37 °C to adhere the cells to the culture plates, 40 µL drug solutions in complete medium were applied to each well at a final concentration range of 0 to 200 µM across each plate. Drugs were tested in triplicate or quadruplicate. The cells were incubated for 24 hours at 37 °C and 5% CO_2 with the drug solutions, which were then aspirated and replaced with 200 µL per well of complete medium for an additional

24 hour incubation under the same conditions. To each well was added 20 µL of resazurin (Alamar Blue) in PBS buffer to a final concentration of 10 µM, and the plates were incubated for 3 hours. Fluorescence was measured at 560 nm excitation and 590 nm emission bands using a Spectramax iD3 plate reader. Fluorescence readings were normalized with respect to the untreated control wells and plotted against the logarithm of drug concentration. An IC_{50} was determined for each compound by fitting this data to a variable slope nonlinear regression curve using Graphpad Prism software (v. 8).

In Vivo Efficacy against Blood Stage Murine Malaria

The *in vivo* ED_{50} and ED_{90} of selected aminoguanidines was measured using a modified 4-day Peters test (Peters 2002). Female CF1 mice from Charles River Laboratories were inoculated intravenously with approximately 2.5-5.0 x 10^4 parasitized erythrocytes (murine malaria *P. yoelii*, Kenya strain MR4 MRA-428) from a donor mouse (experiment day zero). On the following four days (experiment days 1-4), solutions of the test compounds in PEG-300 or SEDDS formulation (Self-Emulsifying Drug Delivery System, 37.5% PEG-400, 37.5% Tween 20, and Capmul MCM-NF) or vehicle only were administered by oral gavage once daily. Aminoguanidines were initially assessed at 2.5, 5, and 10 mg/kg/day, and experiments were repeated to adjust the dose range as needed to obtain an interpolated ED_{50} and ED_{90} value (**1** required a dosing down to 0.1 mg/kg/day to attain this result). Experiments were repeated with doses up to 25 mg/kg/day to obtain a non-recrudescence dose, though only **16** was found to produce a cure in this model. Parasitemia of each mouse was determined by microscopic examination of Giemsa stained blood smears on day 5. ED_{50} and ED_{90} values were assessed by generating dose-response curves relative to untreated controls using Graphpad Prism (v. 8). Mice were monitored regularly for signs of acute toxicity. Mice were considered cured of malarial infection if they maintained 0% parasitemia at experiment day 30. The procedures involved, together with all matters relating to

the care, handling, and housing of the animals used in this study, were approved by the Portland VA Medical Center Institutional Animal Care and Use Committee.

Murine Microsomal Stability

Metabolic stability studies of selected aminoguanidines were performed at ChemPartner, Shanghai, China. Compounds were incubated at 37 °C and 1 μM concentration in murine liver microsomes (Corning) for one hour at a protein concentration of 0.5 mg/mL in potassium phosphate buffer at pH 7.4 containing 1.0 mM EDTA. The metabolic reaction was initiated by NADPH and quenched with ice-cold acetonitrile at 15 minute increments up to one hour. The progress of compound metabolism was followed by LC-MS/MS (ESI positive ion, LC-MS/MS-034(API-6500+)) using a C_{18} stationary phase (ACQUITY UPLC BEH C_{18}(2.1×50 mm, 1.7 μm) and a MeOH/water mobile phase containing 0.25% FA and 1 mM NH_4OAc. Imipramine or Osalmid were used as internal standards, and ketanserin was used as an internal standard for a drug with intermediate stability. Concentration versus time data for each compound were fitted to an exponential decay function to determine the first-order rate constant for substrate depletion, which was then used to calculate the degradation half-life ($t_{1/2}$) and predicted intrinsic clearance value (Cl_{int}) from an assumed murine hepatic blood flow of 90 mL/min/kg.

*Pharmacokinetics Profile of Compound **1***

A pharmacokinetics profile of compound 1 was performed at ChemPartner, Shanghai, China. CD1 mice (6-8 weeks, male, Jihui Laboratory Animal Co.) were dosed either intravenously (1 mg/kg in 50 mM carbonate buffer, pH 9) or by oral gavage (10 mg/kg in PEG-400) with compound 1. Blood (110 μL) was collected at 0, 5, 15, and 30 min after dosing, as well as 1, 2, 4, 8, and 24 hr after injection (N = 3 animals per time point for each administration route) and plasma was isolated from collected samples. Plasma concentration of compound 1 was determined by LC-MS/MS (ESI positive ion, LC-MS/MS-034(API-6500+)) using a C_{18} stationary phase (ACQUITY

UPLC BEH T3 (2.1×50 mm, 1.8 µm) and an ACN/water mobile phase containing 0.1% FA. Diclofenac was used as an internal standard. Plasma concentration of compound 1 versus time data for each administration route were fitted to an exponential decay function to determine the first-order rate constant for substrate depletion, which was then used to calculate the degradation half-life ($t_{1/2}$) and predicted intrinsic clearance value (Cl_{int}). Oral bioavailability was calculated by dividing the area under the curve (AUC) for oral administration by the AUC for IV administration.

In vivo Blood Stage Prophylaxis of ELQ Prodrugs in Murine Malaria

Female Swiss-Webster mice (CFW, Charles River Laboratories. Inc. Raleigh, NC) were used to evaluate malaria prophylaxis of prodrugs. Mice (n = 4 per prodrug per time point) were injected IM in the quadricep with prodrugs in 0.05 mL sesame oil containing 1.2% benzyl alcohol. Doses of each prodrug were normalized to deliver 10 mg/kg of ELQ-300, regardless of total prodrug mass. The prophylactic effect of each prodrug was challenged at different time points with IV injections of 30,000 *P. yoelii*-infected erythrocytes from a donor mouse. Parasitemia was evaluated microscopically with blood smears 5 days after each prophylaxis challenge. Prophylaxis challenges were performed at 1, 2, 3, and 5.5 weeks after dosing using a new group of mice at each time point. Mice were monitored regularly for signs of acute toxicity. In follow-up evaluations, mice that remained free of parasites for 30 days were considered 'not infected.' Mice with detectable parasitemia were considered 'infected' and euthanized. All experiments were approved by the Portland VA Medical Center Institutional Animal Care and Use Committee.

Pharmacokinetics of ELQ Prodrugs

Female Swiss-Webster mice (CFW, Charles River Laboratories. Inc. Raleigh, NC) were used to evaluate malaria prophylaxis of prodrugs. Mice (n = 4 per prodrug per time point) were injected IM in the quadricep with prodrugs in 0.05 mL sesame oil containing 1.2% benzyl alcohol. Doses of each prodrug were normalized to deliver 10 mg/kg of ELQ-300, regardless of total prodrug

mass. Blood samples were collected from the mice at 30 days, 70 days, and 77 days after dosing. Pharmacokinetics measurements were performed by the OHSU Pharmacokinetics Core. Plasma concentrations of ELQ-300 were measured by LCMS/MS (QTRAP 4000, ESI positive mode) using a Dacapo DX-C18 column with a water/acetonitrile mobile phase containing 0.1% formic acid. Plasma concentration curves were fitted using Graphpad Prism 7. All experiments were approved by the Portland VA Medical Center Institutional Animal Care and Use Committee.

Protein Target Identification with a Photoactivatable Probe

Plasmodium falciparum Tm90-C2B parasites were isolated from erythrocytes in culture by selective lysis of the erythrocyte membrane using 0.1% saponin (Ansorge 1996, Baumeister 1999). Free parasites were resuspended in PBS containing a protease inhibitor cocktail (Protease Inhibitor Cocktail III, CalBioChem). Aliquots of parasites at a protein concentration of 2 mg/mL were incubated for one hour with the probe compound **86** at concentrations of 0, 0.1, 1, 10, and 100 μM in the dark at 4 ^{o}C. 50 μL of each sample was irradiated under UV light at 350 nm for 3 min. Another 50 μL aliquot of the 100 μM **86** sample was not irradiated as a control. In all samples containing **86**, the probe was conjugated to TAMRA N3 (Click Chemistry Tools) via copper catalyzed alkyne azide click chemistry. The reaction mixtures contained 300 μM TBTA, 3 mM $CuSO_4$, 5 mM TAMRA N3, 3 mM TCEP, and 30 μL of each sample, and the reaction was carried out in PBS at room temperature in the dark for 1 hr. The reactions were quenched with 15 μL 4X SDS PAGE sample buffer and all six samples were heated at 95 ^{o}C for 10 minutes. An all blue ladder and each sample in duplicate were added to wells of an SDS PAGE gel and run for 80 min at 165 V. The gel was imaged and later stained with Coomassie Blue.

Variation: Initial Probe Experiment

Plasmodium falciparum Dd2 parasites were isolated from erythrocytes as described and resuspended in PBS with no protease inhibitor. Protein concentration was not confirmed. Parasites were incubated with 0 or 100 μM **86** as described. Seven 50 μL aliquots of the parasite

mixture containing **86** were prepared. Samples were irradiated under UV light at 350 or 400 nm for 1, 3, or 5 min, with one sample receiving no irradiation. The samples were conjugated to TAMRA N3, quenched, and loaded onto an SDS PAGE gel as described. The gel was imaged and stained with Coomassie Blue.

Chapter 3 : Robenidine Analogs are Potent Antimalarials in Drug-Resistant *Plasmodium falciparum*

The text, figures, schemes, and tables from this chapter are previously published in ACS Infectious Diseases under the same title (Krollenbrock 2021) and are reprinted with permission. *In vivo* efficacy experiments were performed by Dr. Yuexin Li. Metabolic stability experiments were performed by Chem Partner (Shanghai, China). All other experiments were performed by the author.

Introduction

Robenidine (Figure 3-1a) is a veterinary drug used in the poultry industry to treat coccidiosis caused by parasites in the *Eimeria* genus. Though this compound and related aminoguanidines have recently been studied in other pathogens, the chemotype has not been systematically explored to optimize antimalarial activity despite the close genetic relationship between *Eimeria* and *Plasmodium* (both are members of the Apicomplexa phylum of unicellular, spore-forming parasites).

In the study described in this chapter, a library of 38 structurally diverse aminoguanidines was created and compared for *in vitro* anti-plasmodial activity as well as mammalian cell cytotoxicity. The series was evaluated in both drug-sensitive and drug-resistant malaria strains. Compounds with promising selective activity were further evaluated *in vivo* against murine *Plasmodium yoelii* in mice. Multiple aminoguanidines from this library were found to have high potency *in vitro* which translated to robust efficacy *in vivo*. One compound, **1** (Figure 3-1b),

exhibits single-digit nanomolar IC_{50} values against *P. falciparum* strains with an *in vivo* ED_{50} value of 0.25 mg/kg/day vs. murine malaria in a standard 4-day test. Among aminoguanidines with potent *in vitro* activity, murine microsomal stability was found to correlate with *in vivo* efficacy.

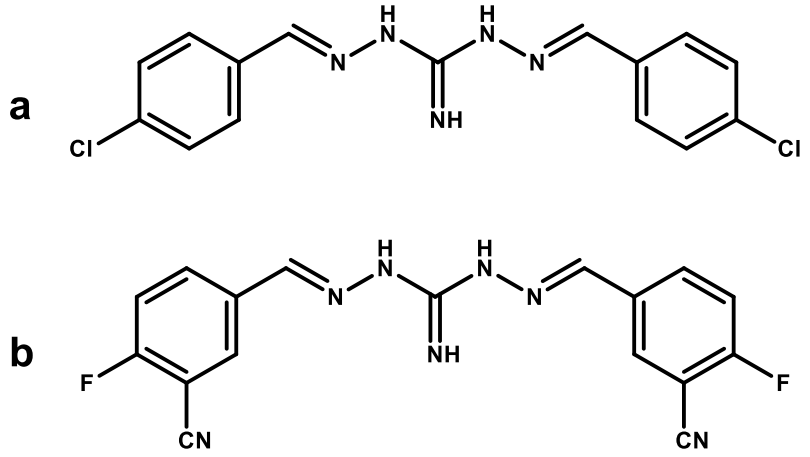

Figure 3-1: a: Robenidine; b: compound **1**.

Results and Discussion

The aminoguanidine robenidine is an effective antimalarial in vitro

To gain an initial assessment of robenidine as a potential antimalarial drug, it was evaluated *in vitro* for the ability to inhibit the growth of *P. falciparum* strain D6, a drug-sensitive strain. Blood stage parasite cultures were incubated in a range of concentrations of robenidine, and 72 hour parasite growth was measured by SYBR green staining relative to untreated controls (Smilkstein 2004). In this assessment, robenidine exhibited an average *in vitro* IC_{50} of 324 nM (Figure 3-2). This value represents an excellent starting point for further evaluation of structure activity relationships of robenidine analogs. Notably, the concentration-response curve was characterized by a steep slope at the IC_{50} inflection point, similar to the control drug chloroquine.

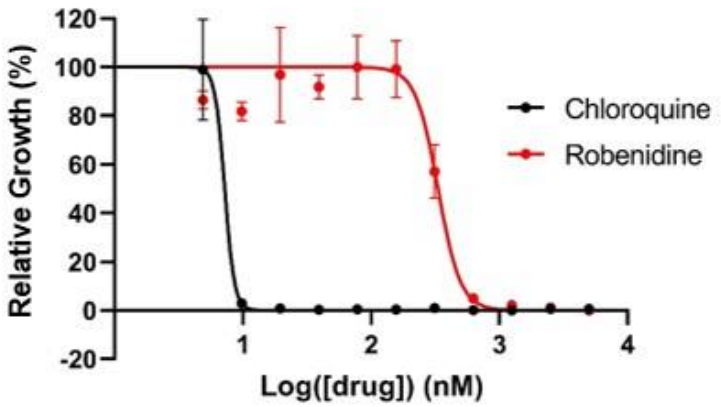

Figure 3-2: IC_{50} curve of robenidine in D6 compared with chloroquine. Y values represent fluorescence relative to untreated controls.

Synthesis of aminoguanidine robenidine analogs

Given the successful initial evaluation of robenidine *in vitro*, a series of 38 robenidine analogs were designed and synthesized to determine the potential for improved antimalarial activity within the aminoguanidine chemotype. Robenidine analogs were synthesized in a single step route starting from commercially-available substituted benzaldehydes or acetophenones with the synthetic approach utilized in robenidine's initial discovery (Kantor 1970). Two equivalents of each starting material were refluxed in ethanol with 1,3-diaminoguanidine hydrochloride (Scheme 1). The resulting symmetrical aryl aminoguanidine products (formed as HCl salts) were precipitated from solution using diethyl ether, filtered, and washed with diethyl ether. Compounds were purified by recrystallization from ethanol.

As evidenced by the continued commercial success of robenidine as a veterinary drug, this synthetic approach is highly amenable to affordable, large-scale synthesis, an important attribute given that any new antimalarial drug must be inexpensive for use in resource poor regions where the disease is endemic. It is noteworthy that the aminoguanidines can be prepared in a single step from commercially available starting materials, and no chromatographic

separations are required for their purification. This is a significant advantage over other antimalarial drug candidates requiring multiple steps and/or complex separations.

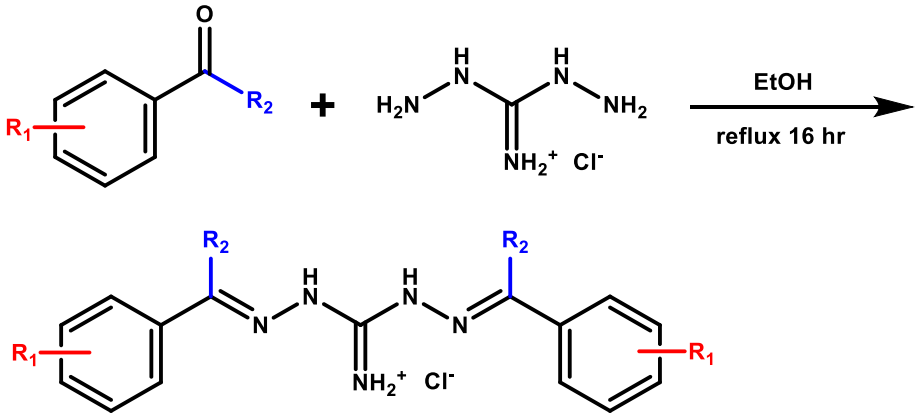

Scheme 3-1: A general synthesis of aminoguanidine robenidine analogs. Compounds were prepared by refluxing benzaldehydes or acetophenones with 1,3-diaminoguanidine hydrochloride in ethanol.

Structure activity relationships of aminoguanidines in vitro

The *in vitro* activity of each compound in the aminoguanidine library was assessed against asynchronous cultures of *Plasmodium falciparum* parasites replicating within human erythrocytes (Tables 3-1 - 3-3). As the chemical development of robenidine was not discussed in its original publication in 1970 (Kantor 1970) and limited structural information is available regarding its mechanism of action (Wong 1972), profiling was guided primarily by *in vitro* potency against the *P. falciparum* D6 strain cultured in human erythrocytes as described above.

Robenidine is structured as a diarylaminoguanidine with symmetrical 4-chloro (para relative to the aminoguanidine moiety) substituents on its two phenyl rings. Our SAR studies primarily focused on the potential to improve antimalarial activity by exchanging these 4-chloro substituents for different functional groups at the same position. All compounds are symmetrical

and take the form shown in Scheme 1 unless otherwise noted. A halogen series (Table 3-1) was prepared to examine the effects of both halide type and position on antiplasmodial activity. Within this series, chloro and bromo substituted aminoguanidines were more active than fluoro substituted compounds, with position effects varying among the halides. The ortho-fluoro compound **2** displayed much lower activity than robenidine, and the para-bromo compound **9** showed moderately improved activity.

Other replacement functional groups for robenidine's 4-chloro substituents were varied widely for size, lipophilicity, and electron withdrawing vs. donating effects on the adjacent phenyl ring. Compounds with promising activity were also prepared as their ortho and meta isomers to investigate positional effects for these functional groups. Similarly, promising compounds were prepared with additional methyl groups on the benzyl carbons of the aminoguanidine moieties as shown in Scheme 1 (the R_2 position) by starting from the analogous acetophenones rather than benzaldehydes.

The 4-methoxy robenidine derivative **11** was among the earliest compounds to show improved potency over robenidine. To further pursue this activity, the methyl (**10**), trifluoromethyl (**12**), trifluoromethoxy (**16**), and difluoromethoxy (**18**) derivatives were also prepared along with their R_2-methyl analogs (Table 3-2). Among these compounds **16** was the most potent, quickly becoming the frontrunner with a nearly ten-fold reduction in IC_{50} value (39 nM vs. D6) relative to robenidine (324 nM vs. D6). Conversion of the R_2 moiety from H to methyl did not have a consistent effect, improving activity for the trifluoromethyl derivative (**12** vs. **13**) while reducing activities of the trifluoromethoxy and difluoromethoxy derivatives (**16** vs **17** and **18** vs **19**, respectively). The ortho (**14**) and meta (**15**) variants of **16** were also prepared and demonstrated significantly reduced antimalarial activity in comparison with the para isomer.

The early success of **16** led to an interest in exploring other electron withdrawing groups at the para position. The nitro (**27**) and cyano (**22**) derivatives were significantly more active than robenidine. **22** in particular had activity in the same range as the early hit compound **16**, so the

ortho (**20**) and meta (**21**) analogs were prepared to explore the position effects of the nitrile group. This series was expected to show a similar pattern to the trifluoromethoxy compounds, and so it came as quite a surprise when the 3-CN analog **21** was found to have IC_{50} value of 7 nM, much lower than any other aminoguanidine evaluated up to that point. The R_2-methyl analog (**23**) of this compound was prepared and found to be less active than the R_2-H original.

A few general trends were observed for *in vitro* antimalarial activity. In general, substitution at the ortho position dramatically reduced antimalarial activity, possibly by sterically constraining rotation of the aryl rings. The carboxylic acid **29** and tetrazoles **34** and **35** were inactive against all tested *P. falciparum* strains. Electron withdrawing substituents appear to have a positive effect on antimalarial activity, though the biphenyl analog **26** is unusually potent and the dimethylamino (**28**) and propynoxy (**32**) compounds also exhibit respectable antiparasitic activity.

All aminoguanidines synthesized were also evaluated against three multi-drug resistant *P. falciparum* strains (Dd2, Tm90-C2B, and A6) and for mammalian cell cytotoxicity. Robenidine and the lead compounds **16**, **21**, and **22** were further evaluated *in vivo* to guide optimization resulting in the design of **1**, the overall series lead. The results of these experiments are listed in Tables 2-4 and discussed below.

Table 3-1: Aminoguanidine halogen series and antimalarial drugs[a]

Compound	R_1	R_2	cLog(P)	IC_{50} D6 (nM)	IC_{50} Dd2 (nM)	IC_{50} Tm90-C2B (nM)	IC_{50} A6 (nM)	IC_{50} Cytotoxicity (μM)	IVTI
2	2-F	H	2.40	2866	4593	>5000	1893	>200	>100
3	3-F	H	2.40	767	>5000	>5000	426	49	64
4	4-F	H	2.40	1016	3792	4904	369	24	24
5	2-Cl	H	3.54	334	961	1219	348	>200	>100
6	3-Cl	H	3.54	202	567	664	237	35	>100
Robenidine	4-Cl	H	3.54	324	814	1317	410	30	93
7	2-Br	H	3.84	280	715	974	876	94	>100

8	3-Br	H	3.84	572	1516	1838	502	62	>100
9	4-Br	H	3.84	277	876	899	269	38	>100
Atovaquone	N/A	N/A	4.88	<1	<1	>5000	>5000	72	>100
Chloroquine	N/A	N/A	5.06	10	70	297	16	181	>100

[a]See Scheme 1 for the aminoguanidine scaffold and sites of modification. *P. falciparum* IC_{50} values are the average of two to four determinations, each carried out in quadruplicate (a more granular view of this data is provided in the supporting information). D6, *P. falciparum* pan-sensitive strain; Dd2, multi-drug resistant *P. falciparum* strain; Tm90-C2B, multi-drug resistant *P. falciparum* clinical isolate that is also resistant to atovaquone; A6, *P. falciparum* in-house derived mutant line resistant to respiratory antagonists.[40] Cytotoxicity assays were carried out with human hepatoma derived HepG2 cells and performed in quadruplicate. IVTI = *In Vitro* Therapeutic Index, defined as cytotoxicity/D6 IC_{50}. N/A = not applicable.

Table 3-2: Aminoguanidine methyl, methoxy, fluoromethyl, fluoromethoxy, and nitrile series[a]

Compound	**R_1**	**R_2**	**cLog(P)**	**IC_{50} D6 (nM)**	**IC_{50} Dd2 (nM)**	**IC_{50} Tm90-C2B (nM)**	**IC_{50} A6 (nM)**	**IC_{50} Cytotoxicity (μM)**	**IVTI**
10	4-CH_3	H	3.11	905	2427	2529	>5000	43	48
11	4-OCH_3	H	1.95	263	1602	>5000	289	>200	>100
12	4-CF_3	H	3.88	614	1536	2742	567	40	65
13	4-CF_3	CH_3	5.39	211	414	451	283	114	>100
14	2-OCF_3	H	4.17	1080	2328	>5000	391	156	>100
15	3-OCF_3	H	4.17	670	1571	2988	689	61	91
16	4-OCF_3	H	4.17	39	83	114	52	11	>100
17	4-OCF_3	CH_3	5.68	140	526	458	182	9	64
18	4-$OCHF_2$	H	2.84	71	191	193	87	19	>100
19	4-$OCHF_2$	CH_3	4.36	99	403	315	171	3	30
20	2-CN	H	0.98	1024	2097	1990	969	31	30
21	3-CN	H	0.98	7	20	31	24	7	>100

22	4-CN	H	0.98	58	166	312	76	>200	>100
23	3-CN	CH_3	2.49	47	70	104	17	9	>100
1	3-CN, 4-F	H	1.27	4	12	16	14	8	>100

[a]See Table 3-1 legend and Experimental section.

Table 3-3: Other aminoguanidines[a]

Compound	R_1	R_2	cLog(P)	IC_{50} D6 (nM)	IC_{50} Dd2 (nM)	IC_{50} Tm90-C2B (nM)	IC_{50} A6 (nM)	IC_{50} Cytotoxicity (μM)	IVTI
24	H	H	2.11	705	4298	>5000	581	>200	>100
25	4-OH	H	0.78	143	240	286	278	39	>100
26	4-Ph	H	5.89	15	87	71	33	>200	>100
27	4-NO_2	H	1.60	96	198	247	85	>200	>100
28	4-NMe_2	H	2.44	118	264	213	122	20	>100
29	4-COOH	H	1.60	>5000	>5000	>5000	>5000	>200	N/A
30	4-$CONH_2$	H	1.60	527	405	727	516	42	80
31	4-SO_2NH_2	H	-1.56	>5000	>5000	>5000	>5000	>200	N/A
32	4-Propynoxy	H	2.79	102	199	376	153	>200	>100
33	4-Morpholino	H	1.03	131	329	295	116	>200	>100
34	3-Tetrazole	H	1.10	1645	>5000	>5000	4790	107	65
35	4-Tetrazole	H	1.10	838	>5000	>5000	>5000	>200	N/A
36	(2,2-DiFluoro) 2,3-Dioxazole	H	5.22	250	800	905	235	>200	>100
37	2,4-OMe, 5-Cl	CH_3	3.52	360	1247	1180	216	3	8
38	mono 2-F[b]	H	2.26	1028	2202	>5000	833	>200	>100

[a]See Table 3-1 legend and Experimental section.

[b]Compound **38** has a 2-Fluoro substituent at only one R_1 site. The other R_1 site is unsubstituted (4-H).

Aminoguanidines retain in vitro activity in drug-resistant strains of malaria

In addition to the drug-sensitive *P. falciparum* D6 strain, the aminoguanidines were assessed against three drug-resistant strains (Tables 2-4). *P. falciparum* Dd2 is a multidrug resistant strain sensitive to atovaquone but resistant to chloroquine as well as the antifolate combination of pyrimethamine + sulfadoxine. *P. falciparum* Tm90-C2B is a multidrug resistant clinical isolate including resistance to both atovaquone and chloroquine (Looareesuwan 1996). *P. falciparum* A6 is derived from D6 and is resistant to respiratory antagonists such as atovaquone and antimycin A but sensitive to chloroquine (Smilkstein 2008)

The degree of cross resistance observed for the MDR strains Dd2 and C2B with the tested aminoguanidine series ranged from extensive (e.g., ~19-fold for **11**), to intermediate (e.g., 6.5-fold for **3**), to modest (2-4-fold for **1** and **23**) relative to the drug sensitive D6 strain of *P. falciparum*. The general lack of significant cross-resistance is consistent with expectations given that robenidine and other aminoguanidines are not clinically prescribed for malaria or even administered directly to humans for any indication (it is possible that trace amounts of robenidine have passed into humans via the consumption of poultry treated for coccidiosis, though these trace amounts are unlikely to drive antimalarial resistance).

Aminoguanidines have high in vitro therapeutic indices

The aminoguanidines were evaluated for cytotoxicity against human hepatoma derived HepG2 cells (Tables 2-4). In this assay, HepG2 cells were incubated with test compounds for 24 hours, followed by a 24-hour recovery period and subsequent staining to evaluate for cytotoxic effects with resazurin. The ratio of the resulting HepG2 IC_{50} value to the *P. falciparum* D6 IC_{50} value can be considered an '*in vitro* therapeutic index,' or IVTI.

Cytotoxicity in Hep2G did not track proportionally with antimalarial activity in any of the four tested *P. falciparum* strains. Overall, substitution at the 3 (meta) position resulted in increased cytotoxicity relative to the 2 (ortho) and 4 (para) positions, though the cyano substituent was

shown to be an exception to this trend. Several of the aminoguanidines, including the active compound **21**, had no measurable effect on Hep2G activity at concentrations as high as 200 μM. Most aminoguanidines in the series had HepG2 IC_{50} values above 10 μM, and nearly all active aminoguanidines had an *in vitro* therapeutic index of over 1000-fold (this value cannot be calculated for those aminoguanidines having no antimalarial activity). It is noteworthy that **1**, with the greatest antiplasmodial activity among compounds in this series, exhibits an IVTI value of 2,000 which is indicative of its highly selective antiparasitic action.

Aminoguanidines do not show Atovaquone synergy observed with linear biguanides

One of the features of the aminoguanidines that initially captured our interest was their structural resemblance to the biguanide antimalarial drug proguanil (Figure 1-5e). When dosed *in vivo*, proguanil undergoes a cyclization reaction to form cycloguanil, a metabolite responsible for its reported mechanism of action as a DHFR inhibitor (Figure 3-3) (Carrington 1951, Shearer 2005). However, it appears that proguanil may exhibit antimalarial activity by a separate and unknown mechanism when in its original linear form. Further, this linear-form activity is synergistic with the anti-respiratory drug atovaquone (Figure 1-5f) (Srivastava 1999). Notably, atovaquone and proguanil are co-administered as a malaria prophylactic with the commercial name Malarone (Looareesuwan 1996).

Our group has explored this synergistic activity with several analogs of proguanil lacking the ability to cyclize. This activity is achieved by replacing the isopropyl moiety with a tert butyl moiety. One especially active linear biguanide is the compound LT-31 (Figure 3-3), which has an aryl trifluoromethyl group in place of proguanil's chlorine.

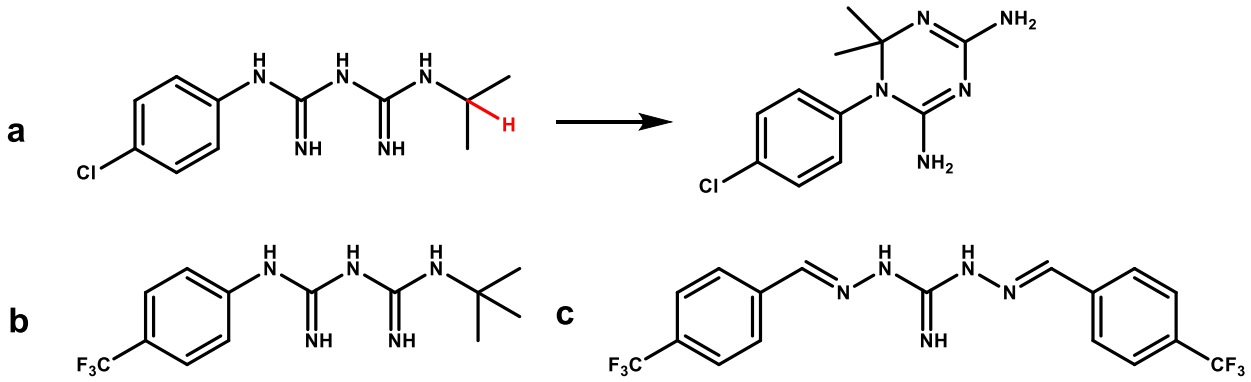

Figure 3-3: a: proguanil is converted to cycloguanil *in vivo* by a mechanism involving the abstraction of the proton shown in red, b: LT-31 cannot cyclize by the same mechanism because a tert-butyl group is used in place of proguanil's isopropyl group, c: the aminoguanidine **13** is structurally similar to LT-31.

The synergistic effect between the linear biguanides and atovaquone can be demonstrated using the A6 *Plasmodium falciparum* strain, which is resistant to atovaquone and the biguanides on their own. Atovaquone has an IC_{50} of <1 nM in the drug sensitive D6 strain but is inactive at concentrations greater than 5 μM in the resistant A6 clone (Table 3-4). Similarly, LT-31 has an IC_{50} of 95 nM in D6, but 1345 nM in A6 (Figure 3-4, Table 3-4). The activity of atovaquone and LT-31 can be restored in A6 if they are administered in combination. With a fixed atovaquone concentration as low as 10 nM, the A6 IC_{50} of LT-31 shifts from 1345 nM to 20 nM, even lower than its D6 IC_{50} of 95 nM.

The same comparison (IC_{50} in D6 vs. A6 vs. A6 with atovaquone) was evaluated for the aminoguanidines **13** and **16**. Like LT-31, **13** has a trifluoromethyl group para to its nitrogenous core (Figure 3-4, **16** has a trifluoromethoxy rather than a trifluoromethyl substituent).

The aminoguanidines did not show the same atovaquone synergy observed for linear biguanides like LT-31 and proguanil. The A6 IC_{50}s for compounds **13** and **16** were somewhat higher than their D6 IC_{50}s (Table 3-4), though there is much less resistance for these compounds

than for the biguanides and atovaquone in this strain. The addition of 10 nM atovaquone moderately shifted the IC_{50} for **13** and had no effect on the activity of **16**. These findings indicate distinct mechanisms of action for the linear biguanides and the aminoguanidines.

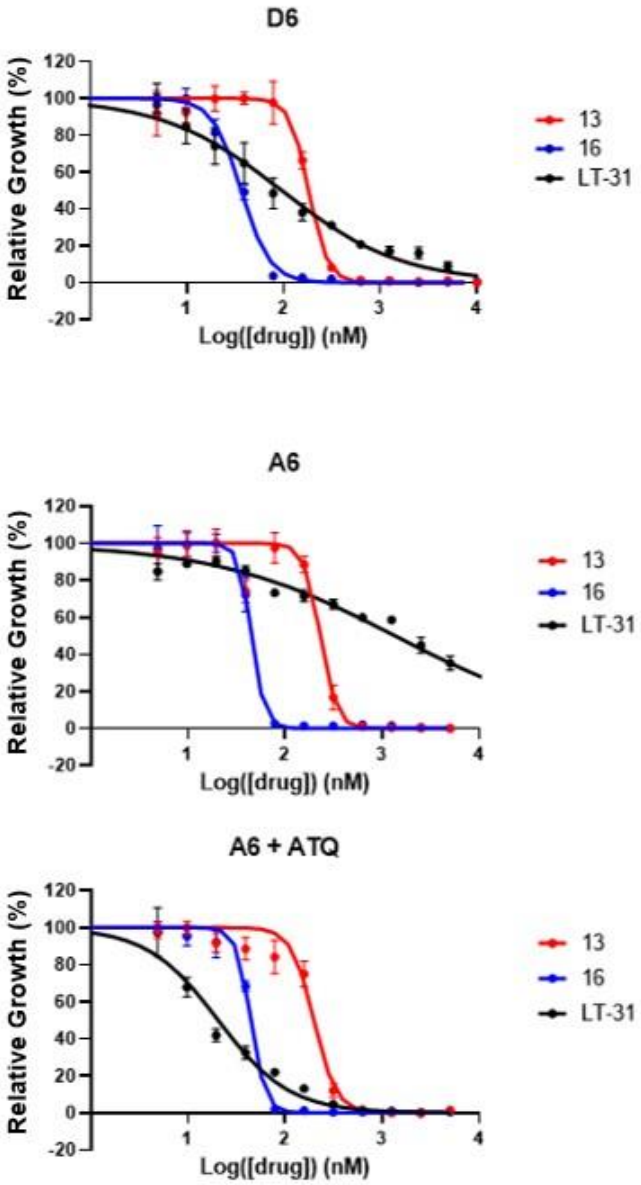

Figure 3-4: The concentration-response curve of the linear biguanide LT-31 shifts significantly from the drug-sensitive D6 *P. falciparum* strain to the drug-resistant A6 strain. Activity is restored

in A6 with the addition of 10 nM atovaquone (ATQ). Conversely, the concentration-response curves of the aminoguanidines **13** and **16** do not shift significantly between the three test conditions.

Table 3-4: Atovaquone synergy of aminoguanidines and the linear biguanide LT-31

Compound	IC_{50} D6 (nM)	IC_{50} A6 (nM)	IC_{50} A6 + ATQ (nM)
13	182	230	192
16	36	45	44
LT-31	95	1345	20
Atovaquone	<1	>5000	-

Aminoguanidine activity is concentration dependent but not time dependent

Many drugs have activity dependent on their exposure time in addition to concentration, and antimalarial potency is frequently stage-specific. To determine whether the aminoguanidines acted by a time-dependent mechanism against malaria parasites, the SYBR Green activity assay was adapted to include additional incubation intervals. Two potent aminoguanidines, **16** and **21**, were incubated with *P. falciparum* Dd2 infected erythrocytes for 48, 72, or 96 hours (Figure 3-5). Notably, this assay measures drug-treated parasite growth during the incubation time relative to untreated parasites. A shorter incubation time allows for less parasite growth for all drug conditions, producing data with proportionally greater variability or 'noise.' Conversely, longer incubation times reduce noise in the resulting data.

IC_{50} values for both **16** and **21** were somewhat higher at 48 hours than at longer drug incubation times (Table 3-5), though this may be the result of noise in the data associated with the short incubation time. This finding may also stem from the use of asynchronous parasite cultures, wherein one life-cycle stage may be more impacted than another (**16** in particular

appears to exhibit a biphasic concentration-response curve, indicative of stage specificity). IC_{50} values for both compounds were virtually identical between 72-hour and 96-hour incubation time points. These results indicate that a 72-hour incubation may be required to attain full *in vitro* activity, but that no additional benefit is construed with longer incubation times. Aminoguanidine activity appears to be driven primarily by drug concentration rather than by lengthening drug incubation time. Additional experiments are planned to explore for possible stage-specific activity of the most active compounds in this series however our results combine to suggest that the molecules are not acting in a manner consistent with a "delayed death" phenotype as shown for other drugs such as doxycycline and azithromycin (Dahl 2007).

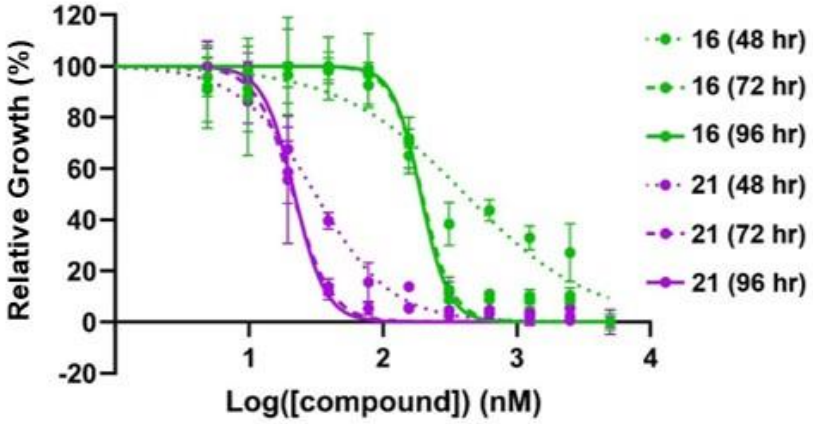

Figure 3-5: Inhibition of *P. falciparum* Dd2 growth by 16 (green) and 21 (purple) at 48 hr (dotted curves), 72 hr (dashed curves), and 96 hr (solid curves) time points.

Table 3-5: *Pf* Dd2 IC_{50} of 16 and 21 vs drug incubation length[a]

Compound	IC_{50} Dd2 (nM)		
	48 hr	72 hr	96 hr
16	410	195	192
21	31	21	22

[a]See Table 3-1 legend and Experimental section.

Lead aminoguanidines have high in vivo efficacy in a mouse model of malaria

Aminoguanidines exhibiting high *in vitro* antimalarial potency and robenidine were assessed for *in vivo* efficacy in a murine model of malaria (*Plasmodium yoelii*, Table 3-6). In this modified 4-day Peters test (Peters 2002), mice were inoculated with parasites from a donor mouse (day 0), and then dosed orally with drugs on each of the subsequent four days (days 1-4). On day 5 of the experiment, the parasitemia for each mouse was determined microscopically by examining methanol-fixed and Giemsa-stained blood smears. The ED_{50} represents the interpolated dose of a compound at which parasitemia was suppressed to one half that of untreated controls. Similarly, the ED_{90} represents the dose at which parasitemia is suppressed ten-fold. Mice were considered cured of their infection if no parasites were detected in the blood 30 days from the first drug administration, and the non-recrudescence dose (NRD) represents the lowest dose to achieve a cure.

Robenidine, **16**, **22**, and **21** were evaluated for *in vivo* antimalarial efficacy. That robenidine exhibited respectable in vivo antimalarial activity was somewhat surprising given that it is poorly absorbed and known to accumulate in the gastrointestinal tract (Zulalian 1973). The early hit compound **16** (the 4-OCF_3 analog, ED_{50} 1.2 mg/kg/day) showed improved *in vivo* activity over robenidine (ED_{50} = 1.6 mg/kg/day), while **22** (the 4-CN analog, ED_{50} = 2.7 mg/kg/day) did not. Unexpectedly, **21** (the 3-CN analog, ED_{50} = 7.1 mg/kg/day) was six-fold less efficacious than **16** *in vivo*, despite being six-fold more active than **16** *in vitro*. For comparative purposes consider that the ED_{50} of chloroquine in this system is 1.5 mg/kg/day (Pou 2012).

The only aminoguanidine which produced a cure in this model was **16** with NRD of 12.5 mg/kg/day, while other compounds were not curative (including compound **1** described below). It is important to note that failure to produce a cure in this model and by this dosing regimen is not predictive of clinical failure. Indeed, several approved clinical drugs such as chloroquine are not curative in this model at any dose level.

Table 3-6: *in vivo* ED_{50} and ED_{90} of lead aminoguanidines[a]

Compound	*P. yoelii* ED_{50} (mg/kg/day)	*P. yoelii* ED_{90} (mg/kg/day)	*P. yoelii* NRD (mg/kg/day)
Robenidine	1.6	4.9	>25
16	1.2	3.7	12.5
22	2.7	7.7	>25
21	7.1	9.4	>25
1	0.25	0.28	>25

[a]In vivo activity values were determined from a modified 4-day Peters test. Compounds were administered by oral gavage up to 25 mg.kg/day, near the solubility limit of the PEG delivery vehicle. NRD = non-recrudescence dose (cure dose). Compounds were tested up to 25 mg/kg/day, and no acute toxicity was observed in the animals.

1 *is a highly potent antimalarial in vitro and in vivo*

The discrepancy between the *in vitro* success (Table 3-2) and *in vivo* mediocrity (Table 3-6) of **21** remained a mystery which we later explored. From previous *in vivo* SAR studies on other scaffolds, we had noted that aryl groups without protective substitutions at the para positions were metabolically unstable. While **16** was substituted at the para position, **21** was not, potentially leaving this position vulnerable to hepatic microsomal degradation.

To interrogate this hypothesis, an analog of **21** was prepared with an additional para-fluoro substituent (**1**, 3-CN, 4-F). Given the low activity of **4** (4-F), this substitution was expected to have little effect on *in vitro* potency while potentially improving upon the *in vivo* activity of **21**. Unexpectedly, **1** had excellent *in vitro* activity, becoming the new series lead in potency. **1** had a single-digit nanomolar IC_{50} value against D6 (4 nM), IC_{50} values in the low double digits for the drug resistant strains, and an *in vitro* therapeutic index of 2000-fold.

The *in vivo* efficacy of **1** was even more pronounced with an ED_{50} value of 0.25 mg/kg/day, fivefold lower than its nearest competitor **16**. The single atom difference between **21** (3-CN, 4-H) and **1** (3-CN, 4-F) resulted in a nearly 30-fold improvement in *in vivo* efficacy.

Murine microsomal stability of aminoguanidines correlates with in vivo activity

To investigate the relationship between the aminoguanidines' *in vivo* efficacy and their metabolic properties, the murine microsomal stability of a selection of aminoguanidines was evaluated (Table 3-7). Robenidine, **16**, **21**, **1**, and the control compound ketanserin were incubated with pooled murine liver microsomes and monitored for degradation by LC/MS/MS for one hour. The concentration vs. time plot for each compound was used to determine its biological half-life ($t_{1/2}$) and predicted intrinsic clearance (Cl_{int}).

For all of the aminoguanidines evaluated, murine microsomal stability correlated with *in vivo* efficacy. Robenidine, **16**, and **1** were all biologically stable with half-lives above 150 min (with the same rank order for *in vivo* activity and stability). **21** was metabolically unstable in the presence of murine microsomes, with a half-life of only 58.18 min.

This data supports the notion that **1** is more efficacious *in vivo* than **21** due in part to improved stability. Substituting the 4-position H for F resulted in a three-fold increase in metabolic stability. Presumably the prolonged presence of **1** in the bloodstream contributes to its excellent performance *in vivo*.

Table 3-7: Murine Microsomal Stability of Aminoguanidines[a]

Compound	Murine Microsomal Stability, $t_{1/2}$ (min)	Predicted Cl_{int} (mL/min/kg)
Ketanserin	14.47	377.20
Robenidine	158.65	34.40
16	172.16	31.70

21	58.18	93.80
1	186.15	29.32

[a]Data from ChemPartner Co. Ltd, Shanghai, P.R. China. See Experimental section for full details.

Conclusion

1 is a robenidine derivative with excellent *in vitro* potency, virtually no cross-resistance in multi-drug resistant strains, and a high *in vitro* therapeutic index. In a murine model of malaria, **1** displayed robust *in vivo* antimalarial activity propelled by a combination of high intrinsic potency and biological stability. Although speculative at this time it also possible that the nitrogen atoms in the aminoguanidine bridge of 1 exhibit diminished basicity (i.e., ionizeabilty) due to the presence of two strongly electron withdrawing groups (F and CN) at the para and meta positions of the flanking aromatic rings which may in turn enhance oral bioavailability.

Further exploration of the aminoguanidine scaffold is certainly warranted, as is developing more knowledge of its antimalarial properties including the mode of action. Assessing the *in vivo* activity of these compounds in humanized mice may refine predictions of clinical success. Assessing the compounds against synchronous parasites will elucidate potential stage-specific potency effects. Beyond the blood stage, evaluating the aminoguanidines against other stages of the malaria life cycle such as the liver stage will provide valuable information useful for their potential development for use in humans. Systematically exploring the mechanism of action including chemical biology techniques and resistance studies can further guide SAR for this chemotype, and we are currently engaged in this work. Potential synergy with other antimalarial compounds such as artemisinin, atovaquone, and ELQ-300 will also be assessed.

As we look for new entries in the antimalarial pipeline, it may be useful to reexamine drugs and chemotypes effective in related parasites and pathogens. This appears to be the case with robenidine, a drug discovered in 1970 but which has not been methodically explored in malaria using a medicinal chemistry approach until this point. Though robenidine itself has reasonably good antimalarial activity *in vitro* and *in vivo*, it did not take long to improve upon this activity in both settings. In this study, a second look at an old drug efficiently produced a new and promising chemical lead.

Chapter 4 : Structure Activity Relationships and Drug Action of the Aminoguanidines in Malaria

In vivo efficacy experiments were performed by Dr. Yuexin Li. Metabolic stability experiments and pharmacokinetics experiments were performed by Chem Partner (Shanghai, China). All other experiments were performed by the author.

Introduction

With the highly potent and effective compound **1** in hand, several questions remained regarding its potential as an antimalarial drug. A series of experiments was carried out to further explore the antimalarial activity of the aminoguanidine chemotype, including microscopic observation of parasites treated with **1**, testing of aminoguanidines against specific stages within the erythrocytic cycle, and evaluating potential synergy between **1** and other antimalarial compounds. A full pharmacokinetic profile of **1** was also obtained.

Several series of novel aminoguanidines were also prepared. First, major modifications to the generic aminoguanidine structure were performed to test the limits of its antimalarial activity and to identify key structural elements. Second, a series of bicyclic and heterocyclic aminoguanidines was created to explore the unanticipated success of the biphenyl aminoguanidine **26**. Third, a series of targeted compounds designed to understand and improve upon the positive attributes of **1** and **16** was prepared including an asymmetrical hybrid of the two

compounds. Fourth, a small set of chemical probe compounds was designed to further investigate the aminoguanidine mechanism of action. Fifth, alternative salts and free bases of selected aminoguanidines were formed.

Compounds showing promising *in vitro* activity via the SYBR Green fluorescence assay described in the previous chapter were further evaluated *in vivo* using a 4-day Peters test (Peters 2004, see previous chapter). Selected aminoguanidines were also assessed for metabolic stability. Finally, an initial validation experiment for the multifunctional probe compound **86** was performed.

Results and Discussion

*Visual Appearance of Plasmodium Parasites Treated with Compound **1***

A blood-stage culture of *P. falciparum* Tm90-C2B parasites was treated with 400 nM **1** for 24 hr, then visualized under a light microscope after staining drug-treated parasites with Giemsa. There were no obvious phenotypic differences between treated (Figure 4-1b) and untreated (Figure 4-1a) parasites within erythrocytes, however a significant quantity of lysed parasite material was present outside of the erythrocytes, demonstrating the lethal effect of **1**. It is possible that the morphological effects of aminoguanidine action only become apparent after exposure for longer periods, e.g., 48 to 72 hours.

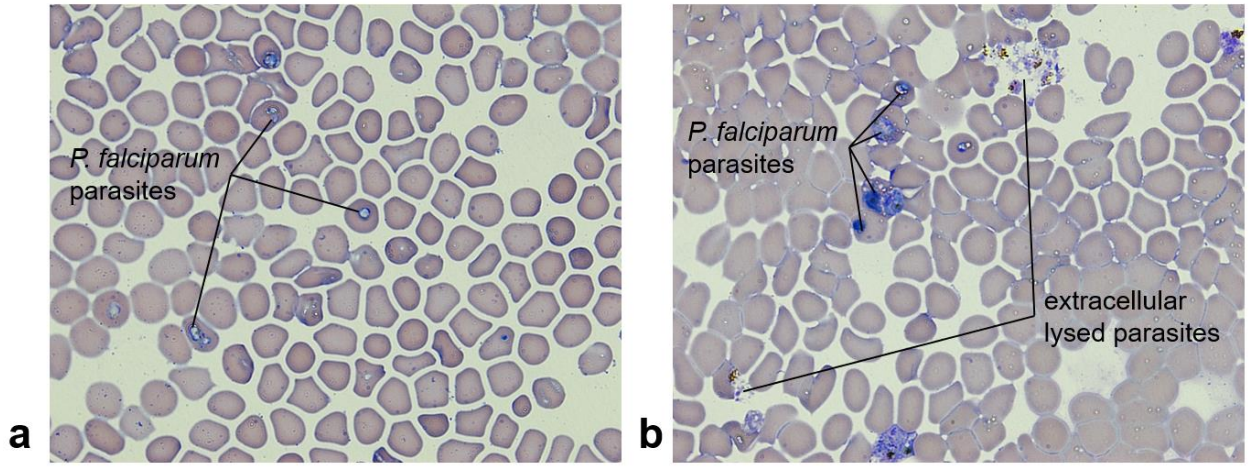

Figure 4-1: Light microscope images of Geimsa-stained blood smears of *P. falciparum* Tm90-C2B-infected erythrocytes; a: untreated parasites; b: parasites incubated for 24 hr with 400 nM **1**.

*Synergy of Compound **1** with Commercial Antimalarial Drugs*

To evade the onset of clinical resistance, antimalarial drugs are nearly always prescribed as combination therapies such as atovaquone-proguanil (also called Malarone) and sulfadoxine-pyrimethamine (also called Fansidar). One indicator of success as a drug combination is *in vitro* synergistic activity, in which the *in vitro* activity of a combination of compounds is greater than either compound on its own. Any given pair of compounds can be synergistic (the combination is greater than the sum of its parts), antagonistic (the combination is worse than the sum of its parts), or indifferent (the combination is the same as the sum of its parts) with one another.

To assess potential partner drugs for **1**, *in vitro* synergy was measured using the fixed-ratio isobologram method (Fivelman 2004). Briefly, **1** was combined with atovaquone (ATQ), chloroquine (CQ), or ELQ-300 in the following ratios: 0:5, 1:4, 2:3, 3:2, 4:1, and 5:0. IC_{50}s for each combination were determined in *P. falciparum* Tm90-C2B parasites using the SYBR Green assay described in Chapter 3. Changes in the IC_{50} of each compound in the presence of the partner compound were quantified as fractional inhibitory concentrations (FICs) as described by

Fivelman et al. (note that FICs are unitless ratios of concentrations). FICs for **1** were plotted against those of each partner drug to form isobolograms (Figure 4-2).

An isobologram that forms a straight line indicates partner drugs that interact in an indifferent manner, whereas an isobologram that forms a concave curve indicates synergy and a convex curve indicates antagonism. Correspondingly, a mean FIC for all combination ratios close to 1 indicates indifference, mean FIC less than 1 indicates synergy, and mean FIC greater than 1 indicates antagonism.

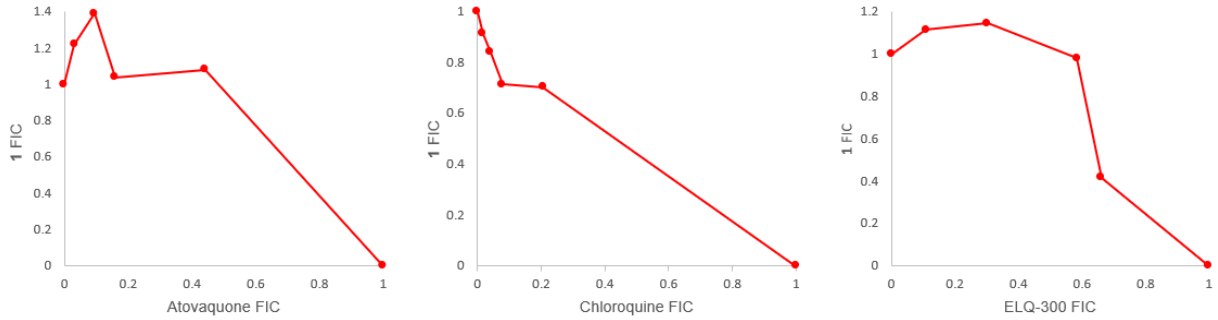

Figure 4-2: Isobolograms measuring the synergy of **1** with Atovaquone (left), Chloroquine (center), and ELQ-300 (right) in *P. falciparum* Tm90-C2B.

The isobolograms of **1**-atovaquone and **1**-ELQ-300 combinations were somewhat convex and mean FICs were 1.37 and 1.33 respectively (Figure 4-2, Table 4-1). These values are still fairly close to 1, indicating indifference tending toward antagonism. Notably, atovaquone and ELQ-300 both target *P. falciparum* cytochrome bc_1, though they do so at distinct binding sites (Stickles 2015). Conversely, the combination **1**-chloroquine had a slightly concave isobologram and mean FIC of 0.88, indicating indifference tending toward synergy. As a reference point, the strong synergy between atovaquone and proguanil has an FIC reported as 0.29 in strain T996 and 0.17 in strain K1 (Fivelman 2004).

Table 4-1: Mean FICs of **1** combined with Atovaquone, Chloroquine, or ELQ-300

Compound Combination	Mean FIC
1 + Atovaquone	1.37
1 + Chloroquine	0.88
1 + ELQ-300	1.33

Taken together, these data support the choice of chloroquine, or a novel 4-aminoquinoline, as a partner drug for **1** over either atovaquone or ELQ-300, though the mild antagonism that the latter drugs exhibit is not sufficient to preclude them from consideration. Other factors, such as compatible biological half-lives and drug-drug interactions must also be taken into account when preparing a drug combination therapy.

Aminoguanidines in Synchronous Blood Stage Parasites

P. falciparum parasites undergo a series of physical changes during the erythrocytic cycle as they transform from the ring stage to the trophozoite stage to schizonts containing the next generation of erythrocyte-invading merozoites. The physical differences between these life-cycle stages may coincide with varied susceptibility to antimalarial compounds.

The *in vitro* potency of the aminoguanidines was generally assessed in asynchronous parasite cultures. To evaluate potential stage-specificity of the aminoguanidines, cultures of *P. falciparum* D6 and Dd2 were synchronized by repeated treatments with sorbitol as described by Lambros (Lambros 1979). Parasites synchronized to either the ring stage or trophozoite stage were treated with **1**, **16**, atovaquone, or chloroquine and IC_{50}s were determined using the previously described SYBR Green assay (Figure 4-3).

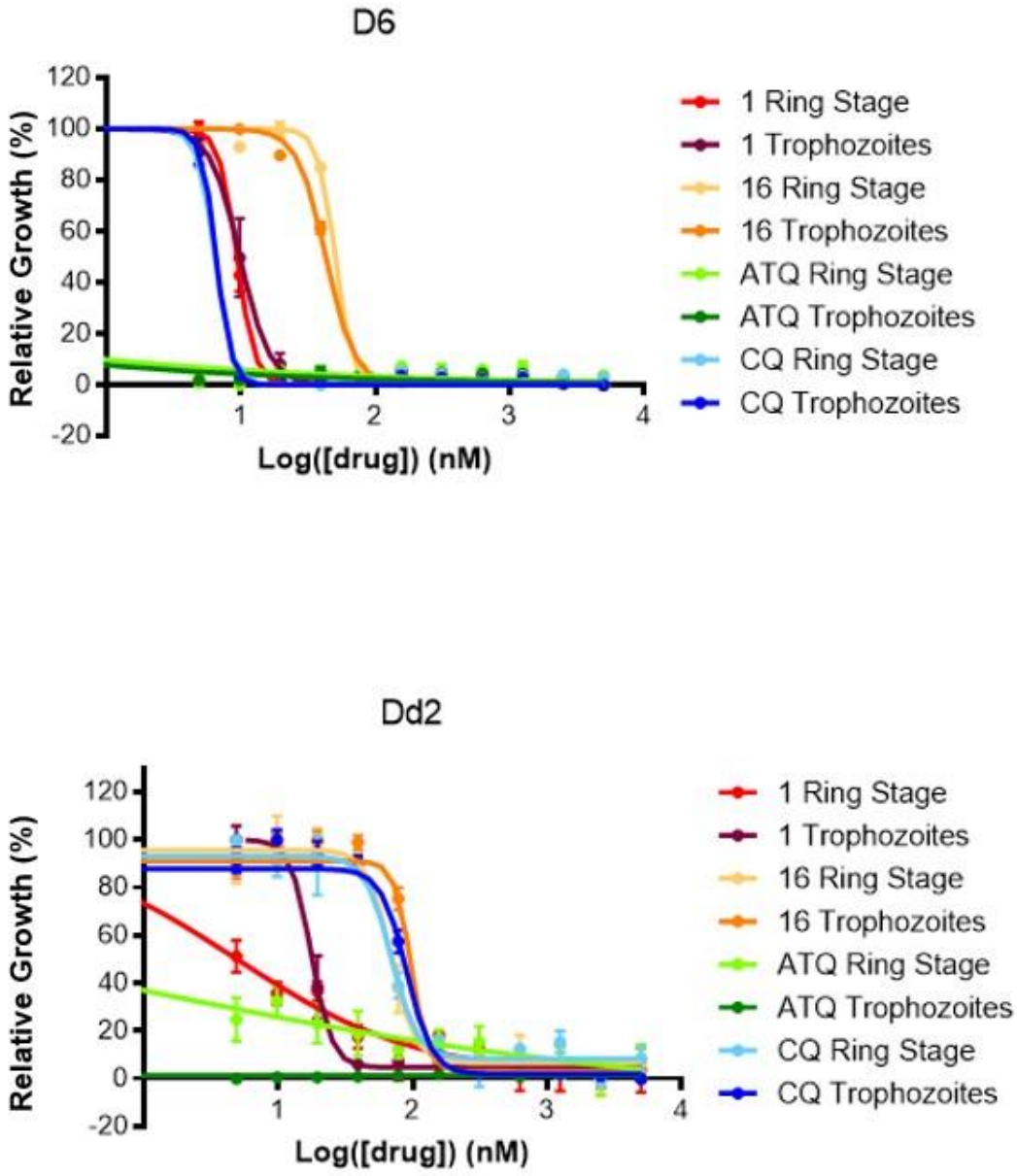

Figure 4-3: IC_{50} curves of **1**, **16**, atovaquone (ATQ), and chloroquine (CQ) in parasites synchronized to the ring stage or the trophozoite stage. *P. falciparum* D6 (top) parasites are drug sensitive, while Dd2 parasites are chloroquine resistant but atovaquone sensitive.

There were no significant differences between activity against ring stage parasites and trophozoites in the sensitive *P. falciparum* D6 strain for any of the four tested compounds (Figure 4-3, Table 4-2). Compound **1** was moderately more active against ring stage parasites than

trophozoites in the drug resistant strain *P. falciparum* Dd2. Chloroquine and **16** were slightly more active against ring stage Dd2 parasites. Atovaquone appeared slightly less active in ring stage Dd2 than in Dd2 trophozoites, though both IC_{50}s fell below the tested range of concentrations. These minor activity differences between stages may explain some of the variability between trials of the aminoguanidine IC_{50} assays, as the population of parasites in asynchronous culture is often skewed towards one life cycle stage over another.

Table 4-2: IC_{50}s of **1**, **16**, atovaquone, and chloroquine in synchronous parasites.

Compound	D6 IC_{50} (nM) Ring Stage	D6 IC_{50} (nM) Trophozoite	Dd2 IC_{50} (nM) Ring Stage	Dd2 IC_{50} (nM) Trophozoite
1	9	10	5	18
16	50	43	69	97
Atovaquone	<4	<4	<4	<4
Chloroquine	6	7	69	90

*Pharmacokinetics of Compound **1***

To succeed as a clinical therapeutic, a drug must have viable pharmacokinetics *in vivo* in addition to potency. A pharmacokinetics profile was compiled by Chem Partner (Shanghai China) for **1**. To complete this profile, two pharmacokinetics experiments were performed. In the first, male CD1 mice were dosed IV with 1 mg/kg **1** in carbonate buffer and plasma concentration was monitored until **1** was no longer detectable (Table 4-3). The second experiment was performed similarly but with an oral dose of 10 mg/kg **1** in PEG-400. Oral bioavailability (%F) of **1** was determined by dividing the area under the plasma concentration curve (AUC, Figure 4-4) of the oral experiment by that of the IV experiment (scaled up by a factor of 10 to account for the different doses). Clearance (CL), steady state volume of distribution (V_{ss}), half life ($t_{1/2}$), mean residence time (MRT), oral maximum concentration (C_{max}), and time at oral maximum concentration (T_{max}) were also calculated (Table 4-4).

Table 4-3: Plasma concentration of IV and oral **1** over time in CD1 mice

Sample Time (hr)	Plasma Concentration 1 mg/kg IV Compound 1 (ng/mL)	Plasma Concentration 10 mg/kg Oral Compound 1 (ng/mL)
Pre-dose	BQL[a]	BQL
0.083	547	3.09
0.25	423	26.5
0.5	267	47.1
1	116	61.8
2	47.5	60.2
4	18.7	56.3
8	4.74	50.7
24	BQL	2.51

[a] BQL = Below Quantification Limit

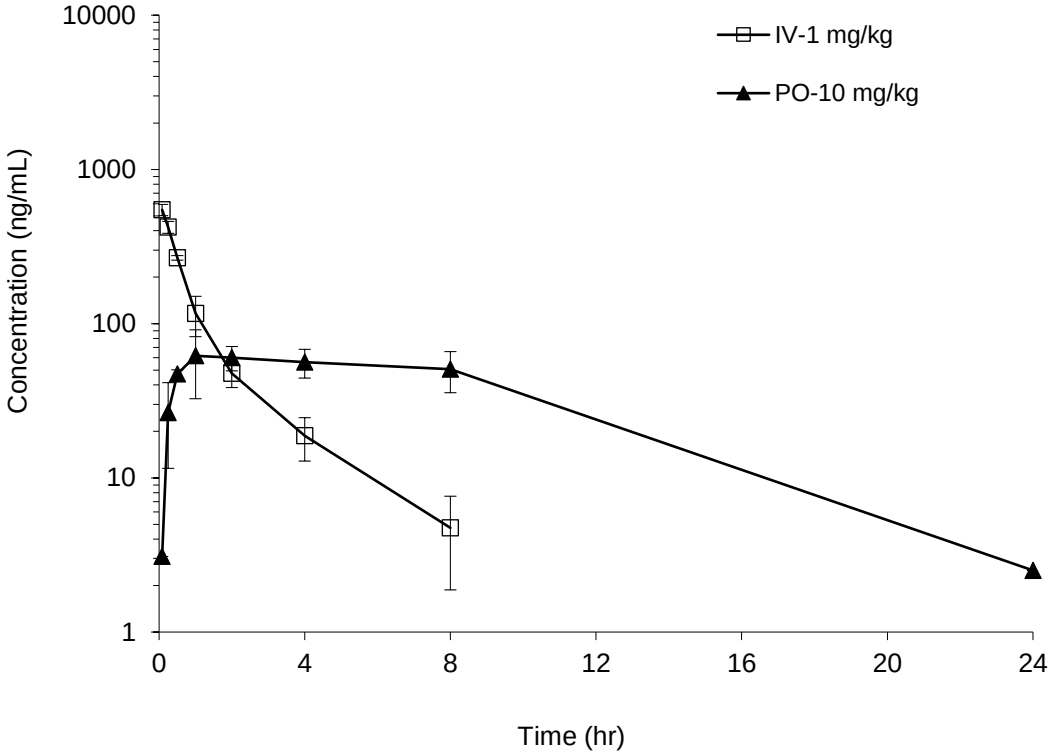

Figure 4-4: Plasma concentration-time curves for oral and IV **1**.

In the IV experiment, **1** showed a moderate clearance (32.1 mL/min/kg) and moderate volume of distribution (2.75 L/kg). In the oral experiment, the maximum plasma concentration (61.8 ng/mL or 176 nM) was reached at 1 hr after dosing. In both experiments, **1** exhibited relatively short biological half-lives (1.83 hr for IV administration and 4.21 hr for oral administration) and correspondingly moderate residence times (1.43 hr IV and 6.78 hr oral). These values are unsurprising given the relatively moderate murine microsomal stability reported in the previous chapter.

Table 4-4: Pharmacokinetic parameters of **1**.

PK Parameter	1 mg/kg IV Compound 1	10 mg/kg Oral Compound 1
CL (L/hr/kg)	1.93	N/A
CL (mL/min/kg)	32.1	N/A
V_{ss} (L/kg)	2.75	N/A
Regression Points (hr)	2~8	4~24
$T_{1/2}$ (hr)	1.83	4.21
AUC_{last} (hr*ng/L)[a]	507	856
AUC_{INF} (hr*ng/L)[b]	519	872
MRT_{last} (hr)[a]	1.20	6.37
MRT_{INF} (hr)[b]	1.43	6.78
T_{max} (hr)	N/A	1.00
C_{max} (ng/mL)	N/A	61.8
F (%)	N/A	16.8

[a]AUC_{last} indicates the area under the plasma concentration curve calculated from the last detected data point. MRT_{last} indicates the mean residence time calculated from AUC_{last}.

[b]AUC_{INF} indicates the area under the curve extrapolated to infinite time. MRT_{INF} indicates the mean residence time calculated from AUC_{INF}.

Somewhat unexpectedly given its *in vivo* efficacy and stability, the oral bioavailability of **1** was low (16.8%). While the biological half-life was moderate in the murine system, oral dosing in PEG-400 failed to deliver high plasma concentrations of **1**. This data on its own does not counter indicate **1** as a promising antimalarial, but more work will need to be done to find a more viable oral formulation. Promisingly, in later *in vivo* efficacy experiments SEDDS formulation was found to be a more suitable oral vehicle for the aminoguanidines than PEG-400. If other vehicles fail to improve oral bioavailability, there are other strategies that can be employed, including the use of prodrugs, alternate administration routes, and the use of formulation technology such as spray dried dispersion or particle size reduction. These techniques are discussed in greater detail in chapter 5 as they relate to another class of antimalarials, the endochin-like quinolones. Efforts to improve the metabolic stability of aminoguanidines are discussed below.

Major Modifications to the Aminoguanidine Structure

In the study described in the previous chapter, a series of aminoguanidine analogs of Robenidine was prepared by the general synthesis in Scheme 4-1. The previously prepared structures were nearly all symmetrical, singly substituted phenyl aminoguanidines, with R_2 as either a proton or methyl group and R_3 as an immine nitrogen. With some exceptions, these molecules had moderate to potent antimalarial activity *in vitro*. To find the structural limitations of this antimalarial activity, a series of compounds was prepared with more substantial deviations from this generic structure.

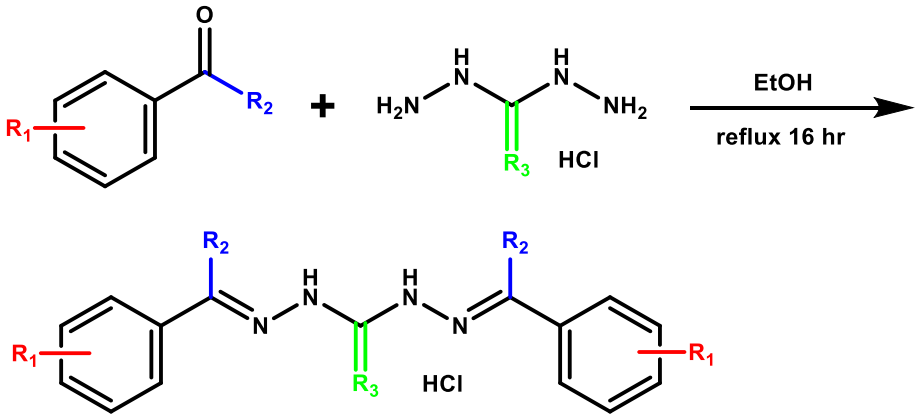

Scheme 4-1: General synthesis of aminoguanidines, carbohydrazides, and thiocarbohydrazides.

First, the role of the central immine nitrogen in the aminoguanidine core was analyzed. The five most potent aminoguanidines from the previous series had R_2 = H and included the following substitutions at R_1: 4-OCF_3, 3-CN, 4-CN, 4-Ph, and the disubstituted compound **1** with 4-F and 3-CN. A series of analogs of these compounds was prepared with either oxygen or sulfur at R_3, changing the central aminoguanidine core to either a carbohydrazide core or a thiocarbohydrazide core, respectively. The same synthetic conditions were employed, substituting carbohydrazide or thiocarbohydrazide for 1,3-diaminoguanidine to form these altered products. All compounds in this series were obtained with high purity, with varying yields which closely resembled those of their aminoguanidine analogs.

Table 4-5: *in vitro* activity of carbohydrazides, thiocarbohydrazides, and other modified aminoguanidines.

Compound	R_1	R_2	R_3	cLog(P)	IC_{50} D6 (nM)	IC_{50} Dd2 (nM)	IC_{50} Tm90-C2B (nM)	IC_{50} Cytotoxicity (μM)
39	4-OCF_3	H	O	6.65	>5000	>5000	>5000	>200
40	4-OCF_3	H	S	7.07	>5000	>5000	>5000	>200
41	3-CN	H	O	3.46	3724	4806	>5000	>200
42	3-CN	H	S	3.88	394	1429	1087	>200
43	4-CN	H	O	3.46	>5000	>5000	4179	>200

44	4-CN	H	S	3.88	2781	4283	4195	>200
45	4-Ph	H	O	8.37	4259	4463	3146	>200
46	4-Ph	H	S	8.79	2009	2747	1846	>200
47	3-CN, 4-F	H	O	3.74	>5000	>5000	>5000	>200
48	3-CN, 4-F	H	S	4.17	441	1577	869	>200
49	3-NO_2	H	N	1.60	91	210	197	44
50	3-$CONH_2$	H	N	-0.86	1125	654	1742	>200
51	4-Cl	(4-Cl)Ph	N	9.35	>5000	>5000	>5000	>200

The *in vitro* activity of the compounds in this series was evaluated using the SYBR Green assay. Both the carbohydrazides and thiocarbohydrazides were significantly less active than the aminoguanidines against *P. falciparum* D6, Dd2, and C2B. The thiocarbohydrazides (R_3 = S) were more potent than the carbohydrazides (R_3 = O), which were in many cases completely inactive. These compounds were generally most active against the sensitive D6 strain and least active against the multidrug resistant Dd2 strain. None of the compounds in this series were cytotoxic against mammalian HepG2 cells. The inactivity of the carbohydrazides and thiocarbohydrazides toward malaria parasites demonstrates the necessity of the central immine nitrogen in the aminoguanidine core for antimalarial activity. Notably, Trott and McCluskey made a similar series of carbohydrazide and thiocarbohydrazide analogs of their aminoguanidines, and similarly found that these substitutions removed antibacterial activity in nearly all cases (Russel 2018).

One of the most prominent structure-activity relationships resulting from the previous series of aminoguanidines was the positive effect of an electron withdrawing group (EWG) substitution at either the 3 (meta) or 4 (para) position of the phenyl ring (R_1). However, the superiority of meta vs para positioning of these EWGs was not consistent. The para trifluoromethoxy compound **16** was more potent than the meta trifluoromethoxy compound **15**,

whereas the para cyano compound **22** was less potent than the meta cyano compound **21**. To further investigate this position effect, two more compounds with meta EWGs were prepared. The meta nitro compound **49** had nearly identical potency to the para nitro compound **27**. The meta amide compound **50** was less potent than the para amide compound **30**, though neither compound was especially active. Neither of these new compounds was cytotoxic.

Two different substituents at R_2 were utilized in the previous aminoguanidine series, H (unsubstituted) or methyl. Generally, compounds with R_2 = methyl were less active than their unsubstituted counterparts, with the exception of compounds where $R_1 = CF_3$ in which **13** was superior to **12**. To evaluate the effect of larger substituents at R_2, the highly symmetrical compound **51** was prepared from the starting material 4, 4'-dichlorobenzophenone, placing a para-chlorophenyl substituent at R_2. This compound was completely inactive against all tested strains of *P. falciparum*, indicating a steric restriction at that position.

Taken together, the structure activity relationships that emerge from this series show that compounds with R_3 = N and R_2 = H have superior antimalarial activity. All subsequent compounds were therefore modified only at R_1.

In vitro Activity of Bicyclic and Heterocyclic Aminoguanidines

In the study described in the previous chapter, the compound with the best *in vitro* and *in vivo* antimalarial activity was **1**. The best compound *in vitro* without a meta cyano substituent was surprisingly the biphenyl compound **26** with a *P. falciparum* D6 IC_{50} of 15 nM. This promising *in vitro* activity did not translate to *in vivo* efficacy, and **26** was inactive against murine malaria at 10 mg/kg/day in a 4-day Peters test (Peters 2002).

It was hypothesized that this *in vivo* inactivity could in part be explained by metabolic instability as was observed for compound **21**, which was unstable due to an unprotected para position on its phenyl rings. Similarly, the biphenyl **26** had no protective substituents on its outer

phenyl rings. To address this issue, a series of four para-substituted biphenyls (**53**-**56**, Table 4-6) was prepared, as well as the undecorated meta biphenyl compound **52**. The substituted biphenyls included fluoro (**53**), chloro (**54**), and bromo (**55**) analogs and the trifluoromethyl compound **56**.

None of the substituted biphenyls or the meta unsubstituted biphenyl had *in vitro* activity approaching that of the unsubstituted para biphenyl **26**. Halogenated biphenyls decreased in potency with increasing halide size, a trend not observed for the simple phenyl aminoguanidines. Out of this series, the fluoro biphenyl **53** had the best *in vitro* activity, and so this compound was assessed *in vivo* in a 4-day Peters test. Like the unsubstituted biphenyl, **53** was inactive at 10 mg/kg/day.

Table 4-6: *in vitro* activity of bicyclic and heterocyclic aminoguanidines.

Compound	**R_1**	**cLog(P)**	**IC_{50} D6 (nM)**	**IC_{50} Dd2 (nM)**	**IC_{50} Tm90-C2B (nM)**	**IC_{50} Cytotoxicity (μM)**
52	3-Ph	5.89	92	1776	169	96
53	4-(4-F Ph)	6.18	62	120	109	46
54	4-(4-Cl Ph)	7.32	322	621	434	>200
55	4-(4-Br Ph)	7.62	1116	1457	788	>200
56	4-(4-CF_3 Ph)	7.66	1256	1498	944	>200
57	4-OPh	6.31	50	105	88	65
58	4-O(4-F Ph)	6.60	127	307	157	98
59	4-O(4-Cl Ph)	7.74	88	249	89	43
60	1-Napthyl[a]	4.46	409	629	563	67
61	2-Napthyl[a]	4.46	818	1494	1427	>200
62	2-Quinoline[a]	1.89	201	463	646	63
63	3-Quinoline[a]	1.89	6	24	17	95
64	4-Quinoline[a]	1.89	58	135	125	>200

65	8-Quinoline[a]	1.89	692	958	1025	33
66	3-Pyridine[a]	-0.88	560	937	1232	>200
67	4-Pyridine[a]	-0.88	1787	2105	>5000	>200
68	3-(7-Cl Quinoline) [a]	3.44	21	29	36	>200
69	4-(7-Cl Quinoline) [a]	3.44	42	65	63	>200

[a]Napthyl, pyridine, and quinoline aminoguanidines are numbered by the position of the aminoguanidine bridge spanning between the ring systems, i.e. 3-quinoline denotes a bis-quinoline connected at the 3 position by an aminoguanidine bridge. See Figure 4-5 for position numbering of each ring system.

Biphenyl groups have a fixed three-dimensional structure, with the two phenyl rings orthogonal to one another due to steric hindrance. Conversely, diphenyl ethers have an additional atom and bond between the rings and can rotate more freely (this does come at the cost of adding additional mass to the molecule). To observe the effect of greater rotational freedom on the multi-cyclic aminoguanidines, a series of para diphenyl ether analogs was prepared.

Overall, the diphenyl ether compounds were more potent than the substituted biphenyls. However, none of these compounds reached potency equivalent to the unsubstituted para biphenyl **26**. Within this series, the unsubstituted diphenyl ether **57** was the most potent. In this case, activity did not decrease with increasing halogen size and the chloro diphenyl ether **59** was more potent than the fluoro diphenyl ether **58**.

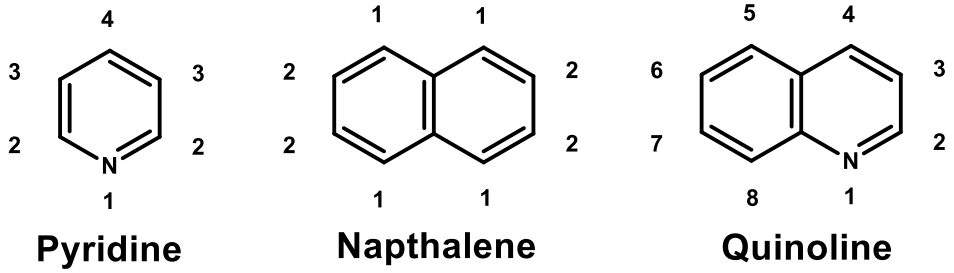

Figure 4-5: The notation of positions around pyridine, naphthalene, and quinoline ring systems. Pyridine and naphthalene are symmetrical and have some positions which are chemically equivalent. Quinoline is asymmetrical and has no chemically equivalent positions.

Diphenyl ethers are more flexible than biphenyl ring systems and have higher mass due to the added oxygen. Conversely, fused ring systems such as naphthalene and quinoline (Figure 4-5) have less mass than biphenyls and are structurally rigid. While the rings of a biphenyl system are orthogonal to one another, the rings of a fused system lay in the same plane.

The fused ring system naphthalene is highly symmetrical and has only two distinct chemical positions (Figure 4-5). When the heteroatom nitrogen is introduced to form a quinoline ring system, the symmetry is removed and all eight positions around the system are chemically distinct.

To investigate the activity of aminoguanidines with fused ring systems, a series of naphthalene and quinoline derivatives was prepared. The quinoline compounds were of particular interest due to the large number of quinoline antimalarial drugs (see chapter 1). These molecules can be considered as a series of bis-napthalenes and bis quinolines connected at different positions around the ring system by a bridge consisting of the aminoguanidine core, and they are described from this standpoint in Table 4-6. For example, the 3-quinoline compound **63** is a bis-quinoline with the two quinolines connected at their 3 positions (Figure 4-5) by an aminoguanidine bridge. Napthyl compounds bridged at each of the two distinct positions were prepared (**61**-**62**), as well as quinolines bridged at position 2, 3, 4, and 8.

The napthyl compounds were not particularly active against malaria parasites *in vitro*, though a position effect was observed as the 1-napthyl compound **61** was about twice as potent as the 2-napthyl **62**. Their potency against *P. falciparum* D6 was similar to the unsubstituted aminoguanidine **24**, but the napthyl compounds maintained better potency in the resistant strains Dd2 and Tm90-C2B.

The position effects observed for the quinoline series were very stark, with a greater than 100-fold span of IC_{50} values. The 3-quinoline **63** stood out as a very potent hit compound, with IC_{50} values that not only surpassed the biphenyl **26** but even reached the level of lead compound **1**. The 4-quinoline **64** was also very potent, though not to the same degree. The 2-quinoline **62** and 8-quinoline **65** were much less potent.

To further explore the success of the 3- and 4-quinolines **63** and **64**, two more sets of compounds were prepared. First, the effect of removing the benzenoid ring was determined by preparing the 3-pyridyl and 4-pyridyl aminoguanidines, **66** and **67** respectively. As expected, these compounds showed dramatically reduced potency compared with their quinoline counterparts, though the superiority of **66** over **67** demonstrated that the same position effect was in place.

Second, 3- and 4- quinoline analogs with 7-chloro substituents were prepared. Many clinical quinoline drugs have a 7-chloro substituent including the bis-quinoline piperaquine, and studies from our own group have indicated that this substituent boosts metabolic stability within this chemotype. Unexpectedly, the addition of the 7-chloro substituent had mixed effects on the aminoguanidine bis-quinolines. While the 4-(7-Cl quinoline) compound **69** was superior to the unsubstituted 4-quinoline **64**, the 7-chloro substituent reduced potency for the 3-quinoline compounds (**68** vs. **63**). This finding may be influenced by the extreme insolubility of **68**, which was insoluble in most common organic solvents and only sparingly soluble in DMSO. To address this issue, alternate salts for this compound were prepared (see below).

Four quinoline aminoguanidines, **63**, **64**, **68**, and **69**, had very potent *in vitro* antimalarial activity. These hit compounds were carried forward for further investigation including *in vivo* efficacy and metabolic stability (see below).

*Analogs of Compound **1** and Compound **16***

Among the compounds described in the previous chapter, two compounds stood out with the most promising *in vitro* and *in vivo* antimalarial activity. The 3-CN, 4-F analog **1** had the best *in vitro* potency, best *in vivo* efficacy, and best metabolic stability of the previous aminoguanidine series. The 4-OCF_3 compound **16** also performed well by these metrics and was the only compound to reach an *in vivo* non-recrudescence dose in which treated mice were still free from parasites 30 days after inoculation (these mice were considered cured at this time point).

Table 4-7: *in vitro* activity of analogs of **1** and **16**.

Compound	**R_1**	**cLog(P)**	**IC_{50} D6 (nM)**	**IC_{50} Dd2 (nM)**	**IC_{50} Tm90-C2B (nM)**	**IC_{50} Cytotoxicity (μM)**
70	3-F, 4-CN	1.27	84	153	161	>200
71	3-CN, 4-Cl	2.15	32	88	73	>200
72	3-CN, 4-CN	-0.15	98	147	126	>200
73	3-CN, 5-CN	-0.15	73	52	52	>200
75	3-I, 4-OCF_3	6.14	1454	1655	2043	78
76	3-CN, 4-OCF_3	3.69	13	25	28	>200
77	3-CN, 4-F, 4'-OCF_3	2.72	6	9	4	>200
78	4-SF_5	4.58	21	47	37	30

A targeted series of aminoguanidines was prepared in an attempt to improve upon, combine, or otherwise explore these positive antimalarial characteristics. First, the positional

isomer of **1**, the 3-F, 4-CN analog **70**, was prepared to determine the significance of the arrangement of the two substituents. As expected, the activity of **70** was significantly reduced compared to **1** (10- to 20-fold depending on the *P. falciparum* strain), indicating the necessity of this particular arrangement (Table 4-7). Second, the 4-F substituent of **1** was replaced with 4-Cl to form **71**. This compound closely resembles the original aminoguanidine robenidine, which has only the 4-Cl substituent. Compound **71** was very potent *in vitro*, though less so than **1**. Third, two dicyano compounds were prepared to see if this modification had an additive effect on activity. Neither the 3, 4-dicyano **72** nor the 3, 5-dicyano **73** were as potent as **1**, though both compounds were fairly active.

Ideally, the superior potency of **1** and the curative ability of **16** could be combined into a single molecule. Two approaches were considered to combine **1** and **16**. In one approach, the 4-F substituent of **1** could be replaced by the 4-OCF_3 substituent of **16** to form the 3-CN, 4-OCF_3 molecule **76**. In another approach, an asymmetrical aminoguanidine could be prepared with 4-OCF_3 on one phenyl ring and 3-CN, 4-F on the other (**77**). The synthesis of each of these molecules presented a unique challenge.

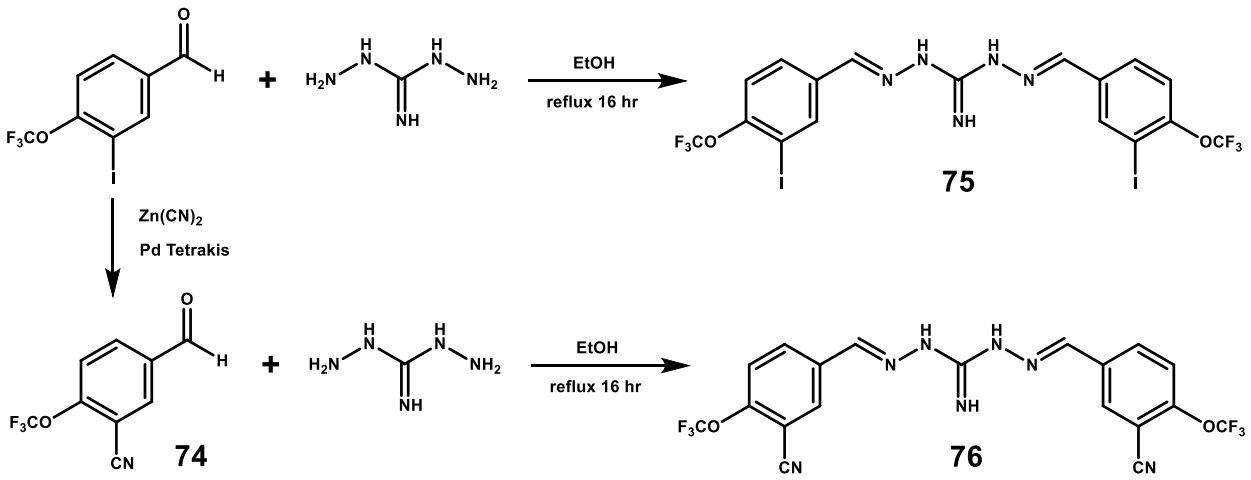

Scheme 4-2: Synthesis of compounds **74**, **75**, and **76**. **74** was prepared by a substitution reaction with zinc dicyanide catalyzed by palladium tetrakis. **75** and **76** were prepared by the general aminoguanidine synthesis procedure.

The 3-CN, 4-OCF3 compound **76** could not be prepared directly because the 3-CN, 4-OCF_3 benzaldehyde necessary as a starting material was not commercially available. Neither were the corresponding acetophenone, benzoic acid, benzyl alcohol, or even toluene. Only one example of this benzaldehyde existed in searchable publication and patent literature, in which it had been prepared via a substitution reaction from 3-I, 4-OCF_3 benzaldehyde (Nagashima 2006). This procedure, involving zinc dicyanide and a large quantity of palladium tetrakis, was replicated successfully to produce 3-cyano-4-trifluoromethoxybenzaldehyde (**74**). This intermediate was utilized to form **76**. This compound was very potent *in vitro*, though about two-fold less so than **1** across all tested *P. falciparum* strains. The original benzaldehyde was also used to form the 3-I, 4-OCF_3 compound **75**, which as expected was much less potent.

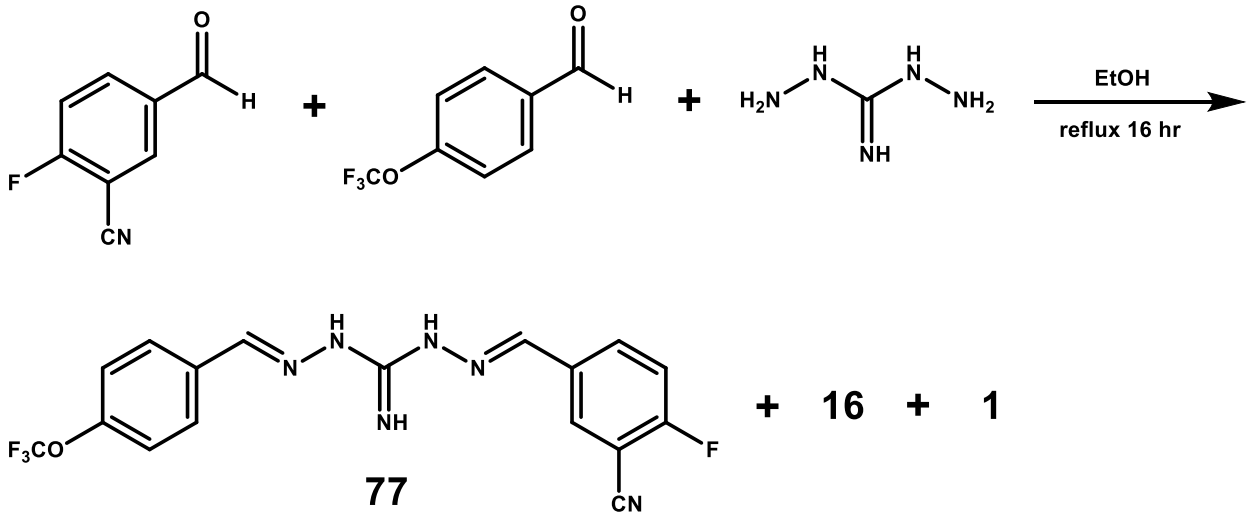

Scheme 4-3: 77 was prepared with a modified aminoguanidine synthesis procedure. One equivalent each of 3-cyano-4-fluorobenzaldehyde, 4-trifluoromethoxybenzaldehyde, and 1,3-diaminoguanidine were refluxed in ethanol, resulting in a 1:2:1 mixture of 16:77:1. This mixture was separated using reverse phase chromatography with a C-18 stationary phase and MeOH/H_2O mobile phase with 0.5% formic acid.

The preparation of **77** posed a different type of synthetic challenge resulting from its asymmetry. In their medicinal chemistry investigation of the antimicrobial properties of the aminoguanidines, Trott and McCluskey prepared several monomeric and asymmetrical structures (Russel 2018). Their approach involved a stepwise synthesis in which a monomeric aminoguanidine was first isolated, and later reacted with a second benzaldehyde to form an asymmetrical product. This approach was not used here because it required the starting materials to be soluble in diethyl ether, which they were not, and sometimes led to multiple products despite the attempt at control. Instead, **77** was intentionally prepared as one of a mixture of products by combining one equivalent each of 4-trifluoromethoxybenzaldehyde, 3-cyano-4-fluorobenzaldehyde, and 1,3-diaminoguanidine. As expected, this procedure led to a mixture of approximately 1:2:1 **1**:**77**:**16**. This mixture could not be separated by recrystallization due to the co-crystallization of the products, and normal phase column chromatography could not be

employed due to the poor solubility of the molecules in nonpolar solvents. Reverse phase column chromatography using a C-18 stationary phase and MeOH/H_2O (0.5% formic acid) mobile phase successfully isolated all three products.

The asymmetrical compound **77** had excellent *in vitro* activity, matching that of **1** in the sensitive *P. falciparum* strain D6 and even surpassing it in the resistant strains Dd2 and Tm90-C2B. Moreover, this compound had reduced cytotoxicity in mammalian HepG2 cells compared with **1**.

Finally, an analog of **16** was prepared with a 4-SF_5 substituent, a bioisostere of a trifluoromethoxy group with even greater electron withdrawing capacity. The 4-SF_5 compound **78** had an IC_{50} of 21 nM in *P. falciparum* D6, approximately two-fold better than **16**. This improvement was maintained in the resistant Dd2 and Tm90-C2B strains. Compound **78** was also less cytotoxic than **16**.

This series contained several very promising hit compounds with high *in vitro* activity. Compounds **71**, **73**, **76**, **77**, and **78** were carried forward for additional testing (see below).

Chemical Tools to Probe the Aminoguanidine Mechanism of Action

A proposed mechanism of action for the anticoccidial drug robenidine was published soon after its discovery in the early 1970s (Wong 1972). In this study, a high concentration of robenidine (20 μM) was incubated with rat mitochondria and found to inhibit the rat mitochondrial ATPase. In the 50 years since this study, no follow-up experiments have been performed to confirm this mechanism, nor have any experiments been conducted to assess the mode of action in the target organism *Eimeria*.

To further explore the aminoguanidine mechanism of action, a series of chemical tools was developed. First, azide aminoguanidines were attempted. The azide functional group can have multiple roles as a chemical biology tool in that it can be irradiated to covalently bind to a

biological target or can participate in an alkyne-azide click chemistry reaction for visualization or isolation of the target. 3- and 4-azidobenzaldehydes were not commercially available, so they were instead prepared via a copper catalyzed substitution reaction from bromobenzaldehydes using sodium azide (Scheme 4-4). These azide intermediates (**79** and **80**) proved difficult to isolate by column chromatography, and moderately impure products were utilized in an attempt to form the aminoguanidines **81** and **82**. The reactions were unsuccessful, instead producing an undesired orange polymer-like material likely caused by chemical transformation of the azides.

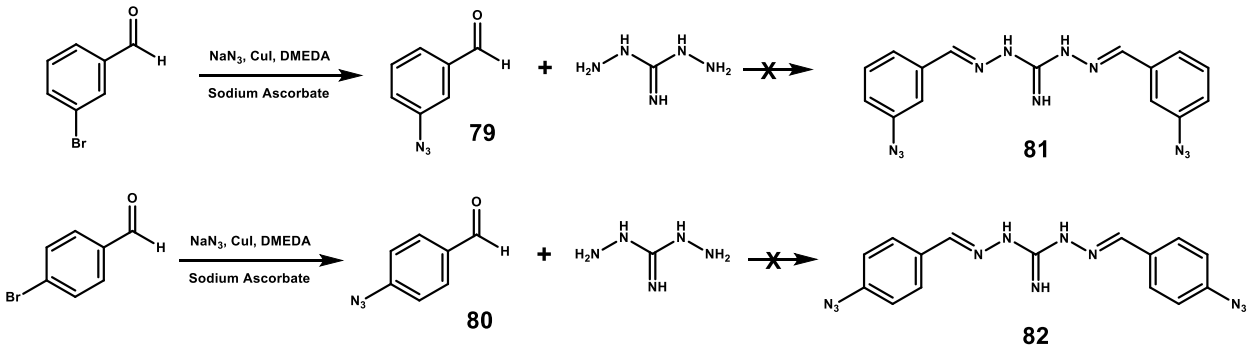

Scheme 4-4: Attempted synthesis of azide aminoguanidines **81** and **82**. Azidobenzaldehydes **79** and **80** were prepared from bromobenzaldehydes via a copper catalyzed substitution reaction using sodium azide, DMEDA, and sodium ascorbate. The corresponding azide aminoguanidines were not produced by the general aminoguanidine synthesis method.

Coumarin is another chemical functionality useful for exploring the biological activity of drug molecules. A bis-coumarin aminoguanidine with the ring systems connected at the coumarin 6 position (**83**) was prepared. Unexpectedly, this compound was found to have excellent *in vitro* antimalarial activity of its own across all tested *P. falciparum* strains (Table 4-8). Many coumarin compounds are fluorescent, and the fluorescence characteristics of **83** were measured. **83** was found to be fluorescent with an excitation maximum of 350 nm and emission maximum of 400 nm. Unfortunately, the absolute fluorescence intensity was not sufficient to visualize subcellular localization of the aminoguanidine compounds in *Plasmodium* parasites *in vitro*.

Table 4-8: *in vitro* antimalarial activity of aminoguanidine chemical tools.

Compound	R_1	cLog(P)	IC_{50} D6 (nM)	IC_{50} Dd2 (nM)	IC_{50} Tm90-C2B (nM)	IC_{50} Cytotoxicity (μM)
83	6-Coumarin	0.66	18	28	55	>200
85	4-Benzophenone	4.19	256	440	517	>200
86	4-Benzophenone, 4'-Propynoxy	3.49	27	68	48	33

Benzophenones are another group of chemical probes that can be conjugated to a biological target. An aldehyde substituted benzophenone was not commercially available, and so it was prepared by oxidation of a benzyl alcohol benzophenone with pyridinium chlorochromate. This particular oxidizing agent was utilized to avoid over-oxidation to form the corresponding benzoic acid. From this aldehyde intermediate **84** (Scheme 4-5), a symmetrical bis-benzophenone aminoguanidine **85** was prepared using the general aminoguanidine synthesis procedure. Promisingly, the large size of this compound did not preclude activity and this compound maintained moderate potency in all strains.

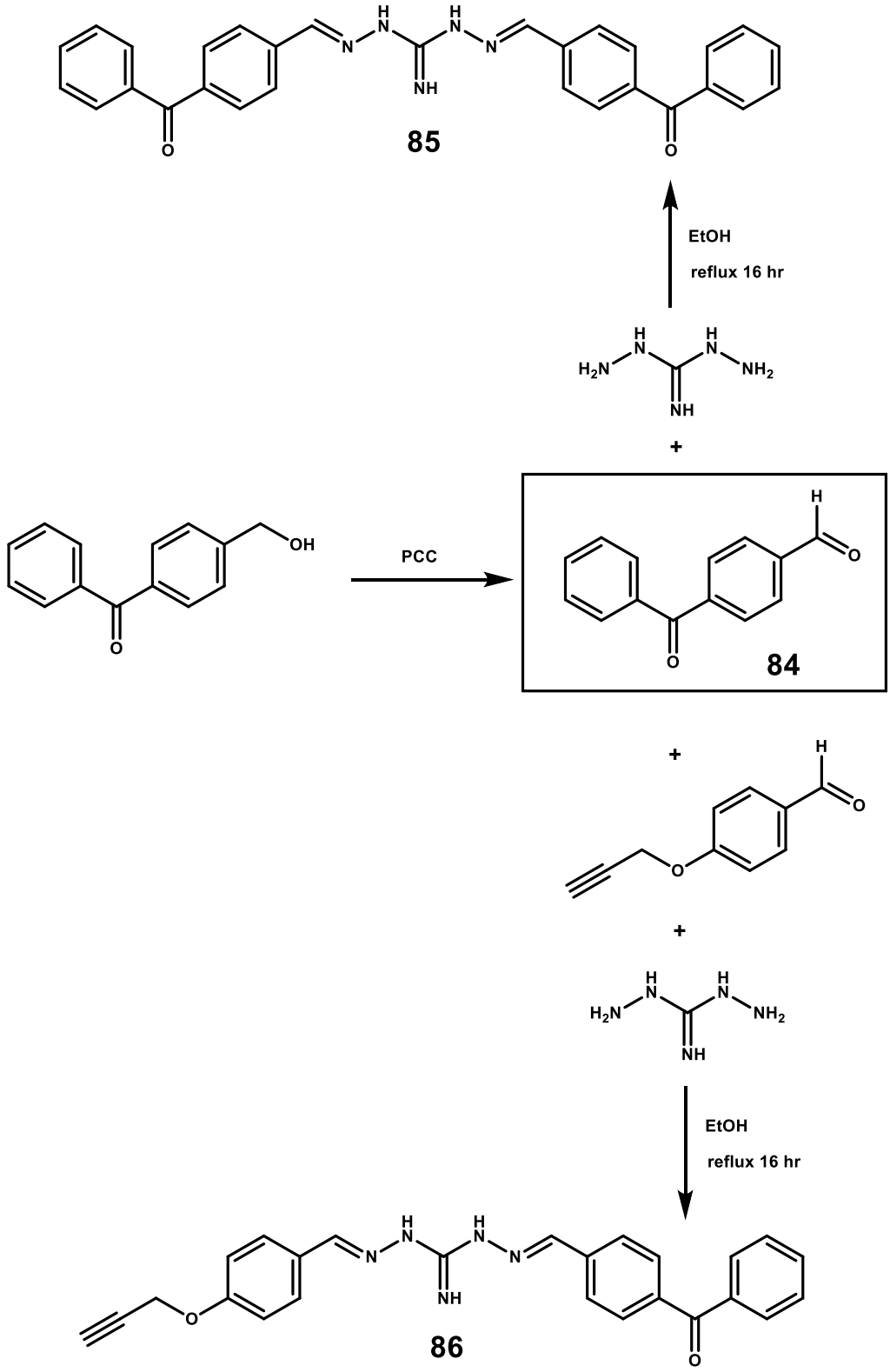

Scheme 4-5: Synthesis of the benzophenone aminoguanidines **85** and **86**. 4-Formylbenzaldehyde (**84**) was oxidized from a benzyl alcohol starting material. Two equivalents

were combined with 1,3-diaminoguanidine to form the symmetrical benzophenone **85** via the general aminoguanidine synthesis method. One equivalent of **84** was combined with 4-propynoxybenzaldehyde and 1,3-diaminoguanidine to produce a 1:2:1 mixture of **32**:**86**:**85**, which was separated by reverse phase chromatography as with compound **77**.

Making a fully functional chemical probe for target identification requires forming a molecule that can covalently bind to a biological target and bind to an identification or purification system such as a fluorescent dye or affinity column. An aminoguanidine probe molecule was envisioned with a benzophenone for target binding and an alkyne for binding to azide chemical tools via click chemistry (recall that in chapter 3 the symmetrical alkyne aminoguanidine **32** was fairly active *in vitro*). Putting both of these functionalities on both sides of the molecule would make it untenably large, so an asymmetrical compound analogous to **77** was pursued (Scheme 4-5).

One equivalent of 4-propynoxybenzaldehyde, one equivalent of the benzophenone intermediate **84**, and one equivalent of 1,3-diaminoguanidine were reacted to produce a 1:2:1 mixture of **32**:**86**:**85**. These compounds were separated using the reverse phase chromatography method developed for **77** (see above) to yield pure **86**. As was observed with **77**, the asymmetrical compound **86** was more potent *in vitro* than either of its symmetrical counterparts **32** or **85**, in this case by a substantial margin.

Though they were developed as chemical tools without potency as an intended goal, both the coumarin aminoguanidine **83** and the probe compound **86** were very potent antimalarials *in vitro* and these compounds were carried forward for testing *in vitro* (see below). Preliminary experiments to determine the functionality of **86** for mechanistic studies were also performed (see below).

Alternative Salts of Aminoguanidines

The chlorinated bis quinoline compound **68** was highly insoluble in water and many organic solvents, and it was hypothesized that this property was negatively influencing its potency. To attempt to improve solubility, alternative salts of this compound were explored (all aminoguanidines in this study are hydrochloride salts unless otherwise specified). First, the free base of **68** was formed by treating the hydrochloride salt with sodium hydroxide. In this formula transformation the color of the product shifted from pale yellow to bright yellow. Second, the phosphate salt of **68** was formed by treating the free base with one equivalent of phosphoric acid. This transformation returned the color to pale yellow. While the phosphate salt of **68** was equally insoluble as the hydrochloride salt, the free base was readily soluble in DMSO and other organic solvents. The *in vitro* activity of these alternate formulations was tested using the SYBR Green assay (Table 4-9). The free base of **68** was approximately equipotent to the hydrochloride salt but outperformed it slightly in head-to-head trials *in vitro*. The phosphate salt showed reduced potency compared with the hydrochloride salt.

Table 4-9: *in vitro* activity of alternative salts of aminoguanidines.

Compound	R_1	IC_{50} D6 (nM)	IC_{50} Dd2 (nM)	IC_{50} Tm90-C2B (nM)	IC_{50} Cytotoxicity (μM)
1-FB[a]	3-CN, 4-F	9	14	13	95
1-PS[b]	3-CN, 4-F	16	38	29	95
68-FB[a]	3-(7-Cl Quinoline)	22	37	30	>200
68-PS[b]	3-(7-Cl Quinoline)	222	174	253	>200

[a]FB = Free base.

[b]PS = Phosphate salt.

To see if the same activity trend was true for other aminoguanidines, the free base and phosphate salt of the lead compound **1** were formed using the same procedures as for **68**. A

similar color change from white to yellow was observed with the conversion to the free base, and conversion from yellow to white was observed with the formation of the phosphate salt. Again, the free base and hydrochloride salt were very similar in potency but the free base was slightly better in head-to-head trials. Also similarly to **68**, the phosphate salt was less potent than the hydrochloride salt. To determine the relative efficacy of the free base and hydrochloride salt *in vivo*, the free base of **1**, notated **1-FB**, was carried forward for additional testing.

In vivo Activity of Selected Aminoguanidines

Among the sets of aminoguanidines described above, there were many compounds which stood out as hits with excellent *in vitro* potency across sensitive and drug-resistant strains of *P. falciparum* while remaining nontoxic to mammalian cells. To help down-select one or more lead compounds from these hits, their blood stage *in vivo* activity was directly compared in a four-day Peters test in the murine *P. yoelii*. The compounds were administered over 4 days at a fixed oral dose of 5 mg/kg/day in SEDDS vehicle (Self-Emulsifying Drug Delivery System, 37.5% PEG-400, 37.5% Tween 20, and 25% Capmul MCM-NF). This study was highly informative for lead selection as the results spanned from 0% inhibition (day 5 parasitemia was indistinguishable from that of untreated controls) to 100% inhibition (mice were completely clear of parasites). No acute toxicity was observed in the animals.

The aminoguanidines with the highest *in vivo* efficacy were the 3-CN, 4-Cl compound **71**, the 3-CN, 4-OCF_3 compound **76**, and the asymmetrical compound **77**. All three compounds fully inhibited parasitemia at 5 mg/kg/day, and all three were structurally related to the lead compound **1** and/or the curative compound **16**. Also high performing were the chlorinated bis quinoline **68** and the 4-SF_5 compound **78**, each of which inhibited parasitemia by more than 80% compared with untreated controls. The asymmetrical probe compound **86** inhibited parasitemia by 51%, in other words its ED_{50} was almost exactly 5 mg/kg/day.

The chlorinated and unchlorinated 4 position bis-quinolines **64** and **69**, the unchlorinated 3 position bis-quinoline **64** were significantly less efficacious than **68**. Notably, the *in vivo* efficacy did not track with *in vitro* potency for the quinoline compounds. This result was further explored by assessing metabolic stability for these four compounds (see below).

The 3,5-dicyano compound **73** and the coumarin compound **83** had negligible efficacy at 5 mg/kg/day. In stark contrast to its positional isomer **1** which has an ED_{50} of 0.25 mg/kg/day, the 3-F, 4-CN compound **70** was completely inactive at 5 mg/kg/day, highlighting the extreme importance of the location of these substituents.

Table 4-10: Day 5 *in vivo* inhibition of parasites at 5 mg/kg/day

Compound	*P. yoelii* % Inhibition at 5 mg/kg/day
63	26
64	14
68	87
69	6
70	0
71	100
73	10
76	100
77	100
78	82
83	2
86	51

Four of the aminguanidines with the most promising *in vivo* activity at the fixed 5 mg/kg/day dose were further assessed in the same model at a range of doses to determine their ED_{50} (see Chapter 3). In this model, **1** had an ED_{50} of 0.25 mg/kg/day. **71**, **76** and **77** were all very active *in vivo* though slightly less so than **1** (Table 4-11). **76** performed marginally better than **77** and

71 *in vivo*, though **77** was superior *in vitro* to **71**, **76** and even the lead compound **1**. As expected given its incomplete parasite suppression at 5 mg/kg/day, the SF_5 compound **78** had a higher ED_{50} of 2.78 mg/kg/day. None of these compounds achieved non-recrudescence at doses up to 10 mg/kg/day, though this is not prohibitive of drug development as some clinical antimalarials such as chloroquine do not achieve non-recrudescence at any dose in this model.

Table 4-11: ED_{50} values of selected aminoguanidines.

Compound	*P. yoelii* ED_{50} (mg/kg/day)
71	0.61
76	0.42
77	0.56
78	2.78
1-FB	0.13

The free base of **1** (**1-FB**) was also assessed *in vivo* in a four-day Peters test to find its ED_{50}. Switching from the hydrochloride salt of **1** to its free base lowered the ED_{50} from 0.25 mg/kg/day to just under 0.13 mg/kg/day, an efficacy improvement of almost exactly 2-fold *in vivo*. **1-FB** has the lowest ED_{50} of all aminoguanidine compounds tested to date. Given this promising finding, the free bases of other potential lead compounds will also be prepared and assessed for antimalarial activity *in vitro* and *in vivo* to see if this trend is maintained.

Metabolic Stability of Aminoguanidines

The quinoline aminoguanidines **63**, **64**, **68**, and **69** were very potent *in vitro* but this did not translate to *in vivo* efficacy, as none of these compounds fully inhibited blood stage parasites at 5 mg/kg/day. This lack of efficacy was also observed for the 3-CN compound **21** and was later explained by its metabolic instability (see Chapter 3). To determine whether this was again the

case for the quinolines, their murine microsomal stability was assessed in pooled liver microsomes (Table 4-12).

The results of this experiment leave little doubt regarding the reason for the quinoline aminoguanidines' lack of *in vivo* efficacy. **63**, which has an *in vitro* IC_{50} of 6 nM in *P. falciparum* D6, has a biological half-life of under 5 minutes. No matter how powerfully the compound kills malaria parasites, it does not exist intact in the mouse long enough to act on them. The other three quinoline compounds fared slightly better but still had very poor stability. These stability values did not correlate directly with *in vivo* antimalarial activity; remarkably **68** cleared 87% of *P. yoelii* parasites with a half-life of less than 30 minutes. For both the 3-quinoline and the 4-quinoline aminoguanidines, the addition of a 7-Cl substituent did improve stability as expected, i.e. **68** was approximately 5-fold more stable than **63** and **69** was approximately 3-fold more stable than **64**. However, the overall stability of the quinolines remained low with none of the biological half-lives exceeding one hour.

Table 4-12: Murine microsomal stability of selected aminoguanidines.

Compound	Murine Microsomal Stability, $t_{1/2}$ (min)	Predicted Cl_{int} (mL/min/kg)
63	4.75	1148.60
64	16.56	329.53
68	24.95	218.75
69	46.35	117.74
76	∞	0
77	279.57	19.52
78	∞	0

The compounds **76**, **77**, and **78** were also evaluated for murine microsomal stability with vastly more promising results. Remarkably, the 3-CN, 4-OCF_3 compound **76** had no detectable degradation throughout the 1 hr length of the experiment. This perfect stability (a very rare

occurrence) significantly exceeds that of its two parent compounds **1** and **16**, which each had half-lives of approximately 3 hr. The asymmetrical compound **77** (3-CN, 4-F on one phenyl ring and 4-OCF_3 on the other) was also very stable, with only marginal degradation observed during the experiment. Its biological half-life of approximately 4.5 hr also exceeds that of **1** and **16**. The SF_5 compound **78** also exhibited perfect stability and was very potent *in vitro* with a *P. falciparum* D6 IC_{50} of 21 nM. It is therefore unusual that this compound did not fully inhibit *P. yoelii* parasites *in vivo* at 5 mg/kg/day, and an unknown alternative such as interspecies differences between *P. falciparum* and *P. yoelii* may be responsible for this finding. The other aminoguanidine with promising *in vivo* activity, **71**, has not yet been assessed for metabolic stability.

Probing the Aminoguanidine Mechanism of Action

The compound **86** was designed as functional chemical probe capable of photoactivation with its benzophenone moiety and click chemistry with its alkyne moiety. This compound also had surprisingly good *in vitro* potency and moderate *in vivo* efficacy. To begin using the probe for target identification for the aminoguanidine mechanism of action, an initial validation experiment was performed.

First, the parasitemia of a blood stage culture of *P. falciparum* Tm90-C2B was measured using a Geimsa-stained blood smear. The culture was treated with 0.1% saponin to selectively lyse the host erythrocytes while the parasites remained intact (Ansorge 1996, Baumeister 1999). The free parasites were resuspended in PBS containing a protease inhibitor cocktail, and parasitemia was measured using a Bradford assay and adjusted to 2 µg/mL. The parasite samples were incubated with the probe compound **86** in concentrations ranging from 0 to 100 µM for 1 hr in the dark.

Next, the samples were irradiated with UV light at 350 nm for 3 min except for a control sample which received no irradiation. In theory, this irradiation caused the benzophenone moiety

of the probe to conjugate to nearby proteins. After irradiation, the samples were incubated in a click chemistry mix containing copper sulfate and the azide-conjugated fluorescent dye tetramethylrhodamine azide (TAMRA N3). In theory, this step covalently linked the azide of the fluorophore to the alkyne of the probe via copper-catalyzed alkyne azide click chemistry. The samples were loaded on a gel and run by SDS PAGE, then imaged and stained with Cooomassie Blue (Figure 4-X).

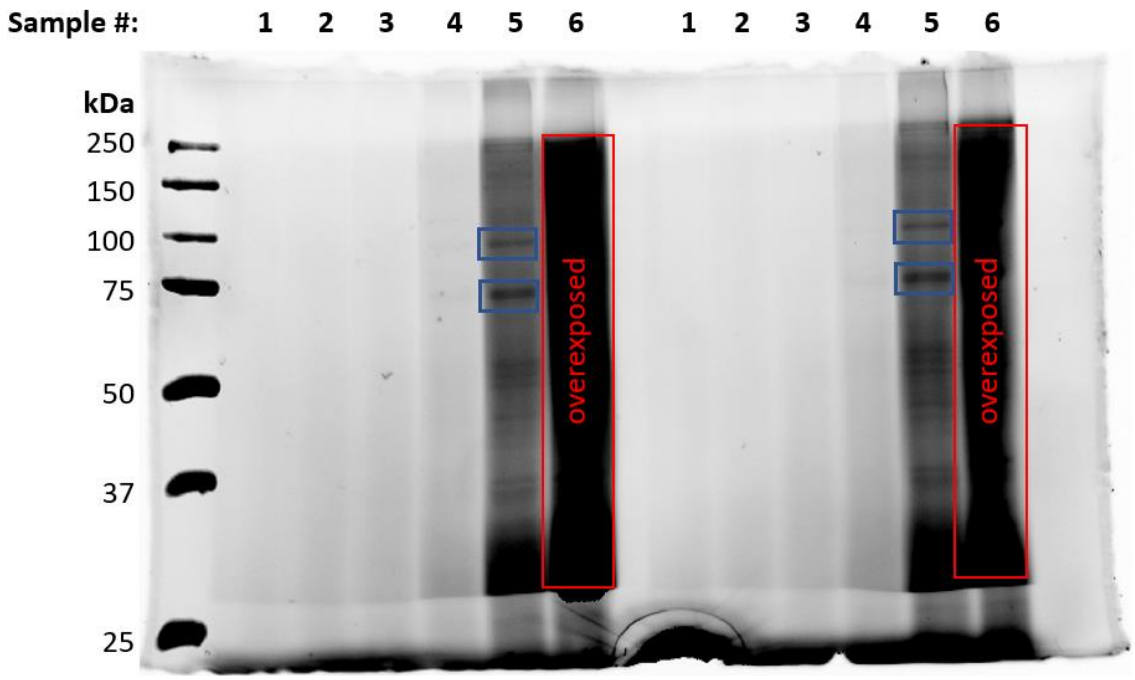

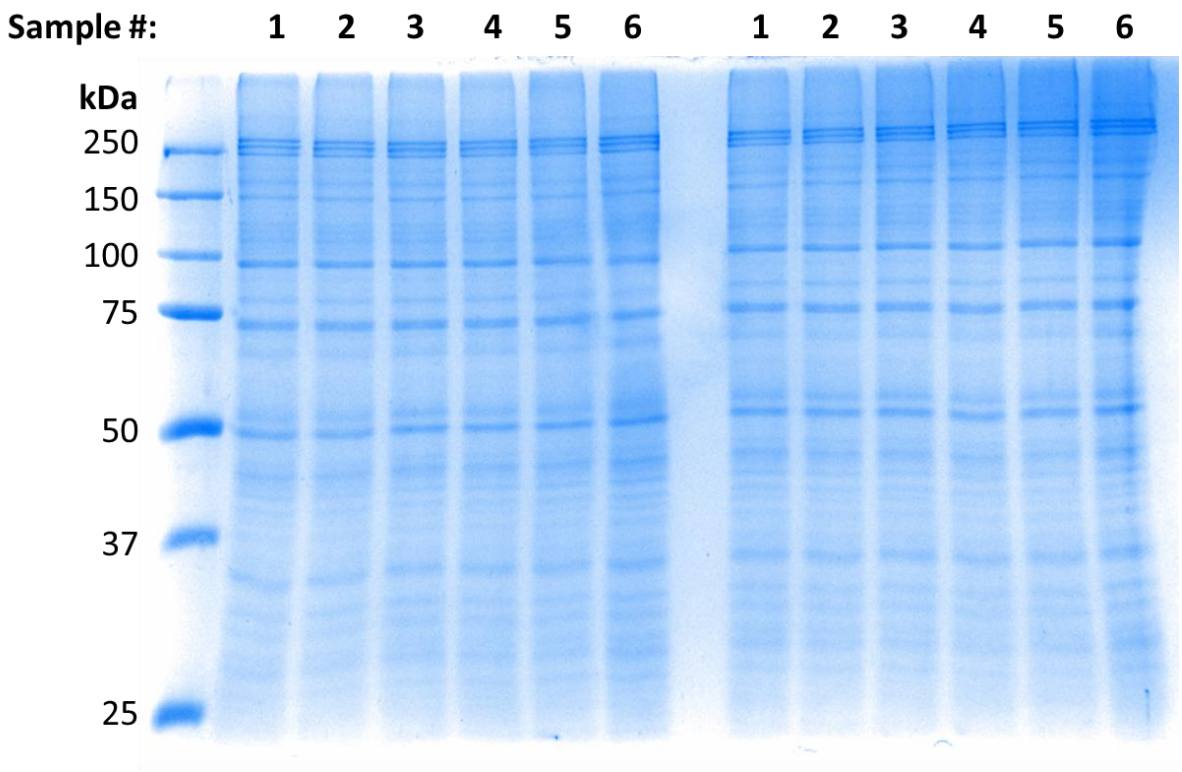

Figure 4-6: Top: a rhodamine fluorescence image (180 sec exposure) of a gel containing *P. falciparum* Tm90-C2B lysates incubated with the probe compound **86**. Lane 1 contains all blue ladder. Sample 1 (lanes 2 and 9) contained lysates with none of the probe compound. Sample 2 (lanes 3 and 10) was incubated with 0.1 μM of the probe, Sample 3 (lanes 4 and 11) with 1 μM, Sample 4 (lanes 5 and 12) with 10 μM, and Sample 5 (lanes 6 and 13) with 100 μM. Sample 6 (lanes 7 and 14) was also incubated with 100 μM of the probe but received no UV irradiation. Lanes 8 and 14 had no samples added. Bottom: a Coomassie Blue stain of the above gel showing the protein contents of the parasite lysates.

Two distinct bands can be observed in the gel image (Figure 4-6) at 75 and 100 kDa. These bands are visible for samples with probe concentration at 100 μM (lanes 5 and 12) with a 180 sec exposure, and the same bands become visible with probe concentrations as low as 1 μM with longer exposure times. The Coomassie stain reveals a high protein concentration across all lanes. For reasons which are still not understood, a very high level of fluorescent signal appears

throughout gel lanes containing sample 6, which contained 100 μM **86** but was not irradiated with UV light. The full length of this lane registered as overexposed even with very short exposure times. Though the samples were kept in the dark except during necessary handling, it is nevertheless possible that ambient UV light was sufficient to activate the probe.

The protein identity of these bands remains to be determined; however, some proteins can be ruled out because of their size. First, the reported target of the aminoguanidines, the mitochondrial ATPase (Wong 1972) has a mass of 53.5 kDa (Sturm 2015), far from the mass of either band. Second, human hemoglobin, which would have been very prevalent in the parasite cultures before erythrocyte removal, has a mass of 64.5 kDa but travels as individual alpha and beta subunits of 14 kDa in an SDS PAGE gel. The lack of bands at either of these masses indicates successful removal of the erythrocytes.

Rather than overinterpreting the significance of the 75 and 100 kDa bands, additional validation experiments are the more appropriate next step for the probe compound **86**. Most importantly, the extent of non-specific binding must be determined by a competition experiment or alternative assay. If such an experiment demonstrates that **86** is as specific as it appears here, the protein target of the aminoguanidines may soon be within reach.

Conclusion

The research described in this chapter sought to further explore the antimalarial activity of the aminoguanidines, expanding the breadth of known structure activity relationships, attempting to improve upon the lead compound **1**, and investigating the qualities of their drug action including mechanism of action. Experiments with **1** revealed that this compound killed parasites *in vitro* within 24 hr of incubation. In drug combinations, **1** was not significantly synergistic or antagonistic with atovaquone, chloroquine, or ELQ-300, but was most active when paired with chloroquine. Minimal activity differences between life cycle stages within the erythrocytic cycle were observed

for **1** and **16**. **1** had a moderate half-life in an *in vivo* pharmacokinetics experiment but had poor oral bioavailability since a low C_{max} was reached with oral dosing in PEG-300.

Major modifications to the aminoguanidine core structure or large substituents at the R_2 position were not well tolerated for *in vitro* antimalarial activity. Bis-quinoline aminoguanidines linked at the 3 or 4 position were active antimalarials *in vitro* but were inactive *in vivo* due to poor metabolic stability even with the addition of a protective 7-Cl substituent. Asymmetrical aminoguanidines were more potent *in vitro* than either of their analogous symmetrical compounds. The hydrochloride salts of the aminoguanidines were more potent than their phosphate salts but less potent than their free bases. An alkyne-benzophenone probe compound **86** identified potential biological targets for the aminoguanidines at 75 and 100 kDa, though additional validation experiments are required to rule out non-specific binding.

Two novel aminoguanidines were identified with excellent *in vitro* potency, *in vivo* efficacy, and metabolic stability: the 3-CN, 4-OCF_3 compound **76**, and the asymmetrical compound **77** with 3-CN, 4-F at one end of the molecule and 4-OCF_3 at the other. Among these two compounds and the previous lead compound **1**, none of the compounds was superior across all of the tested metrics. The 3-CN, 4-Cl compound **71** may also merit consideration as a lead if it shows promising metabolic stability, though this remains to be determined. Further assessments will be necessary to select a lead aminoguanidine compound for preclinical development. Comparisons between these lead compounds are discussed further in Chapter 6.

Chapter 5 : Alkoxycarbonate Ester Prodrugs of the Antimalarial ELQ-300 for Intramuscular Injection

Figure 5-5 was previously published in Malaria Journal (Smilkstein 2019) and is reprinted with permission. *In vivo* efficacy experiments were performed by Dr. Yuexin Li. Pharmacokinetics experiments were performed by Dr. Martin Smilkstein and the Oregon Health and Science University Pharmacokinetics Core. All other experiments were performed by the author.

Introduction

Long term malaria prophylaxis is a major unmet medical need in tropical regions of South America, Africa, and Southeast Asia, a need which is exacerbated by the emergence of widespread resistance to available therapies (WHO 2021, Sachs 2002, Sibley 2014). A novel long-acting injectable (LAI) prophylactic was recently identified by the Medicines for Malaria Venture as one of their most important target candidate profiles (Burrows 2017). Current malaria prophylaxis mainly consists of short term chemoprotection, in which oral medications must be taken daily or weekly to ensure protection from the disease (Burrows 2011).

LAI prophylactics have many potential applications, each of which could significantly further progress toward the goal of global malaria eradication. One LAI application would be protection for armed servicemembers serving abroad in malarious regions. Malarone, the drug cocktail most commonly used for military antimalarial prophylaxis, is an oral formulation which

must be taken daily. Mild to severe side effects including ulcers in the gastrointestinal tract are observed in some users of Malarone. Similarly, LAIs could be given as malaria protection for global health workers during service projects. In larger scale applications for communities native to malarious regions, LAIs could provide protection for communities where malaria is seasonal. LAIs could also be given to pregnant mothers during the gestation period to improve outcomes and prevent fetal acquisition of malaria. Malaria is particularly deadly in young children.

Intramuscular (IM) injection may be the most appropriate administration route for antimalarial LAIs. IM injection is a drug administration route used for therapeutics with many different clinical indications, including HIV, hormone therapies, migraine, and mental disorders (Owen 2016). Typically, IM drugs are administered at large skeletal muscles such as the quadricep and are formulated in highly viscous injection vehicles like sesame oil or castor oil. Unlike intravenous (IV) dosing which distributes the drug to the systemic bloodstream immediately, the vehicle of an IM dosage remains in place in the muscle as an injection 'depot' for up to several weeks or months, dispensing the drug slowly. This administration route is therefore most useful when gradual, sustained drug release is desired.

One antimalarial compound with potential as a LAI is the highly potent preclinical drug candidate ELQ-300 (Figure 5-1d). ELQ-300 functions by inhibiting the *Plasmodium* cytochrome bc_1, a vital component of the mitochondrial cellular respiration complex responsible for the electron transport and recycling of coenzyme Q. The approved antimalarial drug atovaquone inhibits the same target, but resistance selection studies of both compounds indicate that they do so at distinct binding sites. While atovaquone binds to the oxidative Q_o site, ELQ-300 binds at the reductive Q_i site (Stickles 2015). Significantly, ELQ-300 has demonstrated higher potency, lower toxicity, lower resistance propensity, and lower manufacturing cost than atovaquone (Winter 2011, Nilsen 2014, Pou 2021). Despite many positive qualities which make ELQ-300 a late lead drug candidate, clinical development of the drug is hindered by its low oral bioavailability brought

on by low aqueous solubility and high crystallinity. These attributes prevent determination of necessary toxicity data, precluding clinical trials.

To solve the issue of oral bioavailability, medicinal chemistry efforts in the Riscoe group have recently focused on the preparation of ELQ-300 prodrugs designed to disrupt the intra-quinolone hydrogen bonding and pi stacking responsible for its highly crystalline character. The majority of these prodrugs consist of substitutions of ELQ-300 at the quinolone oxygen, and include phosphates, carbamates, amino acid esters, carbonates, and other masking groups (Miley 2015). The most promising prodrug structure thus far is the alkoxycarbonate ester (Figure 5-1c) compound ELQ-331 (Figure 5-1e), which is currently being evaluated for oral delivery in advanced preclinical trials (Frueh 2017). This compound outperforms simple ester (Figure 5-1a) and carbonate ester (Figure 5-1b) prodrugs.

To date the prodrug effort in the Riscoe group has focused on adapting ELQ-300 for oral dosage. However, a recent study demonstrated that prodrugs (structures undisclosed) of ELQ-300 or atovaquone protected mice from malaria sporozoites for 14 days, with a minimum protective concentration for ELQ-300 of 83 nM (Chaterjee 2017). The Riscoe group is uniquely qualified to further pursue these positive results by drawing on knowledge gained from our large base of existing ELQ-300 prodrugs and other endochin-like quinolones, and with support from MMV work has begun to optimize a prophylactic IM ELQ-300 drug product.

The optimal ELQ-300 prodrug structures may be different for oral administration and IM administration. In the research described in this section, a series of alkoxycarbonate ester prodrugs was synthesized and evaluated for properties indicating success as an IM LAI. These properties included crystallinity (as indicated by melting point), solubility in one or more IM injection vehicles, and on-target antimalarial activity (as indicated by having the same resistance profile as ELQ-300). Promising prodrugs were evaluated *in vivo* for long-term prophylaxis in murine malaria (*P. yoelii*).

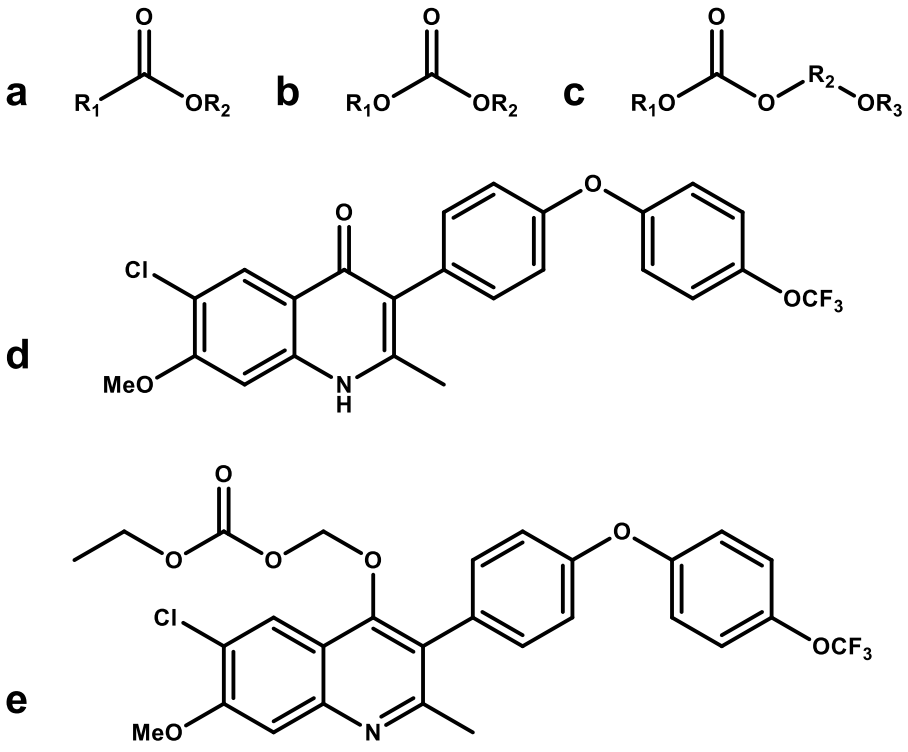

Figure 5-1: a: an ester, b: a carbonate ester, c: an alkoxycarbonate ester, d: ELQ-300, an antimalarial drug candidate, e: ELQ-331, an alkoxycarbonate ester prodrug of ELQ-300.

Results and Discussion

Synthesis of Alkoxycarbonate Ester Prodrugs

A series of nine alkoxycarbonate ester prodrugs of ELQ-300 were prepared in which the terminal carbon chain length of the alkoxycarbonate pro-moiety was varied (Scheme A1). In conjunction with the original alkoxycarbonate ester prodrug ELQ-331 which has a terminal ethyl group, all chain lengths from methyl to decyl were prepared.

The pro-moieties were assembled in one synthetic step and then conjugated to the quinolone oxygen of ELQ-300 in a second synthetic step (Scheme A1). To assemble the pro-moieties, unbranched alcohols ranging from methanol to n-decanol were reacted with

chloromethyl chloroformate under basic conditions in tetrahydrofuran (THF). The highly reactive molecule chloromethyl chloroformate was initially added dropwise at -78 ^{o}C under inert atmosphere and gradually allowed to warm to room temperature. As was previously demonstrated in the development of ELQ-331 (Frueh 2017), the alcohols selectively replace the acyl chloride by an addition-elimination mechanism and do not substitute at the alkyl chloride. Better yields were observed using the organic base triethylamine (TEA) than with potassium carbonate.

To conjugate the resulting chloromethyl alkyl carbonates to ELQ-300, the reagents were combined in the presence of tetrabutylammonium iodide (TBAI) and potassium carbonate and heated at 60 ^{o}C overnight. The resulting substitutions displaced the alkyl chloride, and the ELQ-300 prodrugs were obtained in relatively low yields. Notably, the prodrugs in this series were all solids, however shorter chain prodrugs were crystalline while longer chain prodrugs were waxes that did not retain a fixed shape.

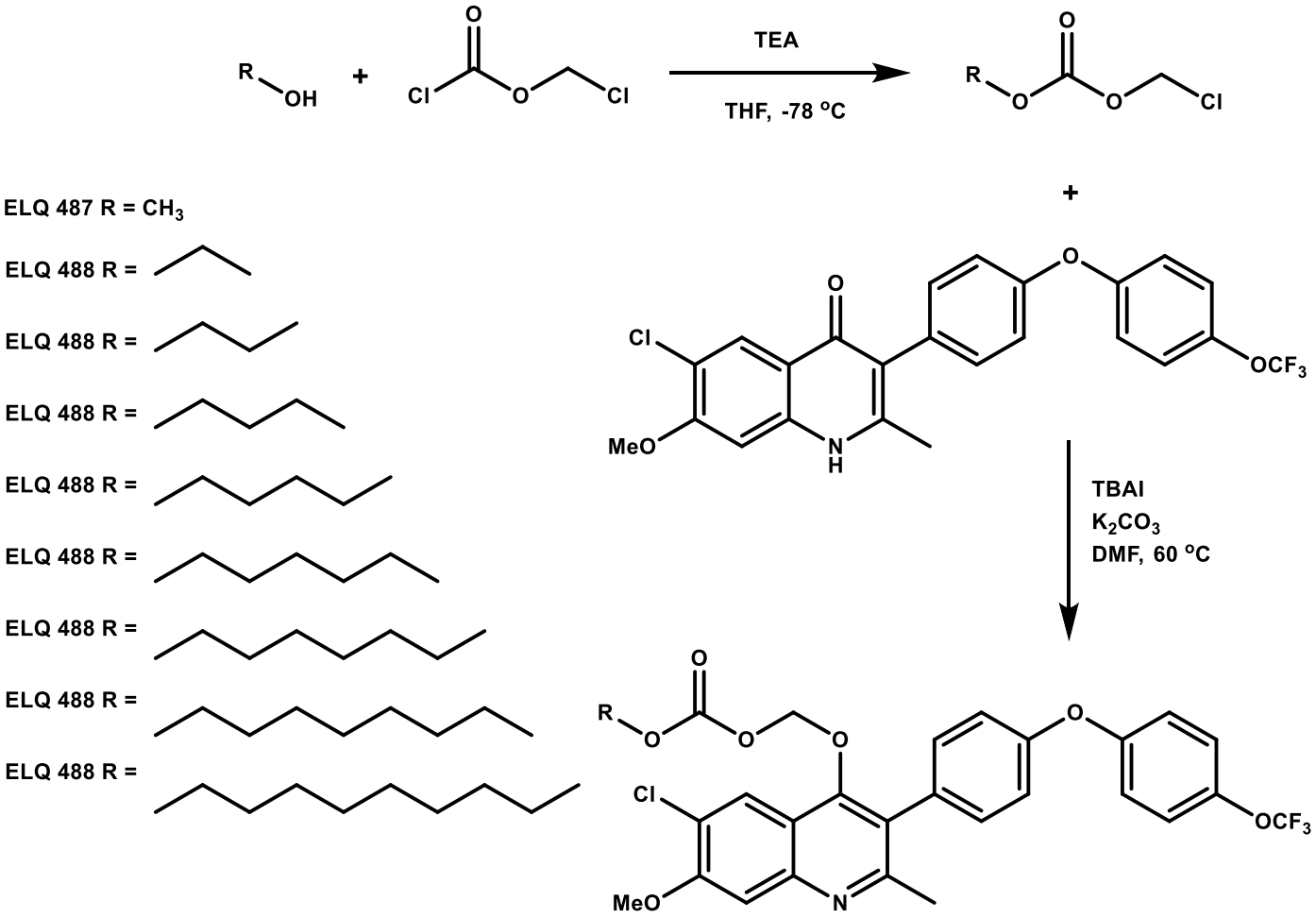

Scheme 5-1: Two step synthesis of alkoxycarbonate ester ELQ=300 prodrugs starting from alcohols, chloromethyl chloroformate, and ELQ-300. R is an unbranched alkyl group ranging from methyl to decyl.

Physiochemical Properties of Alkoxycarbonate Ester Prodrugs

ELQ-300 is highly crystalline and is poorly soluble both in aqueous media and in many IM injection vehicles including sesame oil. A compound's melting point is often a useful indicator of its crystallinity. As an initial assessment for potential success as an IM ELQ-300 prodrug, the melting point of each compound in the alkoxycarbonate ester series was measured (Figure 5-2, top, Table 5-1). As a general trend, the melting points of the alkoxycarbonate esters decreased

with increasing carbon chain length, leveling off around 55 °C. Notably, all compounds in this series have substantially lower melting points than the parent compound ELQ-300, which decomposes around 300 °C. The calculated log of the partition coefficient (cLogP) for each compound was also determined using ChemDraw Professional. The cLog(P) values ranged from 7.4 to 12.2 and increased with increasing carbon chain length (the parent compound ELQ-300 has a cLog(P) of 5.7).

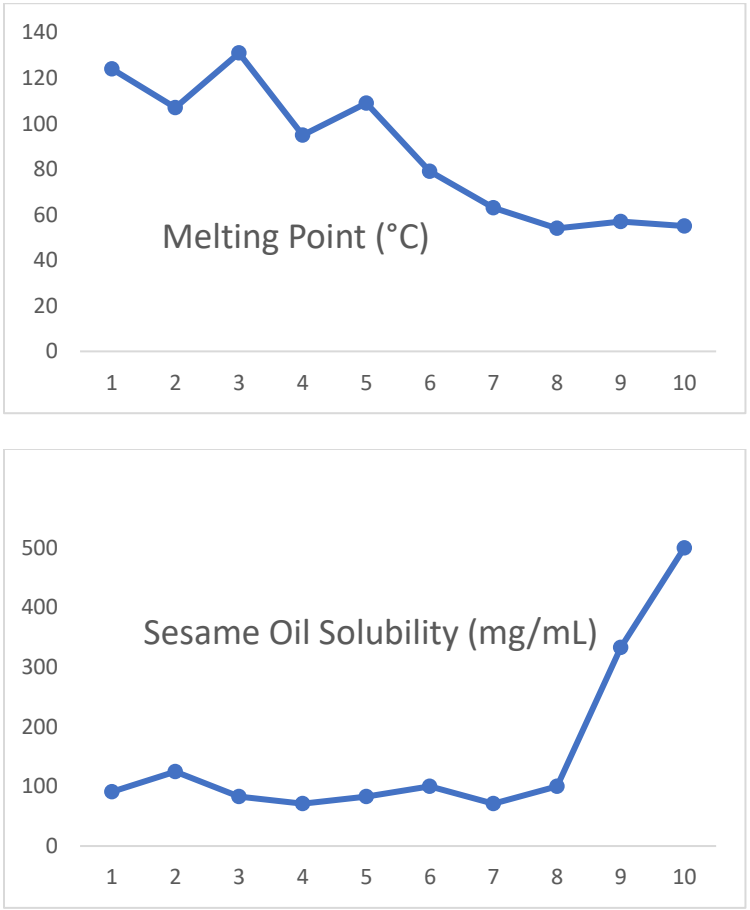

Figure 5-2: Top: melting points of the alkoxycarbonate ester prodrug series. Bottom: sesame oil solubility of the alkoxycarbonate ester prodrug series. The x axis of both graphs refers to the number of carbon atoms in the terminal alkyl chain of the pro-moiety (Scheme A1, R group).

Sesame oil is a common IM injection vehicle. High solubility in the injection vehicle is a desirable attribute for an injectable drug because it allows more drug to be delivered in a smaller volume. The solubility of each alkoxycarbonate ester prodrug was determined by heating increasing masses of each compound in sesame oil and allowing the solutions to cool to room temperature (ELQ-300 did not go into solution even with substantial heat). Compounds that stayed in solution at room temperature at a given concentration for one hour were considered soluble at that concentration. Sesame oil solubility did not track in a linear fashion with terminal alkyl chain length. Rather, solubility remained fairly constant at between 100 and 125 mg/mL for the first 8 compounds, then increased dramatically for the nonyl prodrug (ELQ-494) and decyl prodrug (ELQ-495). ELQ-495 was fully miscible with sesame oil with minimal heating.

Table 5-1: Physiochemical Properties of Alkoxycarbonate Ester Prodrugs of ELQ-300

Compound	R	cLog(P)	MP (ºC)	Sesame Oil Solubility (mg/mL)
ELQ-300	N/A	5.7	310	≤50
ELQ-487	methyl	7.4	124	91
ELQ-331	ethyl	8.0	107	125
ELQ-488	propyl	8.5	131	83
ELQ-489	butyl	9.0	95	71
ELQ-490	pentyl	9.6	109	83
ELQ-491	hexyl	10.1	79	100
ELQ-492	heptyl	10.6	63	71
ELQ-493	octyl	11.1	54	100
ELQ-494	nonyl	11.7	57	333
ELQ-495	decyl	12.2	55	≥500

The solubility of selected alkoxycarbonate ester prodrugs in other IM vehicles was assessed. The parent compound ELQ-300 and the prodrugs ELQ-331 (R = ethyl), ELQ-494 (R = nonyl) and ELQ-495 (R = decyl) was measured as described above in sesame oil, cottonseed oil, castor oil, soybean oil, and the fractionated coconut oil extract Myglyol-812 (Figure 5-3, Table 5-2). ELQ-300 was insoluble in all five vehicles. The solubility of ELQ-331 remained constant at 125 mg/mL for all vehicles. ELQ-494 was more soluble in sesame oil and castor oil compared with Myglyol, cottonseed oil, and soybean oil. ELQ-495 was miscible in all five vehicles.

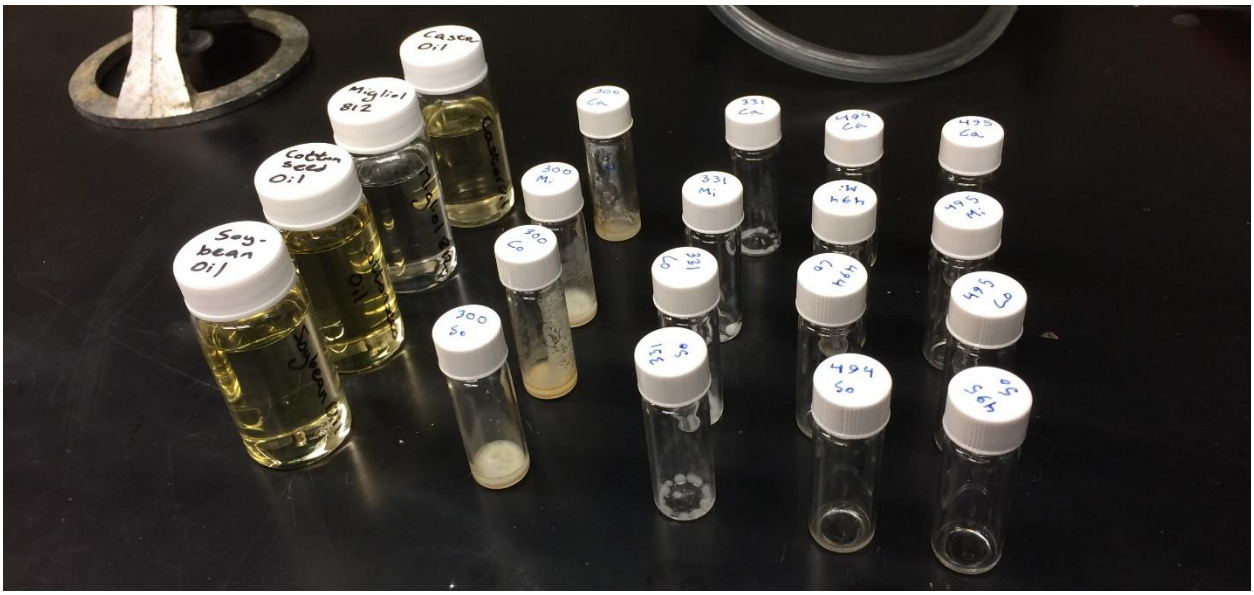

Figure 5-3: Solubility testing of alkoxycarbonate ester prodrugs

Table 5-2: Solubility of alkoxycarbonate ester prodrugs in IM injection vehicles

Compound	R	Sesame Oil mg/mL	Castor Oil mg/mL	Migliol mg/mL	Cottonseed Oil mg/mL	Soybean Oil mg/mL
ELQ-300	N/A	<50	<50	<50	<50	<50
ELQ-331	ethyl	125	125	125	125	125
ELQ-494	nonyl	333	250	125	125	125
ELQ-495	decyl	>500	>500	>500	>500	>500

On-Target in vitro Antimalarial Activity of Alkoxycarbonate Ester Prodrugs

The *in vitro* antimalarial activity of some alkoxycarbonate ester prodrugs was evaluated in both ELQ-300-sensitive and ELQ-300-resistant *P. falciparum* strains. The strain Dd2 is resistant to the antimalarial drug chloroquine and the drug combination pyrimethamine-sulfadoxine but is sensitive to atovaquone and ELQ-300. The strain D1 is sensitive to atovaquone but resistant to ELQ-300. To determine whether the alkoxycarbonate ester prodrugs of ELQ-300 had the same resistance profiles as the parent compound, the prodrugs were tested for *in vitro* potency in both the Dd2 and D1 strains using the SYBR green IC_{50} assay (see Chapter 3).

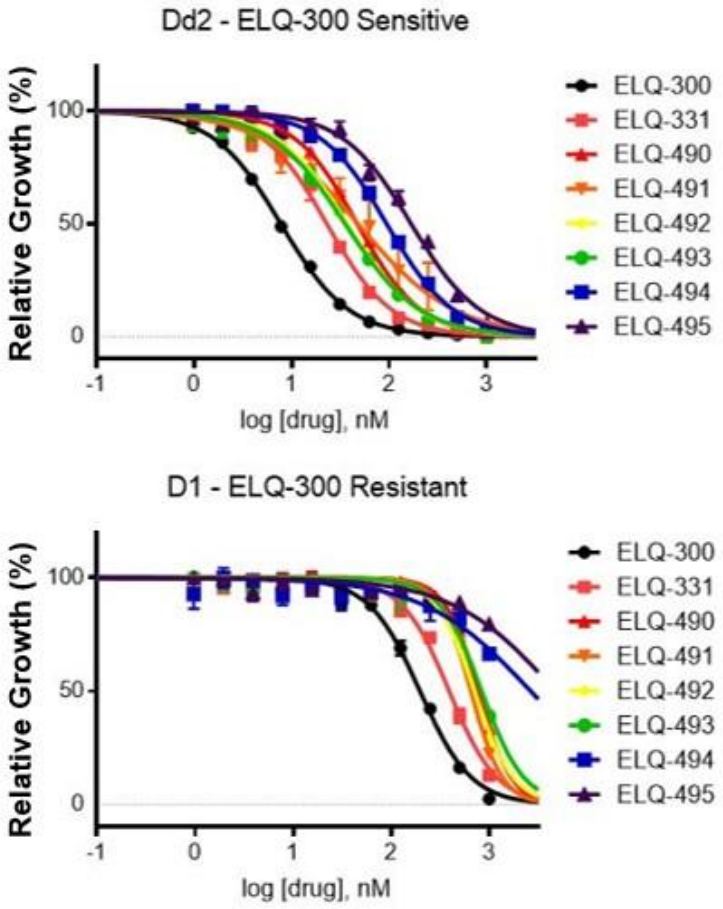

Figure 5-4: IC_{50} curves of alkoxycarbonate ester prodrugs of ELQ-300 in Dd2 (ELQ-300-sensitive) and D1 (ELQ-300-resistant) *P. falciparum*.

All of the alkoxycarbonate ester prodrugs had reduced potency in both Dd2 and D1 as compared with the parent compound ELQ-300 (Figure 5-4, Table 5-3). Overall, potency decreased in both strains with increasing pro-moiety length, though the activity of the pentyl through octyl prodrugs (ELQ-490-493) was relatively comparable. The ethyl prodrug ELQ-331 was more potent than longer chain prodrugs, and the longest prodrugs ELQ-494 and ELQ-495 were less potent, particularly in strain D1.

Table 5-3: *in vitro* activity of alkoxycarbonate ester prodrugs of ELQ-300

Compound	**R**	**Dd2 IC_{50} (nM)**	**D1 IC_{50} (nM)**
ELQ-300	N/A	8	200
ELQ-331	ethyl	22	390
ELQ-490	pentyl	47	770
ELQ-491	hexyl	48	650
ELQ-492	heptyl	37	710
ELQ-493	octyl	36	840
ELQ-494	nonyl	94	2700
ELQ-495	decyl	168	4800

Like the parent compound, the prodrugs all had significantly reduced potency in D1 as compared with Dd2, indicating on-target antimalarial activity. The wide range of activity levels observed with the series indicates that the prodrugs likely remain intact in this *in vitro* system, rather than being cleaved to form the more active ELQ-300.

In vivo Blood Stage Prophylaxis of Intramuscular ELQ-331 and ELQ-492

The *in vivo* prophylactic activity of intramuscular ethyl (ELQ-331) and heptyl (ELQ-492) alkoxycarbonate ester prodrugs of ELQ-300 was assessed in murine malaria (*P. yoelii*). Four groups of mice (n = 4 per group, four groups per compound) were injected IM with the prodrug in sesame oil containing 1.2% benzyl alcohol as a preservative. Dosing for each prodrug was adjusted by prodrug mass to deliver the equivalent of 10 mg/kg ELQ-300. Four control groups were given vehicle only. The parent compound ELQ-300 was insoluble in sesame oil and other IM vehicles and could not be tested directly. At weekly intervals, the prophylactic effect of each prodrug was challenged with an IV injection of *P. yoelii*-infected murine erythrocytes from a donor mouse. New groups of mice were utilized for each prophylaxis challenge. Five days after each prophylaxis challenge, blood was collected from challenged mice and parasitemia was measured using blood smears.

Table 5-4: *in vivo* prophylactic activity of alkoxycarbonate ester prodrugs of ELQ-300

Prodrug	R	1 Wk Post-Injection	2 Wk Post-Injection	3 Wk Post-Injection	5.5 Wk Post-Injection
Control Mouse	N/A	20%	26%	20%	30%
ELQ-331	ethyl	ND	ND	ND	ND
ELQ-492	heptyl	ND	ND	ND	ND

After the first three prophylaxis challenges, there were no parasites visible in mice treated with either ELQ-331 or ELQ-492. Control groups at each time point developed blood stage infections with parasitemia ranging from 20-30 %. Given this initial success, the final group of

mice was given an additional 1.5 weeks before the final prophylaxis challenge, placing it 5.5 weeks after the prodrug treatment. Unexpectedly, even at this extended time point there were no detectable parasites in mice treated with either prodrug. In contrast, the undisclosed prodrugs of the Chaterjee group at CALIBR protected mice for only 14 days (Chaterjee 2017). Further, all prodrug-treated mice in the study remained free of parasites for 30 days after their respective prophylaxis challenges, indicating that no malaria infection had occurred.

Long-Term Pharmacokinetics of ELQ-331, ELQ-494, and ELQ-495

Given the long-lasting prophylactic effects of both tested alkoxycarbonate ester prodrugs of ELQ-300, it was necessary to carry out an additional study to fully determine the duration of protection they provided. In a long-term pharmacokinetics study, mice were dosed IM with ethyl (ELQ-331), nonyl (ELQ-494), or decyl (ELQ-495) prodrugs in sesame oil containing 1.2 % benzyl alcohol (Smilkstein 2019). As in the prophylaxis experiment, dosing was adjusted to deliver 10 mg/kg ELQ-300. Blood samples were taken from the treated mice at 30 days and 70 days after dosing and plasma concentrations of ELQ-300 were measured at the OHSU Pharmacokinetics Core. Notably, it was determined in a previous experiment that the plasma concentration of ELQ-331 is nearly undetectable at any time point because the prodrug is rapidly cleaved to form the active drug in the bloodstream (Smilkstein 2019).

Prodrug dose	Plasma [ELQ-300], nM		
	Day 30	Day 70	Day 77
ELQ-331, 10 mg/kg	290.4 ± 16.4	70.5 ± 8.1	67.5 ± 11.4
ELQ-494, 10 mg/kg	67.5 ± 12.8	21.7 ± 5	n/a
ELQ-495, 10 mg/kg	105.9 ± 18.1	37.7 ± 5.2	n/a

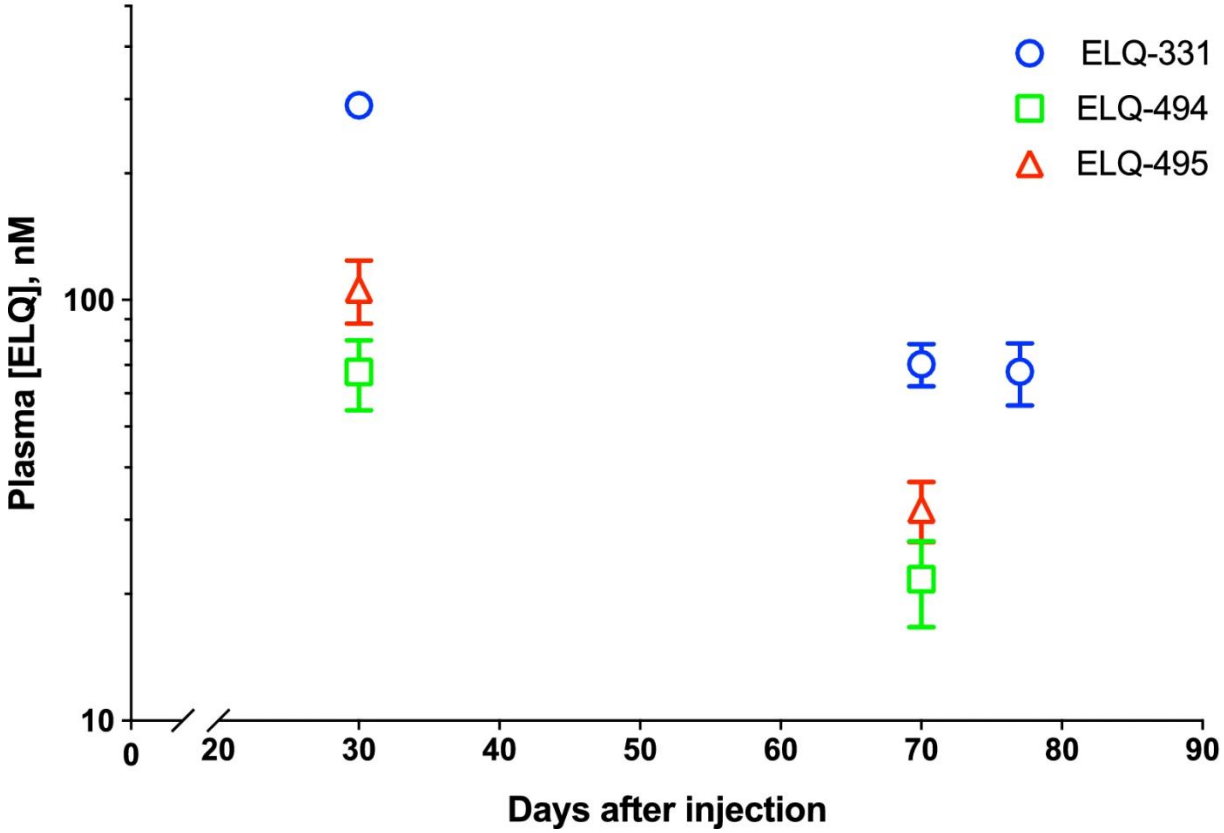

Figure 5-5: Long-term pharmacokinetics of ELQ-300 after dosing IM with the alkoxycarbonate ester prodrugs ELQ-331, ELQ-494, or ELQ-495 (Image from Smilkstein 2019).

At both time points, the ELQ-300 plasma concentration was highest in mice dosed with ELQ-331, followed by ELQ-495, then ELQ-494. This indicates a non-linear relationship between pro-moiety chain length and *in vivo* prodrug activity. Although speculative at this time it would appear that the host esterase that is responsible for cleaving the ELQ alkoxycarbonate ester prodrugs may have a preference for promoieties with a shorter alkyl side chain. Mice dosed with ELQ-331 maintained an ELQ-300 plasma concentration above the estimated minimum effective

concentration (MEC) of 60-80 nM even at 70 days after dosing, so an additional blood sample from these mice was collected at 77 days.

The unusually long decay curve for all three IM prodrugs indicates long-term storage of the prodrugs outside of the bloodstream. There are multiple possibilities which could explain the sustained release of ELQ-300. The prodrugs could remain in the muscle tissue close to the injection site, forming a 'depot' from which small amounts are metered out into the blood (Kalicharan 2016). Alternatively, the prodrugs may enter the bloodstream initially but then quickly become sequestered in a secondary tissue, such as fat (Larsen 2001, Wright 2012). Further exploration of this atypical drug biodistribution will be required to understand the alkoxycarbonate ester prodrugs.

Conclusion

An intramuscular long-acting injectable antimalarial drug would be a highly impactful tool in the fight for global malaria eradication. A drug product of this kind could make significant inroads against seasonal malaria, provide protection for pregnant women, and protect workers moving through malarious regions.

The antimalarial compound ELQ-300 is highly effective against *Plasmodium* parasites *in vitro* and *in vivo*, but is limited by restrictive physiochemical properties. Prodrug strategies led to the development of ELQ-331, an alkoxycarbonate ester prodrug with excellent ELQ-300 delivery with oral dosing.

In optimizing the pro-moiety of the alkoxycarbonate esters for intramuscular delivery, compounds with long terminal alkyl chains appeared to have superior physiochemical properties. Alkoxycarbonate ester prodrugs with long alkyl chains such as ELQ-494 and ELQ-495 showed reduced melting points and dramatically improved solubility in IM injection vehicles such as

sesame oil. All compounds in this series maintained on-target *in vitro* antimalarial activity. All tested alkoxycarbonate ester prodrugs protected mice from developing malaria for 5.5 weeks, the full duration of the study.

Somewhat unexpectedly, IM dosing with the original alkoxycarbonate ester prodrug ELQ-331 led to the longest lasting antimalarial prophylaxis. ELQ-331-treated mice maintained plasma concentrations of ELQ-300 greater than the minimum effective concentration (60-80 nM) for 77 days, a longer duration than mice treated with ELQ-494 or ELQ-495. Despite seemingly inferior physiochemical properties, ELQ-331 remains the optimal candidate for development both as an oral antimalarial and as a long-acting IM injectable. Preclinical development of ELQ-331 in collaboration with the Medicines for Malaria Venture is currently underway.

Chapter 6 : Conclusion

Summary and Conclusions

In 2022, the global fight for malaria eradication stands at a crossroads. On one hand, the first broadly effective malaria vaccine is now available for population-scale application. On the other hand, drug resistance to artemisinin-combination therapies continues to spread and has now emerged in Africa, where the deadly malaria pathogen *Plasmodium falciparum* is prevalent. In the midst of these developments for malaria, the COVID-19 pandemic continues to put additional strain on healthcare infrastructure in malaria-endemic countries, thereby stalling eradication projects like the distribution of insecticide-treated nets. Though the global disease burden of malaria has been gradually declining for decades, the past two years have seen growth in malaria morbidity and mortality. It remains to be seen whether this uptick is a temporary setback or a full-scale reversal of malaria eradication.

Now more than ever, it is necessary to develop novel classes of antimalarial drugs which are effective in drug-resistant malaria. One such class may be the aminoguanidines, structures derived from the anticoccidial drug robenidine. In the research comprising this dissertation, aminoguanidines were evaluated as potential antimalarial drug candidates.

In the first structure-activity relationship study of the aminoguanidines in malaria (Chapter 3), it was determined that robenidine and many of its analogs were active against malaria both *in vitro* and *in vivo*. Compounds with electron-withdrawing groups at the meta or para position of the scaffold were found to be the most active, and a 3-CN substituent was found to have the greatest effect on improving *in vitro* potency. It was also discovered that a substituent at the para position was required to maintain sufficient metabolic stability for *in vivo* efficacy. The 3-CN, 4-F aminoguanidine **1** was identified as a promising lead compound.

A structure-activity relationship study with a second set of compounds expanded on the previous findings (Chapter 4). It was demonstrated that substitution of oxygen or sulfur for the central nitrogen atom of the aminoguanidine core structure removed nearly all antimalarial activity. A series of bicyclic aminoguanidines was prepared with many compounds exhibiting *in vitro* potency, particularly bis-quinolines bridged by the aminoguanidine linker at the 3 or 4 position of the ring system. None of these compounds exhibited efficacy *in vivo*, which in the case of the quinolines was likely due to poor metabolic stability. The asymmetrical compounds **86** and **77** were unusually potent *in vitro* compared with their symmetrical analogs. Conversion from the hydrochloride salt to the free base improved *in vitro* potency for **68** and **1** and dramatically improved *in vivo* efficacy for **1**. Two new potential lead compounds were identified: **76**, a 3-CN, 4-OCF_3 compound, and **77**, an asymmetrical combination of **16** and **1** with 3-CN, 4-F, and 3'-H, 4'-OCF_3.

In a second project on the endochin-like quinolone (ELQ) class of antimalarial drugs, alkoxycarbonate ester prodrugs of the lead drug candidate ELQ-300 were prepared for delivery by intramuscular injection (IM). Prodrugs were prepared with the outer alkoxy moiety extending from one up to ten carbons in length. Melting point decreased and sesame oil (an IM vehicle) solubility increased with increasing carbon chain length. The ethyl (ELQ-331) and heptyl (ELQ-392) alkoxycarbonate ester prodrugs provided prophylaxis to blood stage malaria in mice for 5.5 weeks, the full duration of the study. The ethyl (ELQ-331), nonyl (ELQ-494) and decyl (ELQ-495) prodrugs all remained above a minimum protective concentration for over 30 days, though ELQ-331 retained the longest duration at 77 days post IM injection. ELQ-331 was selected as the most suitable candidate for continued preclinical development. Recently, ELQs even more potent than ELQ-300 have been identified. These compounds are also very crystalline and insoluble, and ethyl alkoxycarbonate pro-moiety of ELQ-331 has been used to facilitate testing of these compounds *in vivo*. The combination of and ELQ together with an aminoquanidine based antimalarial agent is currently under consideration.

Future Directions

Down-selection of a Preclinical Aminoguanidine Drug Candidate

Three of the aminoguanidine compounds had excellent antimalarial properties and show potential for development as antimalarial drug candidates. Among these three compounds (**1**, **76**, and **77**), none of the compounds was superior across all of the metrics considered thus far, including *in vitro* potency, *in vivo* efficacy, and metabolic stability. Each compound has its own strengths and weaknesses as a lead compound.

The 3-CN, 4-F compound **1** can be easily prepared in one synthetic step from commercially available starting materials and requires little to no purification other than filtration out of the reaction mixture. It is highly potent *in vitro* across both sensitive and drug-resistant strains of *P. falciparum* with single digit nanomolar activity in D6. It is highly effective *in vivo* in a four-day Peters test in murine *P. yoelii*. Its metabolic stability is moderate with a half-life of approximately 3 hr. In a pharmacokinetic profile of **1**, the compound showed poor oral bioavailability.

The 3-CN, 4-OCF_3 compound **76** requires two synthetic steps. The first, substitution of 3-iodo, 4-trifluoromethoxybenzaldehyde to form 3-cyano-4-trifluormethoxybenzaldehyde, uses the toxic material zinc cyanide and requires column chromatography for separation (the second step is simpler and is analogous to the synthesis of **1** above). The *in vitro* potency of **76** is moderately high with IC_{50} values in the mid to high double digits depending on the strain, though it is not among the top 10 compounds. The ED_{50} is very low though not as low as for compound **1**. The metabolic stability of **76** is the best out of all tested compounds, with no detectable degradation

after a 1 hr incubation with murine pooled liver microsomes. The oral bioavailability of **76** is not yet known.

The synthesis of the asymmetrical compound **77** requires only one synthetic step, but this step produces a mixture of products that can only be separated by reverse phase column chromatography in very small aliquots at a time. **77** has the best *in vitro* potency of any of the aminoguanidines and is the only compound to achieve single digit nanomolar IC_{50}s across all drug-resistant strains. The *in vivo* ED_{50} of **77** is very close to that of **76** and is slightly higher than that of **1**. The metabolic stability of **77** is better than **1** but slightly worse than **76**. Again, a pharmacokinetic profile of this compound will allow for additional comparisons with **1**.

To summarize, **1** has the most scalable synthesis and best *in vivo* activity but is less metabolically stable (it remains to be seen if metabolism of 1 in pooled human microsomes improves over what is seen in murine microsomes). **76** has the best metabolic stability but is less potent *in vitro*. **77** is the most intrinsically potent but requires a cumbersome purification. Additional testing of these three compounds will be necessary to select a lead compound for preclinical development. First, pharmacokinetics profiles of **76** and **77** should be acquired to directly compare key variables such as oral C_{max}, *in vivo* biological half-life, and oral bioavailability. The free bases of **76** and **77** should also be prepared and tested to see if this form of the compounds improves their activity as it did for **1.** Other properties such as activity against the liver stage, transmission stages in the human and insect hosts, and *in vivo* toxicology could also be deciding factors.

Exploration of the Aminoguanidine Drug Action

The alkyne-benzophenone probe molecule **86** identified two potential biological targets with masses of 75 and 100 kDa in a pilot validation study. The validity of these results must be supported with an additional set of experiments before further action is taken with the potential

targets. First, the fractional protein binding of **86** can be measured to determine the extent of its nonspecific binding. Second, a competition experiment can be performed in which an inactive aminoguanidine is co-administered to the parasite lysates with the probe. If the inactive molecule causes the probe hits to disappear, this indicates that the hits were non-specific. If both of these experiments show that the probe does bind specifically, the experiment can be repeated and the targeted bands can be removed and sequenced by LCMS-MS to reveal the biological target of the aminoguanidines. This technique can be supplemented with additional experiments including drug resistance selection and whole-genome sequencing.

Another set of experiments that will provide additional information about the antimalarial activity of the aminoguanidines includes testing the compounds in other life cycle stages and species of malaria. Assessing liver stage activity was attempted but was unsuccessful for reasons unrelated to the compounds; this information remains a high priority for study. The compounds can also be evaluated for transmission blocking in the mosquito stage or tested in other pathogenic malaria species such as *P. vivax*.

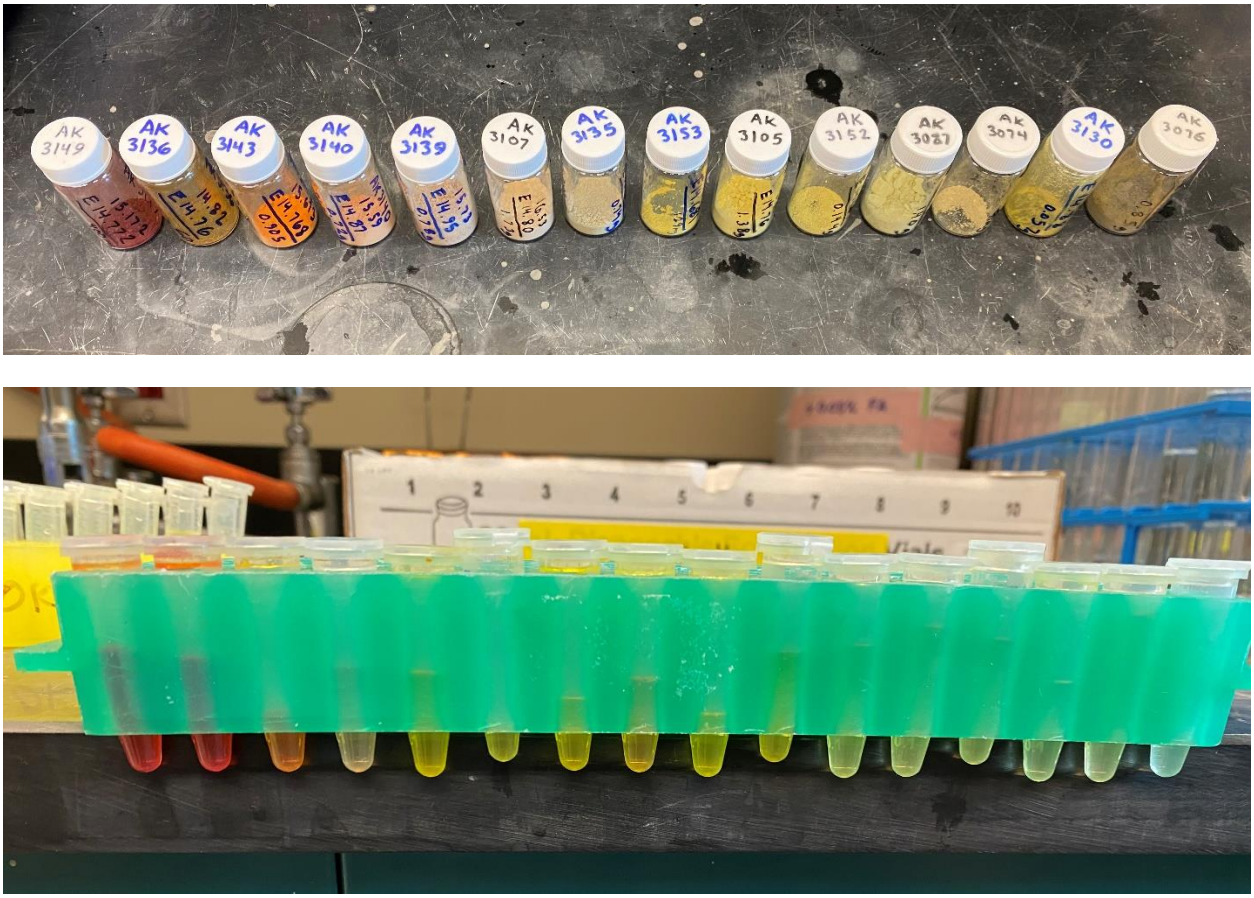

Figure 6-1: Color spectrum of the aminoguanidine library (other compounds were colorless). Top: pure aminoguanidine hydrochloride salts. Bottom: aminoguanidines at 10 mM in DMSO.

Aminoguanidines in Other Pathogens

Several members of the aminoguanidine compound library created during this dissertation research are currently being evaluated in other parasitic pathogens. The full library of compounds is being tested against the toxoplasmosis pathogen *Toxoplasma gondii* by members of Dr. Stone Doggett's research group. Initial results from these experiments show that the only a subset of the malaria hit compounds are also hits in *Toxoplasma*, however the bicyclic aminoguanidines appear to be active against the parasites. The full library is also being tested by Dr. Jenifer Keiser's group in *Schistosoma mansoni*, a parasitic worm. Despite the morphological differences

between these two pathogens, there is a striking level of correlation between antischistosomal and antimalarial activity among the aminoguanidines. A subset of the aminoguanidines was tested in *Leishmania donovani* by Dr. Scott Landfear's group, and the 4-OCF_3 compound **16** and the 4-$N(Me)_2$ compound **28** were identified as selective hits. A subset of the aminoguanidines is also being tested in *Babesia microti* by Dr. Choukri ben Mamoun's group, though no results are yet available. Taken together with the research of this dissertation and the antimicrobial work performed by Trott and McCluskey, these results make it clear that the activity of robenidine and its aminoguanidine derivatives go well beyond *Eimeria*, for which the drug has been used safely and exclusively for over 50 years.

References

Aborode, A. T., David, K. B., Uwishema, O., Nathaniel, A. L., Imisioluwa, J. O., Onigbinde, S. B., & Farooq, F. (2021). Fighting COVID-19 at the Expense of Malaria in Africa: The Consequences and Policy Options. *The American journal of tropical medicine and hygiene*, *104*(1), 26–29.

Abraham, R. J., Stevens, A. J., Young, K. A., Russell, C., Qvist, A., Khazandi, M., Wong, H. S., Abraham, S., Ogunniyi, A. D., Page, S. W., O'Handley, R., McCluskey, A., & Trott, D. J. (2016). Robenidine Analogues as Gram-Positive Antibacterial Agents. *Journal of medicinal chemistry*, *59*(5), 2126–2138.

Abraham, R. J., Abraham, S., Stevens, A. J., Page, S. W., McCluskey, A., Trott, D. J., & O'Handley, R. M. (2019). Aminoguanidines: New leads for treatment of Giardia duodenalis infection. *International journal for parasitology. Drugs and drug resistance*, *10*, 38–44.

Adams, J. H., & Mueller, I. (2017). The Biology of *Plasmodium vivax*. *Cold Spring Harbor perspectives in medicine*, *7*(9), a025585.

Afolabi, M. O., Tiono, A. B., Adetifa, U. J., Yaro, J. B., Drammeh, A., Nébié, I., Bliss, C., Hodgson, S. H., Anagnostou, N. A., Sanou, G. S., Jagne, Y. J., Ouedraogo, O., Tamara, C., Ouedraogo, N., Ouedraogo, M., Njie-Jobe, J., Diarra, A., Duncan, C. J., Cortese, R., Nicosia, A., Sirima, S. B. (2016). Safety and Immunogenicity of ChAd63 and MVA ME-TRAP in West African Children and Infants. *Molecular therapy: the journal of the American Society of Gene Therapy*, *24*(8), 1470–1477.

Ahvazi, B. C., Jacobs, P., & Stevenson, M. M. (1995). Role of macrophage-derived nitric oxide in suppression of lymphocyte proliferation during blood-stage malaria. *Journal of leukocyte biology*, *58*(1), 23–31.

Alemu, A., Shiferaw, Y., Addis, Z., Mathewos, B., & Birhan, W. (2013). Effect of malaria on HIV/AIDS transmission and progression. *Parasites & vectors*, *6*, 18.

Ansorge I., Benting J., Bhakdi S., Lingelbach K. (1996) Protein sorting in Plasmodium falciparuminfected red blood cells permeabilized with the pore-forming protein streptolysin *Organic. Biochemistry Journal* 315, 307–14.

Antinori, S., Galimberti, L., Milazzo, L., & Corbellino, M. (2012). Biology of human malaria plasmodia including *Plasmodium knowlesi*. *Mediterranean journal of hematology and infectious diseases*, *4*(1), e2012013.

Bacchi, C. J., Brun, R., Croft, S. L., Alicea, K., & Bühler, Y. (1996). In vivo trypanocidal activities of new S-adenosylmethionine decarboxylase inhibitors. *Antimicrobial agents and chemotherapy*, *40*(6), 1448–1453.

Bakhtari, S. K., & Jíra, J. (1988). Chemotherapy of experimental toxoplasmosis with special reference to robenidine. *Folia parasitologica*, *35*(3), 193–198.

Bakshi, R. P., Tatham, L. M., Savage, A. C., Tripathi, A. K., Mlambo, G., Ippolito, M. M., Nenortas, E., Rannard, S. P., Owen, A., & Shapiro, T. A. (2018). Long-acting injectable atovaquone nanomedicines for malaria prophylaxis. *Nature communications*, *9*(1), 315.

Baumeister, S., A. Burgwedel, U.G. Maier and Lingelbach, K. (1999) Reconstitution of protein transport across the vacuolar membrane in *Plasmodium falciparum*-infected permeabilized erythrocytes. *Novartis Foundation Symposia* 226, 145–154.

Beck, J. S., Logie, A. W., & McGregor, I. A. (1970). Antigenic changes during the life cycle of *Plasmodium falciparum*. *Experientia*, *26*(12), 1365–1366.

Bendrat, K., Berger, B. J., & Cerami, A. (1995). Haem polymerization in malaria. *Nature*, *378*(6553), 138–139.

Berger, H., Wang, G. T., Shor, A. L., Gale, G. O., & Simkins, K. L. (1974). Safety evaluation of robenidine in the feed of broiler chickens. *Poultry science*, *53*(3), 1013–1015.

Beswick, T. C., Willert, E. K., & Phillips, M. A. (2006). Mechanisms of allosteric regulation of Trypanosoma cruzi S-adenosylmethionine decarboxylase. *Biochemistry*, *45*(25), 7797–7807.

Brun, R., Burri, C., & Gichuki, C. W. (2001). The story of CGP 40 215: studies on its efficacy and pharmacokinetics in African green monkey infected with *Trypanosoma brucei* rhodesiense. *Tropical medicine & international health: TM & IH*, *6*(5), 362–368.

Burrows, J. N., Chibale, K., & Wells, T. N. (2011). The state of the art in anti-malarial drug discovery and development. *Current topics in medicinal chemistry*, *11*(10), 1226–1254.

Burrows, J. N., Duparc, S., Gutteridge, W. E., Hooft van Huijsduijnen, R., Kaszubska, W., Macintyre, F., Mazzuri, S., Möhrle, J. J., & Wells, T. (2017). New developments in anti-malarial target candidate and product profiles. *Malaria journal*, *16*(1), 26.

Camarda, G., Jirawatcharadech, P., Priestley, R. S., Saif, A., March, S., Wong, M., Leung, S., Miller, A. B., Baker, D. A., Alano, P., Paine, M., Bhatia, S. N., O'Neill, P. M., Ward, S. A., & Biagini, G. A. (2019). Antimalarial activity of primaquine operates via a two-step biochemical relay. *Nature communications*, *10*(1), 3226.

Carter, T. E., Mekonnen, S. K., Lopez, K., Bonnell, V., Damodaran, L., Aseffa, A., & Janies, D. A. (2018). Glucose-6-Phosphate Dehydrogenase Deficiency Genetic Variants in Malaria Patients in Southwestern Ethiopia. *The American journal of tropical medicine and hygiene*, *98*(1), 83–87.

de Carvalho, L. P., Groeger-Otero, S., Kreidenweiss, A., Kremsner, P. G., Mordmüller, B., & Held, J. (2022). Boromycin has Rapid-Onset Antibiotic Activity Against Asexual and Sexual Blood Stages of *Plasmodium falciparum*. *Frontiers in cellular and infection microbiology*, *11*, 802294.

Chatterjee, A.K. TCP4: intra-muscular injections for malaria chemoprotection.In: Symposium: what kind of molecules are needed to control and eradicate malaria? (2017) *ASTMH 66th Annual Meeting.* Baltimore, MD.

Chootong, P., Ntumngia, F. B., VanBuskirk, K. M., Xainli, J., Cole-Tobian, J. L., Campbell, C. O., Fraser, T. S., King, C. L., & Adams, J. H. (2010). Mapping epitopes of the *Plasmodium vivax* Duffy binding protein with naturally acquired inhibitory antibodies. *Infection and immunity*, *78*(3), 1089–1095.

Claes, Z., Jonkhout, M., Crespillo-Casado, A., & Bollen, M. (2019). The antibiotic robenidine exhibits guanabenz-like cytoprotective properties by a mechanism independent of protein phosphatase PP1:PPP1R15A. *The Journal of biological chemistry*, *294*(36), 13478–13486.

Coleman, M., Hemingway, J., Gleave, K. A., Wiebe, A., Gething, P. W., & Moyes, C. L. (2017). Developing global maps of insecticide resistance risk to improve vector control. *Malaria journal*, *16*(1), 86.

Collins, W. E., & Jeffery, G. M. (2005). *Plasmodium ovale*: parasite and disease. *Clinical microbiology reviews*, *18*(3), 570–581.

Covell, G. (1960). Relationship between malarial parasitaemia and symptoms of the disease: a review of the literature. *Bulletin of the World Health Organization*, *22*(6), 605–619.

Dahl, E. L., & Rosenthal, P. J. (2007). Multiple antibiotics exert delayed effects against the *Plasmodium falciparum* apicoplast. *Antimicrobial agents and chemotherapy*, *51*(10), 3485–3490.

Das Gupta, R., Krause-Ihle, T., Bergmann, B., Müller, I. B., Khomutov, A. R., Müller, S., Walter, R. D., & Lüersen, K. (2005). 3-Aminooxy-1-aminopropane and derivatives have an antiproliferative effect on cultured *Plasmodium falciparum* by decreasing intracellular polyamine concentrations. *Antimicrobial agents and chemotherapy*, *49*(7), 2857–2864.

Davies, C. S., Pudney, M., Matthews, P. J., & Sinden, R. E. (1989). The causal prophylactic activity of the novel hydroxynaphthoquinone 566C80 against *Plasmodium berghei* infections in rats. *Acta Leidensia*, *58*(2), 115–128.

Dec, M., Puchalski, A., Stępień-Pyśniak, D., Marek, A., & Urban-Chmiel, R. (2020). Susceptibility of chicken *Lactobacillus* bacteria to coccidiostats. *The Journal of veterinary medical science*, *82*(3), 333–336.

Dondorp, A. M., Nosten, F., Yi, P., Das, D., Phyo, A. P., Tarning, J., Lwin, K. M., Ariey, F., Hanpithakpong, W., Lee, S. J., Ringwald, P., Silamut, K., Imwong, M., Chotivanich, K., Lim, P., Herdman, T., An, S. S., Yeung, S., Singhasivanon, P., Day, N. P., White, N. J. (2009). Artemisinin resistance in *Plasmodium falciparum* malaria. *The New England journal of medicine*, *361*(5), 455–467.

Douglas, N. M., Anstey, N. M., Angus, B. J., Nosten, F., & Price, R. N. (2010). Artemisinin combination therapy for *vivax* malaria. *The Lancet. Infectious diseases*, *10*(6), 405–416.

Dvorak, J. A., Miller, L. H., Whitehouse, W. C., & Shiroishi, T. (1975). Invasion of erythrocytes by malaria merozoites. *Science (New York, N.Y.)*, *187*(4178), 748–750.

Fairley, N. H. (1949). Malaria; with special reference to certain experimental, clinical, and chemotherapeutic investigations; the life cycle. *British medical journal*, *2*(4632), 825–830.

Findlay, G.W., & Stevenson, A.C. (1944). Investigations in the Chemotherapy of Malaria in West Africa. II. Malaria Suppression-Quinine and Mepacrine. *Annals of Tropical Medicine and Parasitology, 38*, 168-187.

Fivelman, Q. L., Adagu, I. S., & Warhurst, D. C. (2004). Modified fixed-ratio isobologram method for studying in vitro interactions between atovaquone and proguanil or dihydroartemisinin against

drug-resistant strains of *Plasmodium falciparum*. *Antimicrobial agents and chemotherapy*, *48*(11), 4097–4102.

Fried, M., & Duffy, P. E. (2017). Malaria during Pregnancy. *Cold Spring Harbor perspectives in medicine*, *7*(6), a025551.

Frueh, L., Li, Y., Mather, M. W., Li, Q., Pou, S., Nilsen, A., Winter, R. W., Forquer, I. P., Pershing, A. M., Xie, L. H., Smilkstein, M. J., Caridha, D., Koop, D. R., Campbell, R. F., Sciotti, R. J., Kreishman-Deitrick, M., Kelly, J. X., Vesely, B., Vaidya, A. B., & Riscoe, M. K. (2017). Alkoxycarbonate Ester Prodrugs of Preclinical Drug Candidate ELQ-300 for Prophylaxis and Treatment of Malaria. *ACS infectious diseases*, *3*(10), 728–735.

Fukuda, N., Tachibana, S. I., Ikeda, M., Sakurai-Yatsushiro, M., Balikagala, B., Katuro, O. T., Yamauchi, M., Emoto, S., Hashimoto, M., Yatsushiro, S., Sekihara, M., Mori, T., Hirai, M., Opio, W., Obwoya, P. S., Auma, M. A., Anywar, D. A., Kataoka, M., Palacpac, N., Odongo-Aginya, E. I., Mita, T. (2021). Ex vivo susceptibility of *Plasmodium falciparum* to antimalarial drugs in Northern Uganda. *Parasitology international*, *81*, 102277.

Galinski, M. R., & Barnwell, J. W. (2008). *Plasmodium vivax*: who cares? *Malaria journal*, *7 Suppl 1*(Suppl 1), S9.

Gluzman, I. Y., Francis, S. E., Oksman, A., Smith, C. E., Duffin, K. L., & Goldberg, D. E. (1994). Order and specificity of the *Plasmodium falciparum* hemoglobin degradation pathway. *The Journal of clinical investigation*, *93*(4), 1602–1608.

Grilo, M. L., Vanstreels, R. E., Wallace, R., García-Párraga, D., Braga, É. M., Chitty, J., Catão-Dias, J. L., & Madeira de Carvalho, L. M. (2016). Malaria in penguins - current perceptions. *Avian pathology: journal of the W.V.P.A*, *45*(4), 393–407.

Grande, E. N., Sanchez, A. R., & Sanchez, F. R. (1956). The treatment of malaria with tetracycline. *Antibiotic medicine & clinical therapy (New York, NY)*, *3*(3), 193–196.

Grunnet, L. G., Bygbjerg, I. C., Mutabingwa, T. K., Lajeunesse-Trempe, F., Nielsen, J., Schmiegelow, C., Vaag, A. A., Ramaiya, K., & Christensen, D. L. (2022). Influence of placental and peripheral malaria exposure in fetal life on cardiometabolic traits in adult offspring. *BMJ open diabetes research & care*, *10*(2).

Gutman, J., Kalilani, L., Taylor, S., Zhou, Z., Wiegand, R. E., Thwai, K. L., Mwandama, D., Khairallah, C., Madanitsa, M., Chaluluka, E., Dzinjalamala, F., Ali, D., Mathanga, D. P., Skarbinski, J., Shi, Y. P., Meshnick, S., & ter Kuile, F. O. (2015). The A581G Mutation in the Gene Encoding *Plasmodium falciparum* Dihydropteroate Synthetase Reduces the Effectiveness of Sulfadoxine-Pyrimethamine Preventive Therapy in Malawian Pregnant Women. *The Journal of infectious diseases*, *211*(12), 1997–2005.

Gwadz, R. W., Carter, R., & Green, I. (1979). Gamete vaccines and transmission-blocking immunity in malaria. *Bulletin of the World Health Organization*, *57 Suppl 1*(Suppl), 175–180.

Hadley, T. J. (1986). Invasion of erythrocytes by malaria parasites: a cellular and molecular overview. *Annual review of microbiology*, *40*, 451–477.

Hansen, M., Krogh, K. A., Brandt, A., Christensen, J. H., & Halling-Sørensen, B. (2009). Fate and antibacterial potency of anticoccidial drugs and their main abiotic degradation products. *Environmental pollution (Barking, Essex: 1987)*, *157*(2), 474–480.

Heidelberger, M., & Prout, C. (1946). Studies in human malaria; an attempt at vaccination of paretics against blood-borne infection with *Pl. vivax*. *Journal of immunology (Baltimore, Md. : 1950)*, *53*, 109–112.

Hemingway, J., Ranson, H., Magill, A., Kolaczinski, J., Fornadel, C., Gimnig, J., Coetzee, M., Simard, F., Roch, D. K., Hinzoumbe, C. K., Pickett, J., Schellenberg, D., Gething, P., Hoppé, M., & Hamon, N. (2016). Averting a malaria disaster: will insecticide resistance derail malaria control?. *Lancet (London, England)*, *387*(10029), 1785–1788.

Hooft van Huijsduijnen, R., & Wells, T. N. (2018). The antimalarial pipeline. *Current opinion in pharmacology*, *42*, 1–6.

Huang, Q., Cao, J., Zhou, Y., Huang, J., Gong, H., Zhang, H., Zhu, X. Q., & Zhou, J. (2017). *Babesia microti* Aldo-keto Reductase-Like Protein Involved in Antioxidant and Anti-parasite Response. *Frontiers in microbiology*, *8*, 2006.

Imboden, C. A., Jr, Cooper, W. C., Coatney, G. R., & Jefferey, G. M. (1950). Studies in human malaria. XXIX. Trials of aureomycin, chloramphenicol, penicillin, and dihydrostreptomycin against the Chesson strain of *Plasmodium vivax*. *Journal. National Malaria Society (U.S.)*, *9*(4), 377–380.

Ito, S., Tsunoda, K., & Nishikawa, H. (1974). Effects of robenidine and some other drugs on mice experimentally infected with *toxoplasma*. *National Institute of Animal Health quarterly*, *14*(3), 129–136.

John, C. C., Bangirana, P., Byarugaba, J., Opoka, R. O., Idro, R., Jurek, A. M., Wu, B., & Boivin, M. J. (2008). Cerebral malaria in children is associated with long-term cognitive impairment. *Pediatrics*, *122*(1), e92–e99.

Kalicharan, R. W., Schot, P., & Vromans, H. (2016). Fundamental understanding of drug absorption from a parenteral oil depot. *European journal of pharmaceutical sciences : official journal of the European Federation for Pharmaceutical Sciences*, *83*, 19–27.

Kantor, S., Kennett, R. L., Jr, Waletzky, E., & Tomcufcik, A. S. (1970). 1,3-Bis(p-chlorobenzylideneamino)guanidine hydrochloride (robenzidene): new poultry anticoccidial agent. *Science (New York, N.Y.)*, *168*(3929), 373–374.

Kennett, R. L., Kantor, S., & Gallo, A. (1974). Efficacy studies with robenidine, a new type of anticoccidial, in the diet. *Poultry science*, *53*(3), 978–986.

Khazandi, M., Pi, H., Chan, W. Y., Ogunniyi, A. D., Sim, J., Venter, H., Garg, S., Page, S. W., Hill, P. B., McCluskey, A., & Trott, D. J. (2019). *In vitro* Antimicrobial Activity of Robenidine, Ethylenediaminetetraacetic Acid and Polymyxin B Nonapeptide Against Important Human and Veterinary Pathogens. *Frontiers in microbiology*, *10*, 837.

Köhler, S., Delwiche, C. F., Denny, P. W., Tilney, L. G., Webster, P., Wilson, R. J., Palmer, J. D., & Roos, D. S. (1997). A plastid of probable green algal origin in Apicomplexan parasites. *Science (New York, N.Y.)*, *275*(5305), 1485–1489.

Krollenbrock, A., Li, Y., Kelly, J. X., & Riscoe, M. K. (2021). Robenidine Analogues Are Potent Antimalarials in Drug-Resistant *Plasmodium falciparum*. *ACS infectious diseases*, *7*(7), 1956–1968.

Krylov, M. V., Sokolov, A. N., Zaĭonts, V. I., Korovitskaia, L. A., & Zakharova, N. A. (1976). Khimotsid dlia lecheniia i profilaktiki toksoplazmoza [Khimotsid for treatment and prevention of toxoplasmosis]. *Veterinariia*, (11), 69–71.

Killeen, G. F., Smith, T. A., Ferguson, H. M., Mshinda, H., Abdulla, S., Lengeler, C., & Kachur, S. P. (2007). Preventing childhood malaria in Africa by protecting adults from mosquitoes with insecticide-treated nets. *PLoS medicine*, *4*(7), e229.

Killeen, G. F., Tatarsky, A., Diabate, A., Chaccour, C. J., Marshall, J. M., Okumu, F. O., Brunner, S., Newby, G., Williams, Y. A., Malone, D., Tusting, L. S., & Gosling, R. D. (2017). Developing an expanded vector control toolbox for malaria elimination. *BMJ global health*, *2*(2), e000211.

Kim, J., Tan, Y. Z., Wicht, K. J., Erramilli, S. K., Dhingra, S. K., Okombo, J., Vendome, J., Hagenah, L. M., Giacometti, S. I., Warren, A. L., Nosol, K., Roepe, P. D., Potter, C. S., Carragher, B., Kossiakoff, A. A., Quick, M., Fidock, D. A., & Mancia, F. (2019). Structure and drug resistance of the *Plasmodium falciparum* transporter PfCRT. *Nature*, *576*(7786), 315–320.

Lambros, C., & Vanderberg, J. P. (1979). Synchronization of *Plasmodium falciparum* erythrocytic stages in culture. *The Journal of parasitology*, *65*(3), 418–420.

Larsen, S. W., Rinvar, E., Svendsen, O., Lykkesfeldt, J., Friis, G. J., & Larsen, C. (2001). Determination of the disappearance rate of iodine-125 labelled oils from the injection site after intramuscular and subcutaneous administration to pigs. *International journal of pharmaceutics*, *230*(1-2), 67–75.

Llanos-Cuentas, A., Lacerda, M., Hien, T. T., Vélez, I. D., Namaik-Larp, C., Chu, C. S., Villegas, M. F., Val, F., Monteiro, W. M., Brito, M., Costa, M., Chuquiyauri, R., Casapía, M., Nguyen, C. H., Aruachan, S., Papwijitsil, R., Nosten, F. H., Bancone, G., Angus, B., Duparc, S., Green, J. A. (2019). Tafenoquine versus Primaquine to Prevent Relapse of *Plasmodium vivax* Malaria. *The New England journal of medicine*, *380*(3), 229–241.

Long, P. L., & Millard, B. J. (1978). Studies on Eimeria grenieri in the guinea fowl (Numida meleagris). *Parasitology*, *76*(1), 1–9.

Luzzatto, L., Ally, M., & Notaro, R. (2020). Glucose-6-phosphate dehydrogenase deficiency. *Blood*, *136*(11), 1225–1240.

Mahmoudi, S., & Keshavarz, H. (2018). Malaria Vaccine Development: The Need for Novel Approaches: A Review Article. *Iranian journal of parasitology*, *13*(1), 1–10.

Matuschewski K. (2017). Vaccines against malaria-still a long way to go. *The FEBS journal*, *284*(16), 2560–2568.

McFadden G. I. (2011). The apicoplast. *Protoplasma*, *248*(4), 641–650.

Meis, J. F., Verhave, J. P., Jap, P. H., Sinden, R. E., & Meuwissen, J. H. (1983). Malaria parasites--discovery of the early liver form. *Nature*, *302*(5907), 424–426.

Mendis, K., Sina, B. J., Marchesini, P., & Carter, R. (2001). The neglected burden of *Plasmodium vivax* malaria. *The American journal of tropical medicine and hygiene*, *64*(1-2 Suppl), 97–106.

Miley, G. P., Pou, S., Winter, R., Nilsen, A., Li, Y., Kelly, J. X., Stickles, A. M., Mather, M. W., Forquer, I. P., Pershing, A. M., White, K., Shackleford, D., Saunders, J., Chen, G., Ting, L. M., Kim, K., Zakharov, L. N., Donini, C., Burrows, J. N., Vaidya, A. B., … Riscoe, M. K. (2015). ELQ-300 prodrugs for enhanced delivery and single-dose cure of malaria. *Antimicrobial agents and chemotherapy*, *59*(9), 5555–5560.

Miller, L. H., Baruch, D. I., Marsh, K., & Doumbo, O. K. (2002). The pathogenic basis of malaria. *Nature*, *415*(6872), 673–679.

Molnár, K., & Ostoros, G. (2007). Efficacy of some anticoccidial drugs for treating coccidial enteritis of the common carp caused by *Goussia carpelli* (Apicomplexa: Eimeriidae). *Acta veterinaria Hungarica*, *55*(1), 67–76.

Mukhopadhyay, R., Kapoor, P., & Madhubala, R. (1996). Antileishmanial effect of a potent S-adenosylmethionine decarboxylase inhibitor: CGP 40215A. *Pharmacological research*, *33*(1), 67–70.

Nagashima, A., Kaneda, S. Amada, J., Inoue, T., Ono, A., Nagata, O., Ashizawa, N., Matsumoto, K. (2006). *New pyridazine derivative* (Japanese Patent No. JP2006270450A). Fujiyakuhin Co. Ltd. https://patents.google.com/patent/JP2008088107A/en

Nilsen, A., LaCrue, A. N., White, K. L., Forquer, I. P., Cross, R. M., Marfurt, J., Mather, M. W., Delves, M. J., Shackleford, D. M., Saenz, F. E., Morrisey, J. M., Steuten, J., Mutka, T., Li, Y., Wirjanata, G., Ryan, E., Duffy, S., Kelly, J. X., Sebayang, B. F., Zeeman, A. M., … Riscoe, M. K. (2013). Quinolone-3-diarylethers: a new class of antimalarial drug. *Science translational medicine*, *5*(177), 177ra37.

Nilsen, A., Miley, G. P., Forquer, I. P., Mather, M. W., Katneni, K., Li, Y., Pou, S., Pershing, A. M., Stickles, A. M., Ryan, E., Kelly, J. X., Doggett, J. S., White, K. L., Hinrichs, D. J., Winter, R. W., Charman, S. A., Zakharov, L. N., Bathurst, I., Burrows, J. N., Vaidya, A. B., … Riscoe, M. K. (2014). Discovery, synthesis, and optimization of antimalarial 4(1H)-quinolone-3-diarylethers. *Journal of medicinal chemistry*, *57*(9), 3818–3834.

Noedl, H., Se, Y., Schaecher, K., Smith, B. L., Socheat, D., Fukuda, M. M., & Artemisinin Resistance in Cambodia 1 (ARC1) Study Consortium (2008). Evidence of artemisinin-resistant malaria in western Cambodia. *The New England journal of medicine*, *359*(24), 2619–2620.

Nussenzweig, R. S., Vanderberg, J., Most, H., & Orton, C. (1967). Protective immunity produced by the injection of x-irradiated sporozoites of *plasmodium berghei*. *Nature*, *216*(5111), 160–162.

Nussenzweig, R. S., & Nussenzweig, V. (1984). Development of sporozoite vaccines. *Philosophical transactions of the Royal Society of London. Series B, Biological sciences*, *307*(1131), 117–128.

Oduola, A. M., Weatherly, N. F., Bowdre, J. H., & Desjardins, R. E. (1988). Plasmodium falciparum: cloning by single-erythrocyte micromanipulation and heterogeneity *in vitro*. *Experimental parasitology*, *66*(1), 86–95.

Ogbunude, P. O., & Asiri, S. A. (2001). In vitro effect of diamidines on intracellular polyamines of *Acanthamoeba polyphaga*. *Drugs under experimental and clinical research*, *27*(4), 127–133.

Ogunniyi, A. D., Khazandi, M., Stevens, A. J., Sims, S. K., Page, S. W., Garg, S., Venter, H., Powell, A., White, K., Petrovski, K. R., Laven-Law, G., Tótoli, E. G., Salgado, H. R., Pi, H., Coombs, G. W., Shinabarger, D. L., Turnidge, J. D., Paton, J. C., McCluskey, A., & Trott, D. J. (2017). Evaluation of robenidine analog NCL195 as a novel broad-spectrum antibacterial agent. *PloS one*, *12*(9), e0183457.

Olotu, A., Fegan, G., Wambua, J., Nyangweso, G., Leach, A., Lievens, M., Kaslow, D. C., Njuguna, P., Marsh, K., & Bejon, P. (2016). Seven-Year Efficacy of RTS,S/AS01 Malaria Vaccine among Young African Children. *The New England journal of medicine*, *374*(26), 2519–2529.

Oriero, E. C., Amenga-Etego, L., Ishengoma, D. S., & Amambua-Ngwa, A. (2021). *Plasmodium malariae,* current knowledge and future research opportunities on a neglected malaria parasite species. *Critical reviews in microbiology*, *47*(1), 44–56.

Owen, A., & Rannard, S. (2016). Strengths, weaknesses, opportunities and challenges for long acting injectable therapies: Insights for applications in HIV therapy. *Advanced drug delivery reviews*, *103*, 144–156.

Oxborough R. M. (2016). Trends in US President's Malaria Initiative-funded indoor residual spray coverage and insecticide choice in sub-Saharan Africa (2008-2015): urgent need for affordable, long-lasting insecticides. *Malaria journal*, *15*, 146.

Pagola, S., Stephens, P. W., Bohle, D. S., Kosar, A. D., & Madsen, S. K. (2000). The structure of malaria pigment beta-haematin. *Nature*, *404*(6775), 307–310.

Palatnik-de-Sousa, C. B., & Nico, D. (2020). The Delay in the Licensing of Protozoal Vaccines: A Comparative History. *Frontiers in immunology*, *11*, 204.

Paton, D. G., Childs, L. M., Itoe, M. A., Holmdahl, I. E., Buckee, C. O., & Catteruccia, F. (2019). Exposing Anopheles mosquitoes to antimalarials blocks *Plasmodium* parasite transmission. *Nature*, *567*(7747), 239–243.

Peeters, J. E., Halen, P., & Meulemans, G. (1979). Efficacy of robenidine in the prevention of rabbit coccidiosis. *The British veterinary journal*, *135*(4), 349–354.

Peters, W., Fleck, S. L., Robinson, B. L., Stewart, L. B., & Jefford, C. W. (2002). The chemotherapy of rodent malaria. LX. The importance of formulation in evaluating the blood schizontocidal activity of some endoperoxide antimalarials. *Annals of tropical medicine and parasitology*, *96*(6), 559–573.

Phillips, R. E., & Solomon, T. (1990). Cerebral malaria in children. *Lancet (London, England)*, *336*(8727), 1355–1360.

Pou, S., Winter, R. W., Nilsen, A., Kelly, J. X., Li, Y., Doggett, J. S., Riscoe, E. W., Wegmann, K. W., Hinrichs, D. J., & Riscoe, M. K. (2012). Sontochin as a guide to the development of drugs against chloroquine-resistant malaria. *Antimicrobial agents and chemotherapy*, *56*(7), 3475–3480.

Pou, S., Dodean, R. A., Frueh, L., Liebman, K. M., Gallagher, R. T., Jin, H., Jacobs, R. T., Nilsen, A., Stuart, D. R., Doggett, J. S., Riscoe, M. K., & Winter, R. W. (2021). A New Scalable Synthesis of ELQ-300, ELQ-316, and other Antiparasitic Quinolones. *Organic process research & development*, *25*(8), 1841–1852.

Rafikov, M., Bevilacqua, L., & Wyse, A. P. (2009). Optimal control strategy of malaria vector using genetically modified mosquitoes. *Journal of theoretical biology*, *258*(3), 418–425.

Reid, W. M., Kowalski, L. M., Taylor, E. M., & Johnson, J. (1970). Efficacy evaluations of robenzidene for control of coccidiosis in chickens. *Avian diseases*, *14*(4), 788–796.

Ricketts, A. P., & Pfefferkorn, E. R. (1993). *Toxoplasma gondii*: susceptibility and development of resistance to anticoccidial drugs in vitro. *Antimicrobial agents and chemotherapy*, *37*(11), 2358–2363.

Russell, C. C., Stevens, A., Pi, H., Khazandi, M., Ogunniyi, A. D., Young, K. A., Baker, J. R., McCluskey, S. N., Page, S. W., Trott, D. J., & McCluskey, A. (2018). Gram-Positive and Gram-Negative Antibiotic Activity of Asymmetric and Monomeric Robenidine Analogues. *ChemMedChem*, *13*(23), 2573–2580.

Russell, C. C., Stevens, A., Young, K. A., Baker, J. R., McCluskey, S. N., Khazandi, M., Pi, H., Ogunniyi, A., Page, S. W., Trott, D. J., & McCluskey, A. (2019). Discovery of 4,6-bis(2-((*E*)-benzylidene)hydrazinyl)pyrimidin-2-Amine with Antibiotic Activity. *ChemistryOpen*, *8*(7), 896–907.

Rutgers, T., Gordon, D., Gathoye, A. *et al.* Hepatitis B Surface Antigen as Carrier Matrix for the Repetitive Epitope of the Circumsporozoite Protein of *Plasmodium Falciparum*. *Nat Biotechnol* **6,** 1065–1070 (1988).

Ryley, J. F., & Wilson, R. G. (1971). Studies on the mode of action of the coccidiostat robenidene. *Zeitschrift fur Parasitenkunde (Berlin, Germany)*, *37*(2), 85–93.

Ryley, J. F., & Wilson, R. G. (1972). The development of *Eimeria brunetti* in tissue culture. *The Journal of parasitology*, *58*(4), 660–663.

Ryley, J. F., & Wilson, R. G. (1972). Comparative studies with anticoccidials and three species of chicken coccidia in vivo and in vitro. *The Journal of parasitology*, *58*(4), 664–668.

Sachs, J., & Malaney, P. (2002). The economic and social burden of malaria. *Nature*, *415*(6872), 680–685.

Sibley C. H. (2014). Understanding drug resistance in malaria parasites: basic science for public health. *Molecular and biochemical parasitology*, *195*(2), 107–114.

Sidhu, A. B., Verdier-Pinard, D., & Fidock, D. A. (2002). Chloroquine resistance in *Plasmodium falciparum* malaria parasites conferred by pfcrt mutations. *Science (New York, N.Y.)*, *298*(5591), 210–213.

Sirima, S. B., Mordmüller, B., Milligan, P., Ngoa, U. A., Kironde, F., Atuguba, F., Tiono, A. B., Issifou, S., Kaddumukasa, M., Bangre, O., Flach, C., Christiansen, M., Bang, P., Chilengi, R., Jepsen, S., Kremsner, P. G., Theisen, M., & GMZ2 Trial Study Group (2016). A phase 2b randomized, controlled trial of the efficacy of the GMZ2 malaria vaccine in African children. *Vaccine*, *34*(38), 4536–4542.

Slater, A. F., Swiggard, W. J., Orton, B. R., Flitter, W. D., Goldberg, D. E., Cerami, A., & Henderson, G. B. (1991). An iron-carboxylate bond links the heme units of malaria pigment. *Proceedings of the National Academy of Sciences of the United States of America*, *88*(2), 325–329.

Smilkstein, M., Sriwilaijaroen, N., Kelly, J. X., Wilairat, P., & Riscoe, M. (2004). Simple and inexpensive fluorescence-based technique for high-throughput antimalarial drug screening. *Antimicrobial agents and chemotherapy*, *48*(5), 1803–1806.

Smilkstein, M. J., Forquer, I., Kanazawa, A., Kelly, J. X., Winter, R. W., Hinrichs, D. J., Kramer, D. M., & Riscoe, M. K. (2008). A drug-selected *Plasmodium falciparum* lacking the need for conventional electron transport. *Molecular and biochemical parasitology*, *159*(1), 64–68.

Smilkstein, M. J., Pou, S., Krollenbrock, A., Bleyle, L. A., Dodean, R. A., Frueh, L., Hinrichs, D. J., Li, Y., Martinson, T., Munar, M. Y., Winter, R. W., Bruzual, I., Whiteside, S., Nilsen, A., Koop,

D. R., Kelly, J. X., Kappe, S., Wilder, B. K., & Riscoe, M. K. (2019). ELQ-331 as a prototype for extremely durable chemoprotection against malaria. *Malaria journal*, *18*(1), 291.

Stanley, V. G., Woldesenbet, S., Gray, C., & Hinton, A., Jr (1996). Sensitivity of *Escherichia coli* O157:H7 strain 932 to selected anticoccidial drugs in broiler chicks. *Poultry science*, *75*(1), 42–46.

Stickles, A. M., de Almeida, M. J., Morrisey, J. M., Sheridan, K. A., Forquer, I. P., Nilsen, A., Winter, R. W., Burrows, J. N., Fidock, D. A., Vaidya, A. B., & Riscoe, M. K. (2015). Subtle changes in endochin-like quinolone structure alter the site of inhibition within the cytochrome bc1 complex of *Plasmodium falciparum*. *Antimicrobial agents and chemotherapy*, *59*(4), 1977–1982.

Sturm, A., Mollard, V., Cozijnsen, A., Goodman, C. D., & McFadden, G. I. (2015). Mitochondrial ATP synthase is dispensable in blood-stage *Plasmodium berghei* rodent malaria but essential in the mosquito phase. *Proceedings of the National Academy of Sciences of the United States of America*, *112*(33), 10216–10223.

Taylor-Robinson, A. W., & Smith, E. C. (1999). A role for cytokines in potentiation of malaria vaccines through immunological modulation of blood stage infection. *Immunological reviews*, *171*, 105–123.

Templeton, T. J., Asada, M., Jiratanh, M., Ishikawa, S. A., Tiawsirisup, S., Sivakumar, T., Namangala, B., Takeda, M., Mohkaew, K., Ngamjituea, S., Inoue, N., Sugimoto, C., Inagaki, Y., Suzuki, Y., Yokoyama, N., Kaewthamasorn, M., & Kaneko, O. (2016). Ungulate malaria parasites. *Scientific reports*, *6*, 23230.

Tilley, L., Straimer, J., Gnädig, N. F., Ralph, S. A., & Fidock, D. A. (2016). Artemisinin Action and Resistance in *Plasmodium falciparum*. *Trends in parasitology*, *32*(9), 682–696.

Trager, W., & Jensen, J. B. (1976). Human malaria parasites in continuous culture. *Science (New York, N.Y.)*, *193*(4254), 673–675.

Trager, W., & Jensen, J. B. (1977). Cultivation of erythrocytic stages. *Bulletin of the World Health Organization*, *55*(2-3), 363–365.

Tu Y. (2011). The discovery of artemisinin (qinghaosu) and gifts from Chinese medicine. *Nature medicine*, *17*(10), 1217–1220.

Vaughan A. (2021). Motile mosquito stage malaria parasites: ready for their close-up. *EMBO molecular medicine*, *13*(4), e13975.

Wahlgren, M., Goel, S., & Akhouri, R. R. (2017). Variant surface antigens of *Plasmodium falciparum* and their roles in severe malaria. *Nature reviews. Microbiology*, *15*(8), 479–491.

Ward, R., Rader, D., Lipton, M. M., & Freund, J. (1950). Formation of neutralizing antibody in monkeys injected with poliomyelitis virus and adjuvants. *Proceedings of the Society for Experimental Biology and Medicine. Society for Experimental Biology and Medicine (New York, N.Y.)*, *74*(3), 536–539.

Weinke, T., Trautmann, M., Held, T., Weber, G., Eichenlaub, D., Fleischer, K., Kern, W., & Pohle, H. D. (1991). Neuropsychiatric side effects after the use of mefloquine. *The American journal of tropical medicine and hygiene*, *45*(1), 86–91.

Weiss, D. J., Bertozzi-Villa, A., Rumisha, S. F., Amratia, P., Arambepola, R., Battle, K. E., Cameron, E., Chestnutt, E., Gibson, H. S., Harris, J., Keddie, S., Millar, J. J., Rozier, J., Symons, T. L., Vargas-Ruiz, C., Hay, S. I., Smith, D. L., Alonso, P. L., Noor, A. M., Bhatt, S., Gething, P. W. (2021). Indirect effects of the COVID-19 pandemic on malaria intervention coverage, morbidity, and mortality in Africa: a geospatial modelling analysis. *The Lancet. Infectious diseases*, *21*(1), 59–69.

Wilson, R. J., Denny, P. W., Preiser, P. R., Rangachari, K., Roberts, K., Roy, A., Whyte, A., Strath, M., Moore, D. J., Moore, P. W., & Williamson, D. H. (1996). Complete gene map of the plastid-like DNA of the malaria parasite *Plasmodium falciparum*. *Journal of molecular biology*, *261*(2), 155–172.

Winter, R., Kelly, J. X., Smilkstein, M. J., Hinrichs, D., Koop, D. R., & Riscoe, M. K. (2011). Optimization of endochin-like quinolones for antimalarial activity. *Experimental parasitology*, *127*(2), 545–551.

Wong, D. T., Horng, J. S., & Wilkinson, J. R. (1972). Robenzidene, an inhibitor of oxidative phosphorylation. *Biochemical and biophysical research communications*, *46*(2), 621–627.

Wong, W., Bai, X. C., Sleebs, B. E., Triglia, T., Brown, A., Thompson, J. K., Jackson, K. E., Hanssen, E., Marapana, D. S., Fernandez, I. S., Ralph, S. A., Cowman, A. F., Scheres, S., & Baum, J. (2017). Mefloquine targets the Plasmodium falciparum 80S ribosome to inhibit protein synthesis. *Nature microbiology*, *2*, 17031.

World Health Organization. World Malaria Report 2018. (2018) https://www.who.int/teams/global-malaria-programme/reports/world-malaria-report-2018.

World Health Organization. World Malaria Report 2021. (2021) https://www.who.int/teams/global-malaria-programme/reports/world-malaria-report-2021.

Wright J.C., Burgess D.J., editors. Long-acting injections and implants. (2012) *New York: Springer*.

Yamamoto, D. S., Sumitani, M., Kasashima, K., Sezutsu, H., Matsuoka, H., & Kato, H. (2019). A synthetic male-specific sterilization system using the mammalian pro-apoptotic factor in a malaria vector mosquito. *Scientific reports*, *9*(1), 8160.

Yao, J. M., Zhang, H. B., Liu, C. S., Tao, Y., & Yin, M. (2015). Inhibitory effects of 19 antiprotozoal drugs and antibiotics on *Babesia microti* infection in BALB/c mice. *Journal of infection in developing countries*, *9*(9), 1004–1010.

Yao, F. A., Millogo, A. A., Epopa, P. S., North, A., Noulin, F., Dao, K., Drabo, M., Guissou, C., Kekele, S., Namountougou, M., Ouedraogo, R. K., Pare, L., Barry, N., Sanou, R., Wandaogo, H., Dabire, R. K., McKemey, A., Tripet, F., & Diabaté, A. (2022). Mark-release-recapture experiment in Burkina Faso demonstrates reduced fitness and dispersal of genetically-modified sterile malaria mosquitoes. *Nature communications*, *13*(1), 796.

Yoshida, N., Nussenzweig, R. S., Potocnjak, P., Nussenzweig, V., & Aikawa, M. (1980). Hybridoma produces protective antibodies directed against the sporozoite stage of malaria parasite. *Science (New York, N.Y.)*, *207*(4426), 71–73.

Zhang, Y., & Meshnick, S. R. (1991). Inhibition of *Plasmodium falciparum* dihydropteroate synthetase and growth in vitro by sulfa drugs. *Antimicrobial agents and chemotherapy*, *35*(2), 267–271.

Zulalian, J., & Gatterdam, P. E. (1973). Absorption, excretion, and metabolism of robenz, robenidine hydrochloride (1,3-bis(p-chlorobenzylideneamino)guanidine hydrochloride), in the rat. *Journal of agricultural and food chemistry*, *21*(5), 794–797.

Appendix 1: ^{1}H and ^{13}C NMR Spectra

Compound 1 ^{1}H

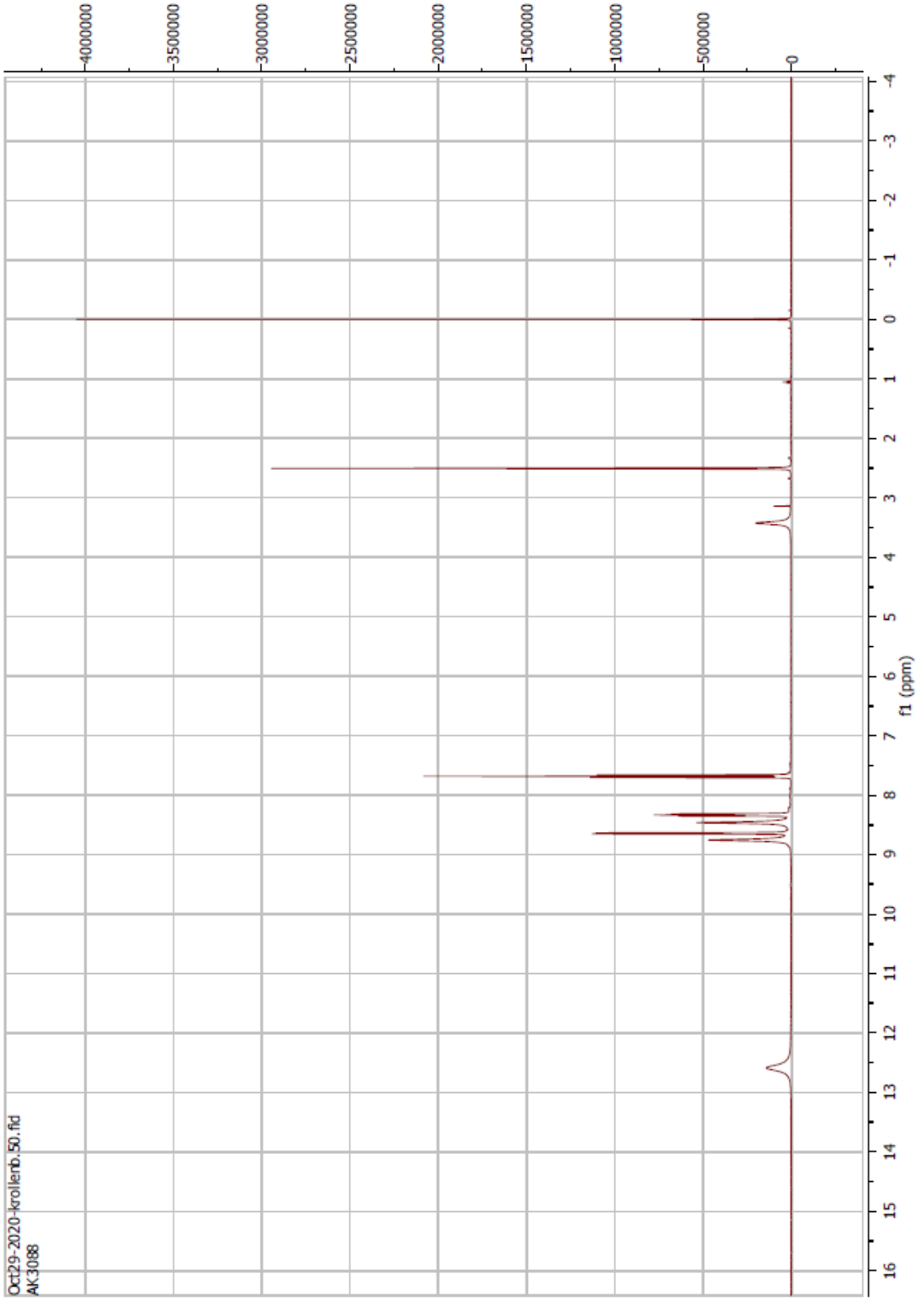

Compound 1 ^{13}C

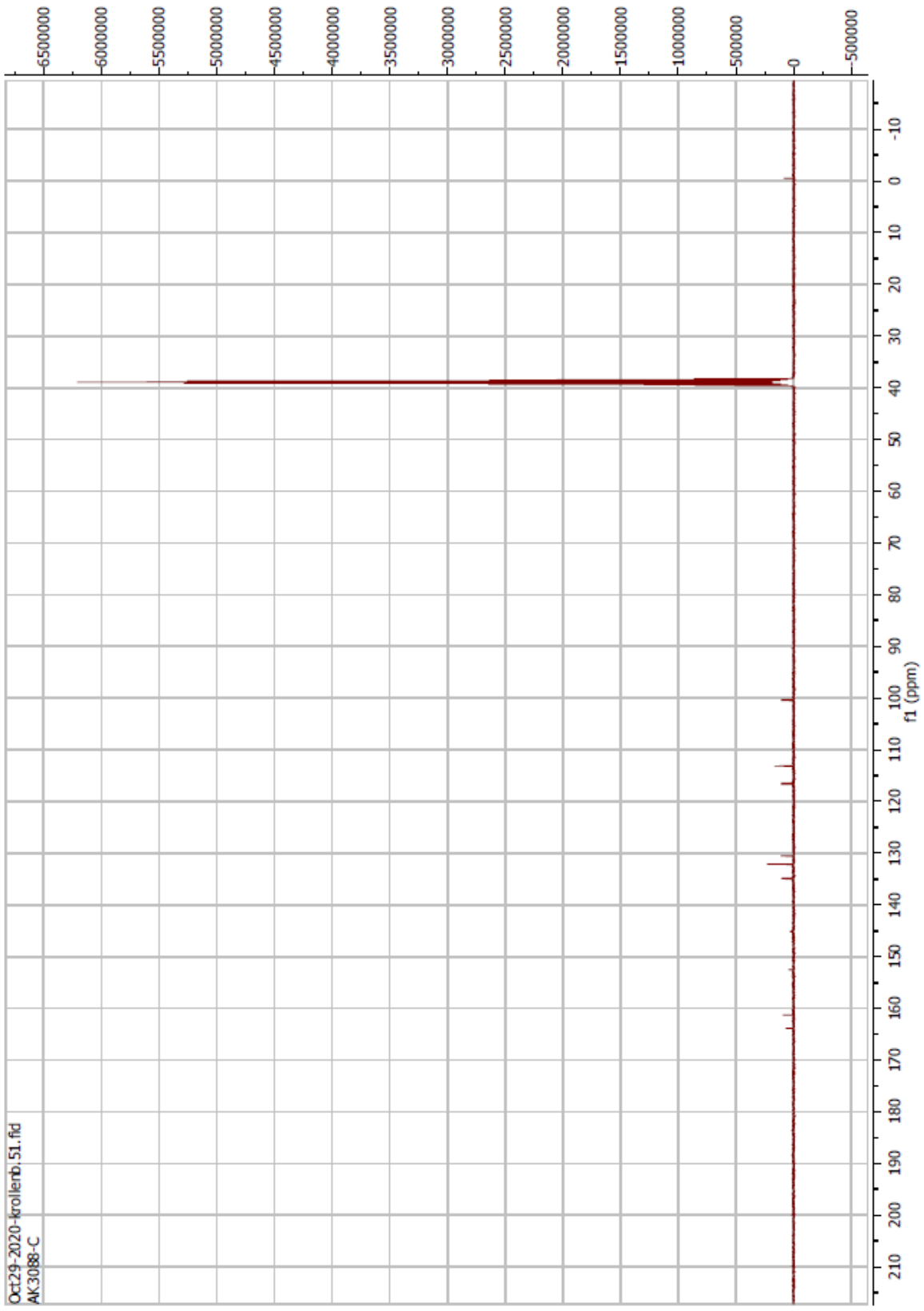

Compound 2 ^{1}H

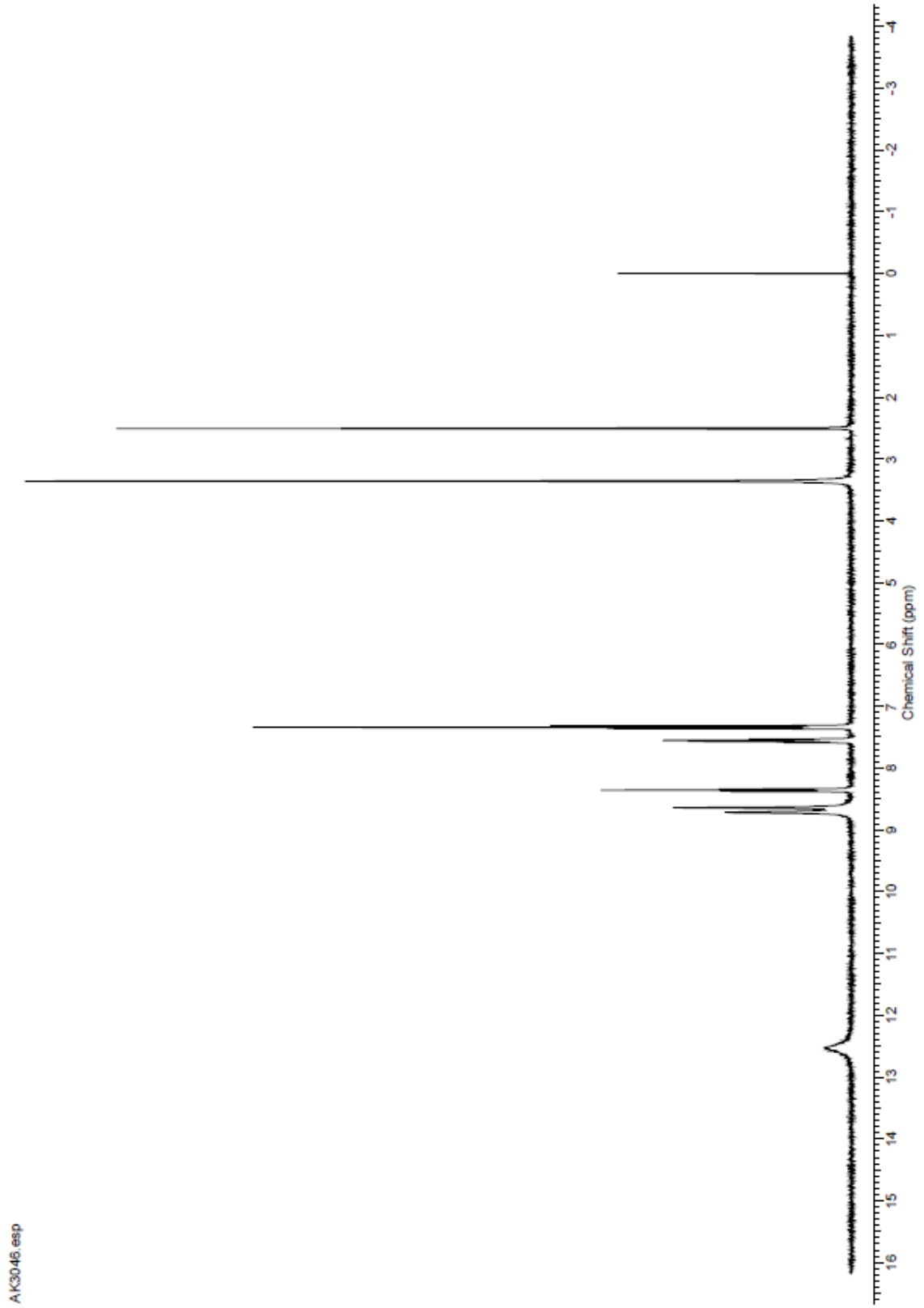

Compound 2 ^{13}C

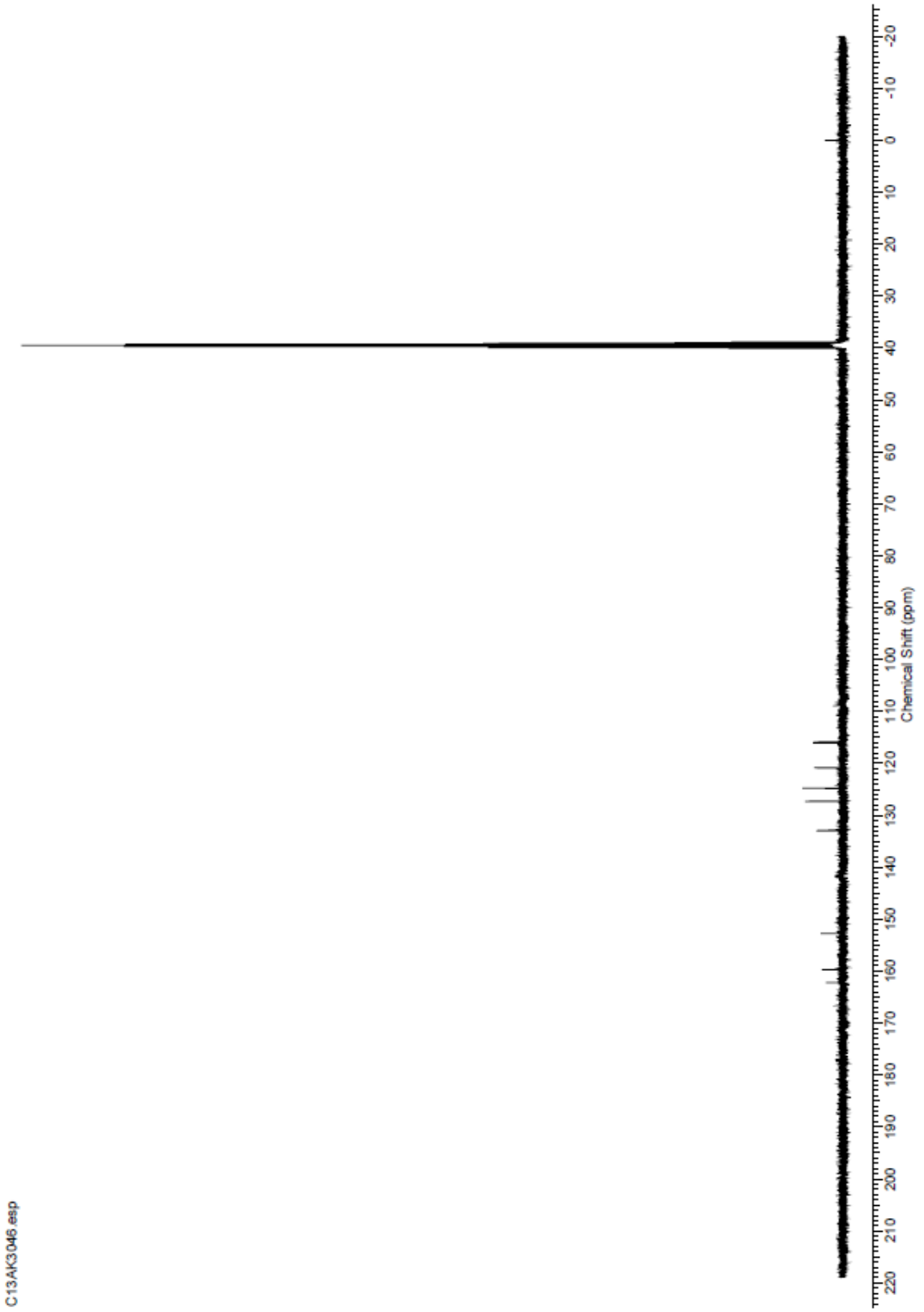

Compound 3 ^{1}H

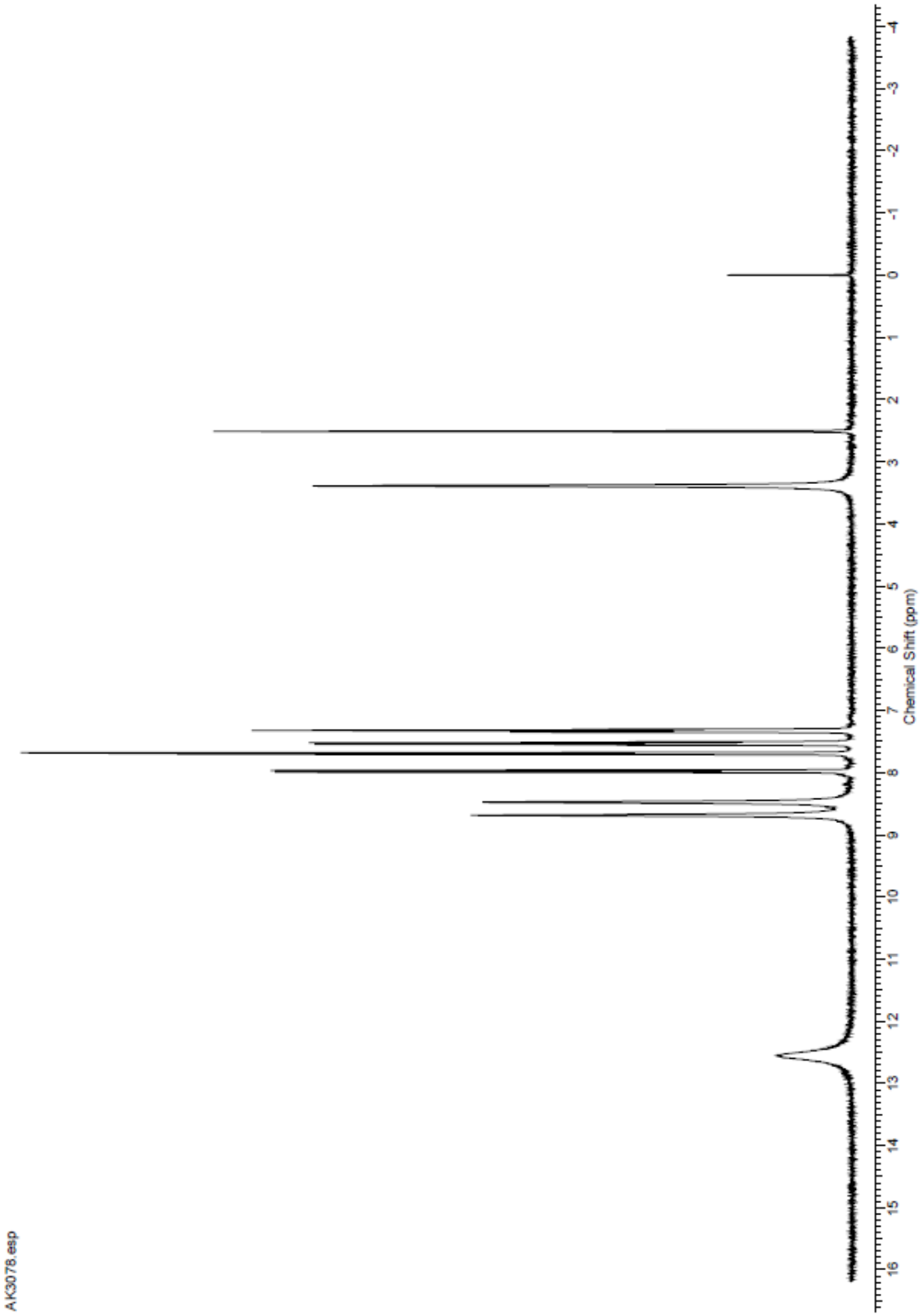

Compound 3 ^{13}C

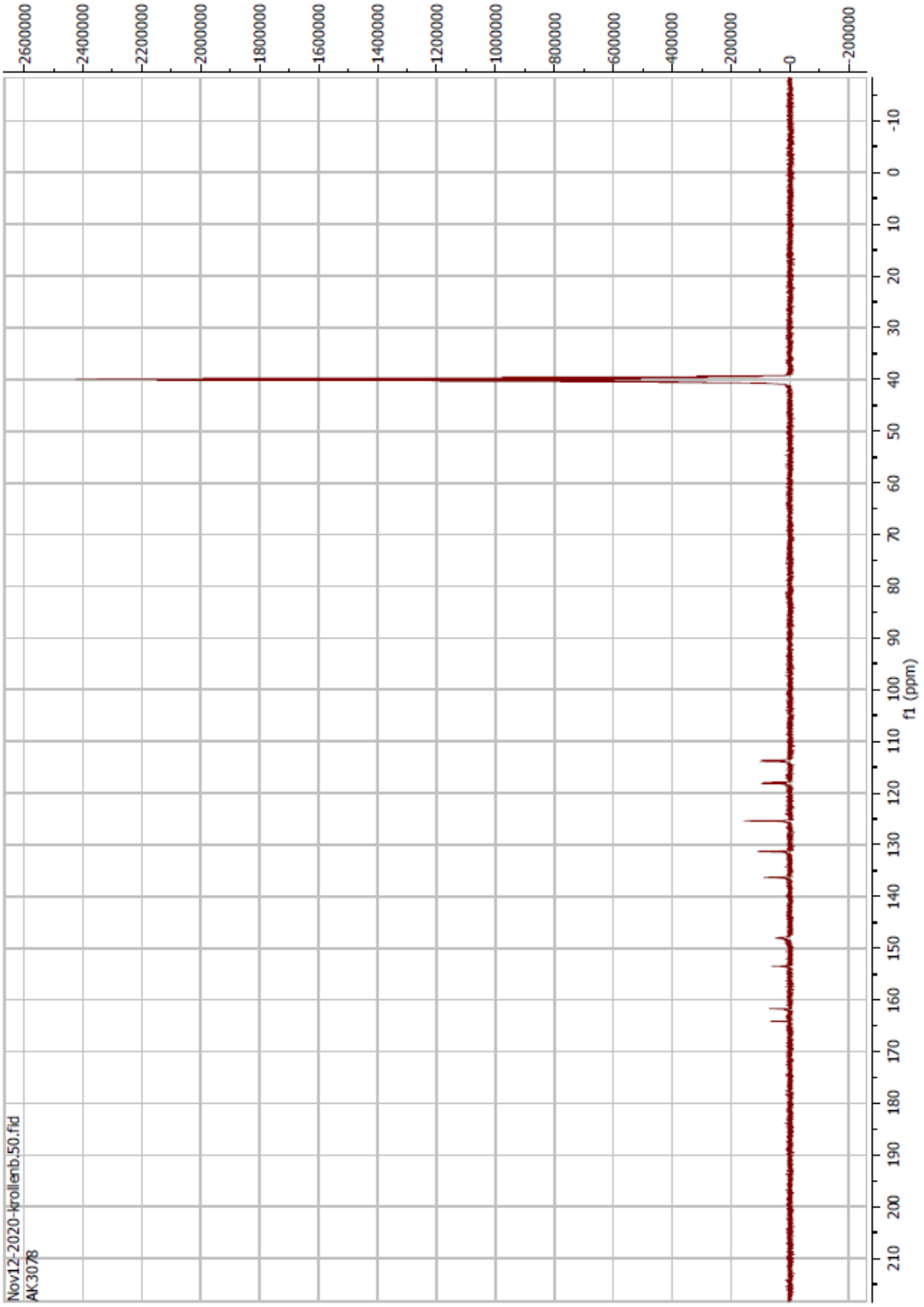

Compound 4 ^{1}H

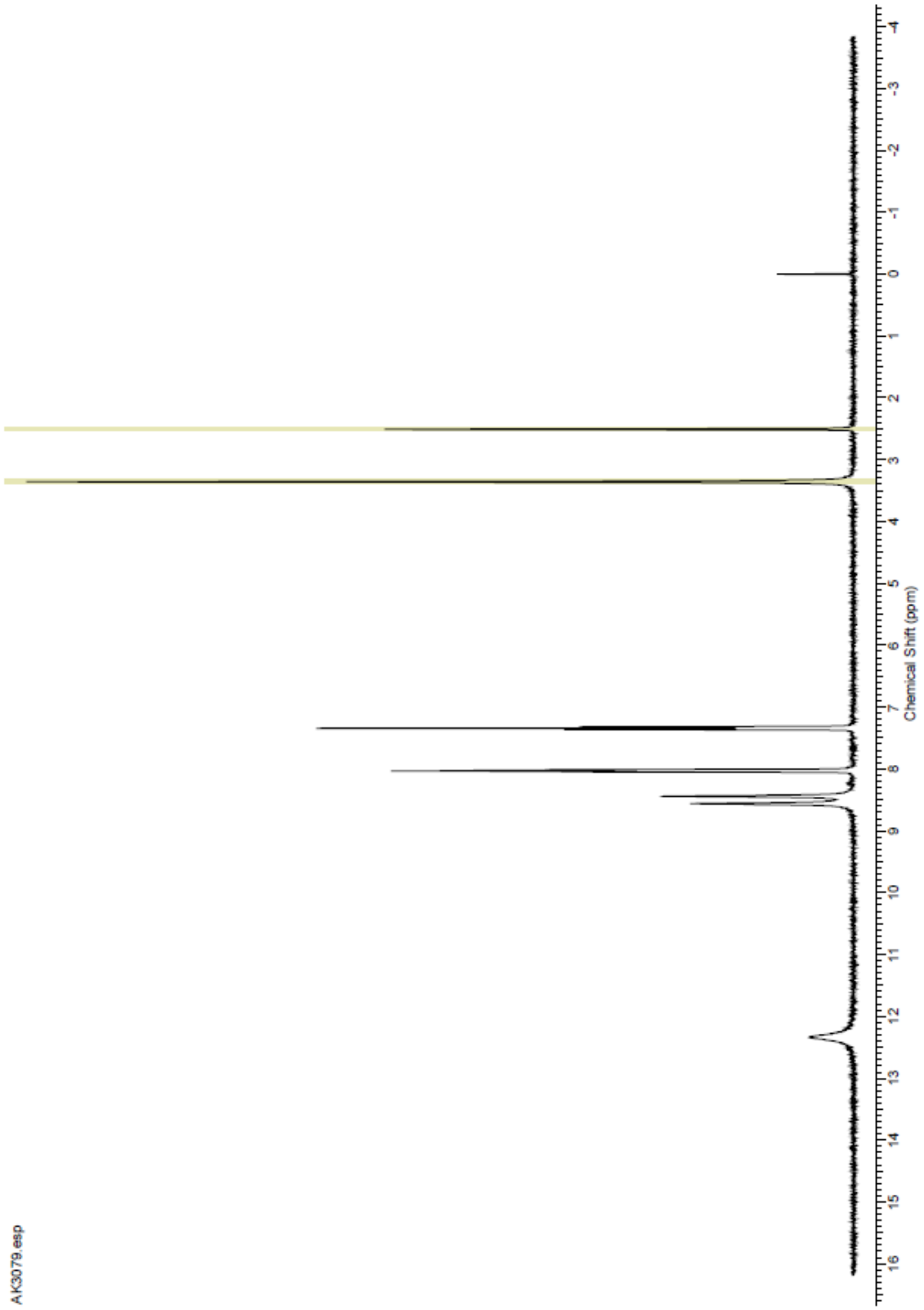

Compound 4 ^{13}C

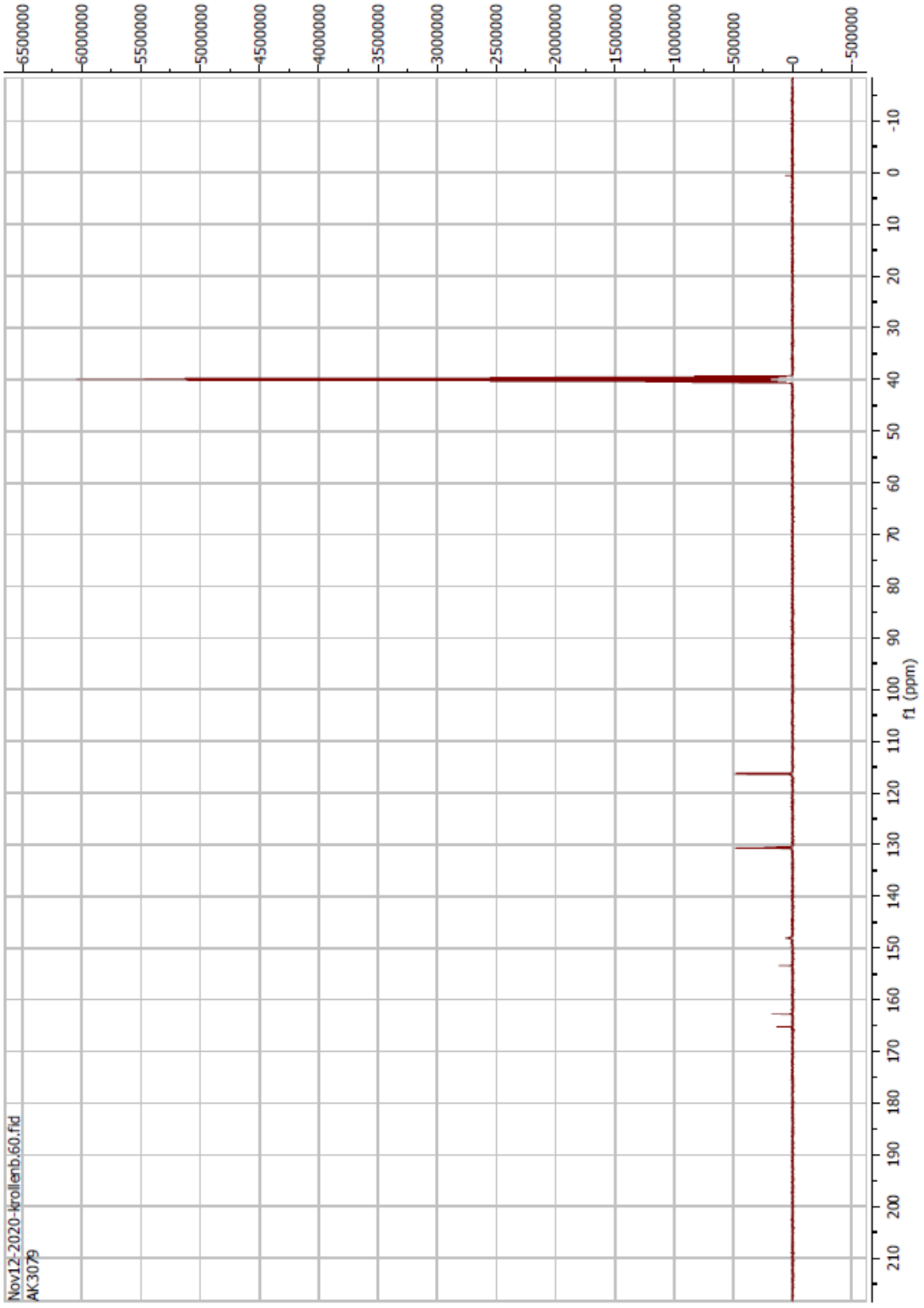

Compound 5 ^{1}H

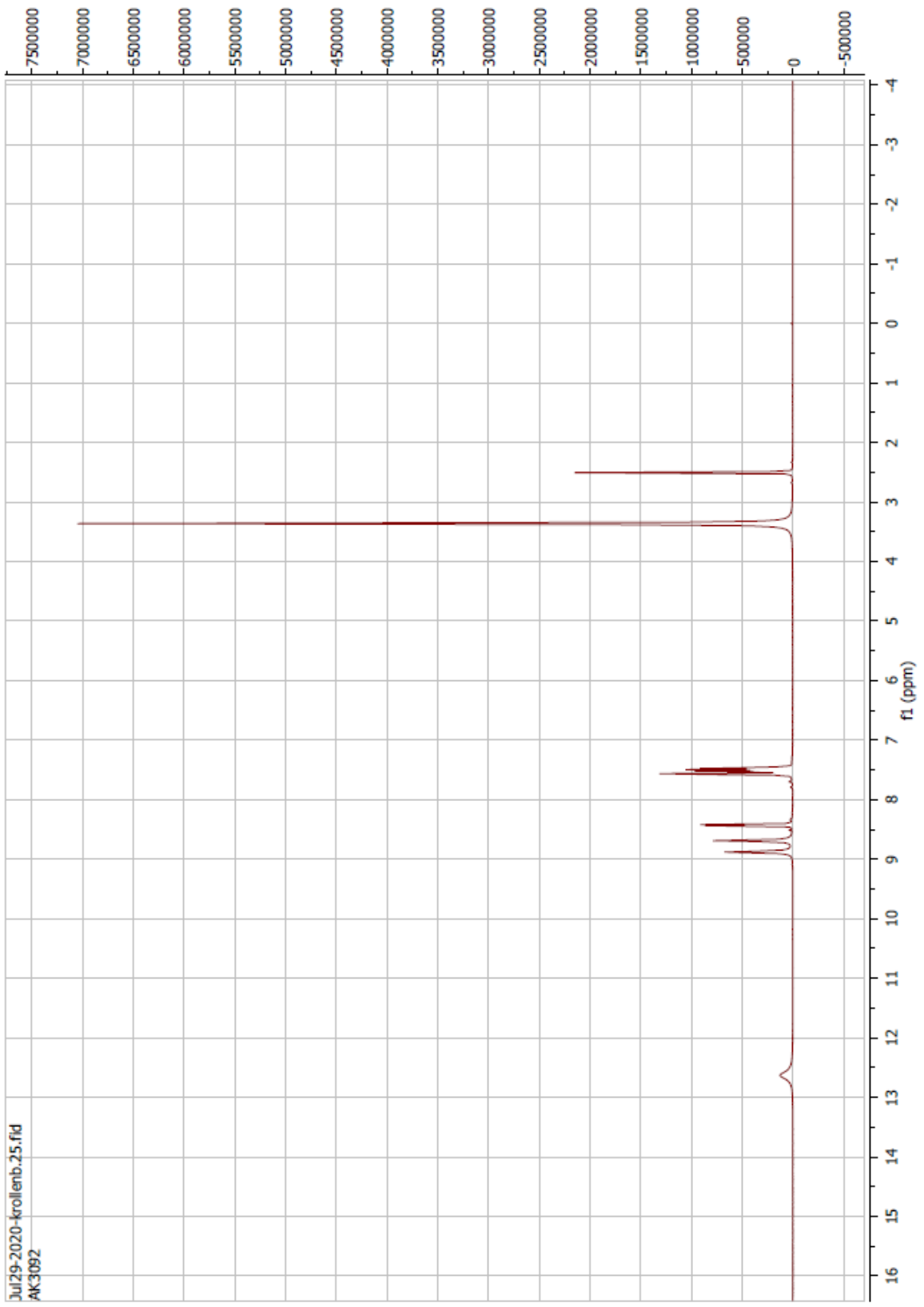

Compound 5 ^{13}C

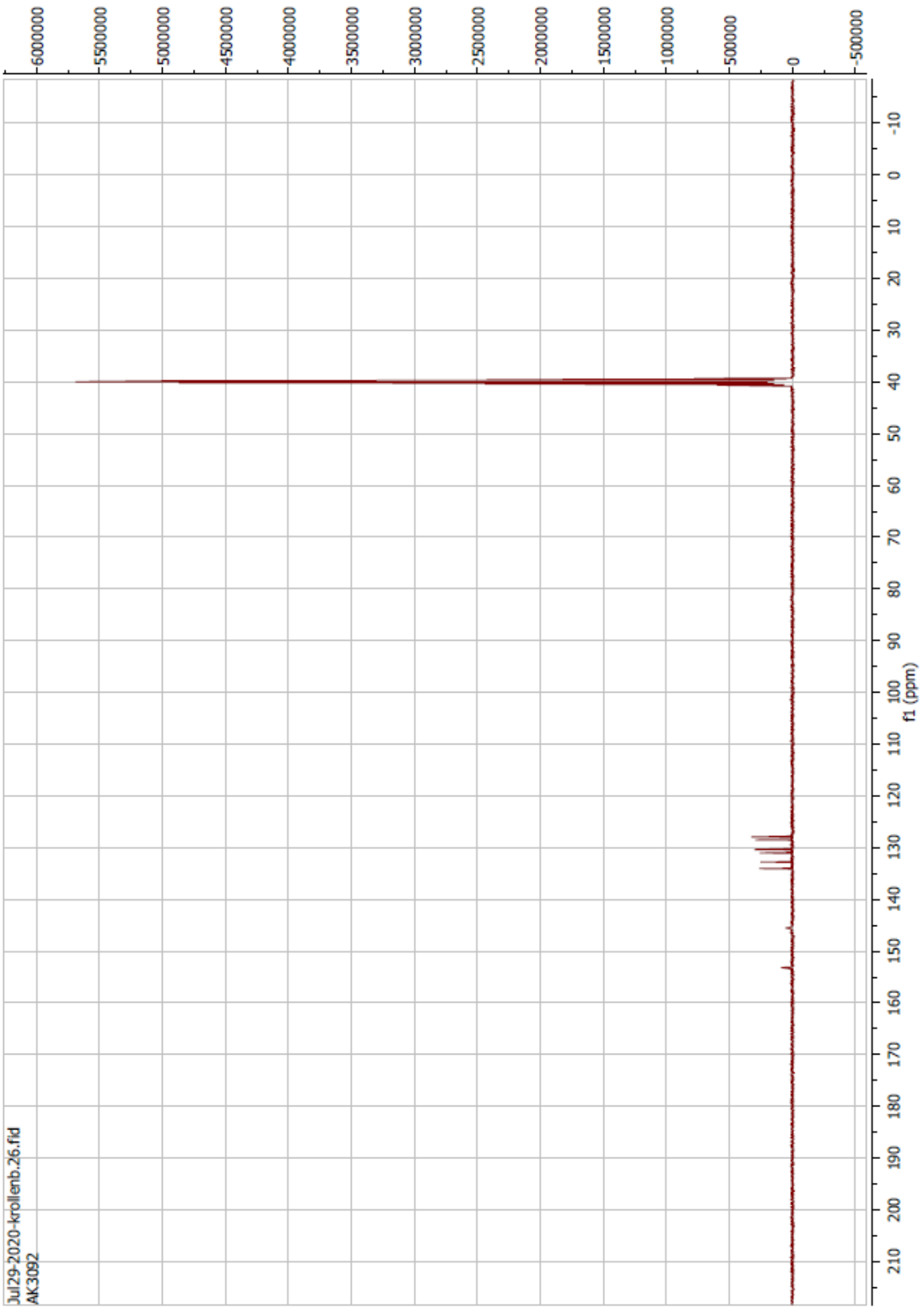

Compound 6 ^{1}H

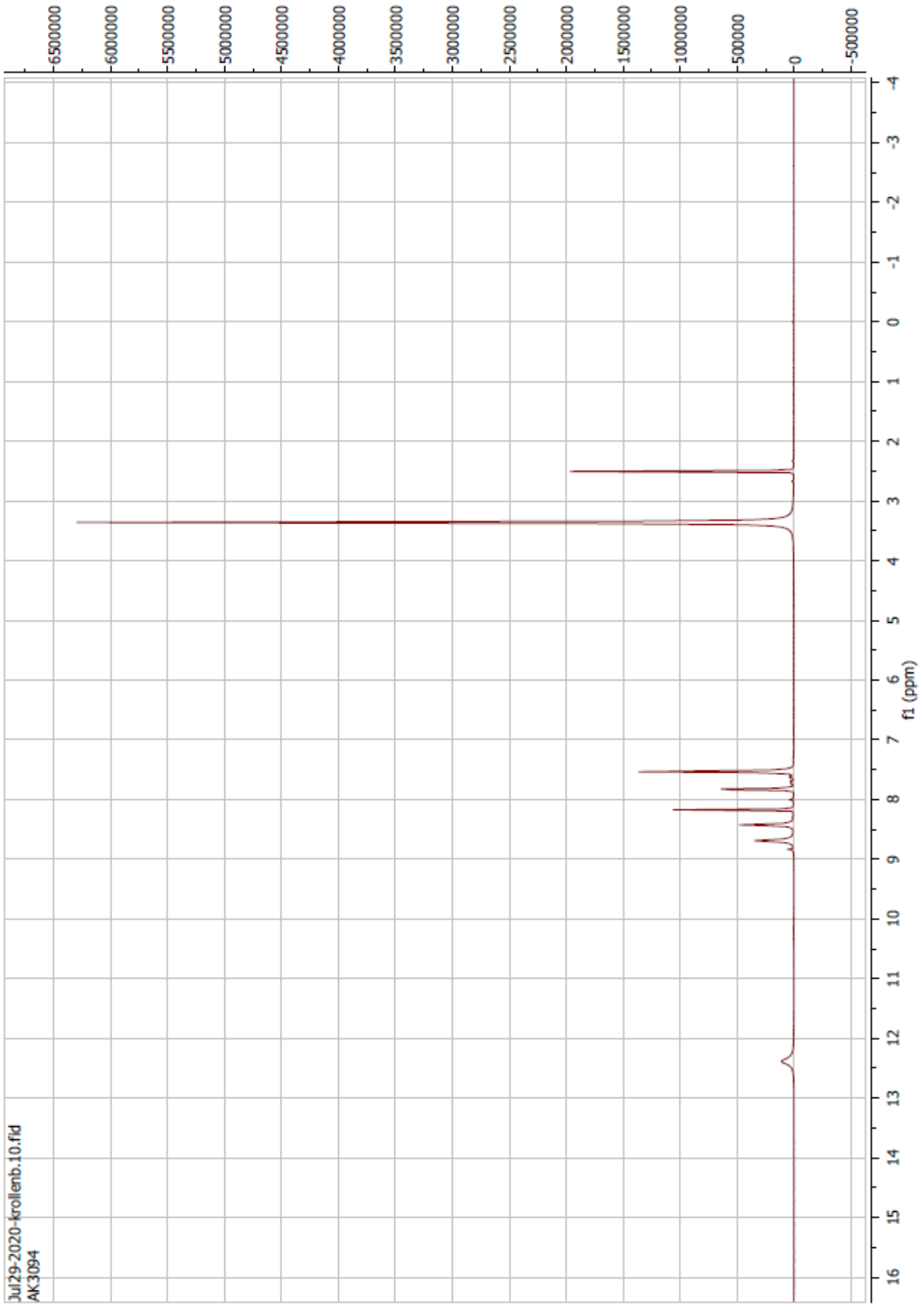

Compound 6 ^{13}C

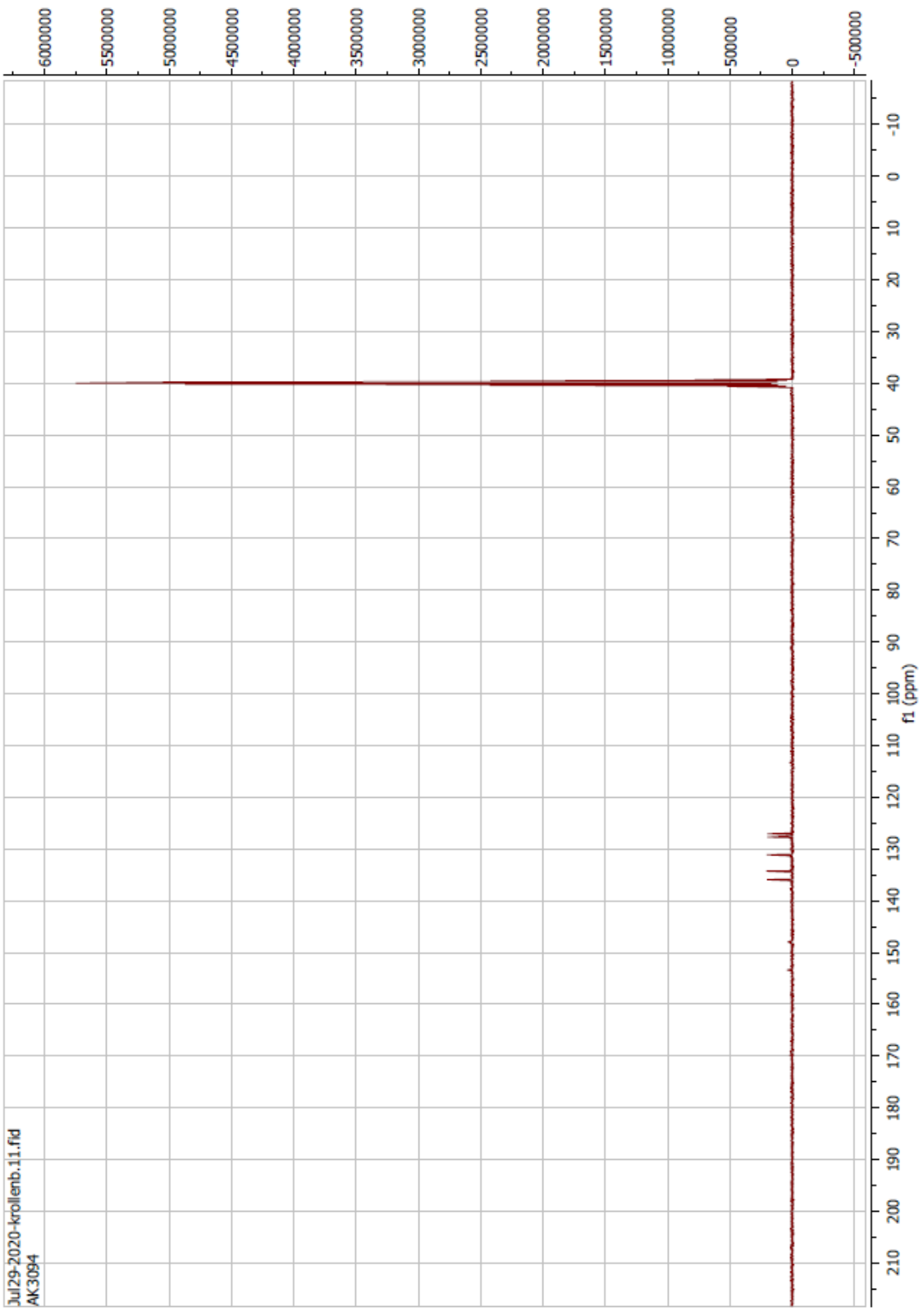

Compound 7 ^{1}H

Compound 7 ^{13}C

Compound 8 ^{1}H

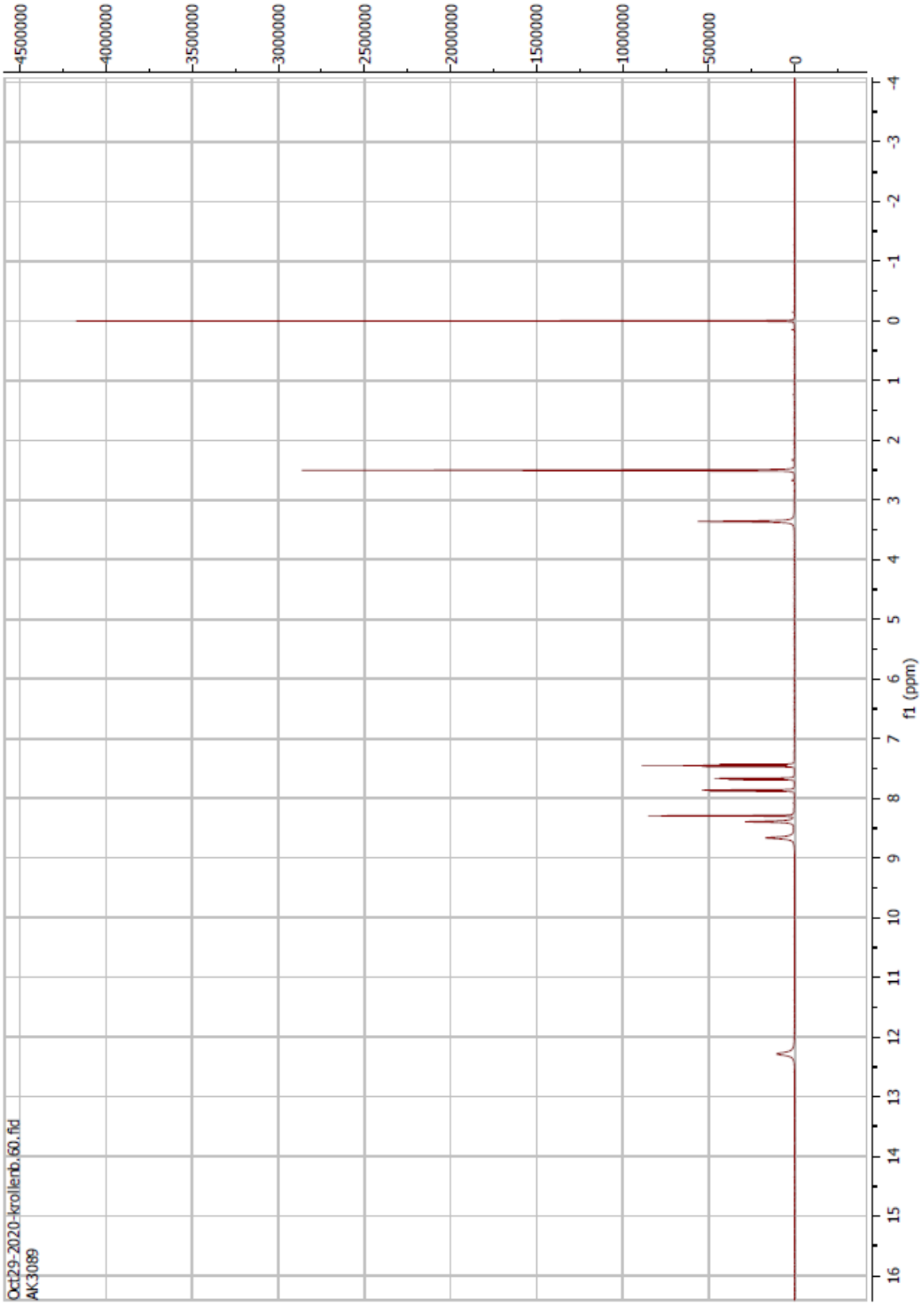

Compound 8 ^{13}C

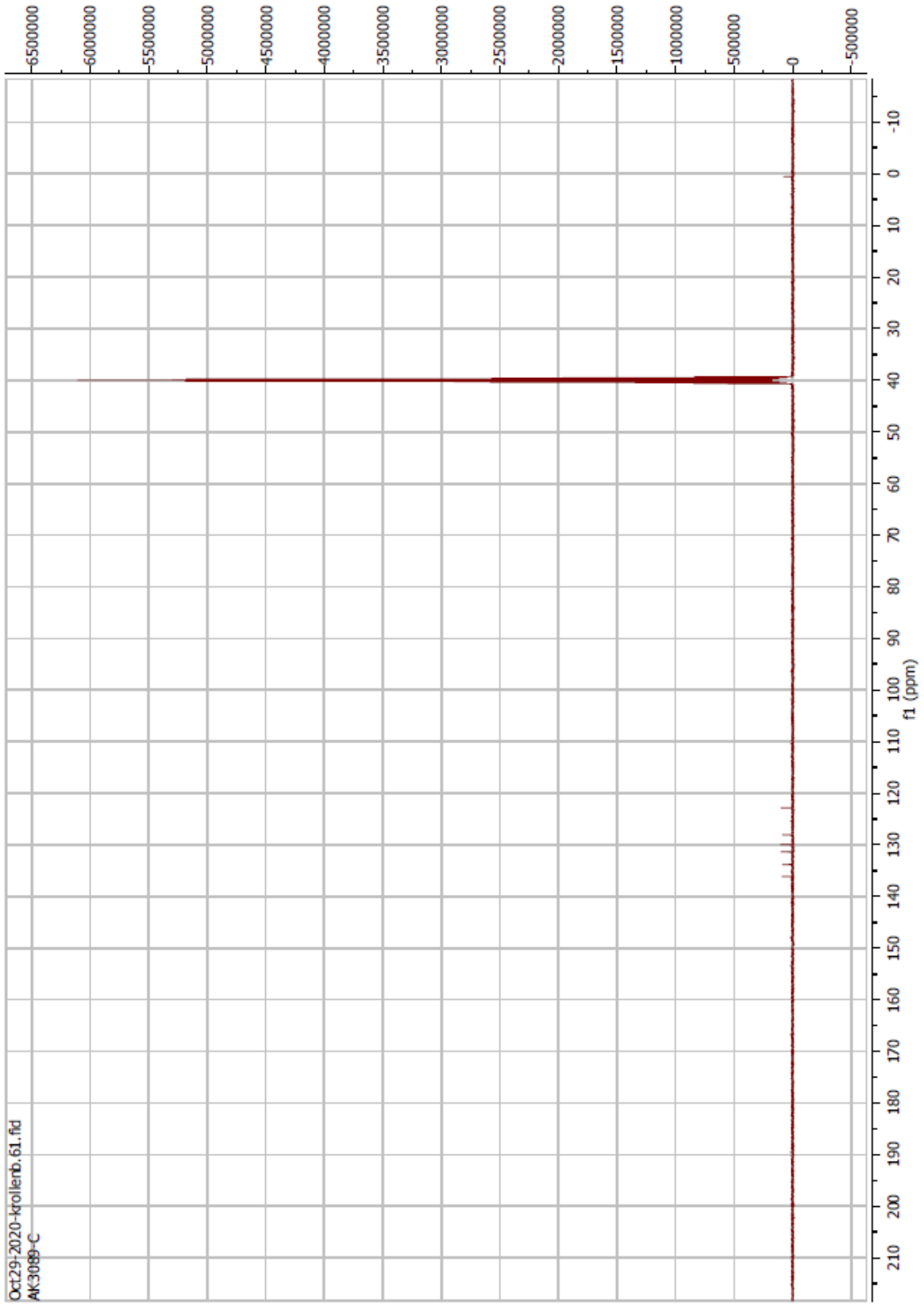

Compound 9 ^{1}H

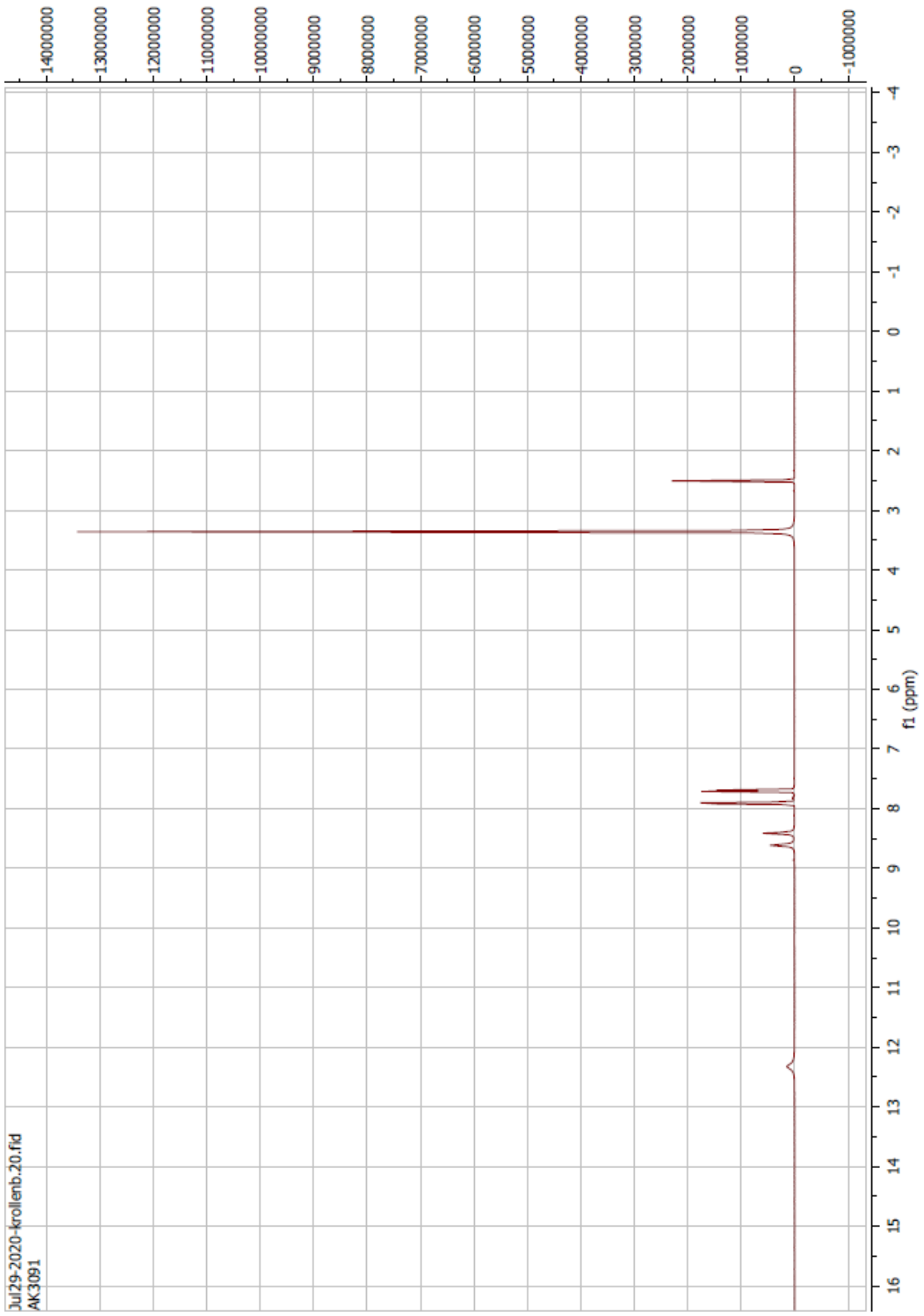

Compound 9 ^{13}C

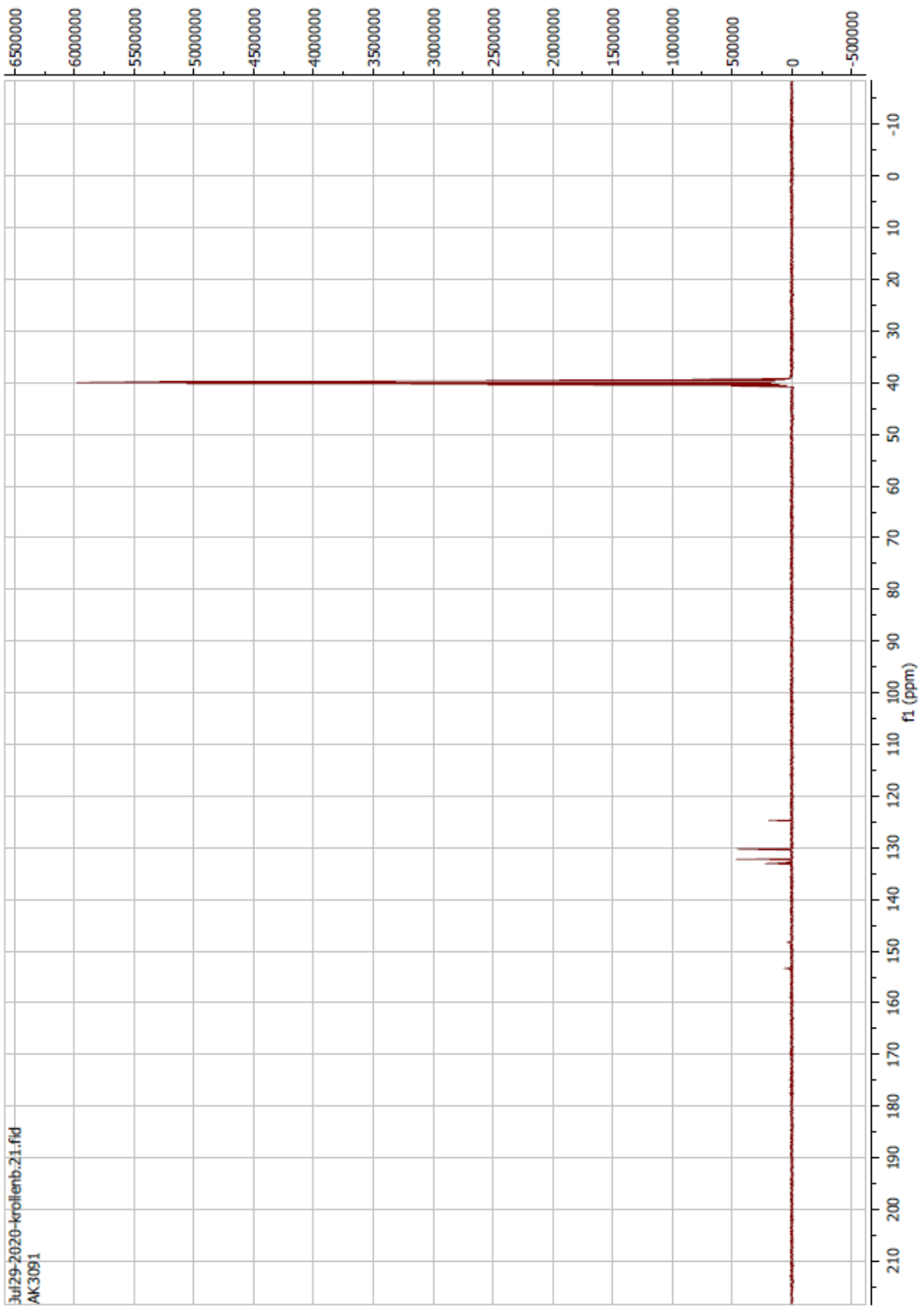

Compound 10 ^{1}H

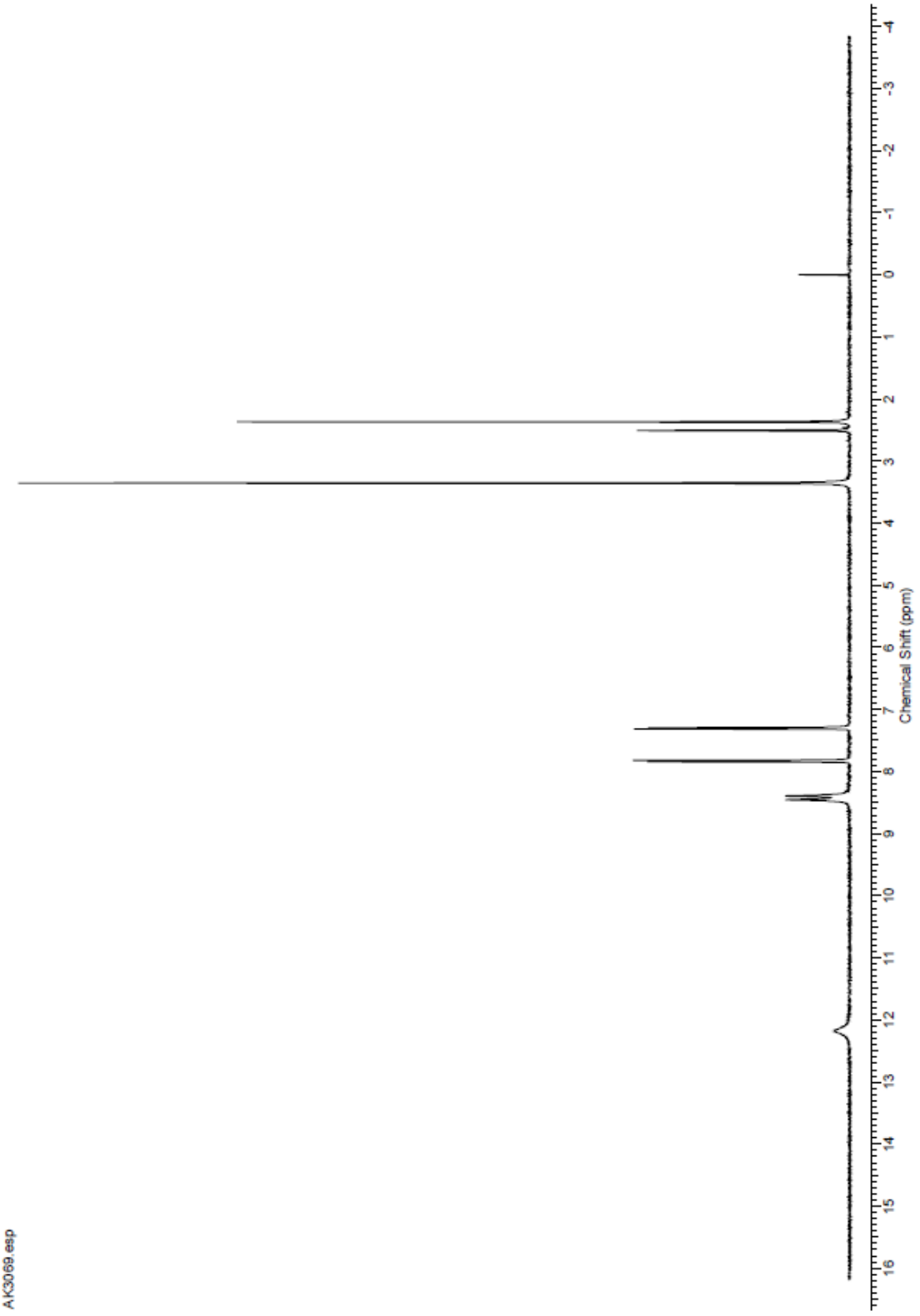

Compound 10 ^{13}C

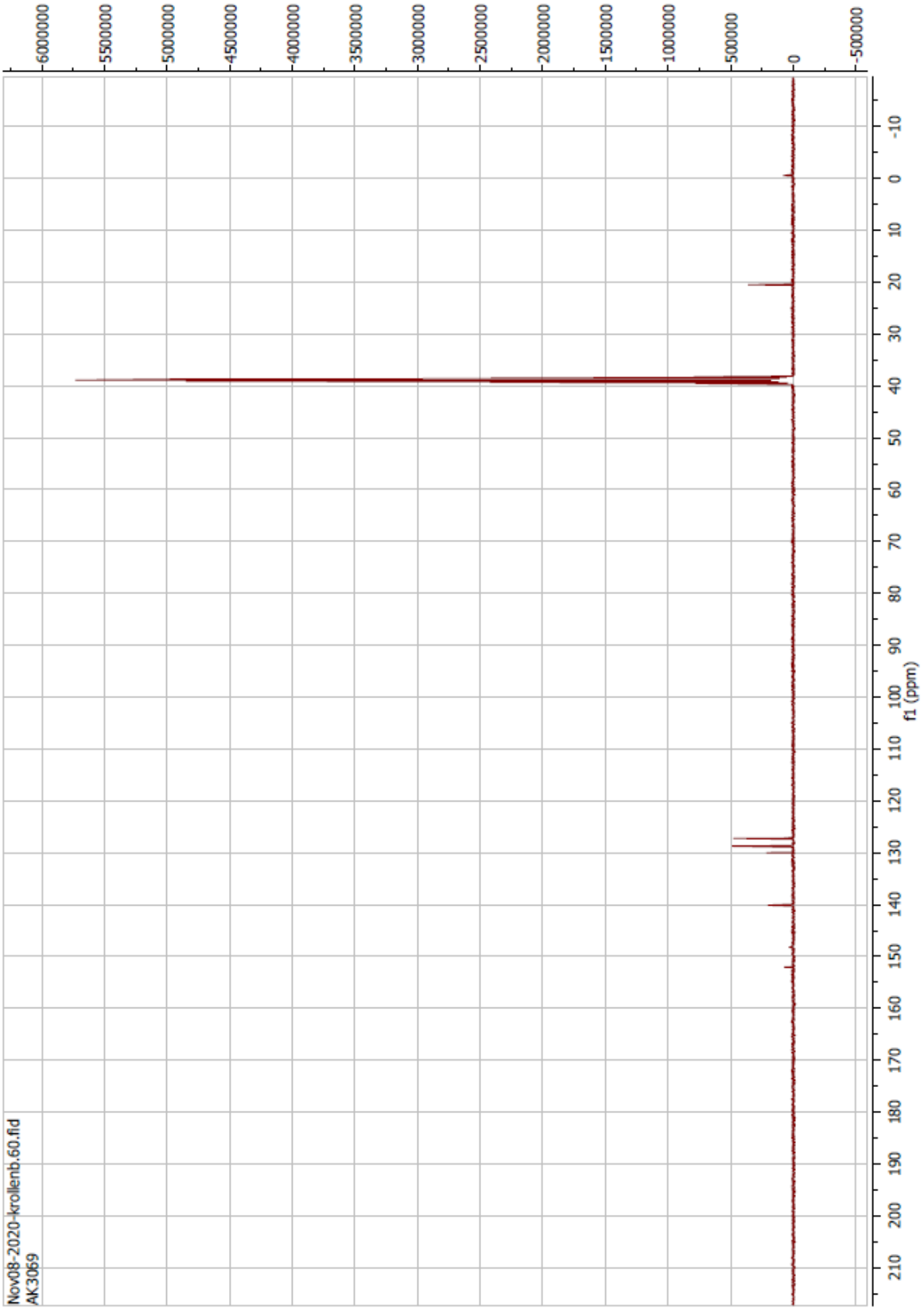

Compound 11 ^{1}H

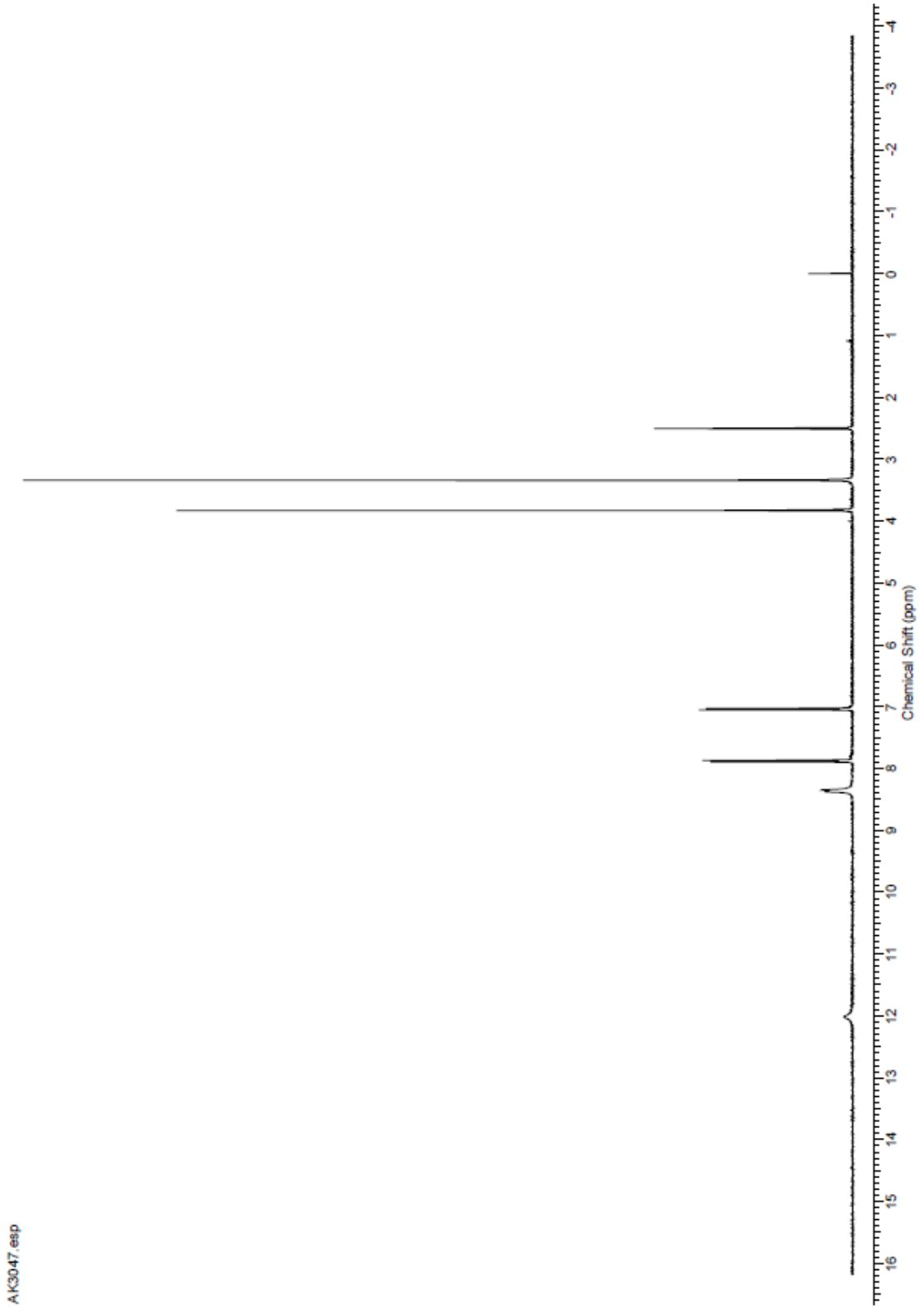

Compound 11 ^{13}C

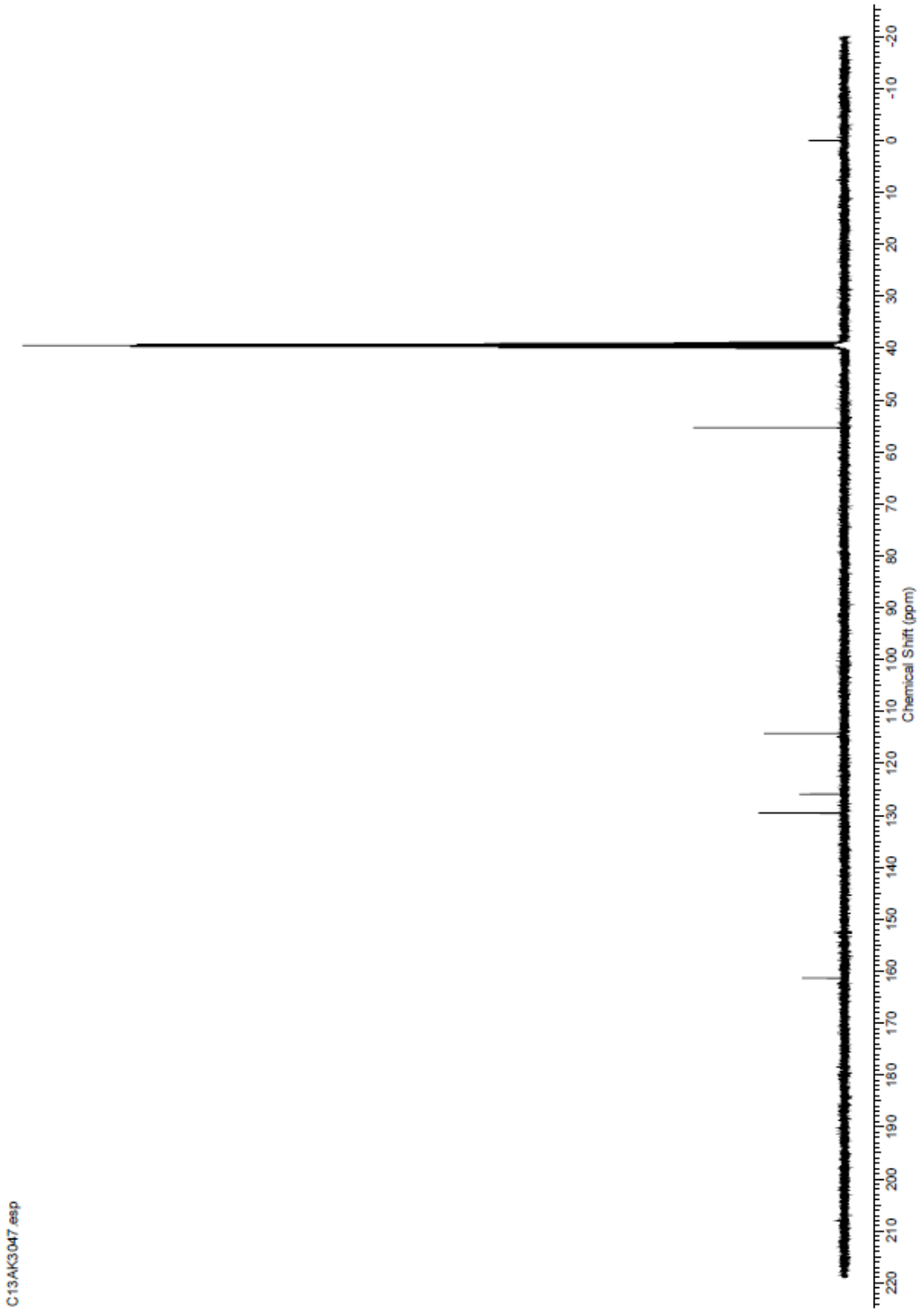

Compound 12 ^{1}H

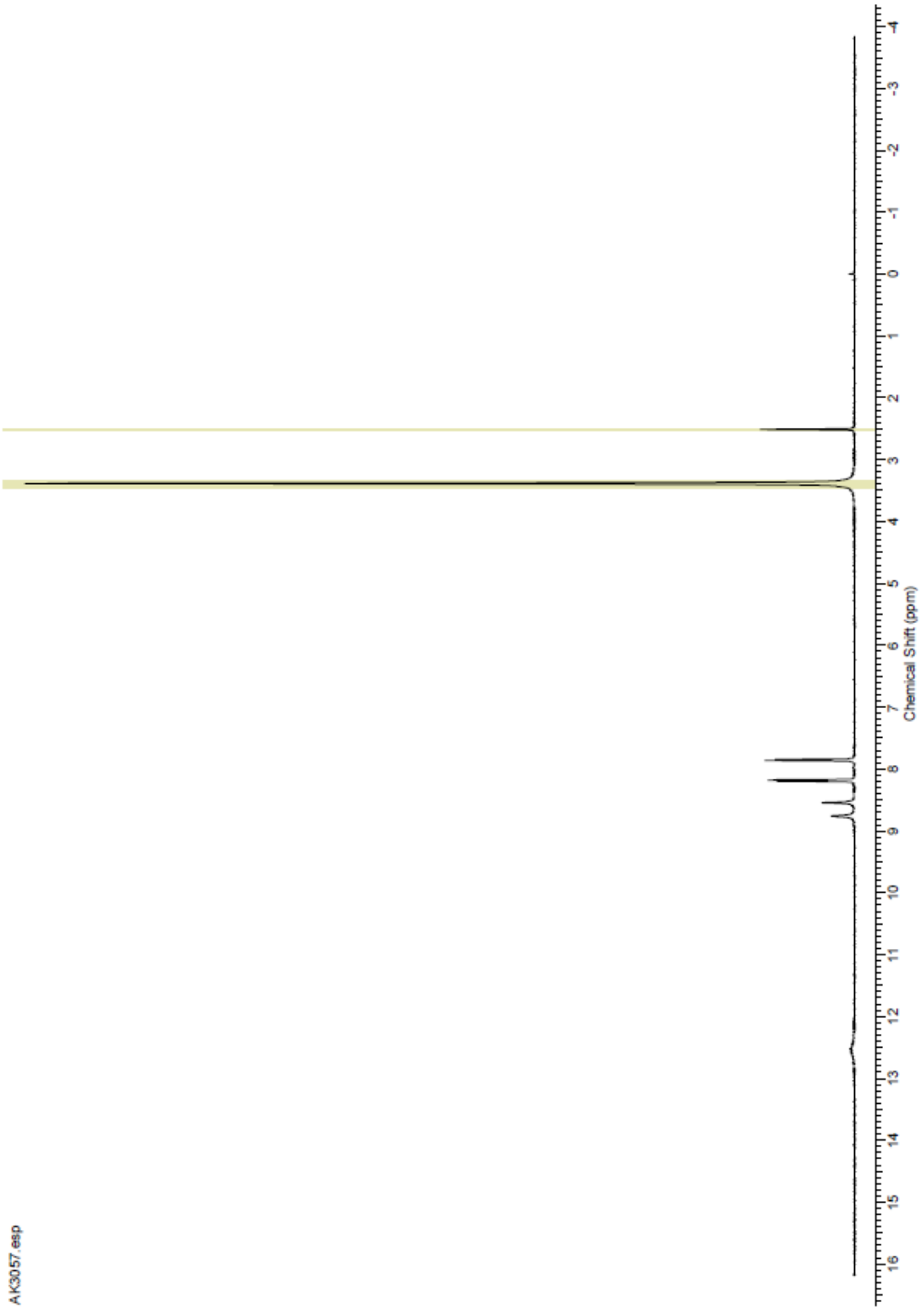

Compound 12 ^{13}C

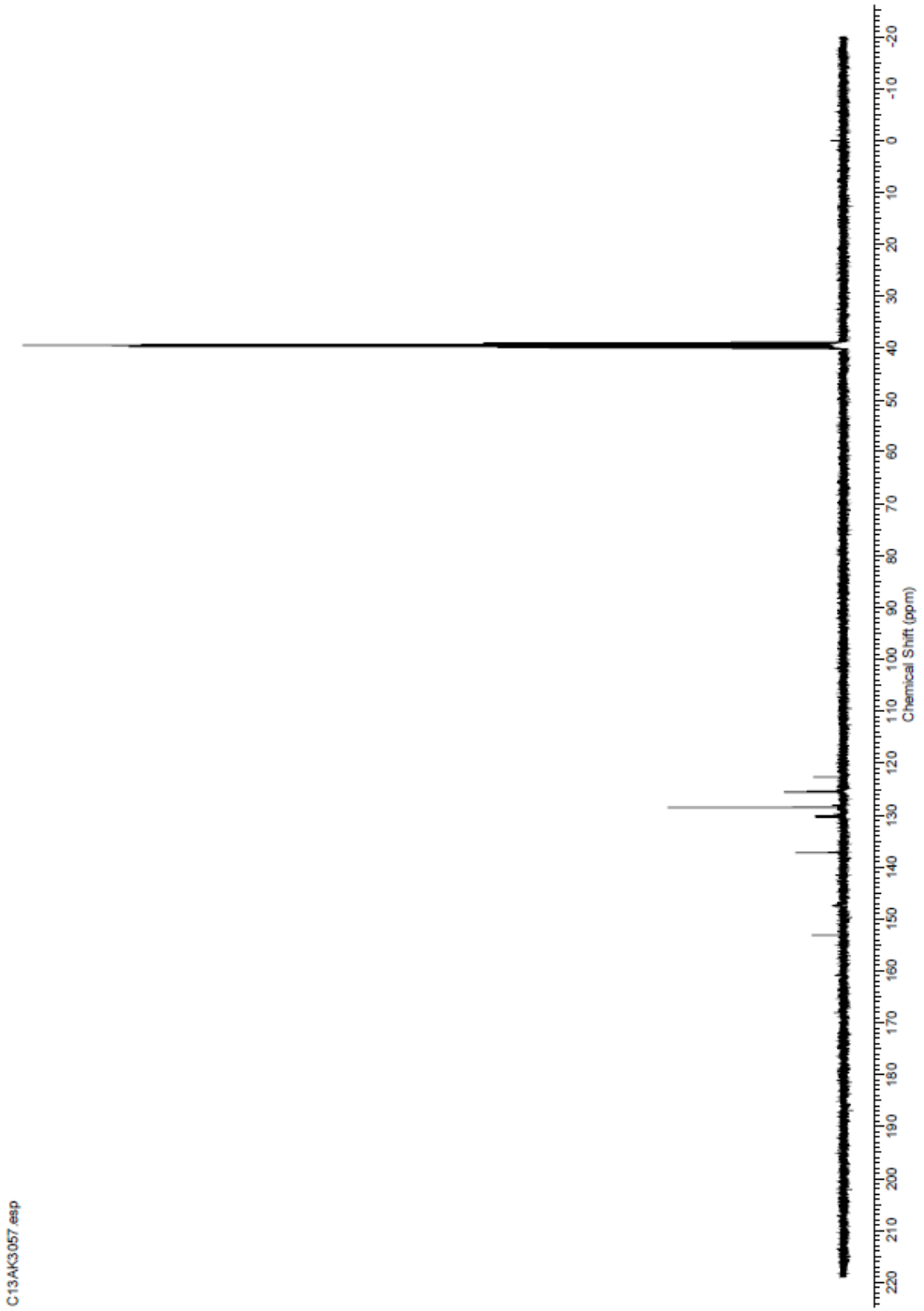

Compound 13 ^{1}H

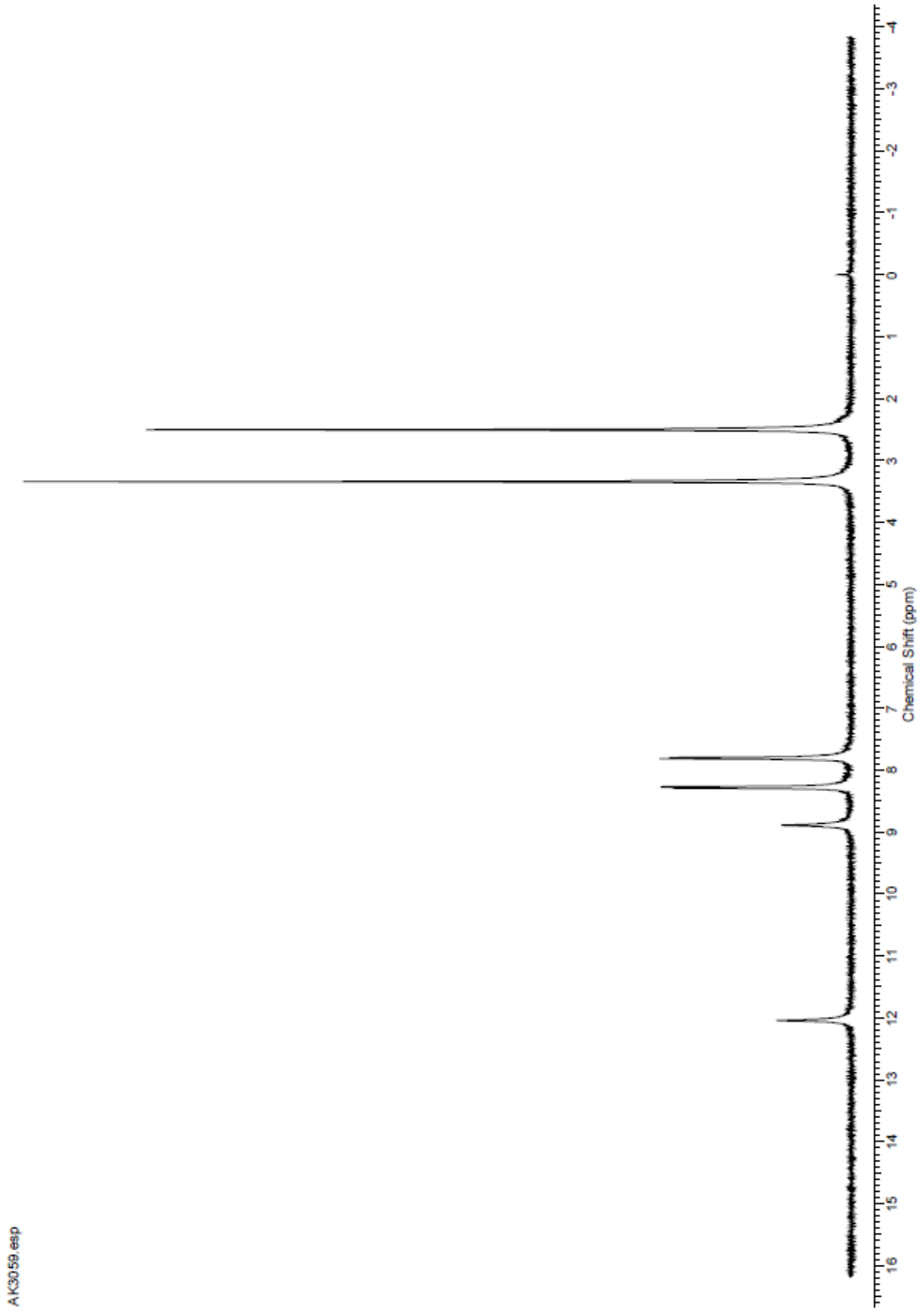

Compound 13 ^{13}C

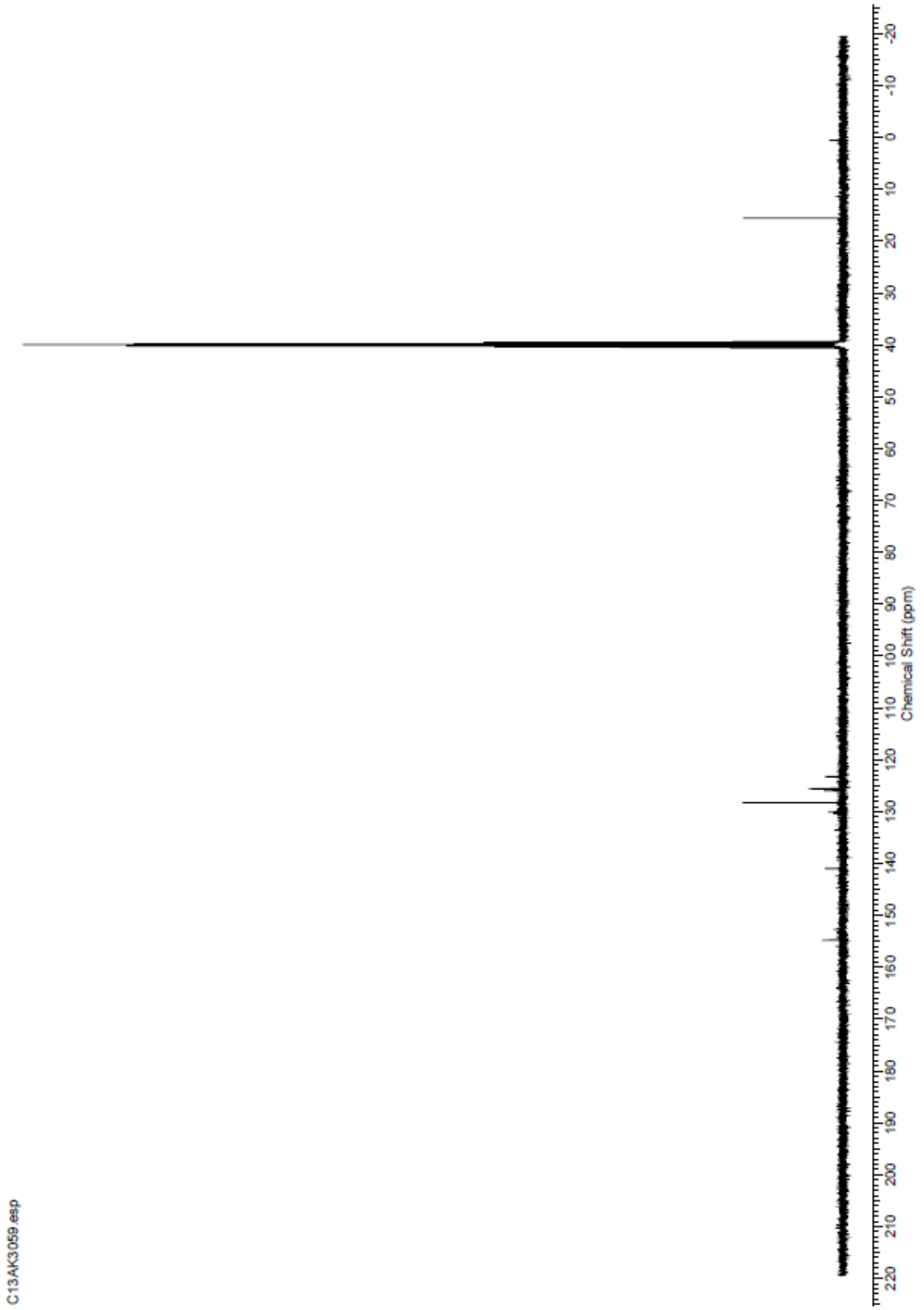

Compound 14 ^{1}H

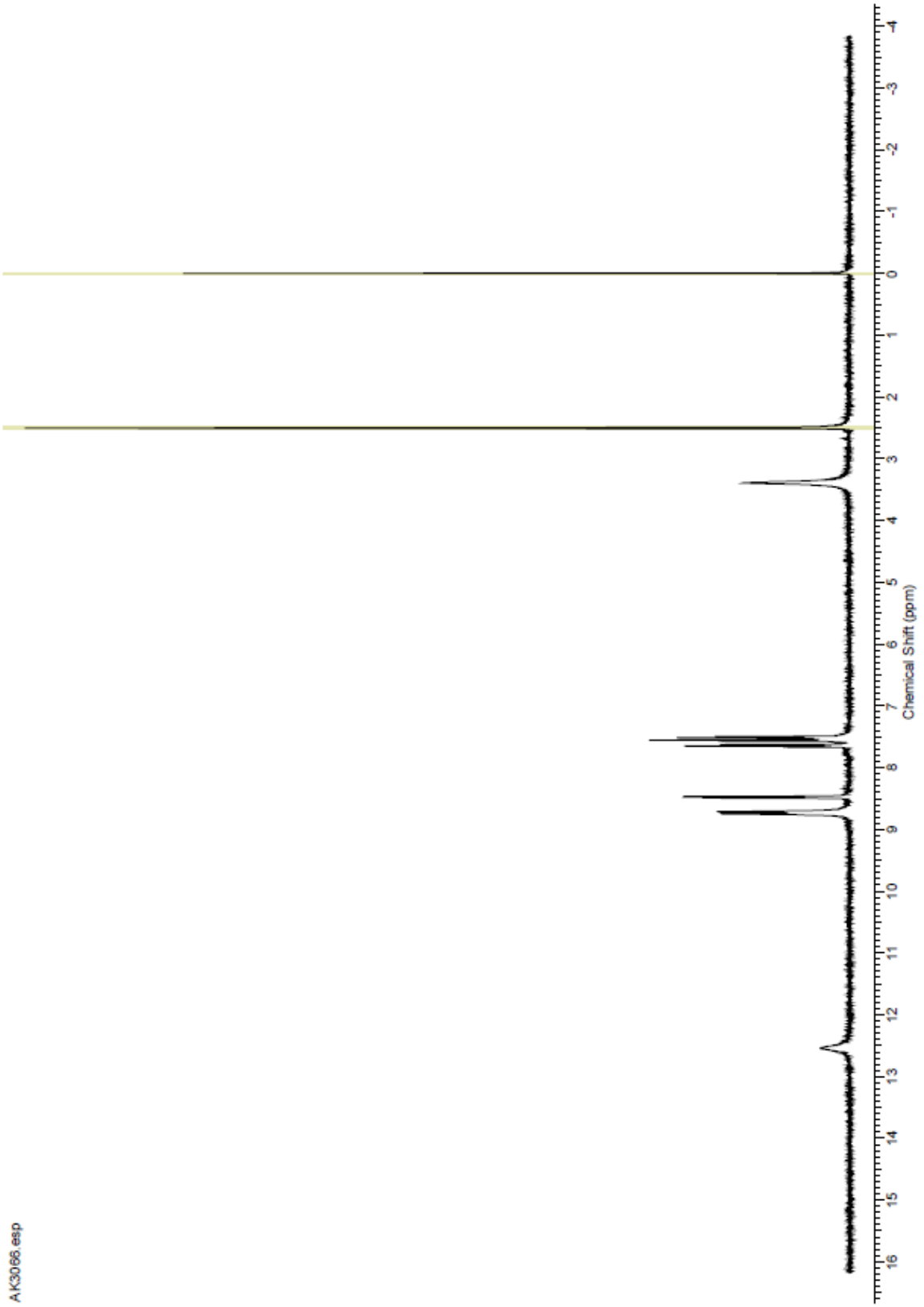

Compound 14 ^{13}C

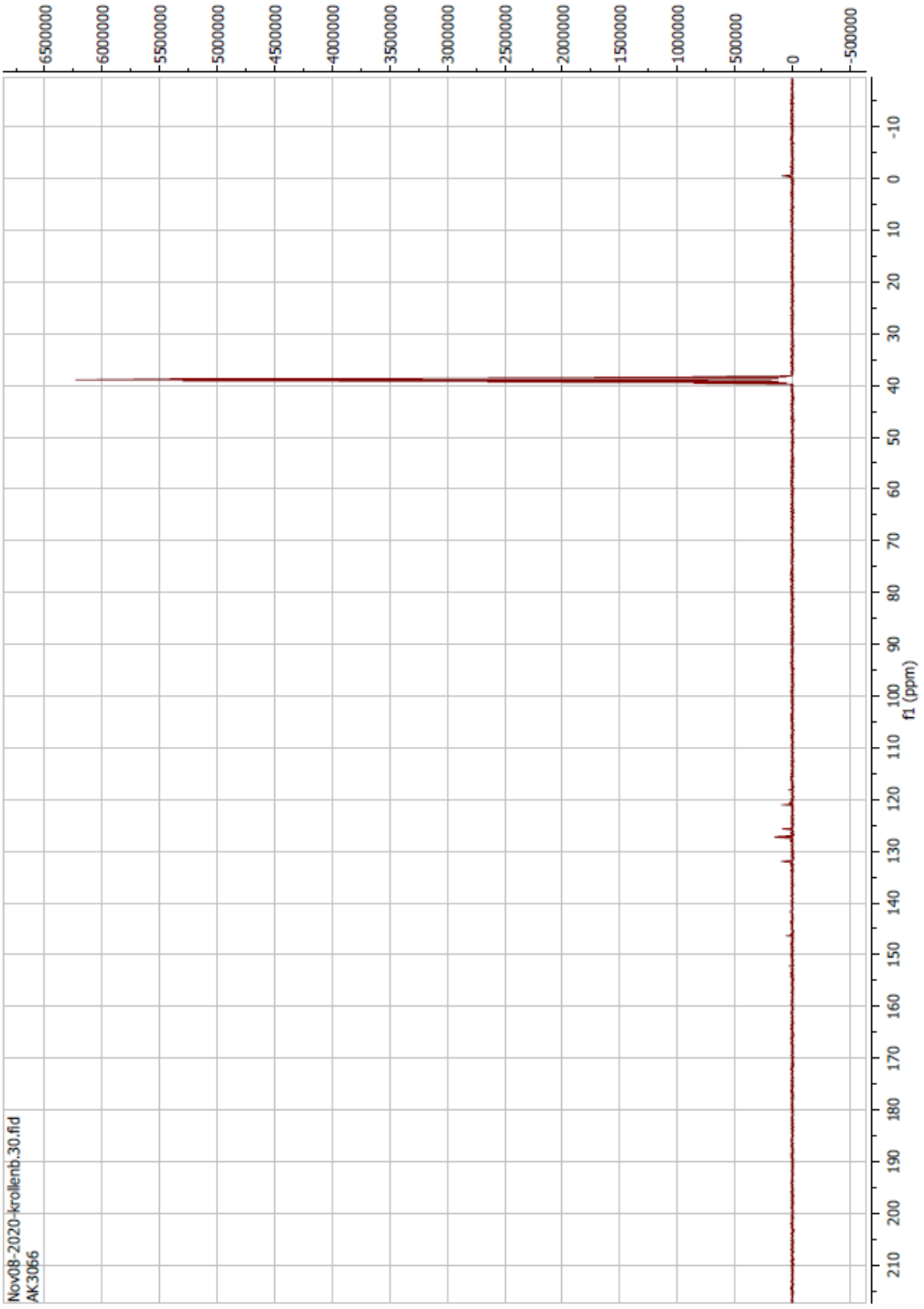

Compound 15 ^{1}H

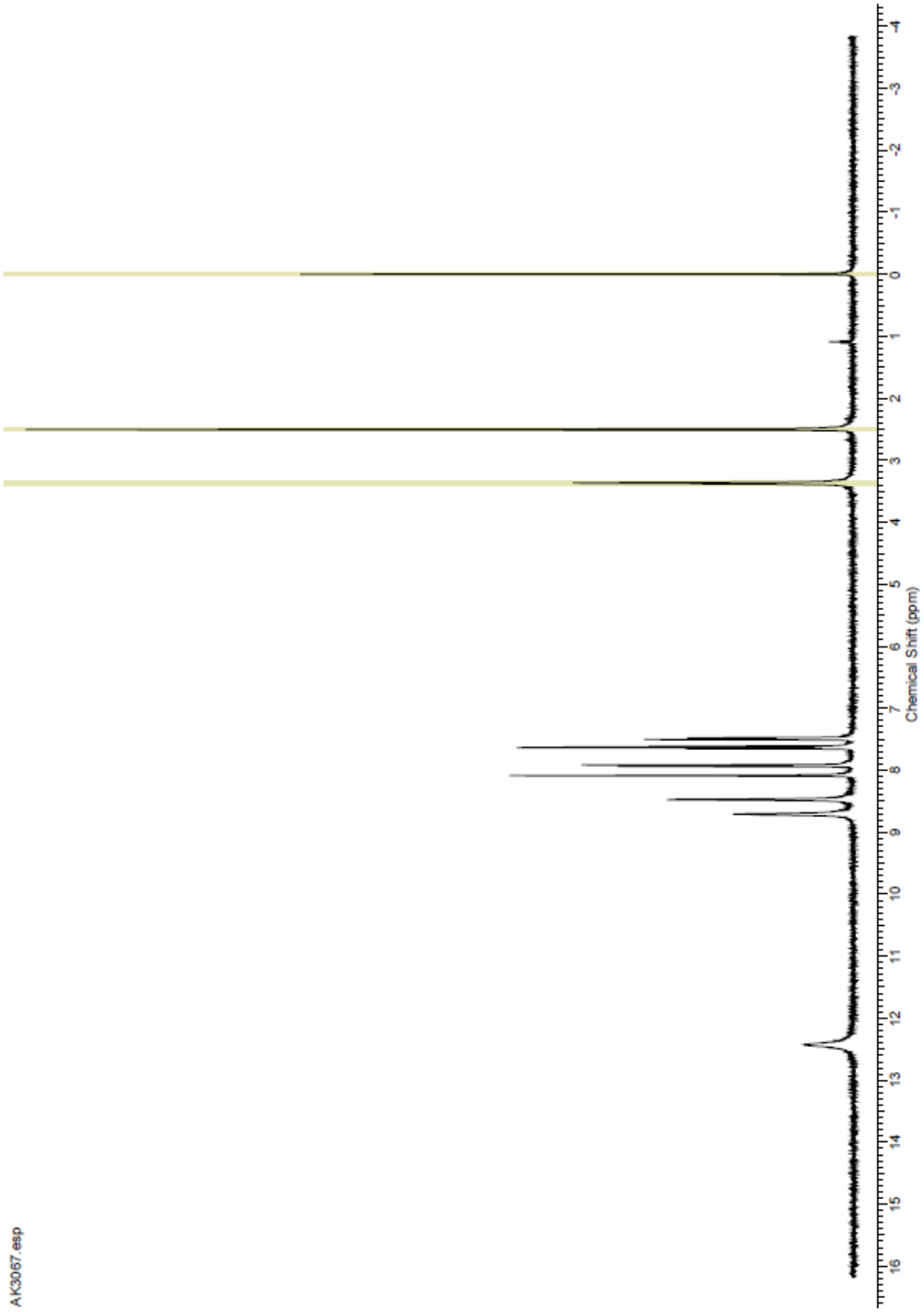

Compound 15 ^{13}C

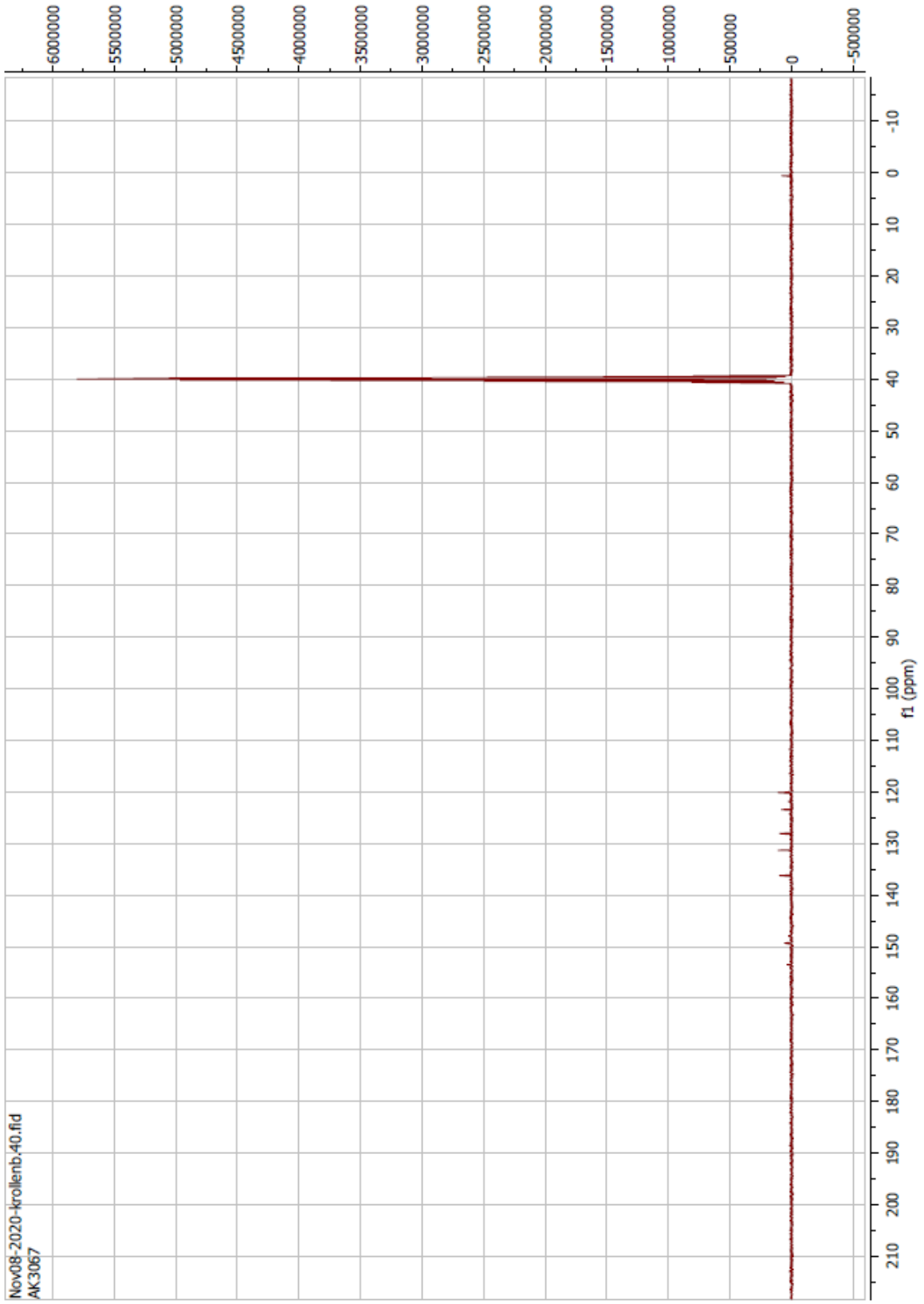

Compound 16 ^{1}H

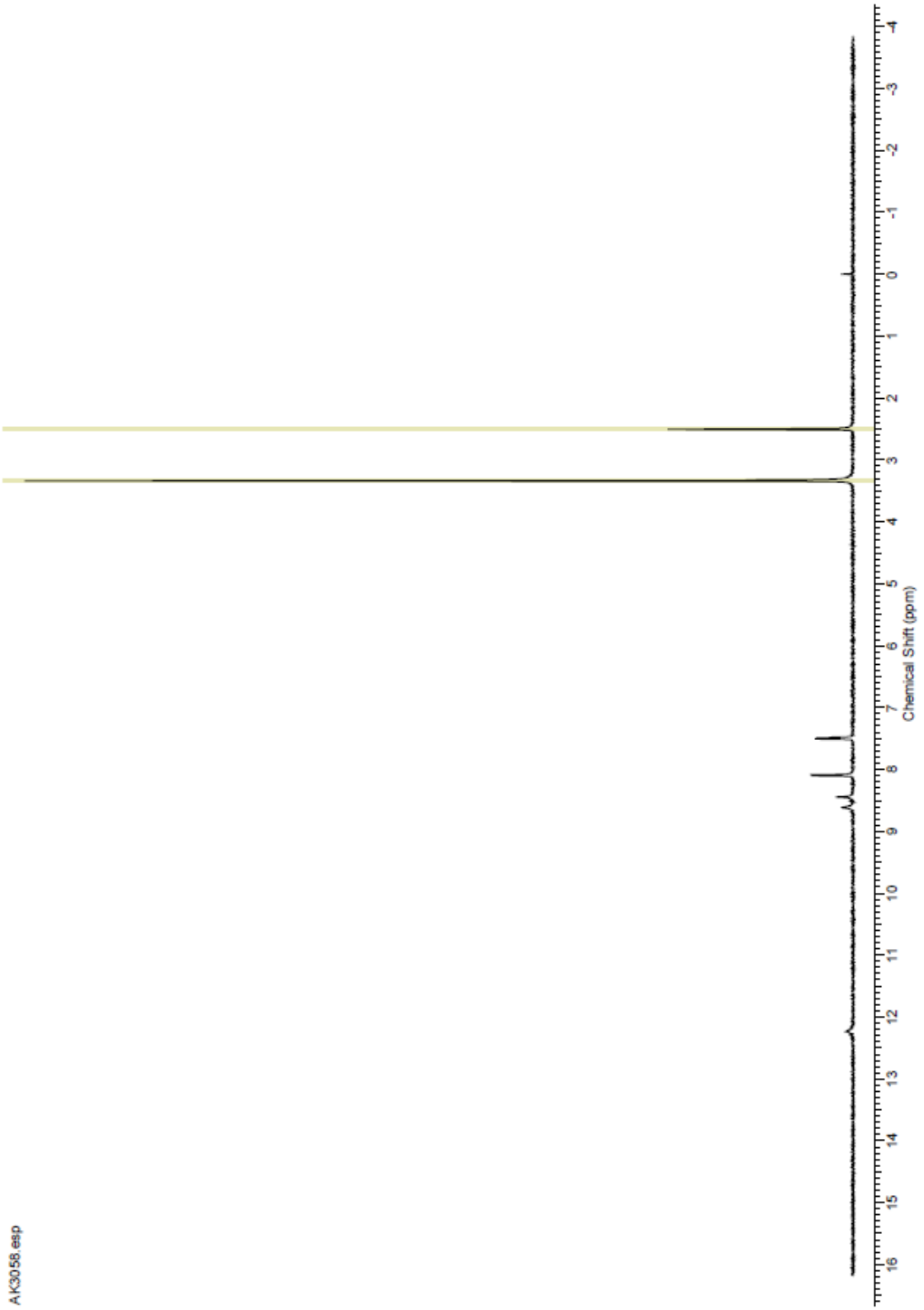

Compound 16 ^{13}C

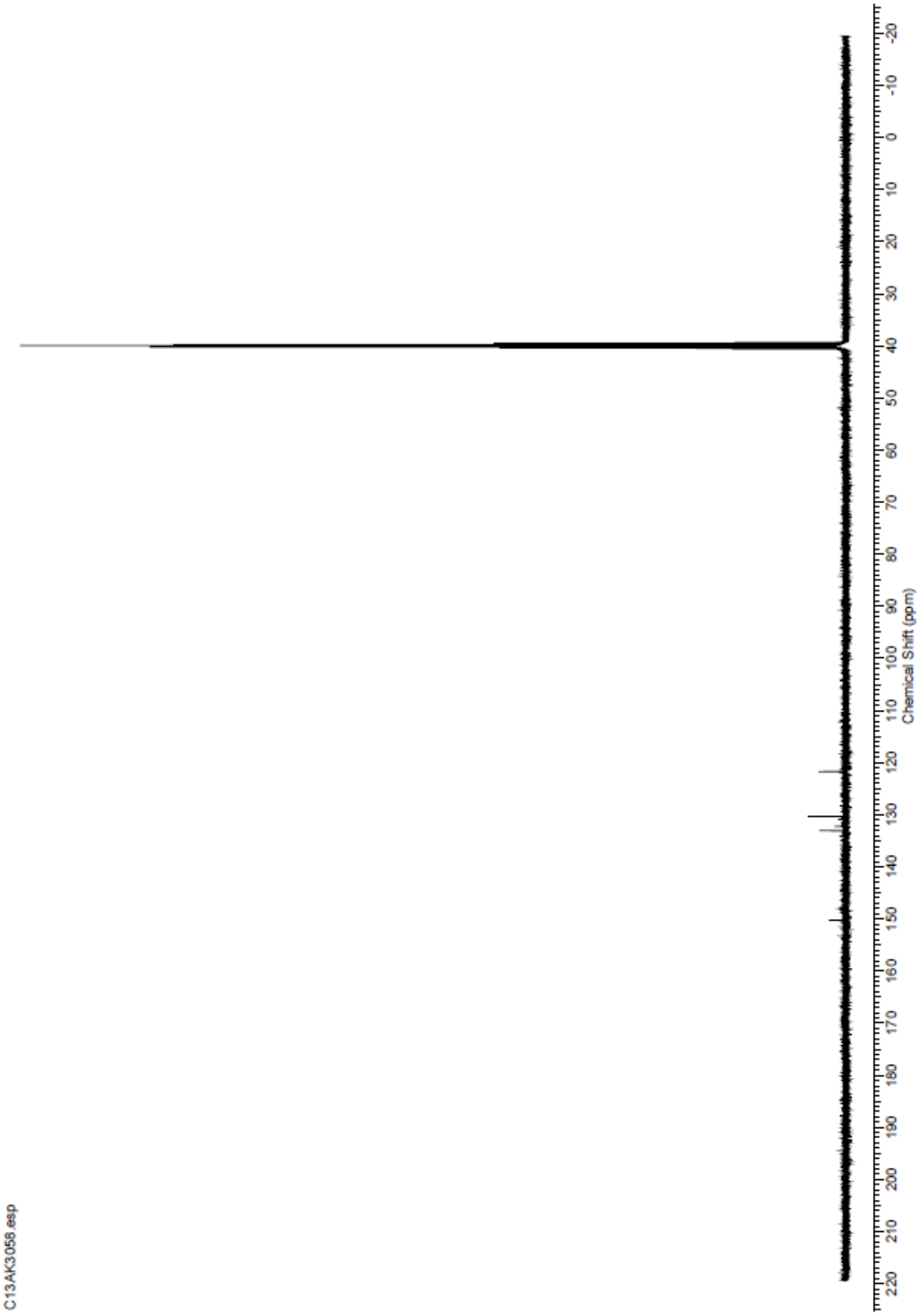

Compound 17 ^{1}H

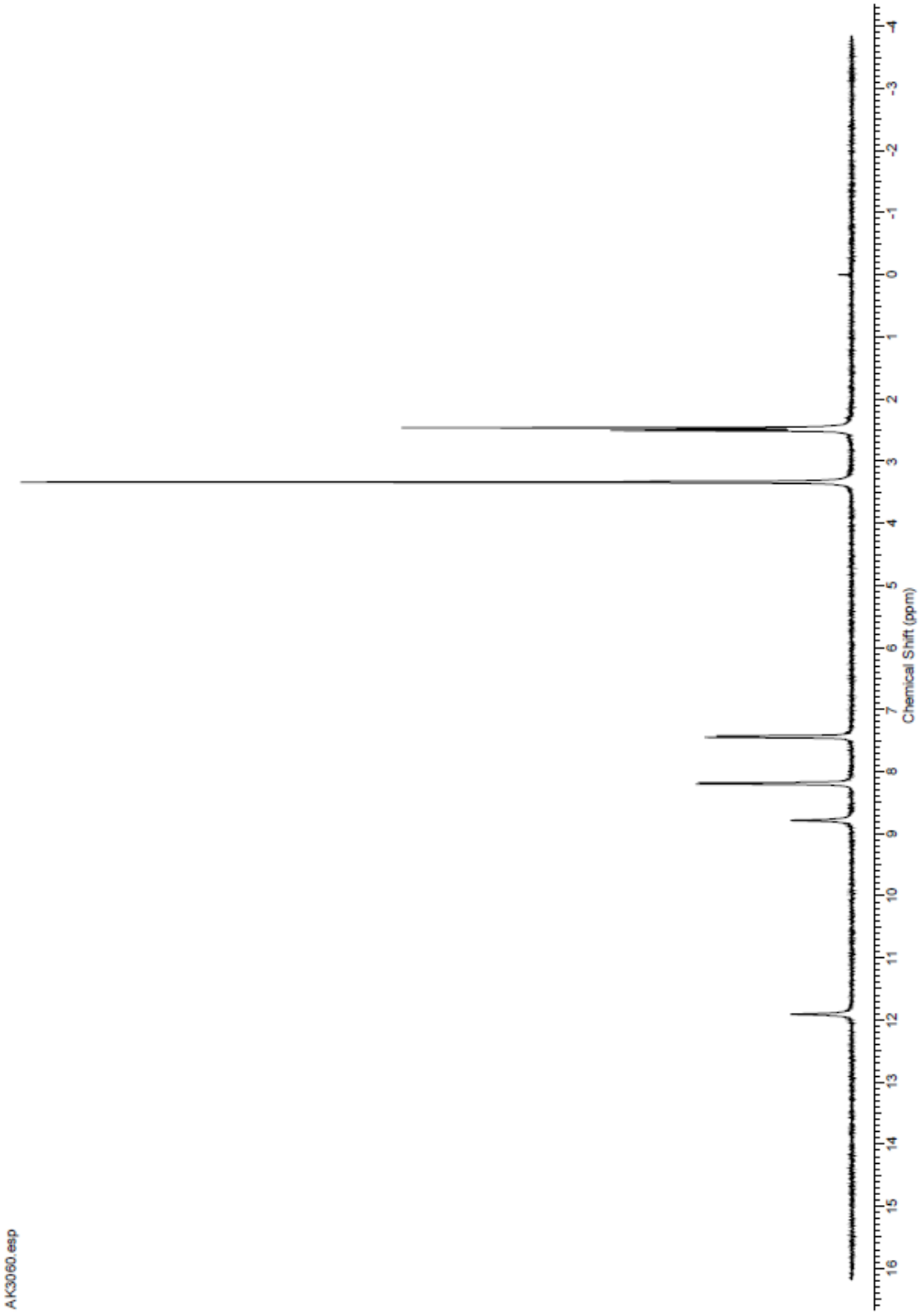

Compound 17 ^{13}C

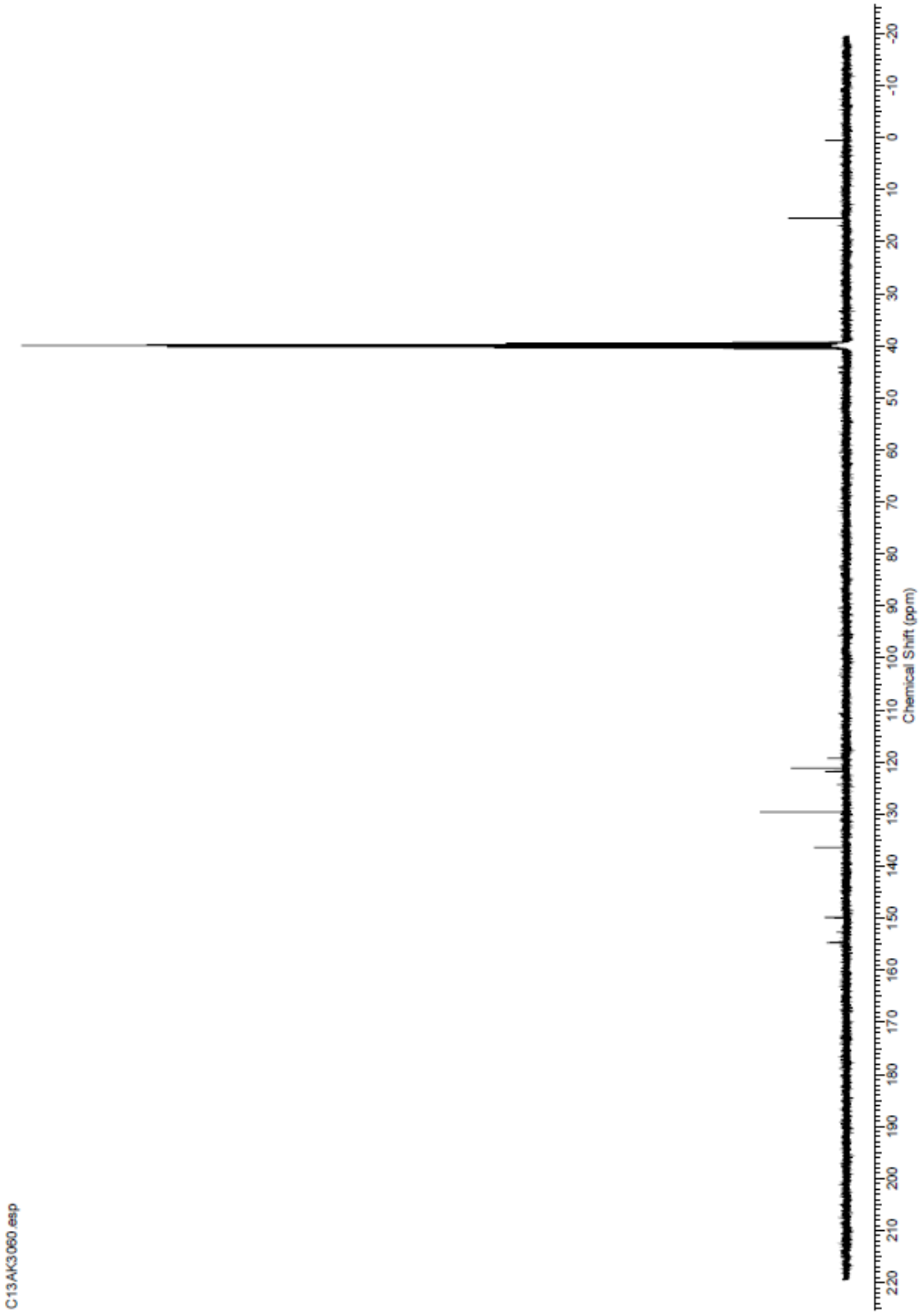

Compound 18 ^{1}H

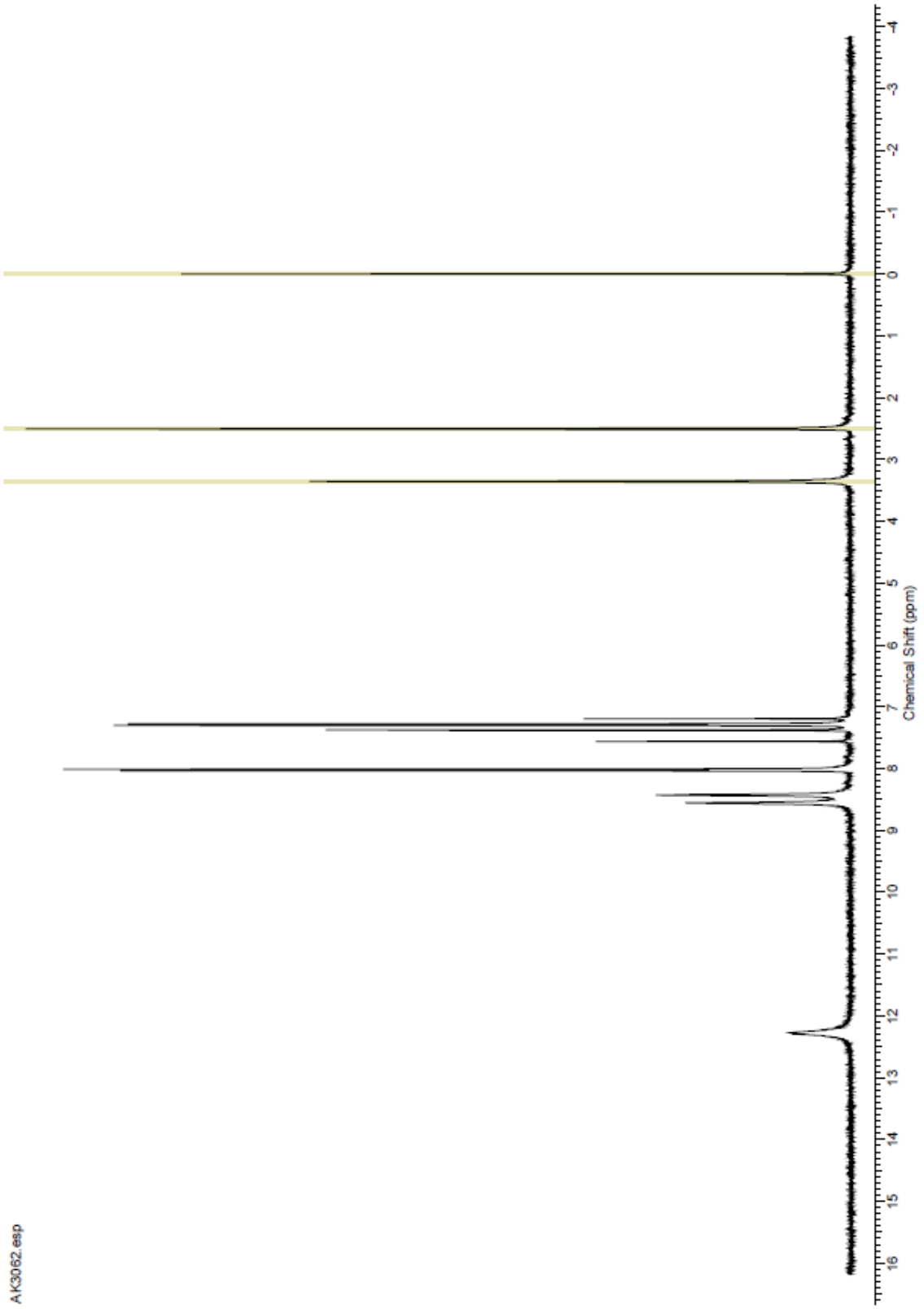

Compound 18 ^{13}C

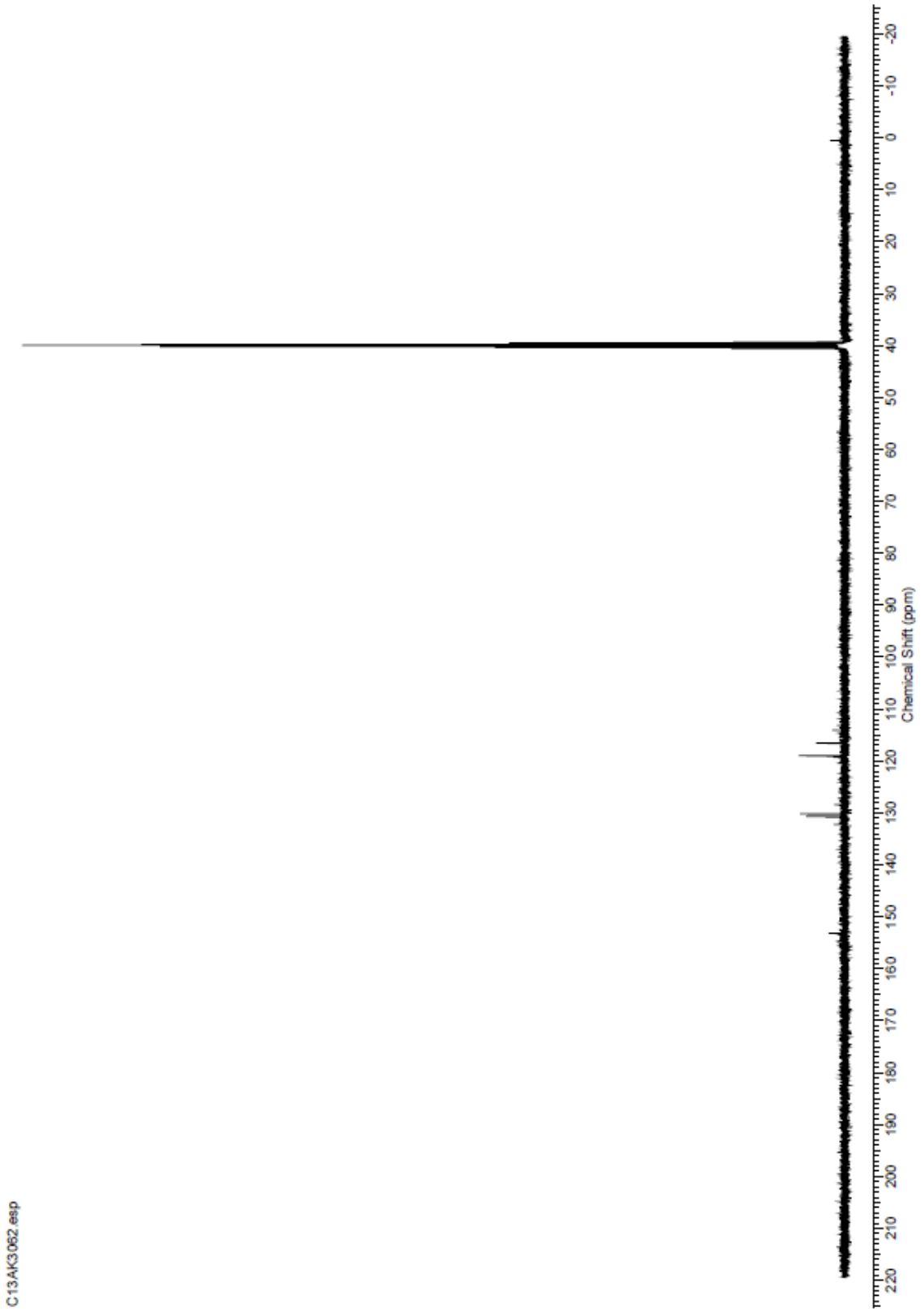

Compound 19 ^{1}H

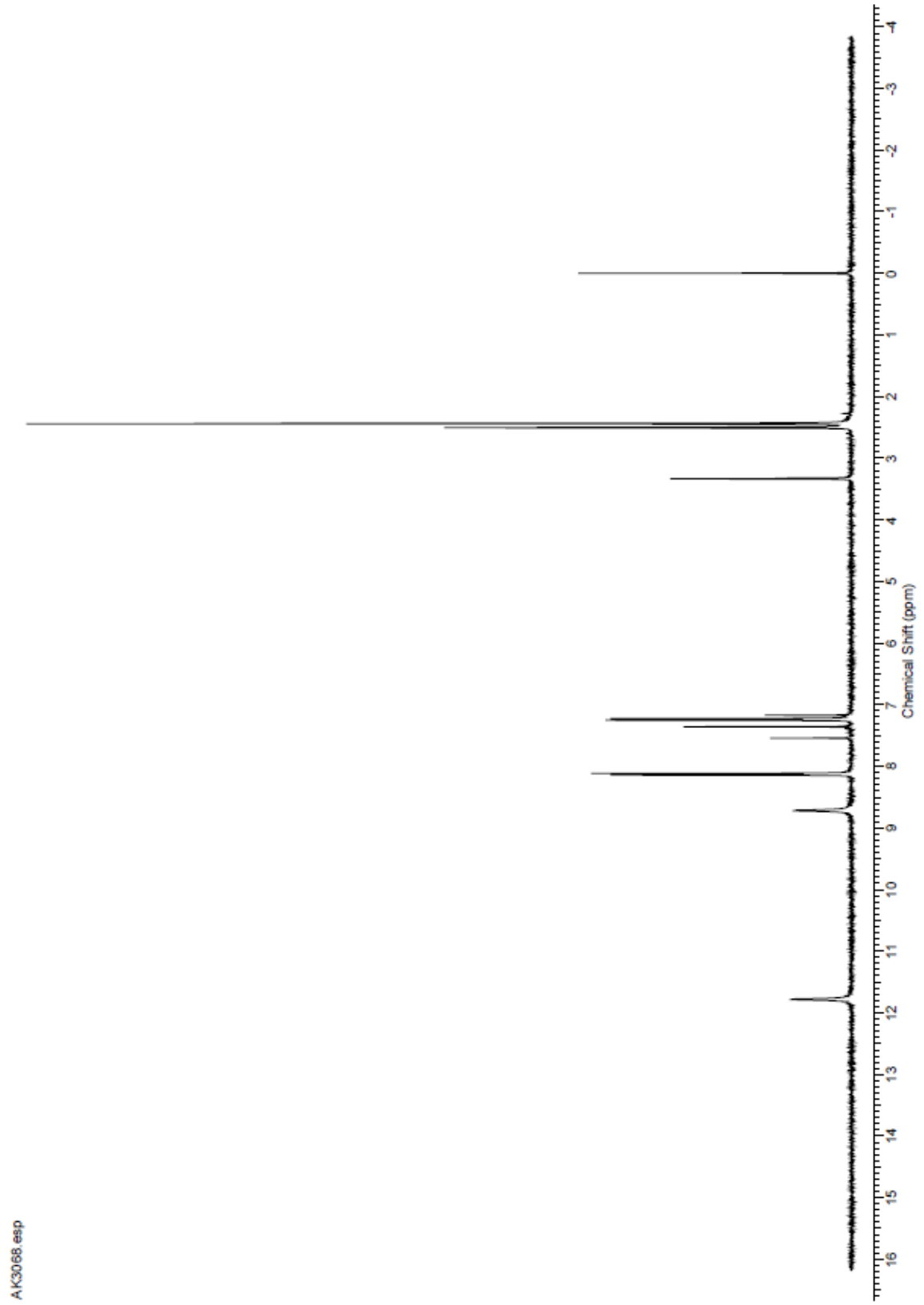

Compound 19 ^{13}C

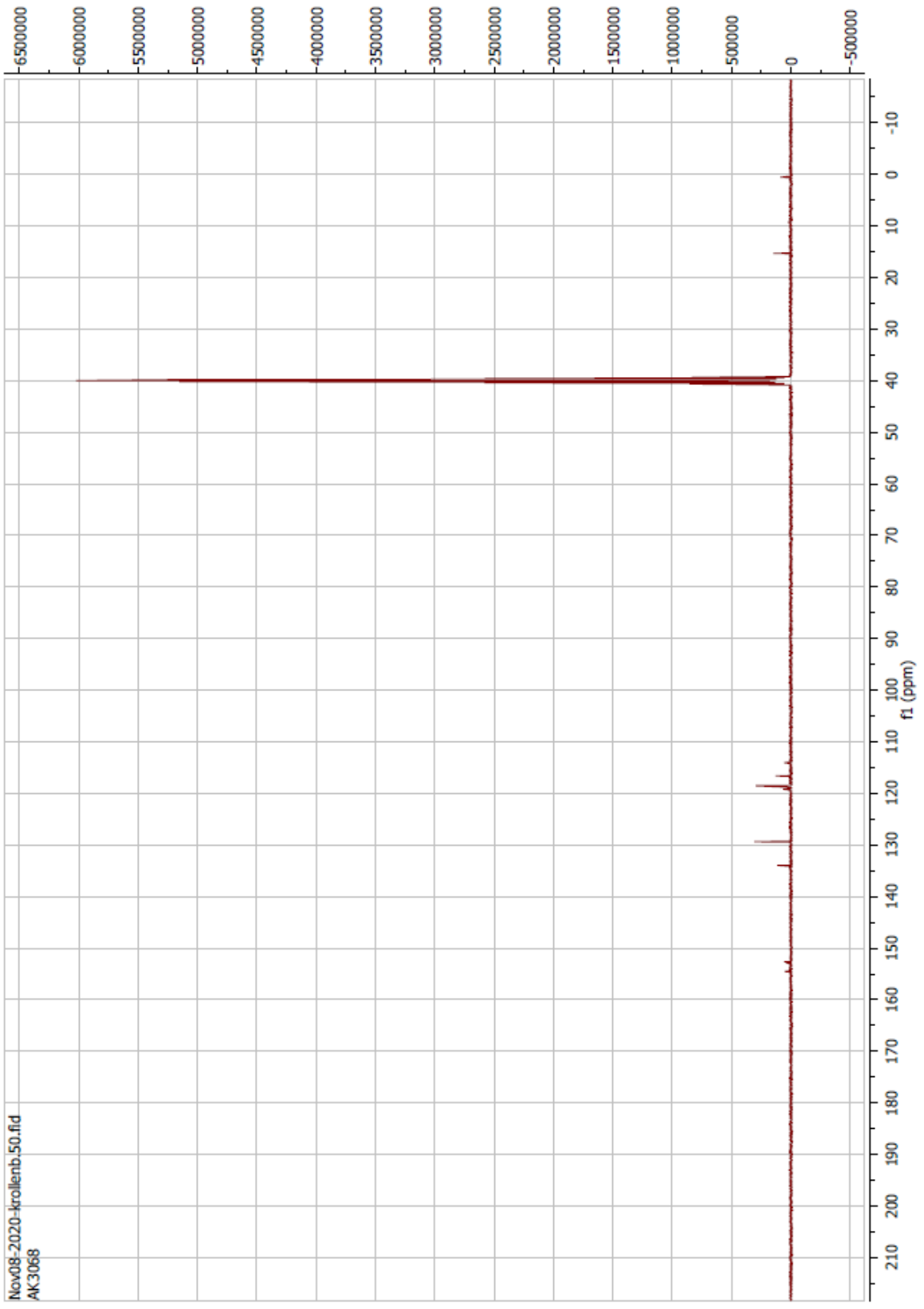

Compound 20 ^{1}H

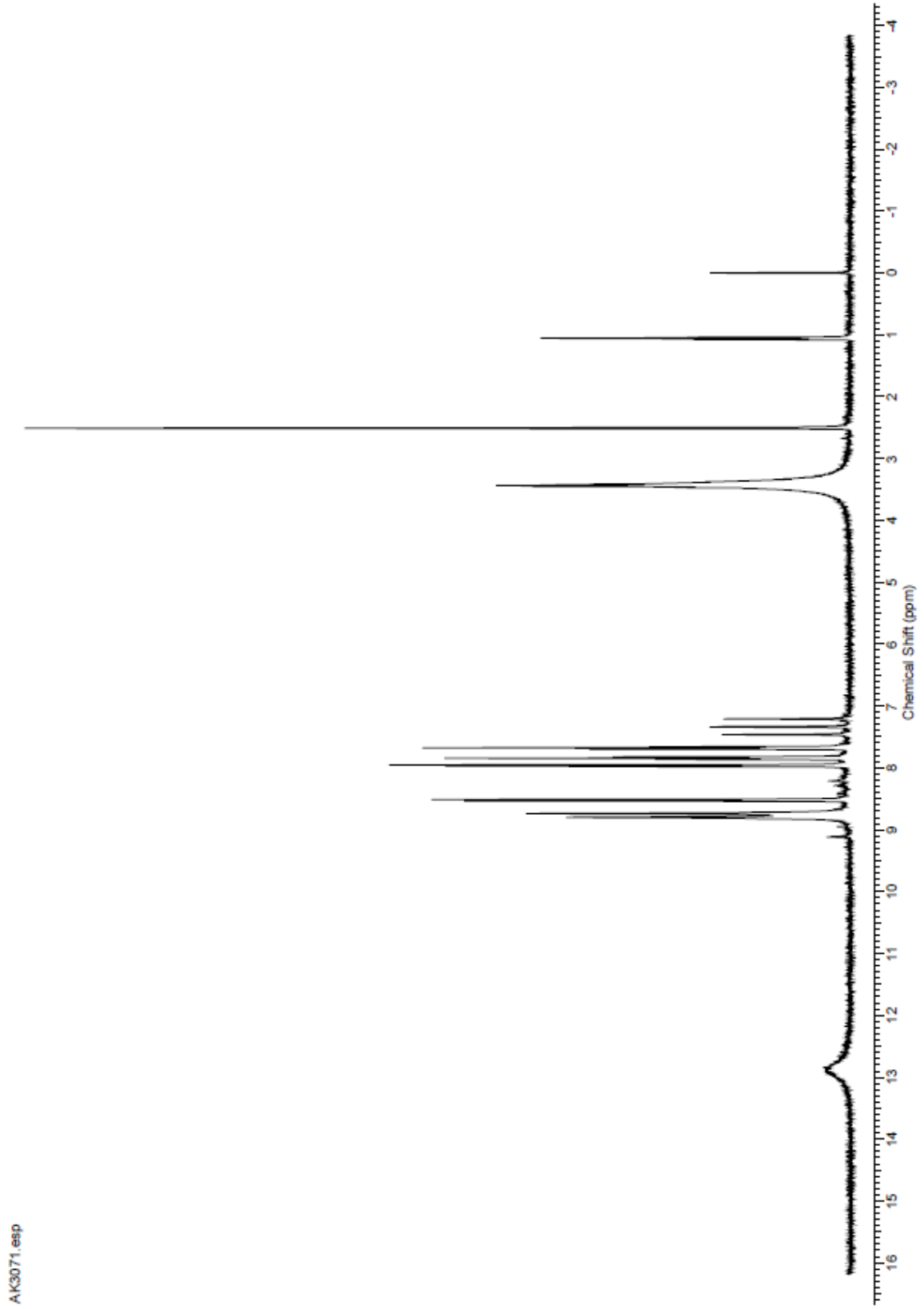

Compound 20 ^{13}C

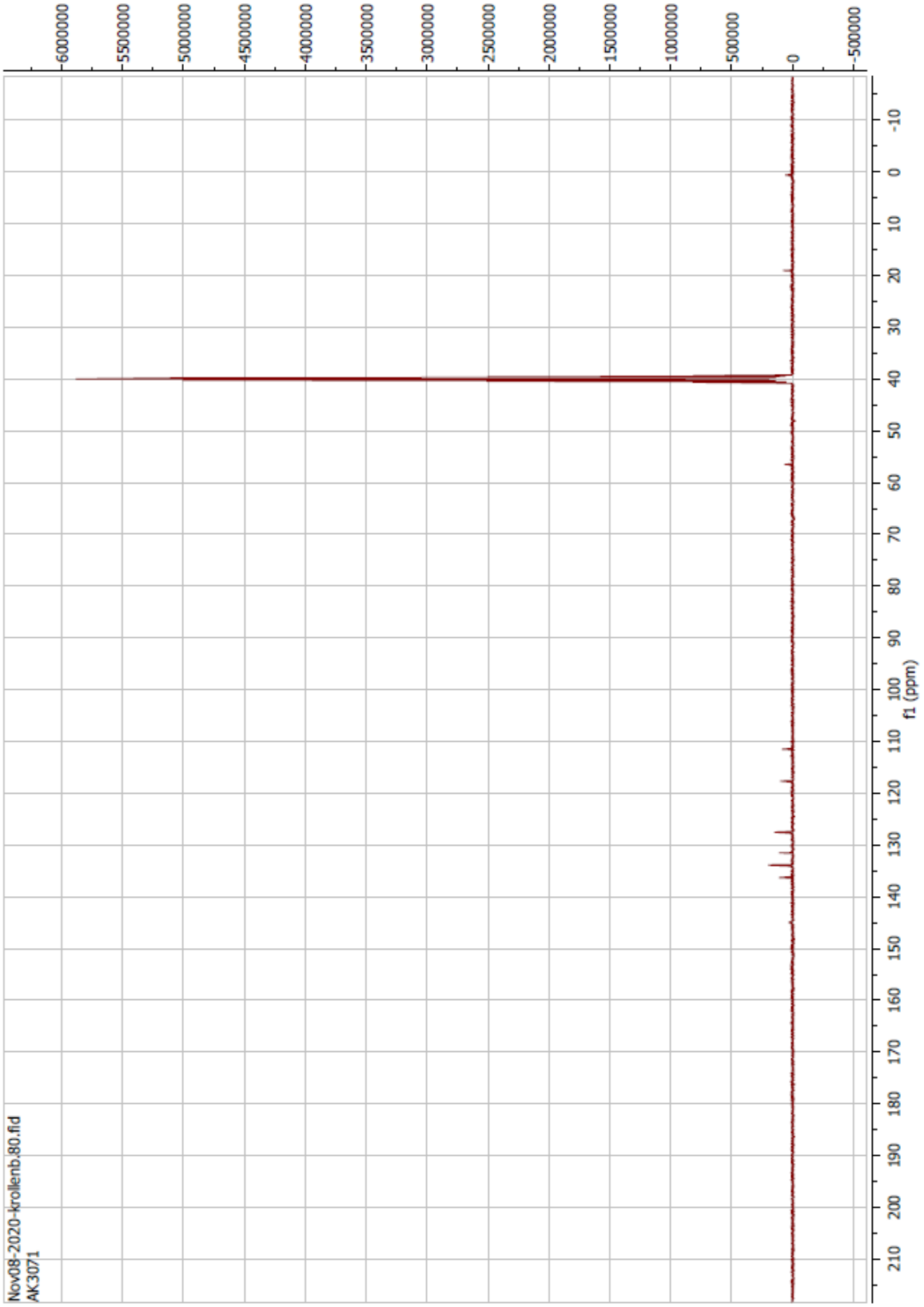

Compound 21 ^{1}H

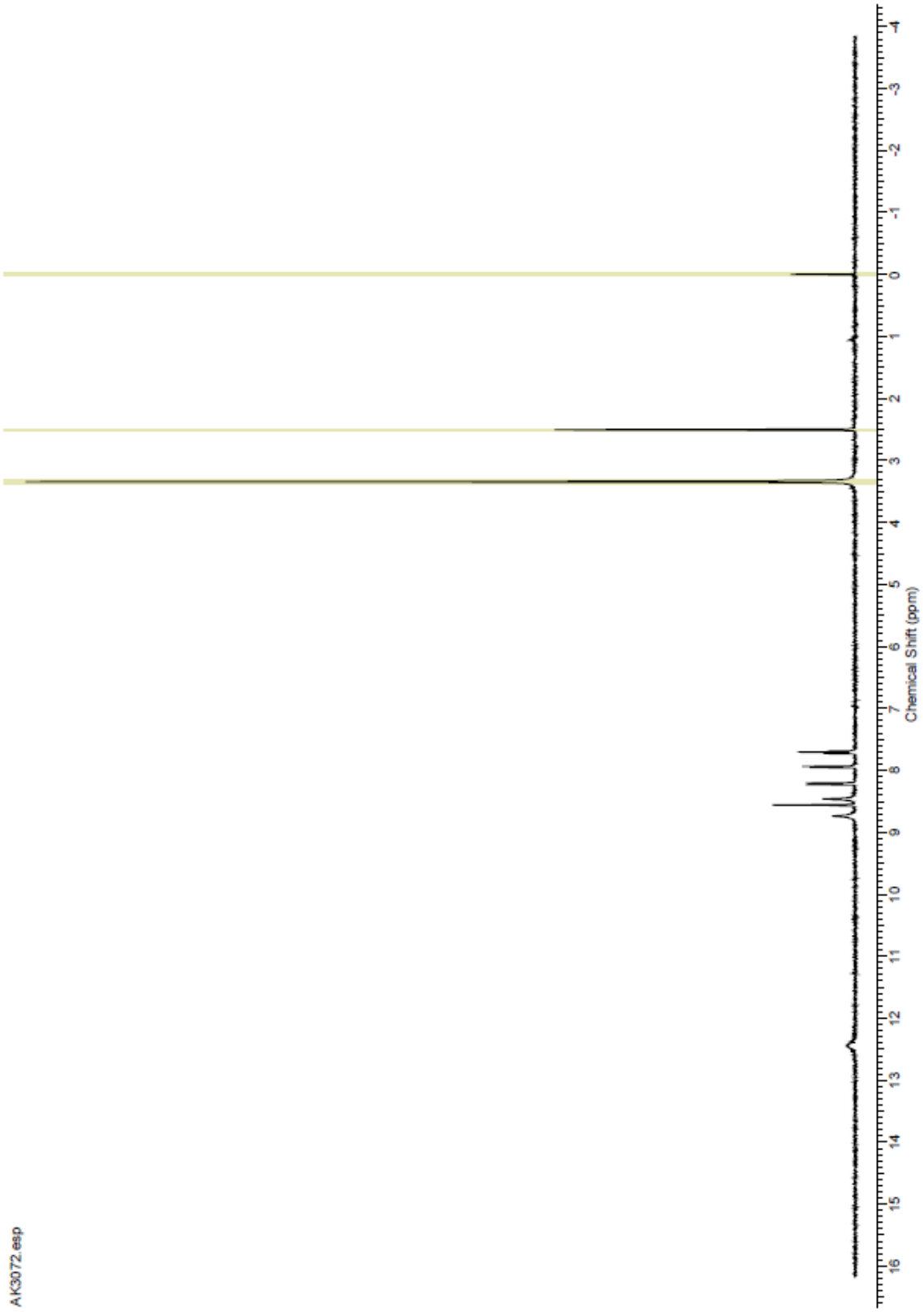

Compound 21 ^{13}C

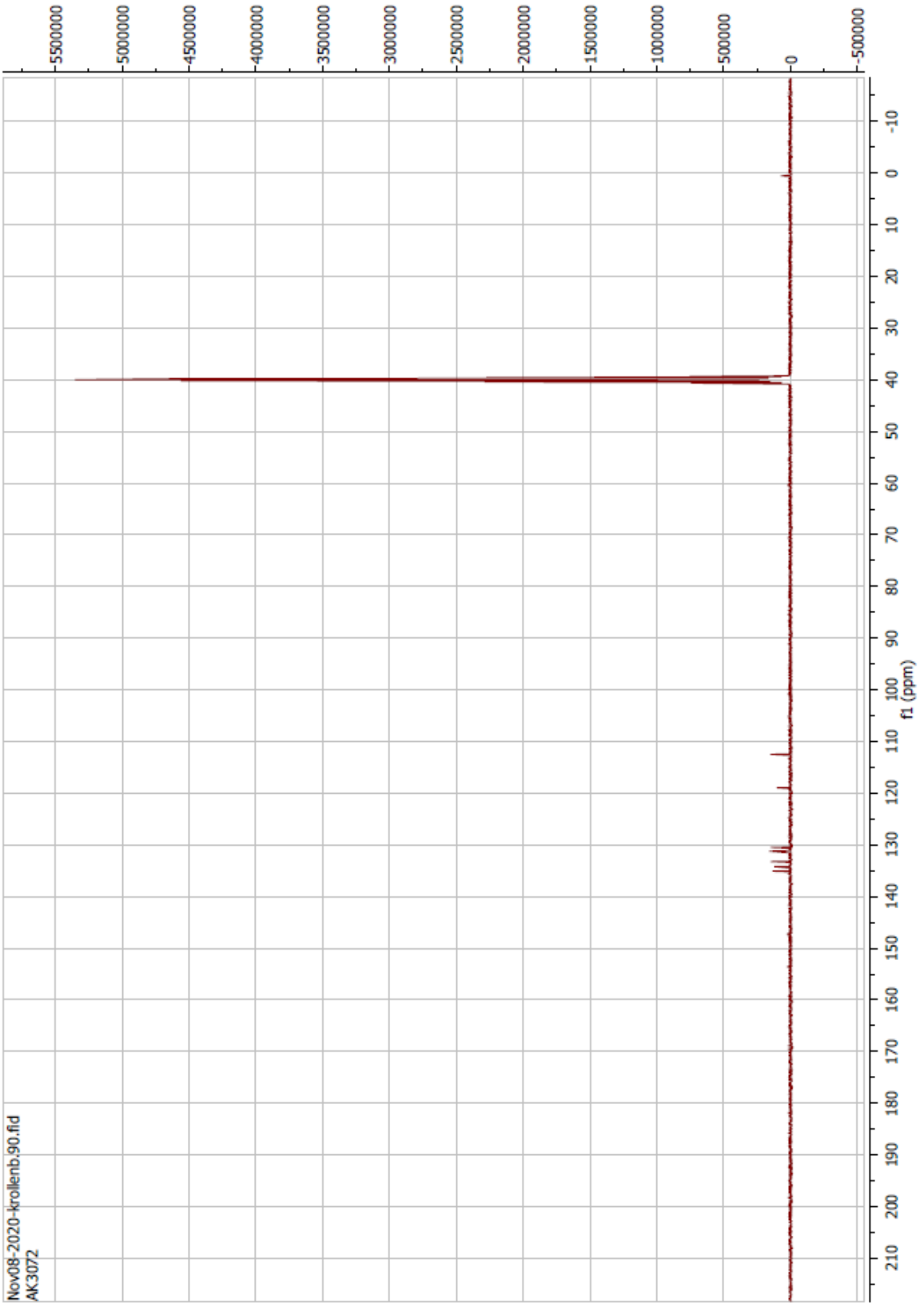

Compound 22 ^{1}H

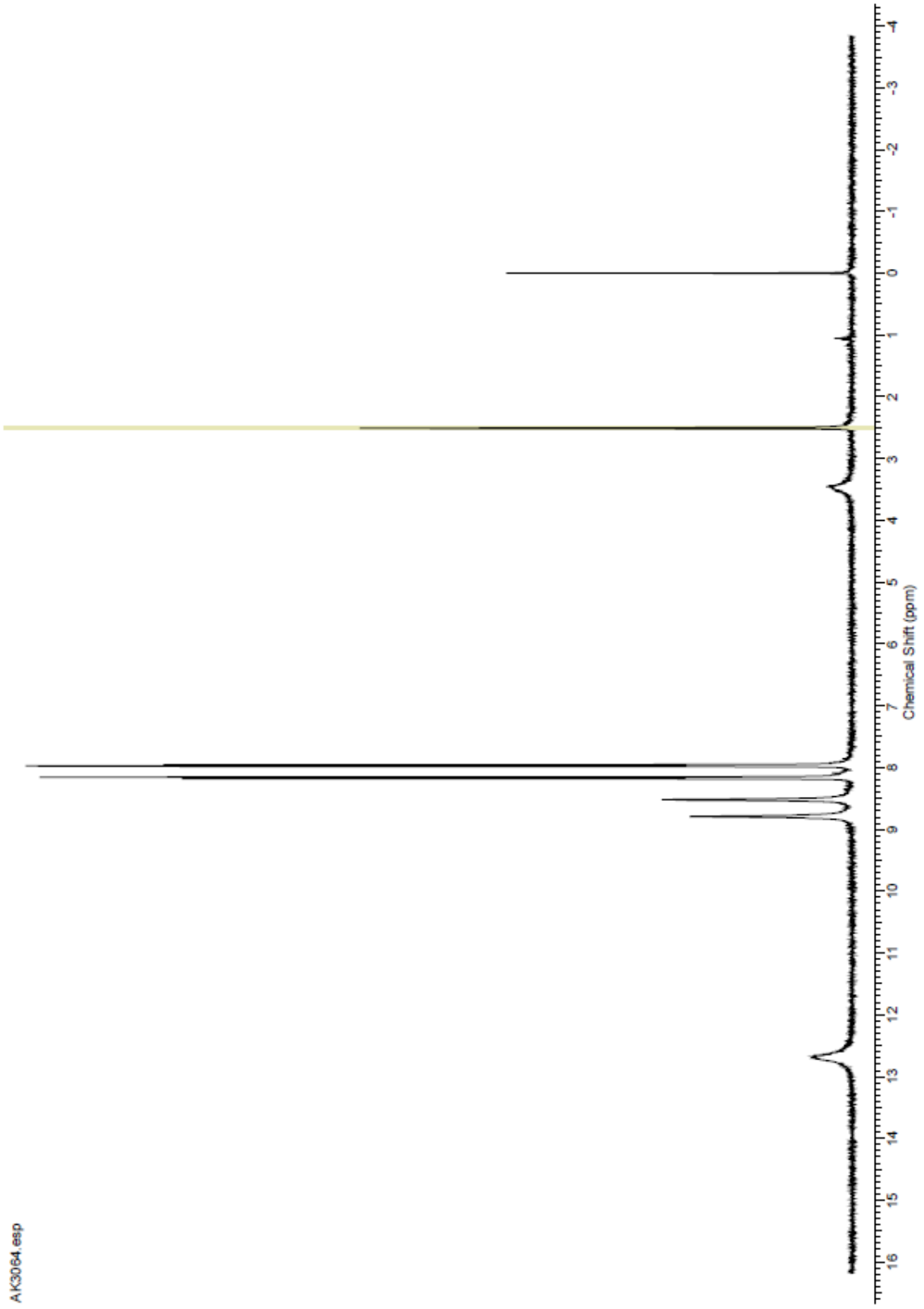

Compound 22 ^{13}C

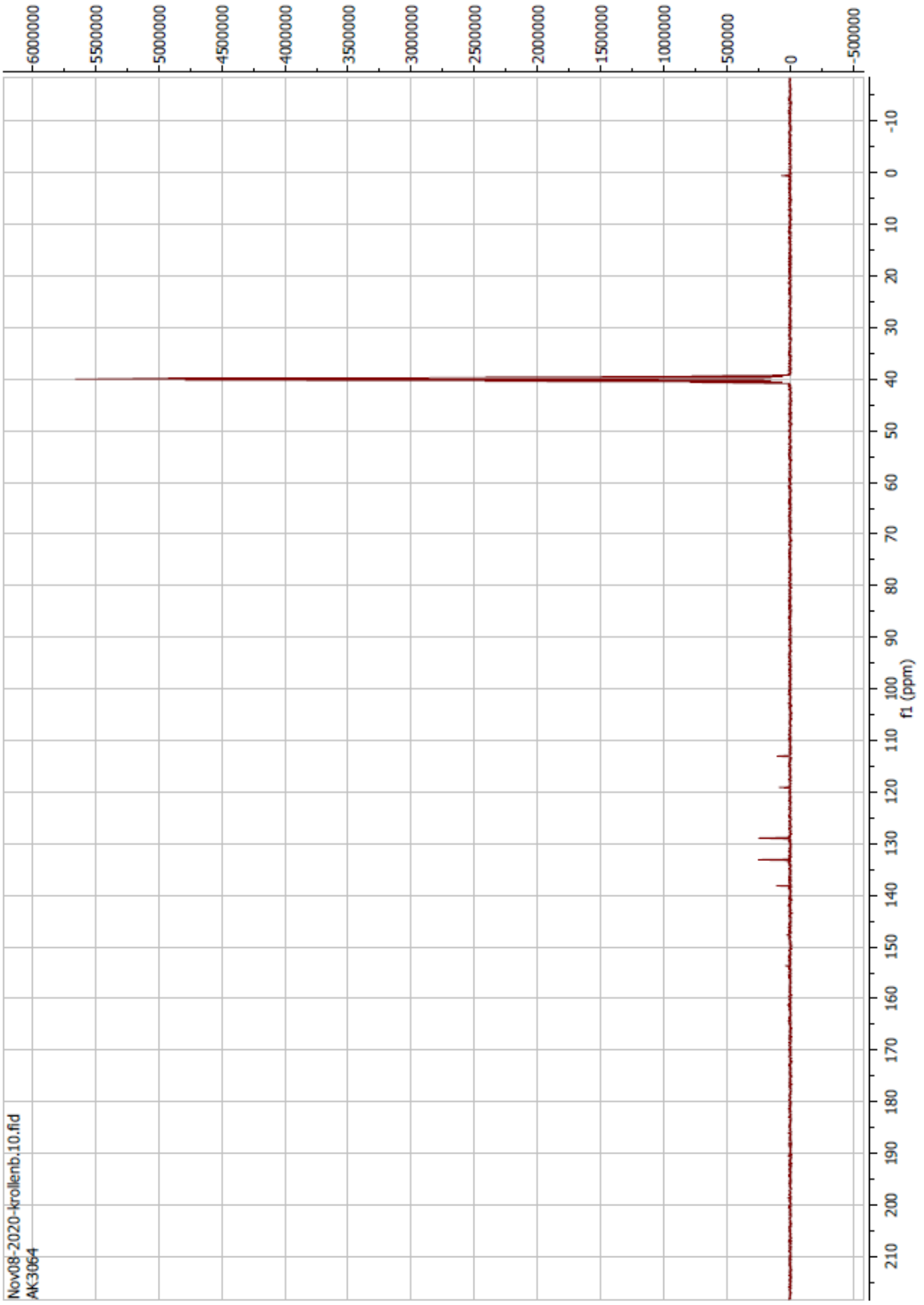

Compound 23 ^{1}H

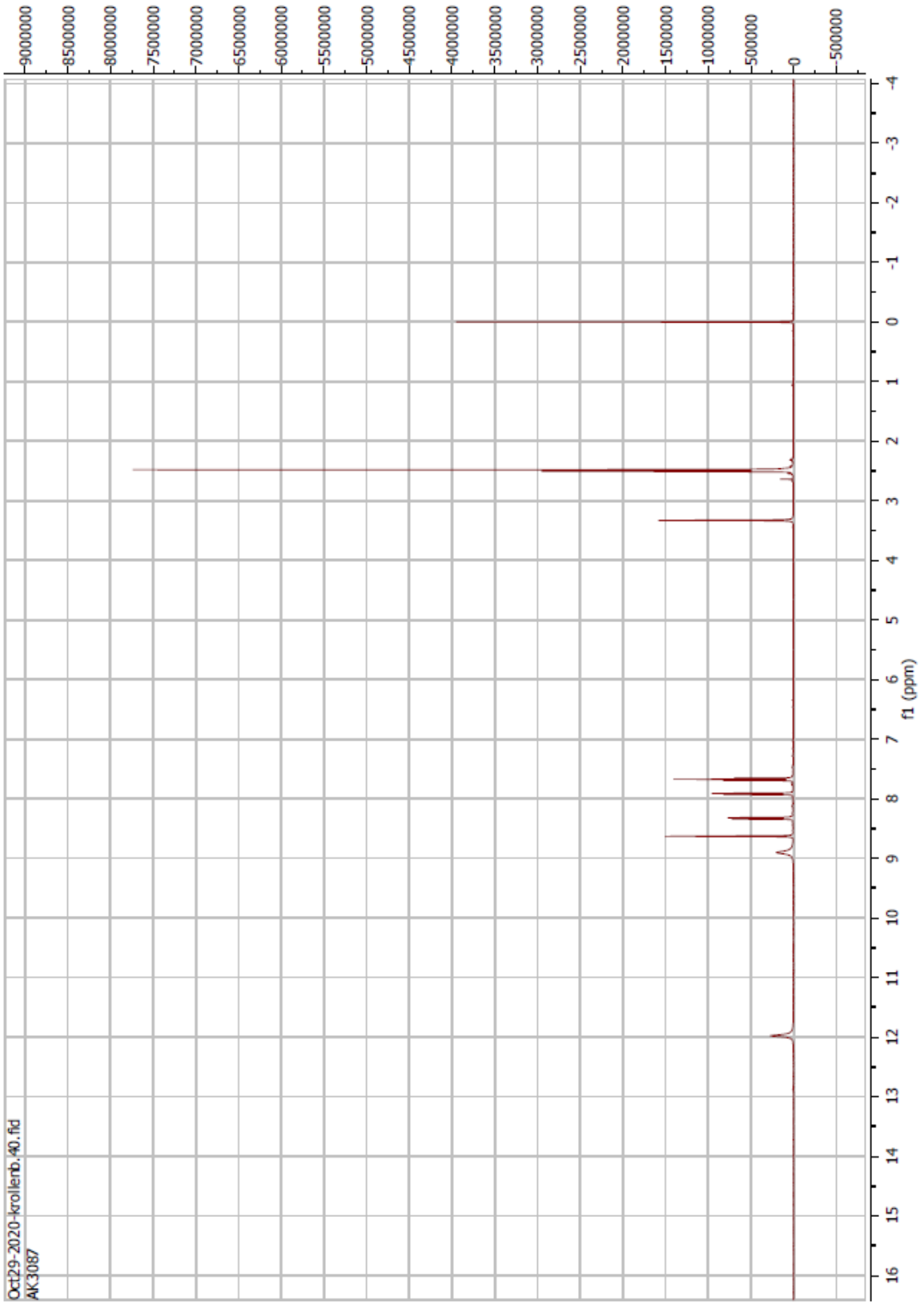

Compound 23 ^{13}C

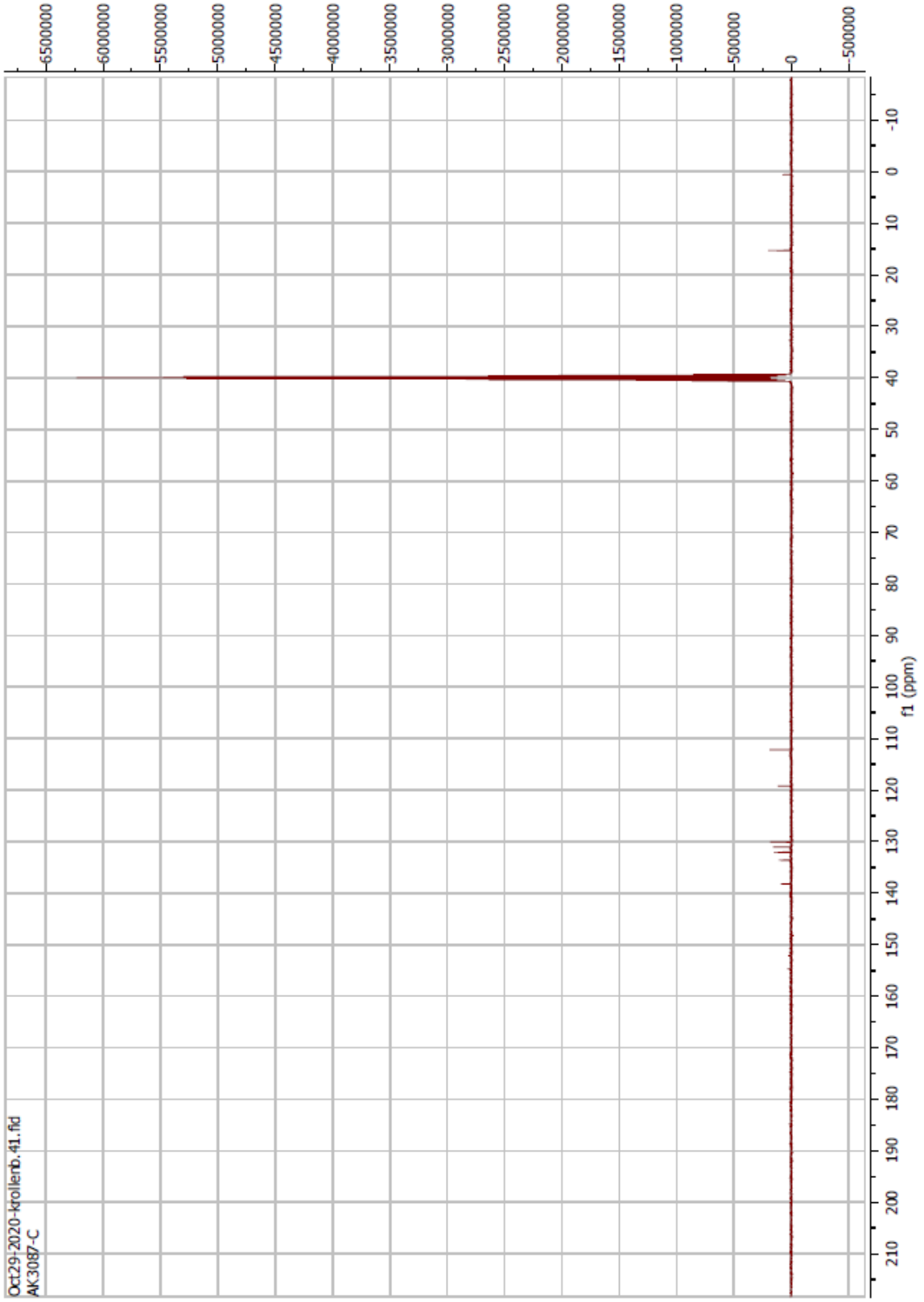

Compound 24 ^{1}H

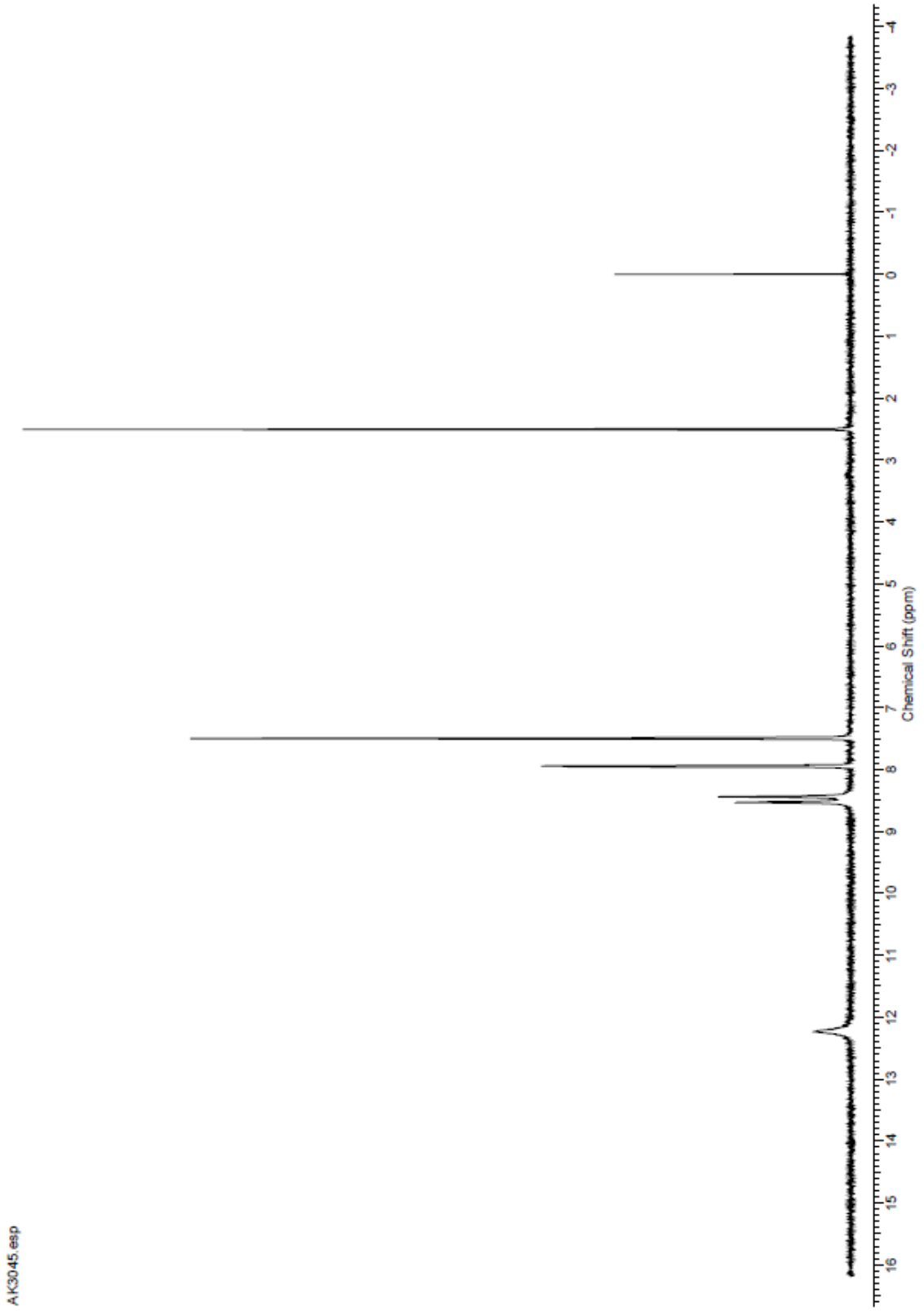

Compound 24 ^{13}C

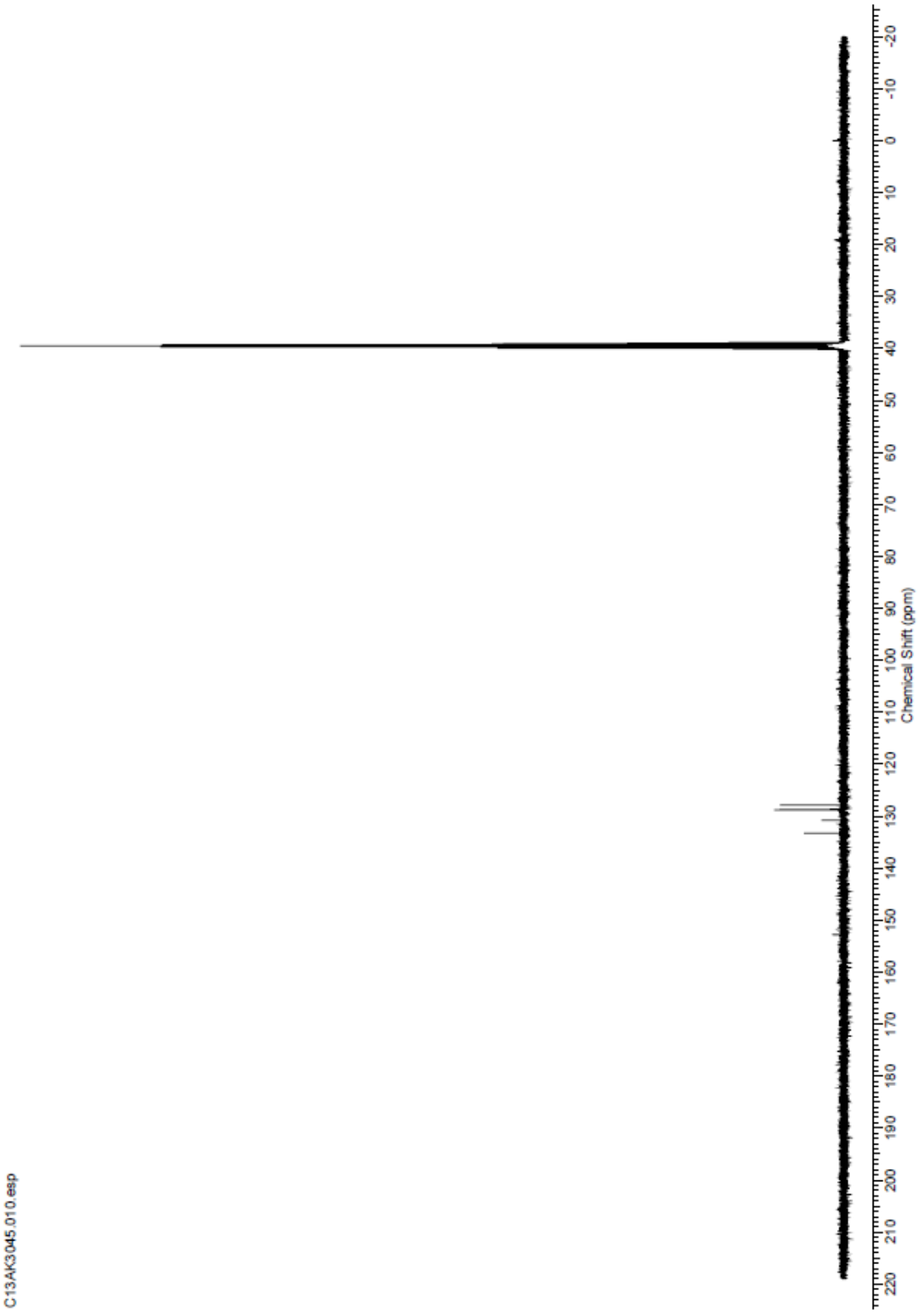

Compound 25 ^{1}H

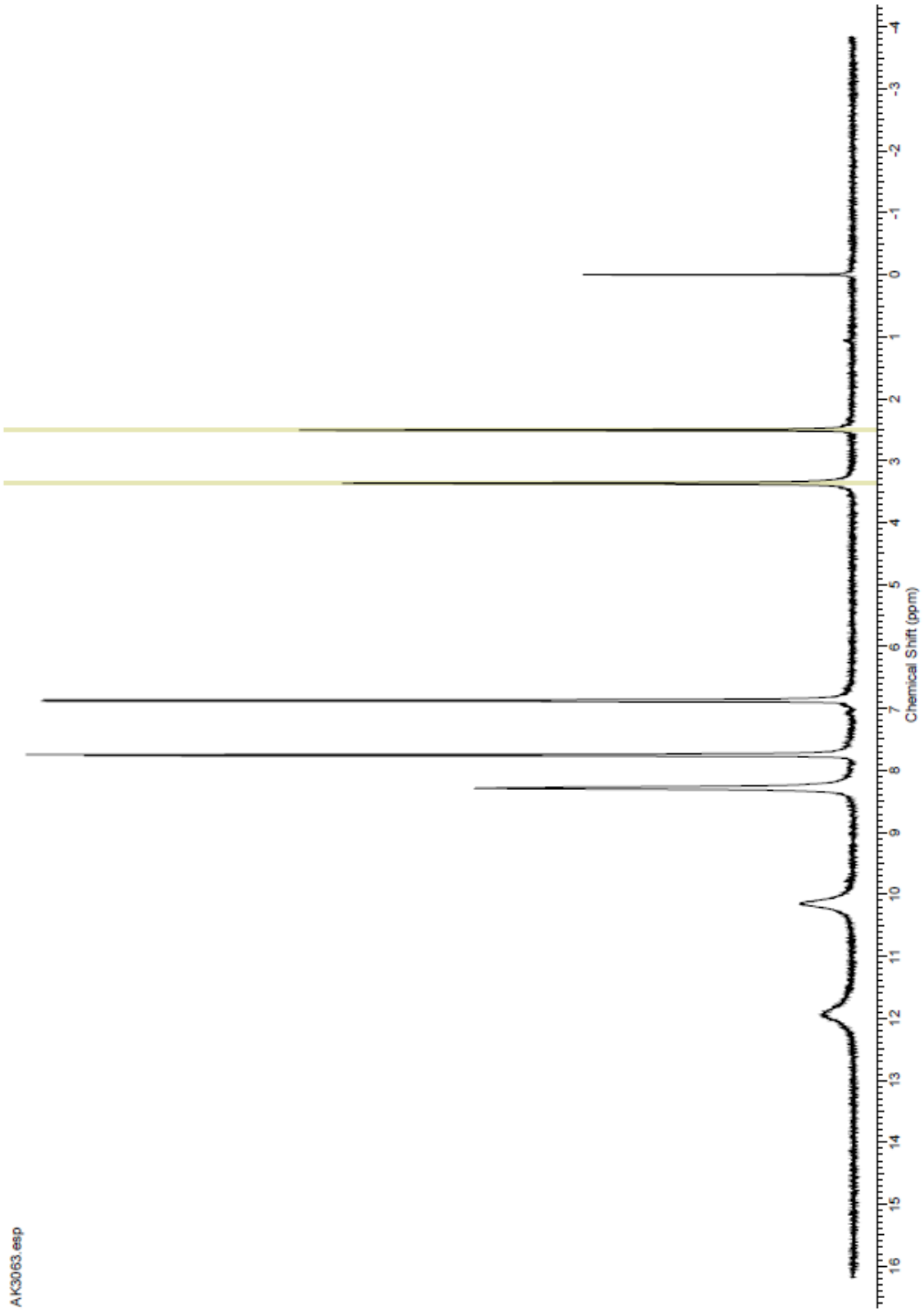

Compound 25 ^{13}C

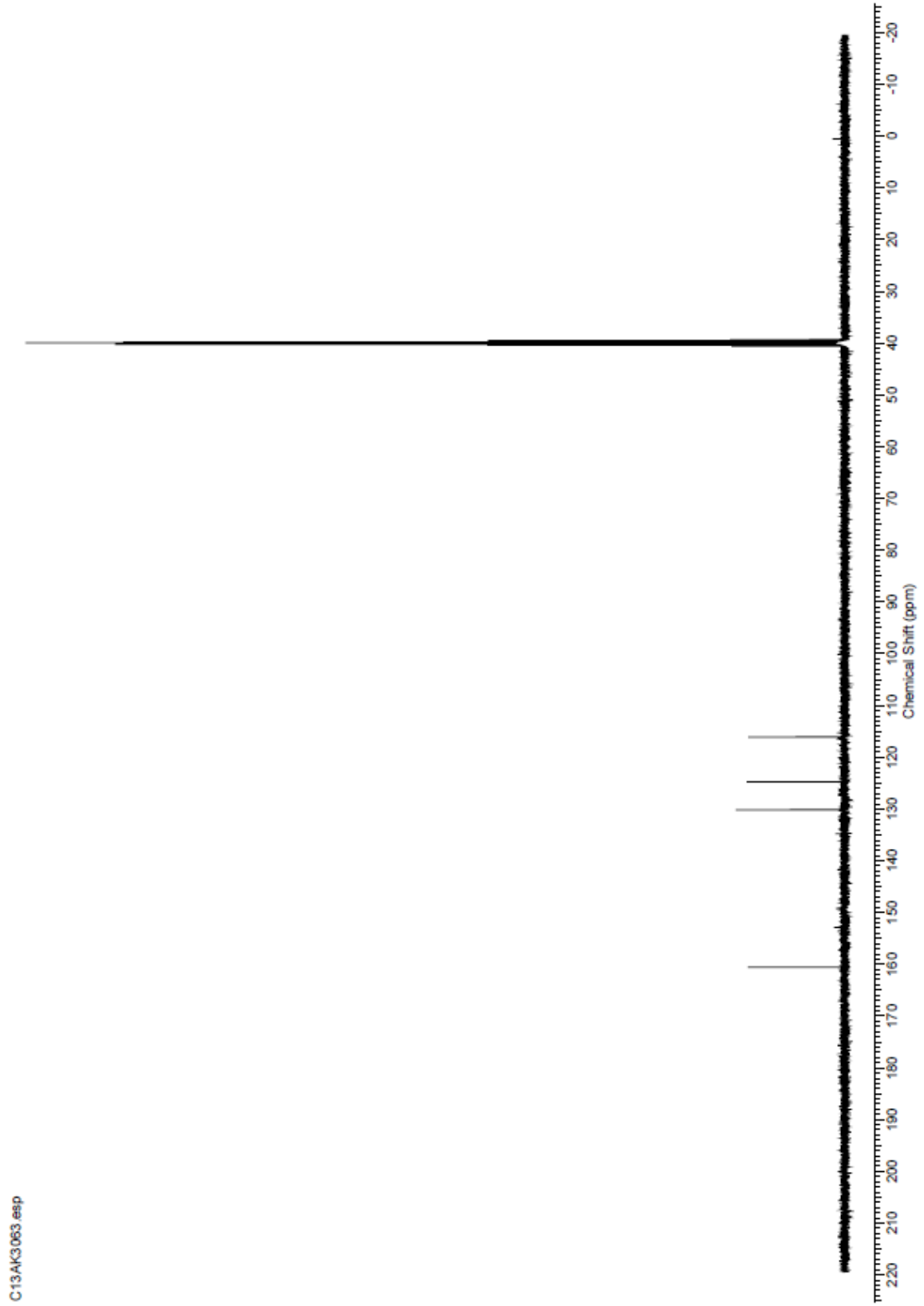

Compound 26 ^{1}H

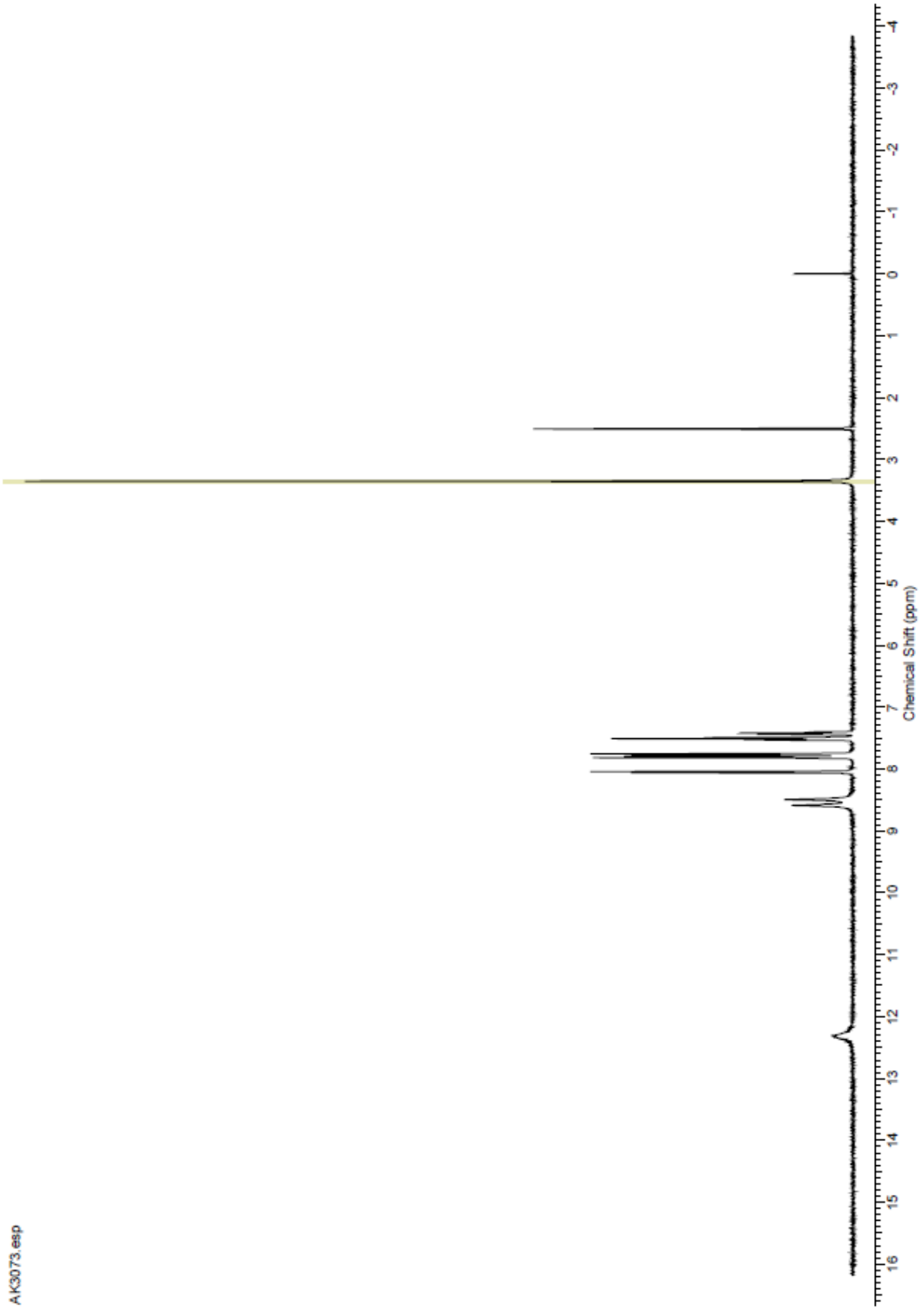

Compound 26 ^{13}C

Compound 27 ^{1}H

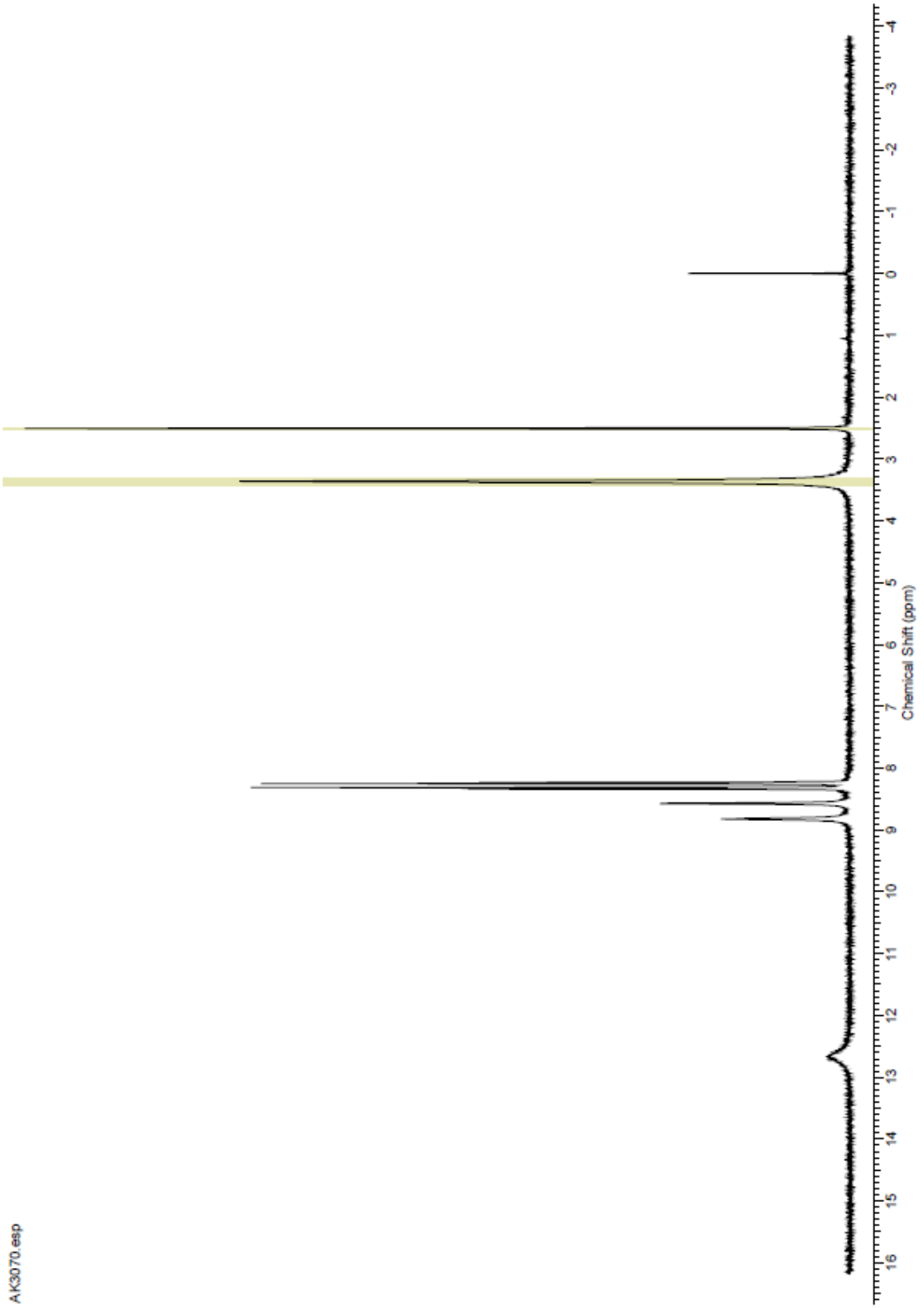

Compound 27 ^{13}C

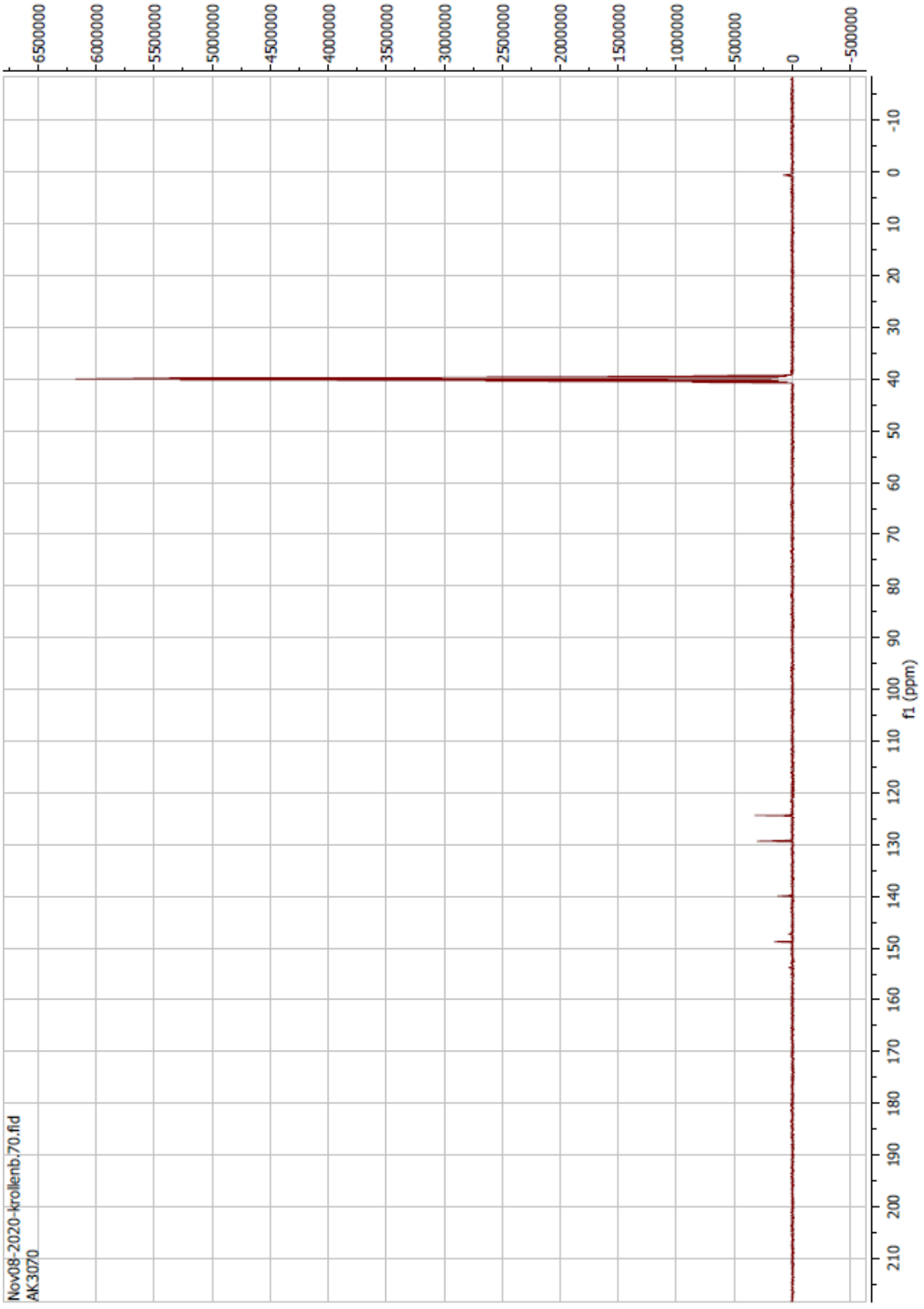

Compound 28 ^{1}H

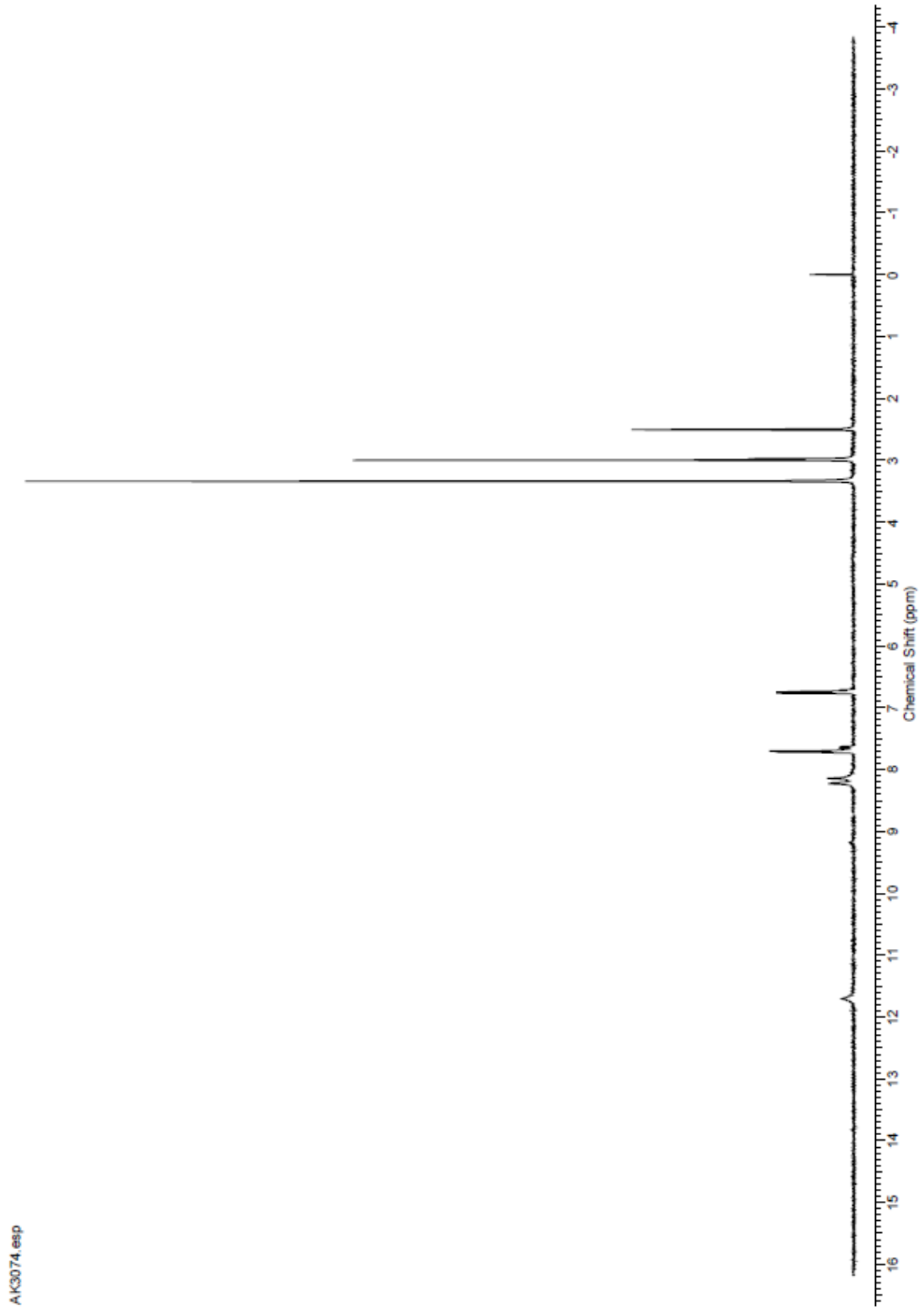

Compound 28 ^{13}C

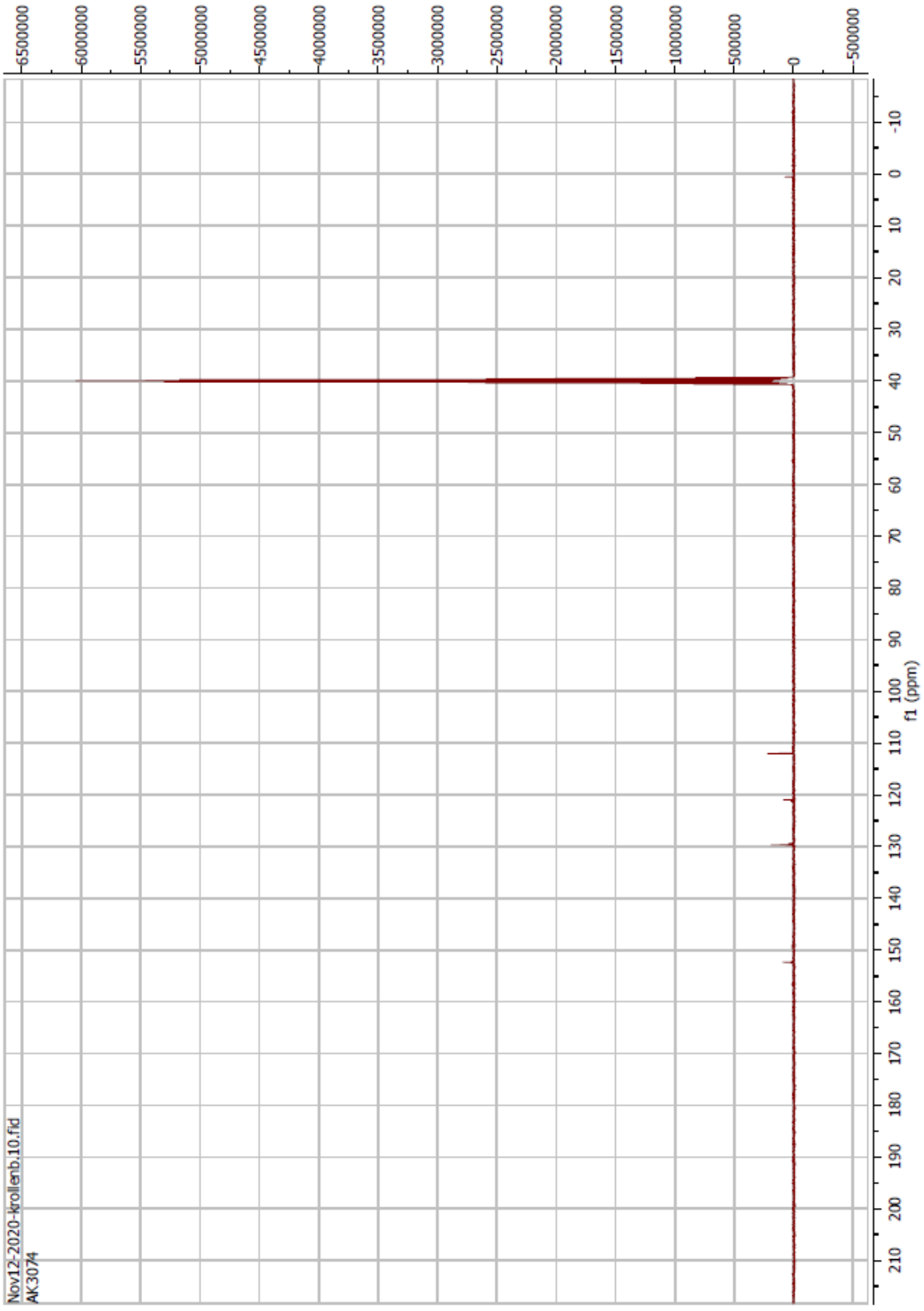

Compound 29 ^{1}H

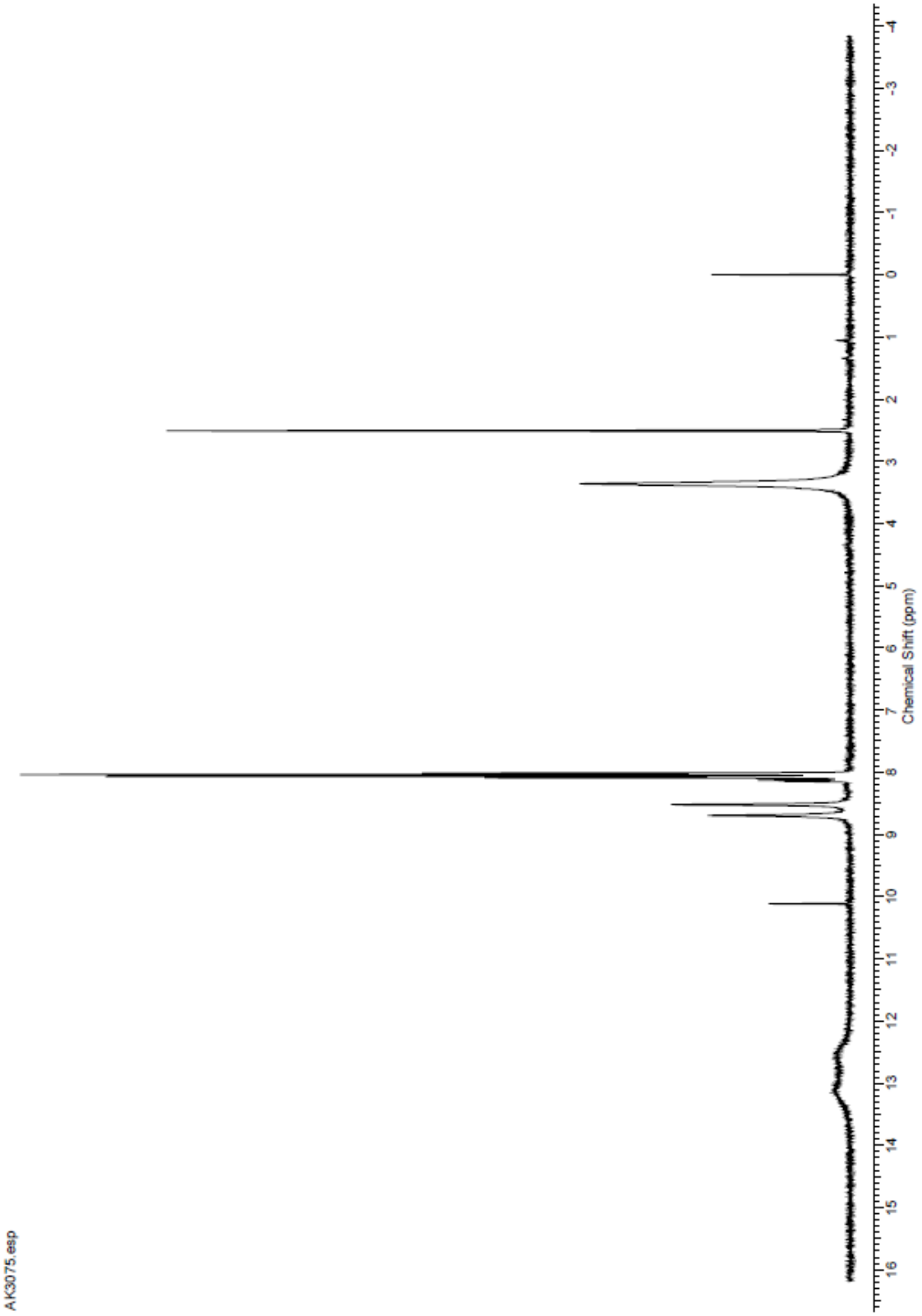

Compound 29 ^{13}C

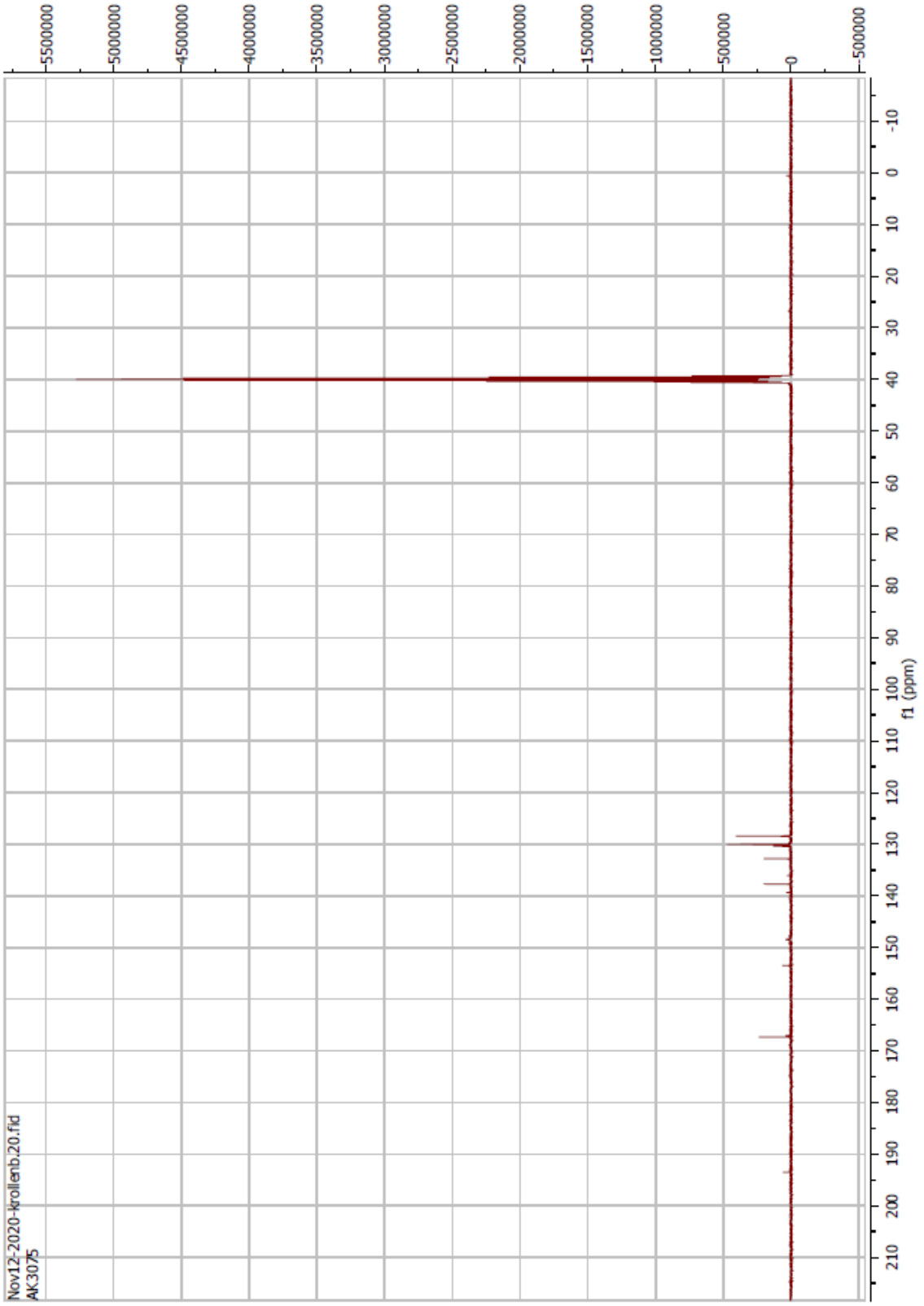

Compound 30 ^{1}H

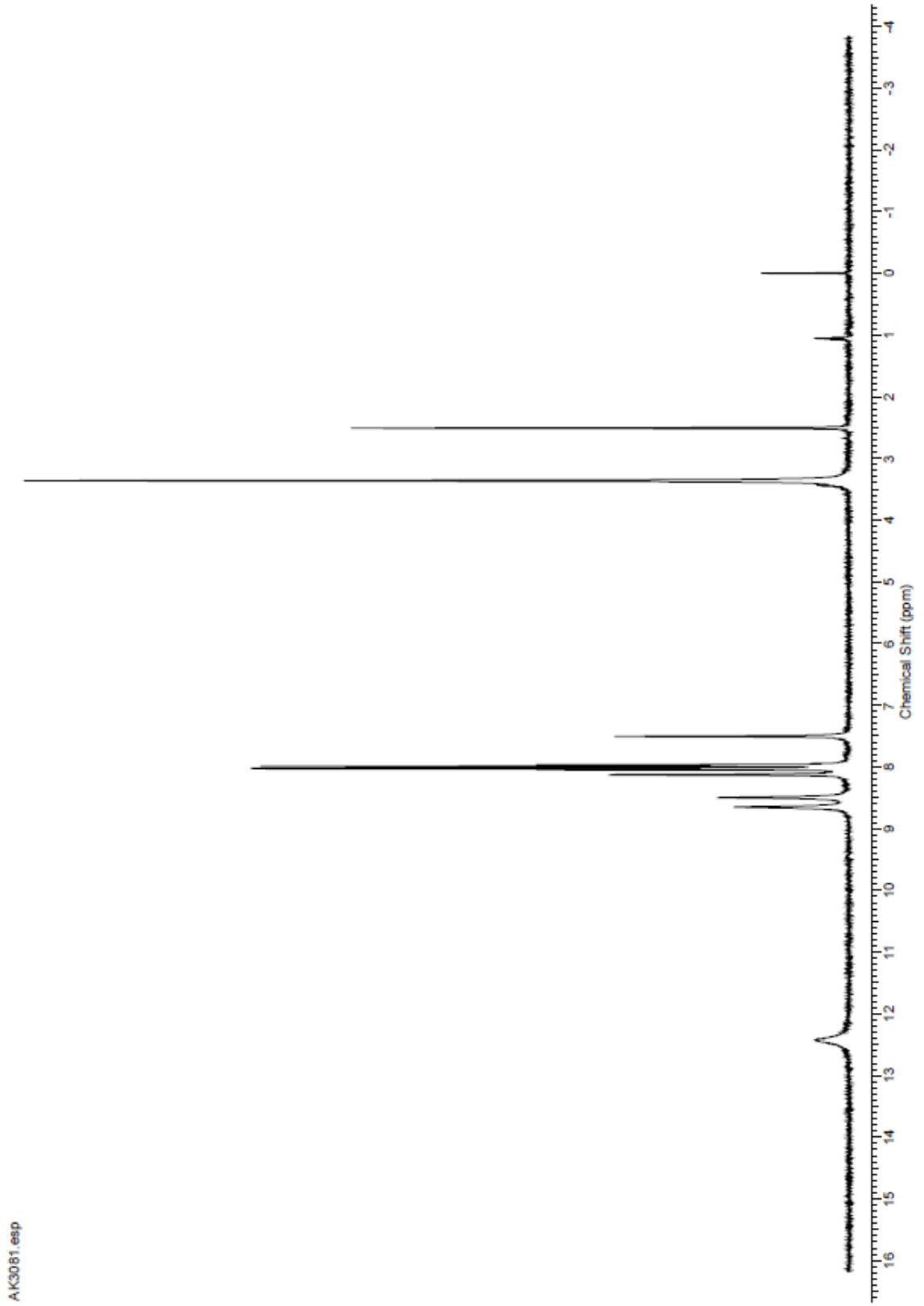

Compound 30 ^{13}C

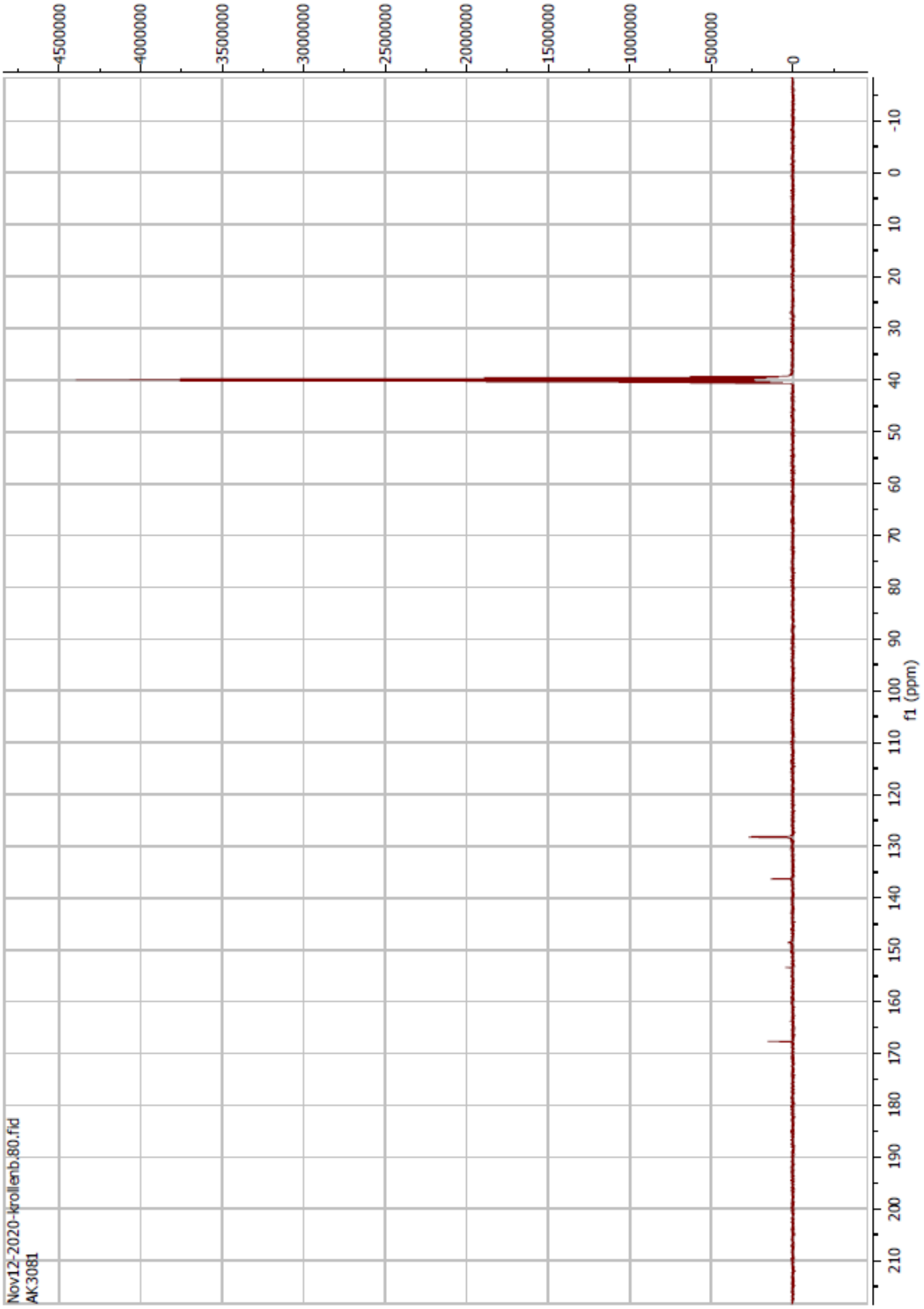

Compound 31 ^{1}H

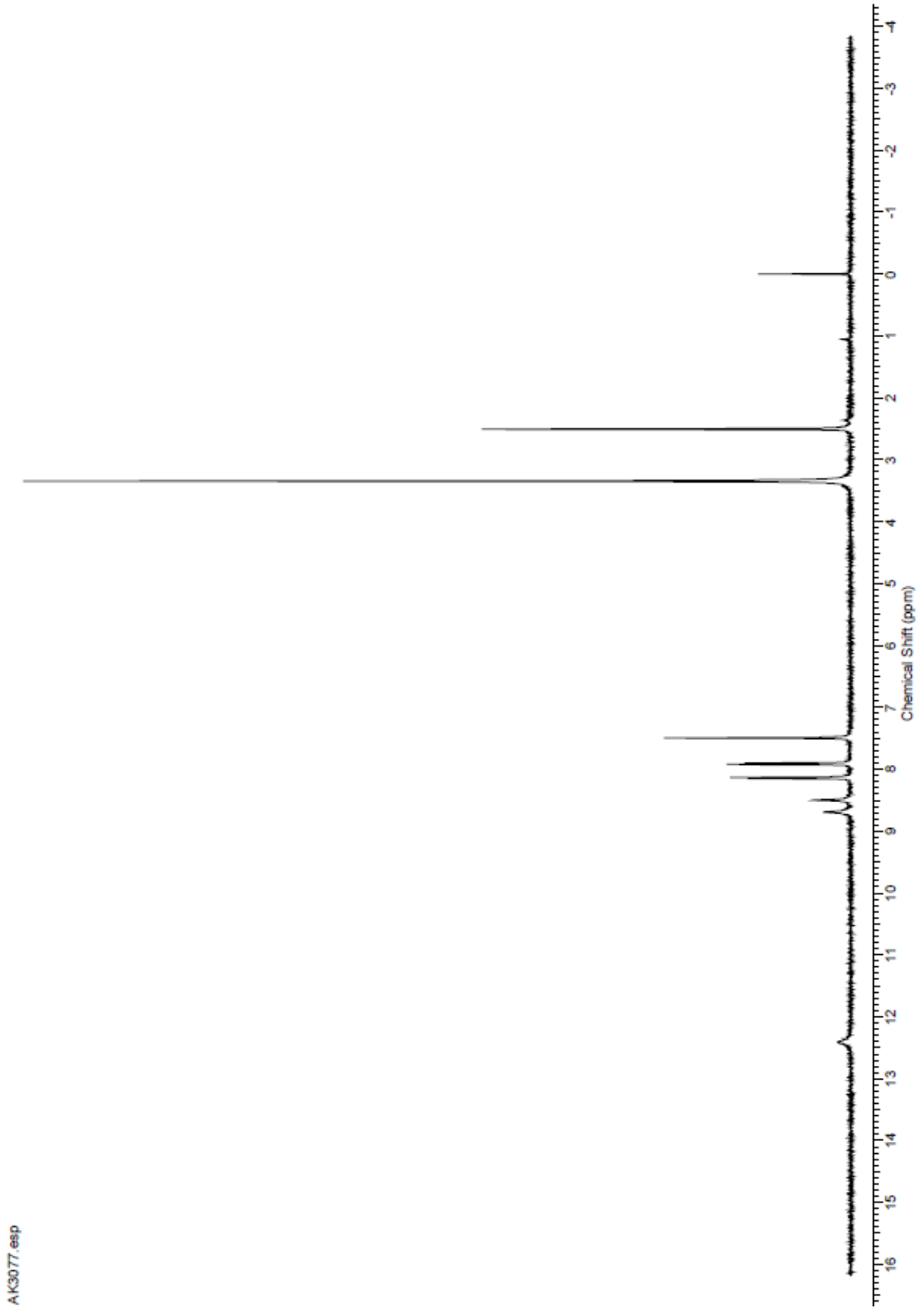

Compound 31 ^{13}C

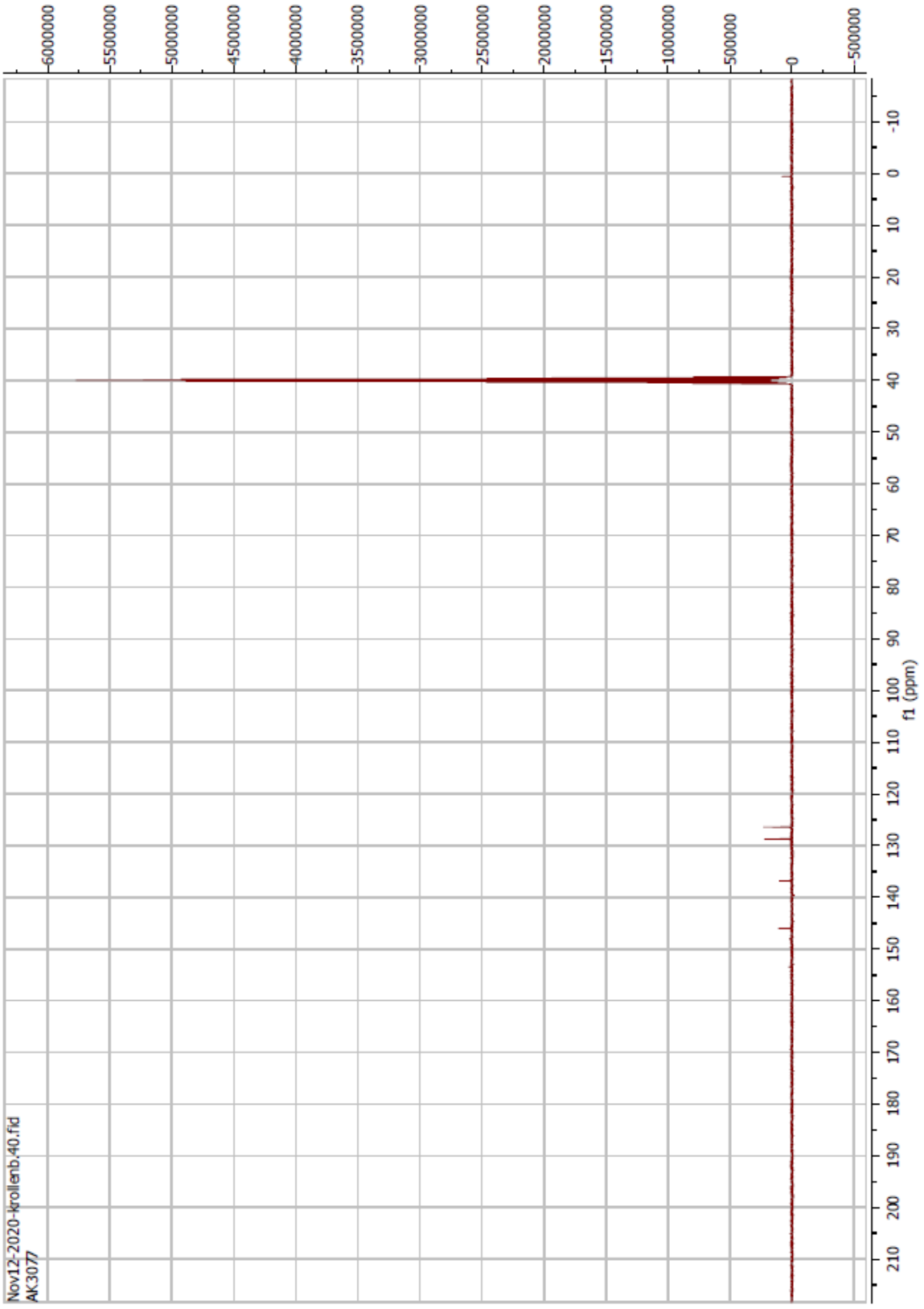

Compound 32 ^{1}H

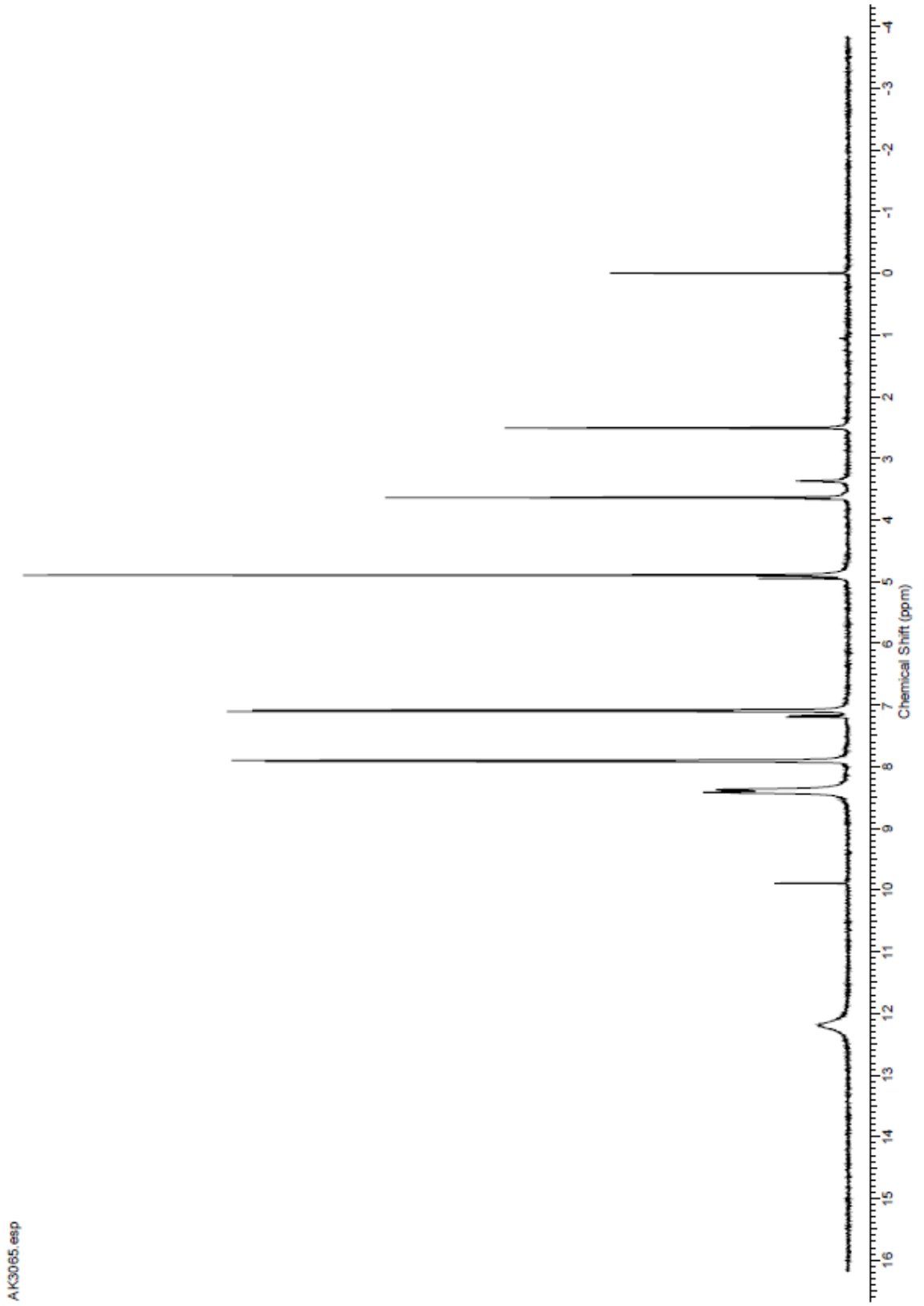

Compound 32 ^{13}C

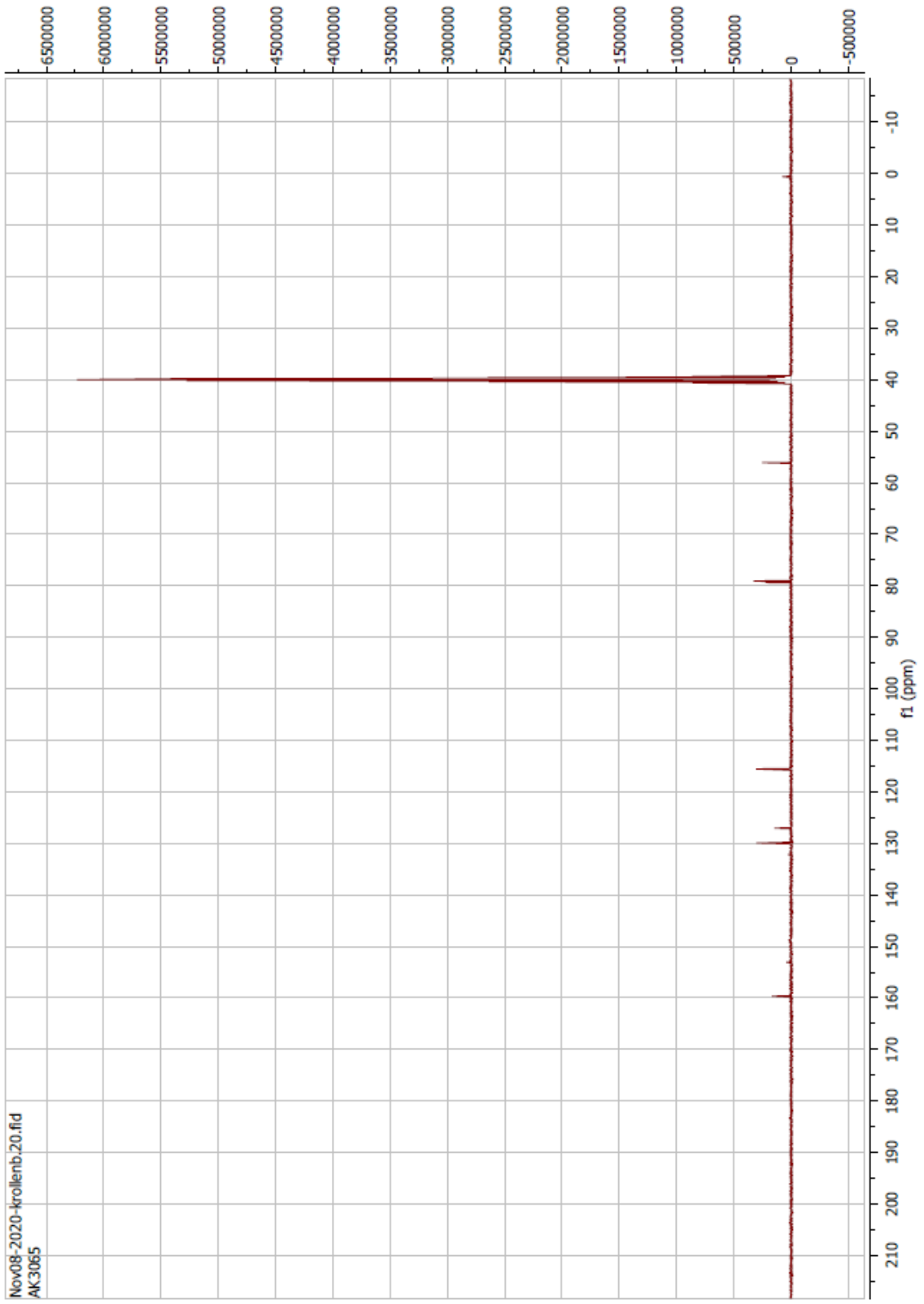

Compound 33 ^{1}H

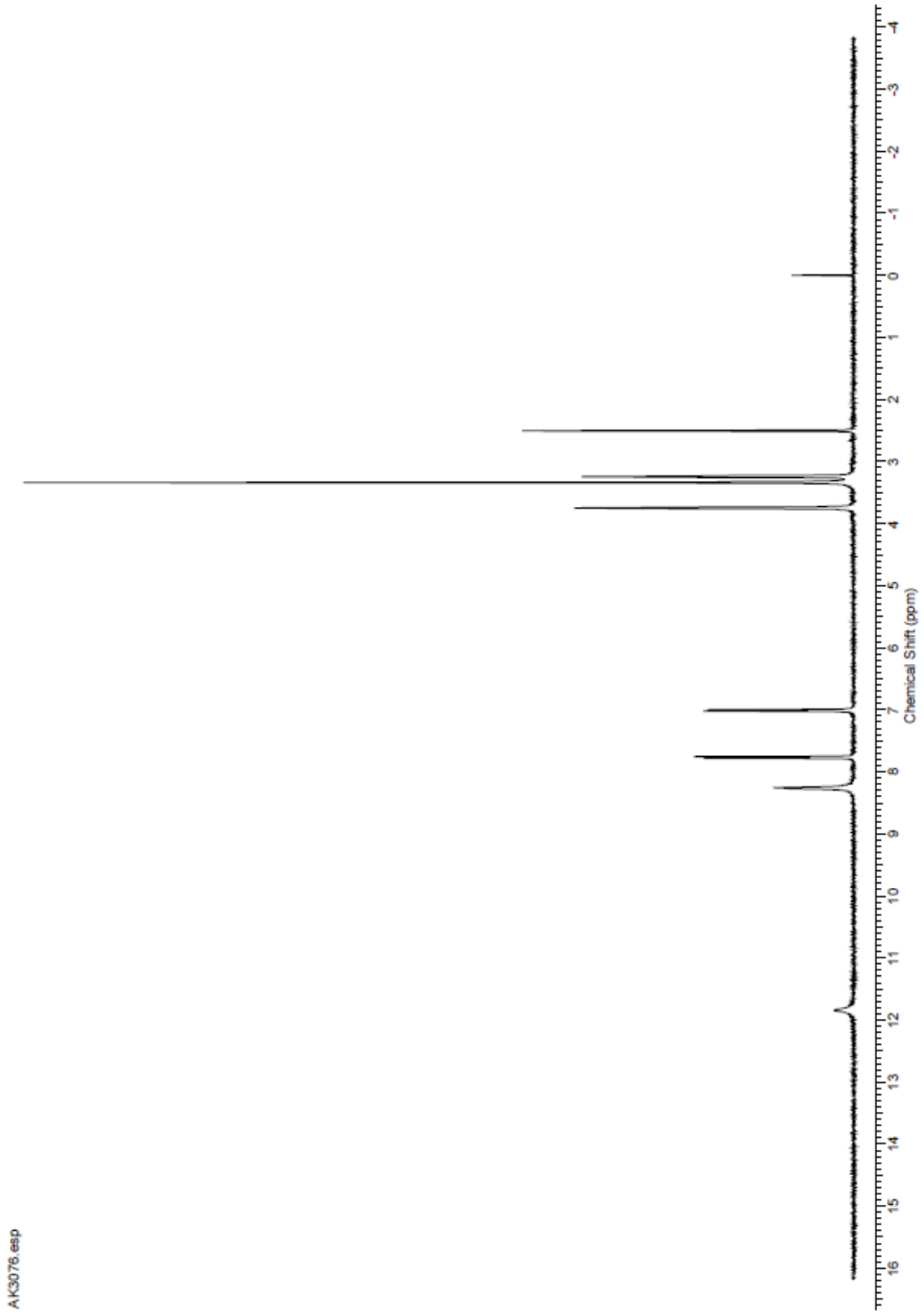

Compound 33 ^{13}C

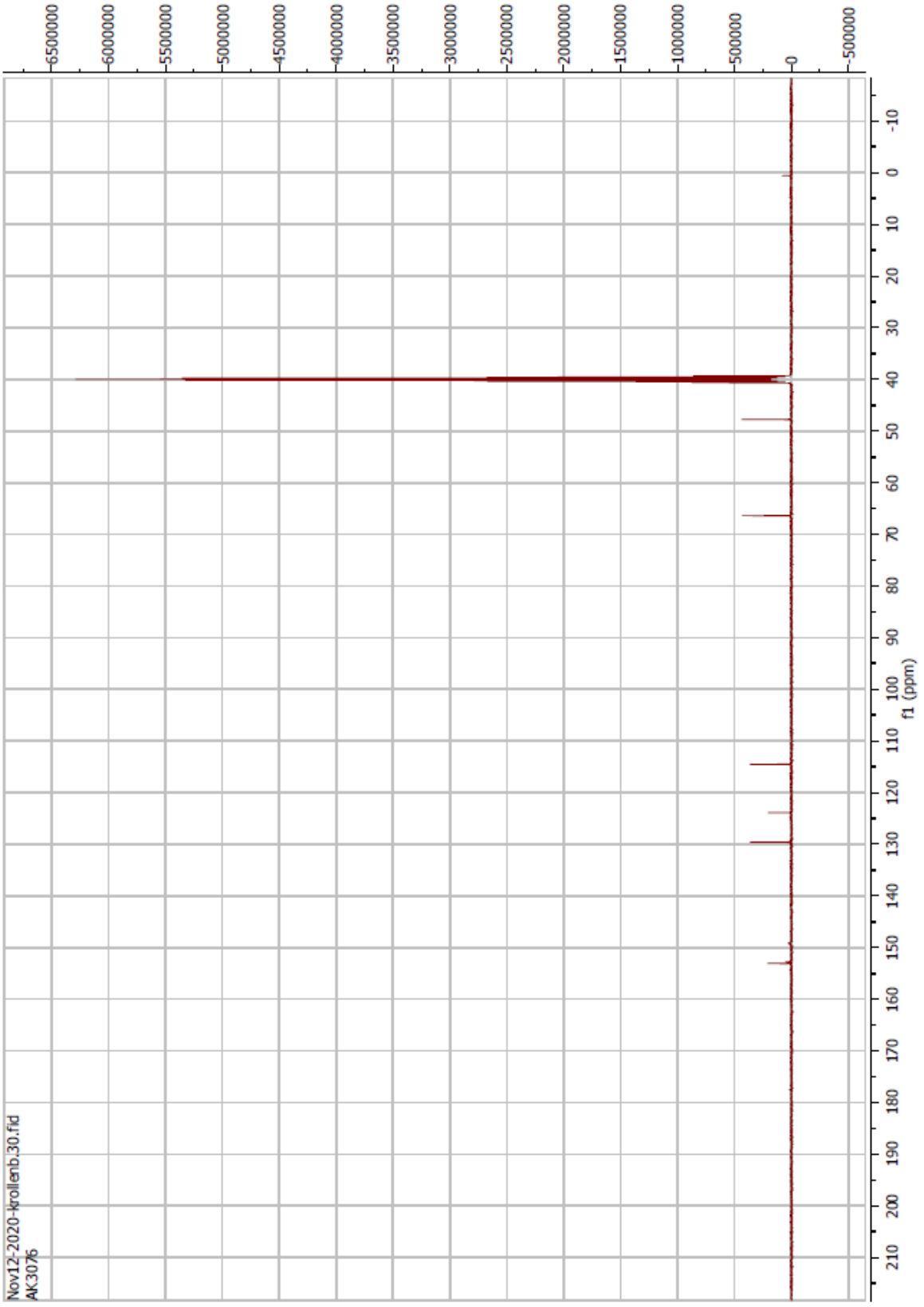

Compound 34 ^{1}H

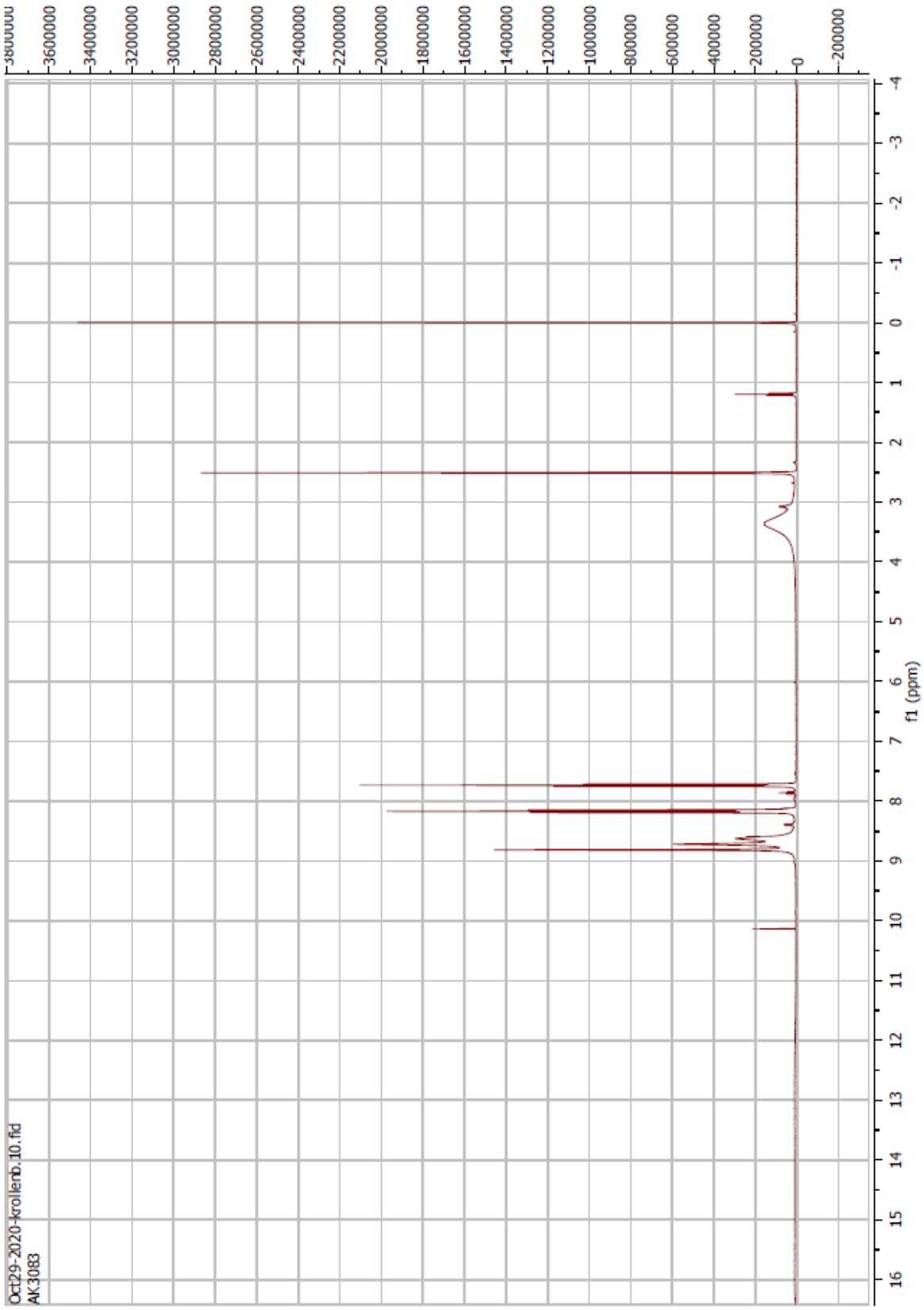

Compound 34 ^{13}C

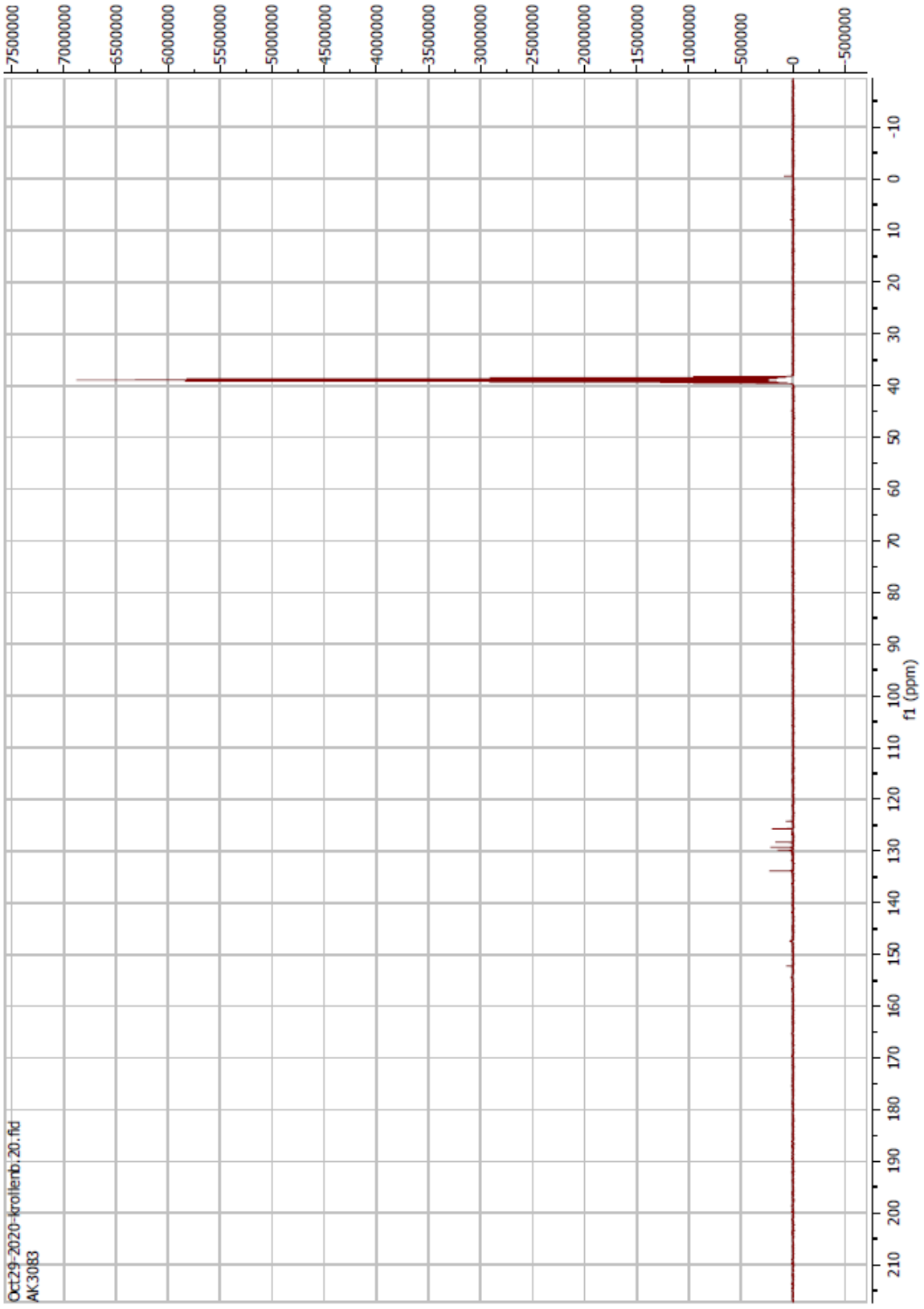

Compound 35 ^{1}H

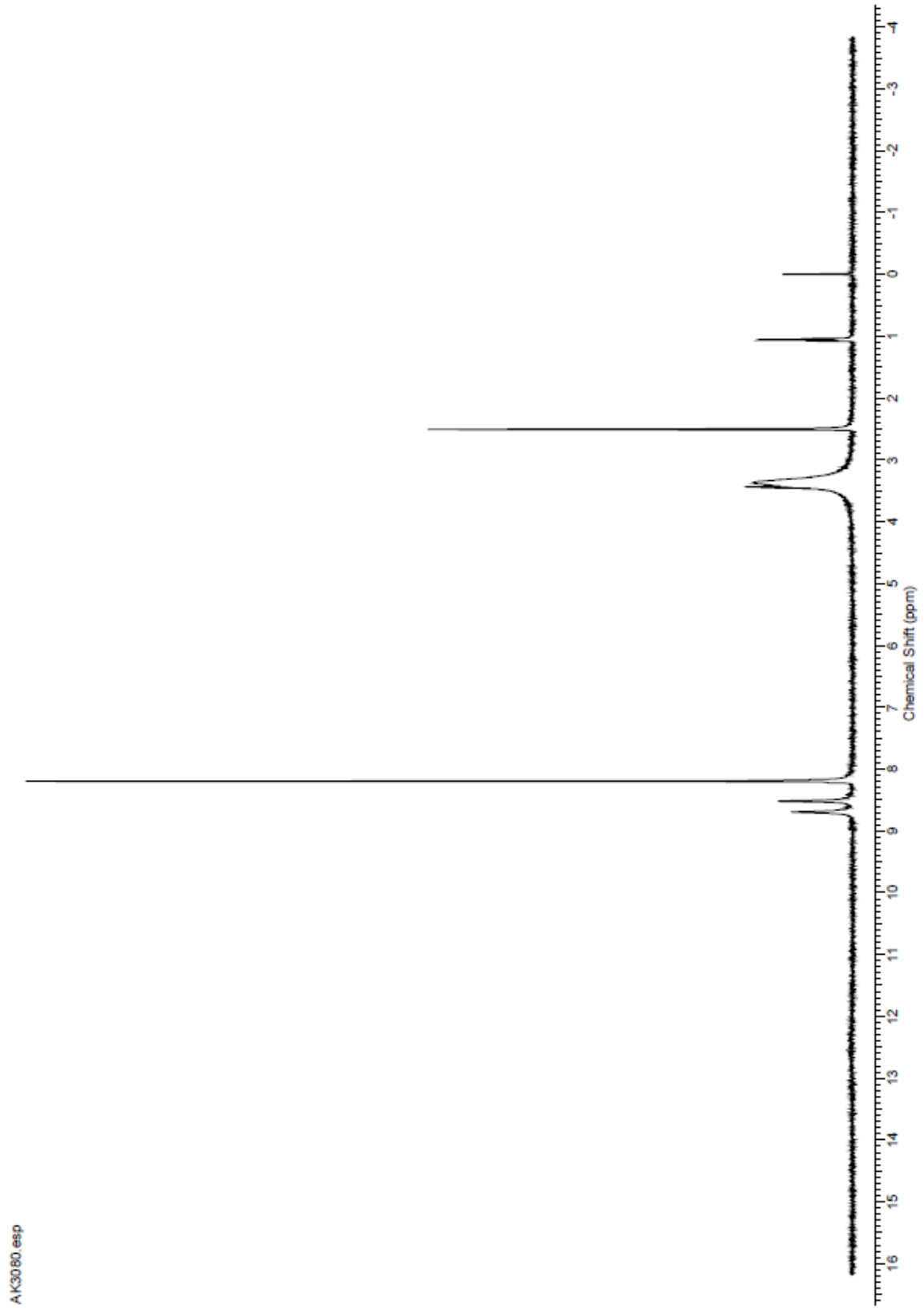

Compound 35 ^{13}C

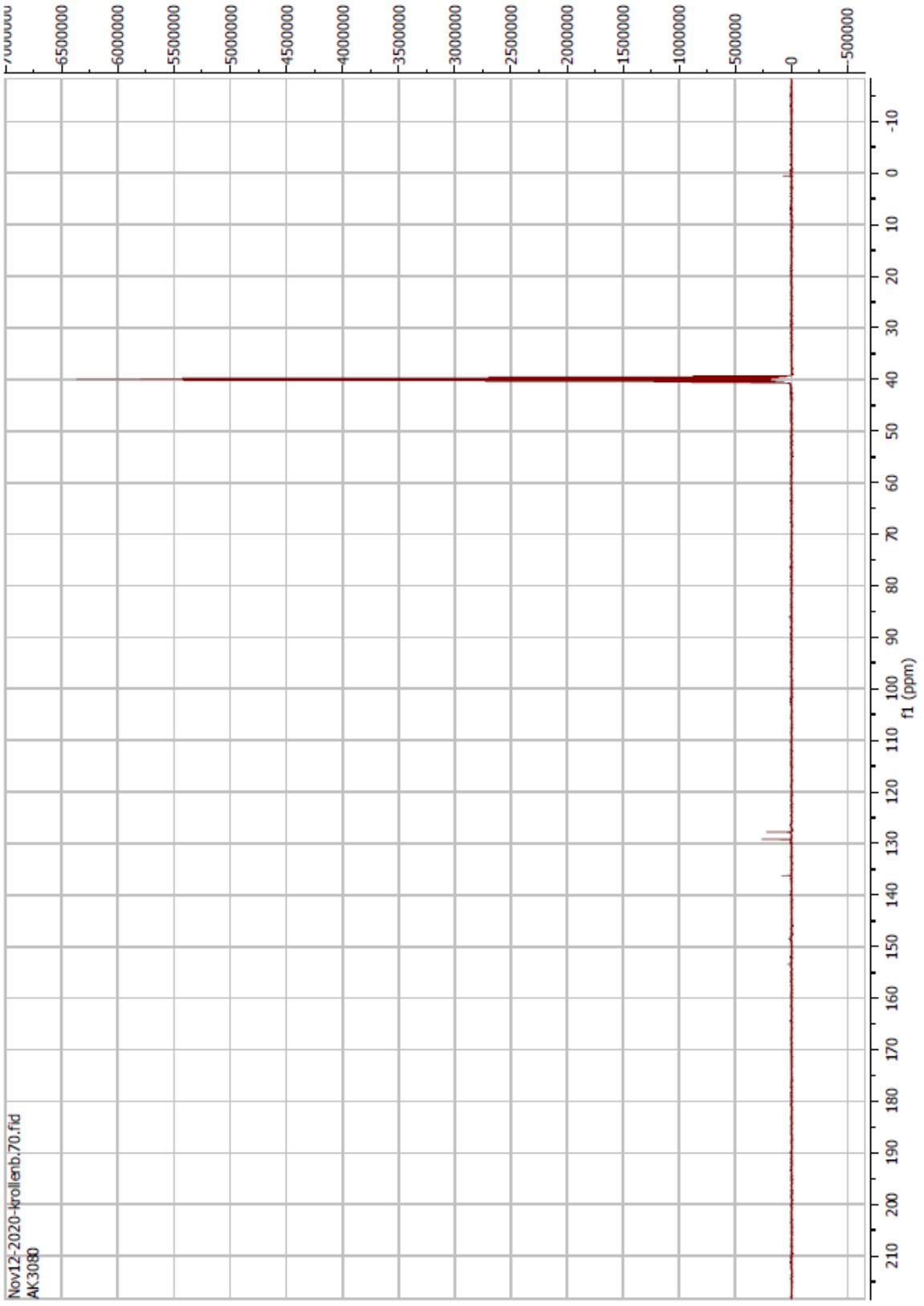

Compound 36 ^{1}H

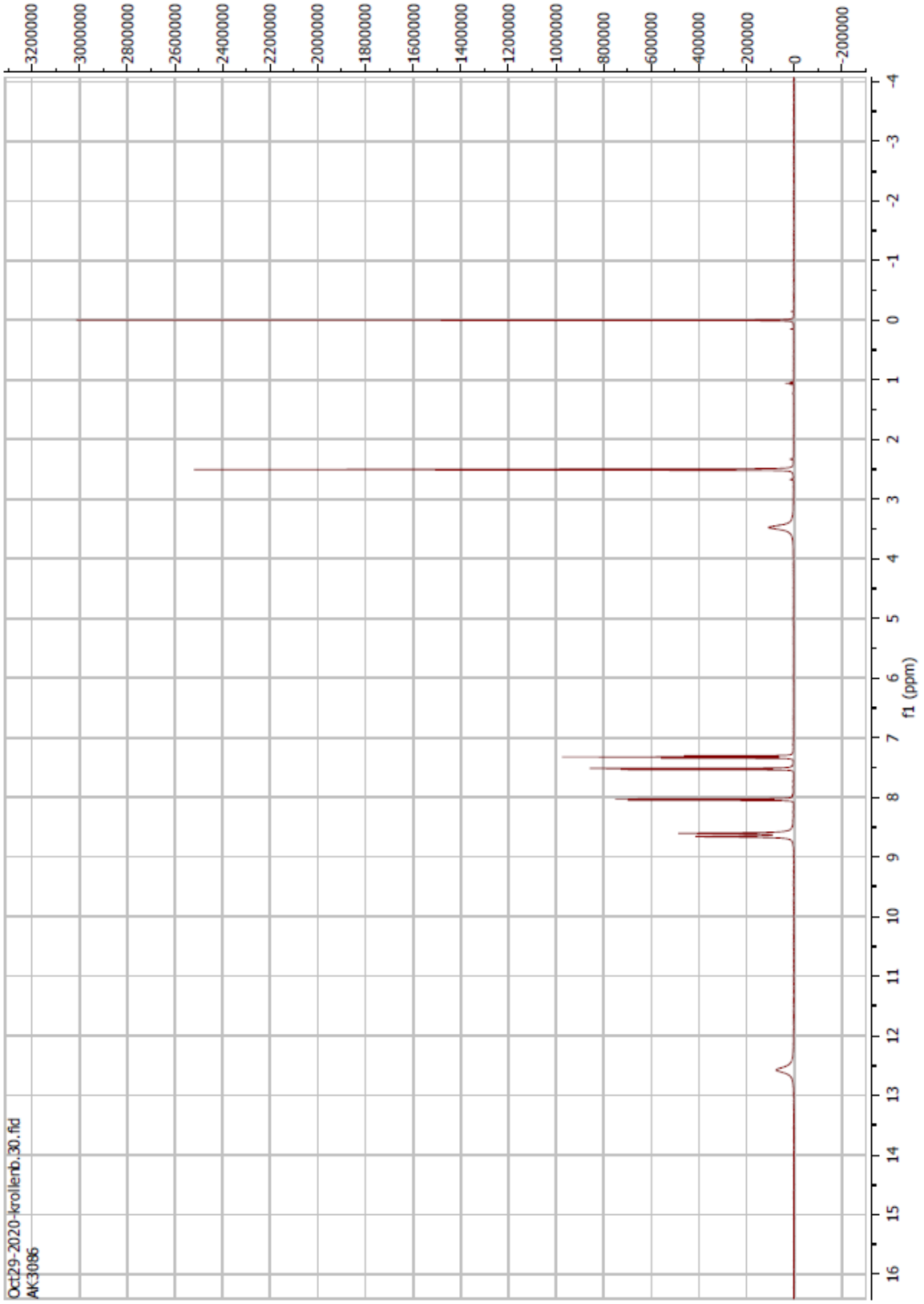

Compound 36 ^{13}C

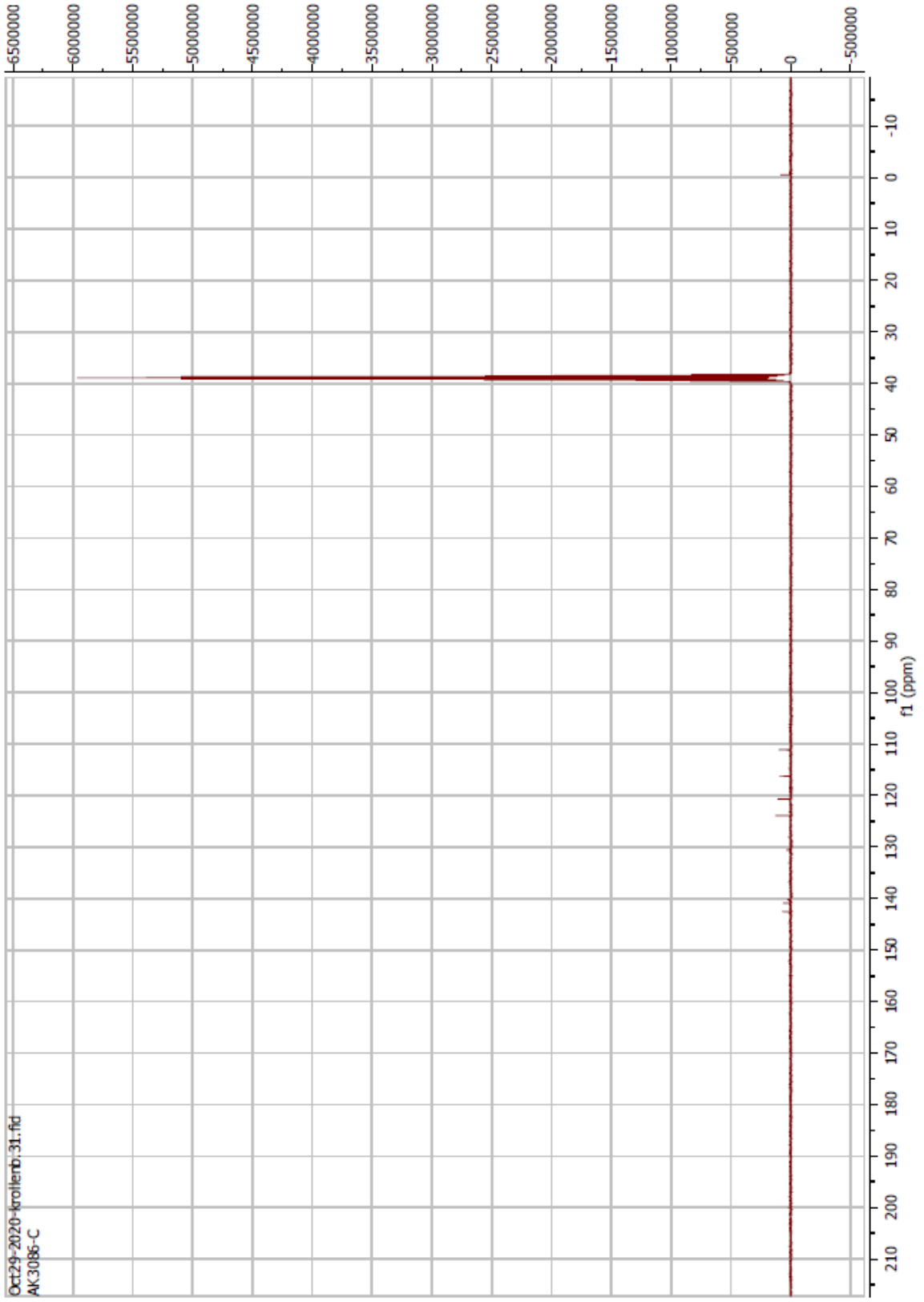

Compound 37 ^{1}H

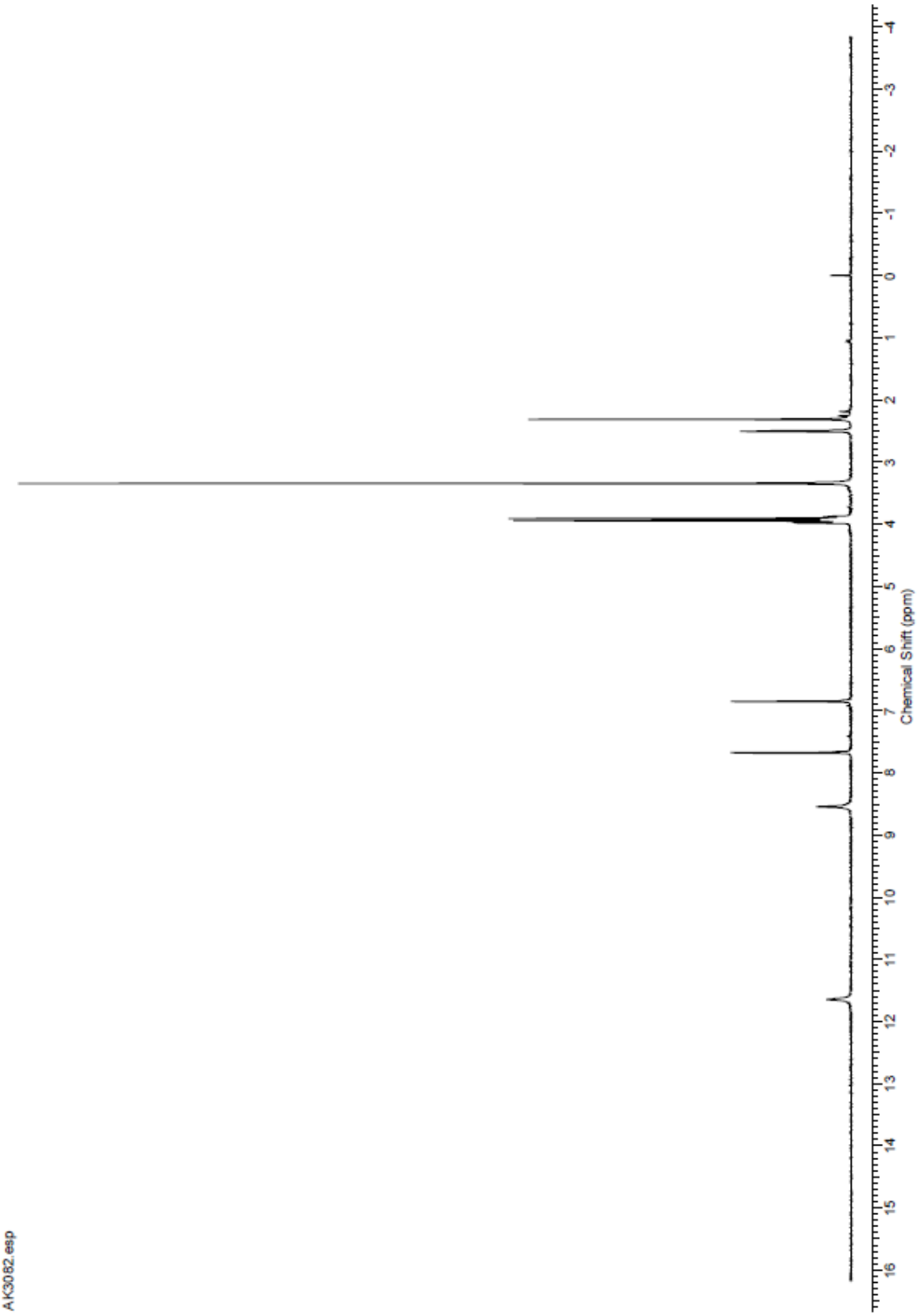

Compound 37 ^{13}C

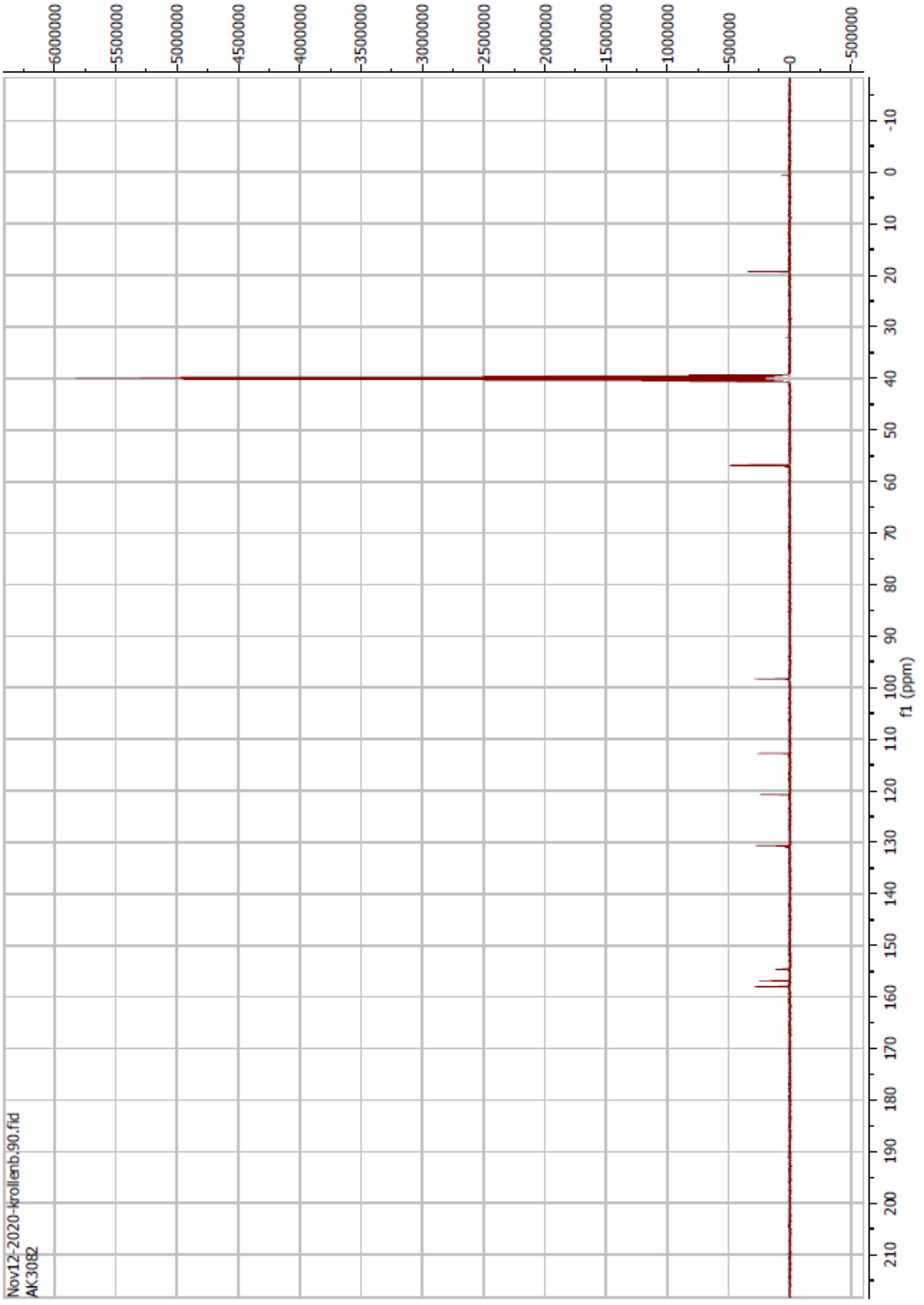

Compound 38 ^{1}H

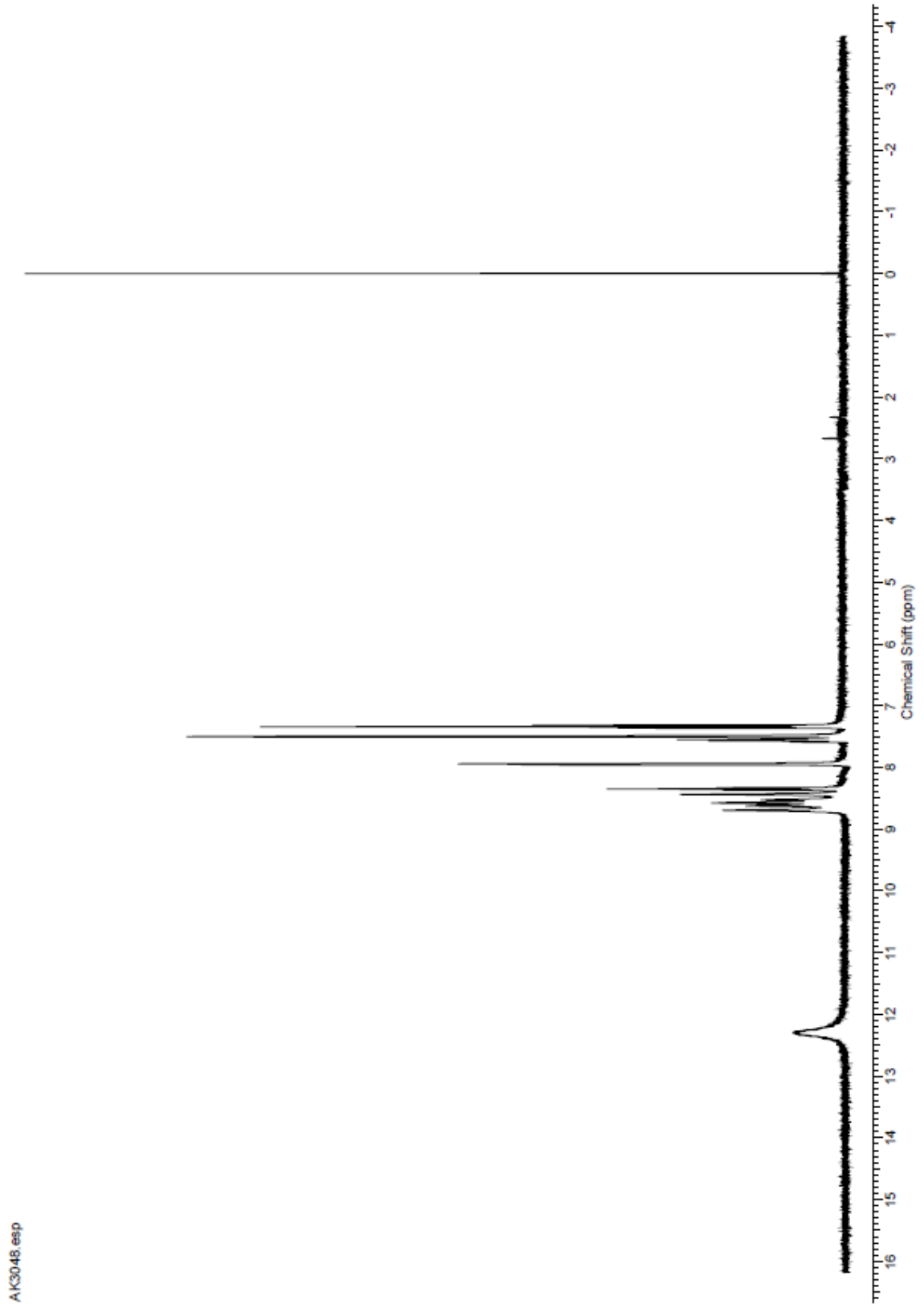

Compound 38 ^{13}C

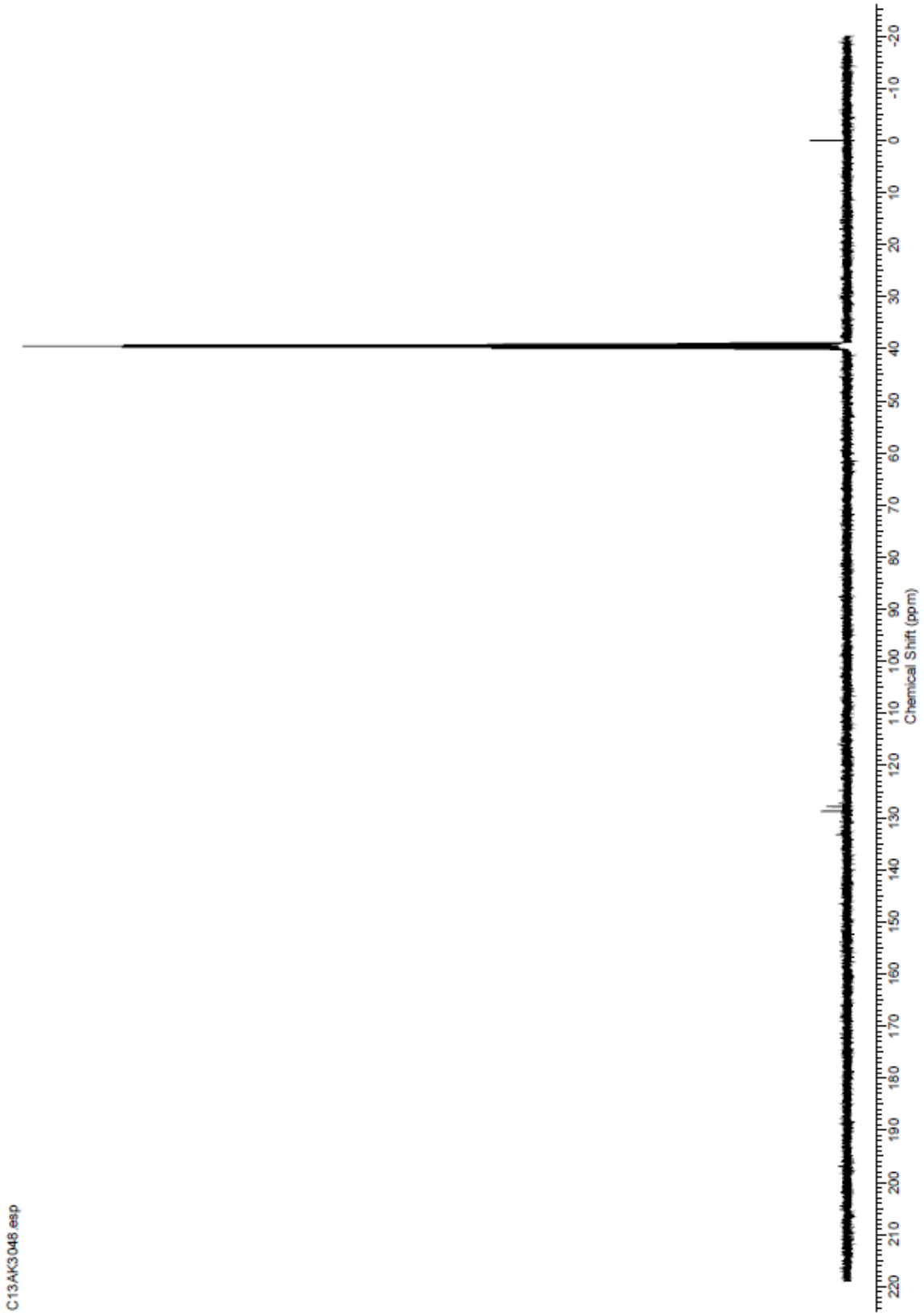

Compound 39 ^{1}H

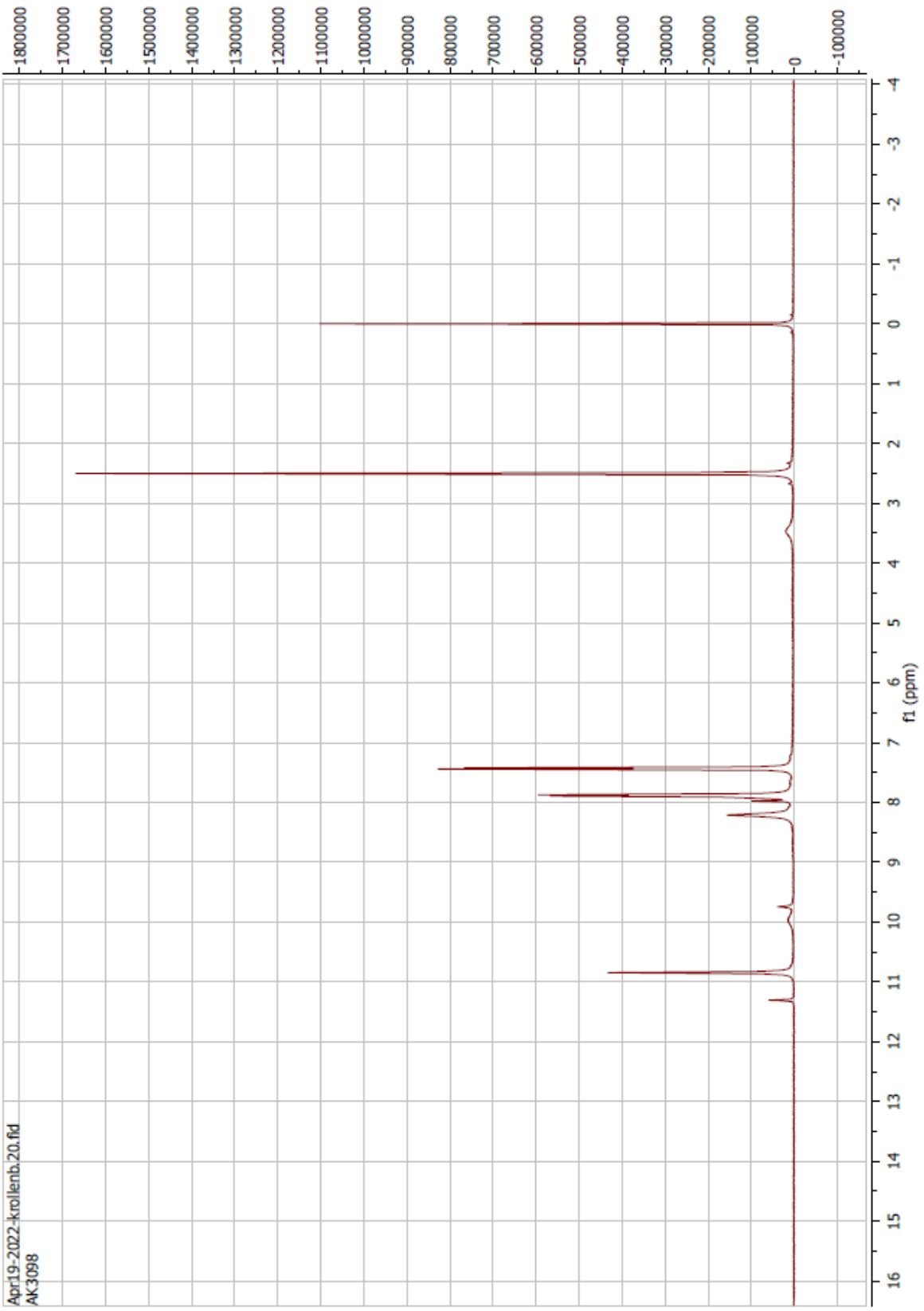

Compound 39 ^{13}C

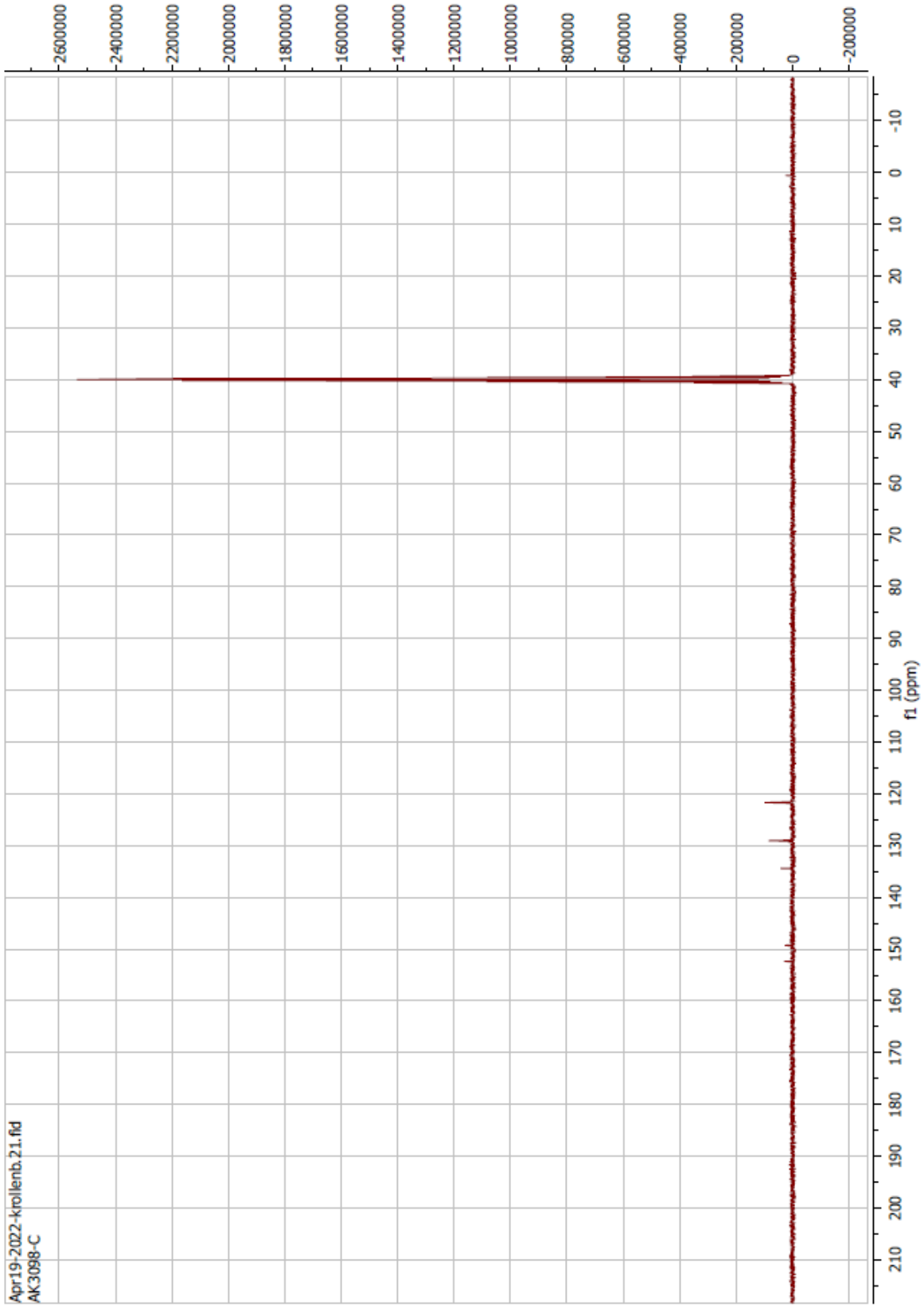

Compound 40 ^{1}H

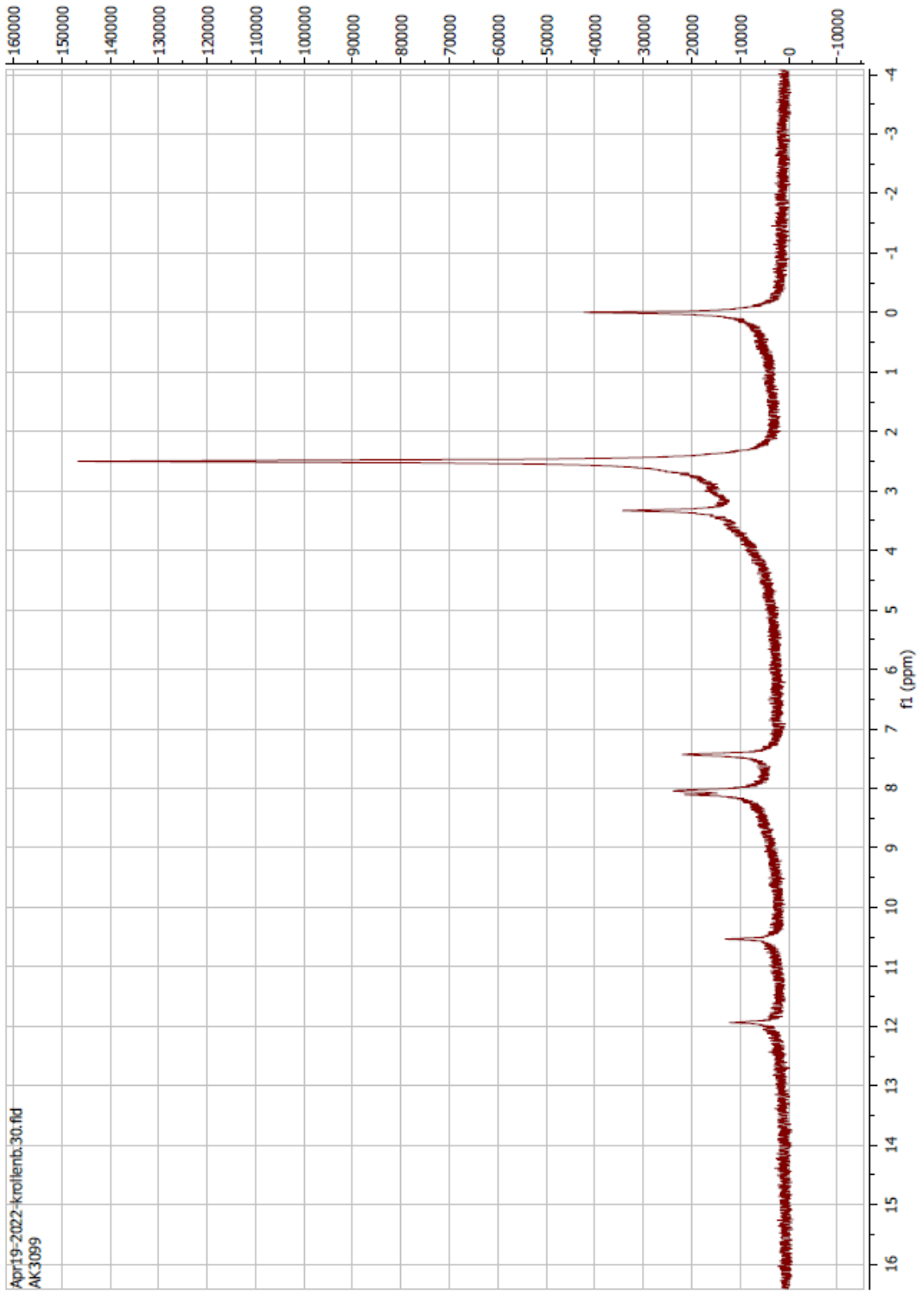

Compound 40 ^{13}C

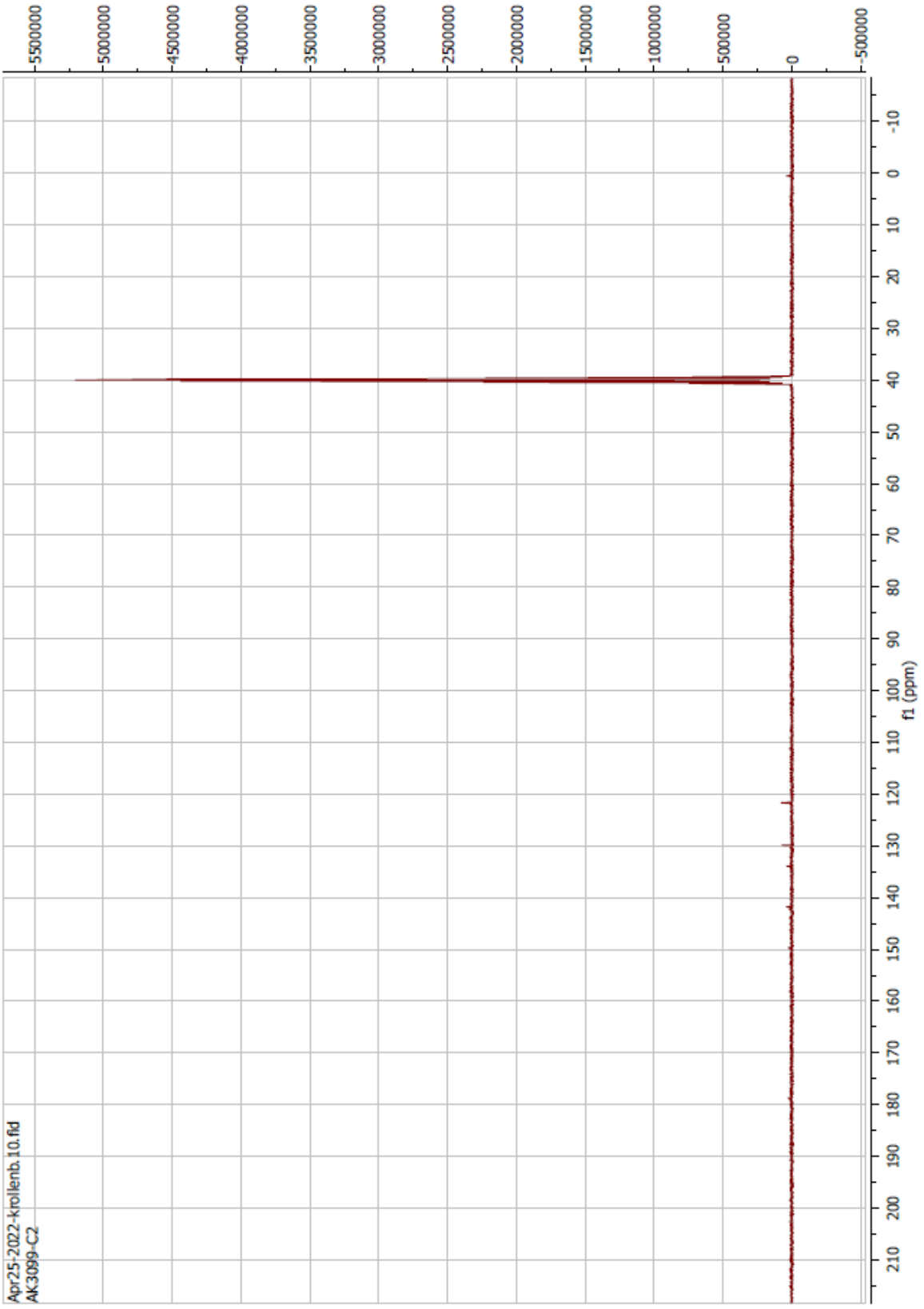

Compound 41 ^{1}H

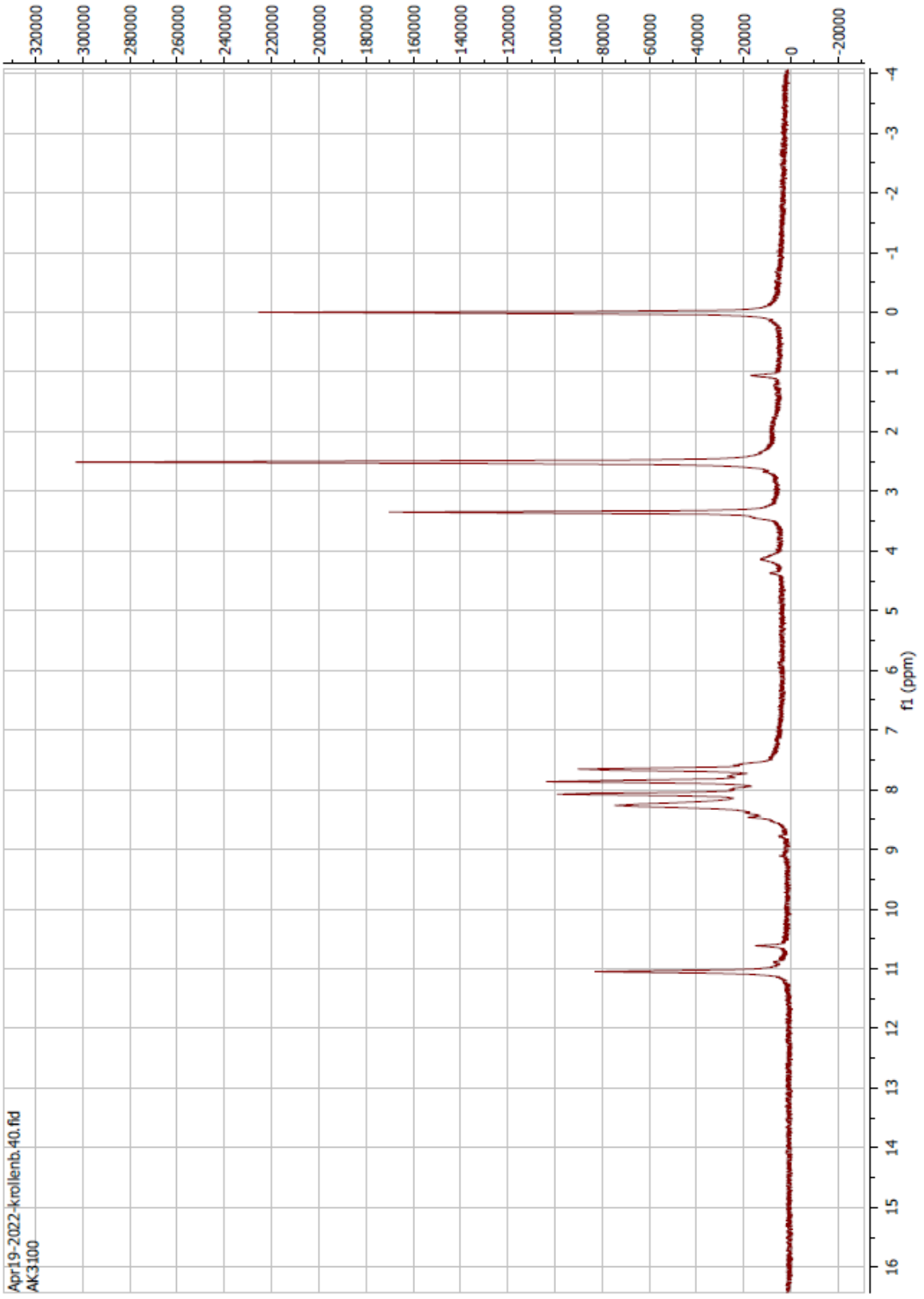

Compound 41 ^{13}C

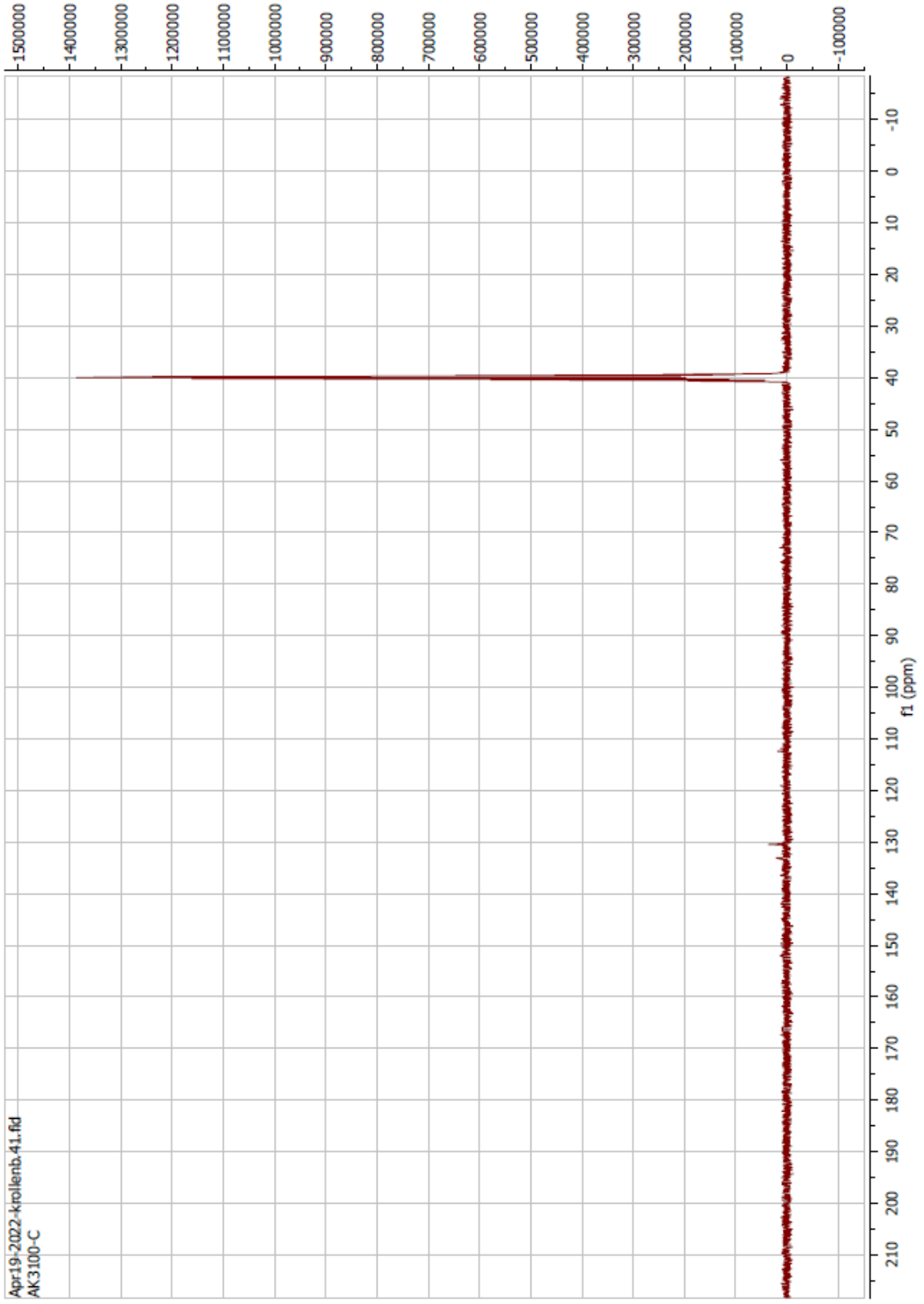

Compound 42 ^{1}H

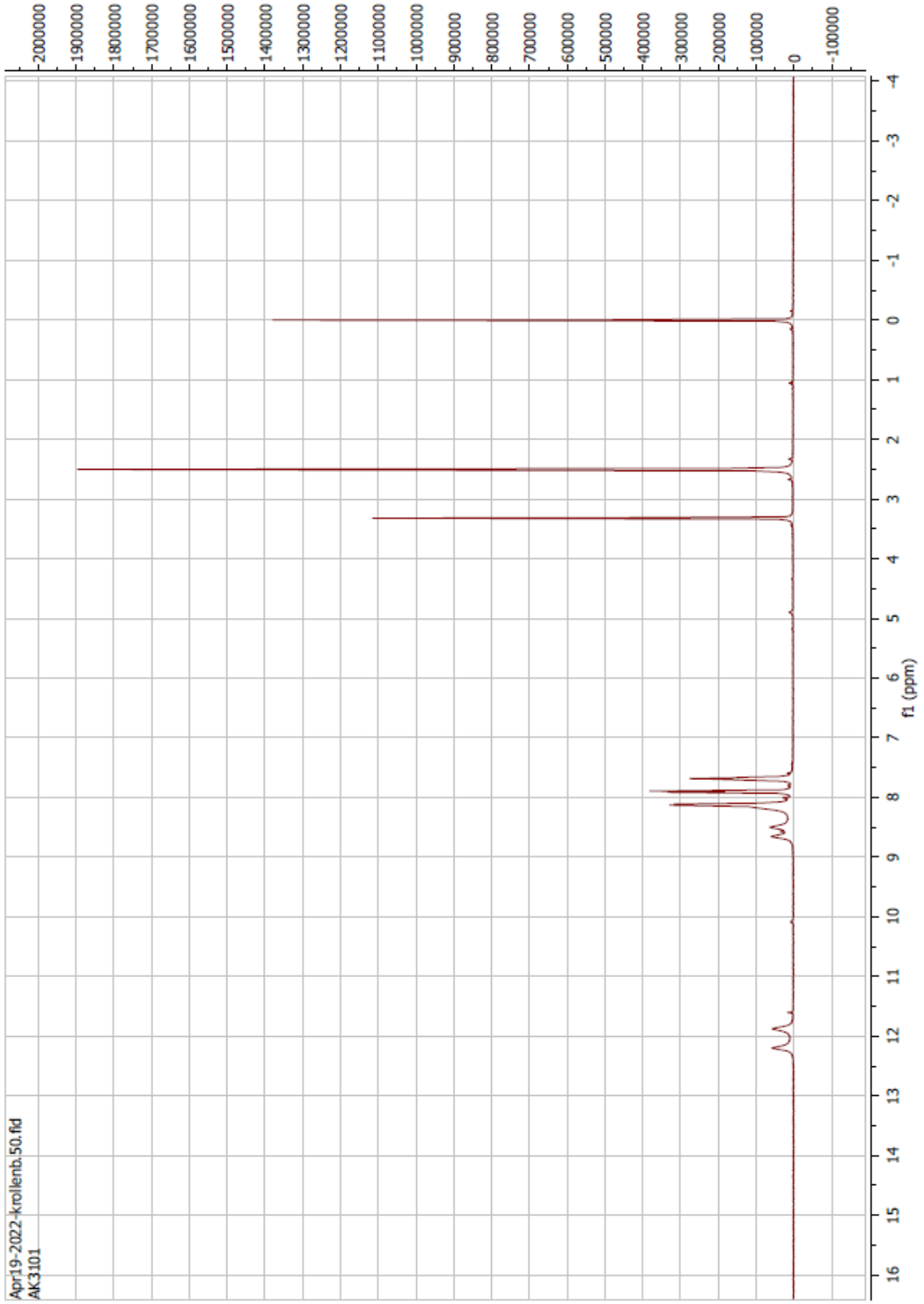

Compound 42 ^{13}C

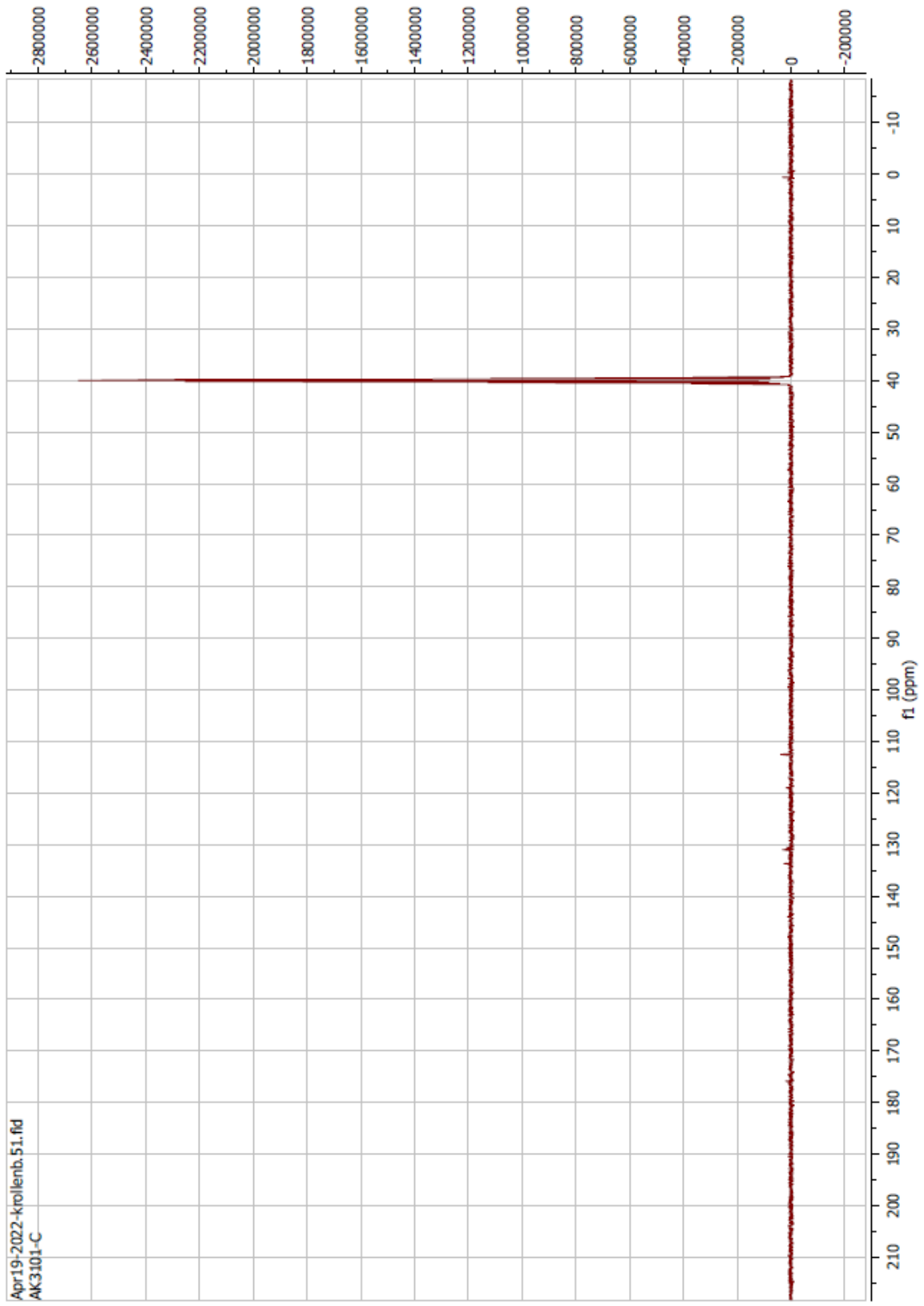

Compound 43 ^{1}H

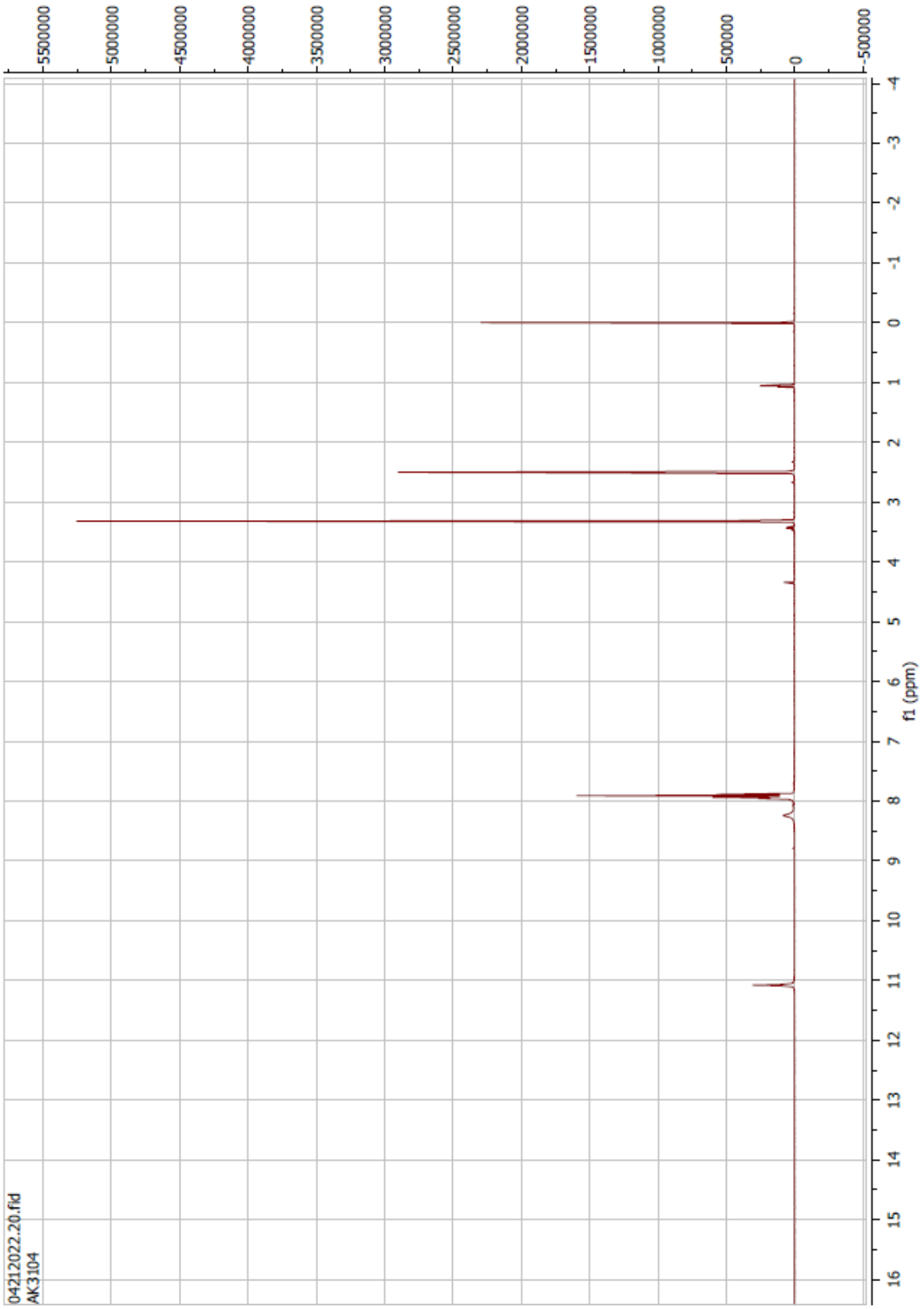

Compound 43 ^{13}C

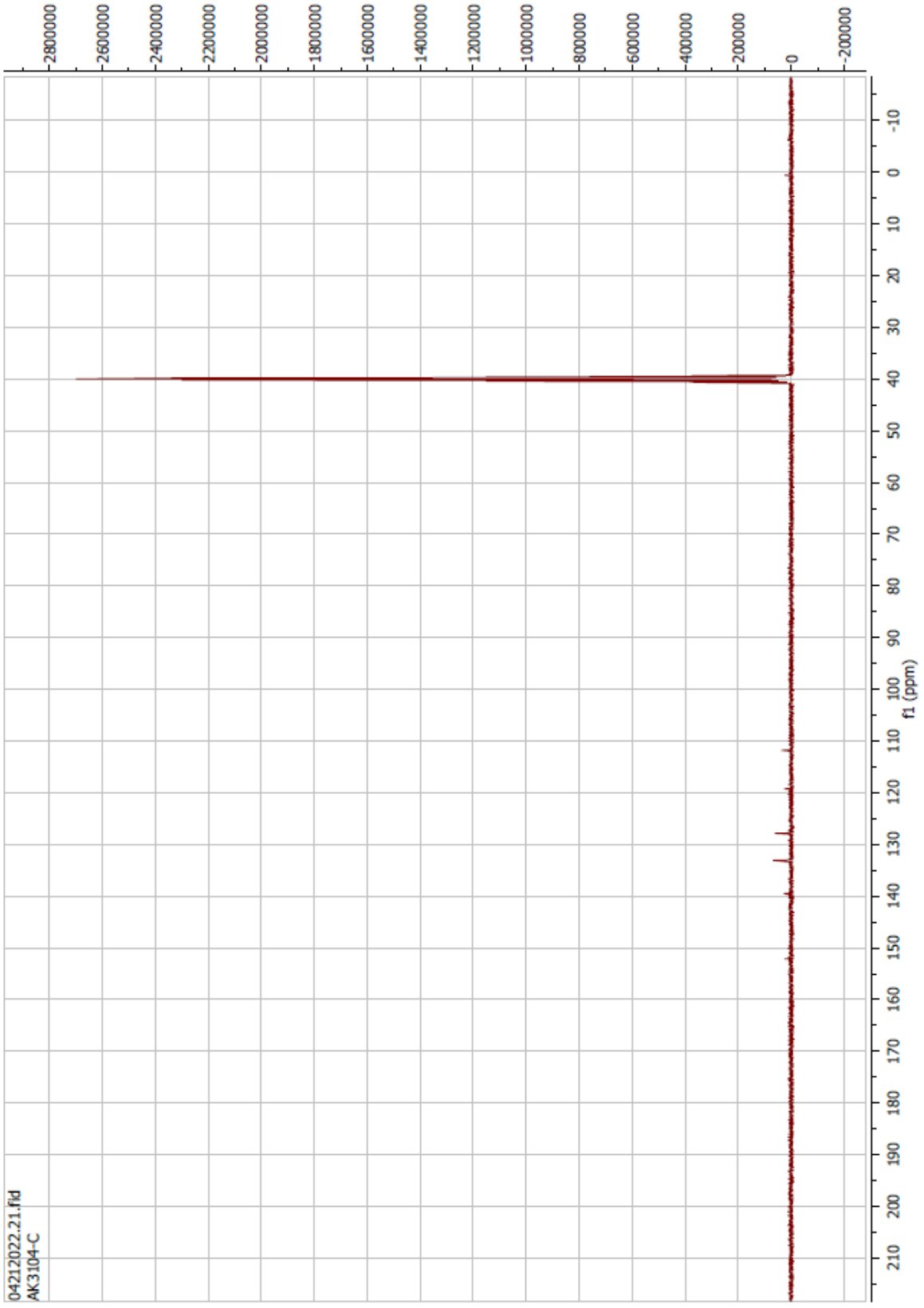

Compound 44 ^{1}H

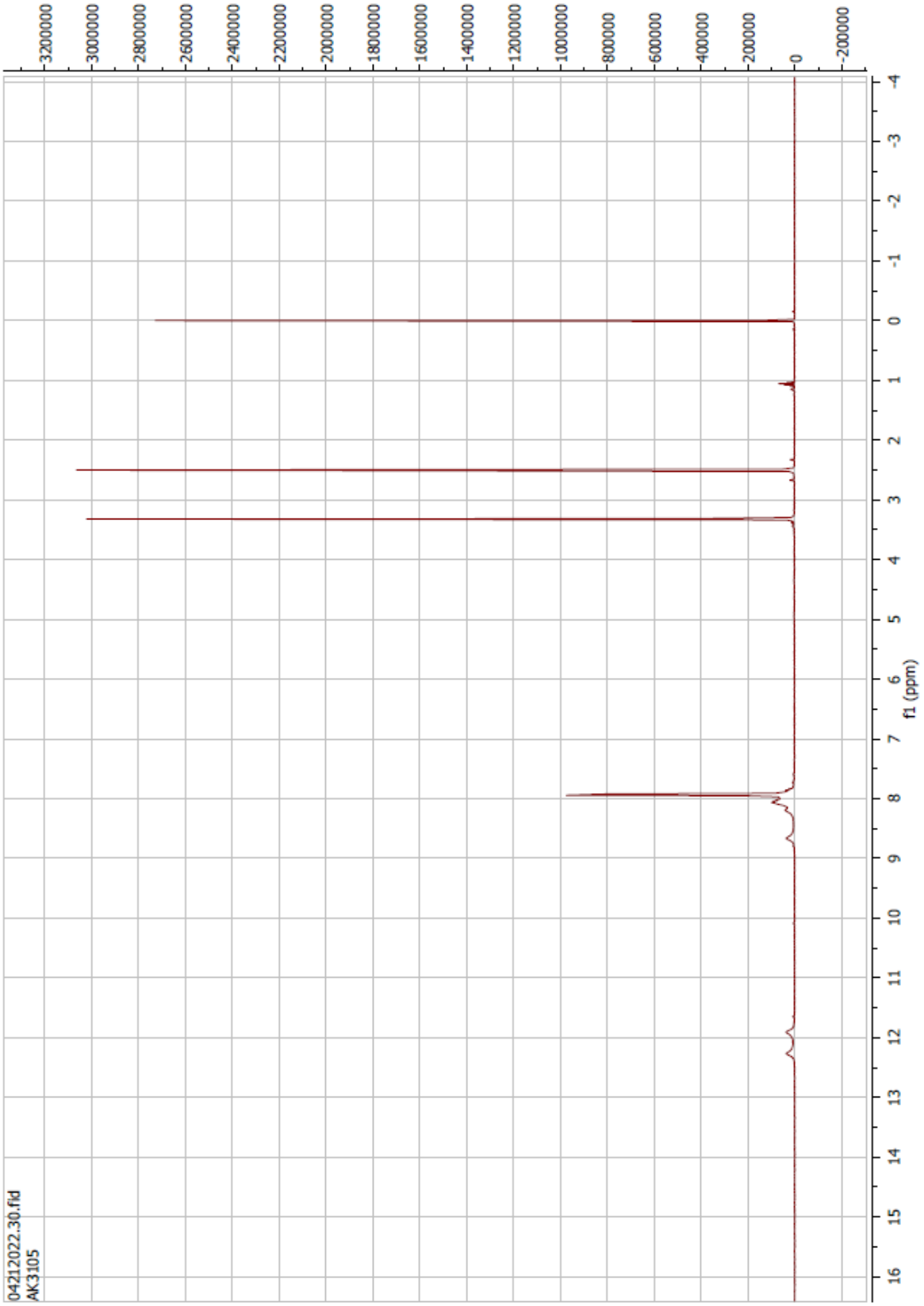

Compound 44 ^{13}C

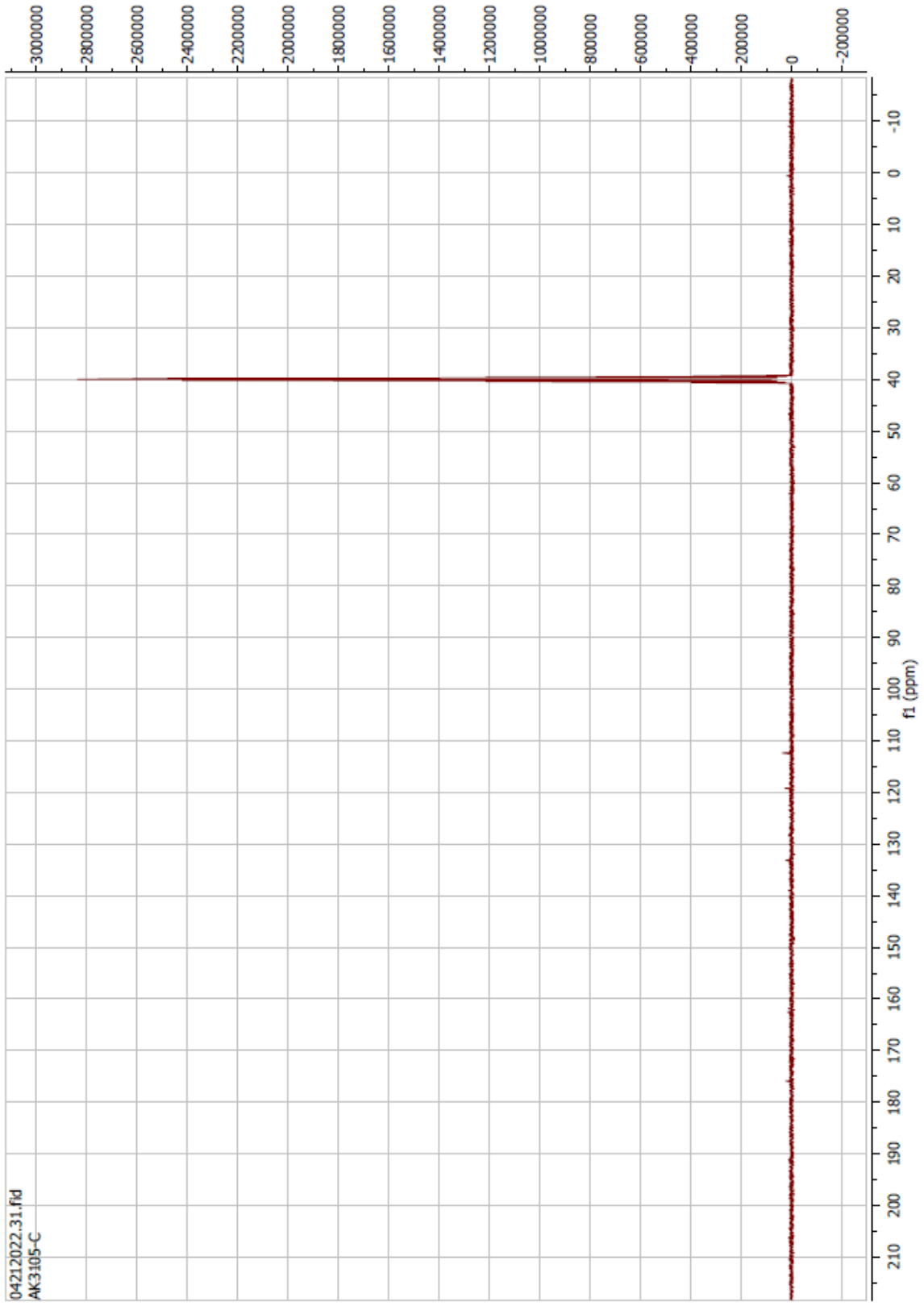

Compound 45 ^{1}H

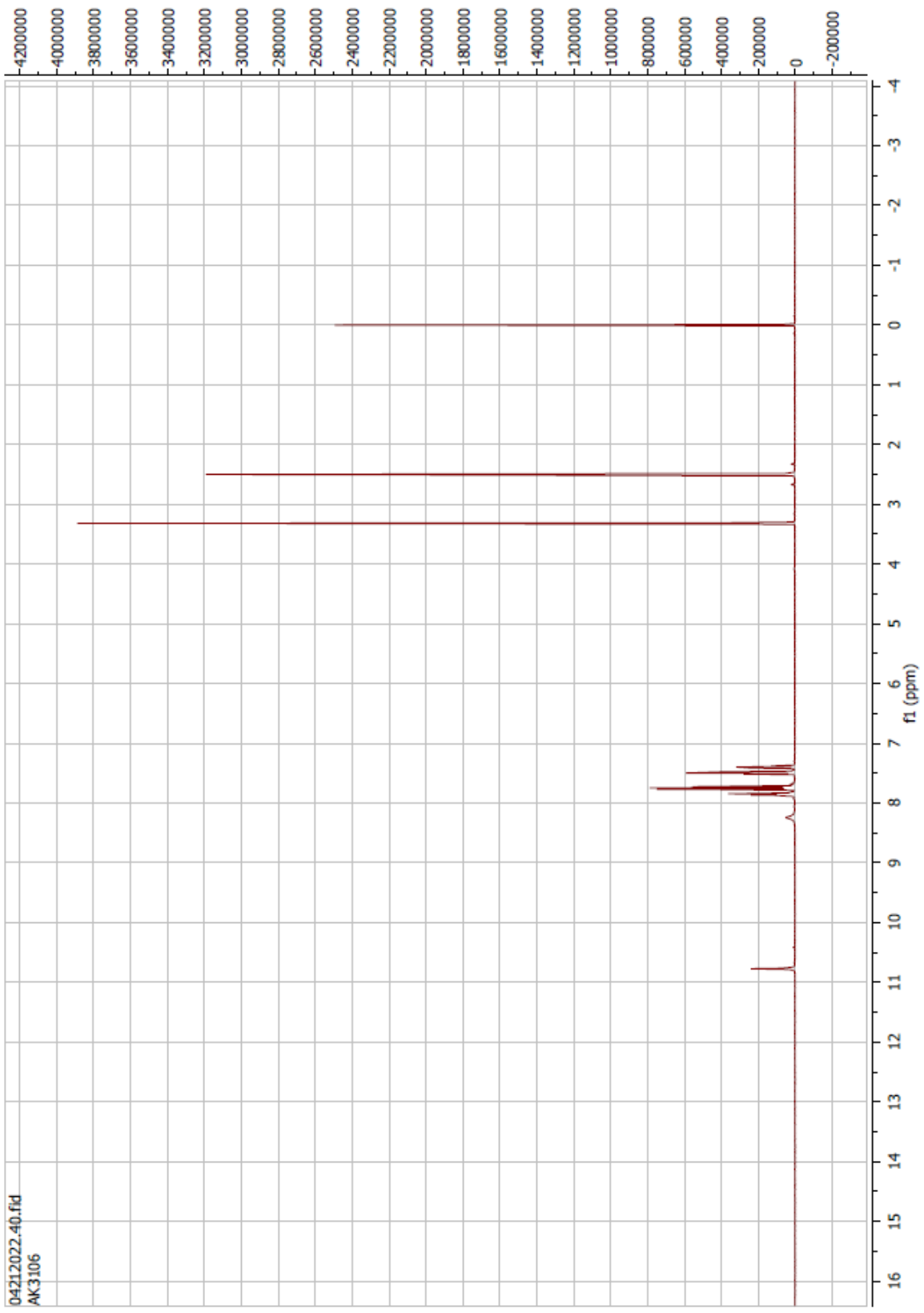

Compound 45 ^{13}C

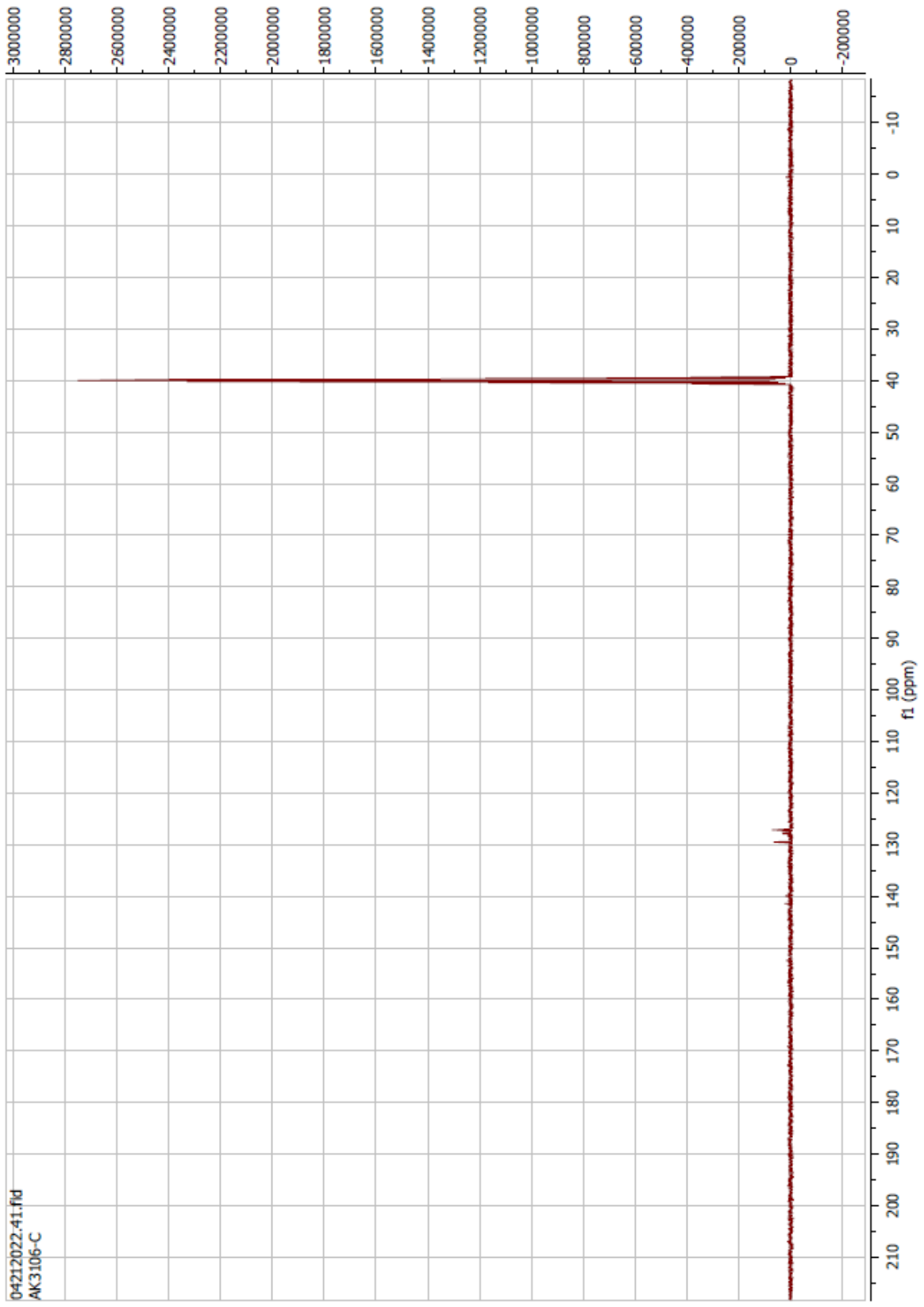

Compound 46 ^{1}H

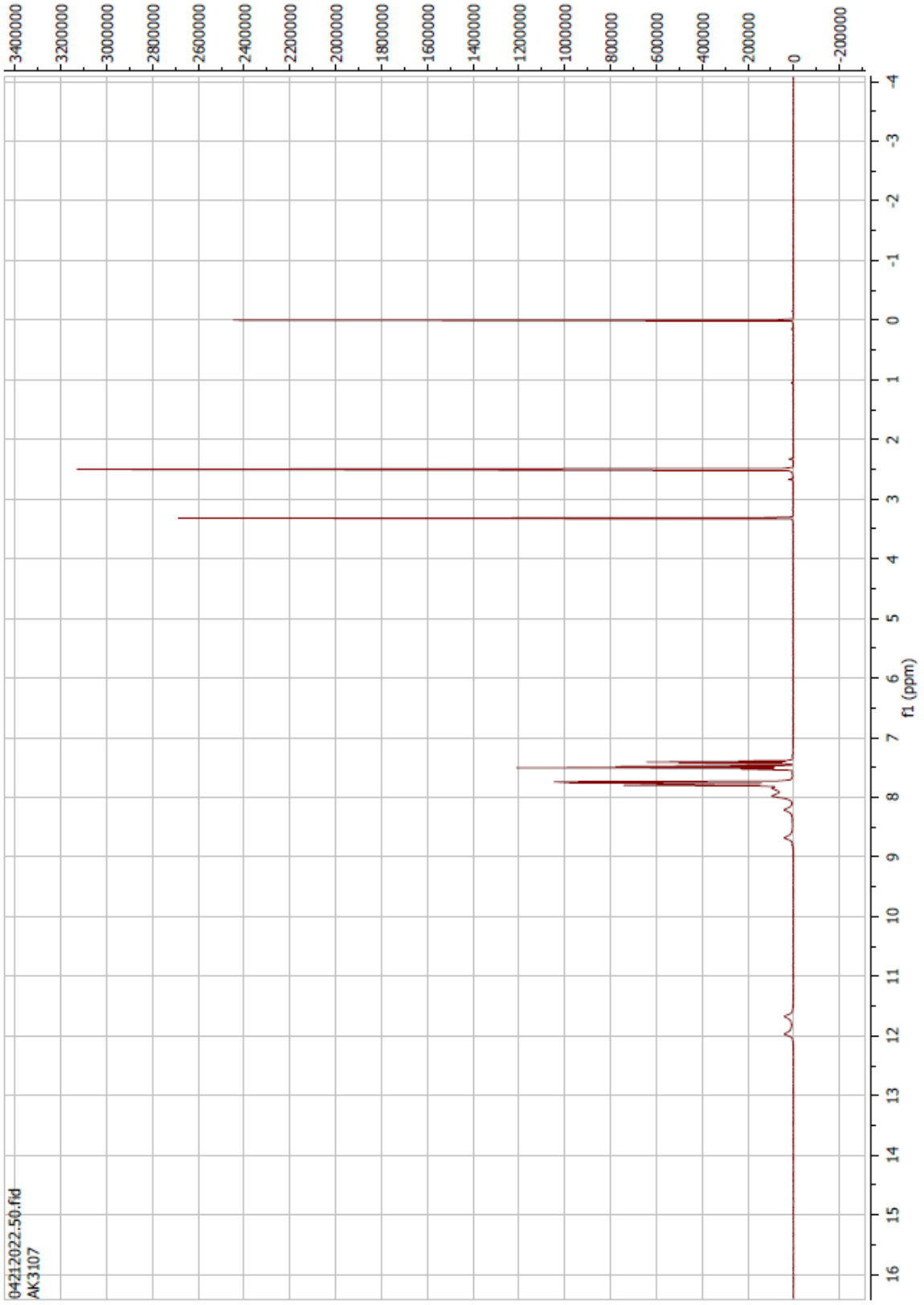

Compound 46 ^{13}C

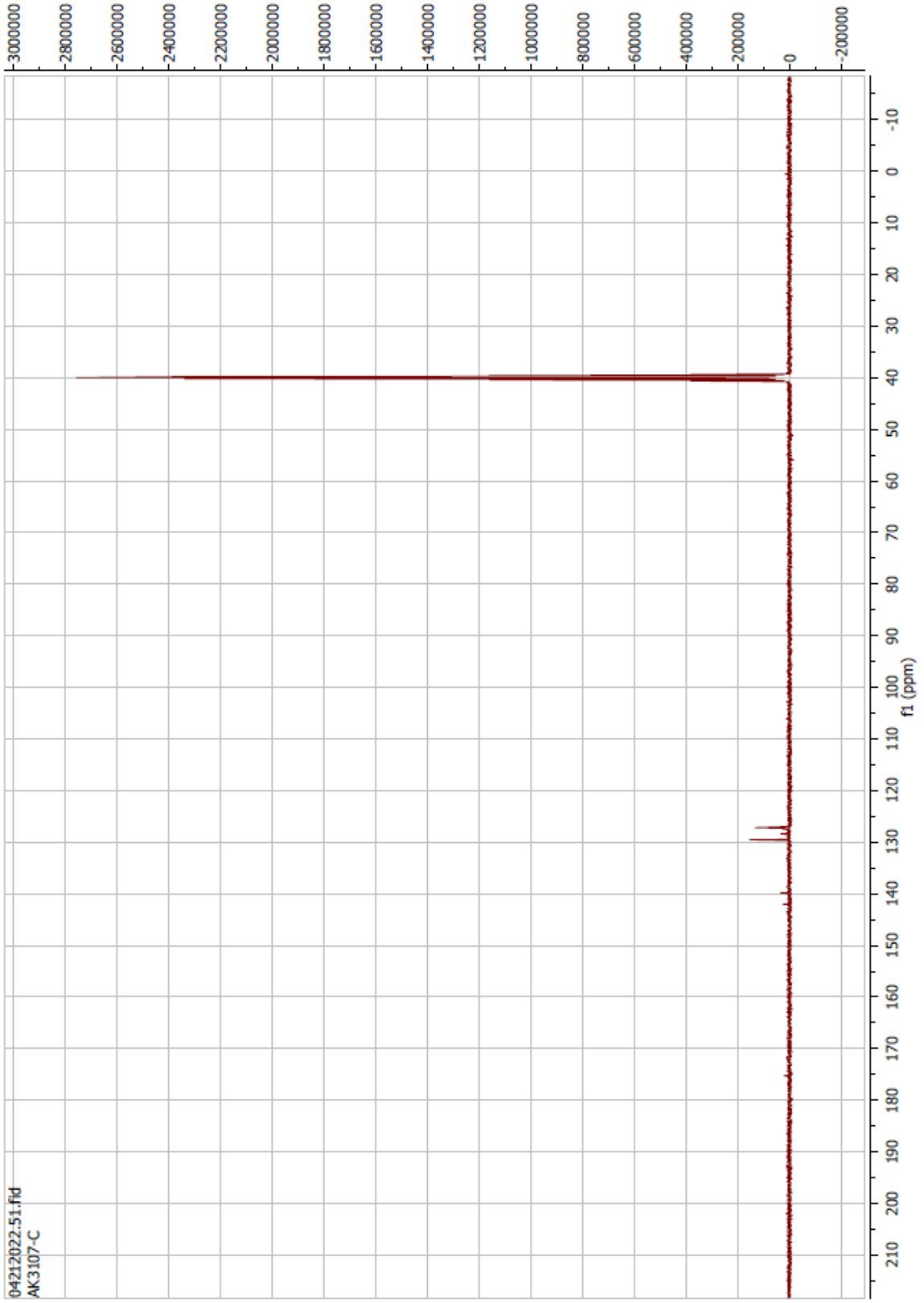

Compound 47 ^{1}H

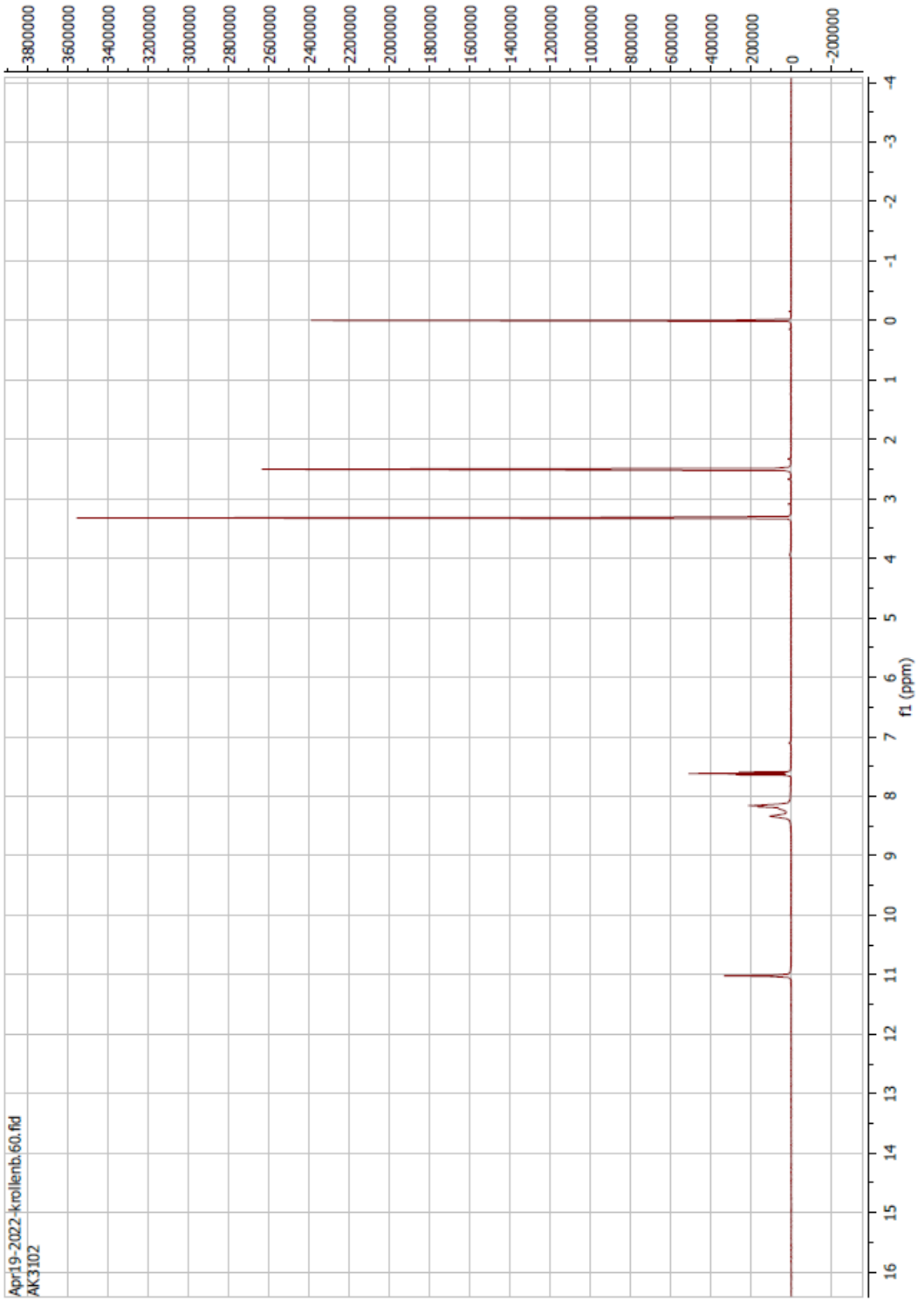

Compound 47 ^{13}C

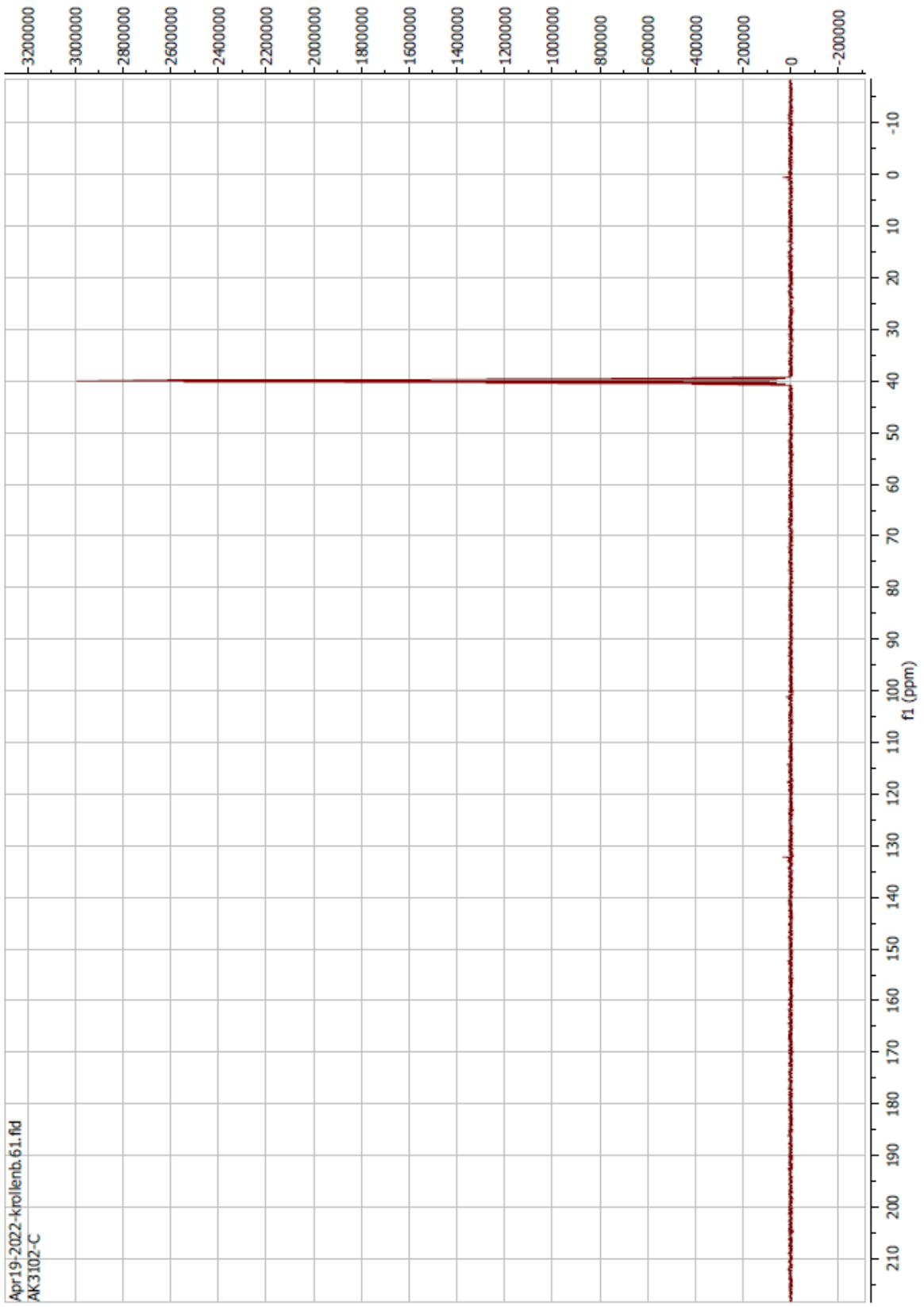

Compound 48 ^{1}H

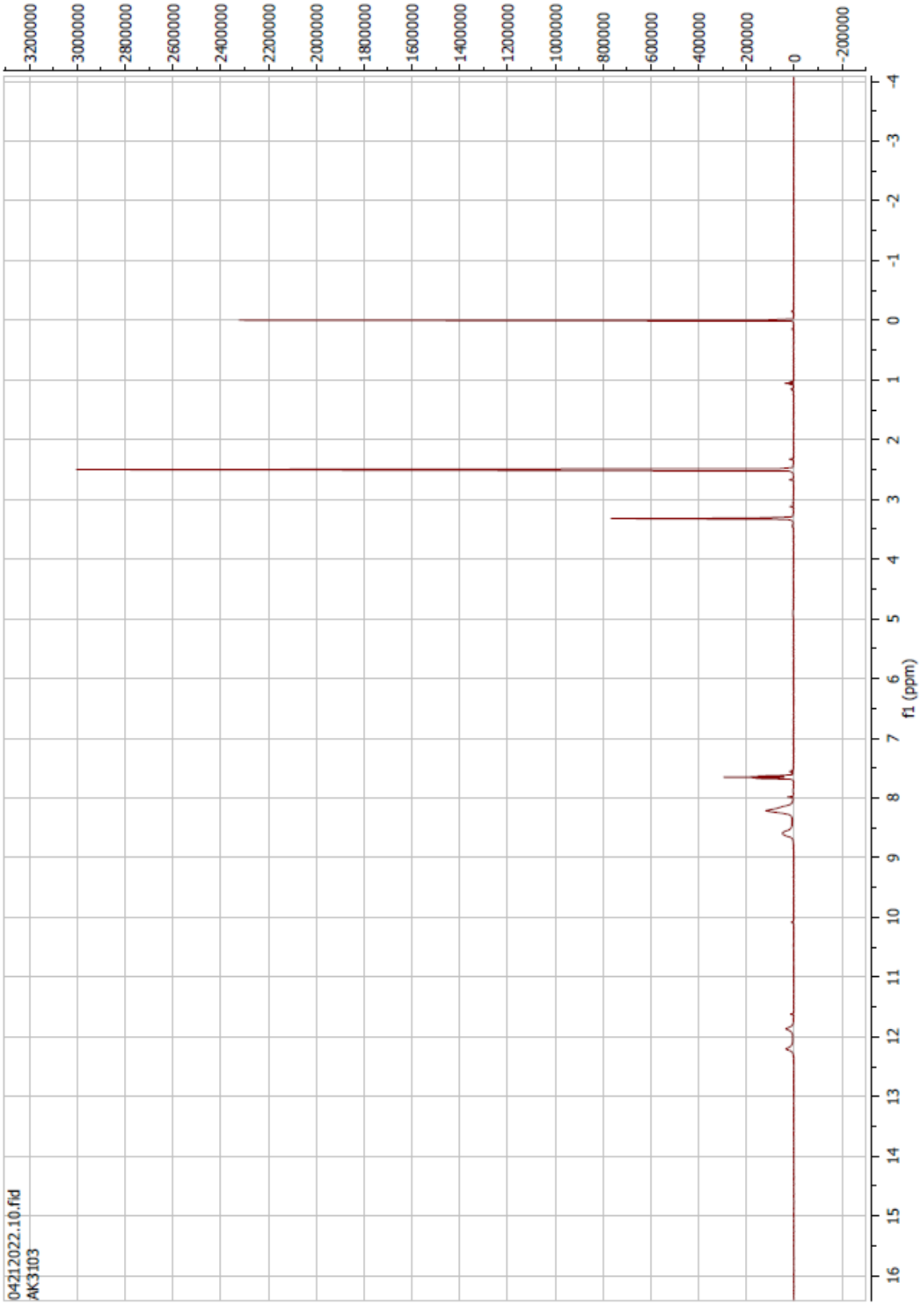

Compound 48 ^{13}C

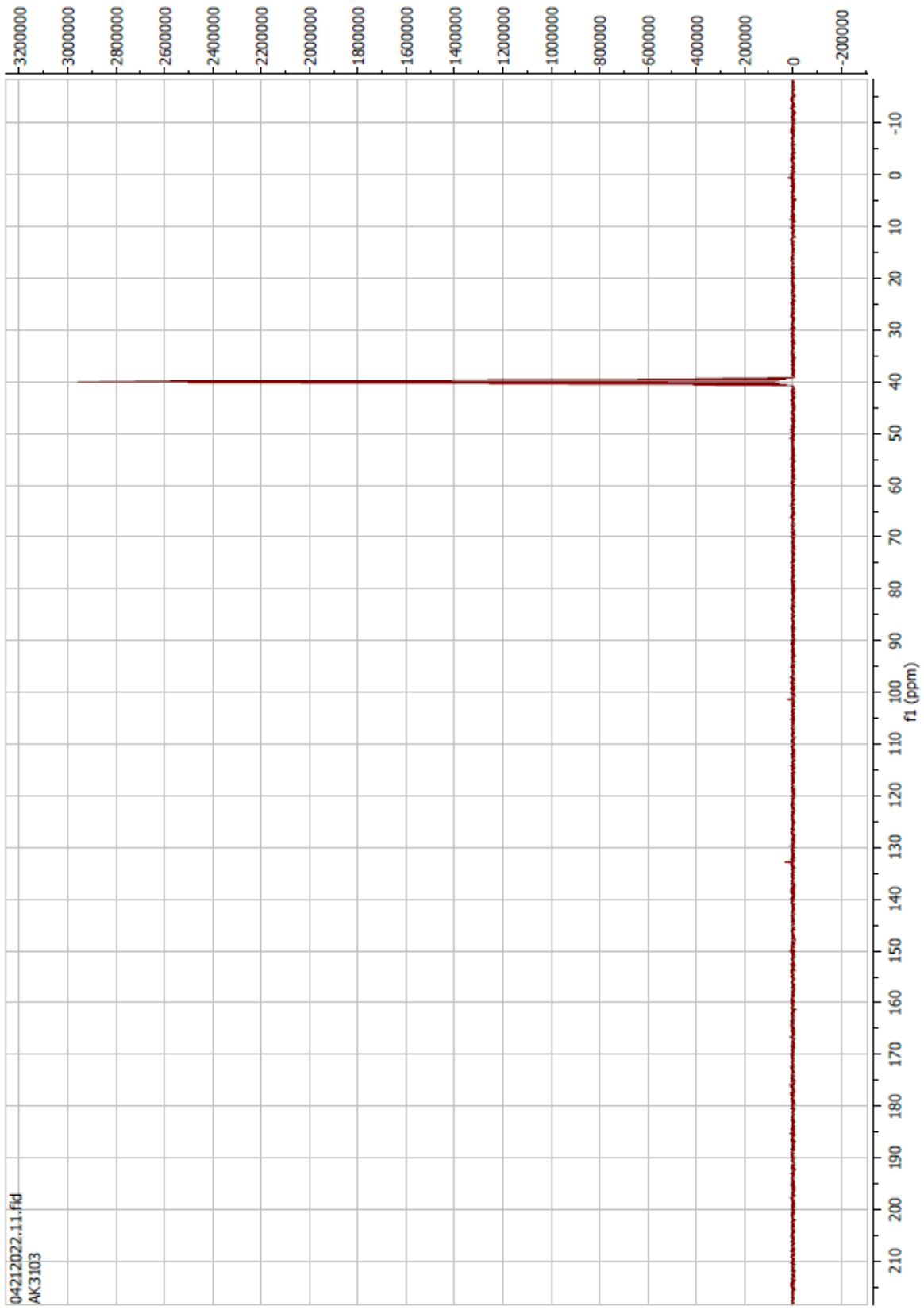

Compound 49 ^{1}H

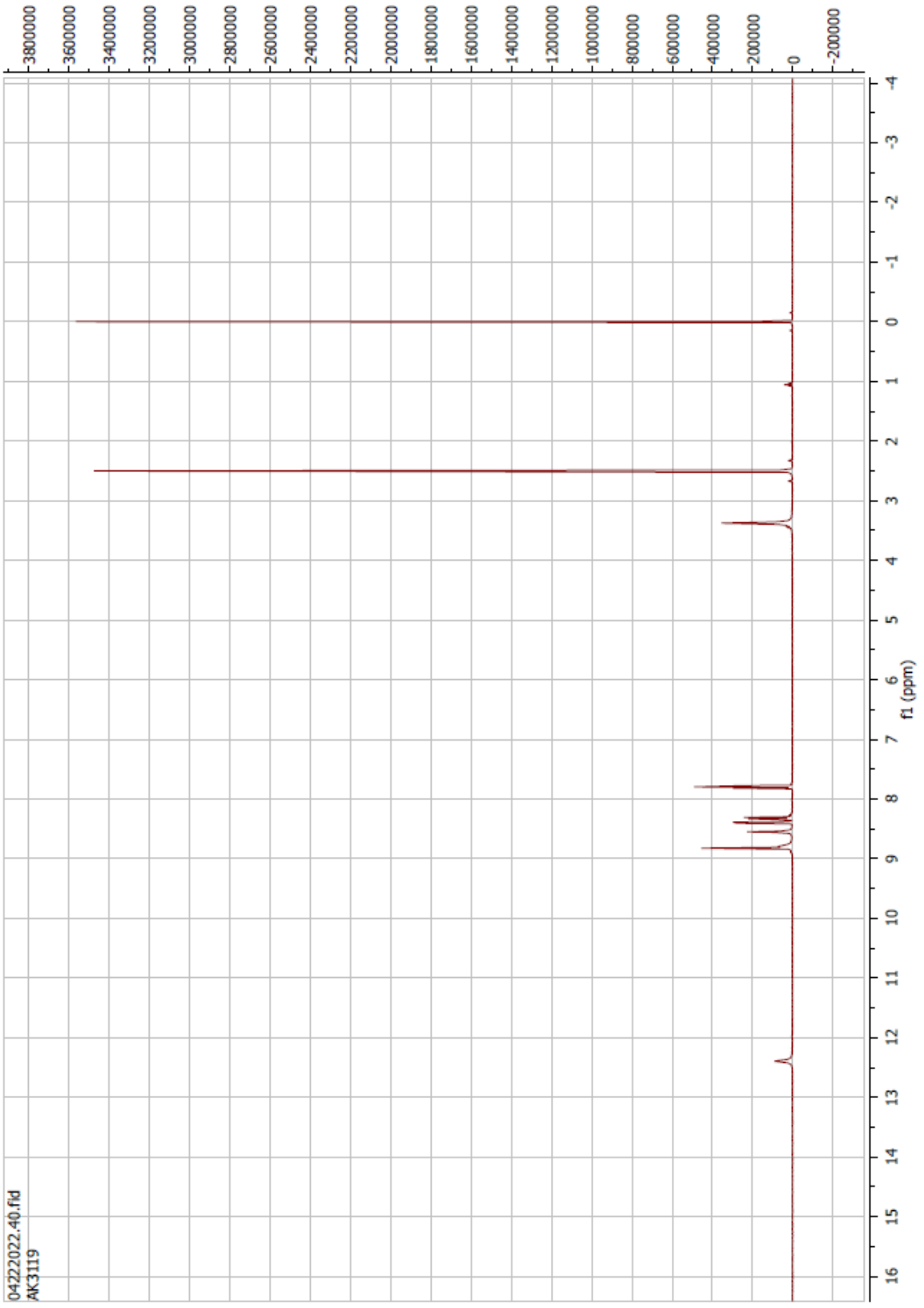

Compound 49 ^{13}C

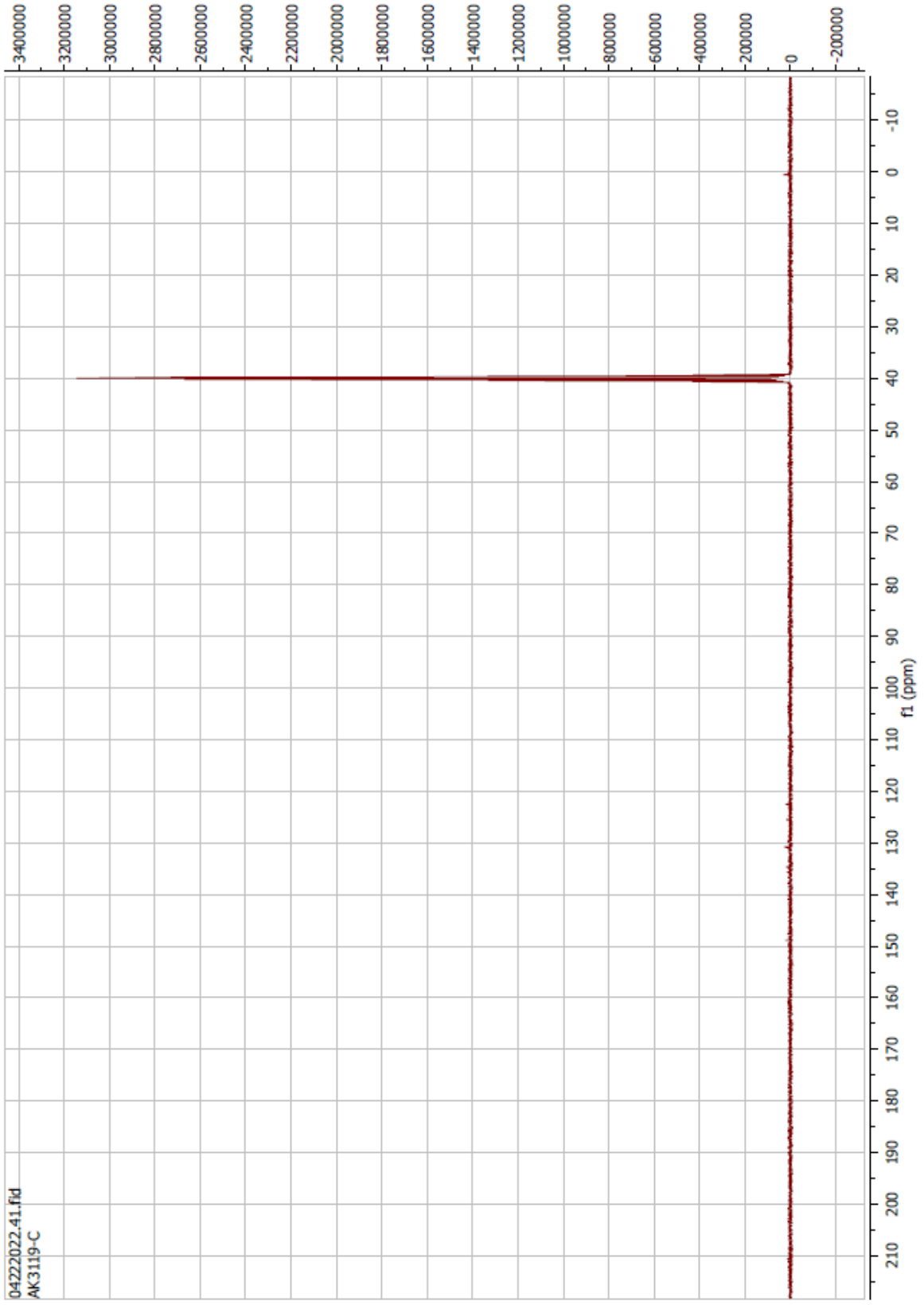

Compound 50 ^{1}H

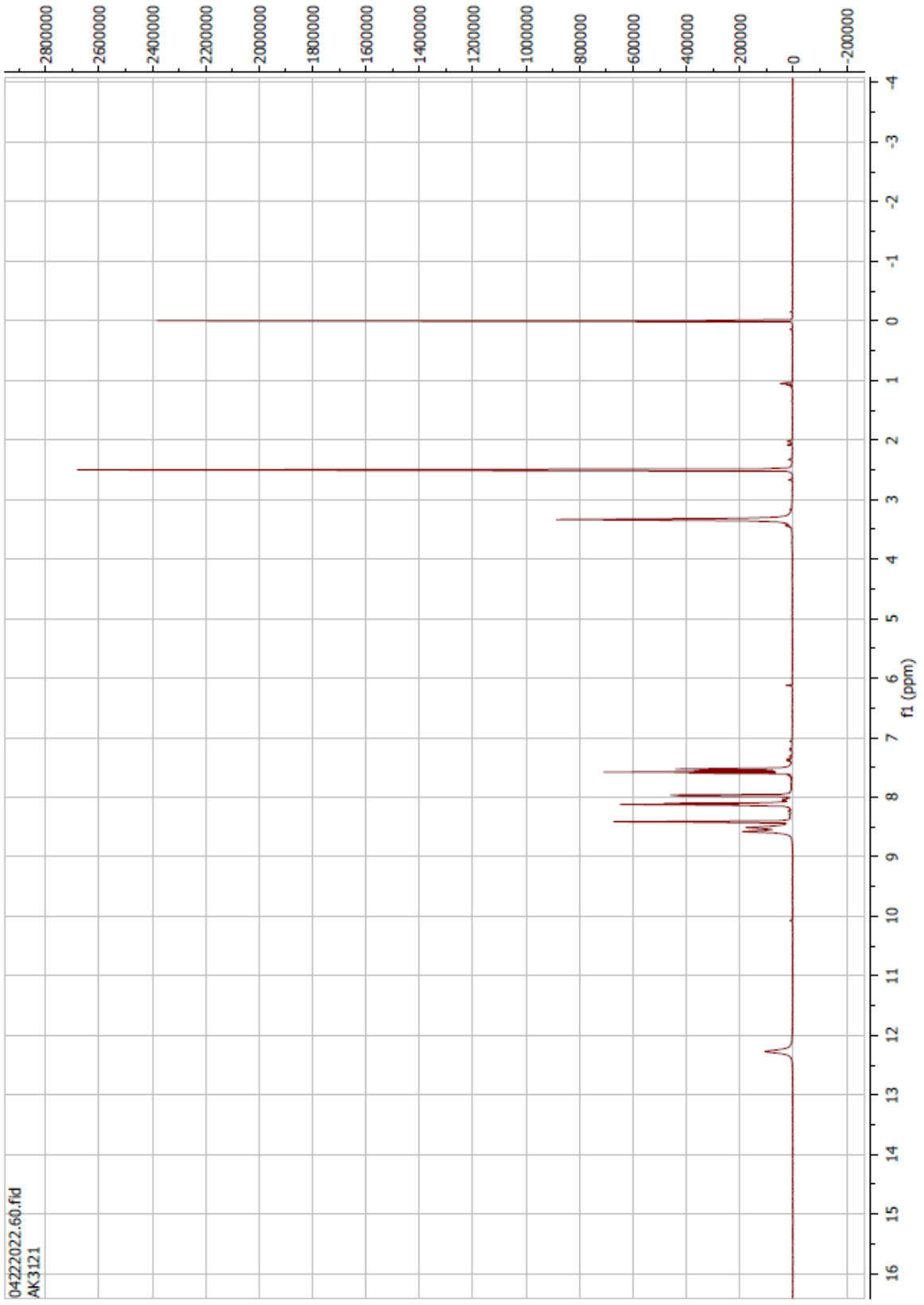

Compound 50 ^{13}C

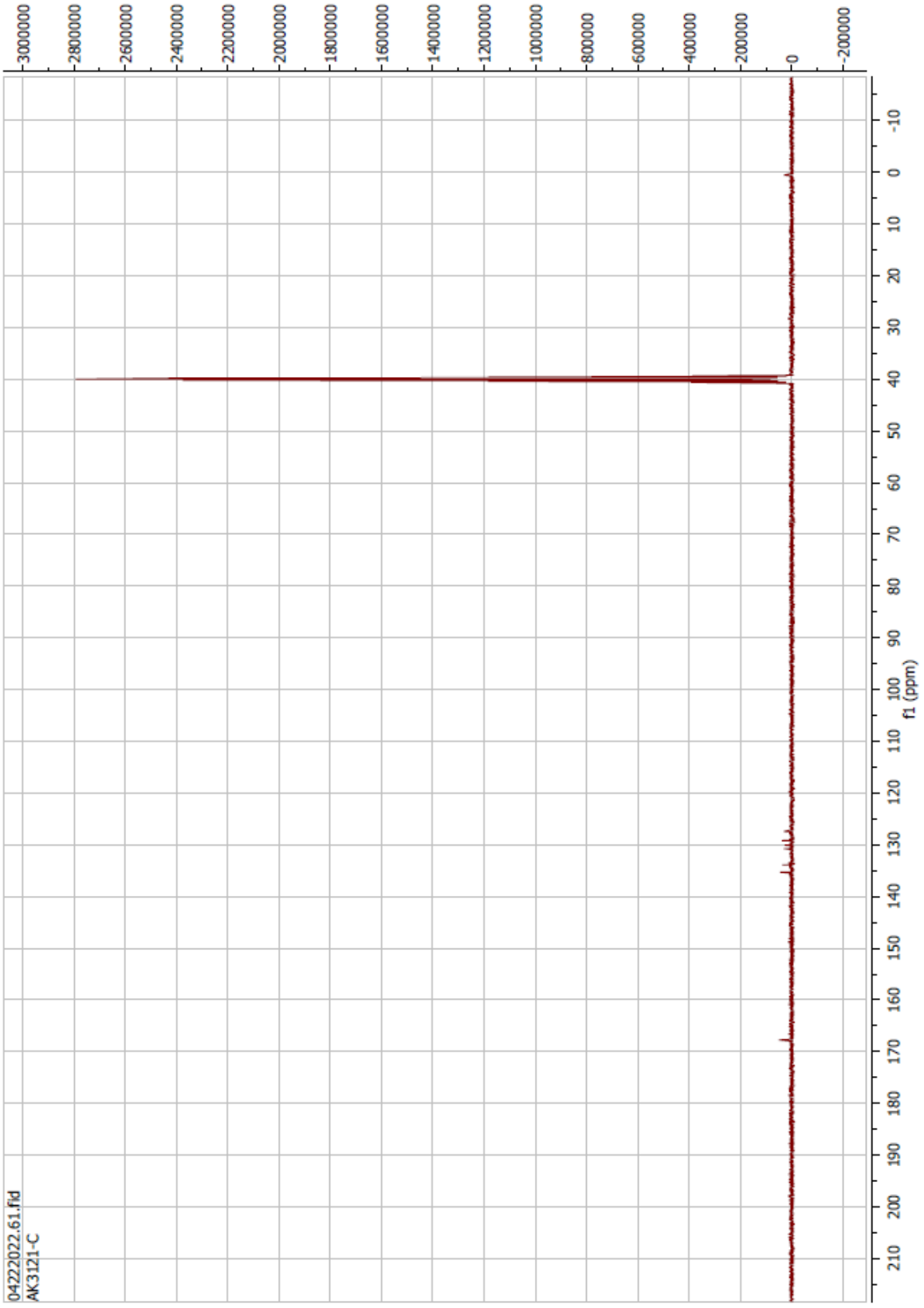

Compound 51 ^{1}H

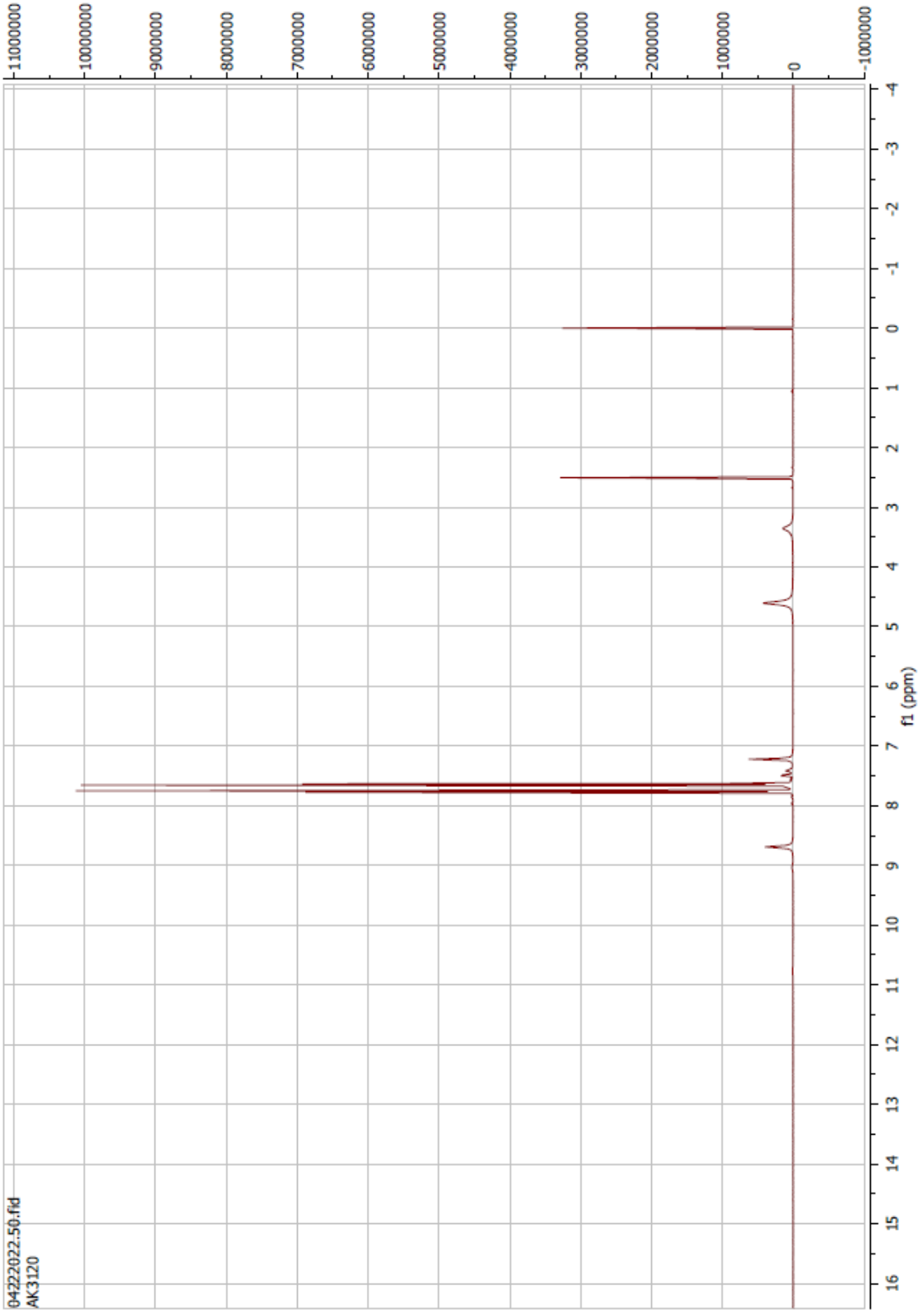

Compound 51 ^{13}C

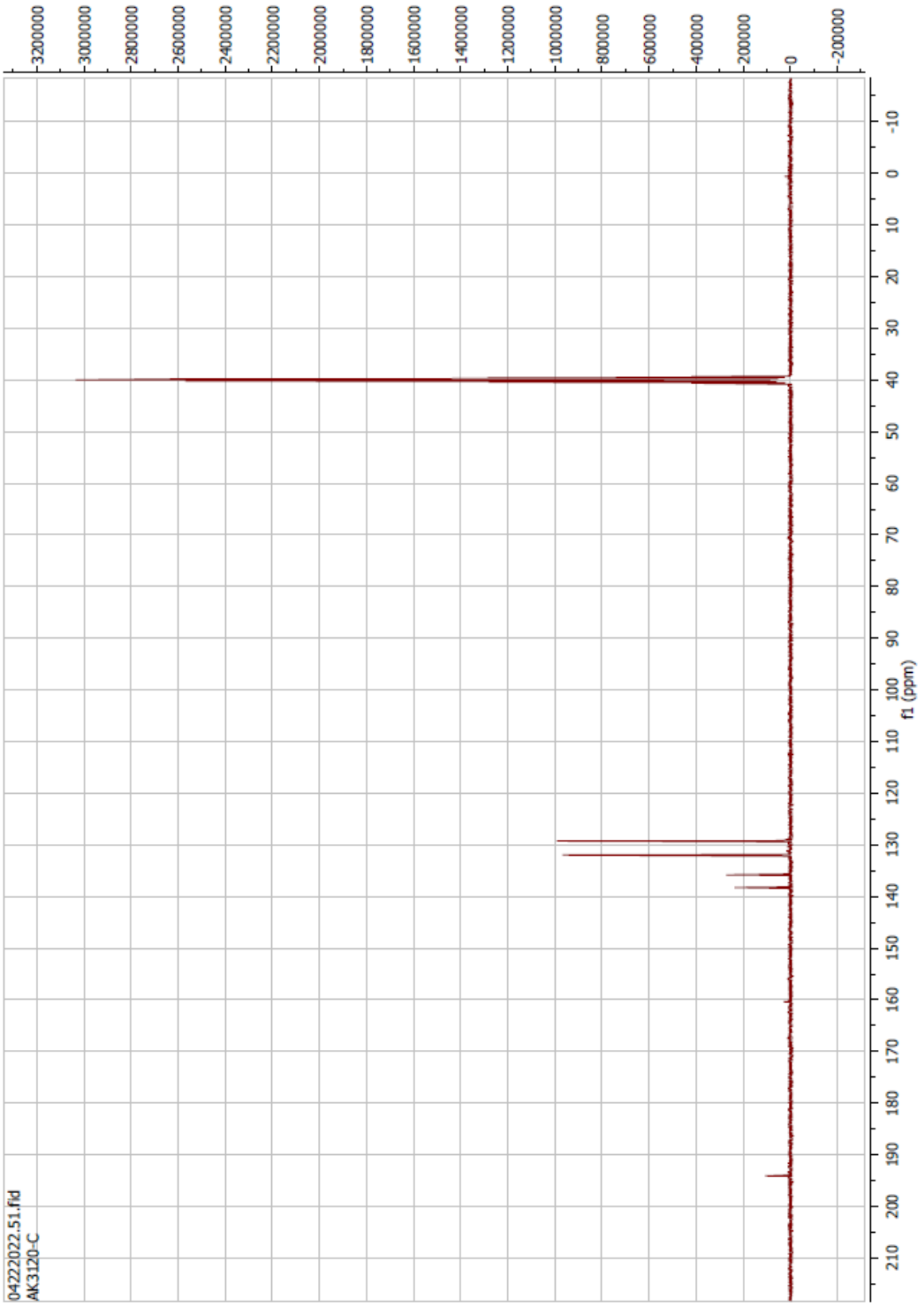

Compound 52 ^{1}H

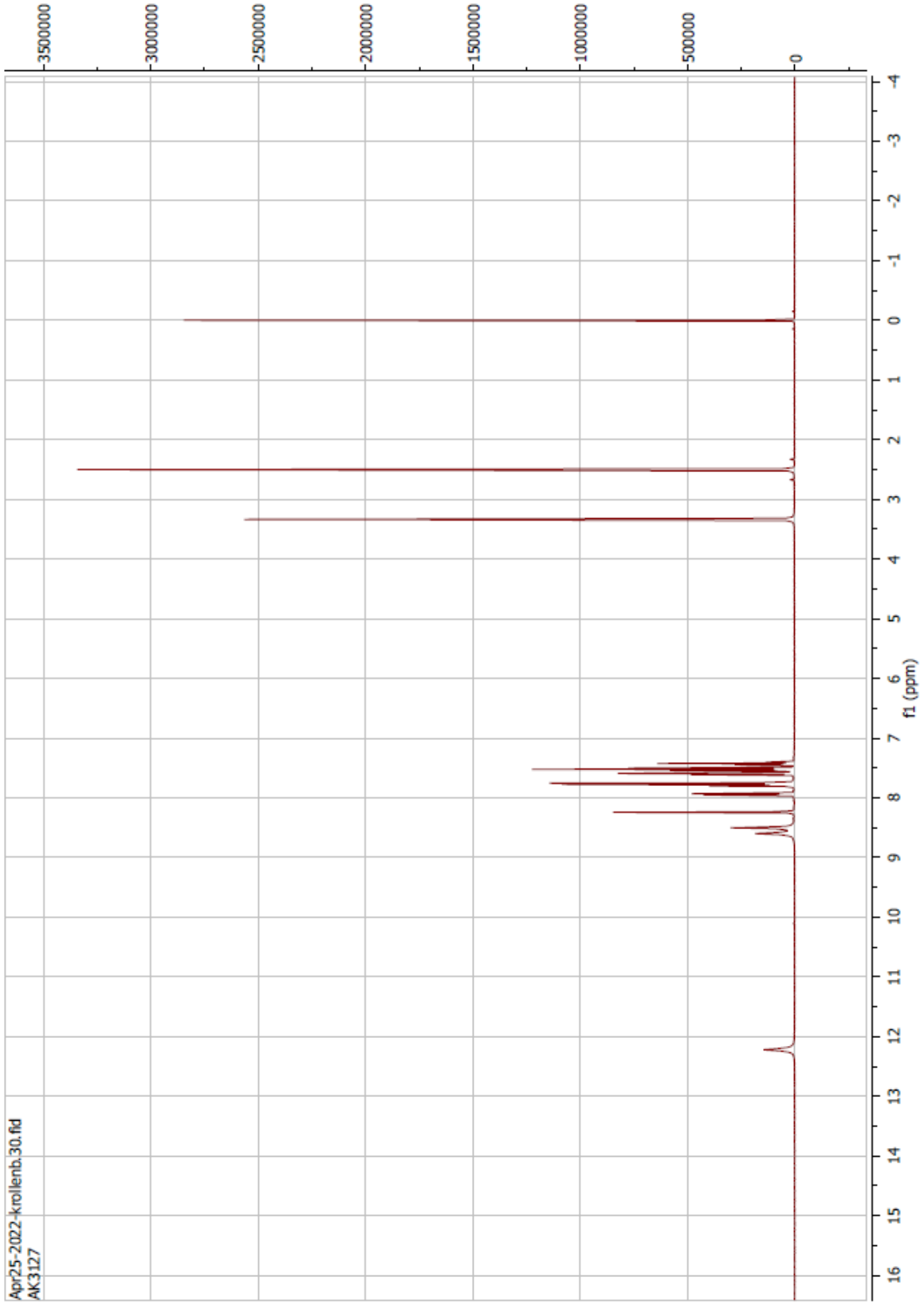

Compound 52 ^{13}C

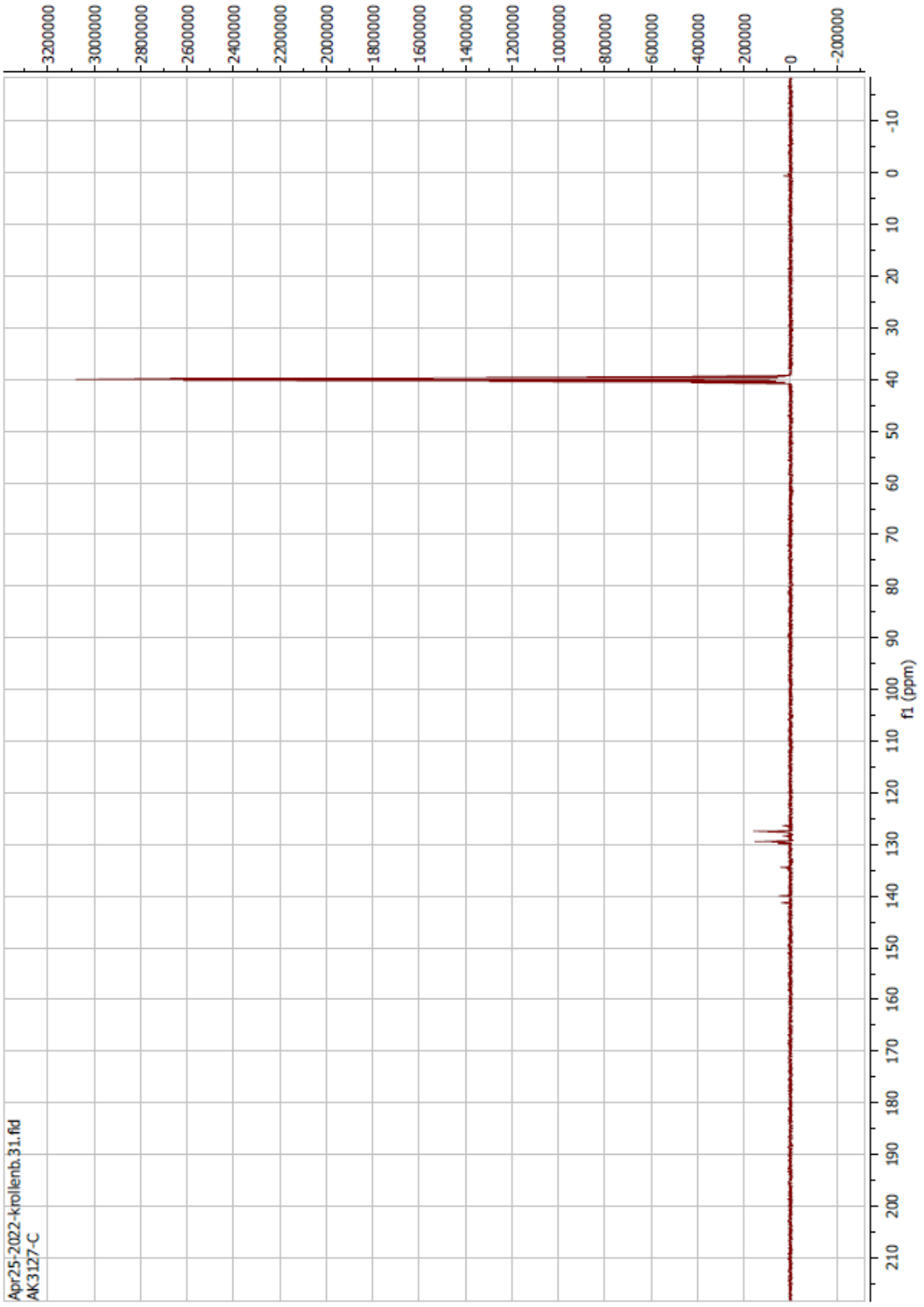

Compound 53 ^{1}H

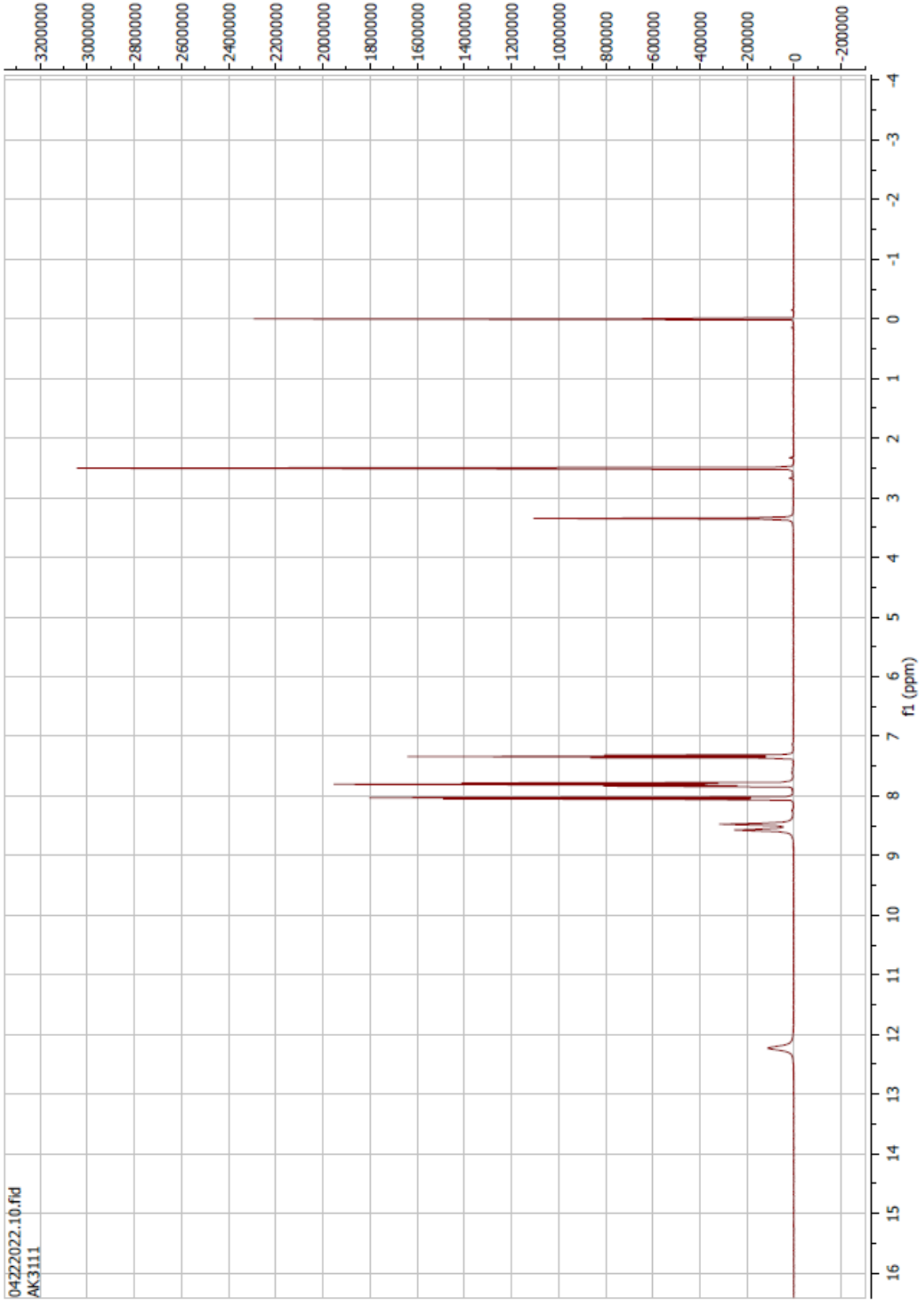

Compound 53 ^{13}C

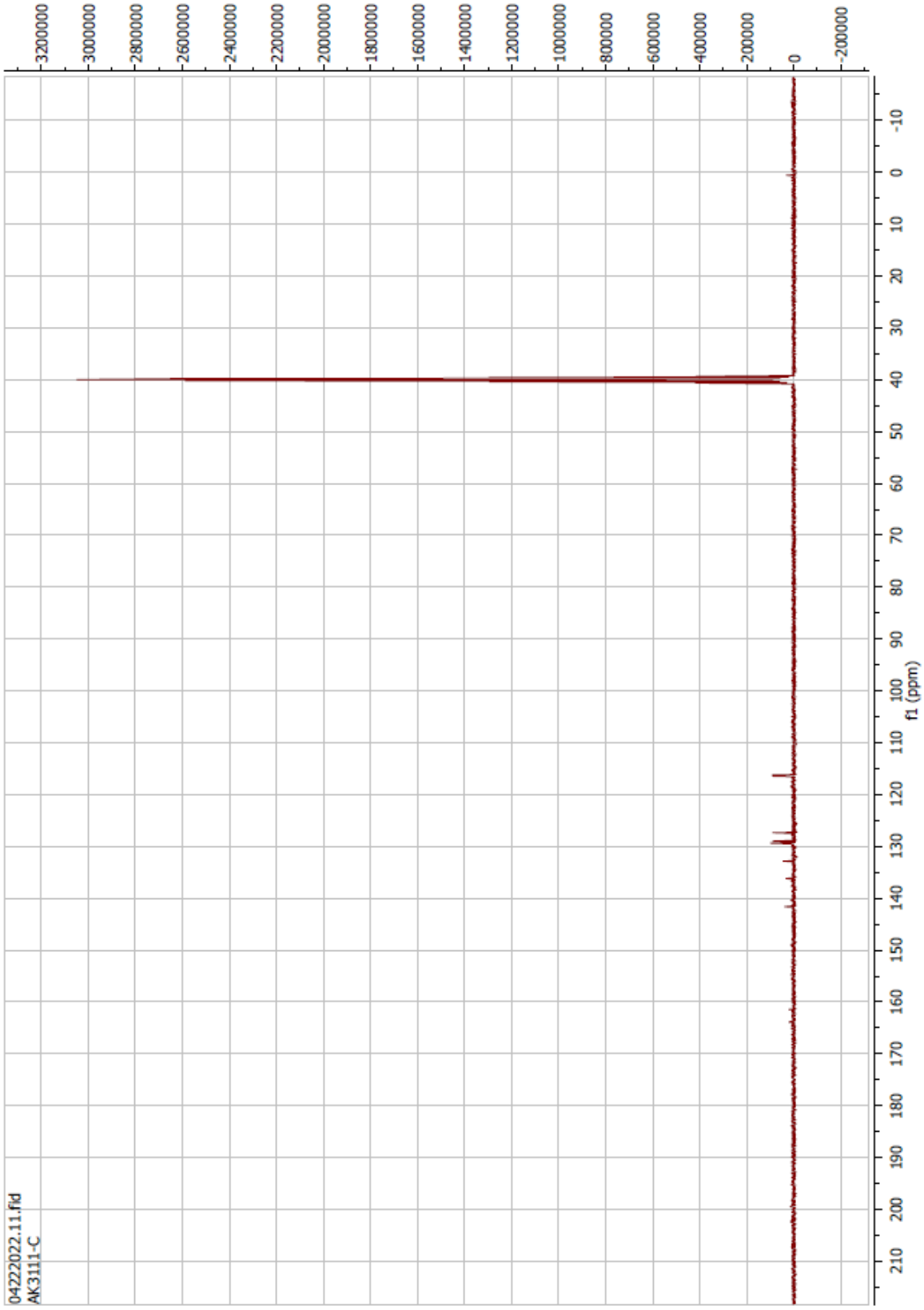

Compound 54 ^{1}H

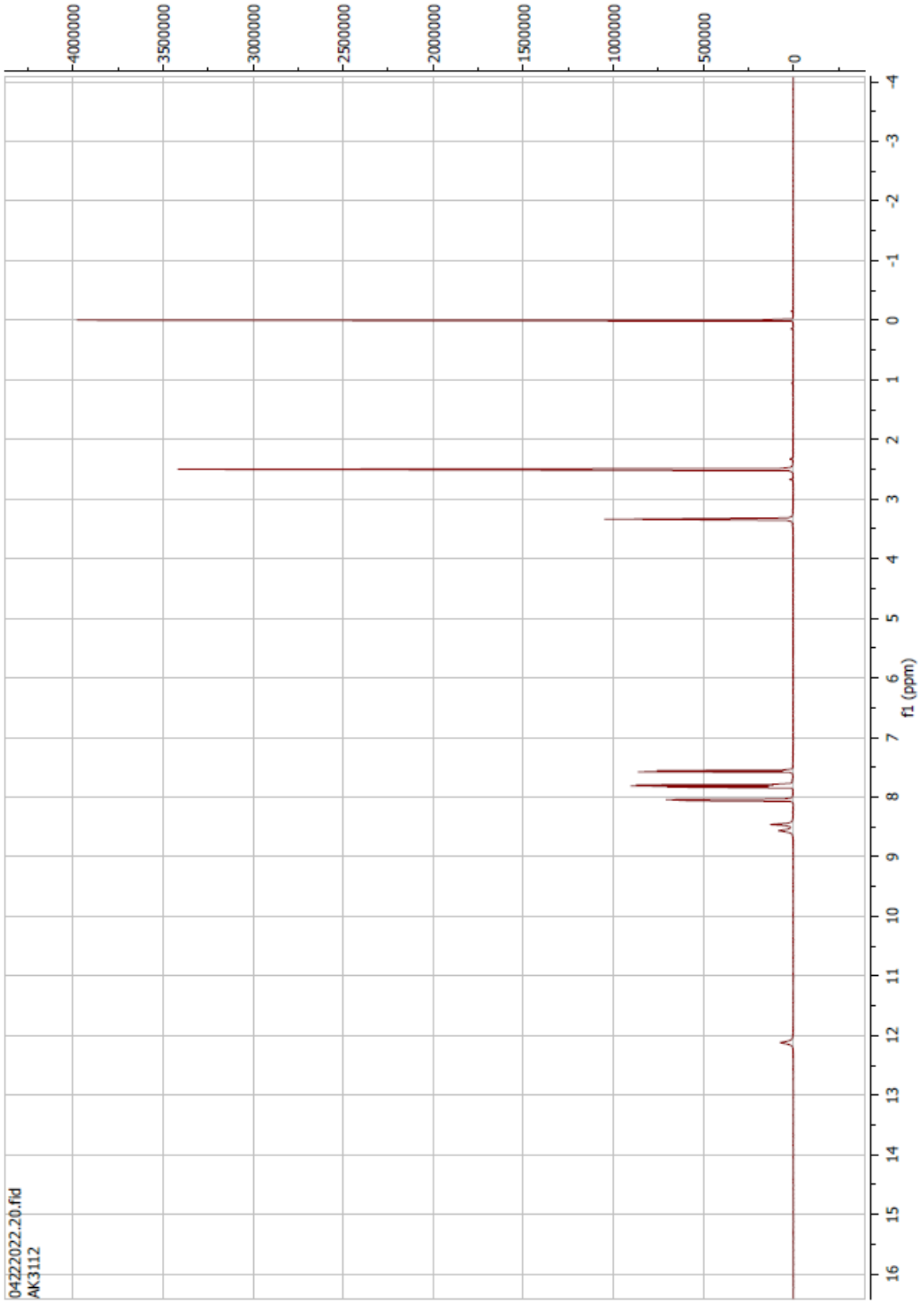

Compound 54 ^{13}C

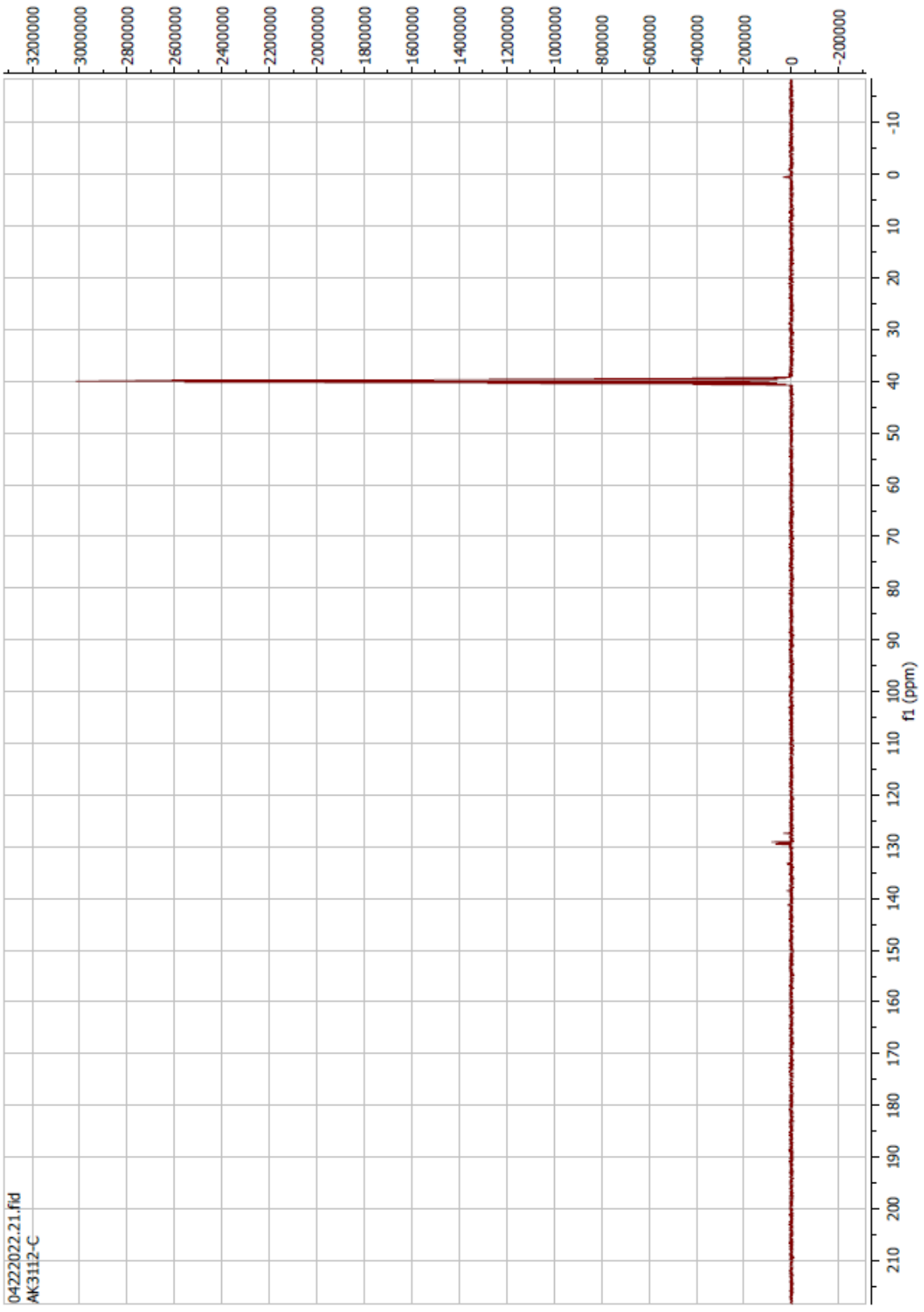

Compound 55 ^{1}H

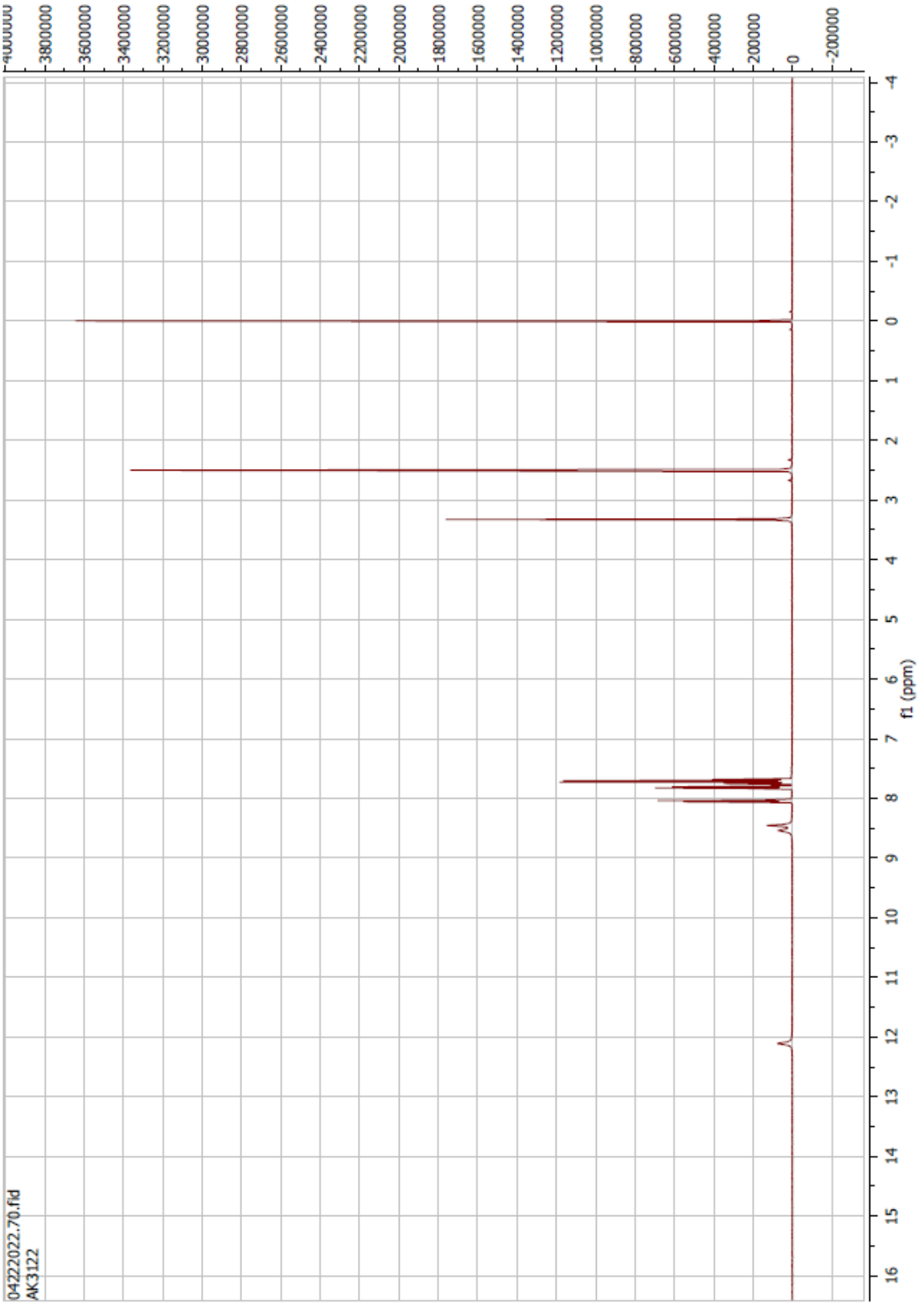

Compound 55 ^{13}C

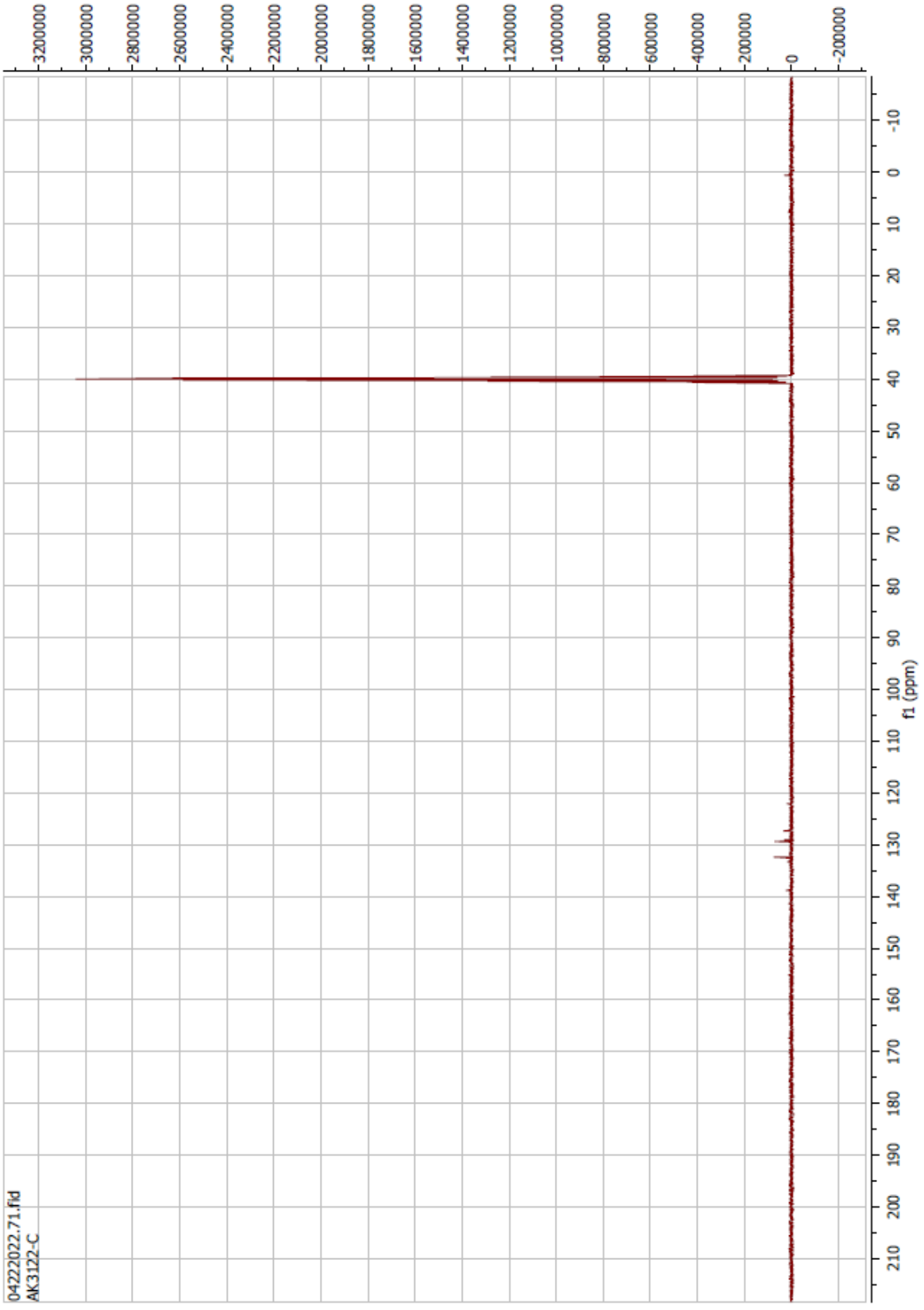

Compound 56 ^{1}H

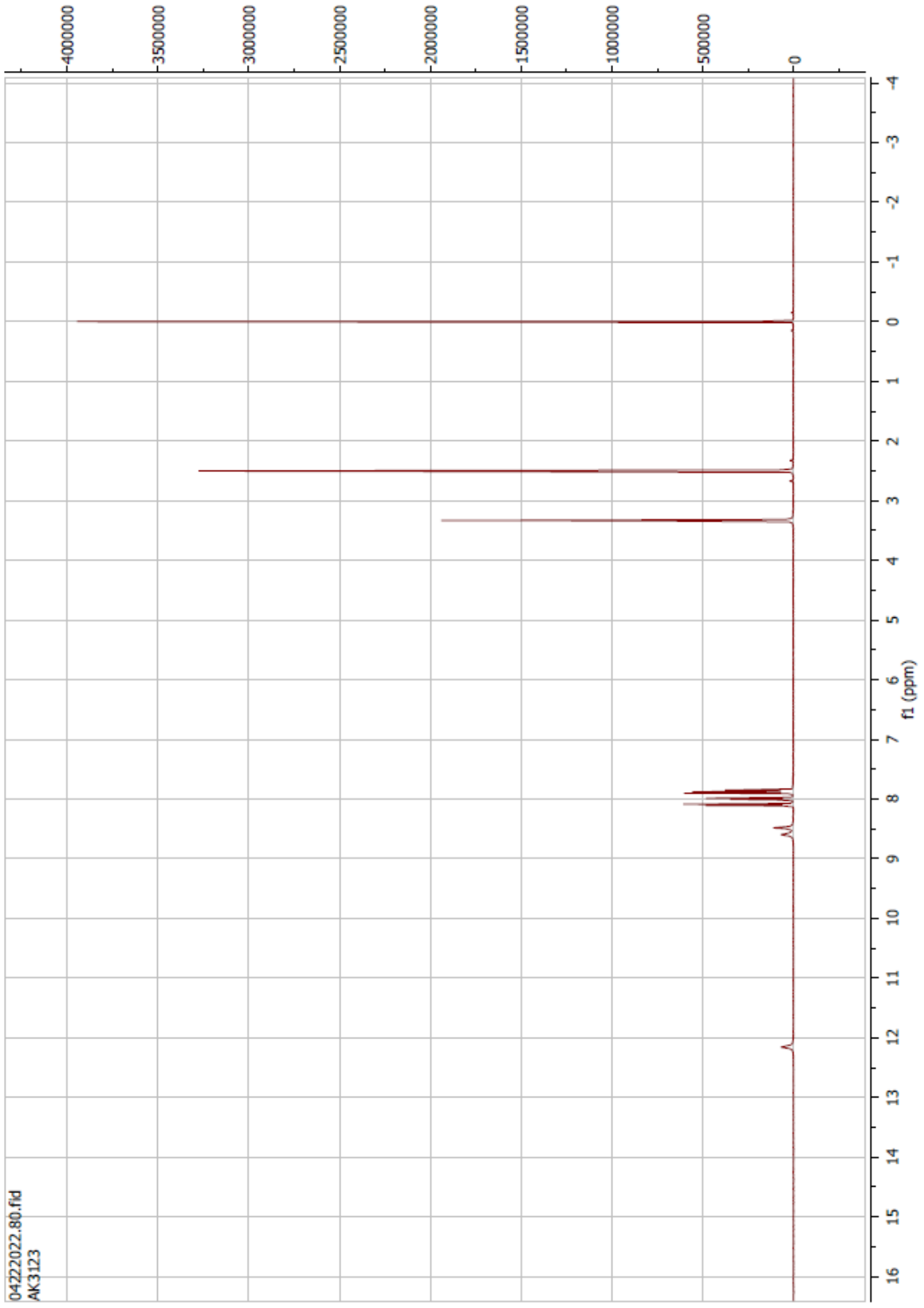

Compound 56 ^{13}C

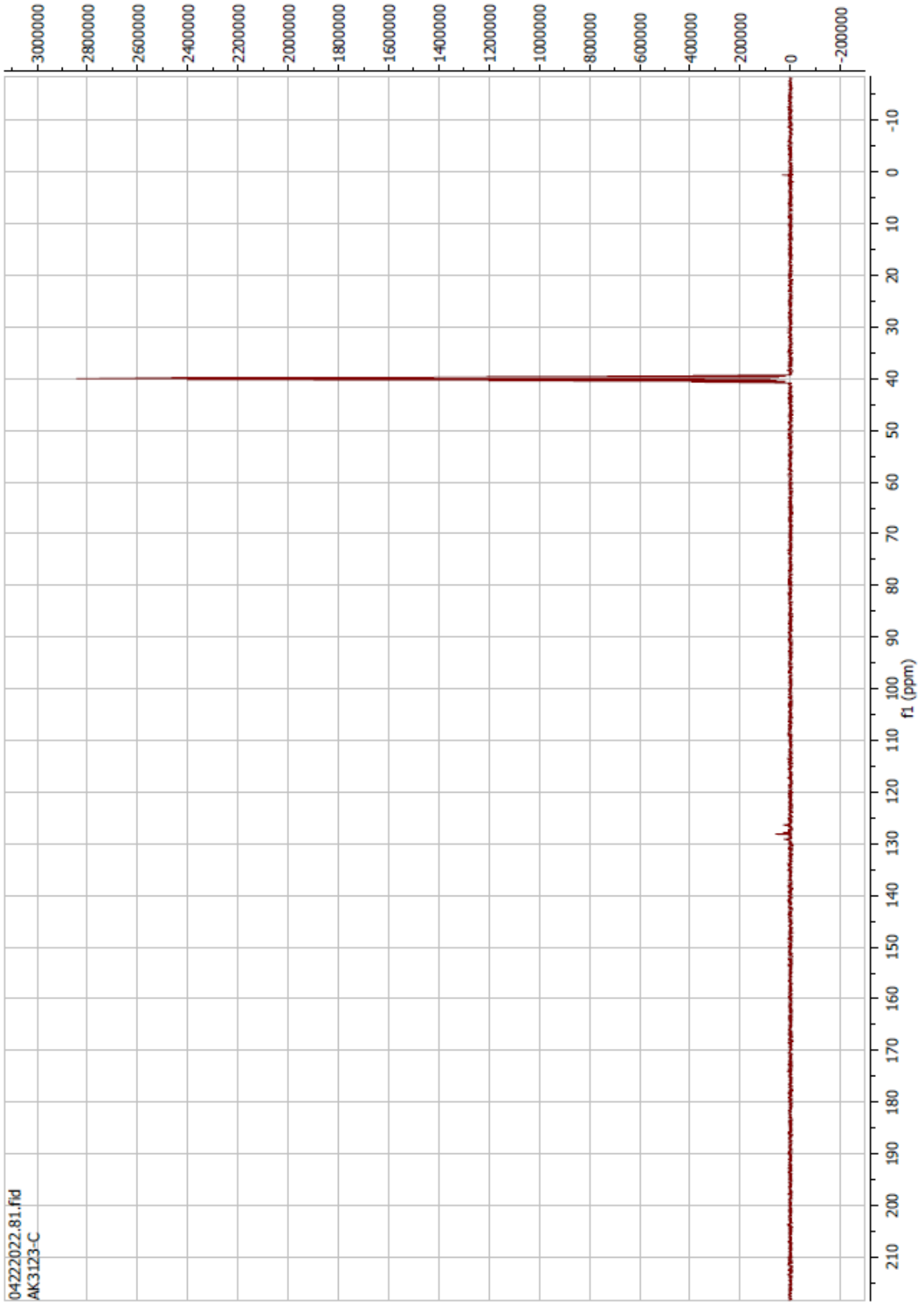

Compound 57 ^{1}H

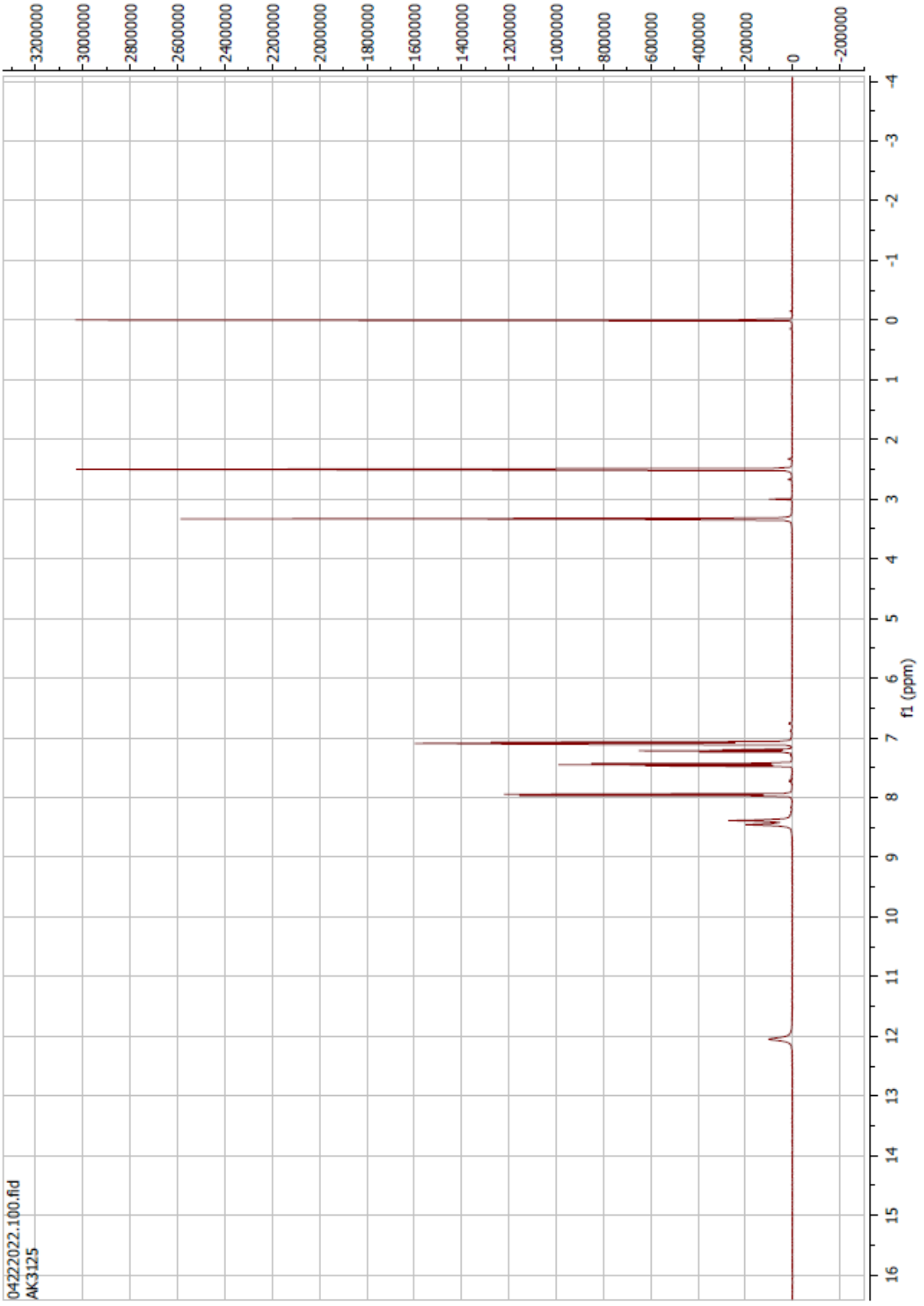

Compound 57 ^{13}C

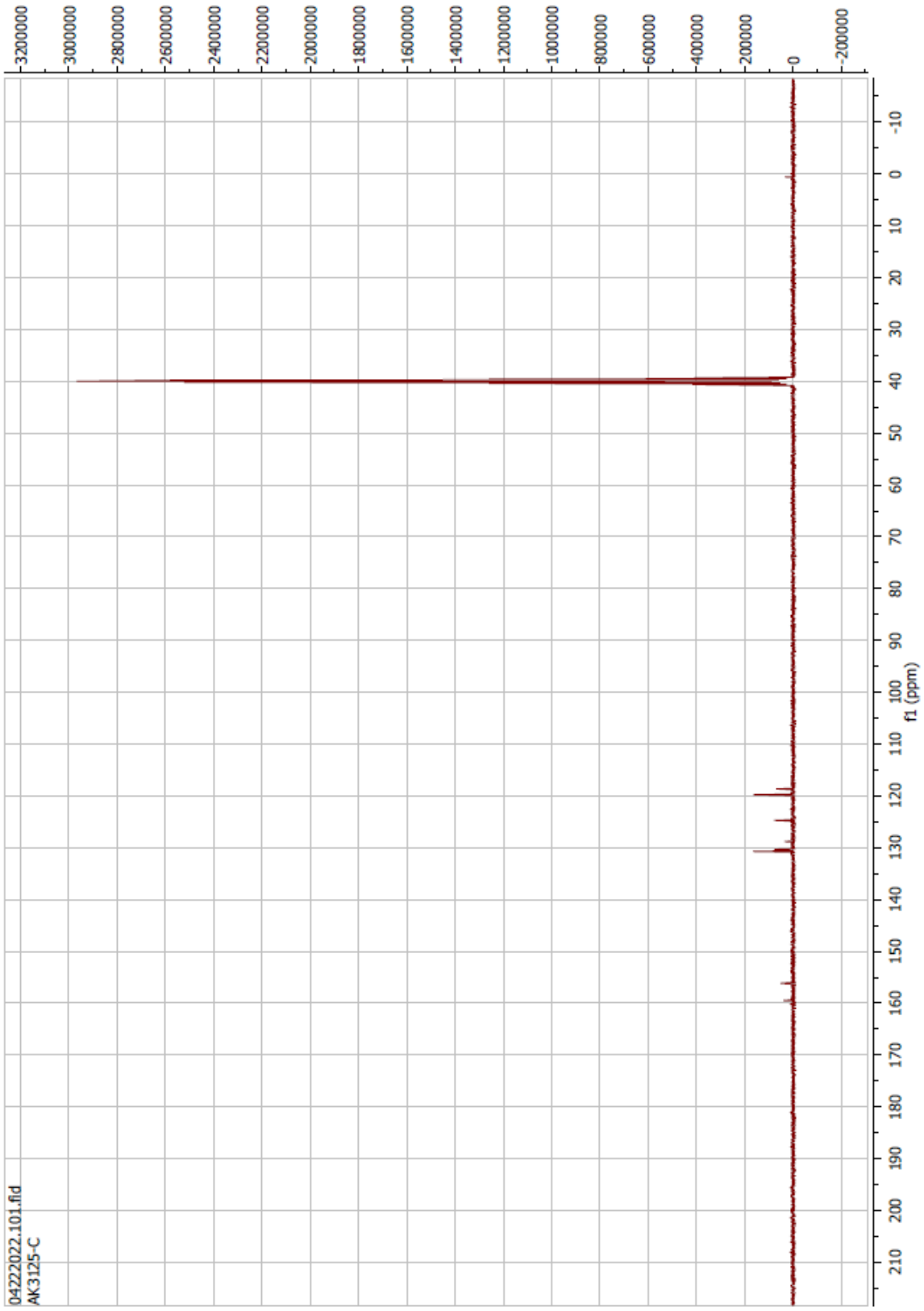

Compound 58 ^{1}H

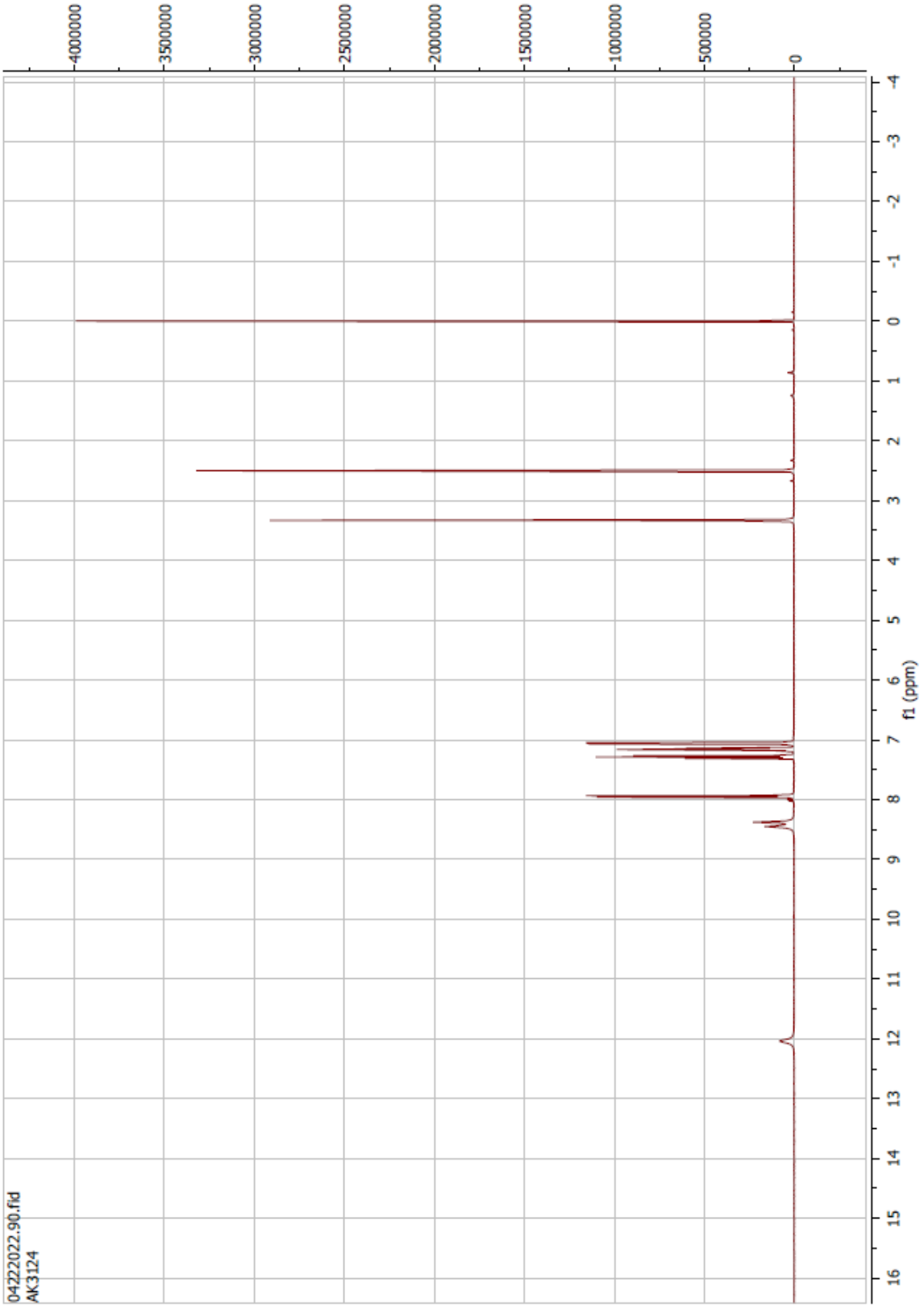

Compound 58 ^{13}C

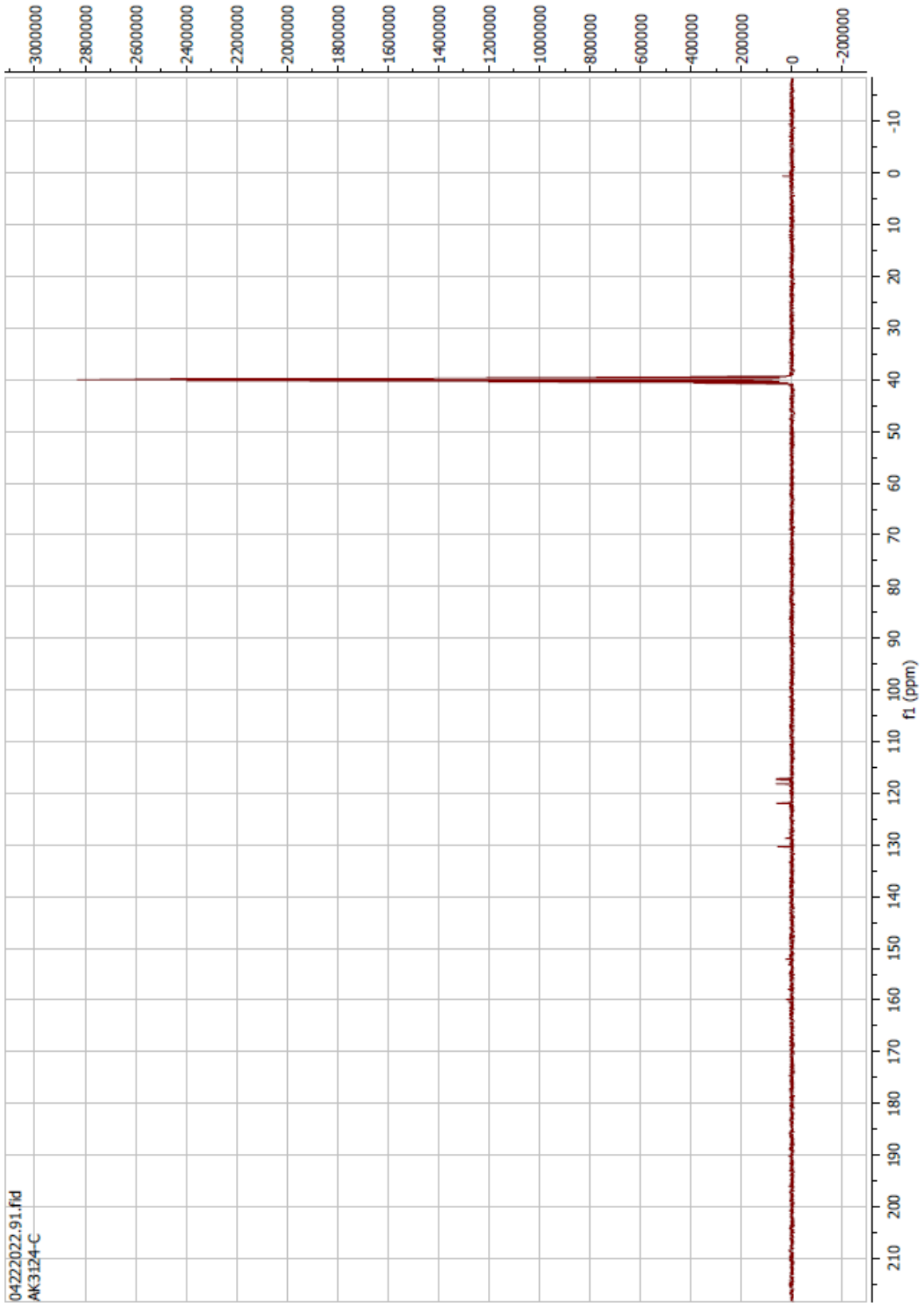

Compound 59 ^{1}H

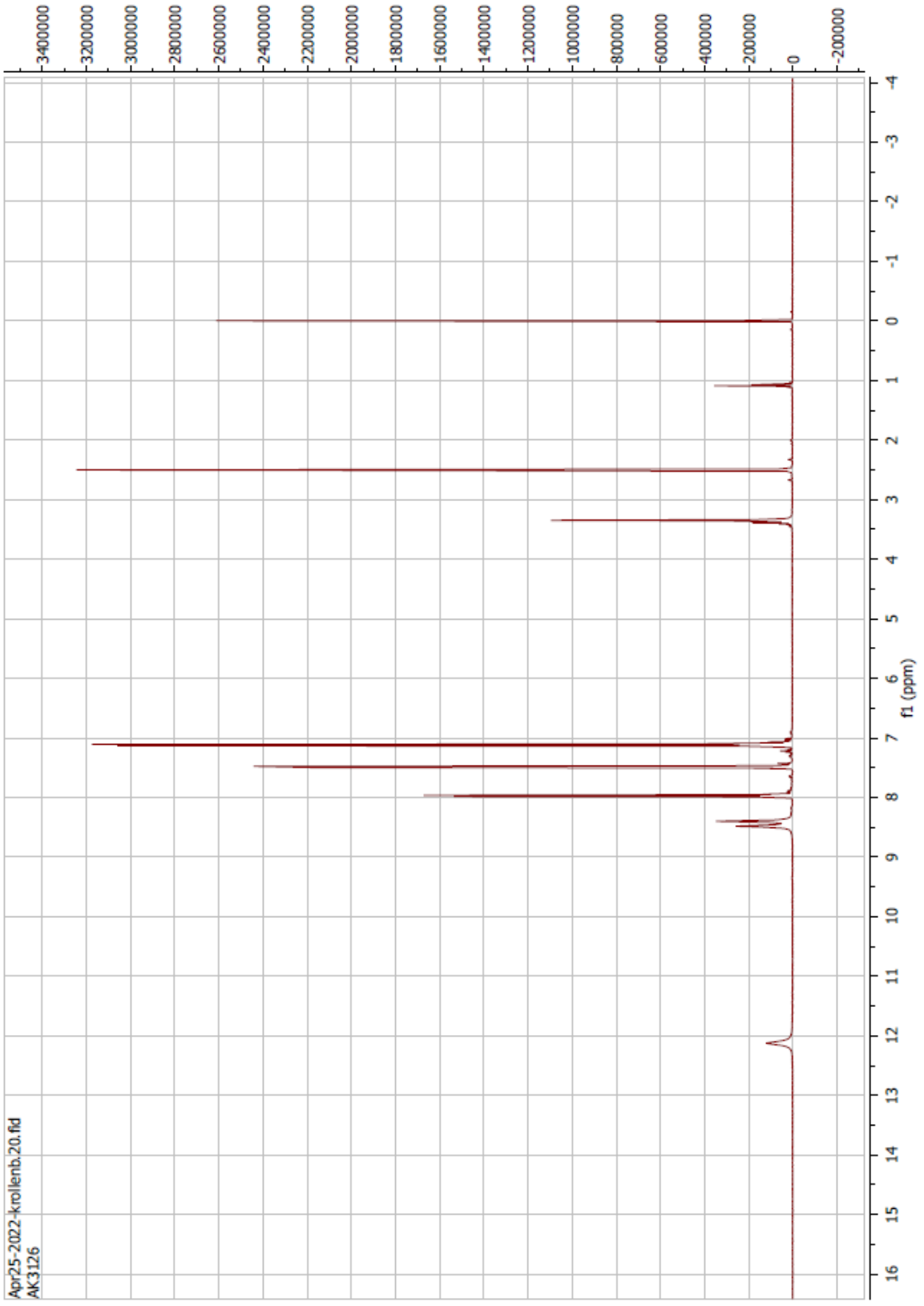

Compound 59 ^{13}C

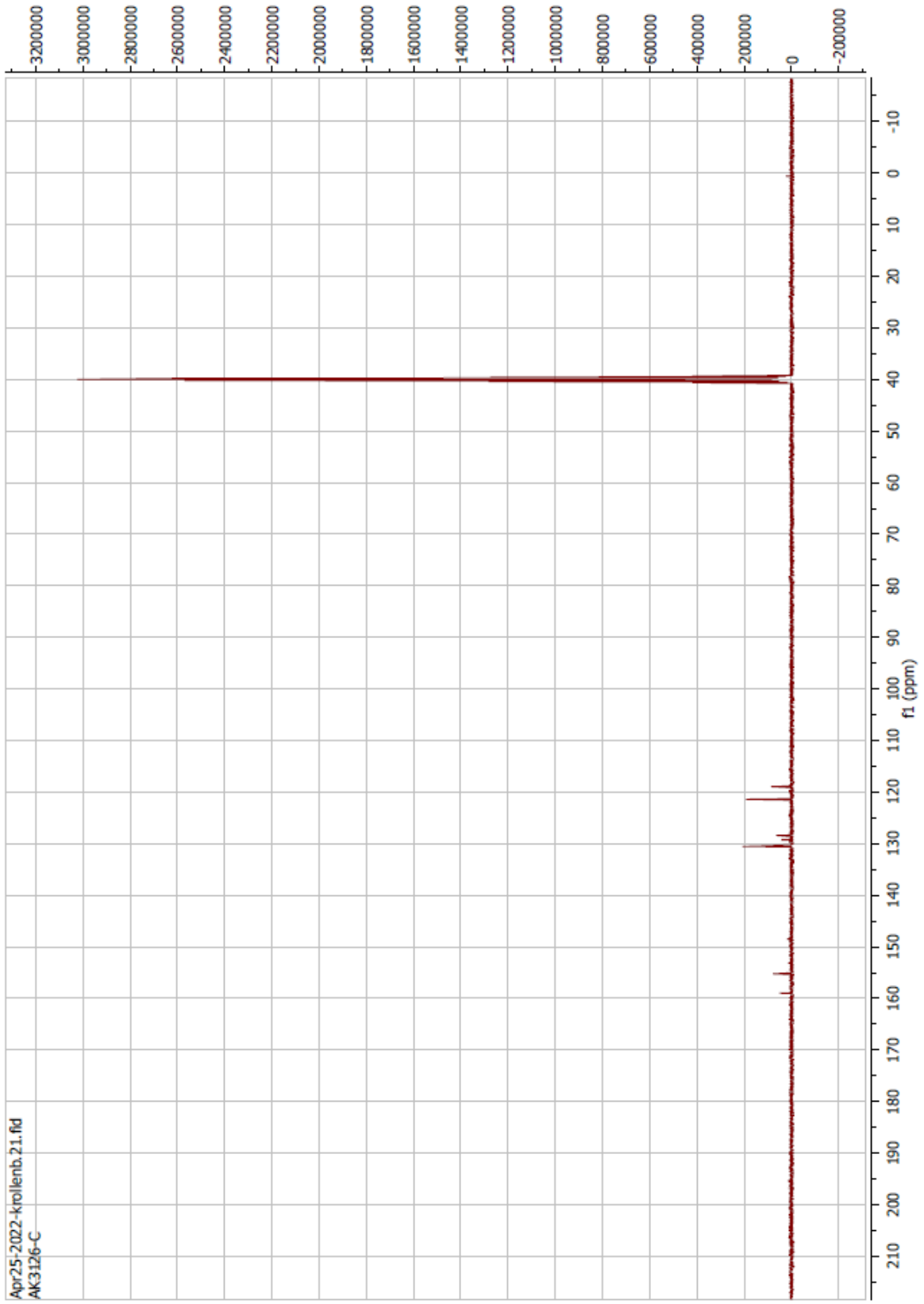

Compound 60 ^{1}H

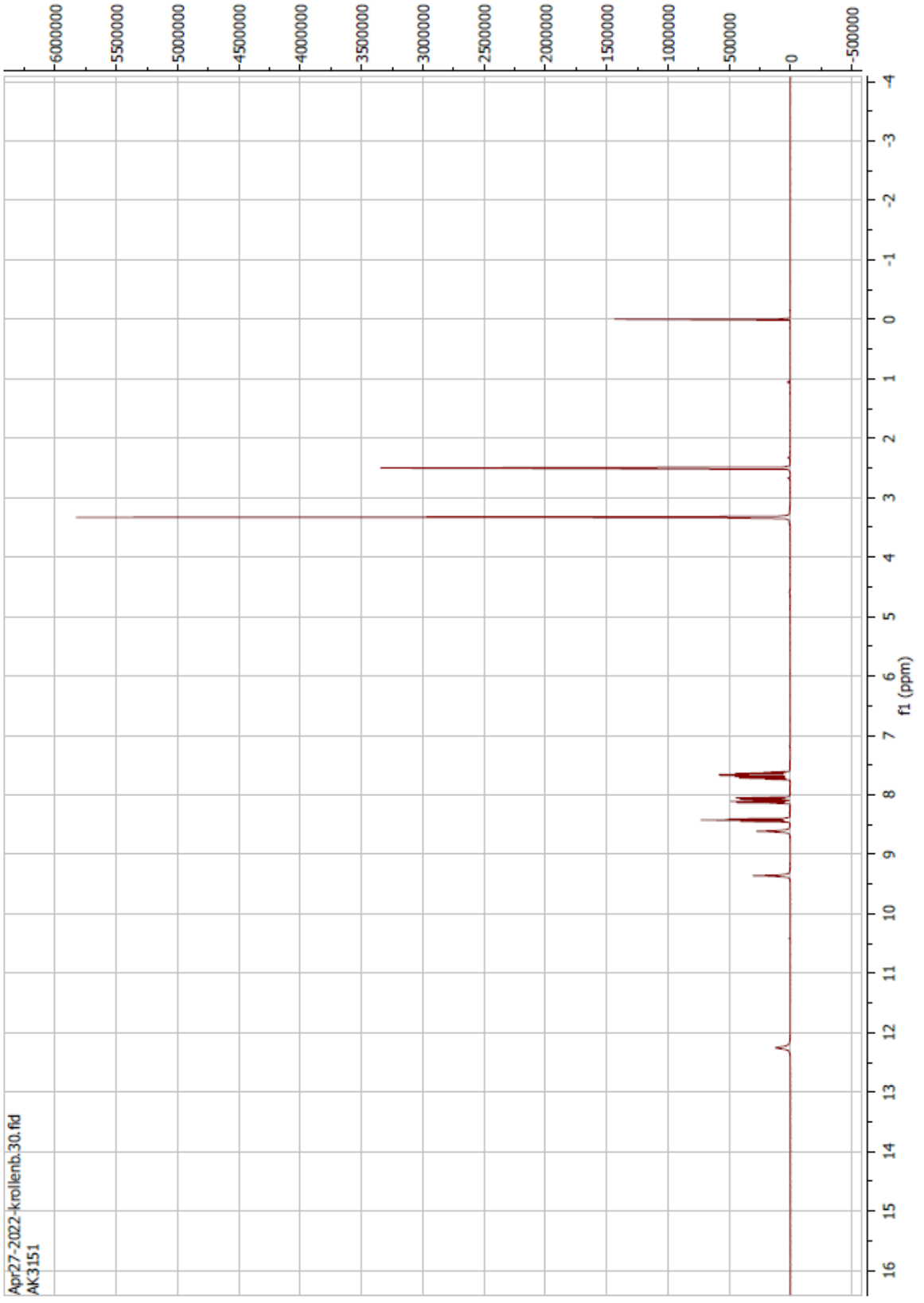

Compound 60 ^{13}C

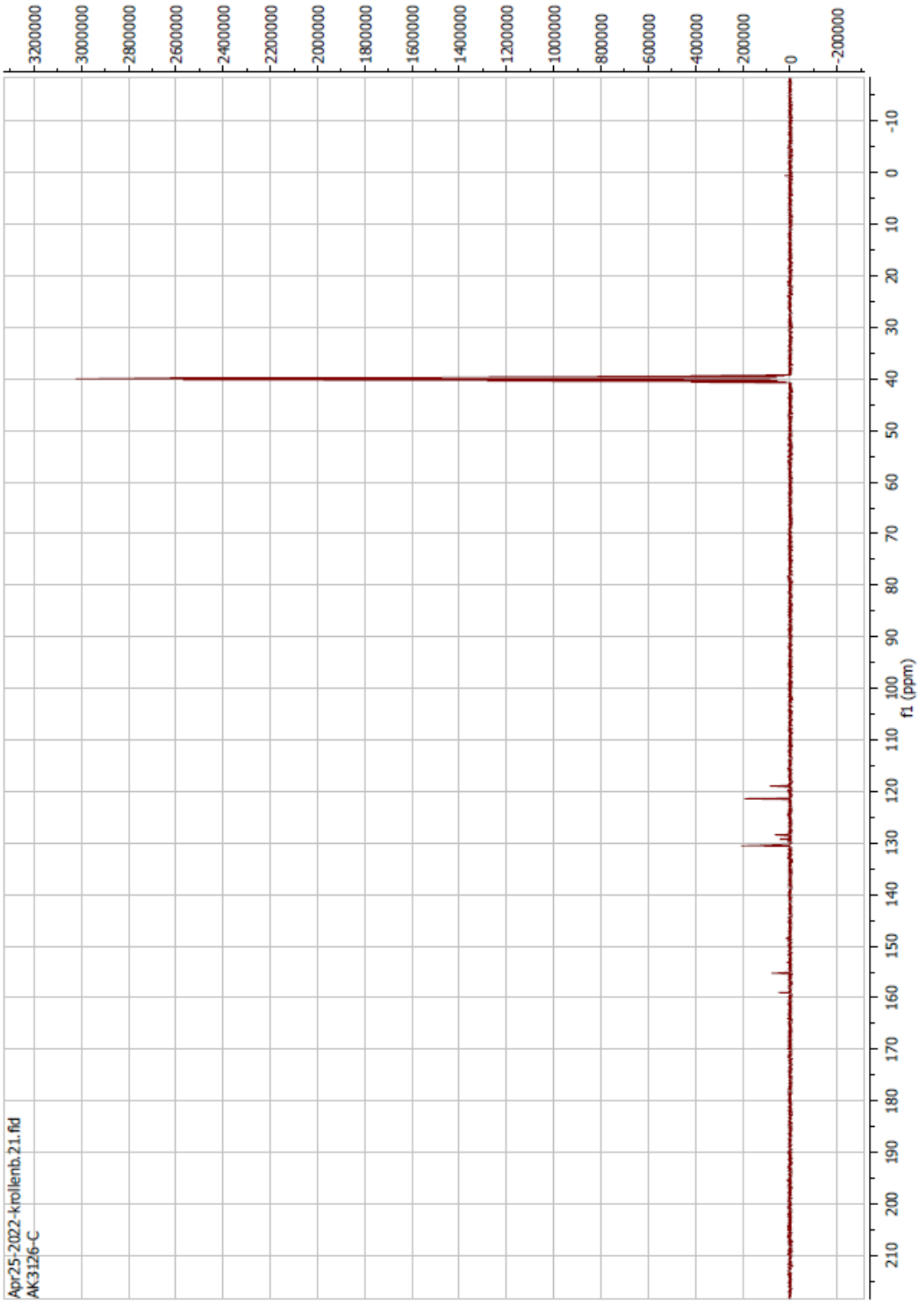

Compound 61 ^{1}H

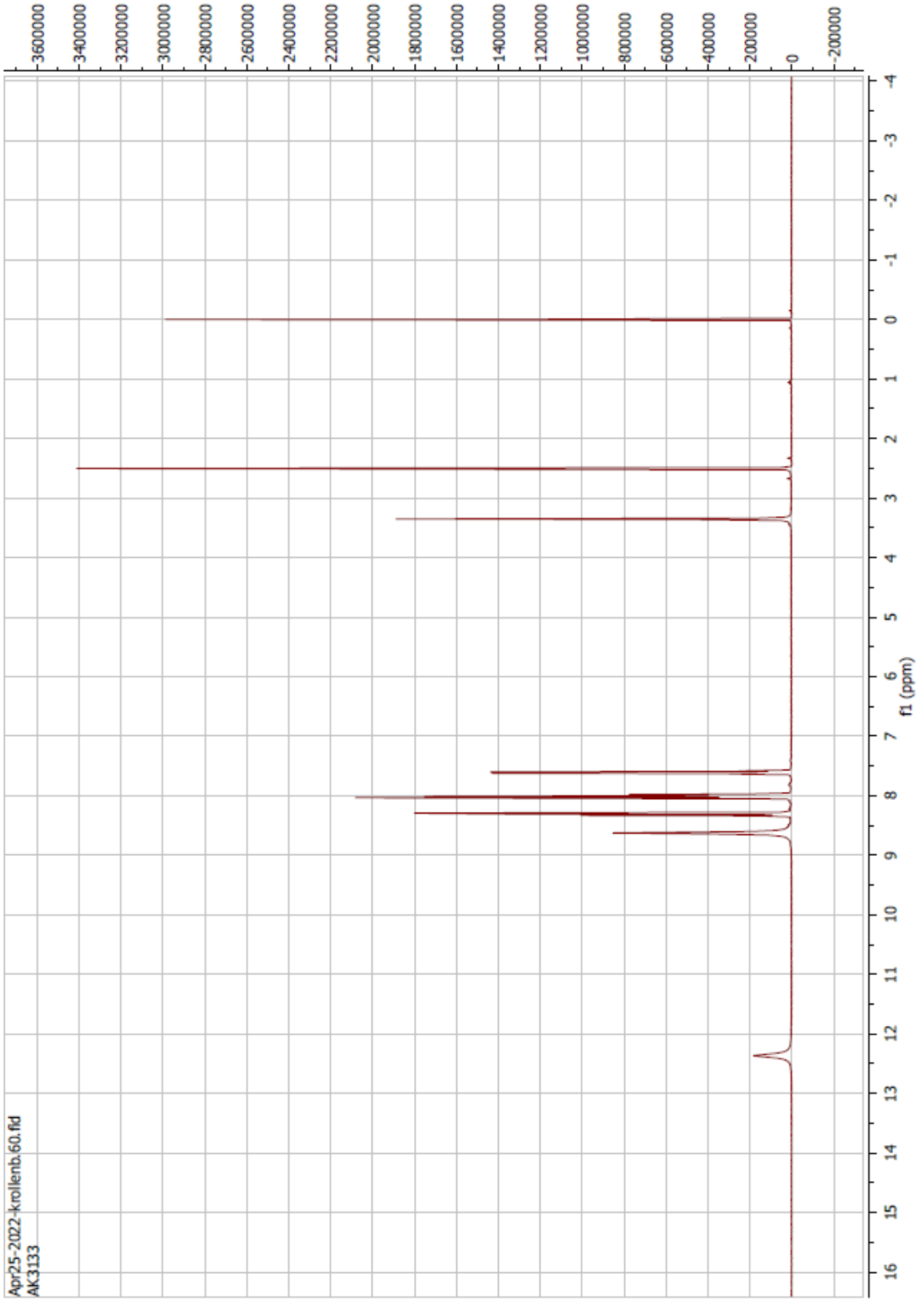

Compound 61 ^{13}C

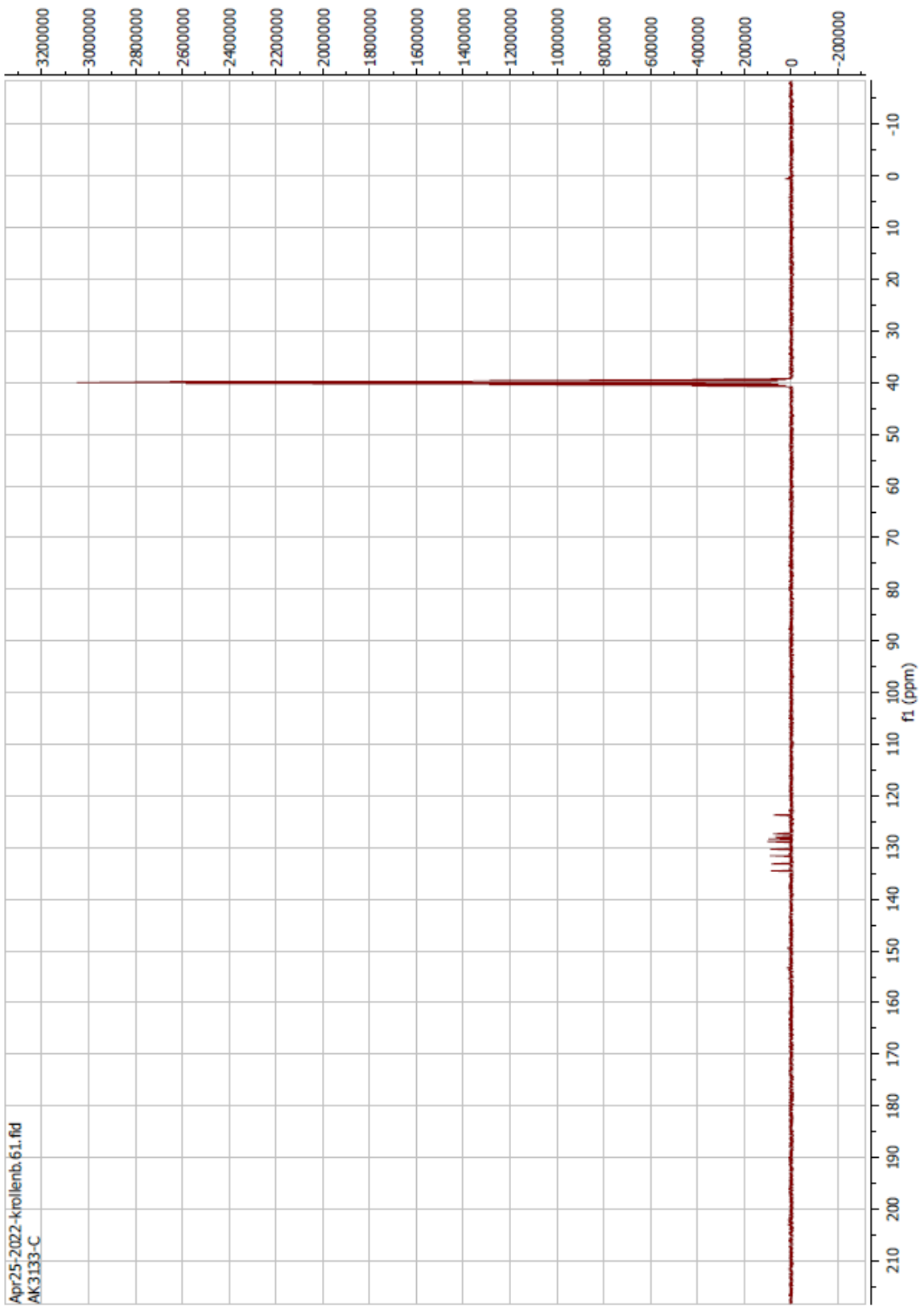

Compound 62 ^{1}H

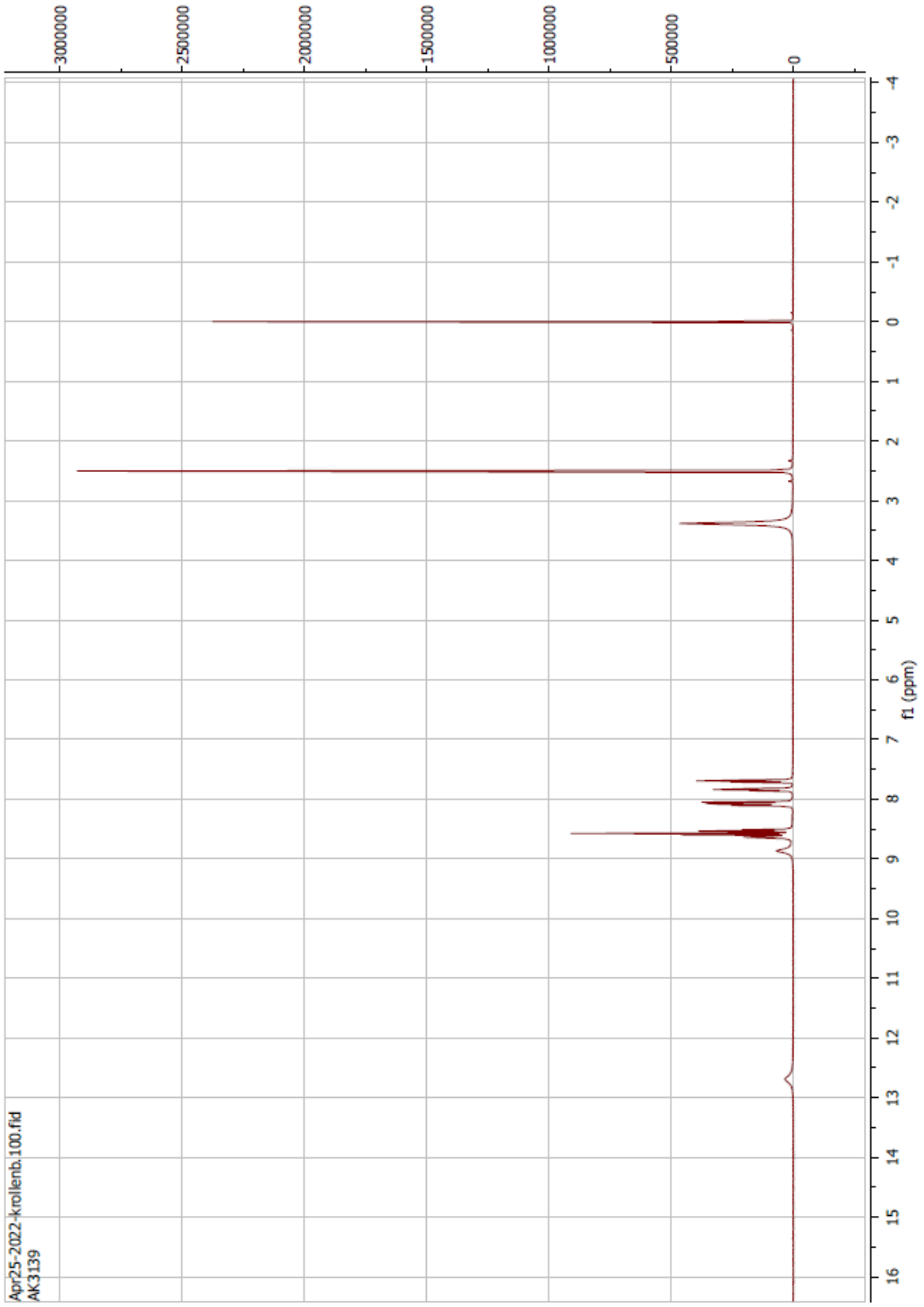

Compound 62 ^{13}C

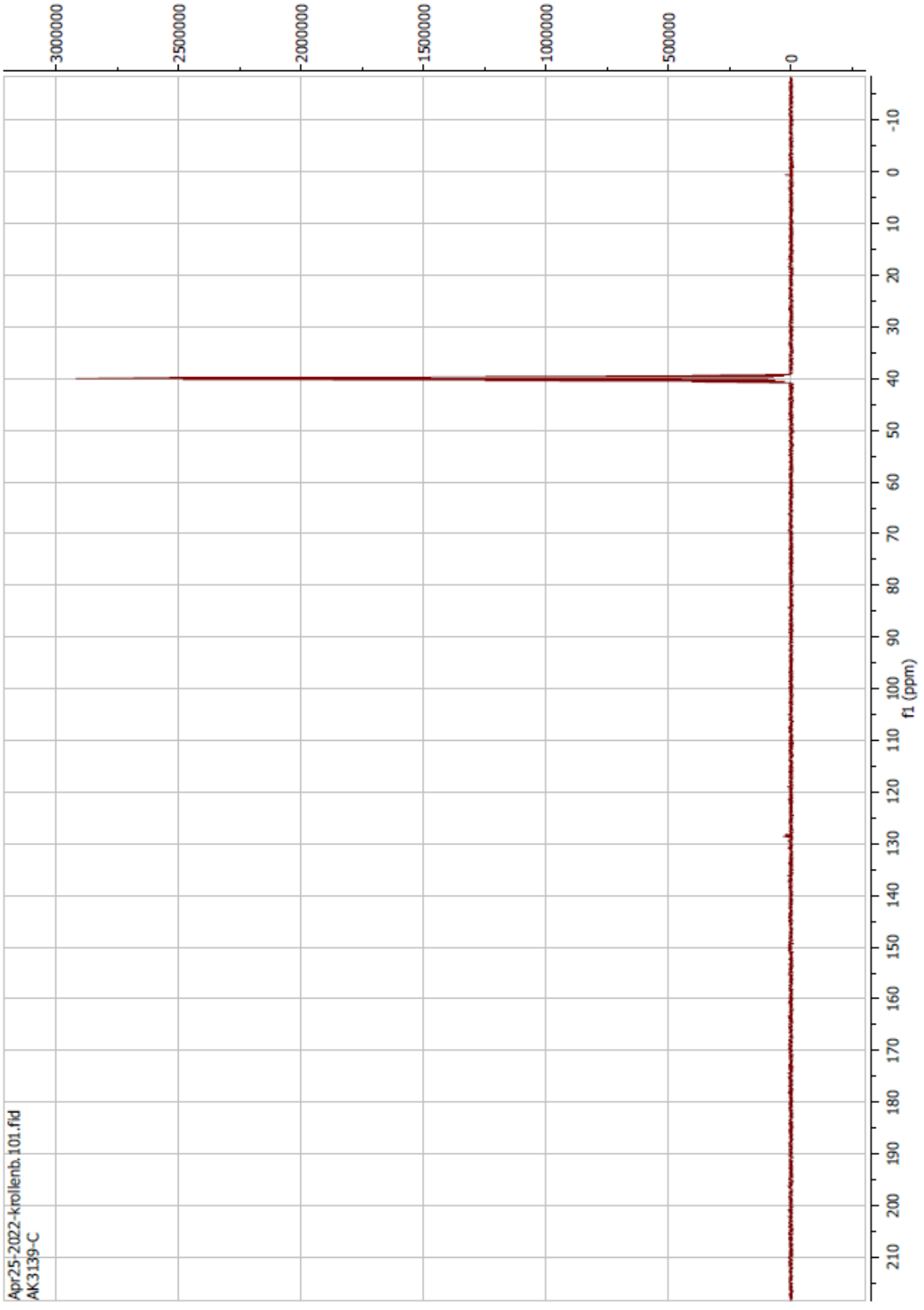

Compound 63 ^{1}H

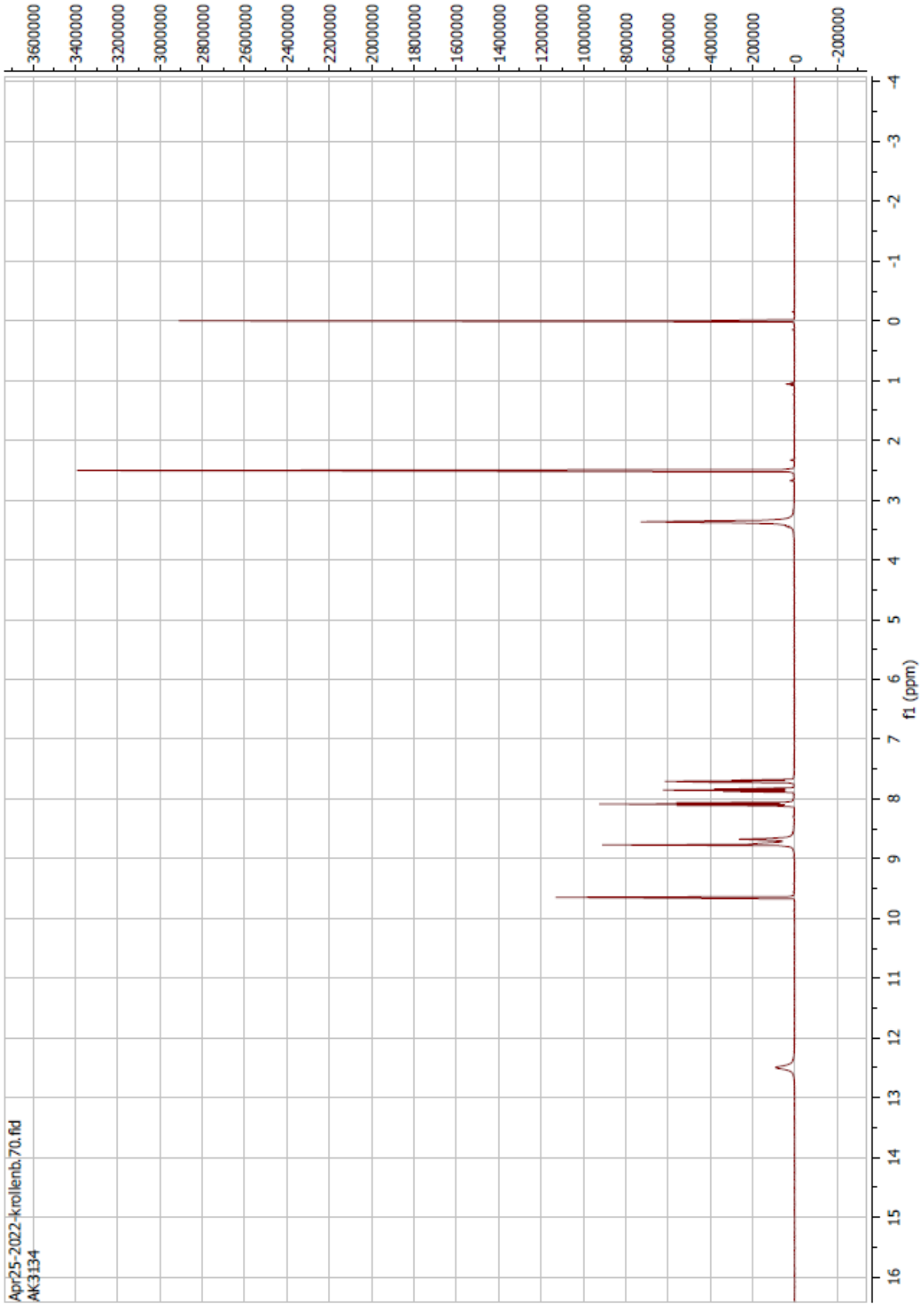

Compound 63 ^{13}C

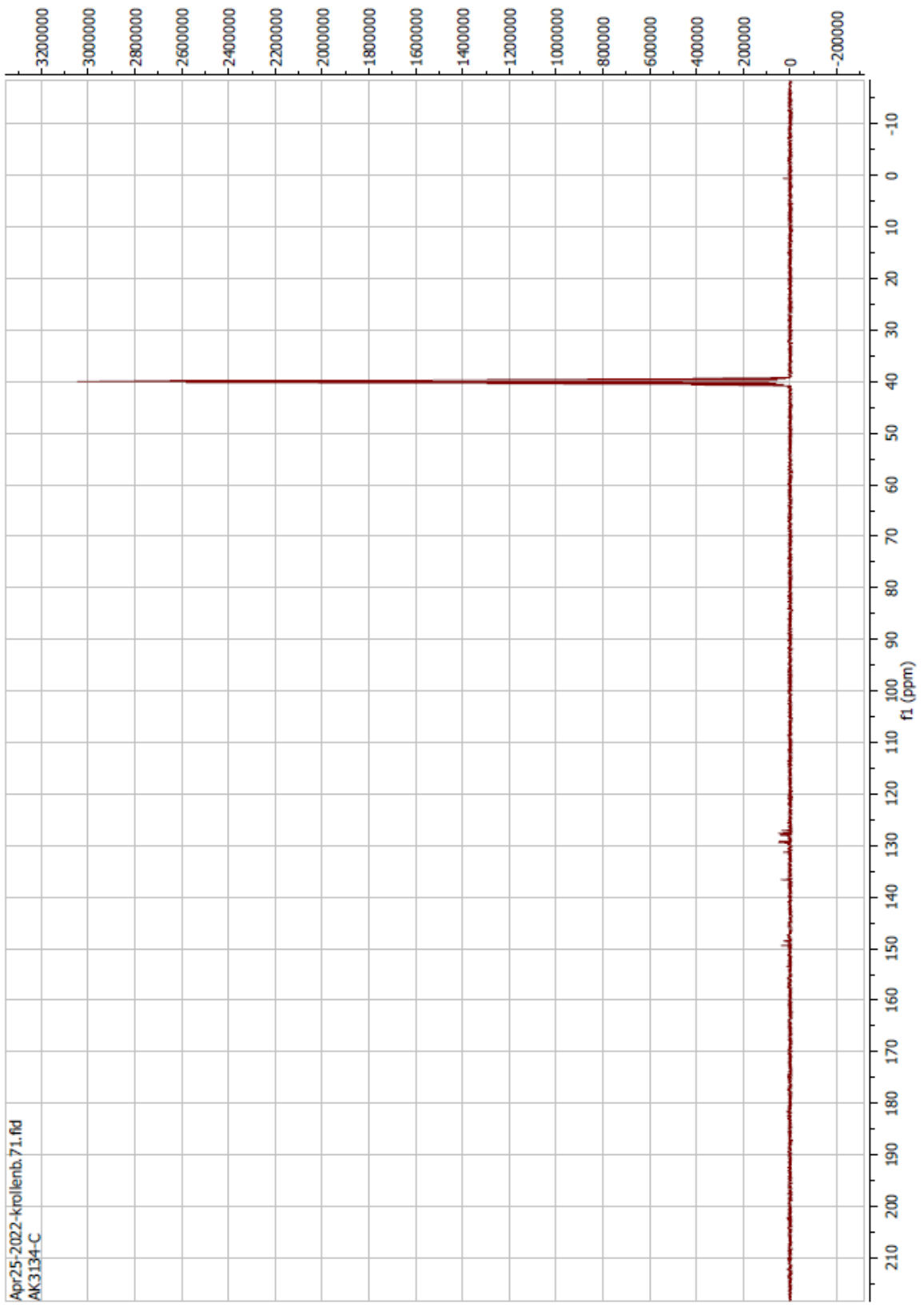

Compound 64 ^{1}H

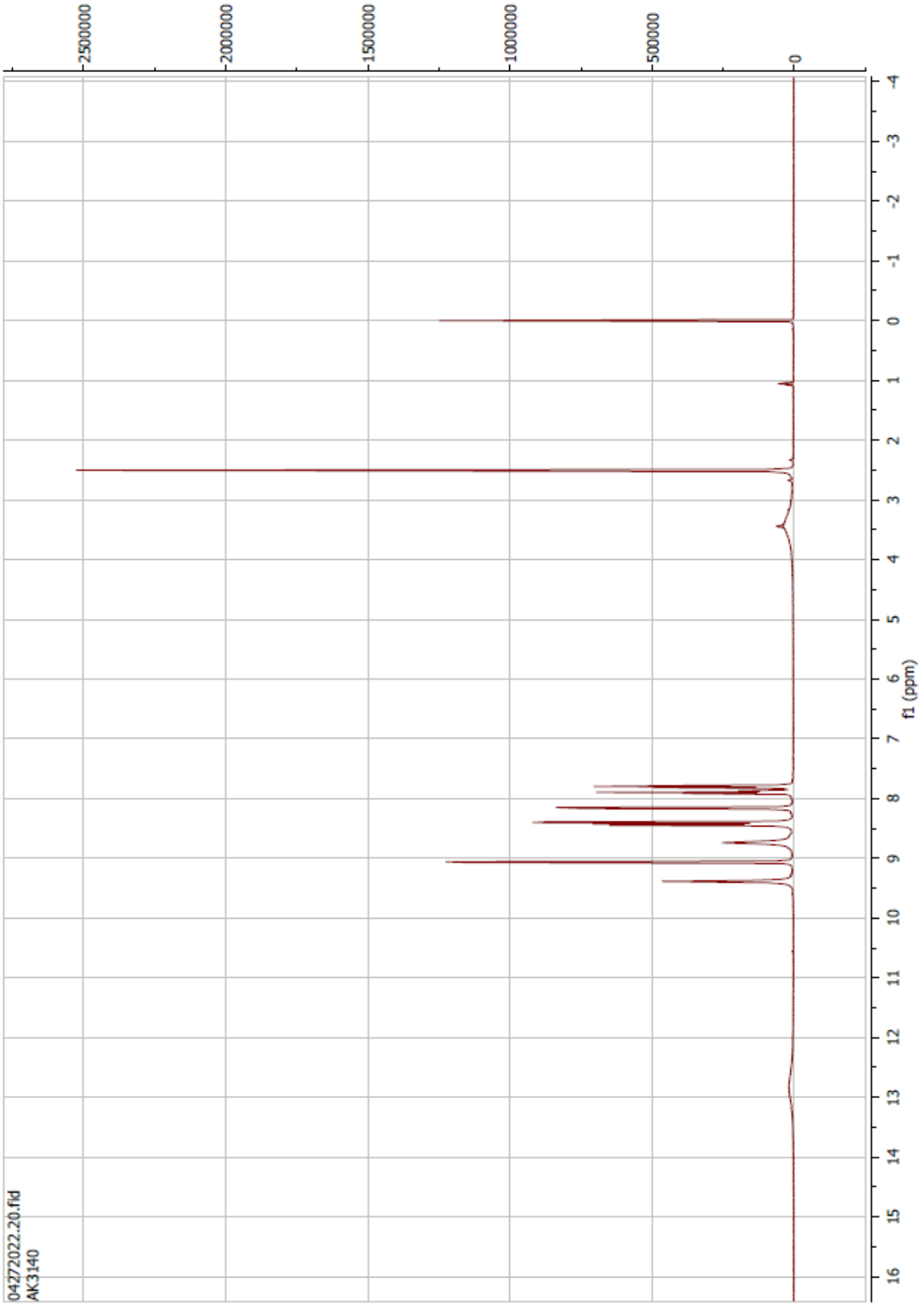

Compound 64 ^{13}C

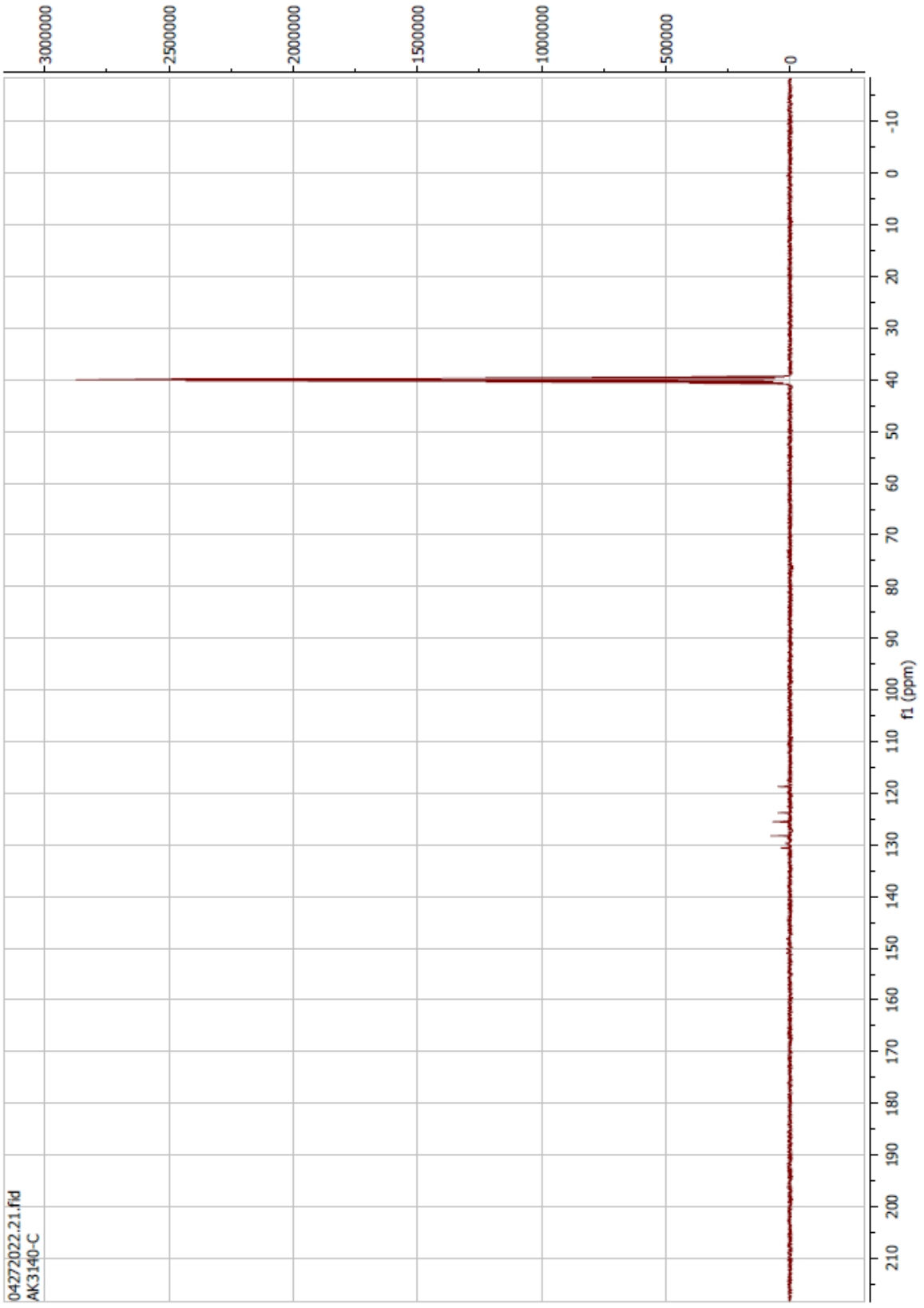

Compound 65 ^{1}H

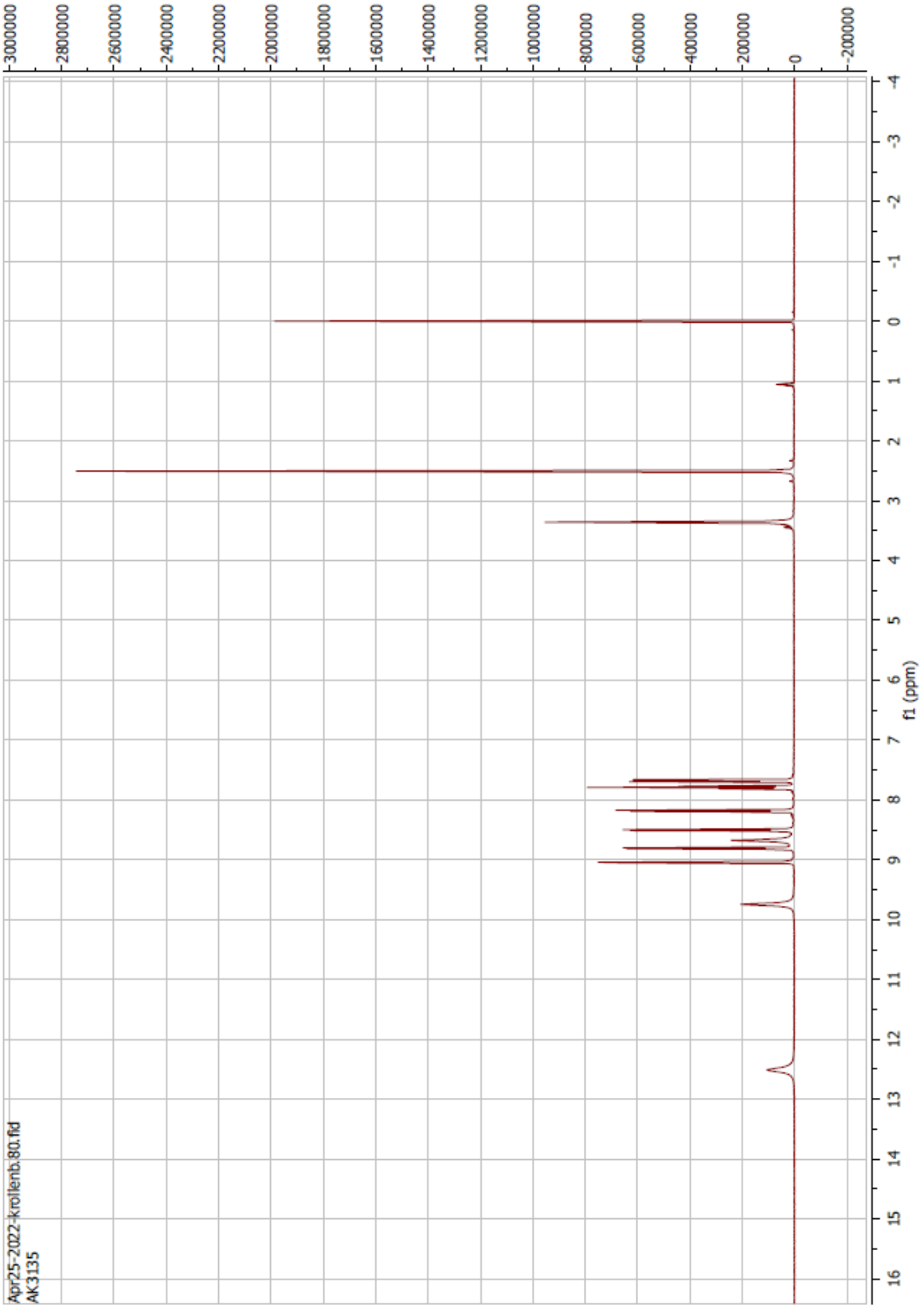

Compound 65 ^{13}C

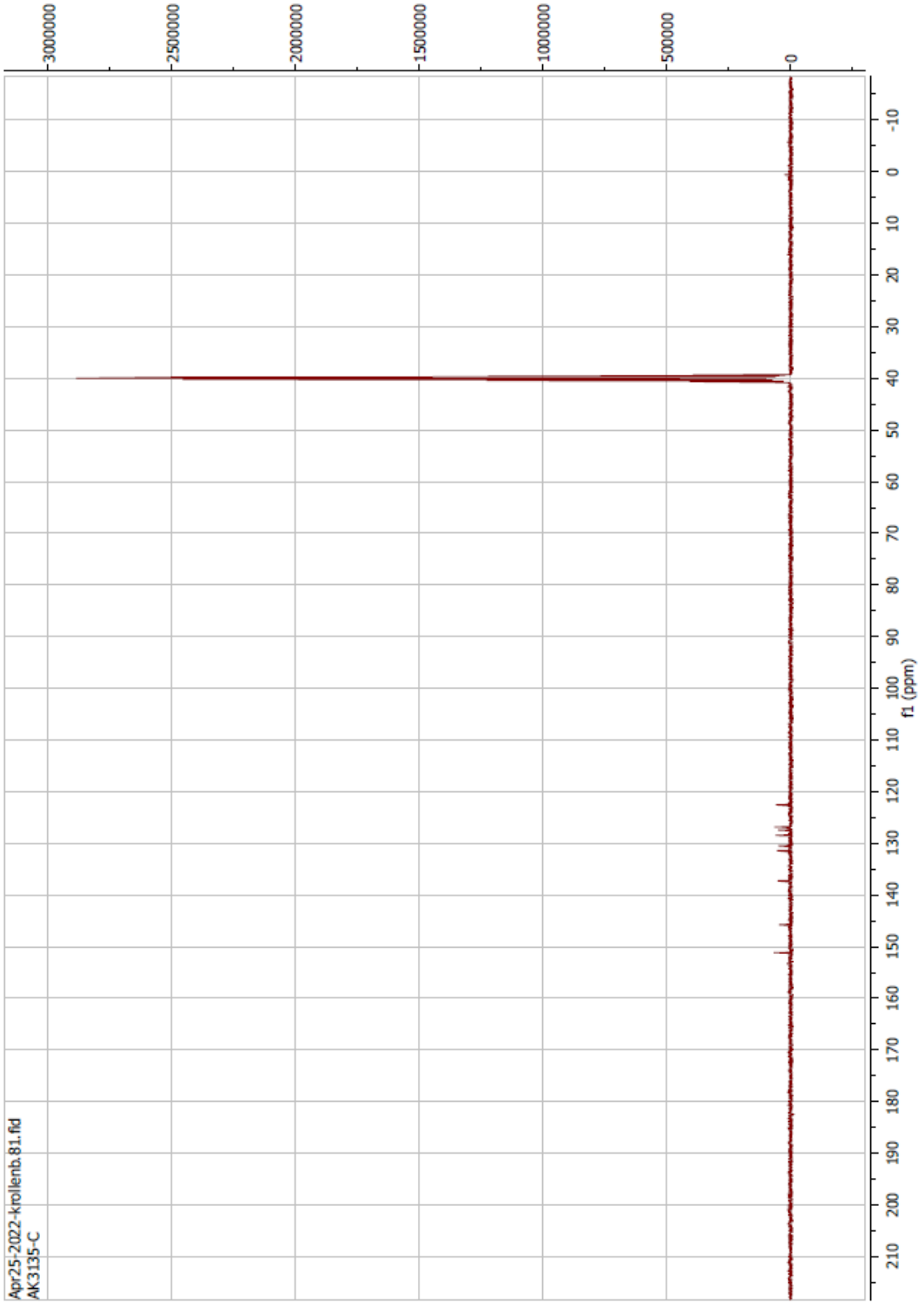

Compound 66 ^{1}H

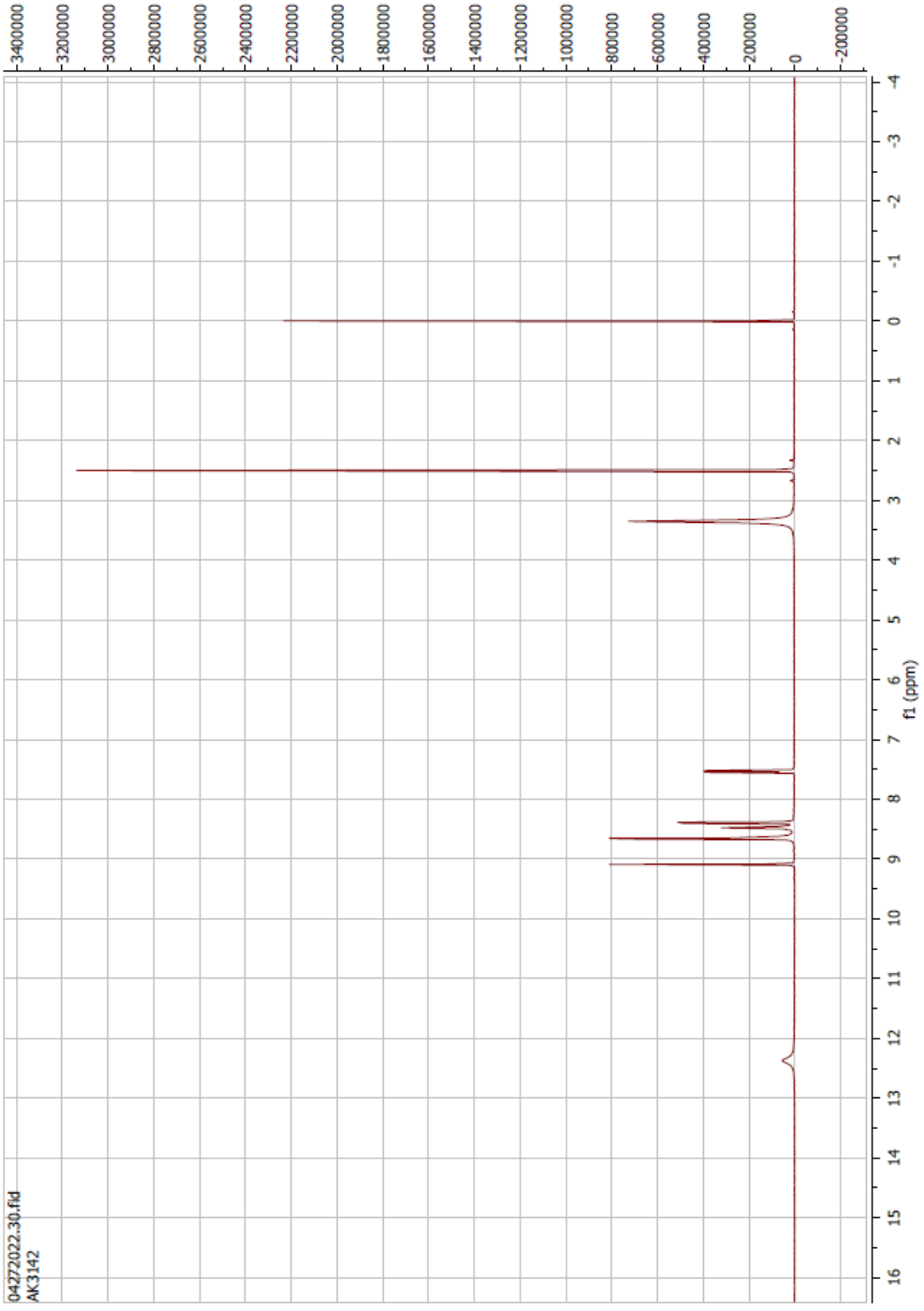

Compound 66 ^{13}C

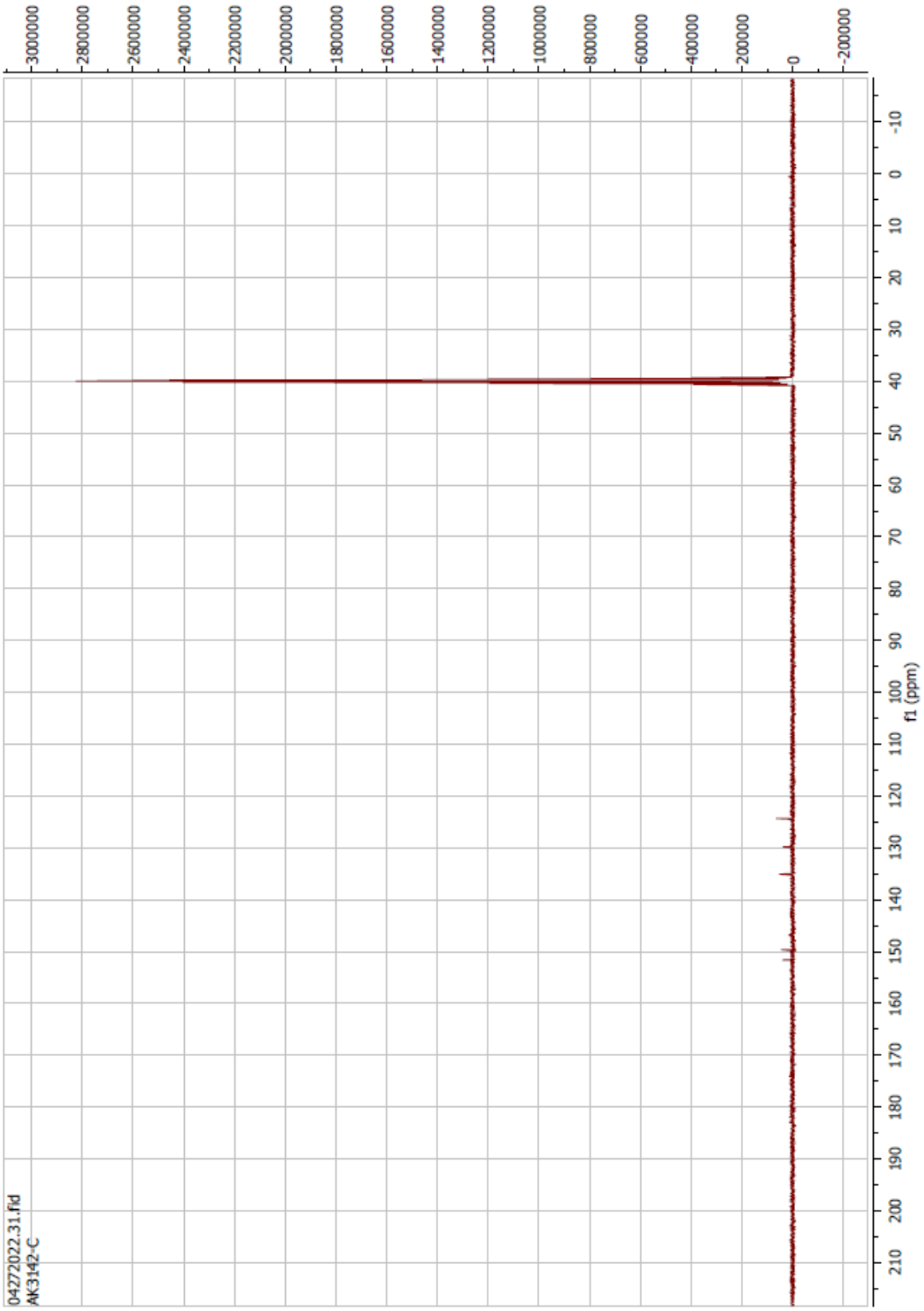

Compound 67 ^{1}H

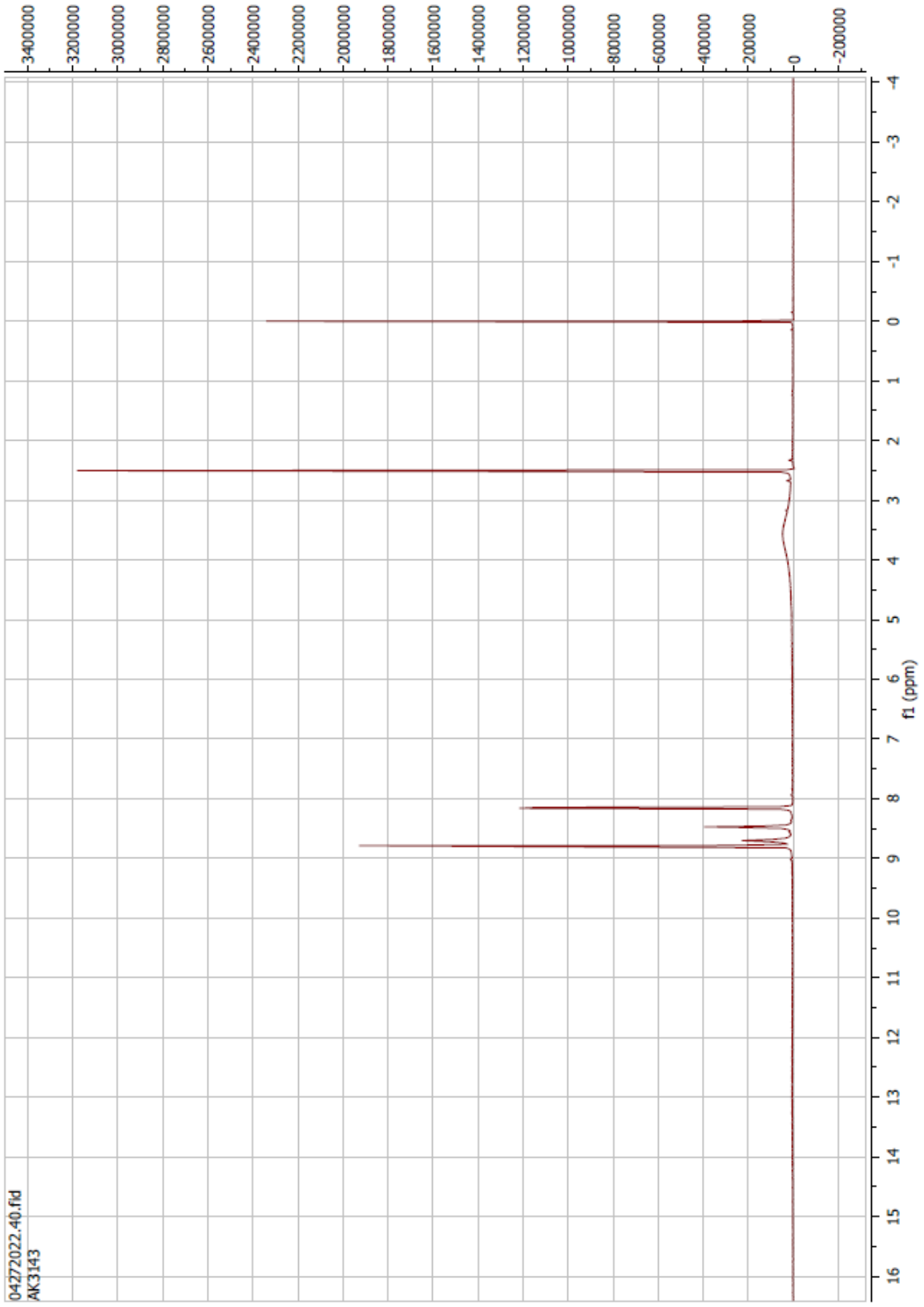

Compound 67 ^{13}C

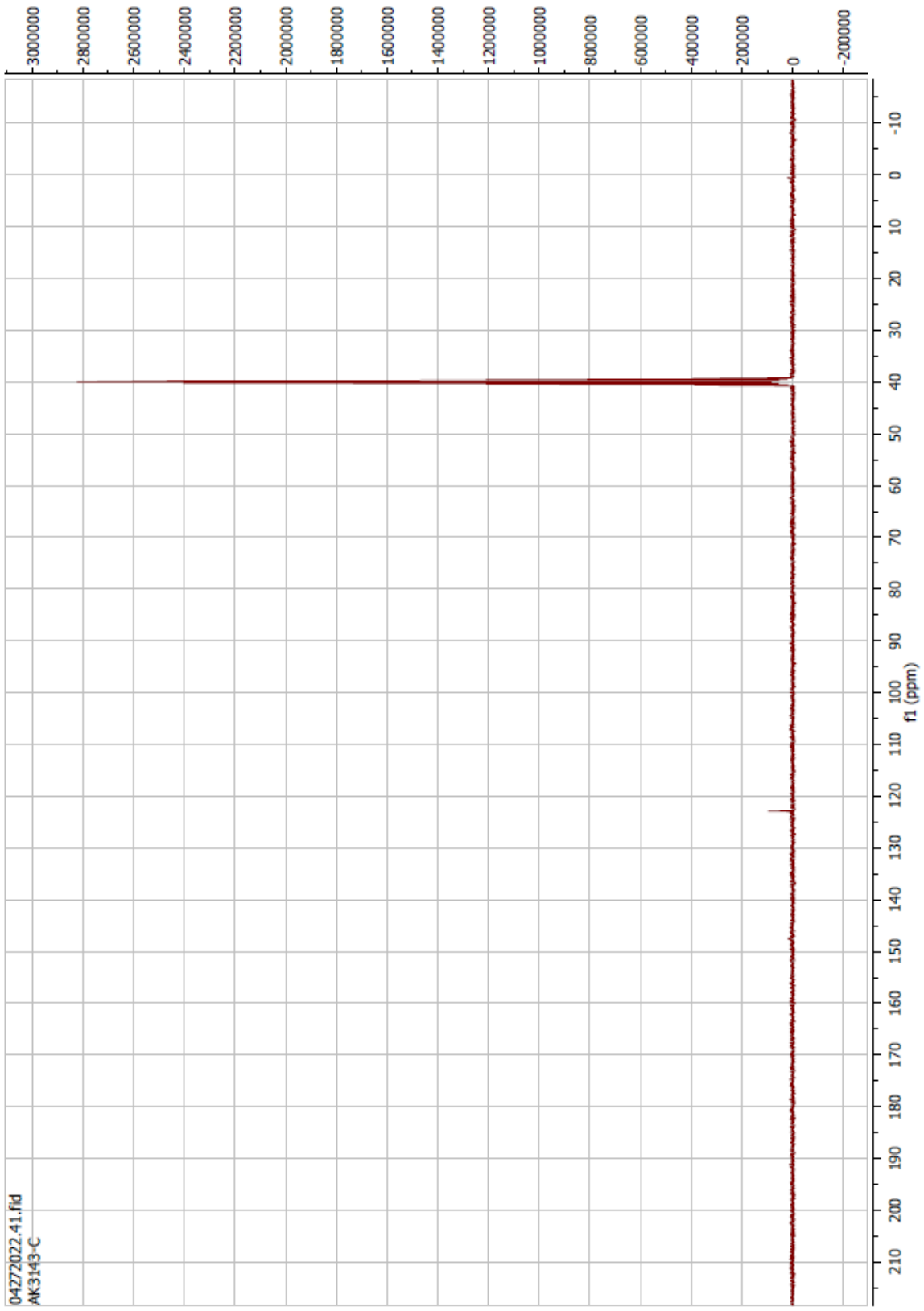

Compound 68 ^{1}H

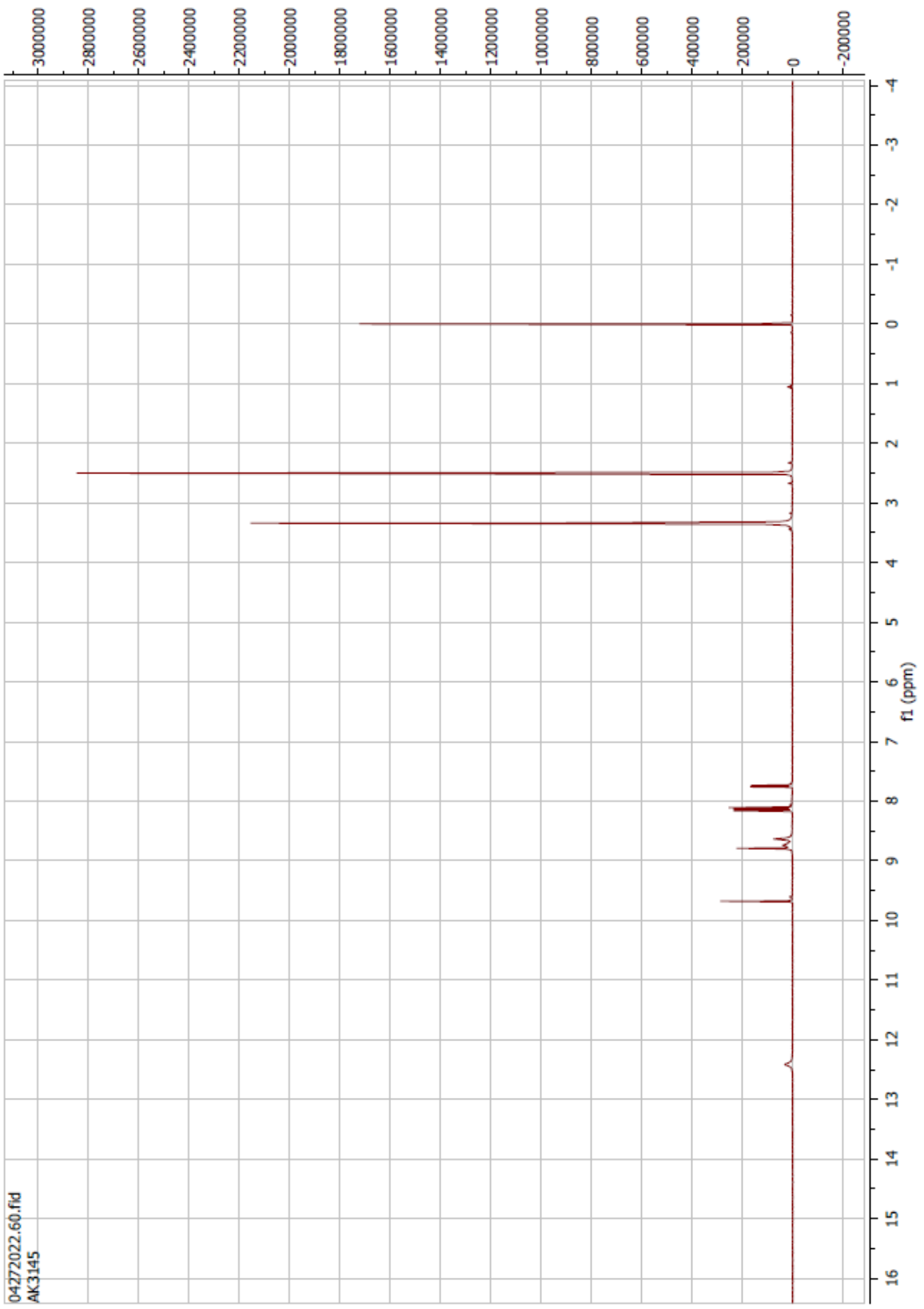

Compound 68 ^{13}C

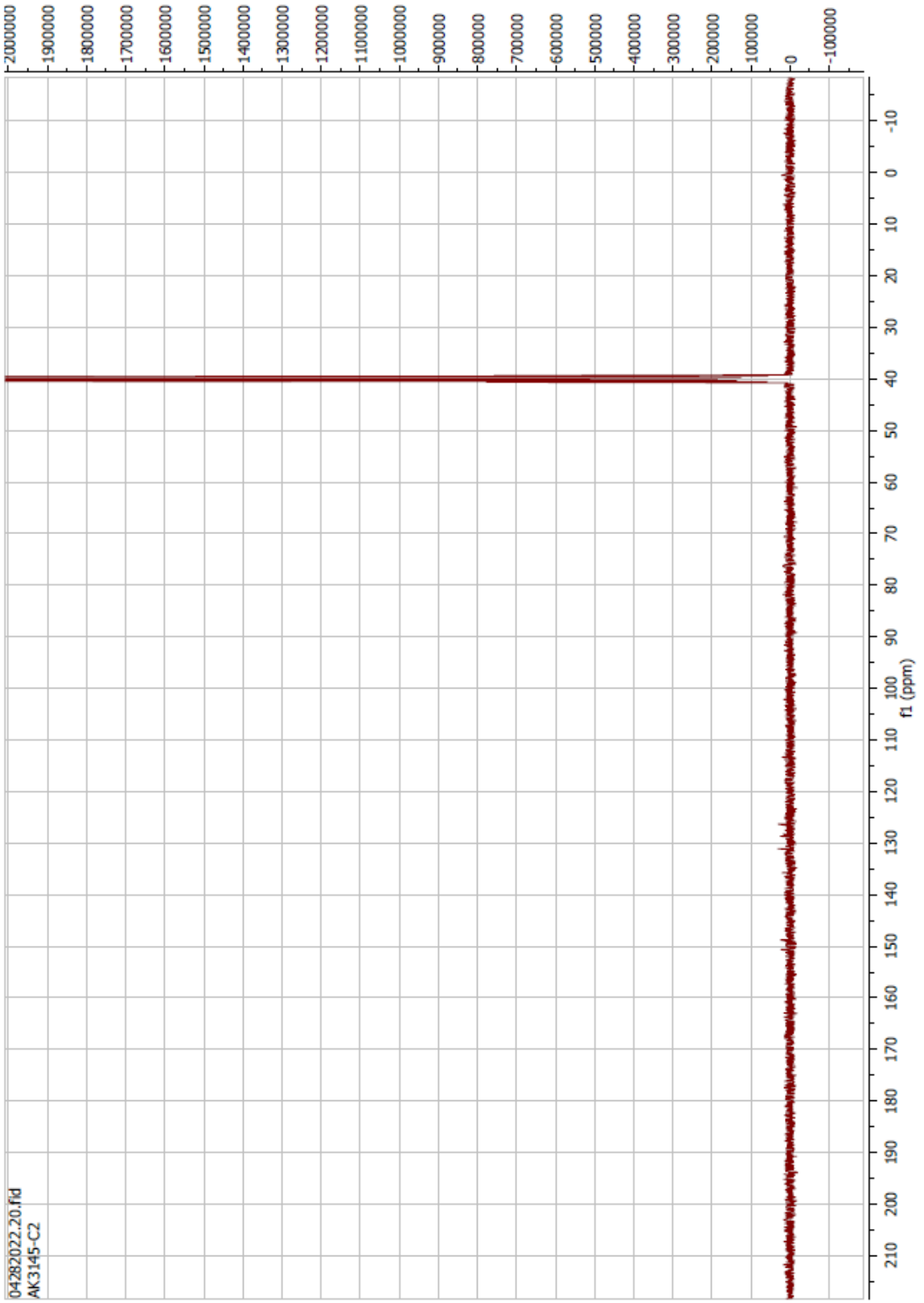

Compound 69 ^{1}H

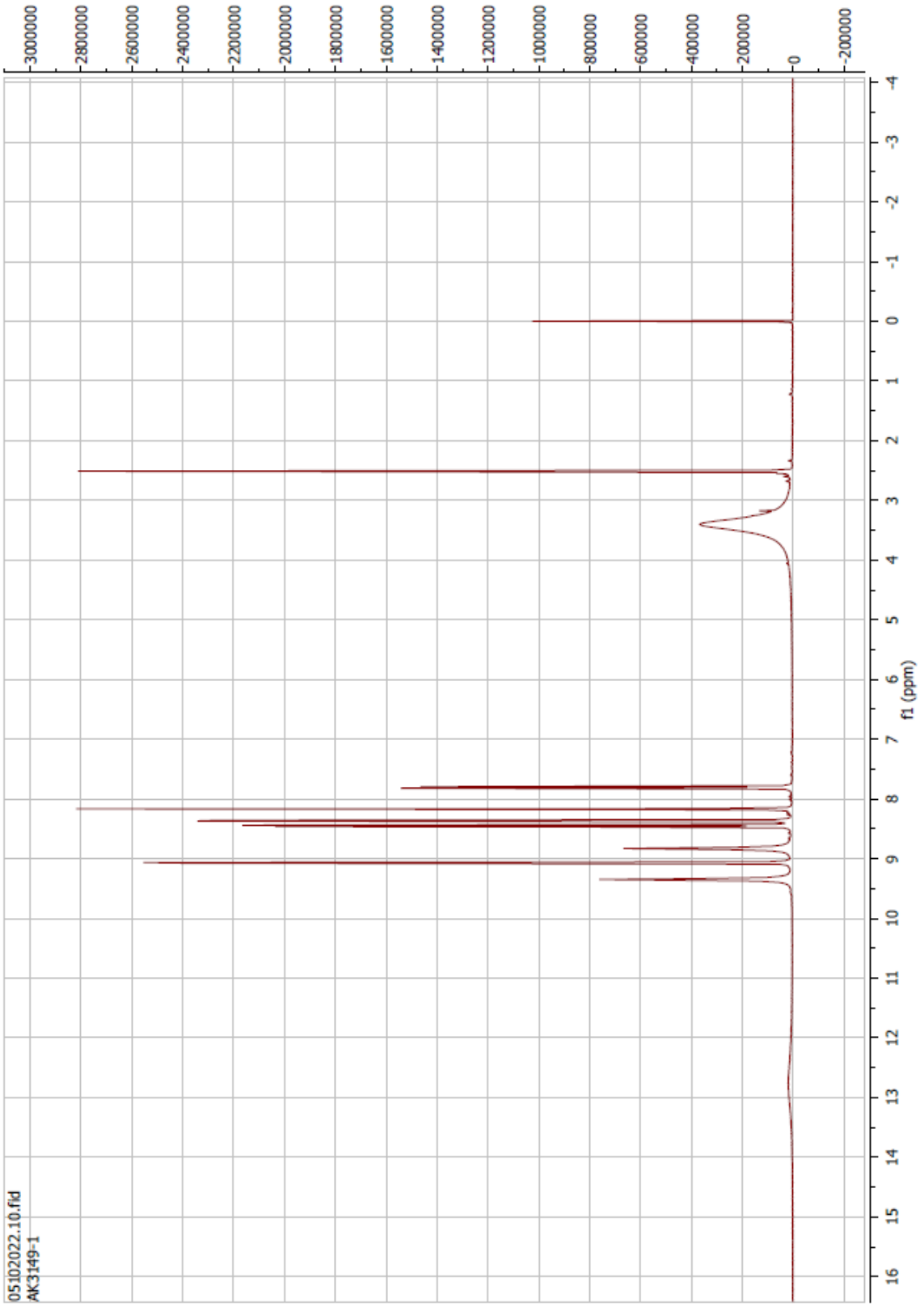

Compound 69 ^{13}C

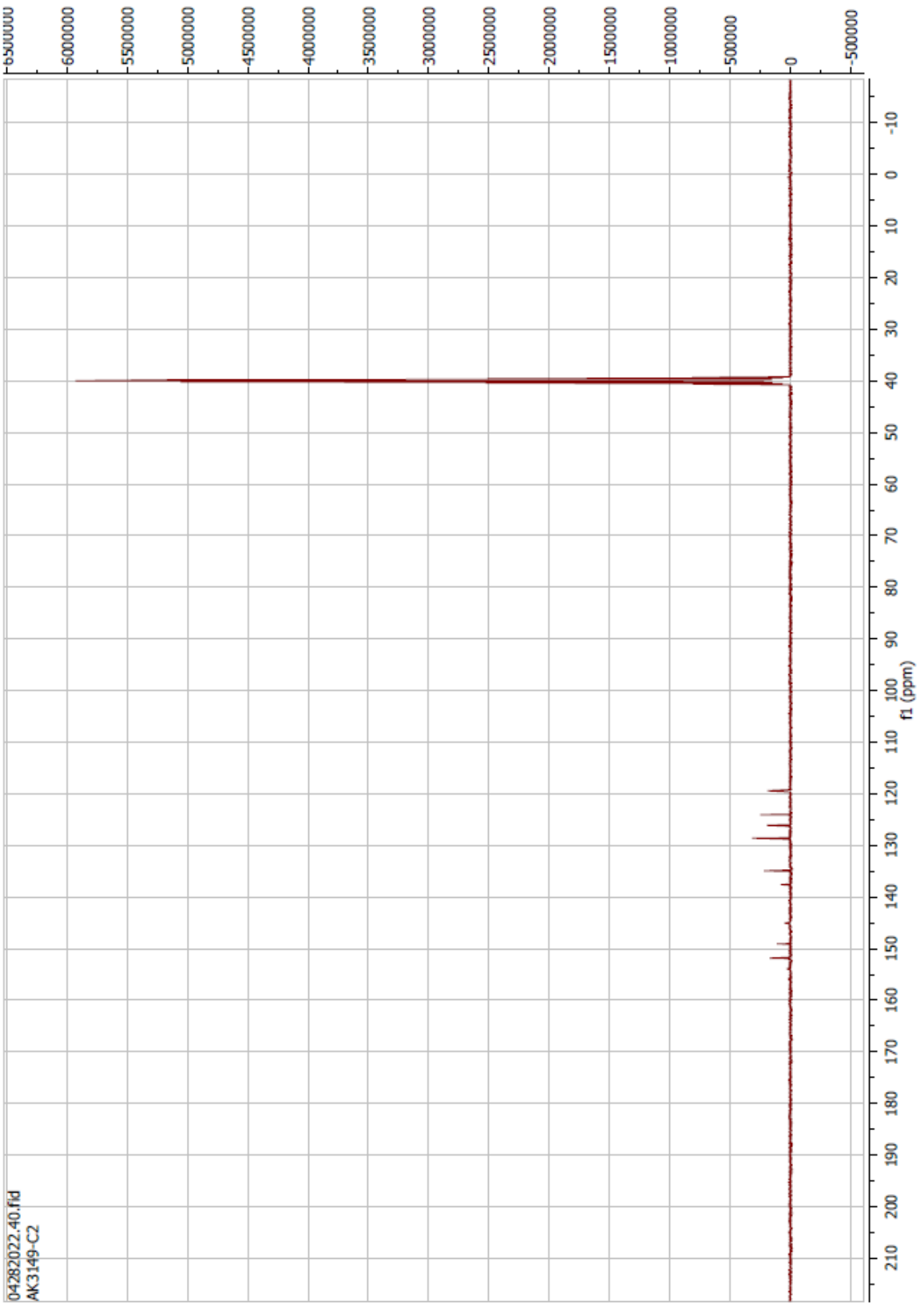

Compound 70 ^{1}H

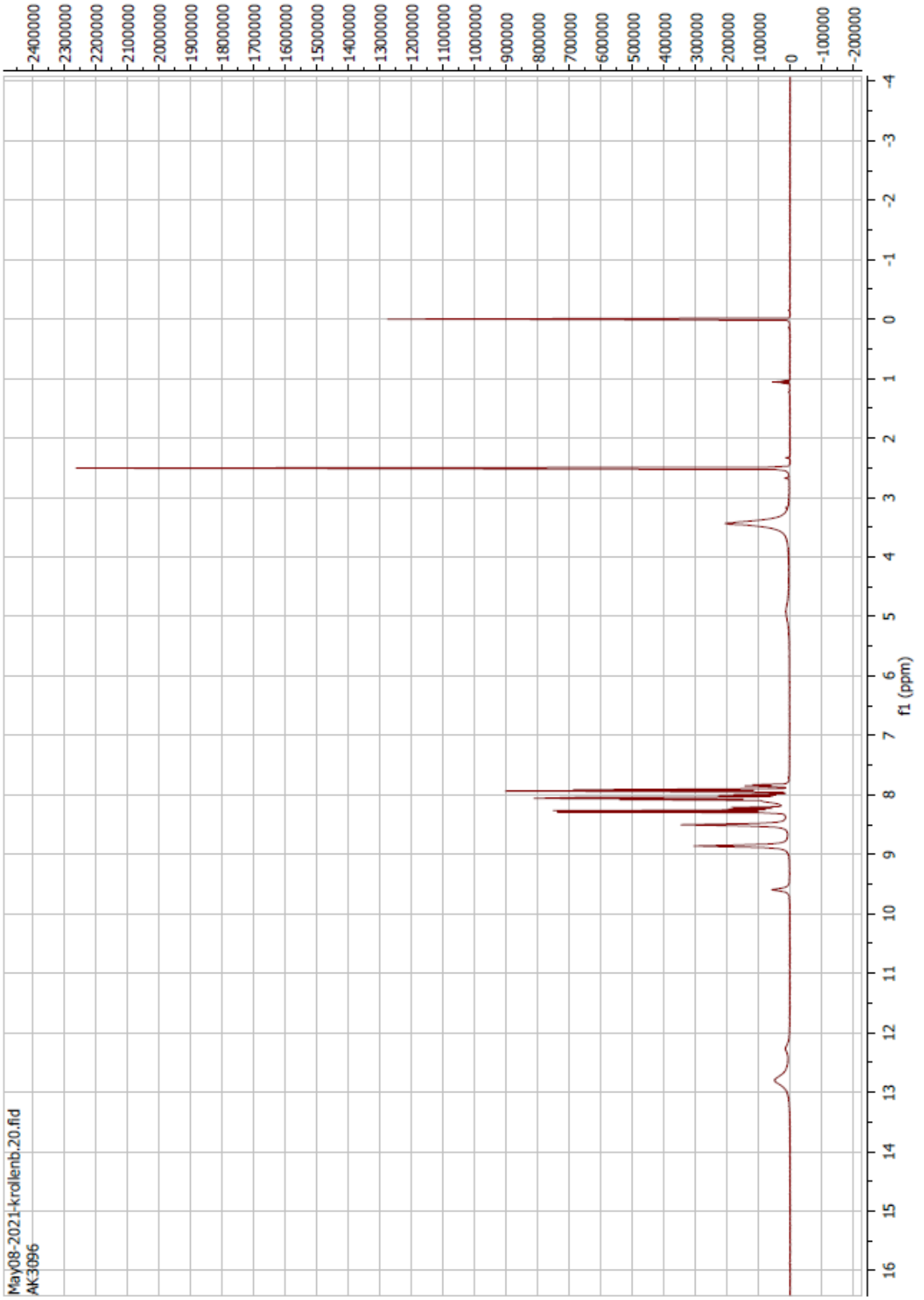

Compound 70 ^{13}C

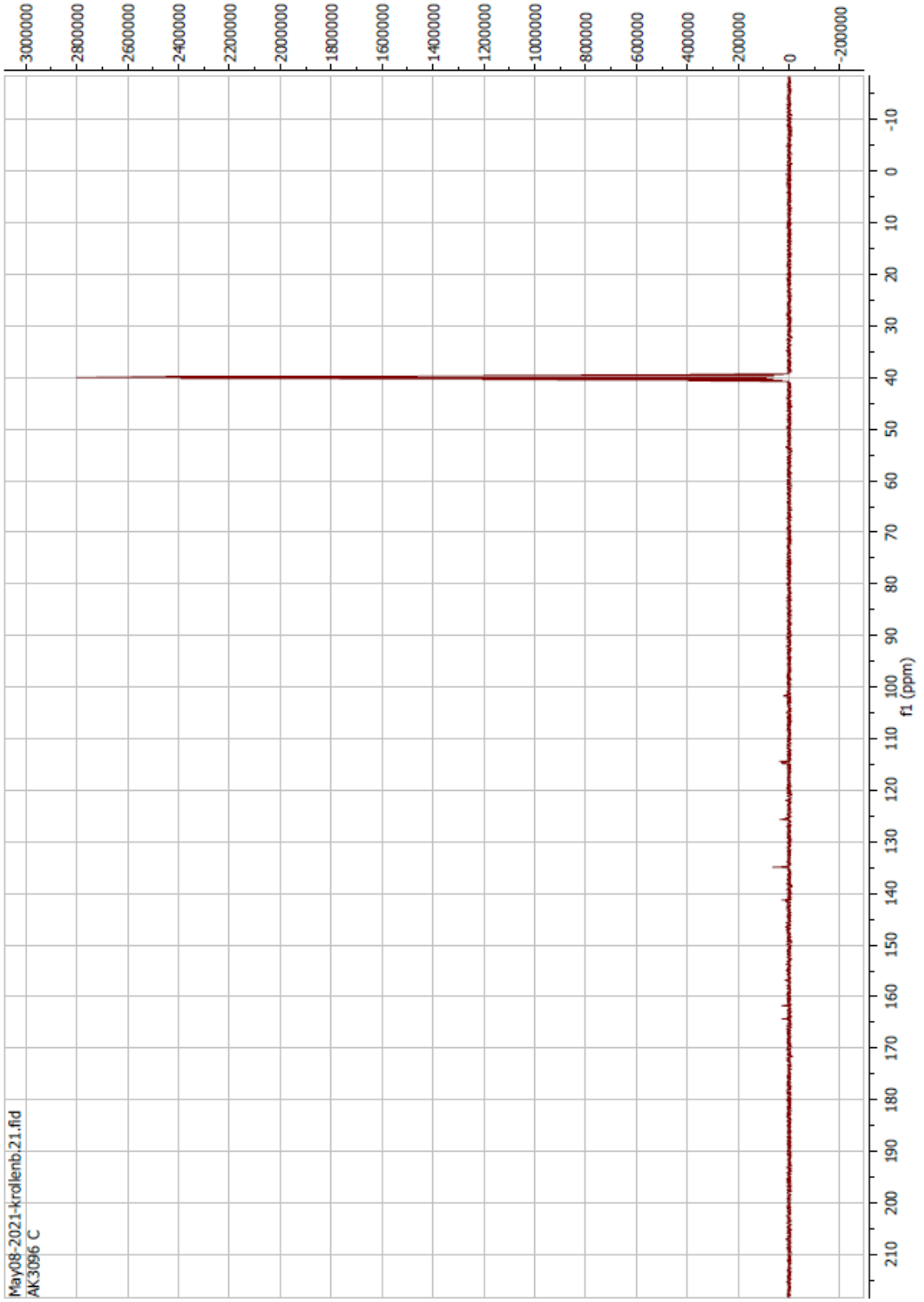

Compound 71 ^{1}H

Compound 71 ^{13}C

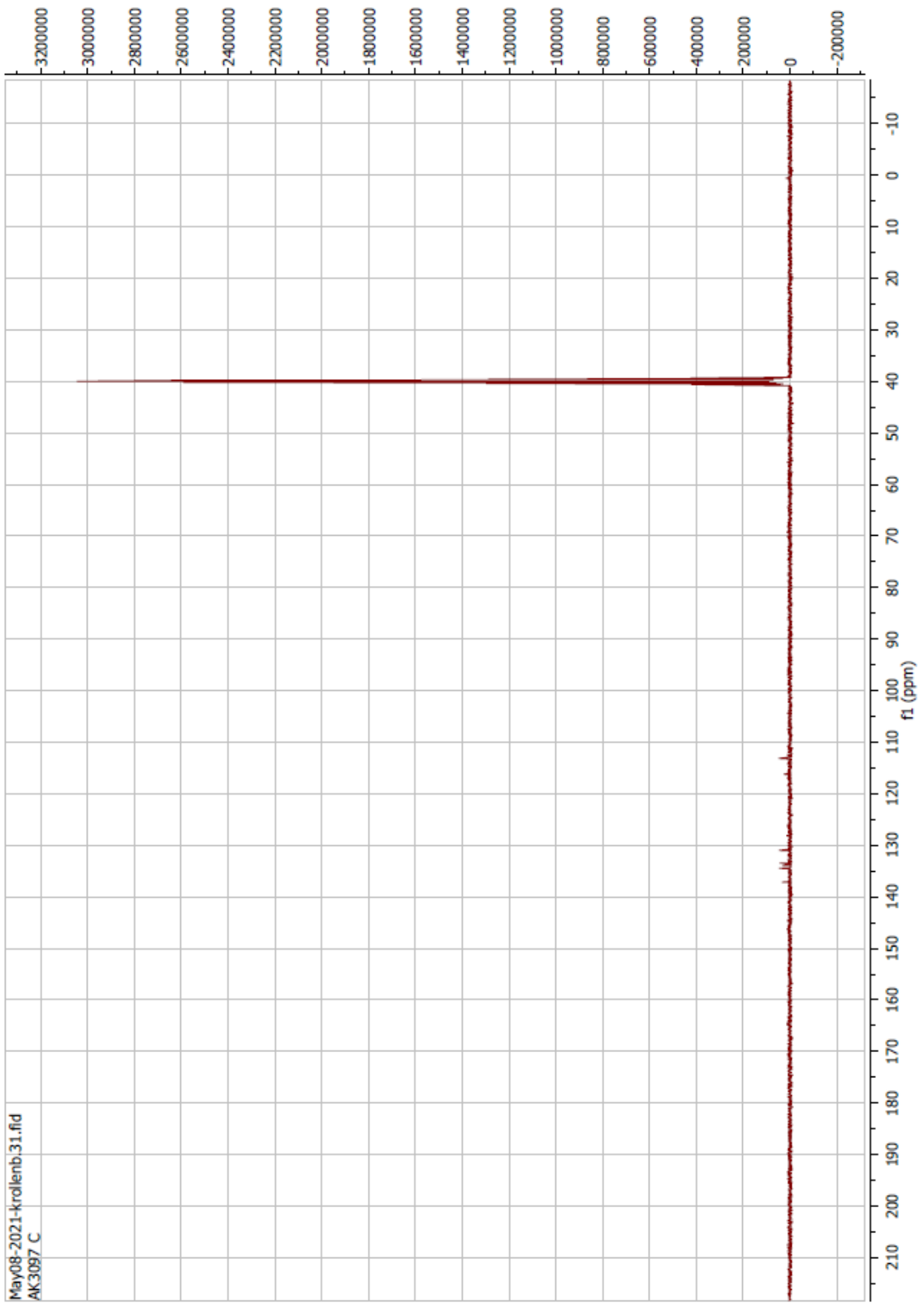

Compound 72 ^{1}H

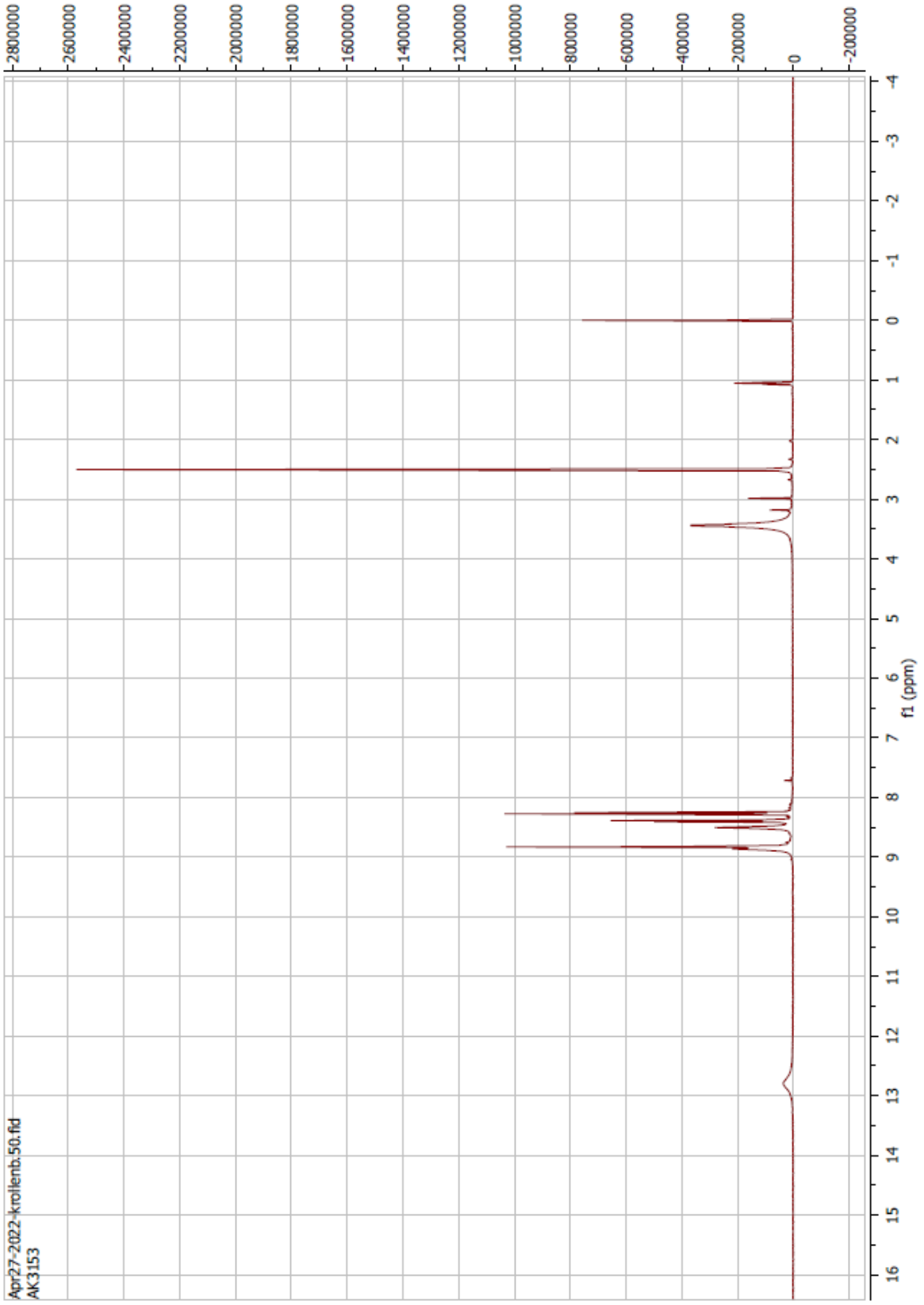

Compound 72 ^{13}C

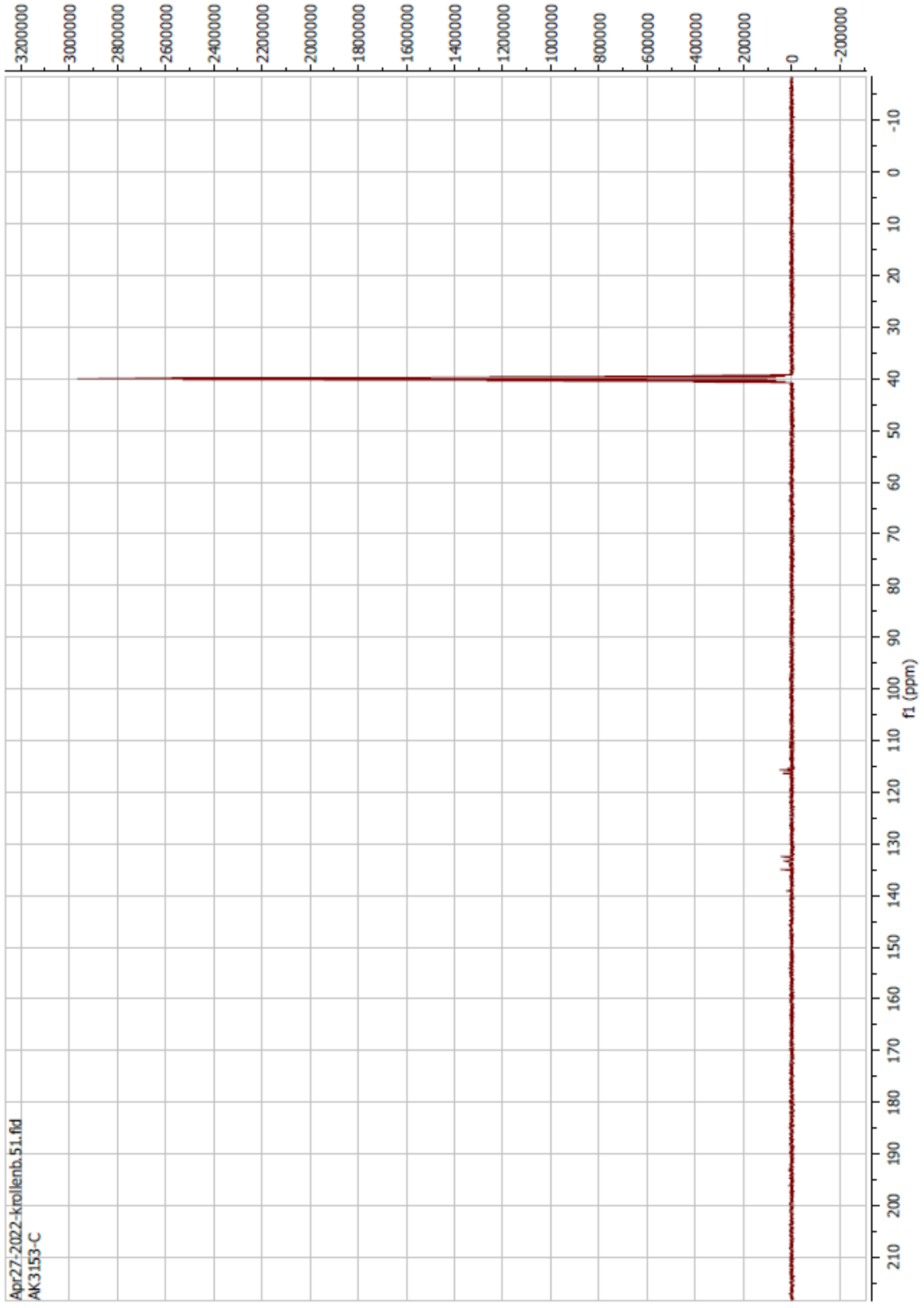

Compound 73 ^{1}H

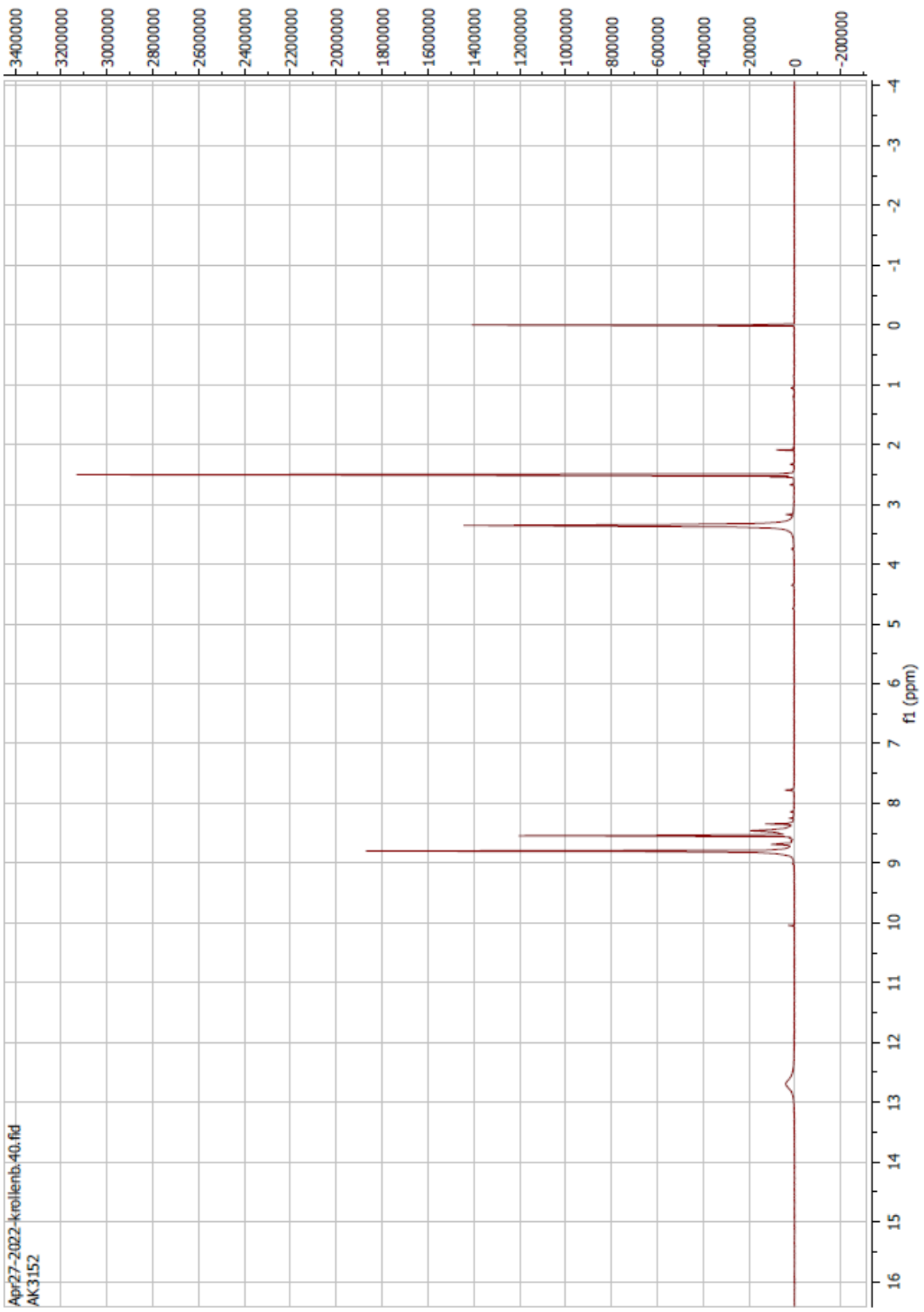

Compound 73 ^{13}C

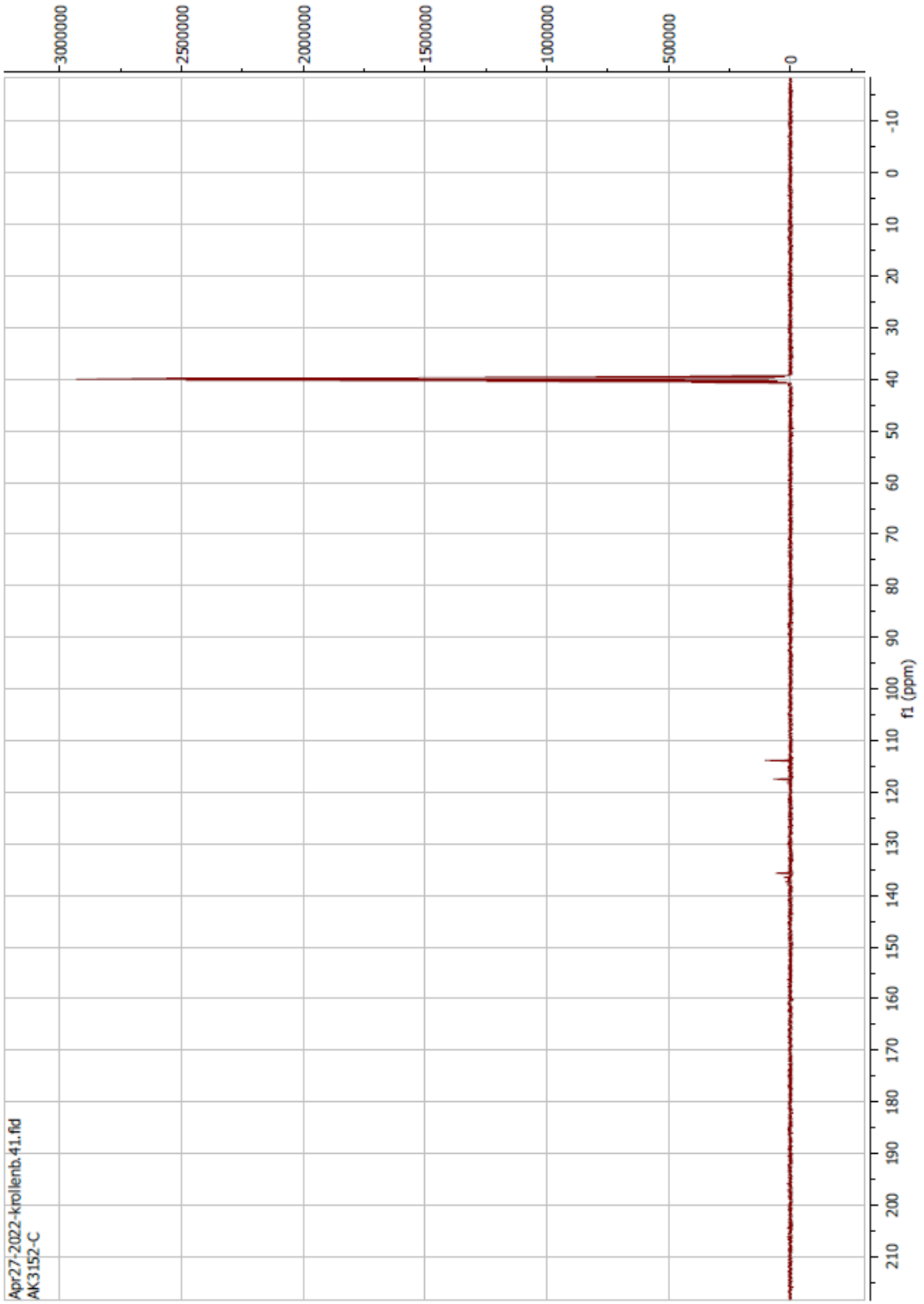

Compound 74 ^{1}H

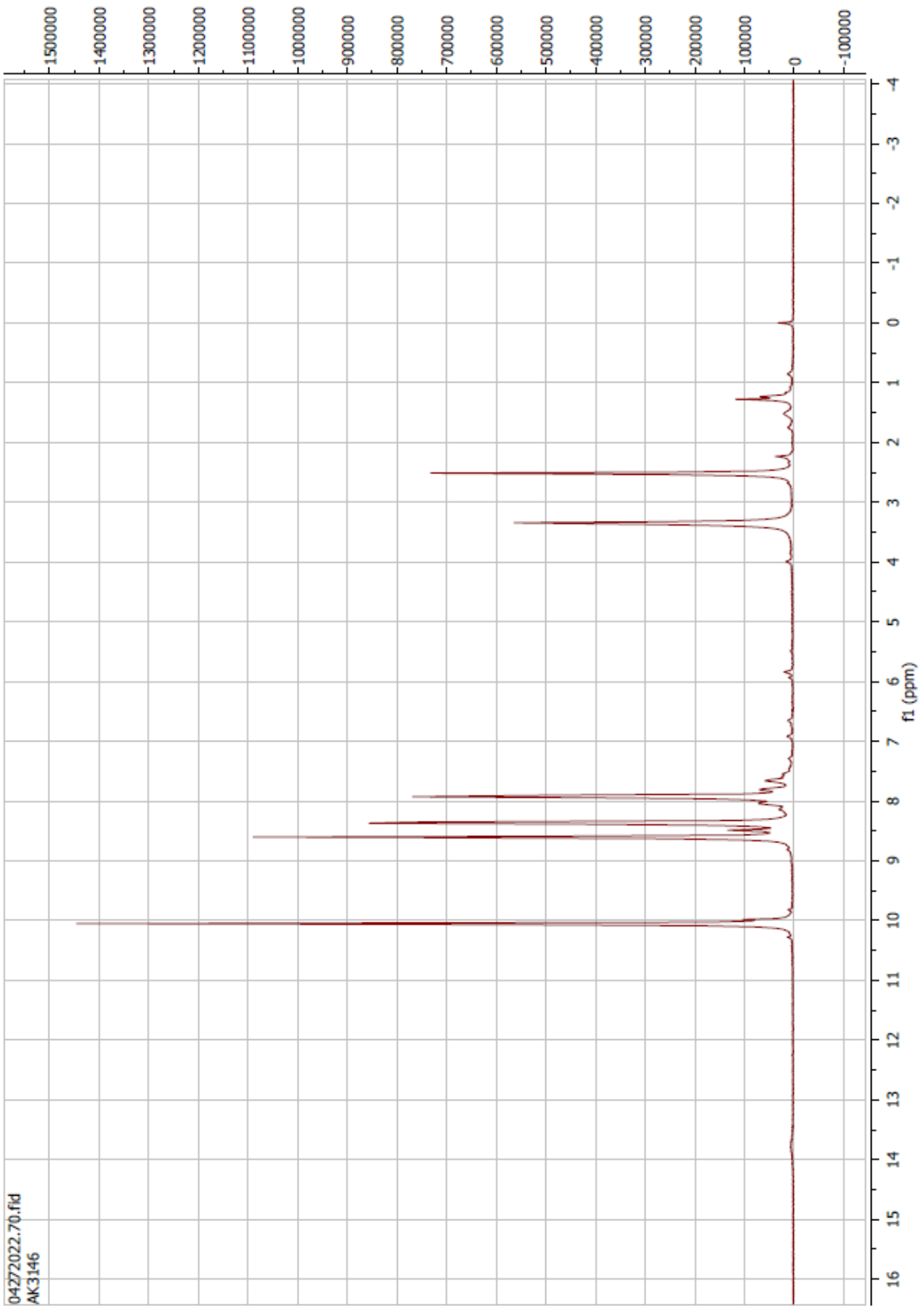

Compound 74 ^{13}C

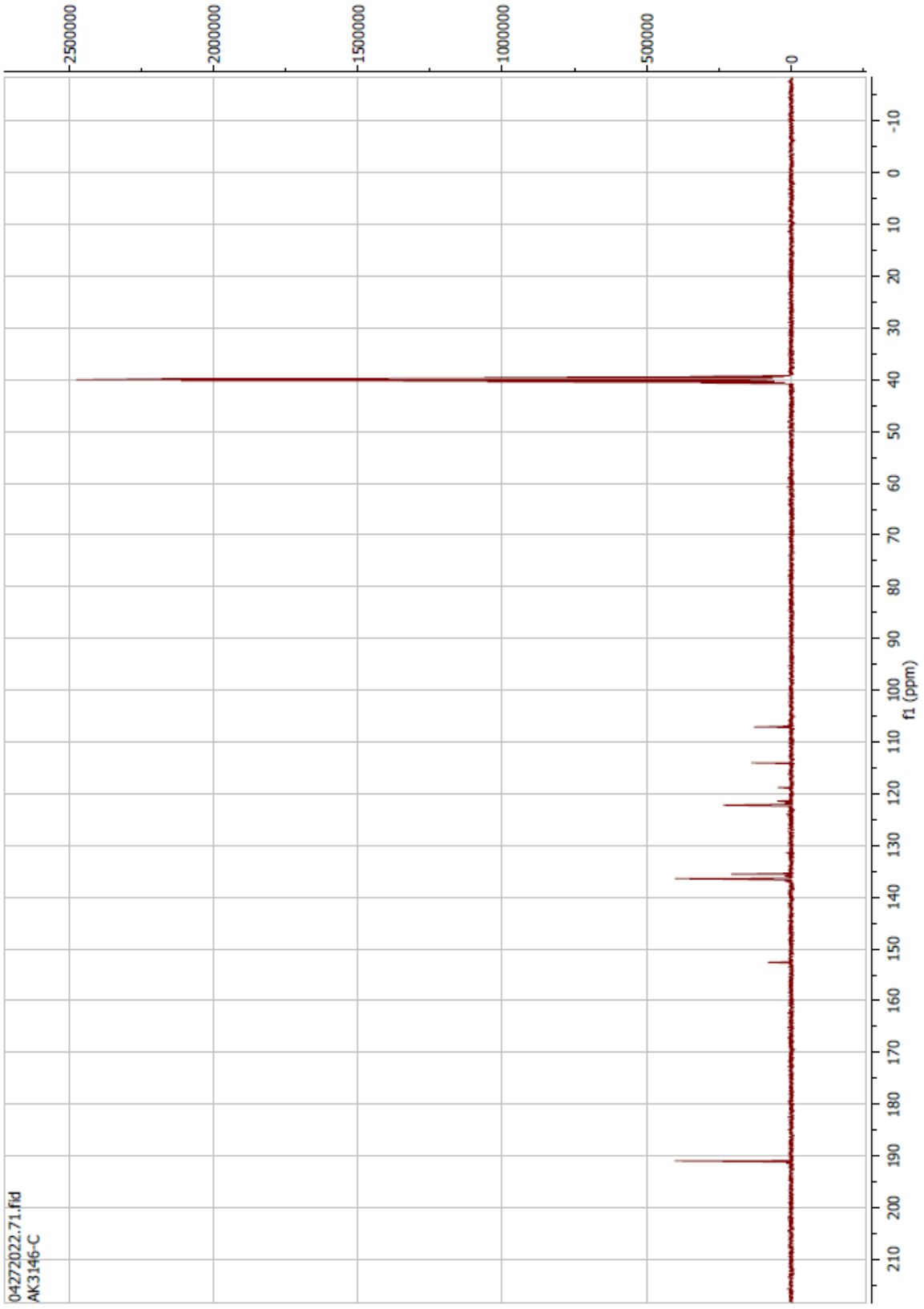

Compound 75 ^{1}H

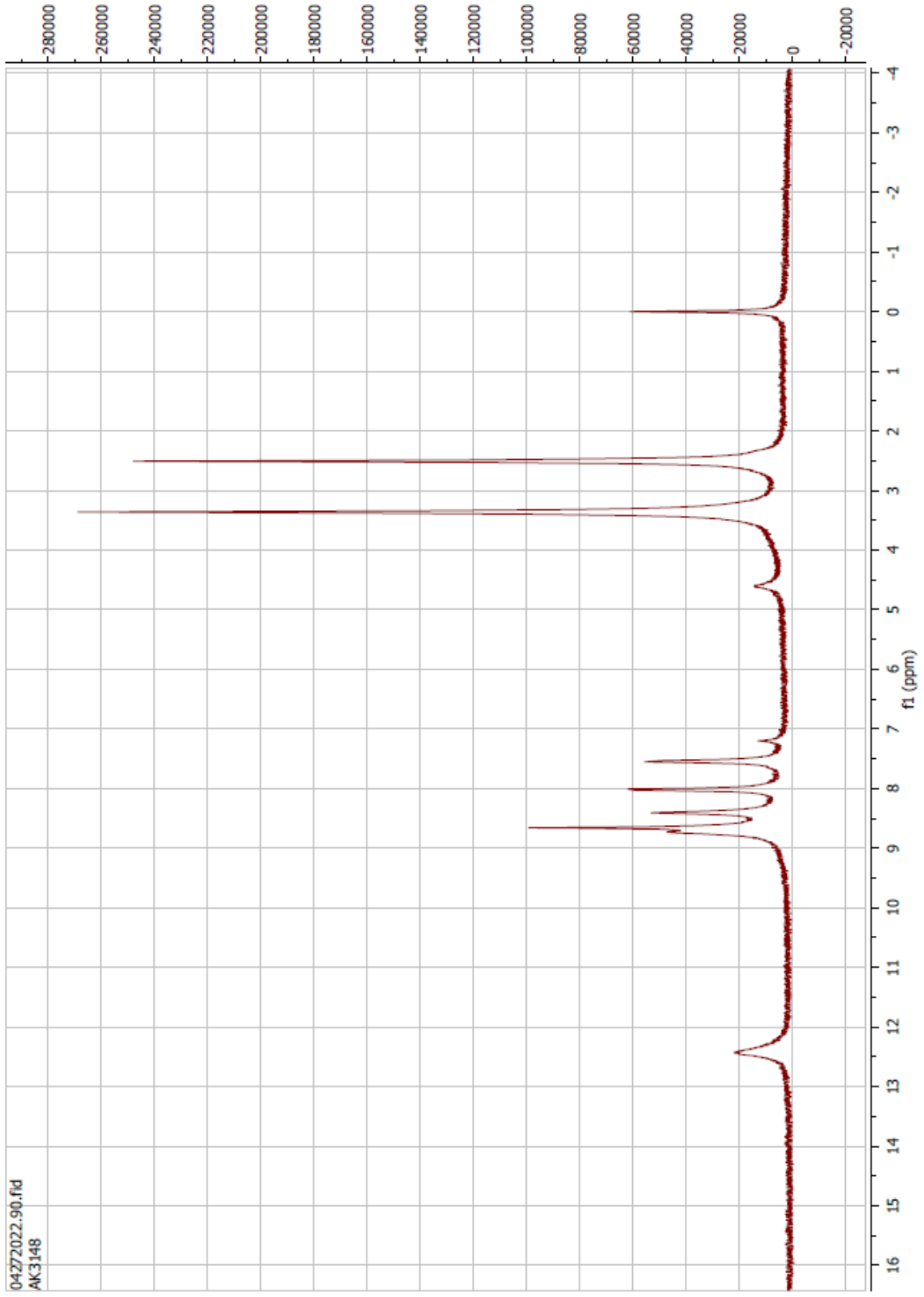

Compound 75 ^{13}C

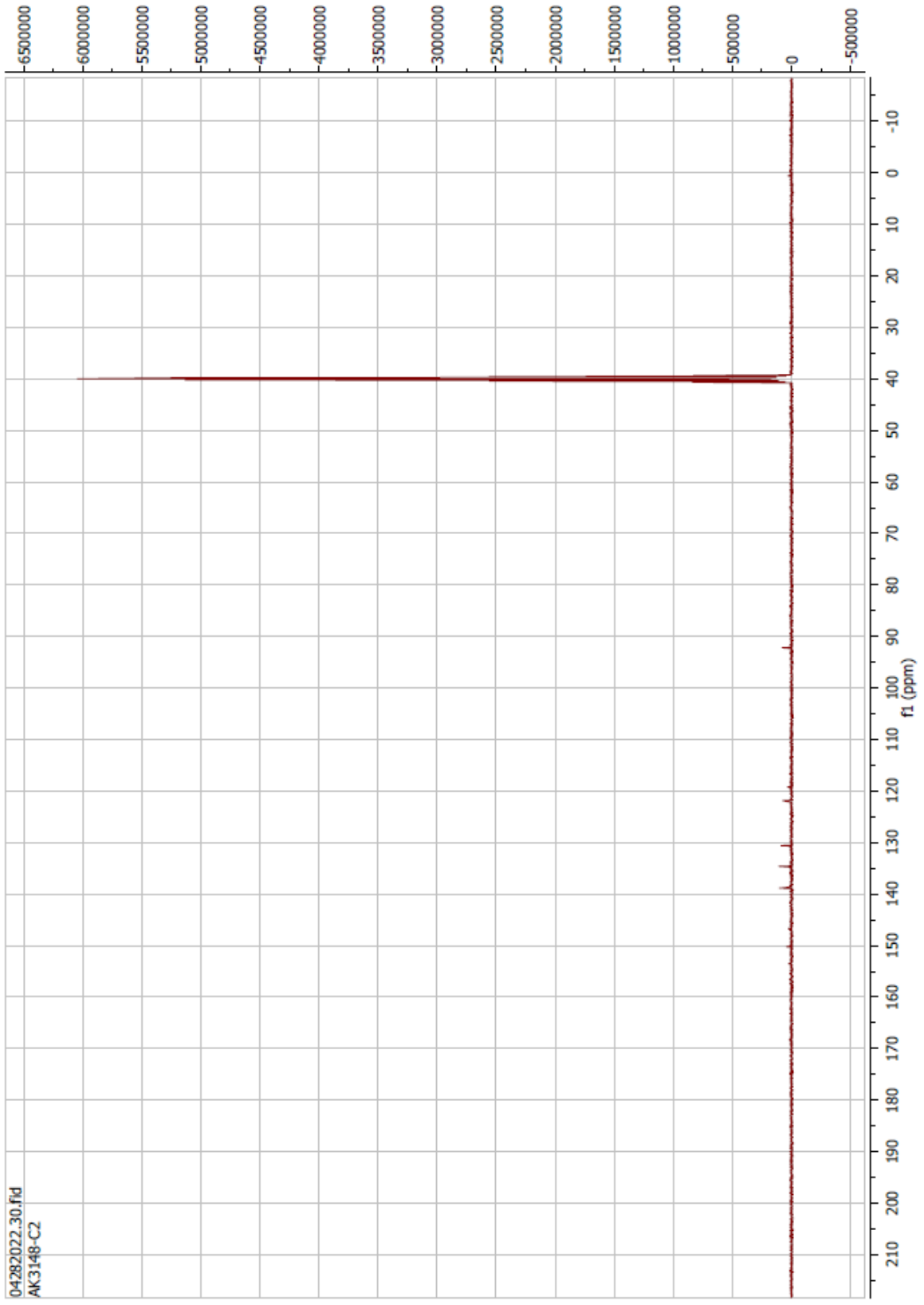

Compound 76 ^{1}H

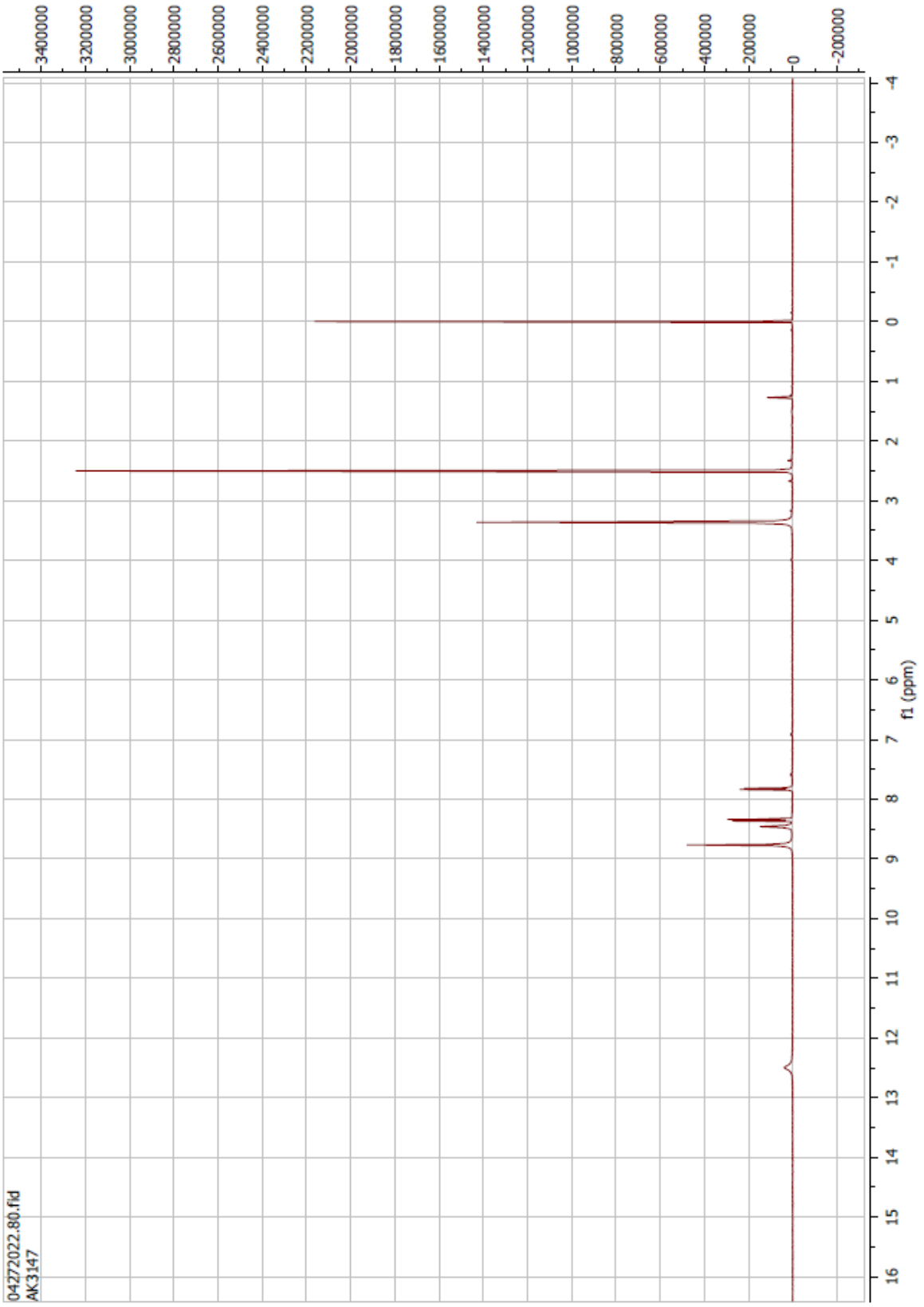

Compound 76 ^{13}C

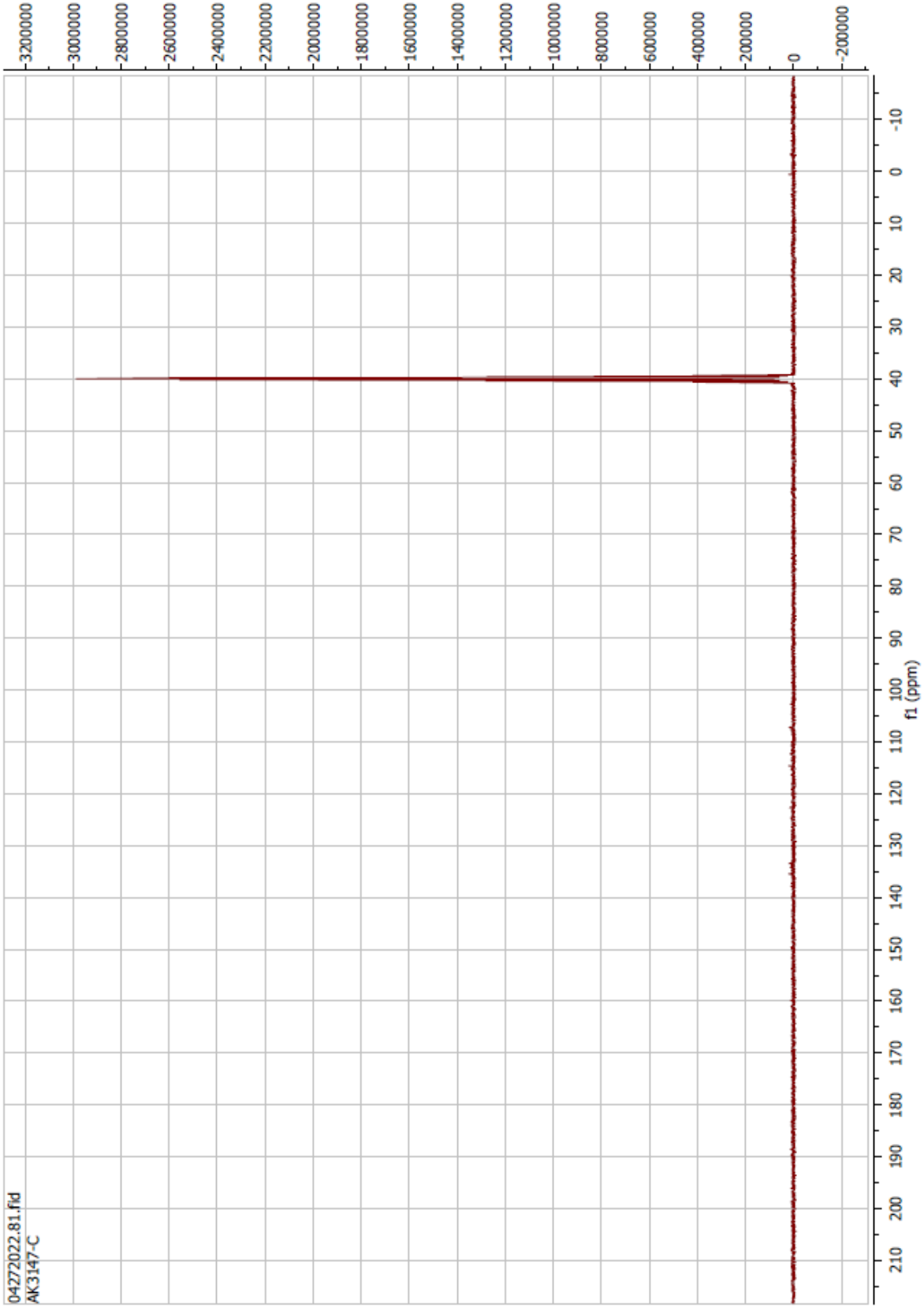

Compound 77 ^{1}H

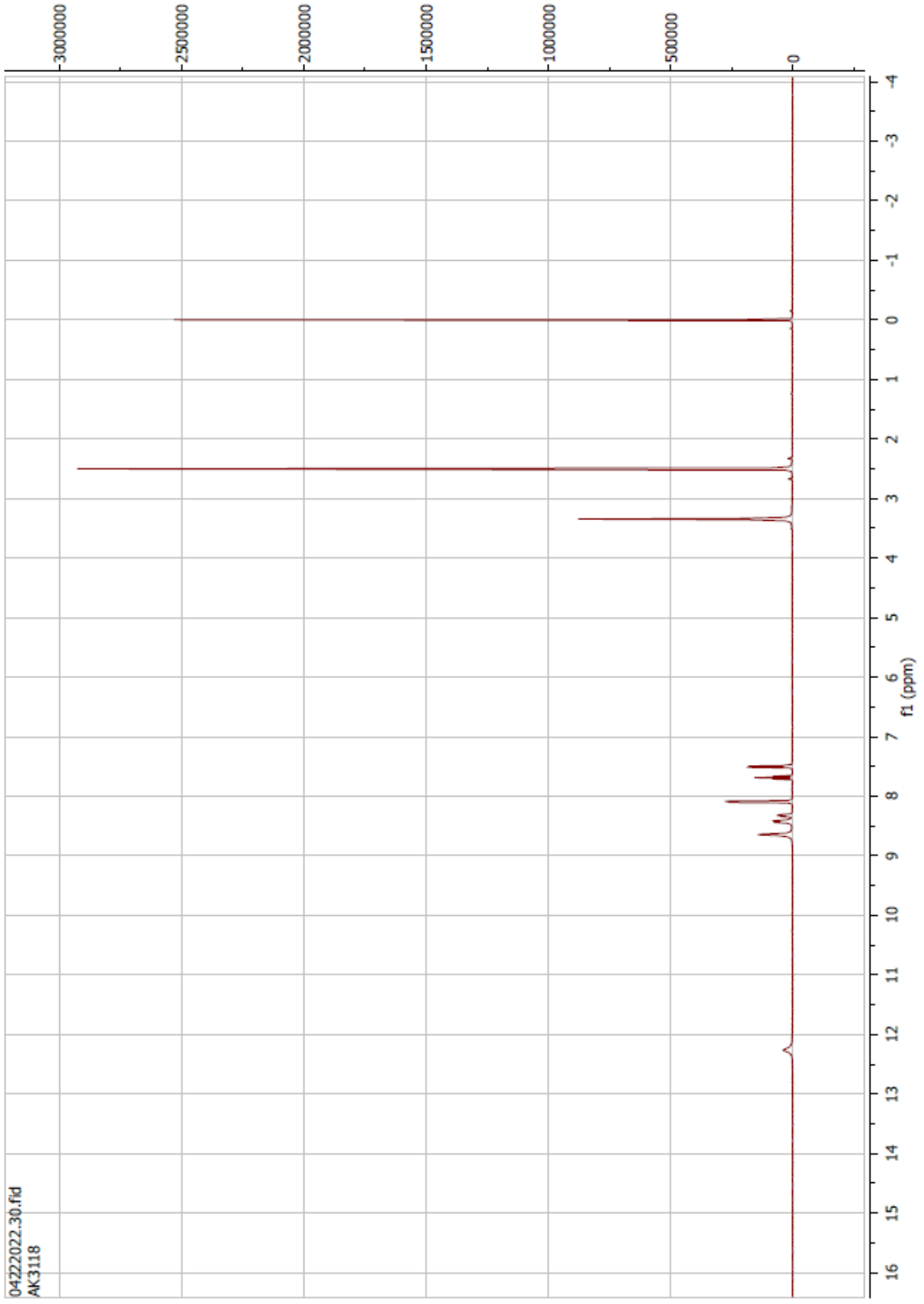

Compound 77 ^{13}C

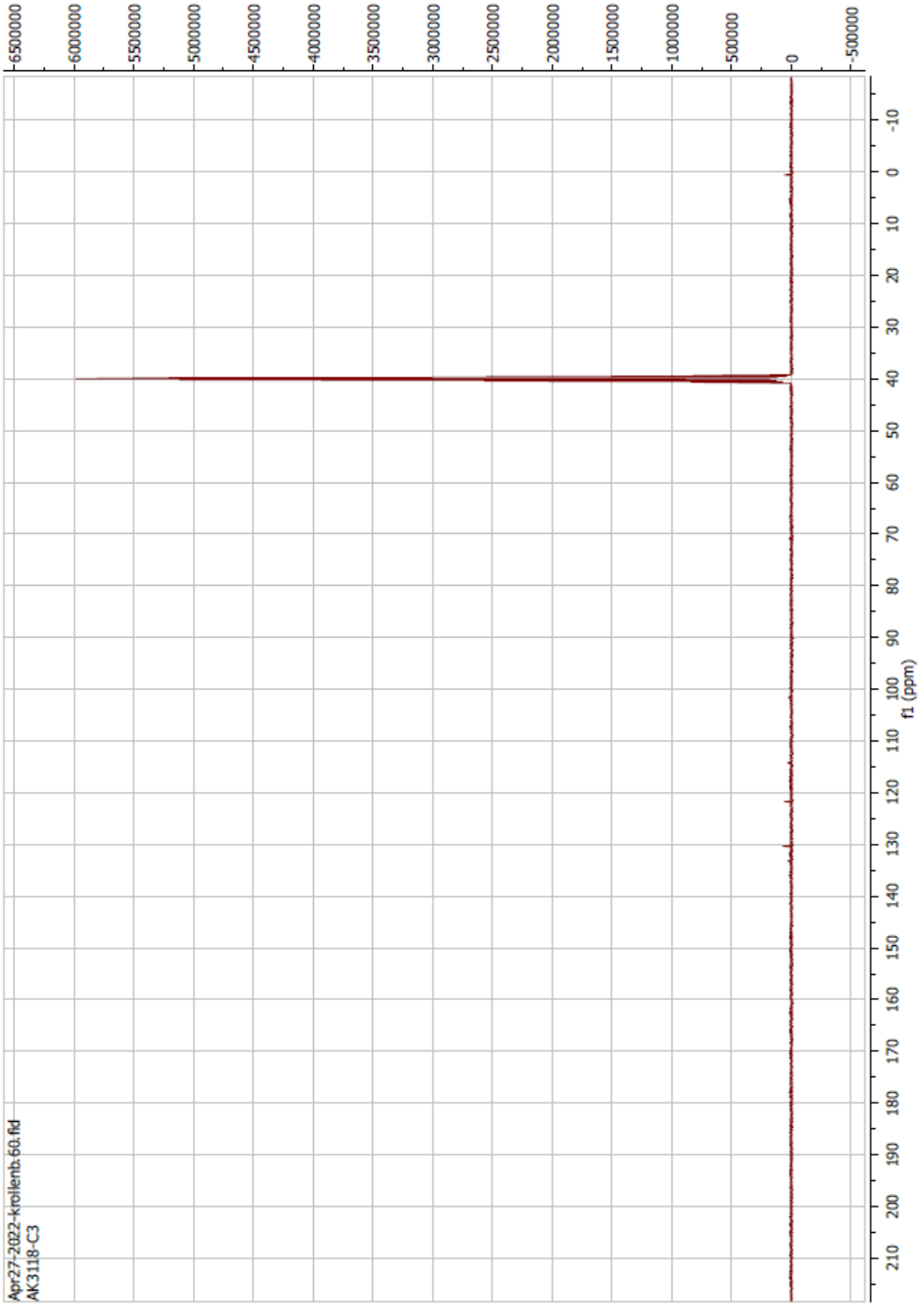

Compound 78 ^{1}H

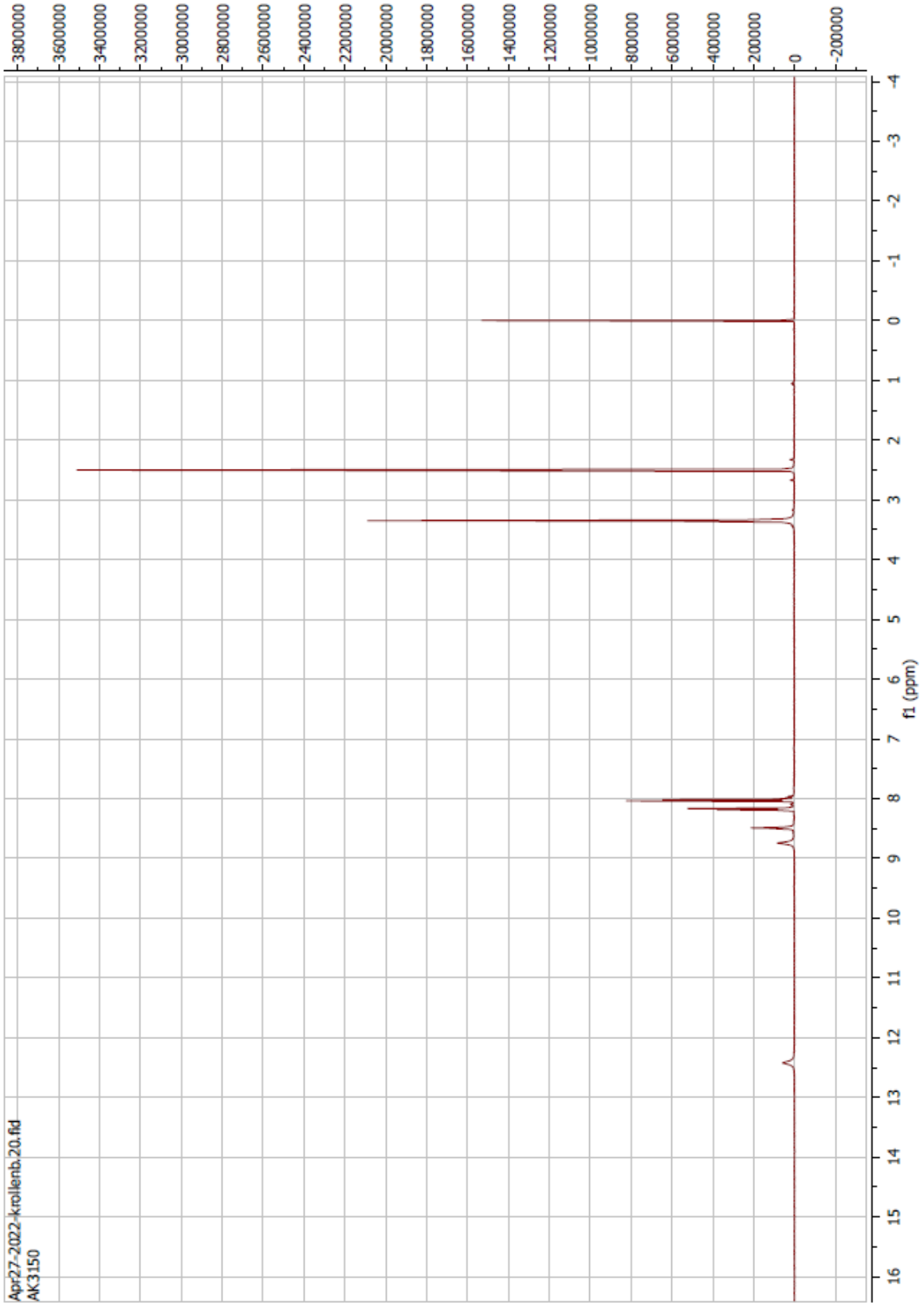

Compound 78 ^{13}C

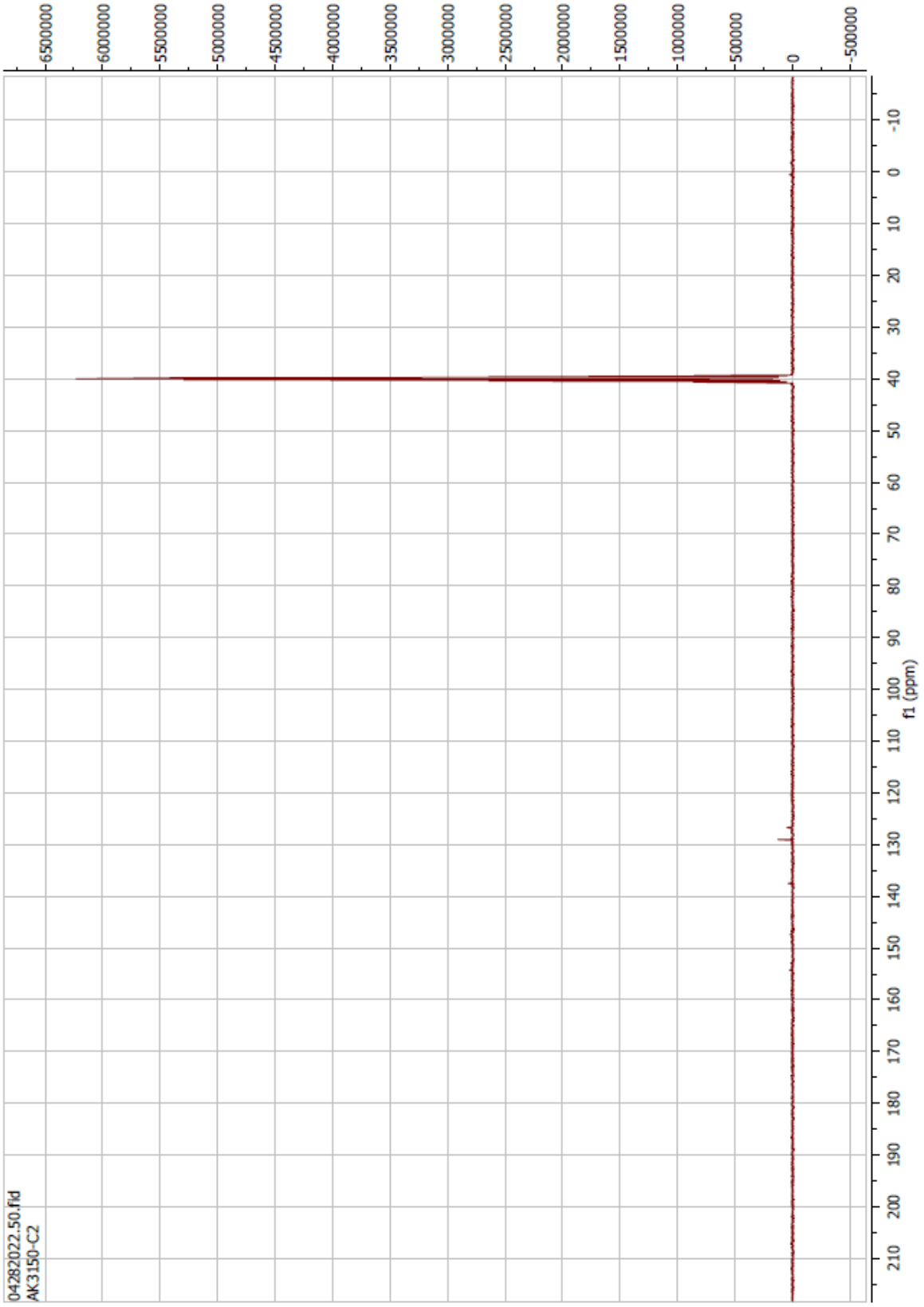

Compound 79 ^{1}H

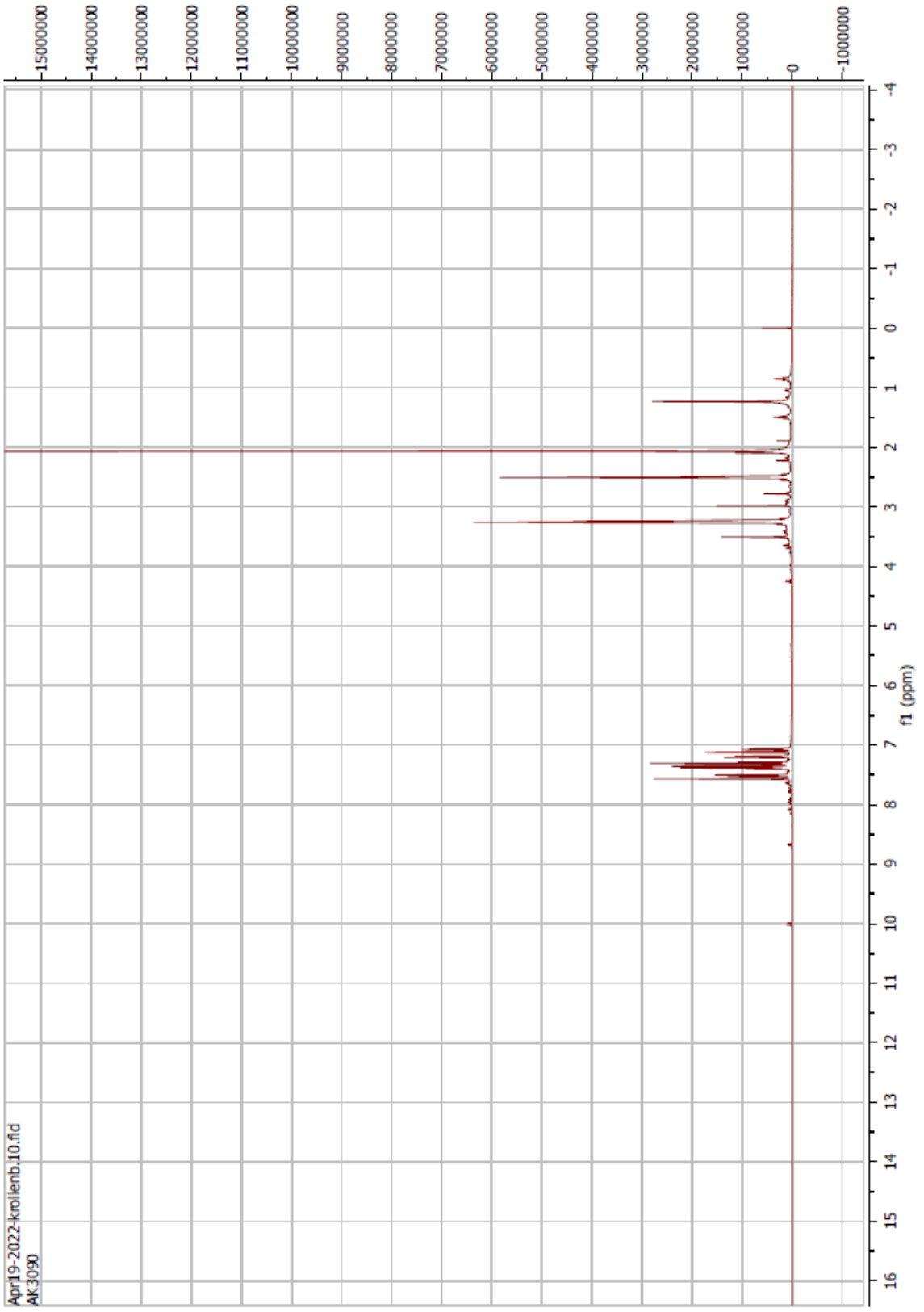

Compound 79 ^{13}C

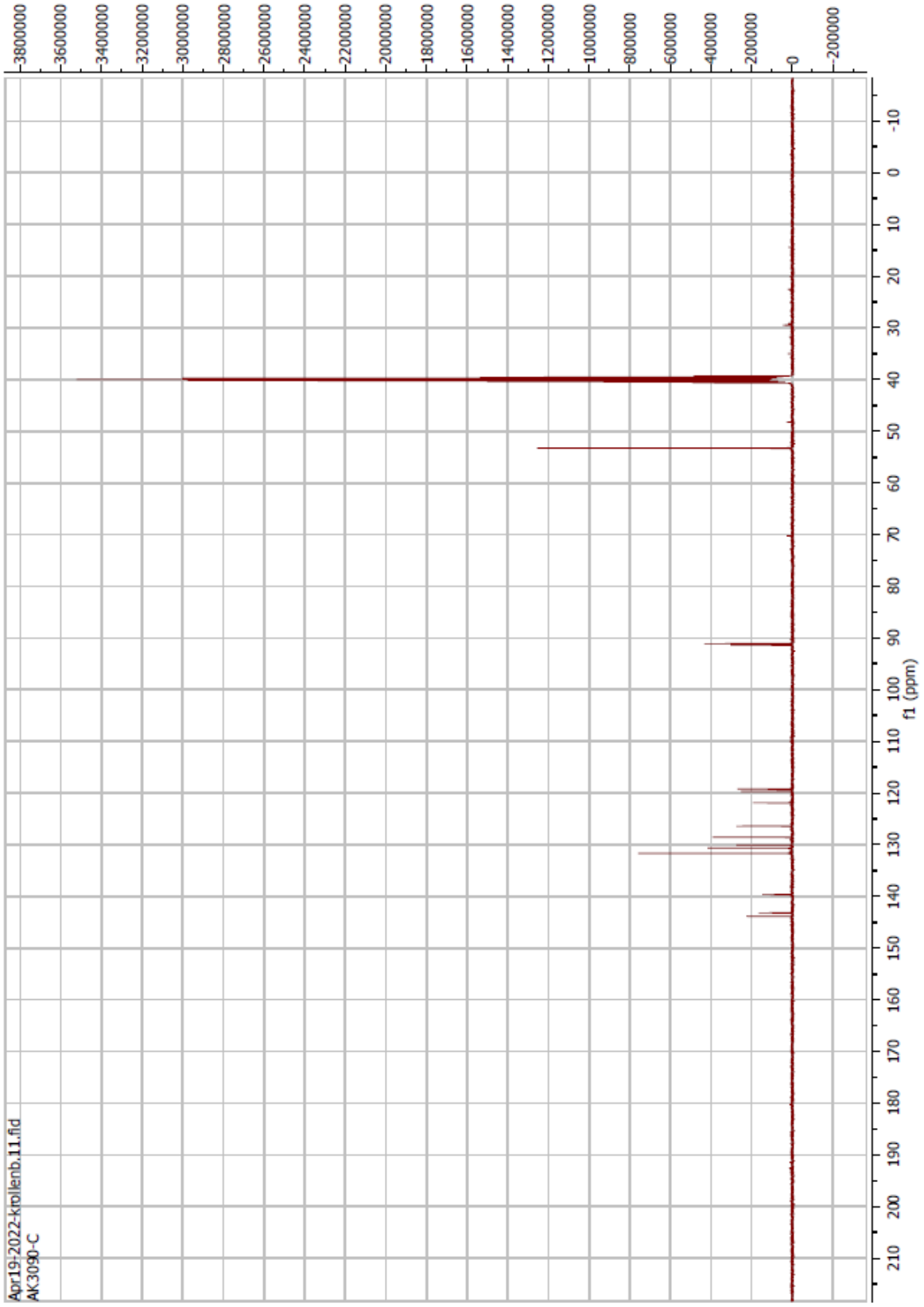

Compound 80 ^{1}H

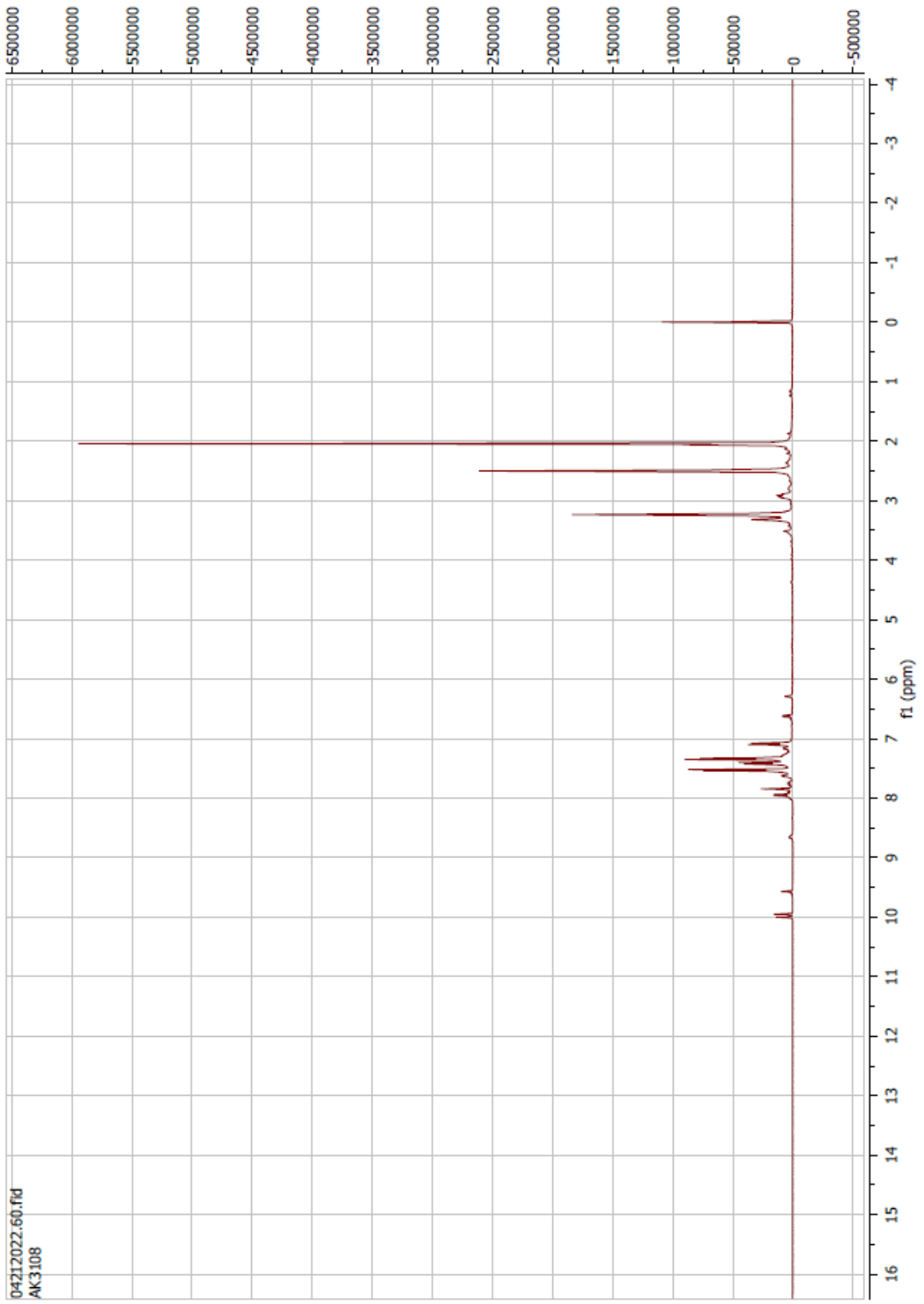

Compound 80 ^{13}C

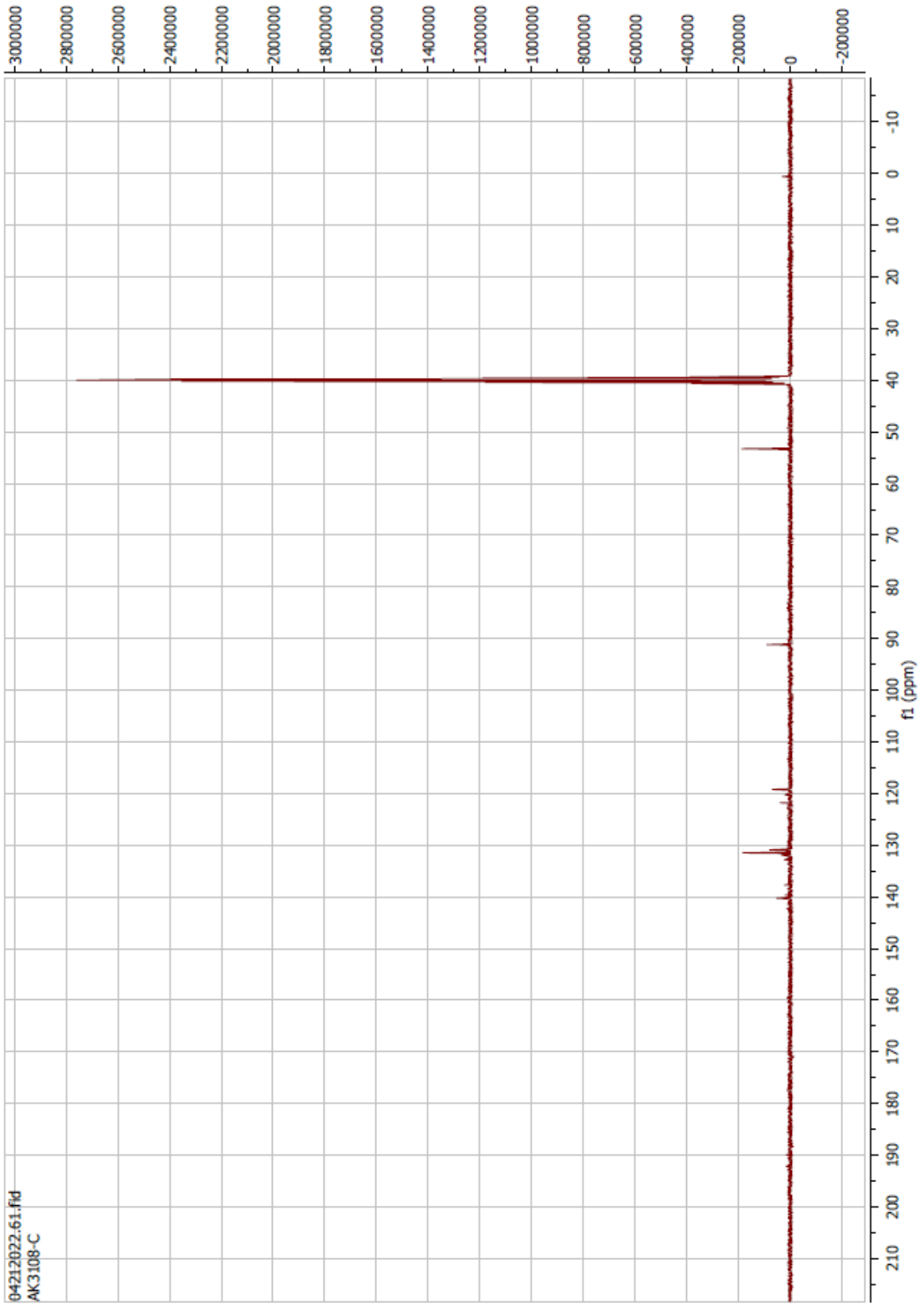

Compound 83 ^{1}H

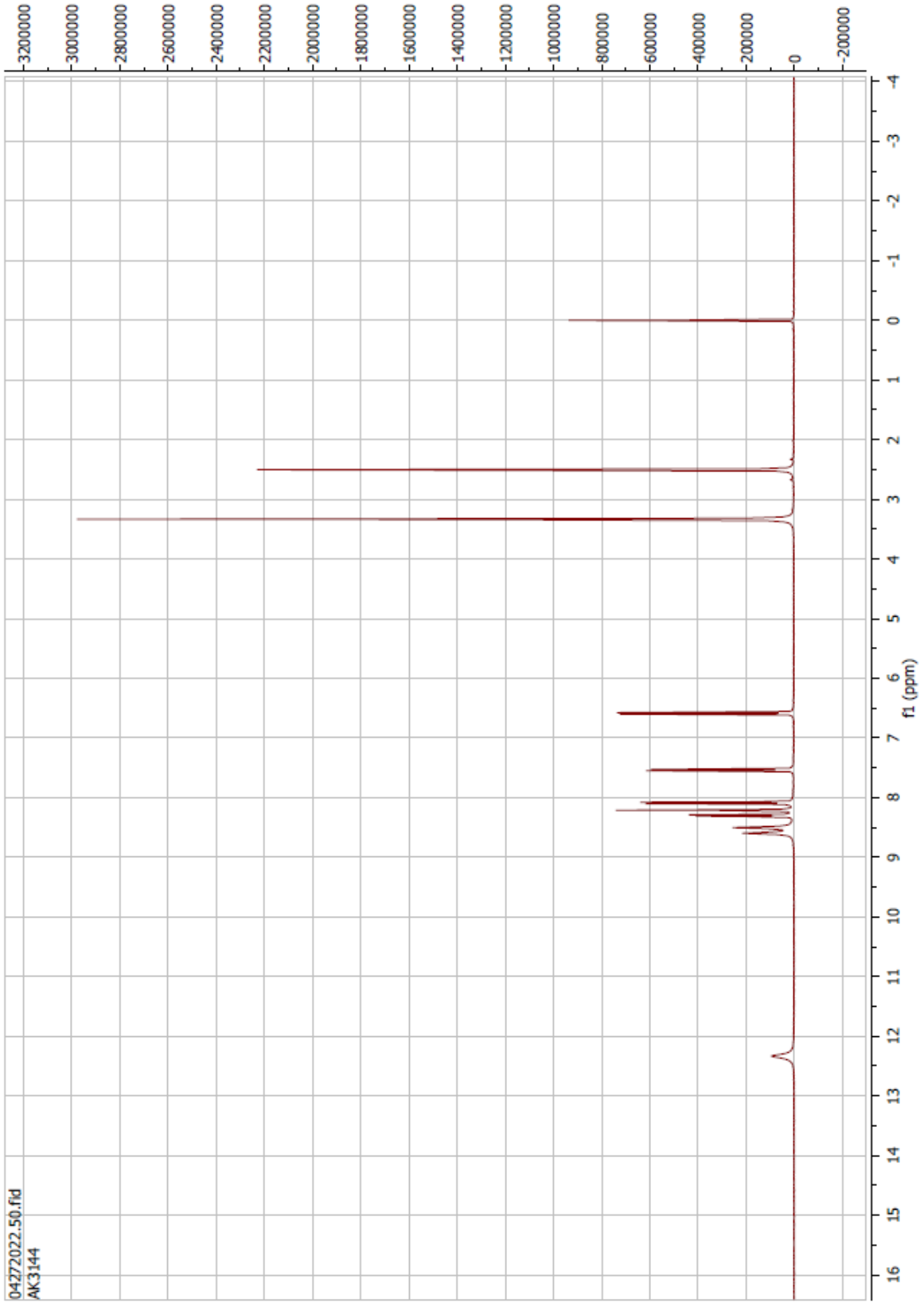

Compound 83 ^{13}C

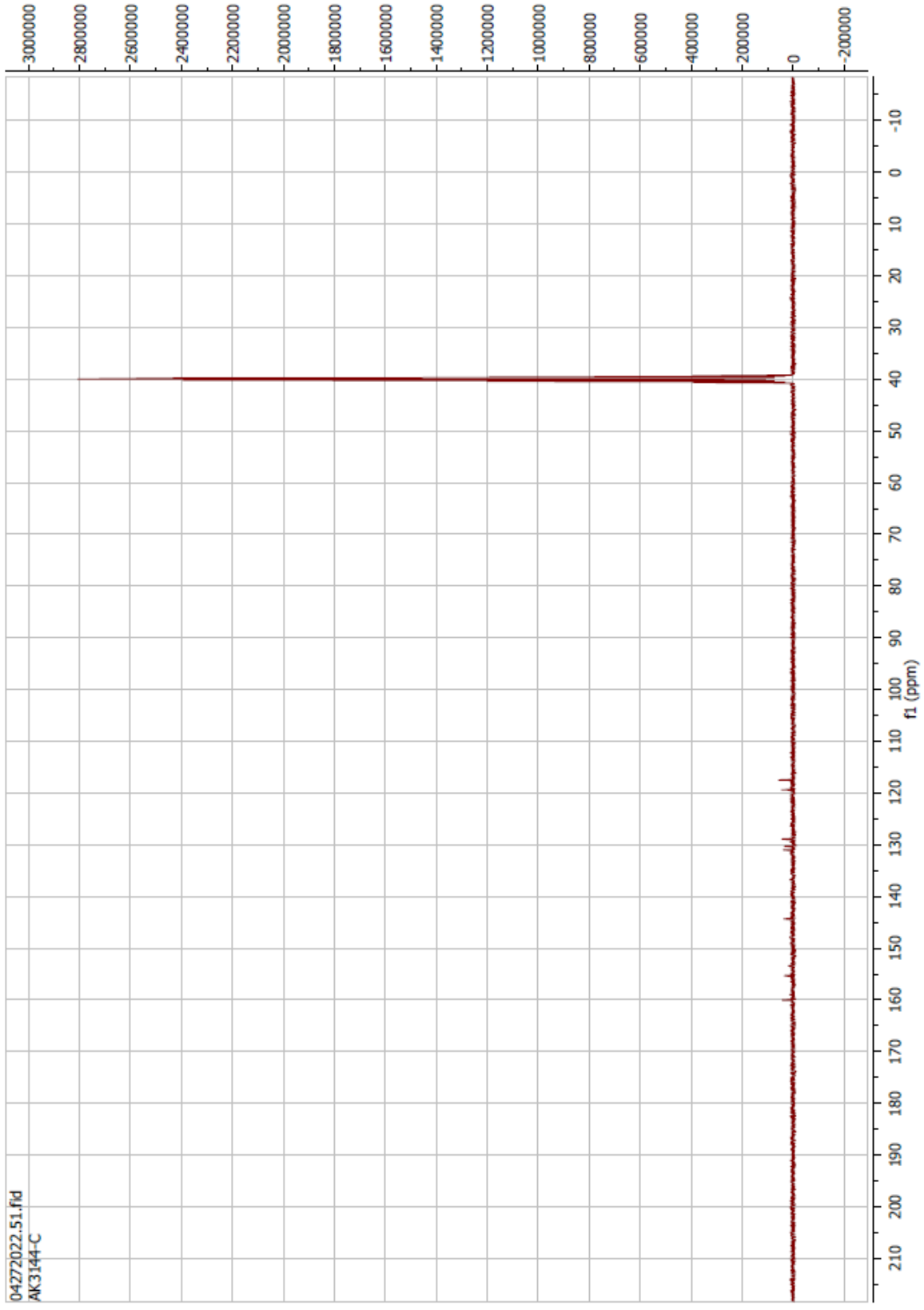

Compound 84 ^{1}H

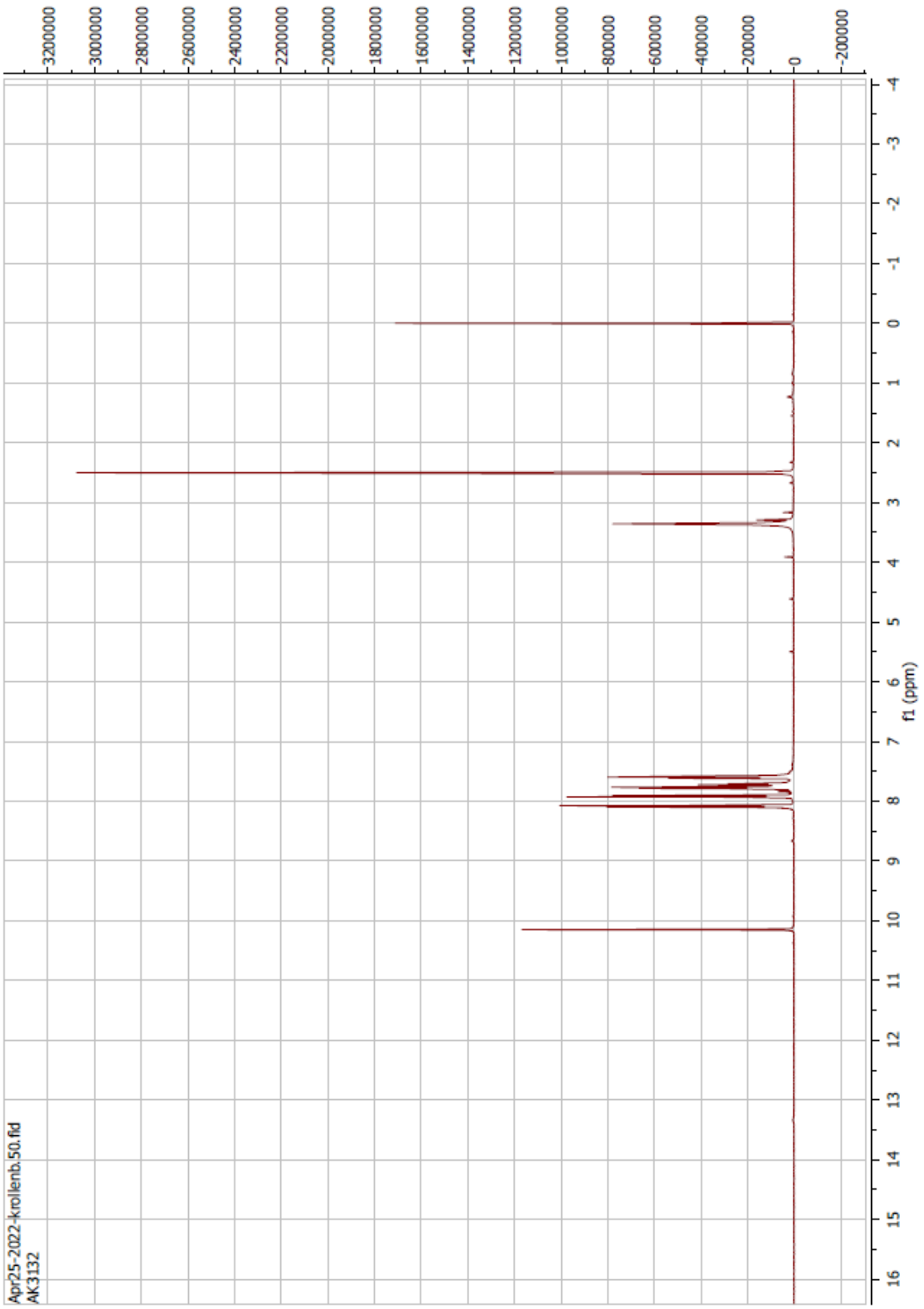

Compound 84 ^{13}C

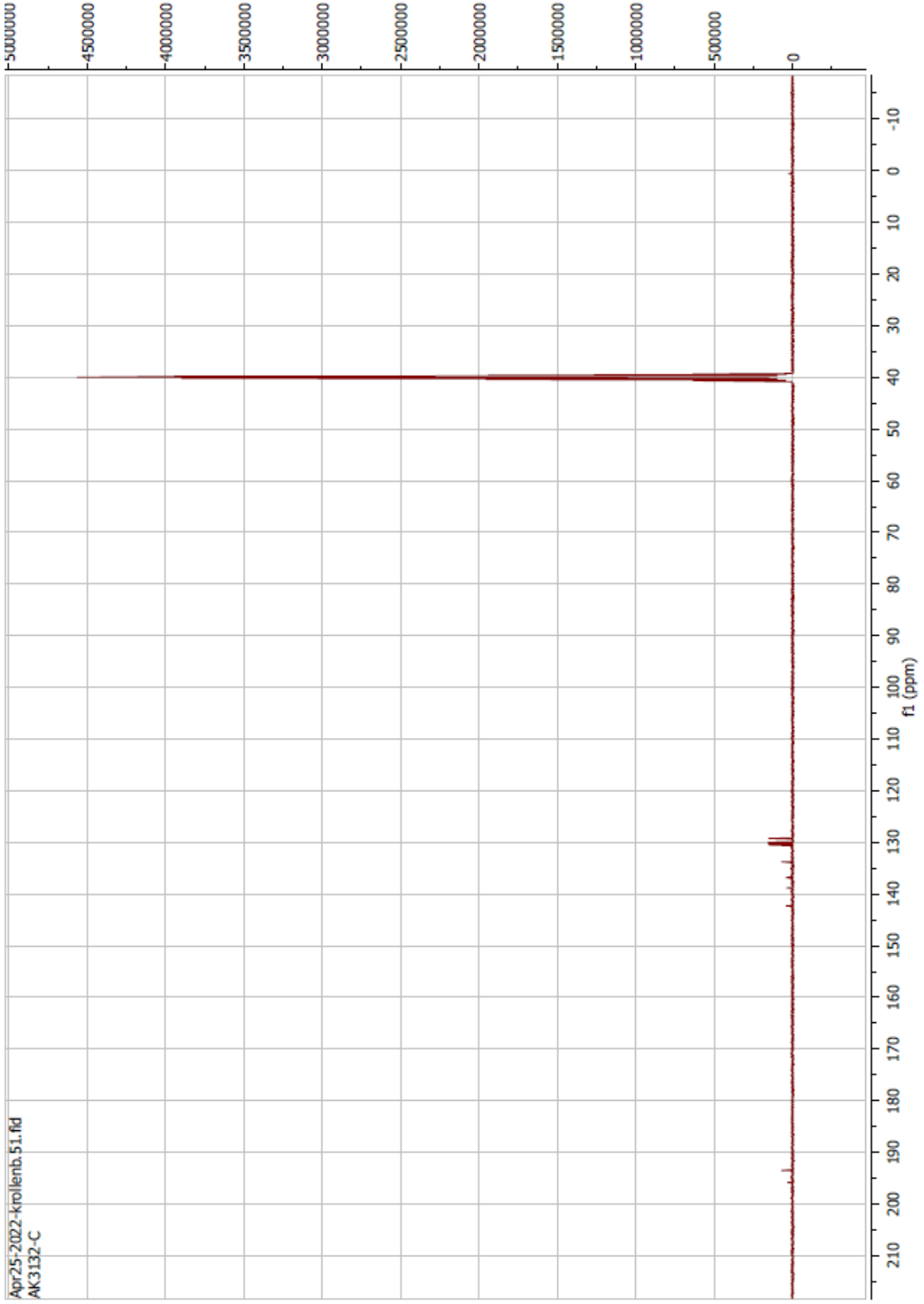

Compound 85 ^{1}H

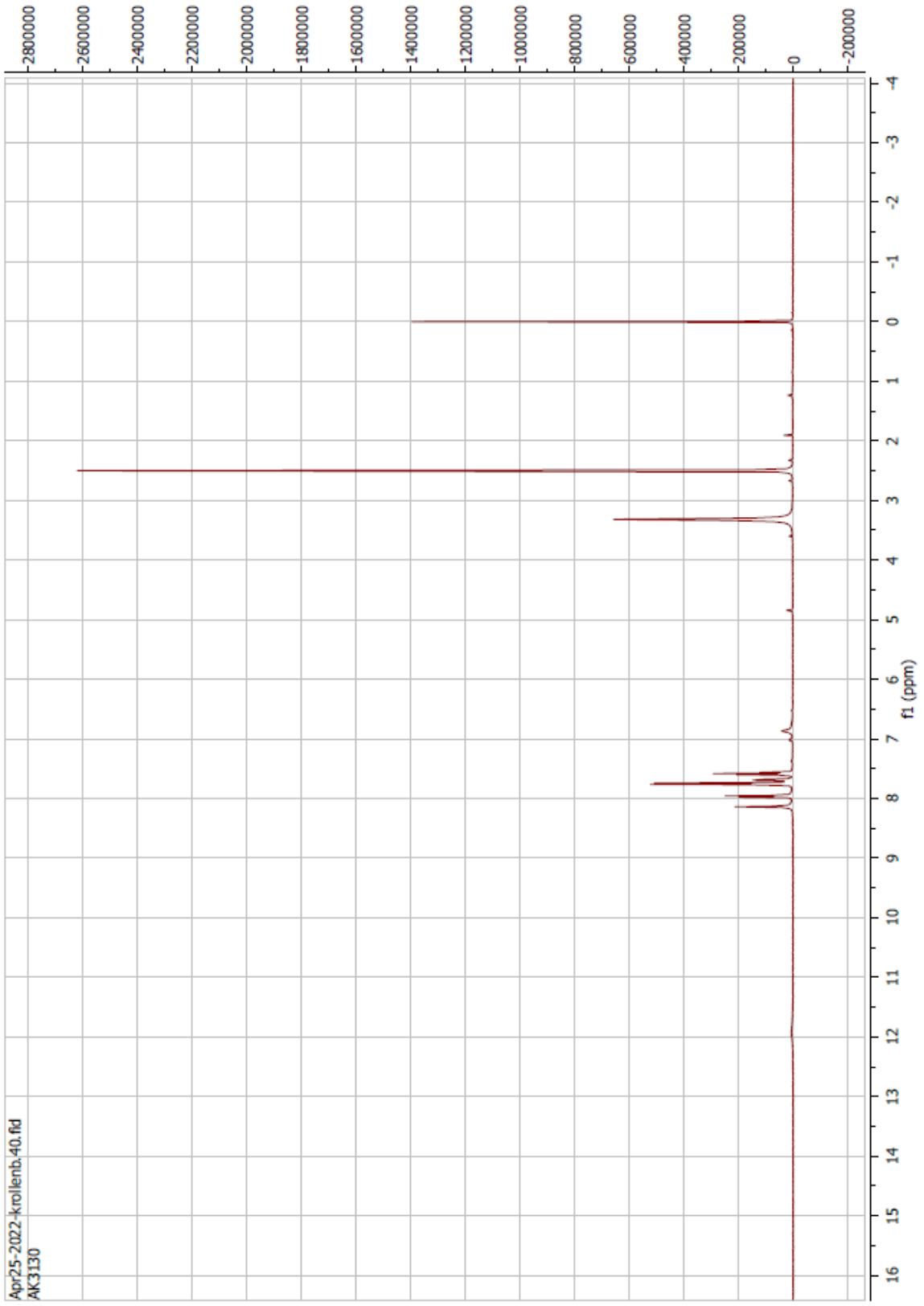

Compound 85 ^{13}C

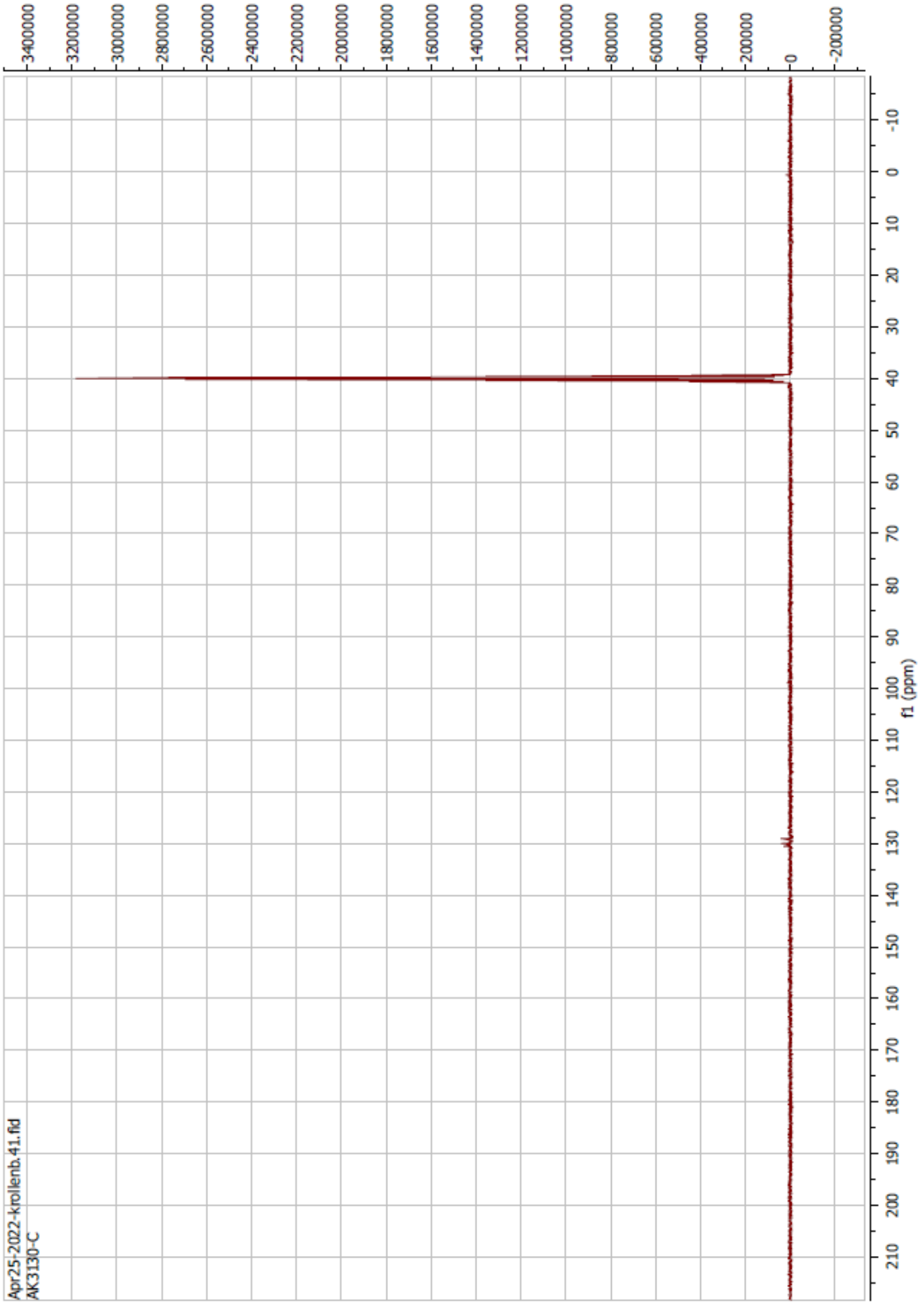

Compound 86 ^{1}H

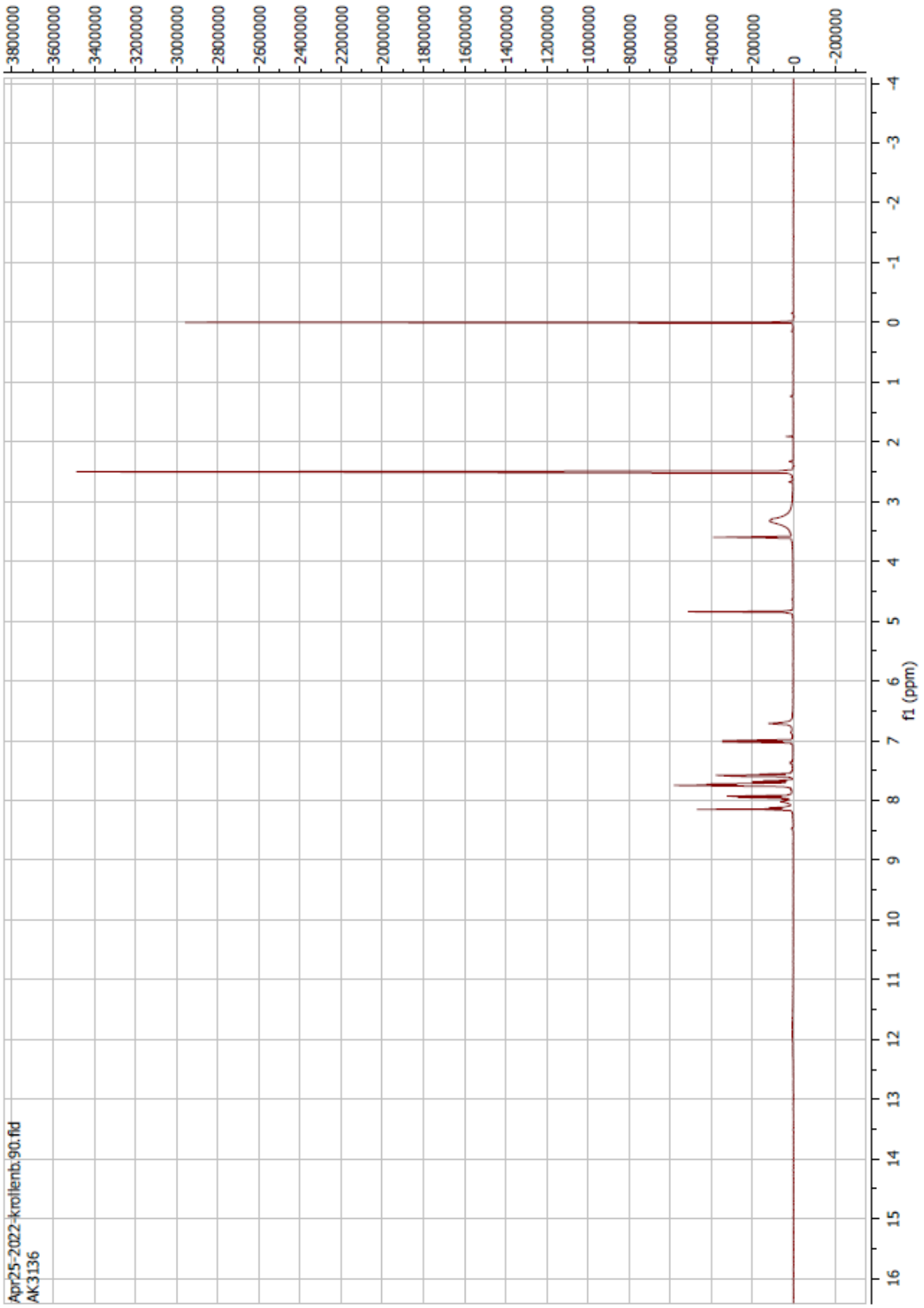

Compound 86 ^{13}C

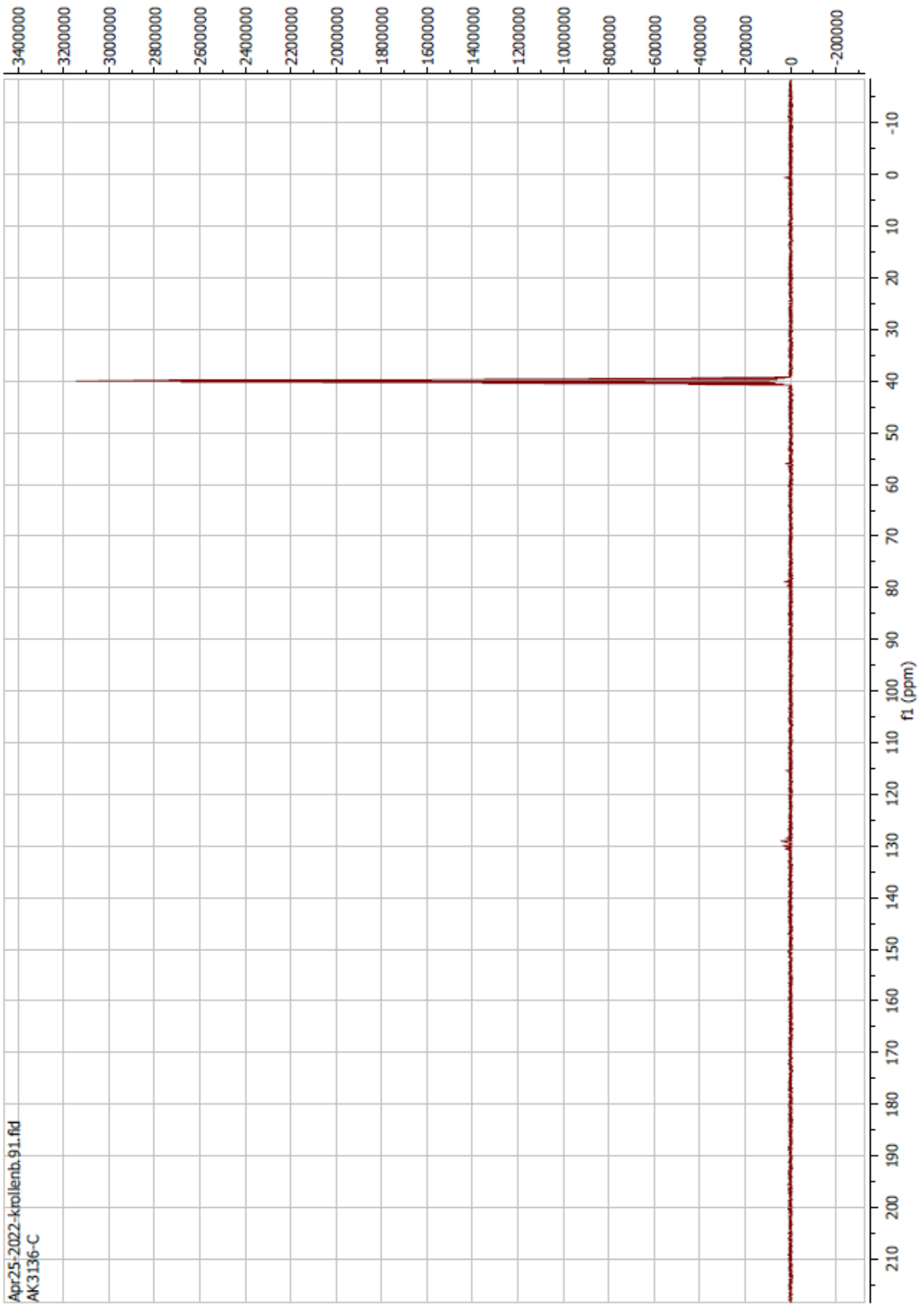

ELQ-487 ^{1}H

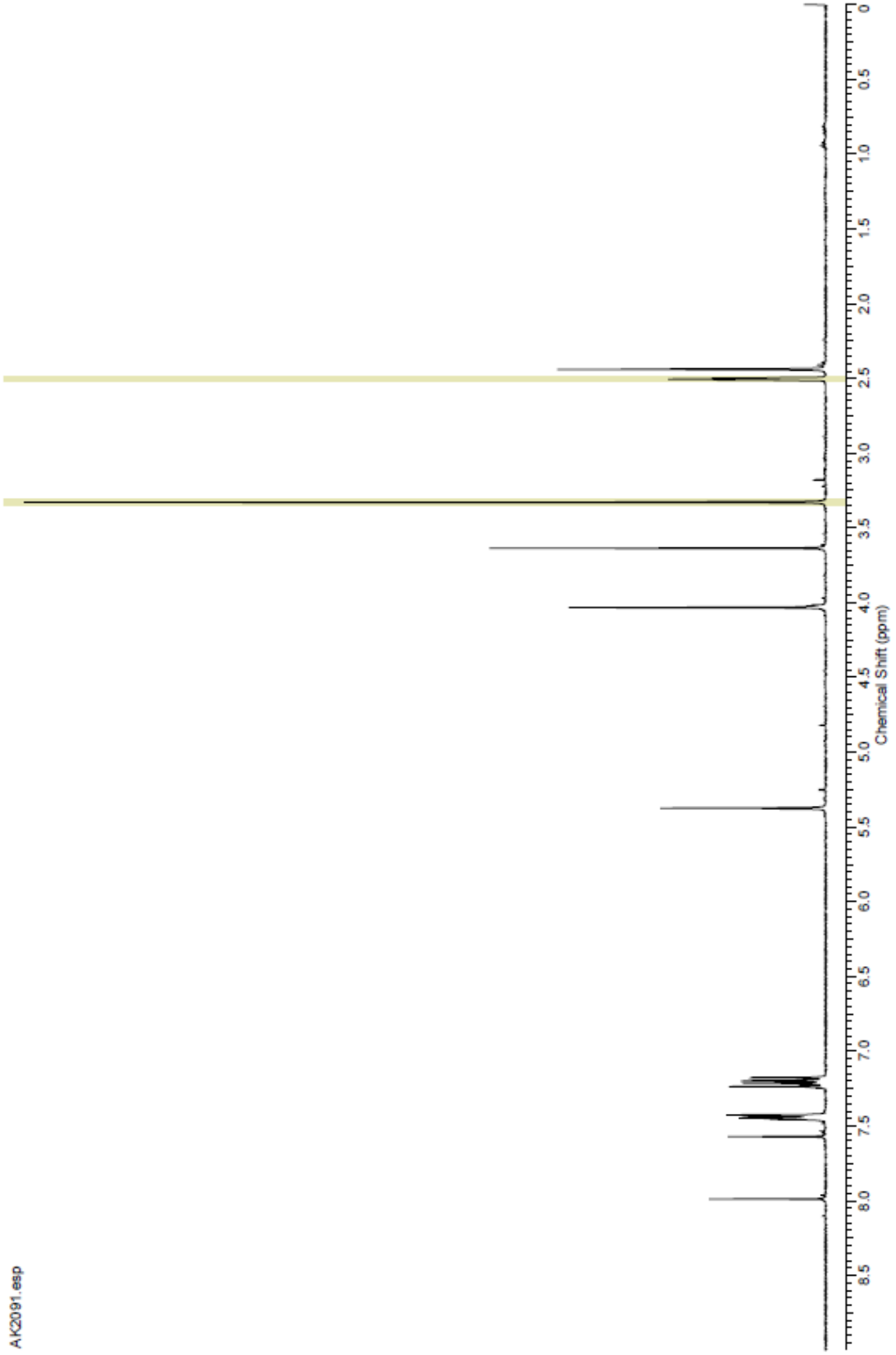
AK2091.esp
Chemical Shift (ppm)
0
0.5
1.0
1.5
2.0
2.5
3.0
3.5
4.0
4.5
5.0
5.5
6.0
6.5
7.0
7.5
8.0
8.5

ELQ-488 ^{1}H

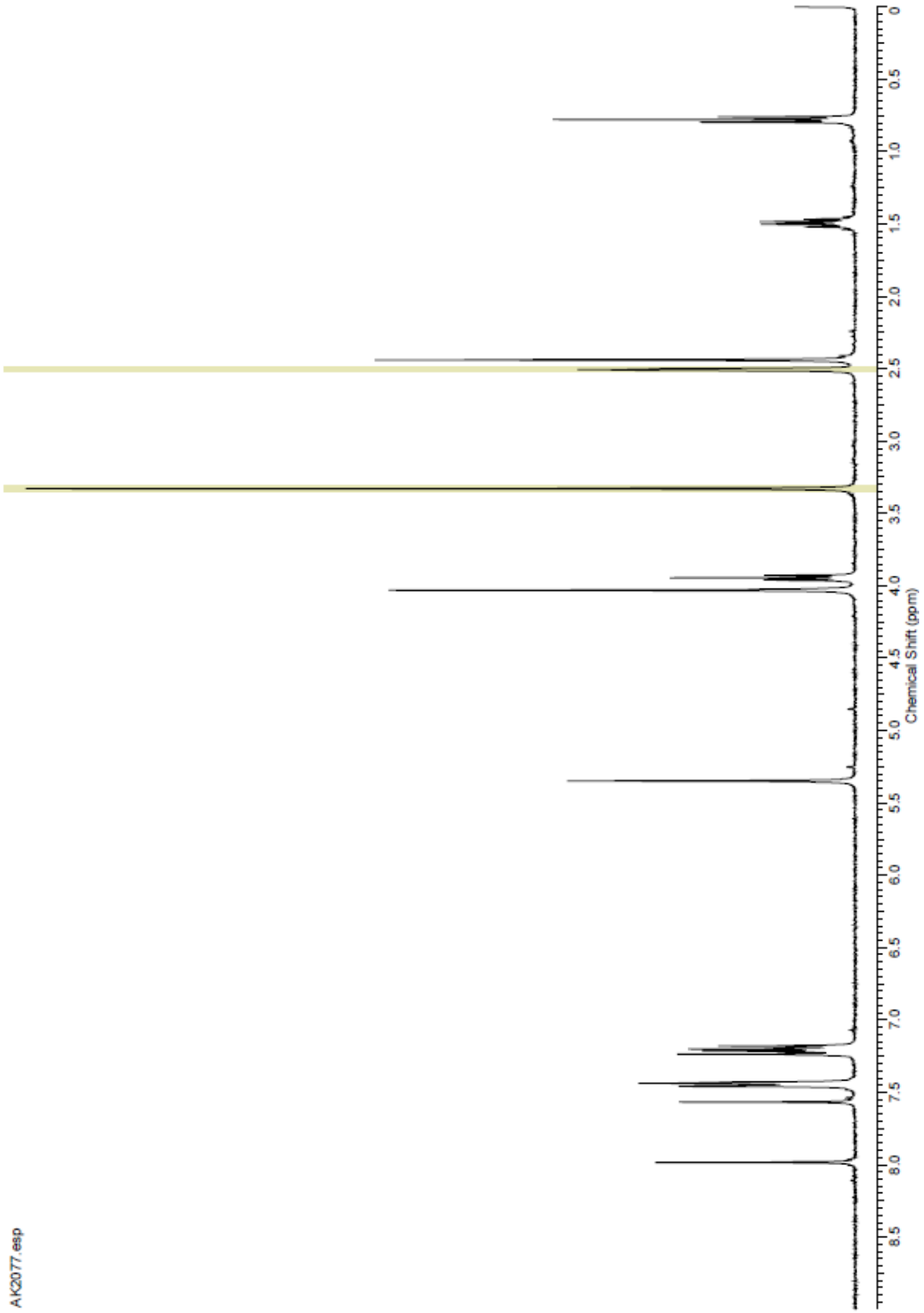
AK2077.esp
Chemical Shift (ppm)
0
0.5
1.0
1.5
2.0
2.5
3.0
3.5
4.0
4.5
5.0
5.5
6.0
6.5
7.0
7.5
8.0
8.5

ELQ-489 ^{1}H

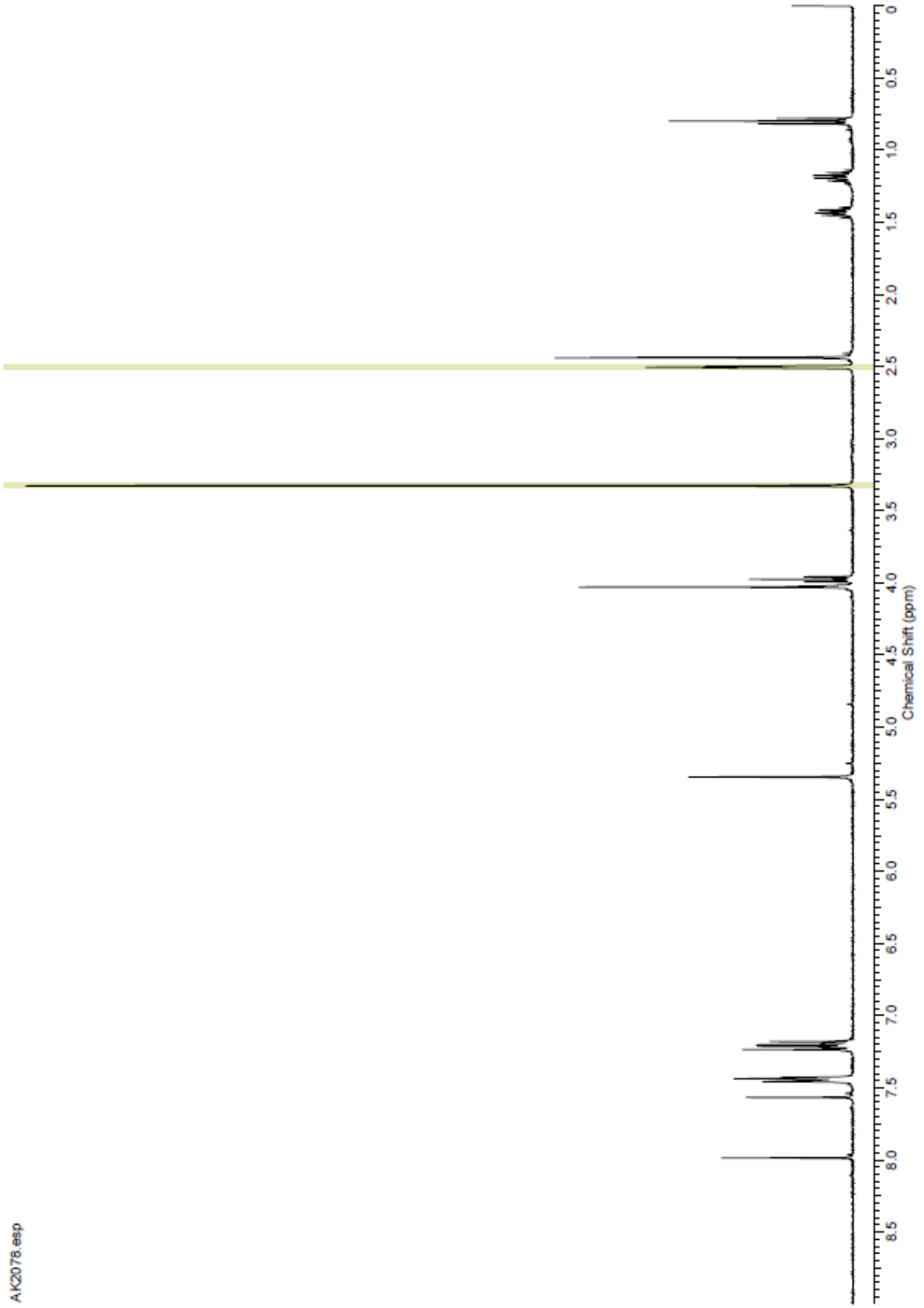
AK2078.esp
Chemical Shift (ppm)
0
0.5
1.0
1.5
2.0
2.5
3.0
3.5
4.0
4.5
5.0
5.5
6.0
6.5
7.0
7.5
8.0
8.5

ELQ-490 ^{1}H

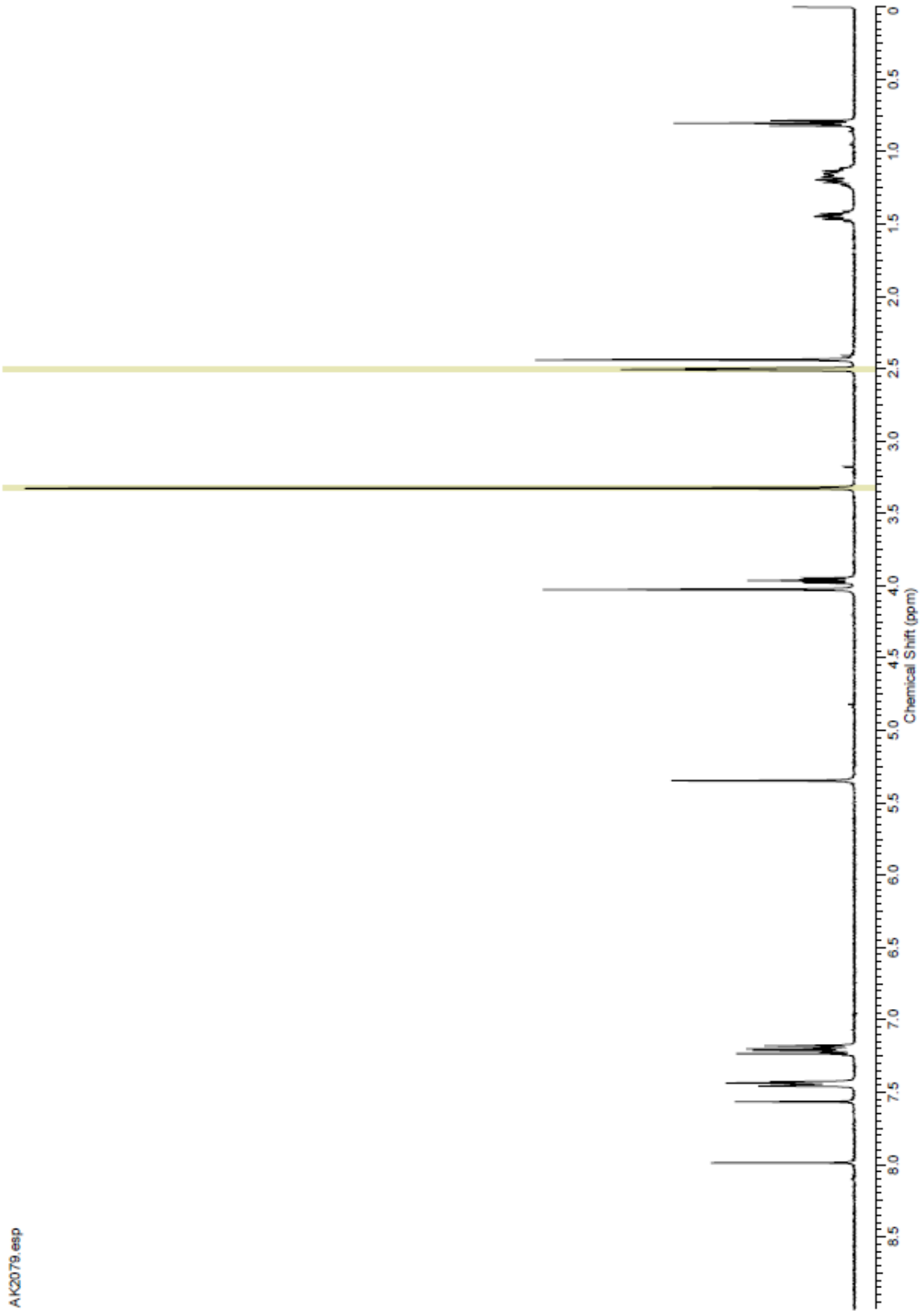
AK2079.esp
Chemical Shift (ppm)
0
0.5
1.0
1.5
2.0
2.5
3.0
3.5
4.0
4.5
5.0
5.5
6.0
6.5
7.0
7.5
8.0
8.5

ELQ-491 ^{1}H

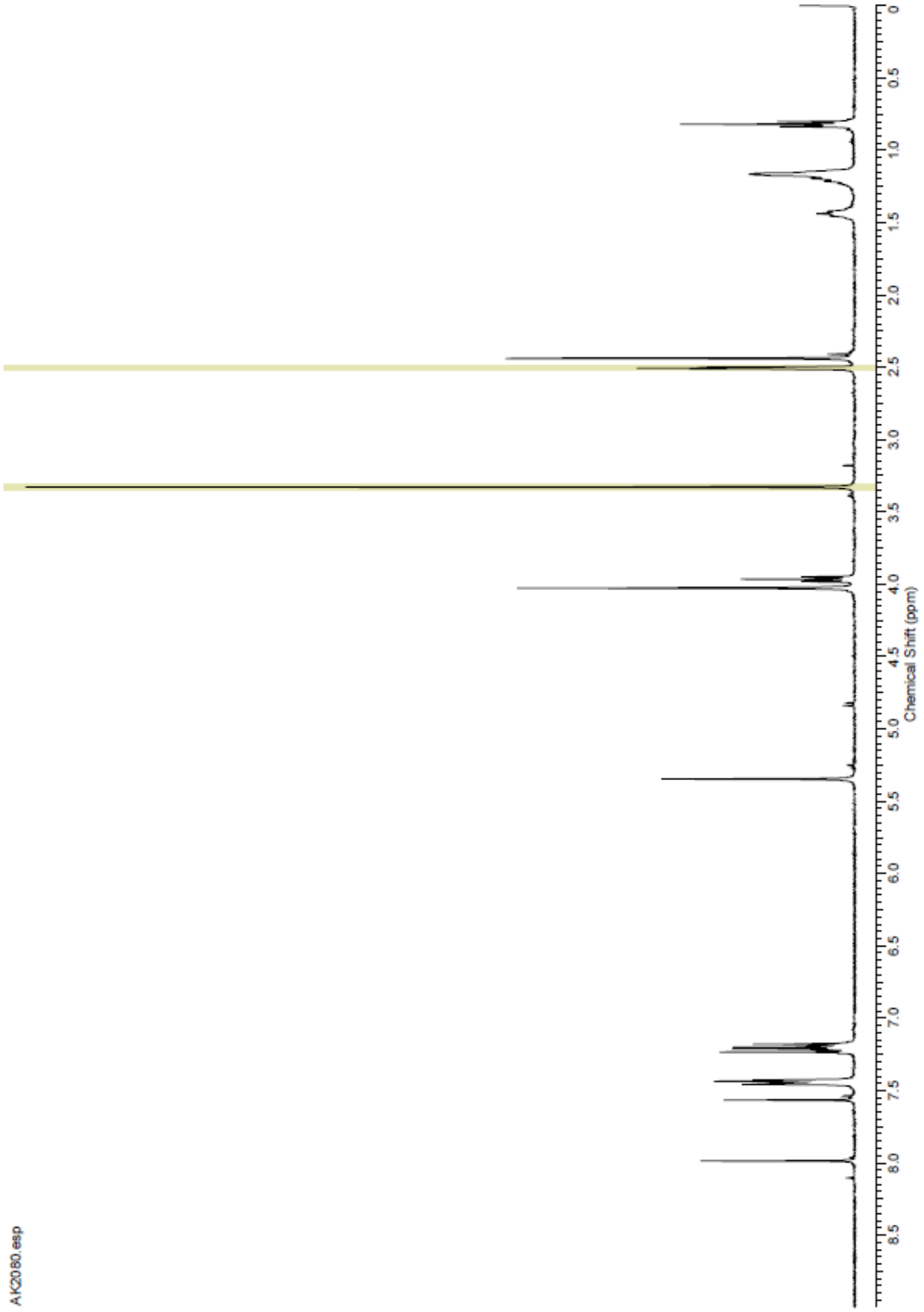
AK2080.esp
Chemical Shift (ppm)
0
0.5
1.0
1.5
2.0
2.5
3.0
3.5
4.0
4.5
5.0
5.5
6.0
6.5
7.0
7.5
8.0
8.5

ELQ-492 ^{1}H

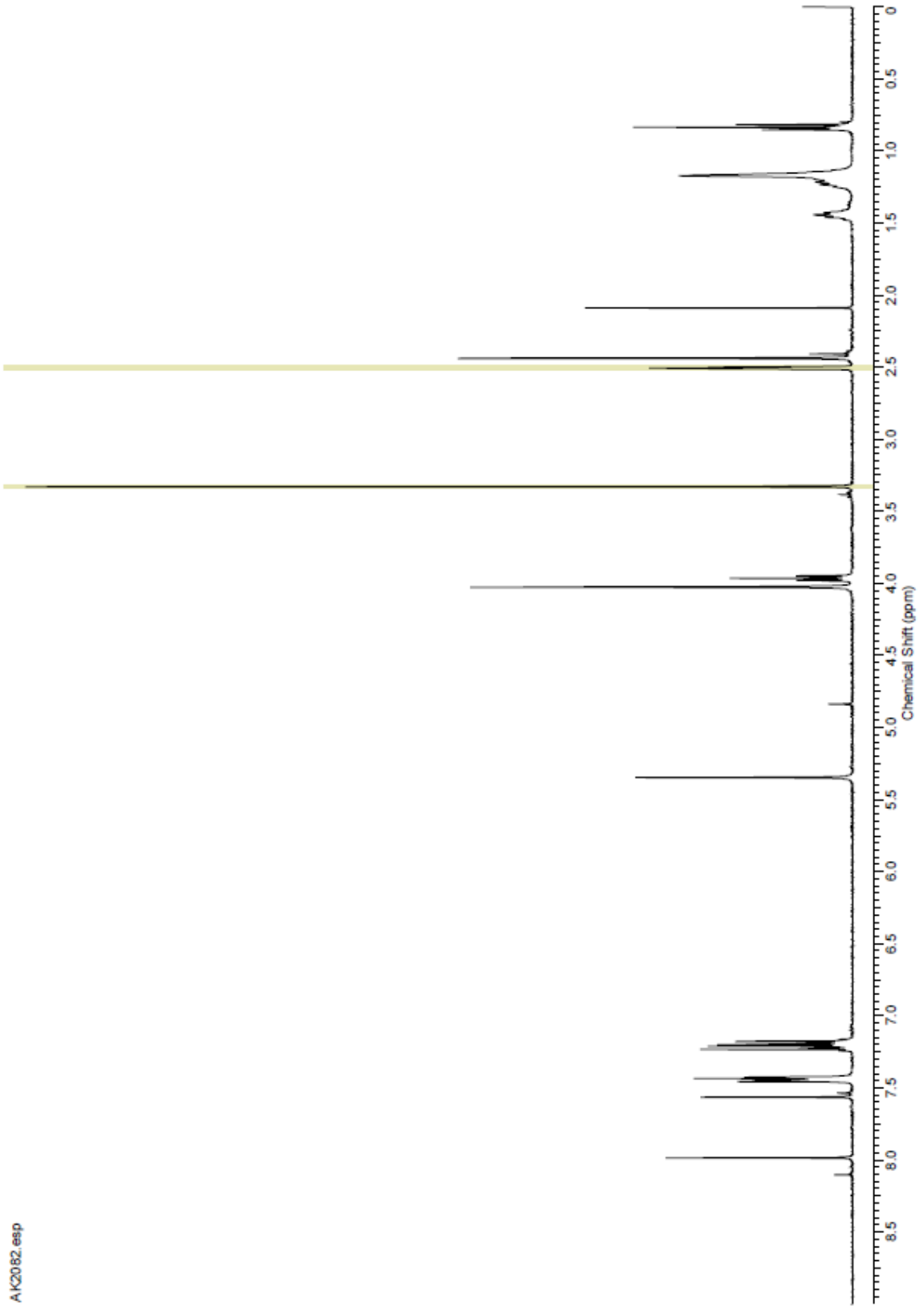
AK2082.esp
Chemical Shift (ppm)
0
0.5
1.0
1.5
2.0
2.5
3.0
3.5
4.0
4.5
5.0
5.5
6.0
6.5
7.0
7.5
8.0
8.5

ELQ-493 ^{1}H

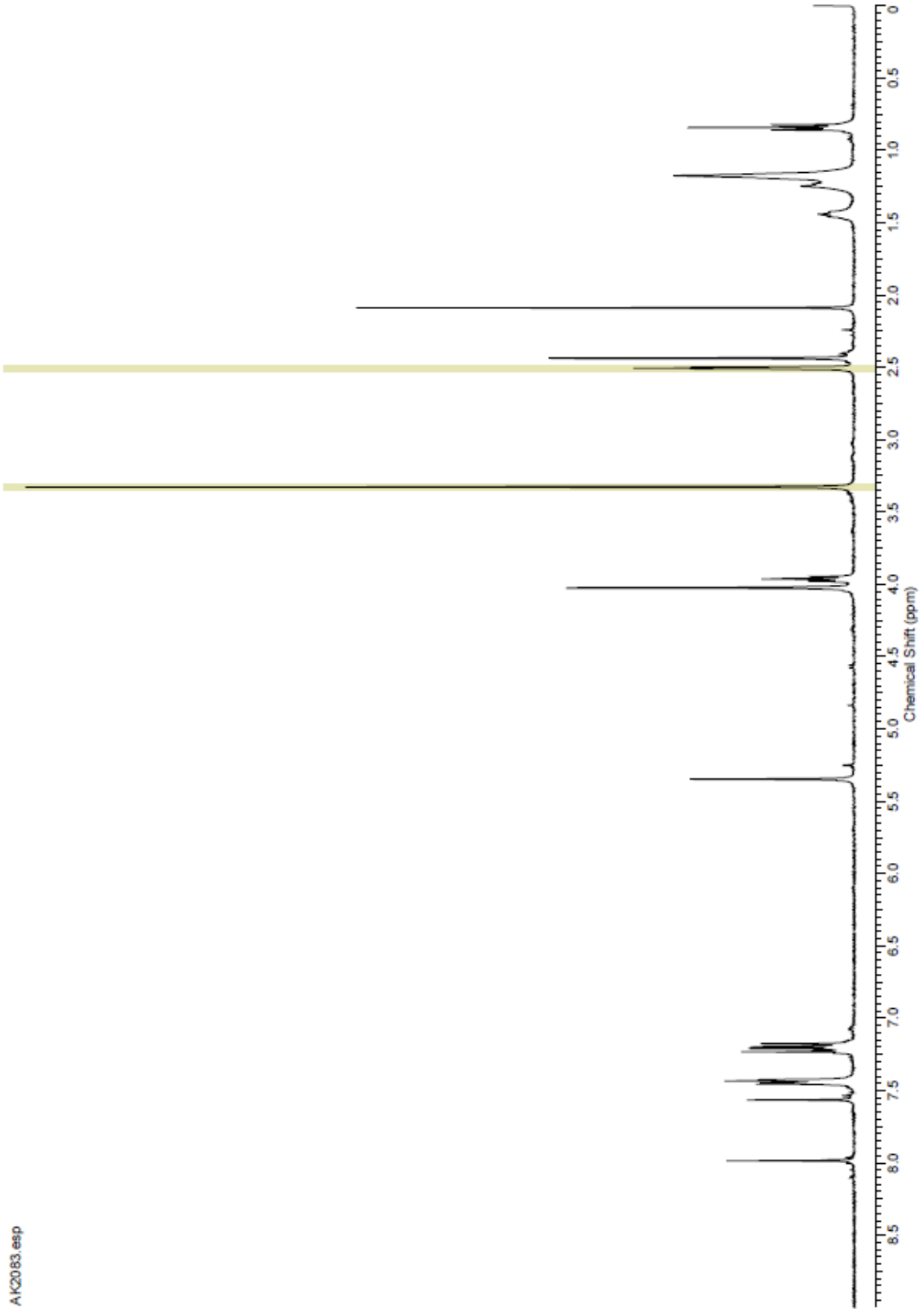
AK2083.esp
8.5
8.0
7.5
7.0
6.5
6.0
5.5
5.0
4.5
4.0
3.5
3.0
2.5
2.0
1.5
1.0
0.5
0
Chemical Shift (ppm)

ELQ-494 ^{1}H

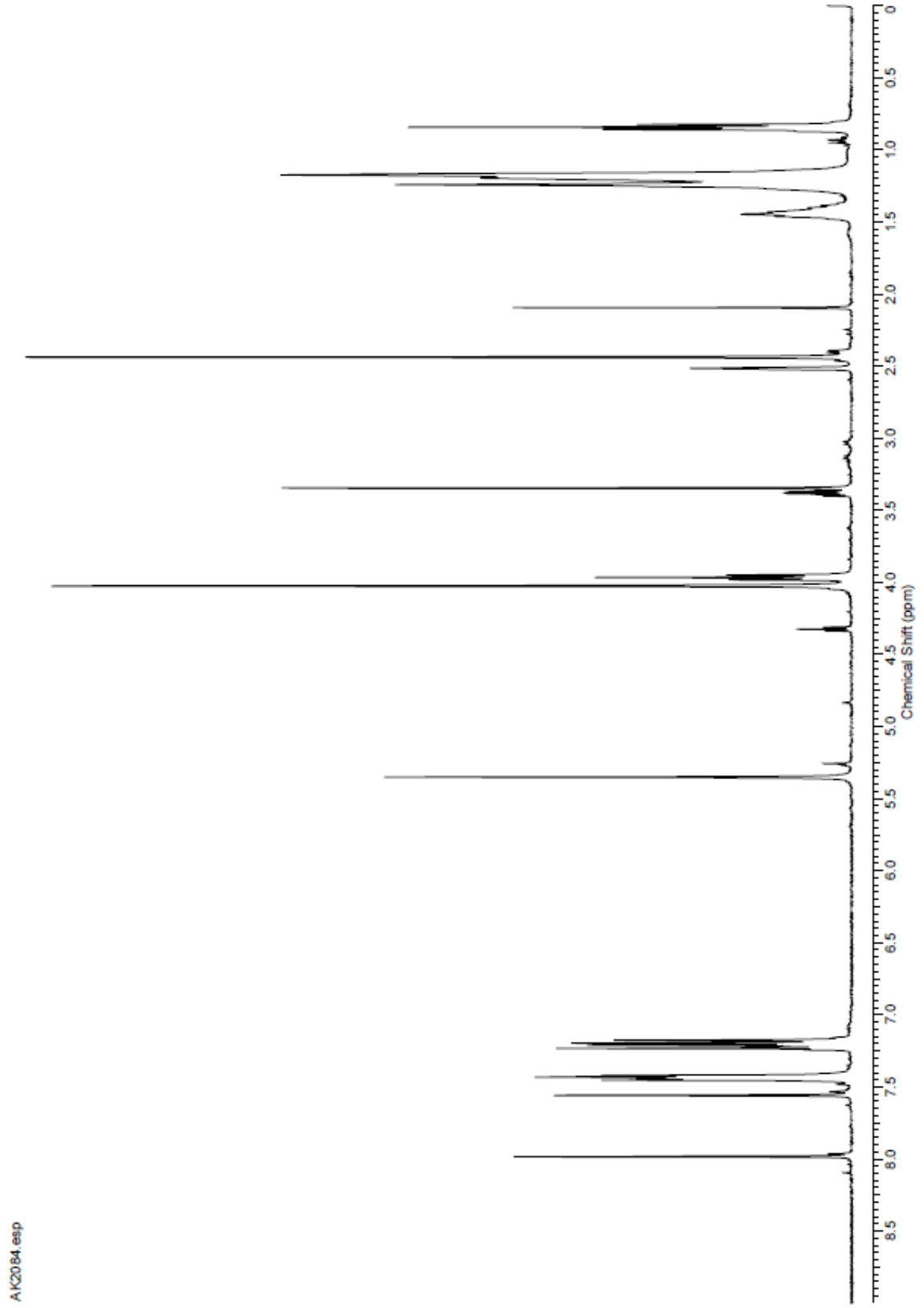
AK2084.esp
Chemical Shift (ppm)
0
0.5
1.0
1.5
2.0
2.5
3.0
3.5
4.0
4.5
5.0
5.5
6.0
6.5
7.0
7.5
8.0
8.5

ELQ-495 ^{1}H

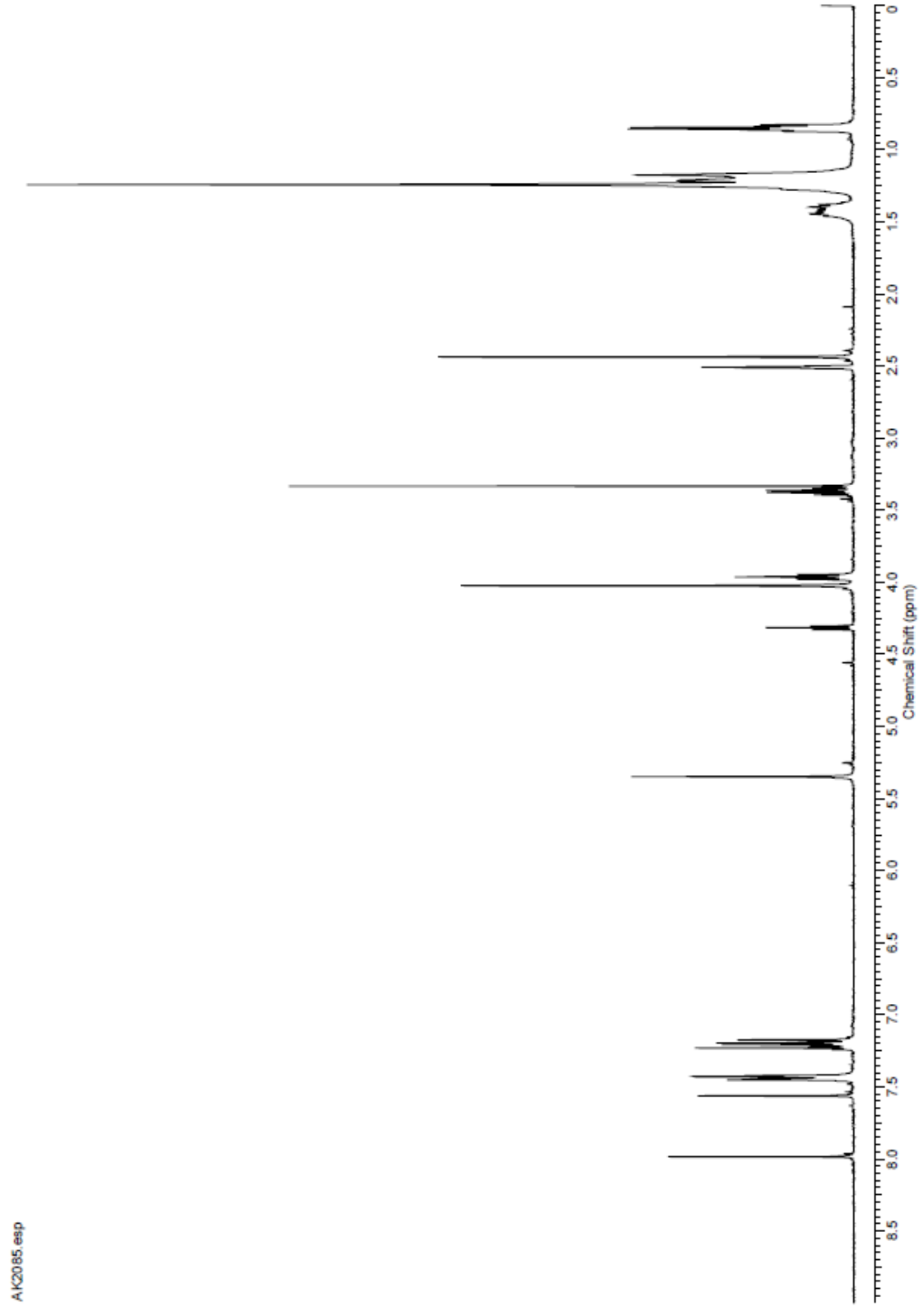
AK2085.esp
Chemical Shift (ppm)
0
0.5
1.0
1.5
2.0
2.5
3.0
3.5
4.0
4.5
5.0
5.5
6.0
6.5
7.0
7.5
8.0
8.5